JOURNAL OF THE MYANMAR ACADEMY OF ARTS AND SCIENCE

Chemistry

Vol. XVI, No.1A, October 2018

Myanmar Academy of Arts and Science

Journal of the Myanmar Academy of Arts and Science
Vol. XVI, No. 1 A

Contents
Chemistry

FABRICATION OF BIMETAL OXIDE HOLLOW NANOSPHERE USING CORE-CORONA MICELLES AS SOFT TEMPLATE*

Min Min Yee[1], Mohammad Mydul Alam[2], Kenichi Nakashima[2]

Abstract

Currently, nanoparticles with controlled morphology have tremendously attracted attention due to their wide application in catalysis, energy storage, and biomedicine. It is well known that hollow nanospheres with controlled size and shape show better performance compared to the conventional dense nanoparticles. In this research, Co/Fe oxide hollow nanospheres with diameter around 27±2 nm have been fabricated by using polymeric micelles of poly (styrene-block-acrylic acid) (PS-*b*-PAA) as a template. The polymer forms spherical micelles with PS-core and PAA-corona in aqueous solutions. According to the transmission electron microscopic (TEM) result, the void space of the fabricated hollow nanospheres is around 17 ±1 nm. The prepared Co/Fe oxide hollow nanospheres became shrunk during calcination. Fourier transform infrared resonance (FTIR) measurements confirm that the template polymer was completely removed during calcination.

Keywords: Nanoparticles, hollow , dense, polymeric micelles, core, corona

Introduction

Compared with dense inorganic nanoparticles, hollow inorganic nanoparticles possess more beneficial properties, e.g., lower density, larger specific area, additional surface permeability, etc. These advantages have intrigued in numerous studies on synthesis and applications of various nanosized inorganic hollow materials. Recently, polymeric micelles have been explored for the synthesis of nanoparticles because the size and morphology of the micelles can

[1] Professor, Dr, Department of Chemistry, University of Mandalay

[2] Professors, Dr, Department of Chemistry, Graduate School of Science and Engineering, Saga University

* **Best Paper Award Winning Paper in Chemistry (2017)**

be tuned by adjusting block size and polymer combination (Chockalingam, 2015). The commonly used polymeric micelles exclusively contain a core-corona architecture formed by AB diblock or ABA triblock copolymers (Bastakoti, 2014). We have reported a facile template for inorganic hollow nanospheres by using ABC triblock polymers as a template, which core-shell--corona structured micelles (Zhai *et al*., 2013). In our method, each domain of the core-shell-corona micelle has its own function. The core acts as a template of the void space of the inorganic hollow nanosphere, the shell serves as reaction field for the precursor of the inorganic material and the corona prevents secondary aggregation of intermediate composite particles of polymeric inorganic material. However, synthesis difficulties and high cost make the triblock copolymer inconvenient to use in scale-up production. To avoid such problems a diblock copolymer poly- (styrene-b-acrylic acid) has been synthesized and used as template for the synthesis of Co/Fe hollow nanospheres. Among inorganic nanoparticles, those of ferrites are materials which combine several remarkable physical properties along with chemical stability and low production cost. In form of nanomaterials, ferrites may have superparamagnetic properties and are currently used in magnetic data storage, magnetic imaging, drug delivery and microwave devices (Segneanu, 2014). In the present contribution, we have synthesized Co/Fe oxide hollow nanospheres using a diblock copolymer, poly(styreneb-acrylic acid) (PS-*b*-PAA), as a template. This diblock polymer forms core-corona type micelles in which the core acts as a template of the void space and the corona acts as reaction site for Co/Fe formation. The synthesized nanospheres have been thoroughly characterized by transmission electron microscopy (TEM), Fourier transformed infrared spectroscopy (FTIR) and Energy Dispersive X Ray spectroscopy (EDX).

Materials and Methods

Materials

The di block polymer poly(styrene-*block*-acrylic acid) ($PS_{(20000)}$-*b*- $PAA_{(7800)}$) has been kindly supported by Professor Yusa, Department of Materials Science and Chemistry, University of Hyogo, Shosha, Himeji, Japan. The number

inside parentheses represents the molecular weight of each block. Ferrous sulphate and cobalt sulphate have been purchased from Sigma Aldrich and Wako Chemicals, respectively. All chemicals were used without any treatment.

Preparation of Co/Fe Oxide Hollow Nanospheres

The core-corona micelle of PS-*b*-PAA has been prepared according to the method described by Khanal *et al*., 2007. In a typical synthesis, 10 mL of micelle solution (1 g L^{-1}) was taken in a conical flask and the pH was adjusted to about 9 using dilute NaOH. It is known that about 90 % of COOH groups of PAA are deprotonated at pH 7 (Nakashima *et al*., 1999). Certain amount of ferrous sulphate and cobalt sulphate (1:1) is added into the micelle solution to make 150 % *DN* (degree of neutralization). *DN* is defined by the following equation,

$$DN(\%) = \frac{\text{Amount of added Co/Fe ion (equivalent)}}{\text{Amount of carboxylate ion in the polymer (equivalent)}} \times 100 \qquad (1)$$

The *DN* is kept at 150 % unless otherwise stated. Due to the electrostatic interaction between cationic Co^{2+}/Fe^{2+} and anionic COO^-, Co^{2+}/Fe^{2+} is preferentially attached to the PAA block. Required amount of dilute NH_4OH is added to the solution for precipitation. The precipitate of Co-Fe hydroxide/polymer composite was separated from the aqueous suspension by centrifugation. The solid product was repeatedly washed with water and ethanol followed by drying at 50 °C. Co/Fe oxide hollow nanospheres were obtained after the polymeric template was removed from Fe/Co hydroxide/polymer composite by calcination at 500 °C for 4 h. Scheme 1 shows the schematic representation of fabrication of Co/Fe oxide hollow nanospheres.

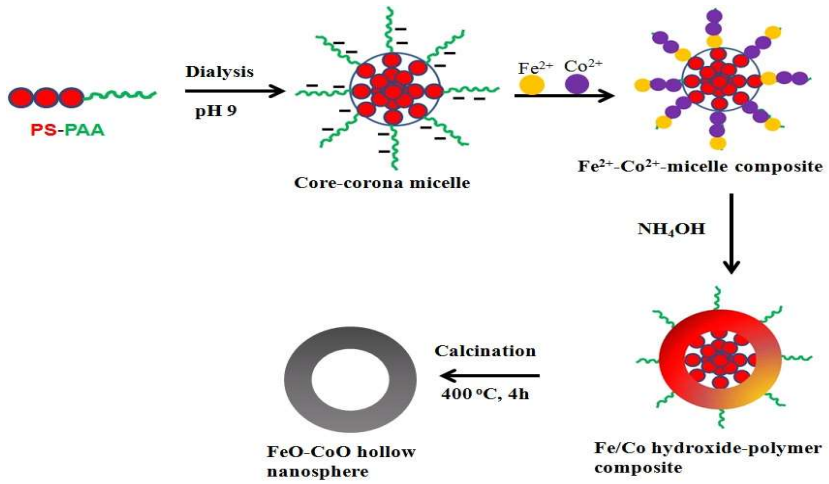

Scheme 1. Preparation of mixed metal oxide nanosphere using core-corona micelle as a template

Characterization of Hollow Particles

Transmission electron microscope (TEM) images were obtained using a JEOL JEM-1210 electron microscope at an accelerating voltage of 80 kV. Fourier transform infrared (FTIR) spectra were recorded on a Jasco FTIR 7300 spectrometer by using a KBr pellet technique. The elemental composition analysis was performed with Energy Dispersive X Ray (EDX) spectroscopy.

Results and Discussion

The formation of PS-*b*-PAA core-corona micelle has been confirmed by TEM. Figure 1 shows the representative TEM image of the core-corona micelle. It can be observed that the micelles are nearly spherical shape with a diameter around 23±2 nm. Similar results was observed by Alam *et al.*2015).

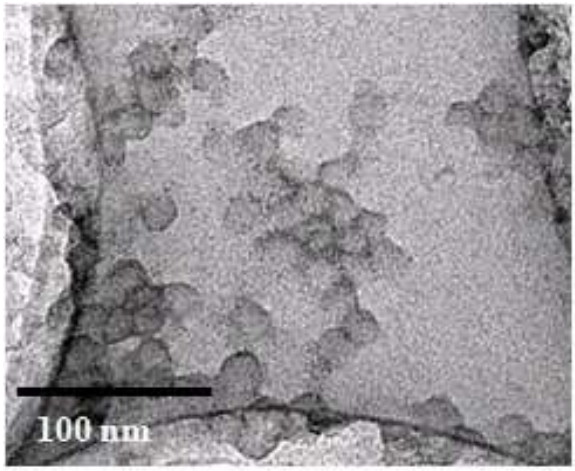

Figure 1. TEM image of the PS-*b*-PAA polymeric micelle stained with phosphotungstic

Figure 2 shows the TEM image of the Co/Fe oxide hollow nanosphere. Nanospheres are spherical shape with outer diameter of around 27±2 nm. The void space is around 17 ±1 nm. It should be noted that the void space is smaller than the core diameter of the micelle, which implies that the nanosphere shrinks during calcination. It can be observed from the TEM image that the some of the nanospheres are connected to each other, however, the morphology of the nanosphere resembles the template polymeric micelle.

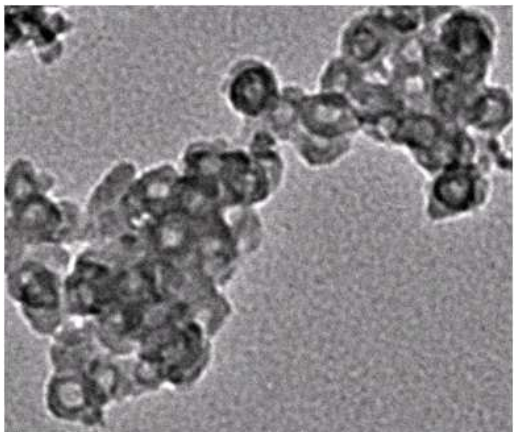

Figure 2. TEM image of the Co/Fe oxide hollow nanospheres after calcination

To confirm the removal of polymer template and the presence of Co/Fe oxide, FTIR analyses have been carried out. Figure 3 shows Co/Fe oxide hollow nanospheres before and after calcination (thick line) at 500 °C for 4 h. As shown in Figure 3, the disappearance of the vibrational bands of the polymer main chain (around 2900 cm^{-1}) and the C=C vibrational band of the phenyl ring (around 1650 cm^{-1}) after the calcination indicates the complete removal of the polymeric template. The presence of two strong M-O stretching and bending frequencies at 1,481 and 831 cm^{-1} shows phase purity of monodisperse one in the face-centered cubic surface.

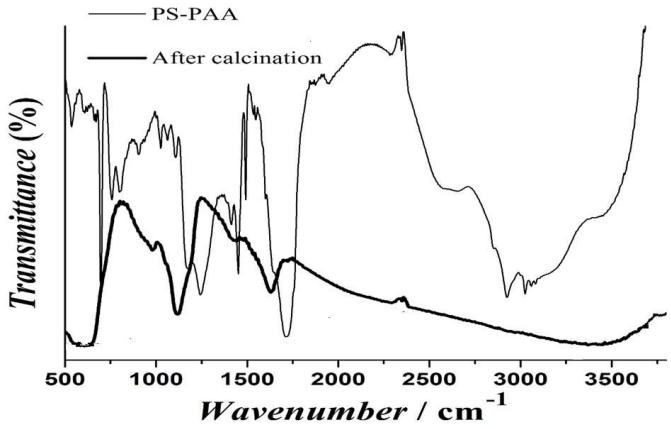

Figure 3. FTIR spectra of the PS-*b*-PAA polymer (thin line), Fe/Co oxide hollow nanosphere after calcination (thick line)

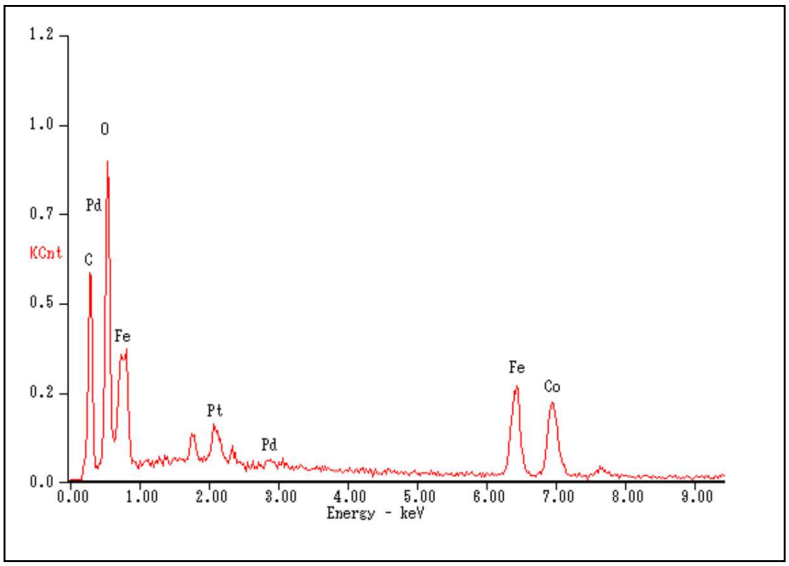

Figure 4. EDX spectrum of Fe/Co oxide hollow nanospheres

Figure 4 represents the EDX spectrum of Fe/Co oxide hollow nanospheres which indicate the existence of Co and Fe in the nanoparticles.

Conclusion

A facile way to fabrication of Co/Fe bimetal oxide hollow nanospheres has been explored by using a diblock copolymer PS-*b*-PAA as a template, which forms core corona micelles in aqueous media. PS-*b*-PAA polymeric micelles are spherical and the size of the PS-core is 23±2 nm. The Co/Fe hollow nanospheres have an outer diameter of 27±2 nm in which the void space diameter and the shell thickness are 17 and 5 nm, respectively. The synthesized Co/Fe nanospheres could allow varieties of applications especially early detection of tumors by magnetic resonance imaging (MRI) where iron oxide bond with various types of ligands such as proteins, peptides and small molecules demonstrate active targeting of tumors via specific molecular recognition.

Acknowledgements

The authors would like to express their profound gratitude to the Department of Higher Education, Ministry of Education, Myanmar, for giving the opportunity to carry out this research work and Myanmar Academy of Arts and Science for giving a chance to present this paper. We gratefully acknowledge the Graduate School of Science and Engineering, Saga University, Saga, Japan for providing research fund by the invitation lecturer program. This work is partly supported by a Grant-in-Aid for Scientific Research (24510139) from the Japan Society for the Promotion of Science (JSPS).

References

Alam, M., Hashimoto, K., Yamaguchi, C., Yusa, S., and Nakashima, K. (2015). "Synthesis of Zinc Borate Hollow Nanospheres Using Polymeric Micelles with Core Corona Architecture as a Template". *Bull. Chem. Soc. Jpn.* vol. 88, pp. 124–126.

Bastakoti, B. P., Guragain, S., Nakashima, K. and Yamauchi, Y. (2014). "Stimuli-Induced Core–Corona Inversion of Micelle of Poly(acrylic acid)- *block* -Poly(*N* -isopropylacrylamide) and Its Application in Drug Delivery". *Macromocular Chem. Phys.*, vol. 51, pp. 65-70.

Chockalingam, A. and Natarajan , U. (2015). "Molecular Dynamics Simulations Investigation of Structure and Thermodynamic Properties of Symmetric Poly(styrene-block-acrylic acid) (PS-b-PAA) Micelle in Salt-Free Aqueous Solution". *Macromol. Theory Simul*., vol. 45, pp.1-15.

Khanal, A., Inoue, Y., Yada, M. and Nakashima, K. (2007). "Synthesis of Silica Hollow Nanoparticles Templated by Polymeric Micelle with Core-Shell-Corona Structure". *J. Am. Chem. Soc.*, vol. 129, pp. 1534-1537.

Nakashima, K., Fujimoto, Y., Anzai, T., Dong, J., and Sato, H. (1999). "Monitoring pH-Dependent Conformational Changes in Aqueous Solutions of Poly(methacrylic acid-b-dimethylsiloxane) Copolymer based on Fluorescence Spectra of Pyrene and 1,3-bis(1-pyrenyl) Propane". *Photochem. Photobiol*., vol. 72, p. 1233.

Segneanu, A. E., Vlazan, P., Svera, P., Grozescu, I. and Sfirloaga, P. (2014). "Magnetic Cobalt Ferrite Nanoparticles: Synthesis and Surface Functionalization with Naturally Small Peptide*". Digest Journ. of Nanomaterials and Biostru*., vol. 9, no. 2, pp. 891 – 898.

Zhai, S., Yusa, S., and Nakashima. K. (2013). "Synthesis of Hollow Zinc Oxide Nanoparticles by Templating Micelles of Poly (styrene-b-acrylic acid-b-ethylene oxide) in Aqueous Solutions". *Bull. Chem. Soc. Jpn.*, vol. 86, no. 7, pp. 884-890.

STUDY ON PHYTOCONSTITUENTS AND BIOACTIVE PROPERTIES OF AVOCADO (*Persea Americana* MILL.) SEEDS

Myo Min[1], Pyae Phyo Kyaw[2]

Abstract

Avocado (*Persea americana* Mill.) is well known traditional medicinal plant and one of the most important fruit crops of the local market in Myanmar. According to the phytochemical investigation of avocado seeds, it was observed that phenolic compounds and flavonoids were present in the fruit seeds. Semi-quantitative elemental analysis of avocado seeds was performed by EDXRF method. Potassium and calcium were present as the considerable amounts in the avocado seeds. The nutritional values of avocado seeds were determined by AOAC method. It was observed that carbohydrate was the highest content and protein, fat and fiber were low contents in the sample. Screening of antimicrobial activities from avocado seeds was carried out by agar well diffusion method. In the screening, different crude extracts such as pet-ether, chloroform, ethylacetate, ethanol, methanol and water of avocado seeds were examined with the six microorganisms. According to the antimicrobial screening, avocado seeds possess antimicrobial activity. The antioxidant activity of water and ethanolic extract from avocado seeds was determined by DPPH free radical scavenging activity method using UV spectrophotometer. The ascorbic acid was used as a standard. The IC_{50} values of standard ascorbic acid, water and ethanolic extract were observed as 37.05, 45.05 and 93.17 μg / mL, respectively. Therefore, the antioxidant activity of water extract from avocado seed was more potent than that of ethanolic extract.

Keywords: avocado seed, nutritional values, antimicrobial activity, antioxidant activity

[1] Associate Professor, Dr, Department of Chemistry, West Yangon University
[2] Captain, Department of Chemistry, Defence Services Academy, Pyinoolwin

Introduction

Persea americana Mill. (Avocado)

The Avocado tree is an evergreen tree that attains heights of 40 to 80 feet and has many branches. The leaves are elliptic or oval in shape and 3 to 10 inches long. Flowers are small, greenish, and perfect (has both male and female parts). The avocado fruit may be round, pear shaped, or oblong, and the skin of the fruit may vary in texture and color. The skin may be pliable to woody, smooth to rough, and green-yellow, reddish-purple, purple, or black in color. The flesh of the fruit is greenish yellow to bright yellow when ripe and buttery in consistency, but inferior varieties may be fibrous. The avocado fruit has one large seed which makes up to 10 - 25% of the fruit weight (Morton, 1987).

Avocado (*Persea americana* Mill.) (Figure 1) is well known traditional medicinal plant and one of the most important fruit crops of the local market in Myanmar. Avocado seeds have more antioxidants than most fruits and veggies on the market and polyphenols like green tea. In fact, avocado seed has 70% of the antioxidants found in the whole avocado fruit, and avocado seed oil is also full of antioxidants, lower cholesterol, and helps fight off diseases.

Figure 1 Plant and flower of Avocado

Scientific Classification

Kingdom	: Plantae
Order	: Laurales
Family	: Lauraceae
Genus	: *Persea*
Species	: *P. americana*
Botanical name	: *Persea americana* Mill
English name	: Avocado
Myanmar name	: Htaw-but-thee

Health Benefits of *Persea americana* Mill (Avocado) Seed

Avocado seed (Figure 2) might offer natural antibiotic and antifungal benefits. In the test-tube study, avocado seed extracts inhibited a variety of pathogens, including Candida and other fungi and the mosquito that carries the tropical disease yellow fever. Seed and skin extracts protected against oxidation of fats and proteins in prepared meats, and moderately inhibited some types of pathogenic bacteria.

Figure 2 Fruit and seed of *Persea americana* Mill. (Avocado)

Avocado seed lowered cholesterol levels and may protect against arterial plaque formation (Pahua-Ramos *et al*., 2012). Then it attributed the cholesterol-lowering benefits to the seed's high content of dietary fiber, which

lowers cholesterol levels by binding to cholesterol in the intestinal tract and preventing absorption. Antioxidant activity of avocado seed might also help prevent cardiovascular disease by inhibiting lipid oxidation, a process that leads to arterial plaque formation .

Avocado seeds have more antioxidants than most fruits and veggies on the market and polyphenols like green tea. In fact Avocado Seed has 70% of the antioxidants found in the whole Avocado, and Avocado Seed Oil is also full of antioxidants, lowers cholesterol, and helps fight off disease. Avocado seed helps to prevent cardiovascular disease, lower cholesterol, and prevent strokes (Gorinstein *et al*., 2011) .

Materials and Methods

The avocado seed samples were collected from Pyinoolwin Township, Mandalay Region. Firstly, phytochemical investigation of avocado seed was carried out by Test Tube method. Then, semi-quantitative elemental analysis of avocado seed was performed by EDXRF method. The nutritional values of avocado seed sample were determined by AOAC method (AOAC, 2000). The antimicrobial activity of avocado seeds was examined by agar well diffusion method (Mar Mar Nyein, *et al*., 1991). The antioxidant properties of water and ethanolic extract from avocado seeds were determined by DPPH method using UV visible spectrophotometer.

Results and Discussion

Phytochemical Constituents of Avocado Seed Sample

The phytochemical tests revealed that alkaloids, α-amino acids, carbohydrates, glycosides, flavonoids, phenolic compounds, reducing sugars, saponins, steroids tannins, and terpenoids were present in the sample. Cyanogenic glycosides were absent in the sample. The results are shown in Table 1.

Semi-quantitative Elemental Analysis of Avocado Seed Sample by EDXRF Method

To determine the heavy toxic metals and macronutrient elements in plant samples, qualitative elemental analysis was carried out by EDXRF. Mineral elements present in dried powder samples of avocado seeds were determined by EDXRF spectrometer. The relative compositions of the elements predominantly found in the sample are presented in Table 2 and Figure 1. It was found that K and Ca were major constituents. S, P and Si were observed as the minor constituents and trace mineral elements such as Fe, Ni and Zn were alos observed in the avocado seed. These elements play an important role for the nutrition and medicinal formulation of human beings. The high content of K is effective for the persons with hypertension.

Table 1 Results of Phytochemical Investigation of Avocado Seed Sample

No.	Constituents	Extract	Test reagent	Observations	Remark
1	Alkaloids	1% HCl	Dragendorff's reagent Mayer reagent Sodium picrate solution	Orange ppt, White ppt, Reddish brown	+ + +
2	α-amino acids	H_2O	Ninhydrin	Purple spot	+
3	Carbohydrates	H_2O	10% α-naphthol, conc: H_2SO_4	Red ring	+
4	Cyanogenic glycoside	Dil H_2SO_4	Sulphuric acid, sodium picrate	No ppt	-
5	Flavonoids	EtOH	Mg turning, conc: HCl	Pink colour	+
6	Glycosides	H_2O	10% Lead acetate solution	White ppt	+
7	Phenolic compounds	H_2O	5% $FeCl_3$ solution	Green solution	+
8	Saponins	H_2O	Distilled water	Frothing	+
9	Steroids	PE	Acetic anhydride, conc: H_2SO_4	Green	+
10	Tannins	H_2O	2% gelatin solution	White ppt	+
11	Terpenoids	$CHCl_3$	Acetic anhydride, conc: H_2SO_4	Pink colour	+

(+) present, (-) absent

Table 2 Relative Abundance of Some Elements in Avocado Seed by EDXRF Method

Elements	Relative abundance (%)
K	65.51
Ca	21.38
S	4.73
P	2.13
Si	2.12
Fe	1.62
Ni	1.57
Zn	0.90

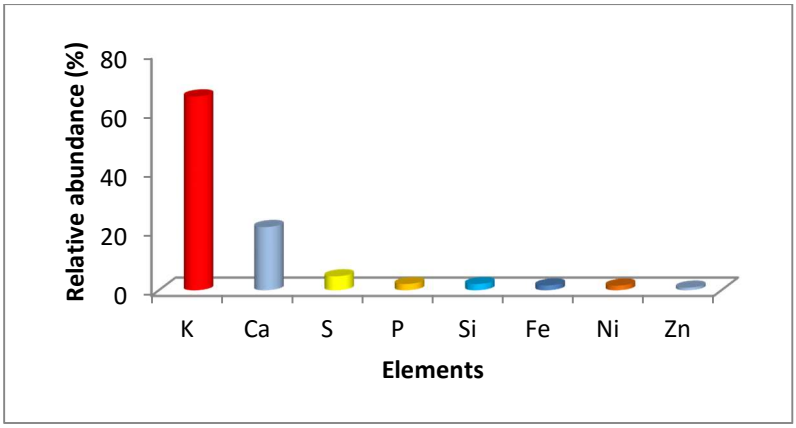

Figure 1 The histogram of elemental contents from avocado seed sample by EDXRF method

Nutritional Values of Avocado Seed

According to the method of AOAC (2000), it was found that the amount of carbohydrate and moisture were highest in the sample. Protein, fat and fibre were observed as minor nutrients. The high content of carbohydrate and low content of fat are required for the human health. The results are shown in Table 3 and Figure 2.

Table 3 Nutritional Values (%) in Avocado Seed Sample

No.	Nutrients	Contents (%)
1	Moisture	10.90
2	Ash	2.38
3	Crude Protein	7.84
4	Crude fiber	1.54
5	Crude fat	5.81
6	Water soluble carbohydrate	71.53

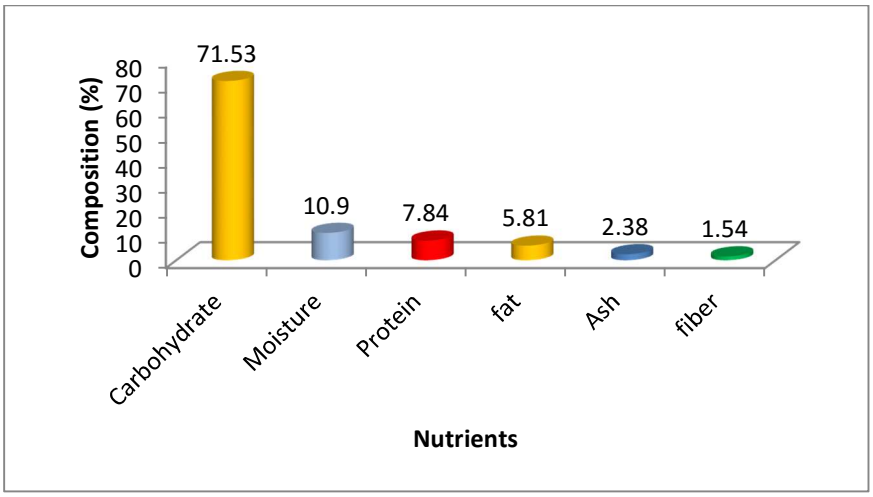

Figure 2 The histogram of nutritional values in avocado seed sample

Screening of Antimicrobial activity

Antimicrobial activities of Pet-ether, $CHCl_3$, MeOH, EtOAc, EtOH and H_2O extracts were screened by agar well diffusion method (Table 4). In this screening, the crude extracts were tested on six species of microorganisms; *Bacillus subtilis, Staphylococcus aureus, Pseudomonas aeruginosa, Bacillus pumilus, Candida albicans* and *E.coli* species.

In the sample of *Persea americana* Mill (avocado) seed, all the extracts are active on all organisms except MeOH and EtOH extracts which are inactive against *Pseudomonas aeruginosa*. The activities of EtOAc extract on all microorganisms are considerably high. The sensitivity of EtOH and H_2O extract are suitable for the medicinal formulation of antimicrobial drugs.

Table 4 Results of Antimicrobial Screening of *Persea americana* Mill (avocado) Seed against Six Microorganisms

Solvent extracts	*B. subtilis*	*S. aureus*	*P. aeruginosa*	*B. pumilus*	*C. albicans*	*E.coli*
Pet-ether	13 mm (+)	18 mm (++)	12 mm (+)	19 mm (++)	18 mm (++)	16 mm (++)
$CHCl_3$	18 mm (++)	13 mm (+)	13 mm (+)	14 mm (+)	12 mm (+)	13 mm (+)
EtOAc	23 mm (+++)	22 mm (+++)	20 mm (+++)	23 mm (+++)	24 mm (+++)	22 mm (+++)
EtOH	18 mm (++)	21 mm (+++)	-	17 mm (++)	15 mm (++)	16 mm (++)
MeOH	18 mm (++)	12 mm (+)	-	16 mm (++)	16 mm (++)	15 mm (++)
H_2O	14 mm (+)	13 mm (+)	25 mm (+++)	13 mm (+)	12 mm (+)	12 mm (+)

Agar well : (10 mm), 10 mm-14 mm (+), 15 mm-19 mm (++), 20 mm-above (+++)

Antioxidant Activity

The DPPH radical scavenging activity of water and ethanolic extracts from avocado seed was compared with ascorbic acid. The reduction capability of DPPH radicals was determined by the decrease in its absorbance at 517 nm, which was induced by antioxidants. Determination of radical scavenging by DPPH method base on the change in absorbance of crude extracts solutions in various concentrations. Six kinds of concentrations 400 µg / mL, 200 µg / mL, 100 µg / mL, 50 µg / mL, 25 µ g/ mL and 12.5µg / mL were prepared by dilution with ethanol as solvent. Ascorbic acid (tablets) was used as standard

sample and ethanol was employed as control. Blank solution was also prepared by mixing sample and ethanol. The absorbance values were measured at wavelength 517nm for different concentration of extracts and the control. These values are used to calculate the percentage inhibition of DPPH radical against the samples. The IC_{50} values of various extracts were calculated from the percentage inhibitions at various concentrations. The results of the free radical scavenging activity of avocado seed assessed by DPPH assay was summarized by IC_{50} using method of linear regression. The lower the value of IC_{50} the higher is the antioxidant property. From the screening, IC_{50} value of standard ascorbic acid was 37.05 µg / mL (Table 5 and Figure 3). It was observed that water and ethanolic extract of avocado seed have the radical-scavenging activity with IC_{50} values of 45.05 µg / mL (Table 6 and Figure 4) and 93.17 µg / mL (Table 7 and Figure 5), respectively. According to the IC_{50} values, water and ethanolic extracts of avocado seeds possess the rich antioxidant properties. It can be seen that the antioxidant activity of water extract is more potent than that of ethanolic extract.

Table 5 % RSA and IC_{50} Value of Standard Ascorbic Acid (Tablet) at 517 nm

Concentration (µg/mL)	%RSA	Absorbance	IC_{50} (µg/mL)
12.5	36.37	0.636	
25.0	45.89	0.658	37.05
50.0	56.63	0.634	
100.0	65.36	0.611	
200.0	76.63	0.550	
400.0	92.26	0.497	

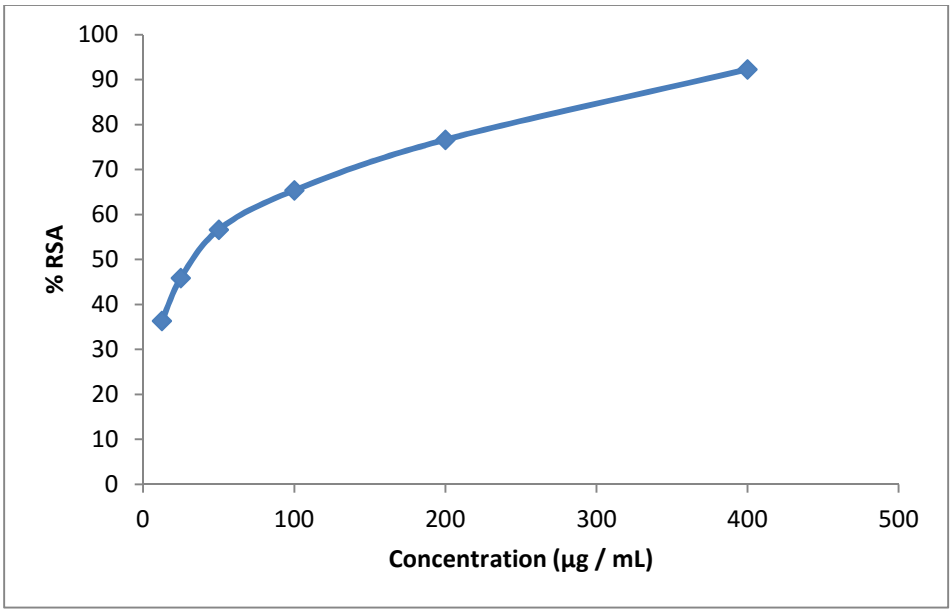

Figure 3 Correlation between DPPH radical scavenging activity and concentration of standard ascorbic acid (tablet)

Table 6 % RSA and IC_{50} Value of Water Extract of Avocado Seed

Concentration (µg/mL)	%RSA	Absorbance	IC_{50} (µg/mL)
12.5	41.01	0.693	
25.0	47.97	0.658	45.05
50.0	52.61	0.634	
100.0	56.67	0.611	
200.0	70.41	0.550	
400.0	80.27	0.497	

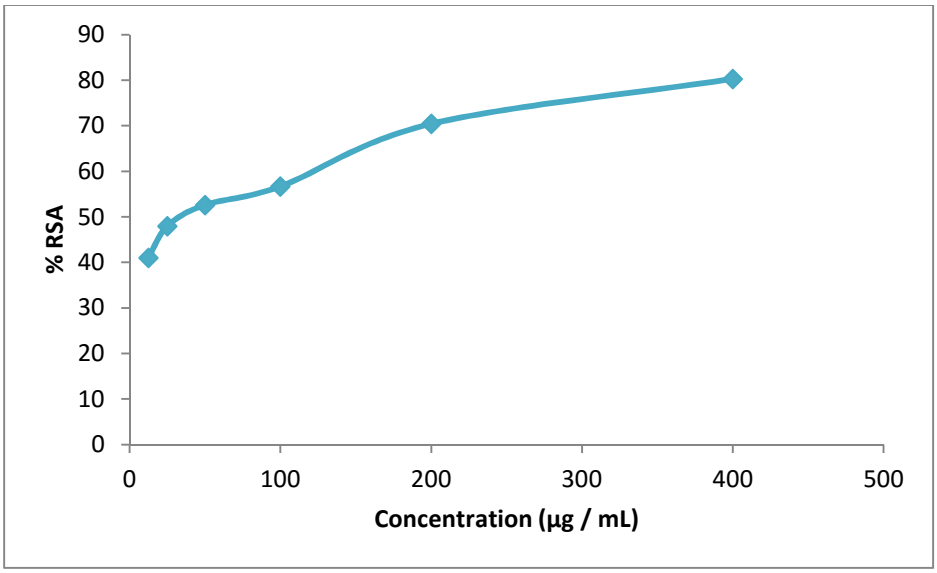

Figure 4 Correlation between DPPH radical scavenging activity and concentration of water extract of avocado seed

Table 7 % RSA and IC_{50} Value of Ethanolic Extract of Avocado Seed

Concentration (µg/mL)	%RSA	Absorbance	IC_{50} (µg/mL)
12.5	30.25	0.260	
25.0	39.35	0.254	
50.0	45.81	0.141	93.17
100.0	54.52	0.002	
200.0	69.19	0.0721	
400.0	98.67	0.025	

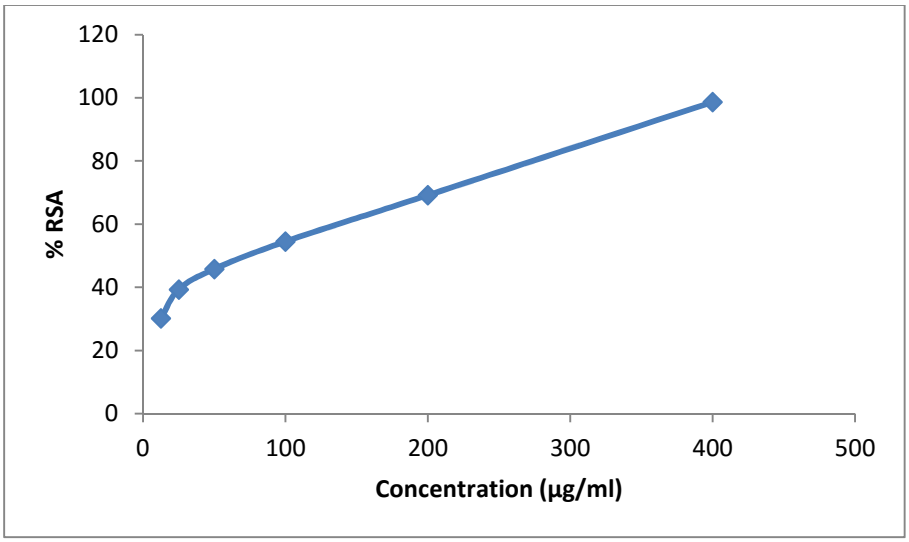

Figure 5 Correlation between DPPH radical scavenging activity and concentration of ethanolic extract of avocado seed

Conclusion

Phytoconstituents such as alkaloids, α-amino acids, carbohydrates, flavonoids, glycosides, phenolic compounds, saponins, steroids, tannins, and terpenoids were present in the avocado seed sample. These phytoconstituents are applicable for the use of human health. But cyanogenic glycosides were not found in the sample. The observed phytochemical constituents are essential compounds for the metabolism and nutrition of human body.

In the study of elemental analysis, the high contents of K (65.51%) and Ca (21.38%) were observed. The high content of K is effective for the persons with hypertension. Ca helps the teeth and bones to be strong for human.

On antimicrobial screening of avocado seed sample, the various crude extracts were examined with six microorganisms such as *Bacillus subtilis, Staphylococcus aureus, Pseudomonas aeruginosa, Bacillus pumilus, Candida albicans* and *E.coli* species. From the screening, EtOAc extract showed the highest activities against all microorganisms. With *Pseudomonas aeruginosa*, MeOH and EtOH extract were inactive. The sensitivities of EtOH and H_2O

extracts are very important for the medicinal formulation of antimicrobial drugs.

The antioxidant activity of avocado seed was continued to determine by DPPH free radical scavenging activity method using UV spectrophotometer. IC_{50} values for the antioxidant activity of the standard ascorbic acid, water and ethanolic extract from avocado seed were 37.05, 45.05 and 93.17 µg / mL, respectively. According to the IC_{50} values of avocado seed, the antioxidant activity of water extract was more potent than that of ethanolic extract. The antioxidant compounds reduce risk for chronic diseases including cancer and heart diseases. Therefore, avocado seeds may be used in the medicinal formulation of human health.

Acknowledgements

The authors would like to express their profound gratitude to the Department of Higher Education (Yangon Office), Ministry of Education, Yangon, Myanmar, for provision of opportunity to do this research and Myanmar Academy of Arts and Science for allowing to present this paper.

References

AOAC, (2000). Official Methods of Analysis of the Association of Official Analytical Chemists. Washington DC: 15th edition

Gorinstein, S. Poovarodom, S. and Leontowicz, H. (2011). "Antioxidant Properties and Bioactive Constituents of Some Rare Exotic Thai Fruits". *Food Research International*, vol. 44, pp. 2222-2232.

Mar Mar Nyein, Chit Maung, Mya Bwin and Tha, S.J. (1991). "*In Vitro* Testing of Various Indigenous Plant Extracts on Human Pathogenic Bacteria". *Myanmar Health Science Research Journal*. vol 3. pp. 89-99

Morton, J.F. (1987). *Fruits of Warm Climates*. Florida: Miami, pp. 91–102

Pahua-Ramos , M. E., Alicia Ortiz-Moreno,A. ,Chamorro-Cevallos,G., Hernández-Navarro,M.D. ,Garduño-Siciliano,L.,Necoechea-Mondragón,H. and Hernández-Ortega,M. (2012). "Hypolipidemic Effect of Avocado (*Persea americana* Mill) Seed in a Hypercholesterolemic Mouse Model". *Plant Foods for Human Nutrition*, vol 67,pp 10-16

COMPARATIVE STUDIES OF ANTIBACTERIAL ACTIVITY AND PHYTOCHEMICAL CONSTITUENTS OF SOME MYANMAR INDIGENOUS MEDICINAL PLANTS

San San Aye[1], Hnin Hnin Aye[2], Daw Hla Ngwe[3], Saw Hla Myint[4]

Abstract

Developing countries, where dysentery and diarrhea are endemic, depend strongly on traditional medicine as a source for inexpensive treatments because it is based on plants which are abundantly available in these countries. Consequently, Myanmar indigenous medicinal plants (*Curcuma longa* L., *Nigella sativa* L. and *Piper betel* L.) which are used for the treatment of dysentery and diarrhea in Myanmar were selected to study in order to find the scientific basis for such use. The selected plants were screened for antibacterial activity by using agar disc diffusion technique. Polar and non-polar extracts of the selected plants were tested on 33 species of standard and hospital bacterial strains. The Minimum Inhibitory Concentration (MIC) of the active extracts was also determined by agar plate dilution method. Three curcuminoids, namely curcumin (5.9 %), desmethoxy curcumin (0.018 %) and bisdesmethoxy curcumin (0.0136 %) were isolated from *C. longa* rhizomes. *N. sativa* seeds were fractionated by column chromatography to give thymoquinone (0.01 %), kaempferol (0.12 %) and quercetin (0.001 %). Eugenol (0.1 %) was isolated from essential oil of *P. betel*. The isolated compounds were identified by UV, FT IR, ^{1}H NMR, ^{13}C NMR and mass spectroscopic methods. The isolated compounds were also found to show bactericidal activity. Thus the extracts of the three plants have high potential for the production of combined formulation to treat infections caused by bacteria.

[1] Associate Professor, Dr,Department of Chemistry, Myingyan Degree College
[2] Professor and Head, Dr, Department of Chemistry, University of Yangon
[3] Professor and Head, Dr. Department of Chemistry, University of Yangon
[4] Professor and Head (Retired),Dr, Department of Chemistry, University of Yangon

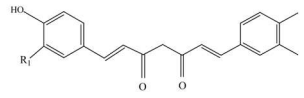

$R_1 = R_2 = OCH_3$: Curcumin
$R_1 = H, R_2 = OCH_3$: Desmethoxy curcumin
$R_1 = R_2 = H$: Bisdesmethoxy curcumin

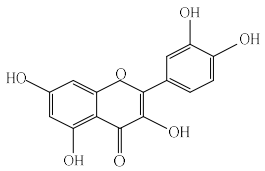

Quercetin

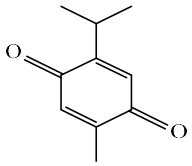

Thymoquinone

Kaempferol

Eugenol

Keywords*:* bactericidal activity, curcuminoids, essential oil, spectroscopic method

INTRODUCTION

Curcuma longa L. (Nanwin)

The medicinal plant (tumeric), *Curcuma longa* L., belonging to the family, Zingiberaceae, is a perennial herb 2 to 3 feet high with a short stem and tufted leaves and is cultivated in India. It is used as a domestic remedy. It is used as a food additive for fish and meat (Burkill, 1996). Major constituents of rhizomes are pale yellow to orange-yellow volatile oil (6 %) composed of a number of monoterpenes and sesquiterpenes including zingiberence, curcumene, α- and β–turmerone (WHO, 1999). The colouring principles

(5 %) are curcuminoids. 50-60 % of which are a mixture of curcumin, desmethoxy curcumin and bisdesmethoxy curcumin. The antioxidant properties of curcuma powder are probably due to the phenolic character of curcumin (FAO/ WHO, 1978).

Nigella sativa L. (Samon-net)

Samon-net (black seed), *Nigella sativa* L., belonging to the family, Ranumculaceae, is an annual herb leaves. Flowers are pale blue on solitary

long stalks. Fruit composed of 5-12 more or less united follicles. It is found in upper Myanmar (Mya Bwin and Sein Gwan, 1973).

Black seed is native to the Mediterranean and is also known as the "Seed of blessing". Black seed has rich nutrient composition which comprises 15 amino acids including all essential acids, carbohydrates and proteins as well as essential fatty acids and minerals: calcium, iron, sodium and potassium. The chief constituents of the seeds are volatile oil and a fixed oil. The seed oil possesses hypotensive effect. *N. sativa* L. seeds have many medicinal properties such as bronchodilator, hypotensive, antibacterial, antifungal, analgesic, anti-inflammatory and are universally accepted as a panacea (Khan, 1999).

Piper betel L. (Kun)

Kun (Betel leaf), *Piper betel* L., belonging to the family, Piperaceae, is shout glabrous climber with leaves of 5-20 cm long broadly ovate, slightly cordate and unequal at the base, shortly accumulate with yellowish or bright green shining on both size. The pungent taste possessed by all organs of the plant is one of the vital characteristics of the genus. This taste owes to the presence of alkaloid piperine and the aromatic odour is due to that of volatile oil (Chopra *et al.*, 1956).

Betel is widely cultivated in South East Asia countries especially in Myanmar for its leaves serve both as indigenous and modern medicines. It is one of the well-known medicinal plants and is widely cultivated for commercial purpose in Myanmar.

Betel leaf oil consists mainly of phenol and terpenes, that relative proportions varying with the original portion of the leaves. The highest the proportion of phenols in the oil, the better the quality. The predominant phenolic constituent in the betel leaf oil is eugenol which is used extensively as a raw material in the synthetic preparation of vanillin and as an antiseptic in pharmaceutical and dental preparation (Guenther, 1960).

Materials and Methods

Plant Materials

The rhizomes of *Curcuma longa* L. and *Nigella sativa* L. were procured from Sandi indigenous medicine shop. The leaves of *Piper betel* L. were collected from Yangon Region market. The rhizomes and seeds were ground to get a fine powder. The drug powders were then stored in an air-tight container. Betel leaves were left in the open air till they were completely dried. The dried sample was ground in a grinding machine.

Chemicals

Column chromatography was run on Kiesel gel 60 (Merck) and TLC on Alufolien Kiesel gel 60 GF_{254} (Merck). Other chemicals were procured from the BDH and E. Merck.

Microbial Strains

The bacterial strains used were obtained from the Department of Medical Research (Lower Myanmar), Yangon.

Instruments

Shinmadzu UV-240, UV-visible spectrophotometer, Perkin-Elmer spectrum GX FT IR spectrophotometer, Bruker 400 MHz NMR spectrometer, autoclave, incubator.

Antibacterial Screening of Crude Extracts

For the examination of *in vitro* antibacterial activity of crude extracts, agar disc diffusion method was used. Discs obtained by filter paper (Toyo No.26, Japan) punched to 8 mm diameter, were used to impregnate the extracts to obtain approximately 20 μg/disc, and prior to adherence on the culture plates. The discs were allowed to dry at 42 ℃ incubator (Finegold and Martin, 1982).

The bacterial suspension from trypticase soy broth was streaked evenly onto the surface of the trypticase soy agar plates with sterile cotton swab. After the inoculums had dried (5 mins), the dried discs were placed on the agar with flamed forceps and gently pressed down to ensure proper contact. A disc impregnated with solvent only was placed alongside the test discs for control and comparing purposes.

The plates were incubated immediately or within 30 mins after inoculation. After overnight incubation at 37 ℃, the zones of inhibition diameter including 8 mm discs were measured.

Determination of mMinimum Inhibitory Concentration (MIC) of the Active Extracts by Agar Plate Dilution Method

The minimum inhibitory concentration (MIC) of the active extracts were determined by plate dilution method (Cruickshank *et. al.,* 1975; Finegold and Martin, 1982).

The active extracts were dissolved with their respective solvents (e.g. ethyl acetate extract with ethyl acetate) and diluted with trypticase soy agar to obtain the following concentrations: 2 mg/mL, 1 mg /mL, 0.5 mg/mL, 0.25 mg/mL, 0.125 mg/mL, 0.0625 mg/mL, 0.03125 mg/mL, 0.015625 mg/mL and 0.0078125 mg/mL.

The bacterial suspension (0.02 mL) was applied as streak/ droplet onto the surface of the prepared agar plates. Then the plates were incubated at 37 ℃ overnight. After overnight incubation, the lowest concentration showing no growth of the organisms was taken as the minimum inhibitory concentration (MIC), expressed in mg/mL. The experiments were repeated three times at exactly the same parameters, and the mean results were taken.

Isolation of Compounds from *C. longa*

The ethyl acetate extract (0.6 g) was chromatographed on a silica gel column using dichloromethane - methanol (95:5) solvent mixture as eluent, Finally, 3 main fractions were obtained after combining the similar fractions.

Isolation of Compounds from *N. sativa*

From the soxhlet extraction ***N.*** *sativa* seed powder (100 g) with PE (60-80 ºC), 40 g of an oil, i.e. 40 % of the drug, were obtained. Thus, oil yielded upon steam distillation was 0.04 g of volatile oil, i.e. 0.04 % of the drug. The volatile oil in turn yielded 0.0632 g of yellow oil of thymoquinone, i.e. 0.01 % based on drug (0.6 g) by column chromatography on a silica gel column with PE-toluene (2:3) solvent mixture as eluent.

The dried seed powder (100 g) was soaked in 500 mL of 70 % ethanol and heated for 10 min on a water bath and kept at room temperature overnight (Harborne, 1984). The mixture was filtered and the filtrate was concentrated to a volume of 100 mL. The solution was extracted twice with 200 mL of PE (60 – 80 ºC). The aqueous layer was evaporated to dryness. The residue was dissolved in 2M hydrochloric acid solution and hydrolyzed for 45 min on a boiling water bath. The mixture was cooled and filtered. The filtrate was extracted with ethyl acetate. The ethyl acetate layer was concentrated to dryness and the residue was used for column chromatographic separation. The ethyl acetate (0.6 g) was chromatographed on a silica gel column using Toluene-EtOAc (70:30) solvent mixture. Finally, quercetin and kaempferol were obtained.

Extraction of Essential Oil from *P. betel*

Extraction of essential oil from *P. betel* was carried out by steam distillation method. The dried powder (100 g) and distilled water (500 mL) were placed in 1 L round-bottomed flask. The flask was fitted for steam distillation and heated. The steam was passed into the flask. The condensed oil and water were collected in a flask and the oil was extracted with PE in a separating funnel. The PE extract was dried over anhydrous sodium sulphate. After filtration, the filtrate was evaporated to get the essential oil which was weighed and kept in air tight bottle for further analysis (Pauli, 2001).

Isolation of Eugenol from *P. betel*

The essential oil of *P. betel* was prepared by steam distillation method. Eugenol was isolated from essential oil of *P. betel* by column chromatographic method using toluene and ethyl acetate (9:1).

Results and Discussion

Antibacterial Activity

It was observed that ethyl acetate and 95 % ethanol extracts of *C. longa* and essential oils of *N. sativa* and *P. betel* showed antibacterial activity on the tested bacteria strains. Therefore, in this screening test, *C. longa*, *N. sativa* and *P. betel* found to possess bactericidal activity (Table 1).

The bactericidal activity of extracts was tested by test tube serial dilution method by determining the turbidity and growth on nutrient agar. All the tested extracts showed the bactericidal activity which coincide with the MIC values. The minimum inhibitory concentrations of EtOAc extract of *C.longa* ranged from 1 to 〉2 mg/mL. The lowest MIC of 1 mg/mL was obtained with *E.coli* (ID-6), *E.coli* (ID-12), *Proteus morganii* (ID-1), *Salmonella typhi* (ID-3), *Salmonella typhi* (ID-24), *Staphylococcus aureus* (ID-15), *Staphylococcus aureus* (ID-26) and the remaining bacteria had MIC of 〉2 mg/mL.

The MIC's of EtOAc extract of *N.sativa* were in the range of 0.01562 to 〉2 mg/mL. The lowest MIC of 0.01562 mg/mL was obtained from *Shigella boydii* (ID 47). *Staphylococcus aureus* (ID-26) was 0.03125 mg/mL and *E.coli* (ID-35), *Plesiomonas shigelloides* (ID-23), *Salmonella typhi* (ID-3), *Salmonella typhi* (ID-19) and *Shigella boydii* (ID-53), the MIC of 0.0625 mg/mL was observed. The remaining bacteria showed MIC value of 2 mg/mL. The MIC'S of essential oil of *P.betel* were from 〉1 to 〉2 mg/mL. The lowest MIC of 〉1 mg/mL was obtained with *E.coli* (ID-35) and *Shigella boydii* (ID-53). In case of *Plesiomonas shigelloides* (ID-23), *Salmonella typhi* (ID-3), *Salmonella typhi* (ID-19), *Shigella dysenteriae* (ID-25), *Shigella boydii* (ID-22), *Staphylococcus aureus* (ID-15) and *Staphylococcus aureus,* (ID-26), the MIC value was 2 mg/mL and the rest showed 〉2 mg/mL. The minimum inhibitory concentrations (MIC) of antibacterial active extracts of *C. longa*, *N. sativa* and *P. betel* are shown in Table 2.

The isolated compounds namely curcumin from *C. longa*, kaempferol, quercetin and thymoquinone from *N. sativa* and eugenol from *P. betel* were found to show bactericidal activity against *Salmonella typhi, Plesiomonas*

shigelloides, Escherichia coli, Staphylococcus aureus, Shigella boydii, Bacillus subtilis and Salmonella paratyphi (Table 3 and Figure 1).

Identification of isolated compounds

1 (Curcumin) : yellow needles, mp. 183°. MS m/z ; 368 (M^+), 350, 340, 232, 137 (Figure 2). UV λ_{max}^{EtOH} nm 260, 425 ; UV $\lambda_{max}^{EtOH+NaOH}$ nm : 467, FT IR υ_{max}^{kBr} cm^{-1} : 3400 (υ_{O-H}), 2925, 2850 (υ_{C-H} of OCH_3), 1627 ($\upsilon_{C=0}$), 1602, 1510, 1460, 1427, 1280, 1150, 960. ^1H NMR δ (ppm) : 7.61 (2H, d, J = 16 Hz), 7.13 (2H, dd, J = 8.5 & 1.5 Hz), 7.05 (2H, d, J = 1.5 Hz), 6.94 (2H, d, J = 8.5 Hz), 6.5 (2H, d, J = 16.0 Hz), 5.90 (2H, s), 5.80 (1H, s), 3.95 (6H, s)

2 (Desmethoxy curcumin) : mp . 181 - 182°. MS m/z : 338 (M^+), 320, 202, 191, 147, 137 (Figure 3) : UV λ_{max}^{EtOH} nm : 250, 419 ; UV $\lambda_{max}^{EtOH+NaOH}$ nm : 462, FT IR υ_{max}^{kBr} cm^{-1} : 3400 (υ_{O-H}), 2925, 2850 (υ_{C-H} of OCH_3), 1627 ($\upsilon_{C=0}$), 1602, 1510, 1460, 1427, 1280, 1150, 960

3 (Bisdesmethoxy curcumin) : mp . 232 - 234°. MS m/z : 308 (M^+), 290, 202, 161, 147, 107 (Figure 4). UV λ_{max}^{EtOH} nm : 245, 415 ; UV $\lambda_{max}^{EtOH+NaO}$ nm : 443, FT IR υ_{max}^{kBr} cm^{-1} : 3400 (υ_{O-H}), 2925, 1627 ($\upsilon_{C=0}$) 1602, 1510, 1460, 1427, 1280, 1150, 960.

4 (Thymoquinone) : bright yellow crystalline compound mp. 49 - 50°. MS m/z : 164 (M^+), 149, 136, 121, 108, 93. UV λ_{max}^{MeOH} nm : 252, 292, FT IR υ_{max}^{kBr} cm^{-1} : 2922, 1458, 1373, 1636 ($\upsilon_{C=0}$). ^1H NMR (ppm) : 6.5 (1H, s), 6.43 (1H, s), 3.01 (1H, septet, J = 6.6 Hz), 2.02 (3H, s), 1.45 (6H, d, J = 6.6 Hz) (Figure 5).

5 (Kaempferol): Yellow crystalline compound, mp. 275º, MS m/z : 286 (m^+), 285, 258, 257, 241, 229, 213, 184, 153, 134 and 121 (Figure 6). UV λ_{max}^{MeOH} nm : 266, 366, FT IR υ_{max}^{kBr} cm^{-1} : 3422 (υ_{O-H}), 1630 ($\upsilon_{C=O}$), ^1H NMR δ (ppm) : 6.18 (1H, d), 6.38 (1H, d), 6.89 (2H, d), 8.07(2H, d).

6 (Quercetin): Yellow crystalline compound, UV λ_{max}^{MeOH} : 257, 375 (Figure 7), FT IR υ_{max}^{kBr} cm^{-1} : 3421 (υ_{O-H}) , 1647 ($\upsilon_{C=O}$).

7 (Eugenol): UV λ_{max}^{PE} 282 nm (Figure 8),FT IR υ_{max}^{kBr} cm^{-1}:3514((υ_{O-H}),1637 ($\upsilon_{C=O}$), 1268, 1234 (υ_{C-O-C}), 1634 ((υ_{C-O-H}).

Table 1. Antibacterial Activity of *C. longa* L., *N. sativa* L. and *P. betel* L.

No.	Tested bacteria	Inhibition zone diameter (mm)			
		***C. longa* L.**		***N. sativa* L.**	***P. betel* L.**
		EtOAc	**EtOH**	**Essential Oil**	**Essential Oil**
1.	*E. coli*	18	13	28	15
2.	*Salmonella paratyphi*	14	12	28	12
3.	*Shigella dysenteriae*	16	11	16	14
4.	*Vibrio parahaemolytics*	22	20	28	10
5.	*Shigella boydii*	16	18	18	16
6.	*Staphylococcus aureus*	14	16	28	20
7.	*Bacillus subtilis*	12	10	14	18
8.	*Salmonella typhi*	14	12	15	12
9.	*Plesiomonas shigelloides*	15	16	28	14
10.	*Shigella sonnei*	14	12	28	20

Table 2. Minimum Inhibitory Concentration of Active Extracts of *C. longa* L., *N. sativa* L. and *P. betel* L.

Extract (mg/mL)	Tested Bacteria*															
	1	2	3	4	5	6	7	8	9	10	11	12	13	14	15	16
C. longa (EtOAc)	1	>2	1	>2	1	>2	1	>2	1	>2	>2	>2	>2	1	1	>2
N. sativa (EtOAc)	>2	>2	>2	0.06 25	>2	0.06 25	0.06 25	0.06 25	>2	>2	0.5	0.01 562	0.06 25	0.5	0.03 125	>2
P. betel (*E-coli*)	>2	>2	>2	>1	>2	2	2	2	>2	>2	2	2	>1	2	2	>2

*

1. *Escherichia coli* (ID-6)
2. *Escherichia coli* EPEC (ID-7)
3. *Escherichia coli* EHEC (ID-12)
4. *Escherichia coli 0126* (ID-35)
5. *Proteus morganii*
6. *Plesiomonas shigelloides* (ID-23)
7. *Salmonella typhi* (ID-3)
8. *Salmonella typhi*(ID-3)
9. *Salmonella typhi*(ID-19)
10. *Shigella sonnei* (ID-14)
11. *Shigella dysenteriae* (ID-25)
12. *Shigella boydii* (ID-47)
13. *Shigella boydii* (ID-53)
14. *Staphylococcus aureus* (ID-15)
15. *Staphylococcus aureus* (ID-26)
16. *Vibrio fluvialis* (ID-70)

Table 3. Antibacterial Activity of Isolated Compounds from *C. longa* L., *N. sativa* L. and *P. betel* L.

Disc diameter = 8 mm

Isolated Compound	**Inhibition zone diameter (mm)**						
	Tested Bacteria*						
	1	**2**	**3**	**4**	**5**	**6**	**7**
Curcumin	13	NT	13	17	16	-	12
Thymoquinone	15	16	16	25	20	>25	>25
Quercetin	12	12	NT	12	14	10	12
Kaempferol	10	-	-	10	12	16	13
Eugenol	25	17	19	20	24	25	25

*** Bacteria**

1. *Salmonella typhi*
2. *Salmonella paratyphi*
3. *Plesiomonas shigelloides*
4. *Escherichia coli*
5. *Shigella boydii*
6. *Bacillus subtilis*
7. *Staphylococcus aureus*

NT – Not Tested, - = No activity

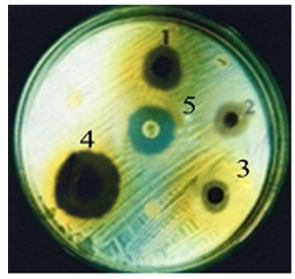

Salmonella typhi

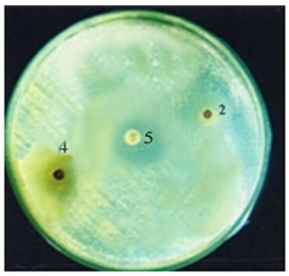

Salmonella paratyphi

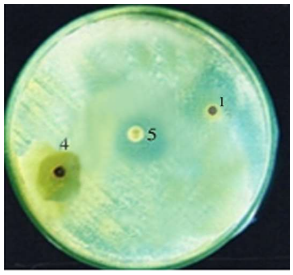

Plesiomonas shigelloides

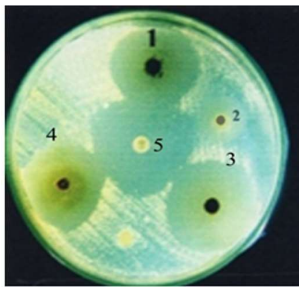

Escherichia coli

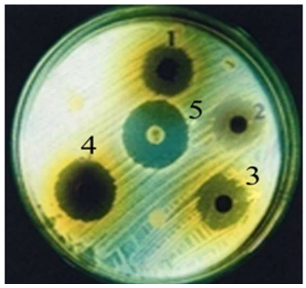

Shigella boydii

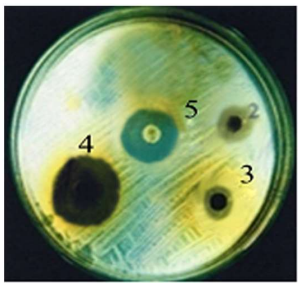

Bacillus subtilis

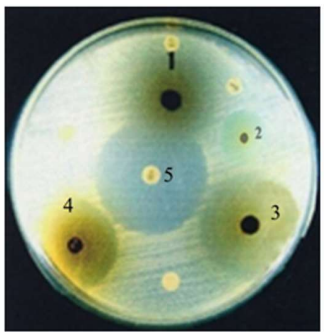

Staphylococcus aureus

1 = Curcumin
2 = Quercetin
3 = Kaempferol
4 = Eugenol
5 = Thymoquinone

Figure 1. Antibacterial activity of isolated compounds

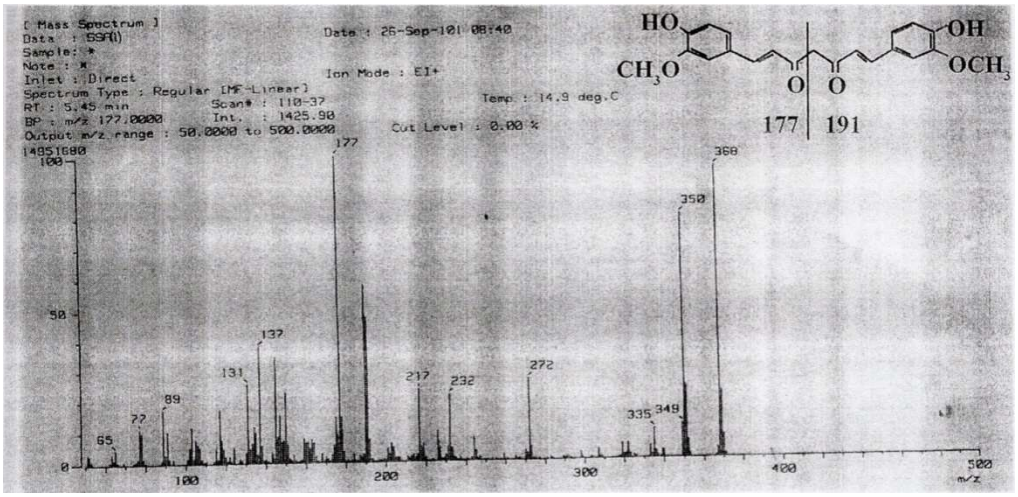

Figure 2. EI mass spectrum of isolated curcumin from *C. longa* L.

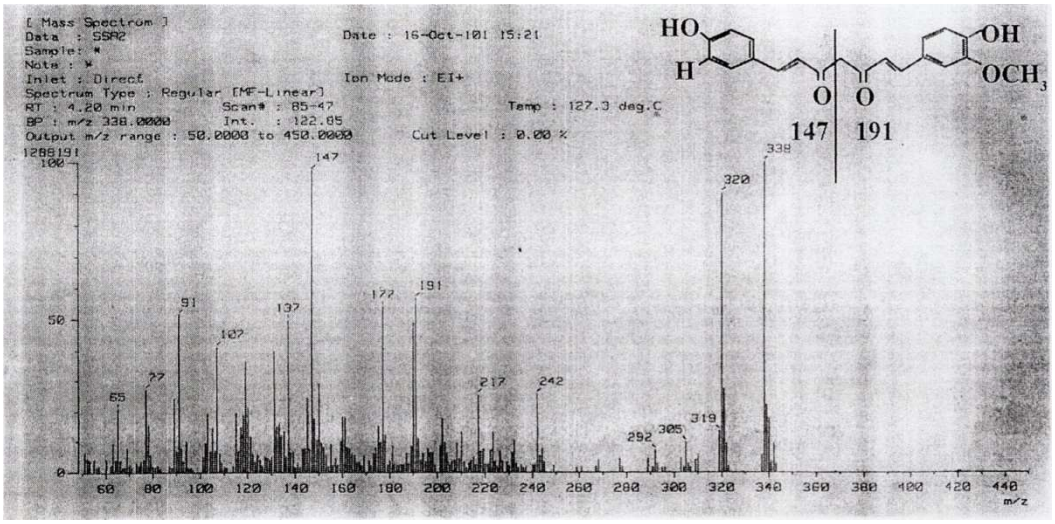

Figure 3. EI mass spectrum of isolated desmethoxy curcumin from *C. longa* L.

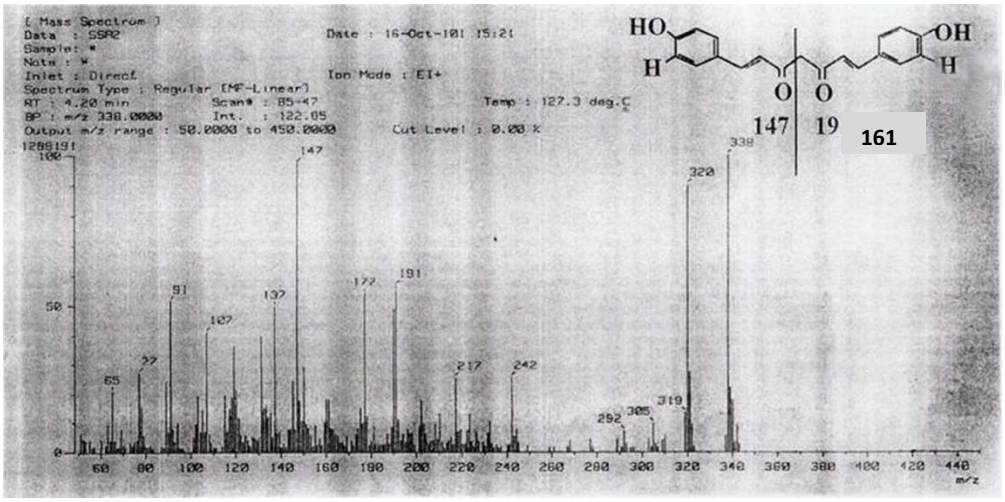

Figure 4. EI mass spectrum of isolated bisdesmethoxy curcumin from *C. longa* L.

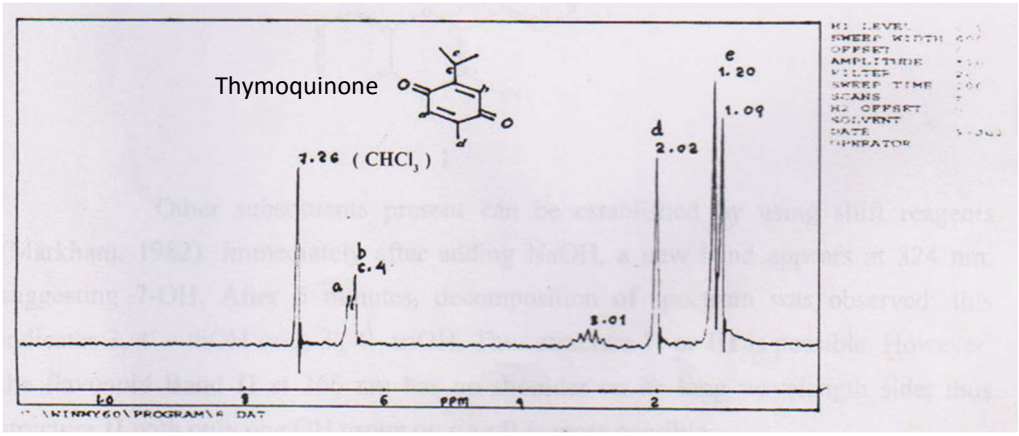

Figure 5. ^{1}H NMR spectrum of isolated thymoquinone from *Nigella sativa* L.

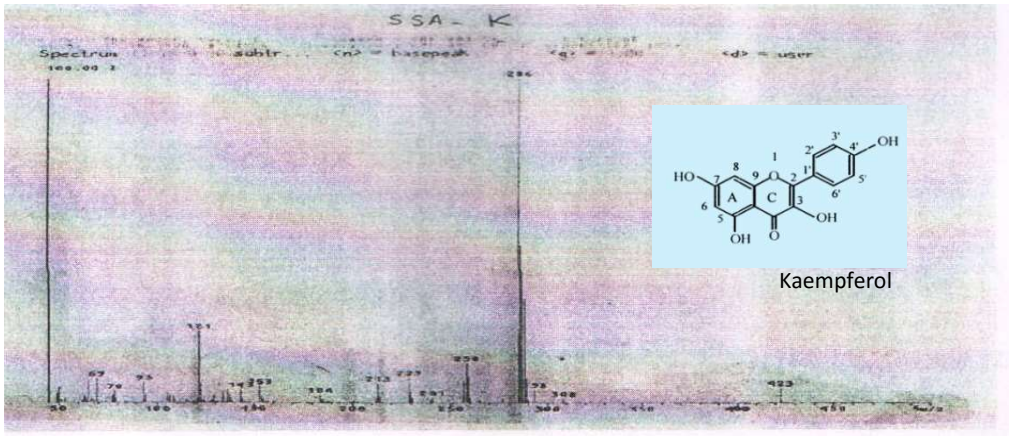

Figure 6. EIMS spectrum of isolated kaempferol from *Nigella sativa* L.

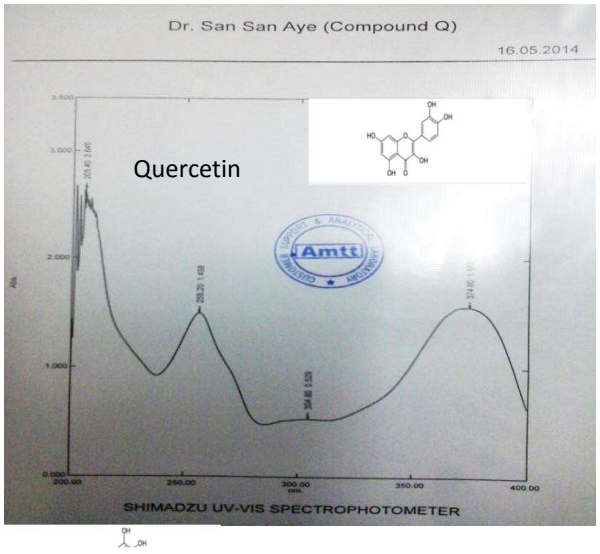

Figure 7. UV spectrum of isolated quercetin from seeds of *Nigella sativa* L. L. (Kun)

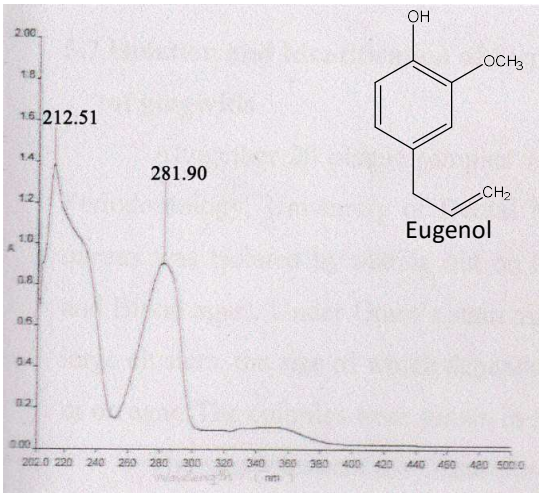

Figure 8. UV spectrum of isolated eugenol from leaves of *Piper betel* L. (Kun)

Conclusion

From the present research work on "Comparative studies of antibacterial activity and phytochemical constituents of some Myanmar indigenous medicinal plants", the following conclusions can be drawn.

Crude extracts have been prepared from *C. longa*, *N. sativa* and *P. betel* by using non-polar and polar solvents. The antibacterial activity of the crude extracts was screened by *in vitro* method using agar disc diffusion techniques on 33 bacteria which include *S. aureus, E. coli, Shigella, Salmonella* and *Vibrio*. Ethyl acetate and ethanol extracts of the *C. longa*, essential oil of *N. sativa* and *P. betel* showed antibacterial activity against all tested organisms.

The minimum Inhibitory Concentration (MIC) of the active extract 1mg/ mL for *C. longa*, 0.0156 mg/ mL for *N. sativa* and 2mg/ mL for *P. betel* were also determined by using serial dilution technique.

Ethyl acetate extract of *C. longa* was separated by column chromatography and curcumin (5.9 %), desmethoxycurcumin (0.018 %) and bisdesmethoxy curcumin (0.0136 %) were obtained in pure form as crystal. Kaempferol (0.12 %) and quercetin

(0.001 %) were isolated from flavonoid extract of *N. sativa* by column chromatographic method.

Essential oil of *N. sativa* was fractionated by column chromatography to yield thymoquinone (0.01 %). Eugenol (0.1 %) was also isolated from essential oil of *P. betel.* The isolated compounds were identified by UV, FT IR, ^{1}H NMR and mass spectroscopic methods.

The antibacterial activity of isolated compounds was tested by agar disc diffusion technique. From the experimental results, all the isolated compounds showed antibacterial activity against all tested organisms (12 mm-25 mm). Among these thymoquinone was found to be the most active compound (> 25 mm).

C. longa (Nanwin), *N. sativa* (Samon-net) and *P.betel* (Kun) may be used for the treatment of dysentery and diarrhea since they have bactericidal action against *Escherichia coli* responsible for diarrhea and *Shigella boydii* responsible for dysentery. These three plants were used in traditional medicine formulation (TMF-06) to treat the diseases caused by bacteria. From the experimental results that *N. sativa* (Samon-net seed) is the most effective plant to treat dysentery and diarrhea. Therefore, these three plants have a good potential for the production of combined formulation to treat diseases caused by bacteria.

Acknowledgements

The authors would like to express their profound gratitude to the Department of Higher Education (Yangon Office), Ministry of Education, Yangon, Myanmar, for provision of opportunity to do this research and Myanmar Academy of Arts and Science for allowing to present this paper.

References

Burkill, I.H. (1966). *A Dictionary of the Economic Products of Malay Peninsula*, Kuala Lumpur, Ministry of Agriculture and Co-operatives, vol. 1, p. 714

Chopra, R. N., Nayar, S. L. and Chopra, I.C. (1956). *Glossary of Indian Medicinal Plants*, New Delhi: CISR, vol. 1, pp.94 - 95.

Cruickshank, R., Mackie, T.J. and McCartney, J.E. (1975). Medical Microbiology, London: Churchill Livingstone Ltd.

FAO/WHO. (1978). "22nd Report of Expert Committee on Food Additives". *Tech. Rep. Ser. Wld.Hlth. Org*., vol. 631,p. 21.

Finegold, S. M. and Martin, W. J. (1982). *Diagnostic Microbiology*. London: The C.V. Mosby Co.

Guenther, E. (1960). *The Essential Oils*, New York: Reinhold, p. 129.

Harborne, J.B. (1984). *Phytochemical methods- A Guide to Modern Techniques of Plant Analysis*, London: Chapman and Hall.

Khan, M.A. (1999). "Chemical Composition and Medicinal Properties of *Nigella sativa* Linn.", *Inflammopharmacology*, vol. 7(1), p. 15-53.

Mya Bwin and Sein Gwan. (1973). *Burmese Indigenous Medicinal Plants*, Burma Medical Research Institute, DMR, No.8.

Pauli, A. (2001). "Antimicrobial Properties of Essential Oil Constituents". *J. Aromatherapy*,vol.11(3),pp.126-133.

World Health Organization. (1999). *W.H.O. Monographs on Selected Medicinal Plants*, Geneva: vol. I, pp.11-14.

SCREENING OF THE ACUTE TOXICITY, ANTIMICROBIAL AND ANTITUMOR ACTIVITIES OF ROOTS OF *Stemona Curtisii* HOOK.F.

Thandar Aung[1], Than Than Myint[2], Aye Win Oo[3]

ABSTRACT

In the present research, roots of *Stemona curtisii* Hook. F., family-Stemonaceae was chosen to be studied. Acute toxicity study of 95% ethanol extract from roots of *Stemona curtisii* Hook. F. was investigated by methods of OECD guidelines for the testing of Chemical 425. Screening of root extract was done with the dosage of 2000 mg/kg, 300 mg/kg and 50 mg/kg body weight in albino mice. Dosage of 2000 mg/kg was discovered lethality within 60 min with symptoms of toxicity like restlessness, convulsion, coma, and death. The results of other groups show no lethality of mice up to fourteen days administration. Antimicrobial activity of pet- ether, methanol, ethyl acetate, 95% ethanol and watery extracts from roots of *S .curtisii* was investigated against six species of microorganisms such as *Bacillus pumilus, Bacillus subtilis, Candida albicans, Escherichia coli, Pseudomonas aeruginosa and Staphylococcus aureus* by agar well diffusion method. Ethyl acetate and methanol extracts of *S. curtisii* exhibited inhibition zone diameter in the ranges of (12~15 mm) and (11~20 mm) against all tested microorganisms, respectively. 95% ethanol extract of *S.curtisii* showed inhibition zone diameters (11 mm) only against *Pseudomonas aeruginosa.* On the other hand, pet-ether and watery extract of sample showed activity against five tested microorganisms in the range of (11~ 14 mm) and (11~20 mm) except *Bacillus subtilis*. Antitumor activity of methanol, ethyl acetate, 95% ethanol, and watery extracts of roots of *S.curtisii* was screened on *Agrobacterium tumefacien* by Potato Disc Assay method. All of extracts from root sample exhibited antitumor activity against *Agrobacterium tumefacien* after 5 days and 7 days periods of observation.

Keywords : *Stemona curtisii* Hook.F., acute toxicity, antimicrobial activity, antitumor activity

---

[1] Associate Professor, Dr,Department of Chemistry, Pathein University

[2] Professor and Head, Dr,Department of Chemistry, Pathein University

[3] Research Scientist, Dr, Laboratory Animal Services Division, Department of Medical Research, Yangon

INTRODUCTION

Stemona curtisii Hook.F. is one of the important monocotyledon plants belonging to the family Stemonaceae and widely distributed in the northern region of Myanmar. The roots of several species in the genus *Stemona* are widely used as medicinal purposes due to the occurrence of various alkaloids. The most important alkaloid is stemofoline which possess bio-insecticide properties. *Stemona* family is one of considerable interest because it is the only source of the unique alkaloids known as stemona alkaloids including stemocurtisine, stemocurtisinol and oxyprotostemonine (Figure 1) which have been isolated from a root extract of *S. curtisii* (Sastraruji, 2006).

The root extracts and the pure alkaloid of *S. curtisii* especially oxyprotostemonine were shown larvicidal activity against *Anopheles minimus* (Mungkornasawakul, 2003). Kaltenegger (2003) reported that the crude extract of *S. curtisii* had insecticidal activities against *Spodoptera littoralis*. The main chemical constituent of the *S. curtisii* Hook.F. is a specific group of Stemona alkaloids, including stemofoline, 2'-hydroxy stemofoline, oxyprotostemonine, dehydroprotostemonine, protostemonine, stemocochinine, stemocurtisine (pyridostemin), stemocurtisinol and oxystemokerrine (Mungkornasawakul, 2004).

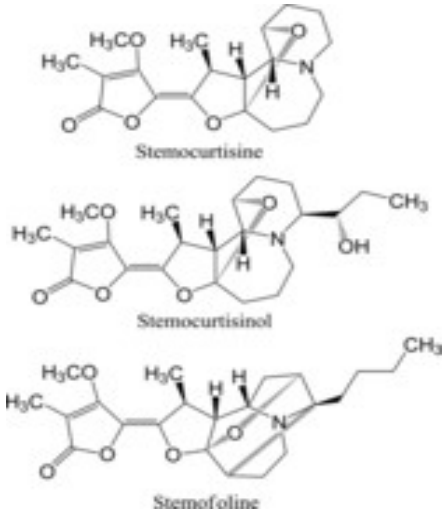

Figure 1 Structures of stemocurtisine, stemocurtisinol and stemofoline

Botanical Aspects of *Stemona curtisii* Hook.F.

Scientific Name	-	***Stemona curtisii*** Hook.F.
Family	-	Stemonaceae
Myanmar Name	-	Thar-myaa-oo
Common Name	-	Non Tai Yak in Thailand
Plant part used	-	Roots

Figure 2. *Stemona curtisii* plant, leaves and roots

Uses of *S.curtisii*

S.curtisii (Family Stemonaceae), a prominent species distributed in the south and southwest of Thailand, has widely been used as a natural pesticide and as treatment for head lice and skin diseases.

Aim and Objectives

The aim of this study was to evaluate acute toxicity, antimicrobial and antitumor activities of root of *S. curtisii*. (Thar-myaa-oo). To fulfill this aim, the research was carried out according to the following objectives.

(1) To extract the sample with various solvents

(2) To determine the phytochemical tests

(3) To investigate the acute toxicity, antimicrobial and antitumor activities of root sample

Materials and Methods

Collection and Preparation of *S. cutisii* Extracts

The roots of *S. curtisii* belonging to the family Stemonaceae were collected from Kalay Township, Sagaing Region in Myanmar, during January to February 2016. The collected roots samples were identified as *S. curtisii* (Thar-myaa-oo) according to the authorized botanist from Department of Botany, Myitkyina University. A total of 5 Kg of *S. cutisii* fresh root samples were scrutinized for any foreign matter and cleaned with distilled water. They were then chopped into small pieces and air dried under shade at the laboratory. When the plant material dried, it was ground into powder using grinding machine. The powdered plant material obtained was stored in clean air tight container.

Preparation of crude extracts by direct extraction methods for screening of some biological activities

Each dried powdered sample (50 g) was extracted with 150 mL of PE (60-80 °C) for 6 h by using soxhlet extractor. The filtrate was concentrated by removal of the solvent under reduced pressure to give the respective pet-ether crude extract. Preparation of ethyl acetate extract, 95% ethanol, methanol, dichloromethane and watery extracts were prepared by similar manner mentioned in above procedure. Each extract was dried at normal pressure on a water bath and stored under refrigerator for screening some bioactivities.

Qualitative screening of the phytochemicals

In order to classify the types of organic constituents present in root samples, preliminary phytochemical tests on samples were carried out according to the series of test tube tests.

(a) Screening of antimicrobial activity of different crude extracts of *S. curtisii* Hook.f.

The antimicrobial activities of different crude extracts such as PE, EtOAc, 95% EtOH, MeOH and H_2O extracts from roots of *Stemona curtisii* Hook.f.were determined against six species of microorganisms such as *Bacillus pumilus* (N.C.I.B - 8982), *Bacillus subtilis* (N.C.T.C - 8236), *Candida*

albicans, Escherichia coli (N.C.I.B - 8134), *Pseudomonas aeruginosa* (6749) and *Staphylococcus aureus* (N.C.P.C - 6371) by employing agar well diffusion at the Pharmaceutical Research Department, Ministry of Industry, Yangon, Myanmar.

(b) Acute toxicity test of the samples on albino mice model

To determine the symptomatology consequent to injection of the plant and to determine the nature and degree of toxicity produced by these extracts and to find out the medium lethal doses (LD_{50}) of the extracts, acute toxicity test was done. Usually the acute lethality of a compound is determined on the basic of deaths occurring in 24 h but the survivors should be observed for at least seven days in order to detect delayed effects. In this study, acute toxicity effect of ethanol extracts of *Stemona* root (three doses) were determined on albino mice, at Laboratory Animal Services Division, Department of Medical Research (DMR), Yangon.

Acute toxicity of different doses of EtOH extract of sample was evaluated by the methods of OECD Guidelines for the Testing of Chemicals 425. According to the test description, total number of adult female albino mice, weighing (25-30 g) were selected and divided into four groups. Each group contained six animals. They were fasted for 18 h before giving the extracts. Group (1) mice were orally administrated with EtOH extract 2000 mg/kg dose. Group (2) mice were given orally with EtOH extract 300 mg/kg dose. Group (3) mice were also administered with EtOH extract 50 mg/kg dose and Group (4) mice performed as a control group and they were treated with clean water and normal laboratory animal food of Laboratory Animal Services Division, at Department of Medical Research. All groups of mice were kept in the four mouse cages in the separated room at the room temperature of 26 ± 1º C. After administration of extracts on each group of animals were observed first 6 h continuously for mortality and behavior changes. Then check the animals each 24 h for fourteen days. The mortality during this period was noted (Nil or percent death). The results obtained from acute toxicity are described in table 2.

(c) Screening of antitumor activity of crude extracts by potato crown gall test or potato disc assay method

The antitumor activity screening of different crude extracts such as ethanol, methanol, ethyl acetate and watery extracts of roots of *Stemona curtisii* Hook.f. was carried out against *Agrobacterium tumefacien* by Potato Crown Gall test or Potato Disc Assay method at the Pharmaceutical Research Department, Ministry of Industry, Yangon, Myanmar.

Fresh, disease free potato tubers were obtained from local market and used within 48 hours of transfer to the laboratory. Tubers of moderate sizes were surface-sterilized by immersion in 50 % sodium hypochlorite (Clorox) for 20 min. The ends were removed and soaked for 10 min more in Clorox. A core of the tissue was extracted from each tuber by using surface-sterilized (ethanol and flame) 105 cm wide cork borer. And, 2 cm pieces were removed from each end and discarded and the remainder of the cylinder is cut into 0.5 cm thick discs with a surface-sterilized cutter. The discs were then transferred to 1.5 % agar plates (1.5 g of Difco agar was dissolved in 100 mL of distilled water, autoclaved and 20 mL poured into each petri dish). Each plate contained three discs. The procedure was done in the clean bench in the sterile room.

100 mg, 200 mg and 300 mg of each extract was separately dissolved in 1 mL of dimethyl sulphoxide (DMSO); this solution was filtered through millipore filters (0.22 μm) into a sterile tube. 0.5 mL of this solution was added to 1.5 mL of sterile distilled water and 2 mL of broth culture of *A. tumefaciens* strain (48 h culture containing $3\text{-}5\times10^{9}$cells/mL) were added aseptically. Controls were made in this way; 0.5 mL of DMSO and 1.5 mL of sterile distilled water were added to the tube containing 2 mL of broth culture of *A. tumefaciens* (from the same 48 h culture).

Using a sterile disposable pipette, 1 drop (0.05 mL) from these tubes was used to inoculate each potato disc, spreading it over the disc surface. The process of cutting the potatoes and incubation must be conducted within 30 min. The plates were sealed with tape to minimize moisture loss and incubated at room temperature for 12 days. After incubation, Lugol's solution (I_2-KI) was added and the tumors were counted with a microscope and

compared with control. The antitumor activity was examined by observation of tumor produced or not.

Results and Discussion

Results of preliminary photochemical analysis of the root extract of *S. curtisii* showed the presence of alkaloids, α-amino acids, carbohydrates, flavonoids, glycosides, phenolic compounds,reducing sugar, saponins, starchs, steroids, tannins, and terpenoids as shown in Table 1.

Table 1. Phytochemicals in Root Extract of *S. curtisii*

Phytochemical Components	**Root extracts of *Stemona curtisii***
Alkaloids	+
α-amino acid	+
Carbohydrates	+
Flavonoids	+
Glycosides	+
Phenolic Compounds	+
Reducing sugar	+
Saponins	+
Starch	+
Steroids	+
Tannins	+
Terpenoids	+
Cyanogenic glycosides	-

+ = Present; – = Absent

Acute Toxicity Study

Acute toxicity screening of EtOH extracts of *Stemona* root was done with the dosage of 2000 mg/kg, 300 mg/kg and 50 mg/kg body weight in albino mice. The condition of mice was recorded after administration in fourteen days. 2000 mg/kg group was discovered lethality within 60 min with symptoms of toxicity like restlessness, convulsion, coma and death. The results of other groups show no lethality of the mice up to fourteen days administration. Other groups of animals were also observed still alive and did not show any visible symptoms of toxicity like restlessness, respiratory disorders, convulsion, aggressive activities, coma and death (Table 2 and Figure 3).

Table 2. Acute Toxicity Effect of Ethanolic Extract of *Stemona* Root on Albino Mice Model after Two Weeks Administration

No	Groups	Dosage of EtOH extract (mg/Kg)	No. of death at day fourteen	% of death at day fourteen
1	Group 1	2000	5/6 (Dead= 5, Alive = 1)	83.33 %
2	Group 2	300	Nil	0 %
3	Group 3	50	Nil	0 %
4	Group 4	Nil	Nil	0 %

Figure 3. Acute toxicity study of ethanolic extract of *Stemona* root on albino mice model

In Vitro Antimicrobial Activity of some Crude Extracts of Root of *S.curtisii* by Agar Well Diffusion Method

In vitro antimicrobial activity of various crude extracts such as PE, MeOH, EtOAc, 95% EtOH and H_2O extracts was investigated by employing agar well diffusion method against six species of microorganisms. The inhibition zone diameter (ID) showed the degree of the antimicrobial activity. The larger the inhibition zone diameters, the higher the antimicrobial activity. The photographs illustrating the inhibition zones provided by crude extracts against six species of microorganisms are presented in Figure 4 and the observed data are summarized in Table 3. Among the tested crude extracts of *S.curtisii*, MeOH and EtOAc extracts showed highest antimicrobial activity against all tested microorganisms. EtOH extract has the antimicrobial activity against only one species of microorganisms, *Pseudomonas aureginosa* (ID: 11mm). However, H_2O extract of *S.curtisii* did not show activity against one species of microorganisms, *Bacillus subtilis*. From this observation, MeOH extract has the most potent antimicrobial activity.

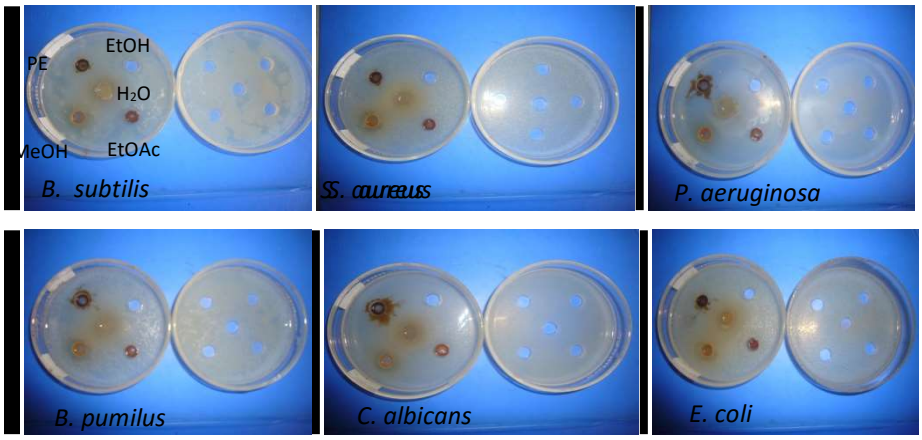

Figure 4. Inhibition well diameter of root extracts of *S.curtisii*

Table 3. *In vitro* Antimicrobial Activity of *S.curtisii* Root by Agar Well Diffusion Method

Table 3. *In vitro* Antimicrobial Activity of *S.curtisii* Root by Agar Well Diffusion Method

Microorganism	**Inhibition Well Diameter(mm)**					
	Crude Extracts of S.curtisii Root					
	I	**II**	**III**	**IV**	**V**	**Control**
Bacillus subtilis	–	11	13	_	_	_
Staphylococcus aureus	11	15	12	–	11	_
Pseudomonas aeruginosa	11	20	15	11	20	_
Bacillus pumilus	13	18	13	_	11	_
Candida albicans	14	16	13	_	11	_
Escherichia coli	12	15	14	_	12	_

I = PE extract
II = MeOH extract
III = EtOAc extract
IV = EtOH extract
V = H_2O extract
VI = Control

Agar Well Diameter-10mm
Inhibition Diameter -10~14mm (+)
Inhibition Diameter -15~19mm (++)
Inhibition Diameter -20 mm above (+++)

Screening of Antitumor Activity of some Crude Extracts from the Roots of S. *curtisii*

The antitumor activity screening of different crude extracts such as methanol, ethyl acetate, ethanol and watery extracts of root sample was carried out against *Agrobacterium tumefacien* by Potato Crown Gall test or Potato Disc Assay method. The photographs illustrating the different concentrations of plant crude extracts against *Agrobacterium tumefacien* are presented in Figures 5 and 6 and the observed antitumor activity of different crude extracts of root sample are summarized in Table 4. Among the tested crude extracts, all extracts of root exhibited antitumor activity against *Agrobacterium tumefacien.*

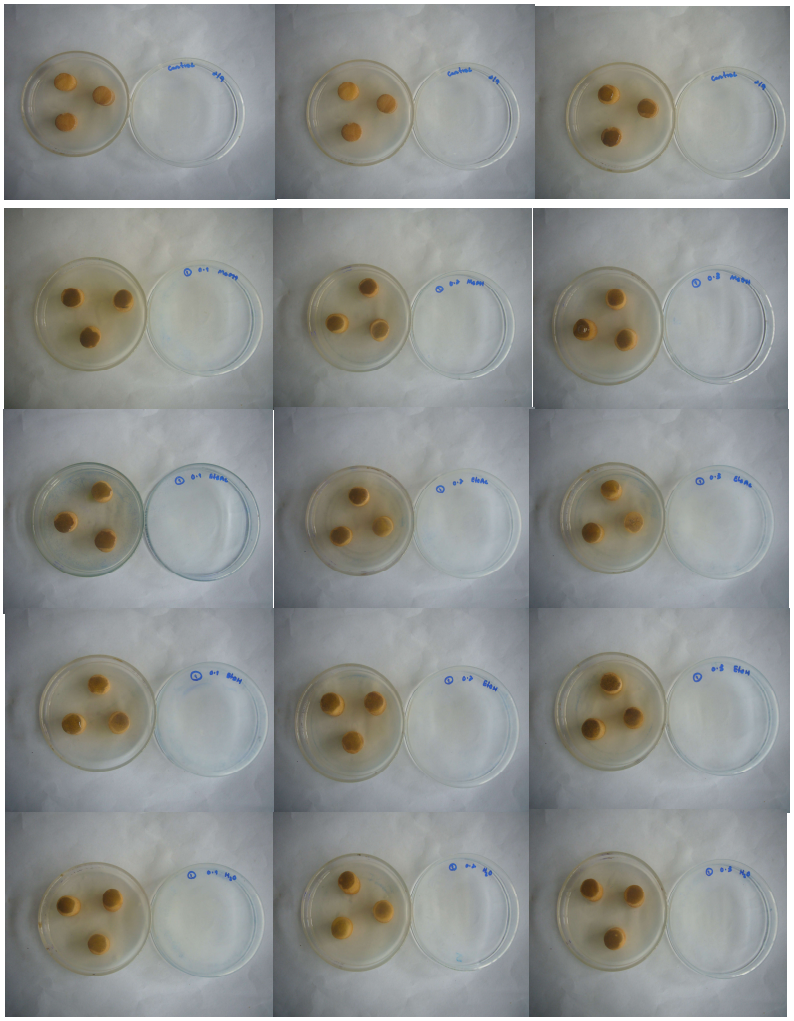

Figure 5. Photographs of observation on antitumor activity of different concentrations of MeOH, EtOAc, EtOH and H_2O extracts of *S. curtisii* on day 5

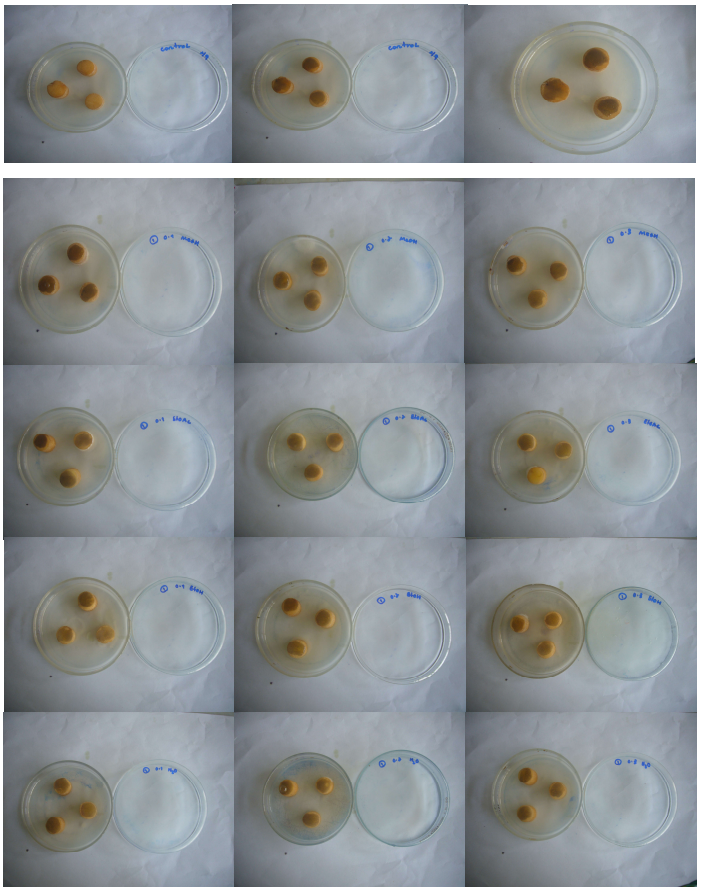

Figure 6. Photographs of observation on antitumor activity of different concentrations of MeOH, EtOAc, EtOH and H_2O extracts of *S. curtisii* on day 7

Table 4. Antitumor Activity of Different Crude Extracts from the Roots of *S. curtisii*

Samples	Concentration of extracts (mg /mL) DMSO	Antitumor Activity	
		Day-5	Day-7
MeOH extract	100	+	+
	200	+	+
	300	+	+
EtOAc extract	100	+	+
	200	+	+
	300	+	+
EtOH extract	100	+	+
	200	+	+
	300	+	+
H_2O extract	100	+	+
	200	+	+
	300	+	+
Control	100,200,300	–	–

(+) = exhibit antitumor activity

(–) = no antitumor activity

Conclusion

From the overall assessments of the present work, the following inferences could be deduced. According to acute toxicity test, 2000 mg/kg group was discovered lethality within 60 minutes with symptoms of toxicity like restlessness, convulsion, coma and death. The results of other groups showed no lethality of the mice up to fourteen days administration. In a study on antimicrobial activity, among the five tested crude extracts of *S.curtisii* Hook. F., MeOH extract exhibited the highest antimicrobial activity against all tested microorganisms. The antitumor activity of MeOH, EtOAc, EtOH and H_2O extracts of *S. curtisii* was screened on *Agrobacterium tumefacien* by Potato Disc Assay method. In *S.curtisii,* all extracts of root exhibited antitumor activity against *Agrobacterium tumefacien* after 5 days and 7 days periods of observation. Therefore, bioactivity of *S. curtisii* Hook. F. is probably due to presence of phytochemical constituents such as terpenoids, saponins, alkaloids and flavonoids. The result obtained from this study strongly indicated that tested crude extract of *S. curtisii* may play an important role in medicinal properties used *in vitro* and may be effective.

Acknowledgements

We would like to thank to the Department of Higher Education, Ministry of Education in Myanmar, for giving us the opportunity to do this research. Our deepest gratitude is expressed to Dr Nyunt Phay, Rector, Pathein University, for his encouragement, kind guidance, and kind help to do this research. We wish to thank Dr Wai Wai Nyunt and Dr Mi Mi Gyi, Pro-Rectors, Pathein University for their invaluable advices and encouragement. Thanks are also extended to Dr Than Than Myint (Professor and Head) and Dr Nilar Kyi (Professor), Department of Chemistry, Pathein University, for their helpful advice, precious suggestions and provision of research facilities at the Department of Chemistry, Pathein University.

References

Kaltenegger, E. (2003). "Insecticizal Pyrido [1,2,-a] Azepine Alkaloid and Related Derivatives from *Stemona*

Species". *Phytochem*., vol. 63, pp. 803-816.

Mungkornasawakul, P. (2003). "Stemocurtisine, the First Pyrido [1,2,-a] Azepine *Stemona* Alkaloid". *J. Nat. Prod.,*vol .66, pp. 980-982.

Mungkornasawakul, P.(2004). "Phytochemical and Larvicidal Studies on *Stemona curtisii*: Structure of A New

First Pyrido [1,2-a] Azepine Alkaloid". *J. Nat. . Prod*., vol. 63, pp.675-677.

Paul, R., Pradad, M. and Sah, N.K. (2011). "Anticancer Biology of *Azadirachta indica* (neem): A Mini

Review." *Cancer Bio Ther* , vol. 12, pp.467-470

Sastraruji,T. (2006). *Bioinsecticide Production, Application in Agricultural Use*. Ph.D. Thesis. Chiang Mai University, Thailand.

ISOLATION OF SOME PHYTOCHEMICAL CONSTITUENTS FROM YACON TUBERS OF TAUNGGYI AREA

Sandar Moe[1], Mu Sein Pan[2]

Abstract

The *Smallanthus sonchifolius* (yacon) tubers were dried at the ambient temperature, chopped into bits and percolated with70% ethanol. Qualitative phytochemical screening was determined by the standard procedure suggested the presence of alkaloids, flavonoids, steroids, polyphenols, terpenoids,α-amino acids, glycosides, phenolic compounds, carbohydrate, saponins, tannins, protein, and reducing sugars. Starch and cyanogenic glycosides were not detected in yacon tubers. The profile of the chemical constituents present was established by thin layer chromatography. Six pure organic constituents namely, stigmasteryl acetate (0.003%), β-sitosteryl acetate (0.005%), hexadecanoic acid (0.009%), β-sitosterol (0.02%), chlorogenic acid (0.12%) and β-sitosterol β-D-glucoside (0.8%) based on ethyl acetate extract were isolated from the ethyl acetate soluble fraction of the 70% ethanol extract of the yacon tuber on a silica gel column by gradient elution with petroleum and ethyl acetate (PE-EA, 99:1 to EA only). The isolated compounds were characterized by UV and FTIR.

Keywords : *Smallanthus sonchifolius*, yacon tuber,percolation, phytochemical screening, ethyl acetate extract, UV, FTIR

Introduction

Yacon, *Smallanthus sonchifolius* (Poepp.&Endl.) H. Robinson, is a plant originally cultivated in South America, and the fresh root is eaten like a fruit in this area. Yacon was introduced to Japan in 1985 and has been gradually paid attention to due to its abundant content of fructooligo saccharide, which has some health-promoting effects such as improvement in the intestinal microflora balance, as a storage sugar in place of starch in its root

[1] Associate Professor, Dr,Department of Chemistry, Taunggyi University
[2] Candidate, MRes, Department of Chemistry, Taunggyi University

(Nakanishi, 1997). Yacon tuber is sometimes used for home cooking but has not been a common foodstuff because of decaying easily or rapid browning of the juice or injured tissues. The browning may be caused by condensation reaction of polyphenols with amino compounds (Yabuta *et al.*, 2001) and enzymatic polymerization of polyphenols (Mayer, 1987). Yacon juice contains 850 ppm polyphenol compounds which generally have anti-oxidative activity and chlorogenic acid was reported as a major antioxidant in yacon as well as tryptophan (Yan *et al.*, 1999). In this study, investigation on ethyl acetate fraction of yacon tubers founds six compounds.

Materials and Methods

Smallanthus sonchifolius (yacon tuber) was collected from Naung Karr Village, Taunggyi Township, Southern Shan State in July 2016 and identified at Department of Botany, Taunggyi University. UV and IR spectra were recorded on Shimadzu 1800 UV-Vis Spectrometer and Shimadzu 8400 Fourier Transform- Infrared Spectrophotometer using KBr pellet. Aluminium backed silica gel GF_{254}precoated plates from Merck were used for TLC analysis.

Isolation of Compounds from YaconTubers

The yacon tuber was dried at ambient temperature and pulverized to coarse grained powder.Dry powder (120 g) was applied to extract with 70% ethanol using percolation method and the resultant crude extract obtained was filtered.The crude extract was concentrated under reduced pressure using a rotary evaporator to obtain a solvent free 70% ethanol extract. This extract (29 g) was stirred with ethyl acetate to obtain ethyl acetate soluble extract (0.5 g), which was separated on silica gel column by gradient elution with PE:EA (99:1, 9:1, 5:1, 3:1, 1:1, 1:2, 1:4 and EA only).Fractions obtained were collected in 10mL flasks. Identical fractions were pooled based on their TLC profiles thus resulting in 6 combined fractions.Further purification using methanol solvent was carried out on fractions that were impure.

Phytochemical Analysis

Qualitative phytochemical screening was carried out to determine the presence or absence of alkaloids, flavonoids, steroids,polyphenols, terpenoids, α-amino acids, glycosides, phenolic compounds, carbohydrate, saponins, tannins, starch, protein, reducing sugars, cyanogenic glycosides and using the standard literature procedure (William and Douglas, 2006).

Spectroscopic Analysis

The isolated compounds were characterized by Fourier transform infrared (FTIR) and ultraviolet spectroscopy. FTIR spectra were recorded in which samples were prepared as KBr pellets at the Universities' Research Centre, Yangon University. UV spectra were recorded on methanol solutions at the Chemistry Department, West Yangon University.

Results and Discussion

Phytochemical Analysis

The dried powder sample of yacon tuber showed the presence of various phytochemicals namely, alkaloids, flavonoids, steroids, polyphenols, terpenoids, α-amino acids, glycosides, phenolic compounds, carbohydrate, saponins, tannins, protein, and reducing sugars. Starch and cyanogenic glycosides were not detected in the sample (Table 1).

Table 1 Phytochemicals Present in Tubers of *Smallanthus sonchifolius*(Yacon)

No.	Test	Extract	Reagent Used	Observation	Remarks
1	Alkaloids	1% HCl	Dragendorff's reagent	Orange ppt.	+
2	Flavonoids	95% EtOH	Mg ribbon and conc: H_2SO_4	Pink color	+
3	Steroids	PE	Acetic anhydride and conc: H_2SO_4	Blue color	+
4	Polyphenols	EtOH	1% $FeCl_3$ and 1% $K_3[Fe(CN)_6]$	Greenish-blue color	+
5	Terpenoids	EtOH	Acetic anhydride and conc: H_2SO_4	Red color	+

No.	Test	Extract	Reagent Used	Observation	Remarks
6	α- Amino acids	EtOH	Ninhydrin reagent	Violet color	+
7	Glycosides	H_2O	10% lead acetate	White ppt.	+
8	Phenolic Compounds	H_2O	10% $FeCl_3$	Brown color	+
9	Carbohydrates	H_2O	10 % α-naphthol and conc: H_2SO_4	Red ring	+
10	Saponins	H_2O	Distilled water	Frothing	+
11	Tannins	H_2O	2% NaCl and 1% gelatin	Yellow brown color	+
12	Starch	H_2O	I_2 solution	No blue color	–
13	Protein	Hot H_2O	NaOH and $CuSO_4$	Yellow ppt.	+
14	Reducing Sugars	H_2SO_4 (dil)	NaOH and Benedict's solution	Brick red ppt.	+
15	Cyanogenic Glycosides	H_2O	conc: H_2SO_4, sodium picrate paper	No brick red	–

(+) = present, (-) = absent, (ppt.) = precipitate

Identification of the Isolated Compounds

After purification of the fractions from the silica gel column with methanol, six pure compounds were obtained. Thin layer chromatograms of six isolated compounds from EA extract of yacon tuber were identified by UV and IR spectroscopic methods. IR spectral database (AIST) was used for comparison.

Compound M_1

The isolated compound **M_1** could not be observed under short and long wavelength UV lights on TLC plate, but it gave a dark violet spot upon heating with anisaldehyde-sulphuric acid reagent (R_f 0.43, Silica gel GF_{254}, PE:EtOAc, 99:1). This suggests a steroid/terpenoid compound. The IR spectrum (Figure 1) of **M_1** showed absorptions at 1739 and 1261 cm^{-1} corresponding to C=O and C-O stretching vibrations of an acetate ester. Apart from this, the remaining bands are very similar to those of stigmasterol. From this observation, it may be deduced that **M_1** is stigmasteryl acetate. The assignment of IR bands is summarized in Table (2). Therefore **M_1** should be stigmasteryl acetate.

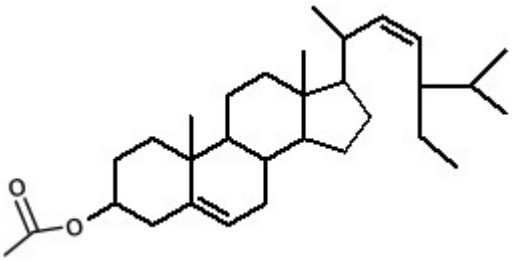

Stigmasteryl acetate (**M_1**)

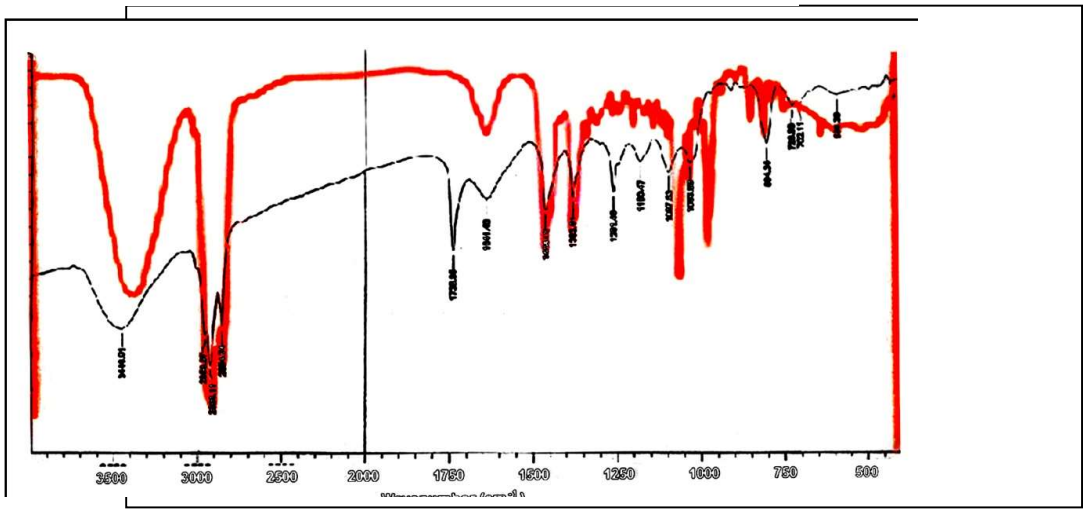

Figure 1 Overlaid IR spectra of M_1(black) and stigmasteryl acetate (red) (AIST)

Compound M_2

The isolated compound **M_2** could not be observed under short and long wavelength UV lights on TLC plate, but it gave a dark violet spot upon heating with anisaldehyde-sulphuric acid reagent (R_f 0.63,Silica gel GF_{254}, PE:EtOAc, 99:1). This suggests a steroid/terpenoid compound. In the IR spectrum (Figure 2) of the compound, the O-H stretching band at 3447 cm^{-1} of β-sitosterol disappeared, while new bands at 1738 cm^{-1} for C = O stretching and 1287 cm^{-1} for C-O stretching showed up, the remaining bands being similar to those of β-sitosterol. This can be seen in the overlaid IR spectra of **M_2** and β-sitosteryl acetate (Figure 2). The assignment of IR bands is summarized in Table (2). Therefore the isolated compound **M_2** should be β-sitosteryl acetate.

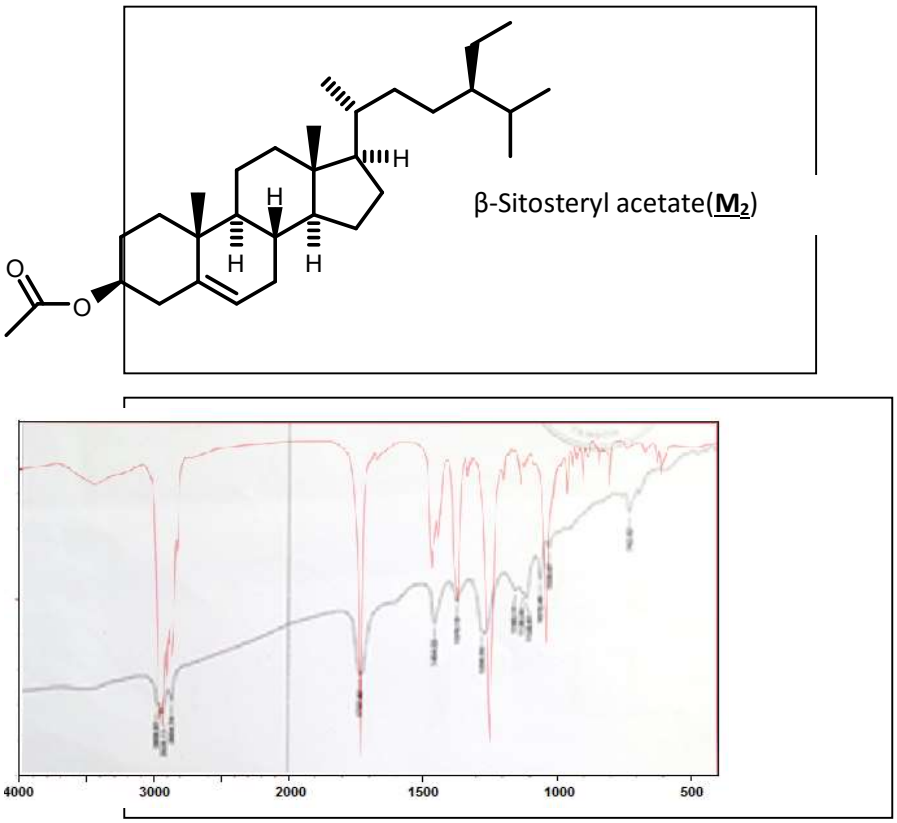

Figure 2 Overlaid IR spectra of M_2 (black) and β-sitosteryl acetate (red) (AIST)

Compound M_3

The isolated compound **M_3** (R_f 0.65, Silica gel GF_{254}, PE:EtOAc, 9:1) was invisible under UV short and long wavelengths on TLC plate, but could be visualized as pink spot upon heating with anisaldehyde-sulphuric acid reagent. The IR spectrum of isolated compound **M_3** suggests a long chain carboxylic acid by the carbonyl stretching band, very broad OH stretching band and an intense CH_2 rocking band, respectively, at 3400-2400, 1697 and 723 cm^{-1} (Figure 3). The assignment of bands is summarized in Table (3). From the close resemblance of the IR spectra (Figure 3) of **M_3** and hexadecanoic acid, **M_3** should be hexadecanoic acid. Hexadecanoic acid is also reported in the plant (Stuardxchange, 2016).

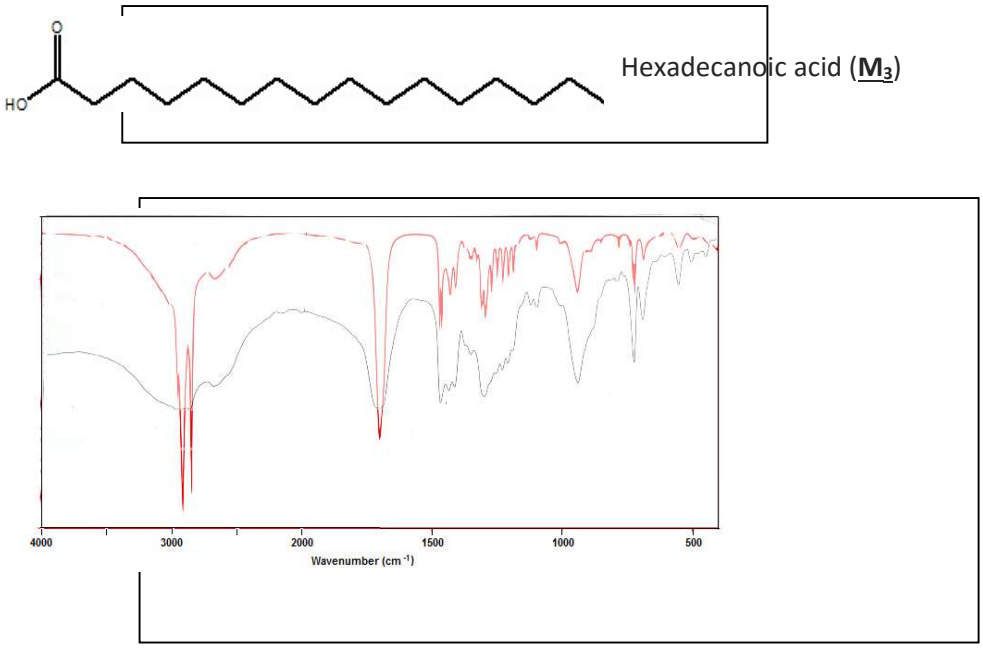

Figure 3 Overlaid IR spectra of M_3 (black) and hexadecanoic acid (red) (AIST)

Compound M4

The isolated compound **M4**(R_f 0.44, Silica gel GF_{254}, PE:EtOAc, 5:1)was invisible under UV short and long wavelengths on TLC plate, but could be visualized as violet spot upon heating with anisaldehyde-sulphuric acid reagent, suggesting a steroid/terpenoid compound. The assignment of absorption bands in IR spectrum (Figure 4) is summarized in Table (2). From the close resemblance between the IR spectra of **M4** and β-sitosterol (Figure 4), **M4** should be β-sitosterol. This is also in accordance with a previous report on the plant (Stuardxchange, 2016).

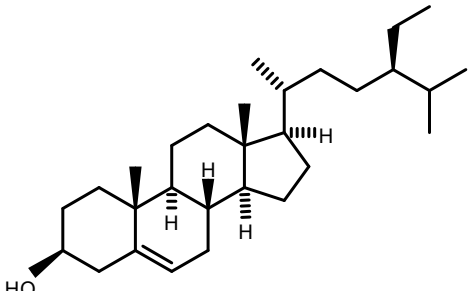

β-Sitosterol (**M4**)

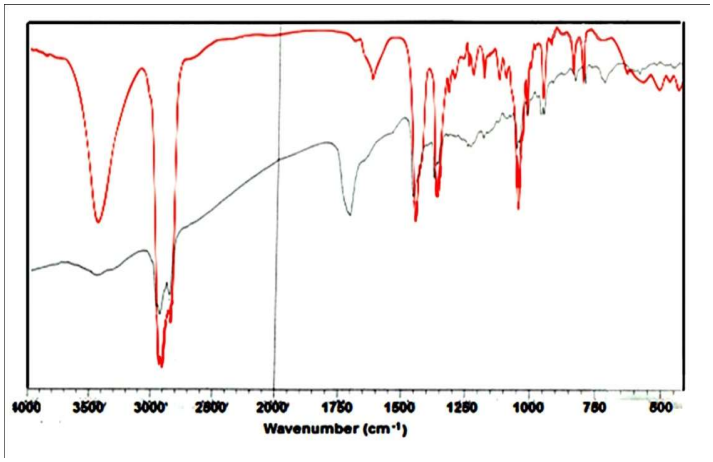

Figure 4 Overlaid IR spectra of M_4 (black) and β-sitosterol (red) (AIST)

Compound M_5

The isolated compound **M_5** (R_f 0.42, Silica gel GF_{254}, PE:EtOAc, 1:4) detectable under UV short wavelength, is a phenolic compound from its positive reaction (an orange spot) on TLC with 10% $FeCl_3$. It also indicated by the alkaline shift from 270 nm (π-π^* transition) to 315 nm (n-π^* transition) of UV absorption bands (Figure 6 and Table 3).The assignment of IR absorption bands (Figure 5) is summarized in Table (2). From the close resemblance between the spectra of **M_5** and chlorogenic acid (Figure 5), **M_5** should be chlorogenic acid. Chlorogenic acid is also previously reported in the plant (Stuardxchange, 2016).

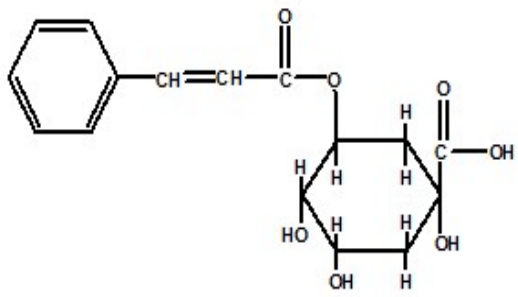

Chlorogenic acid (**M_5**)

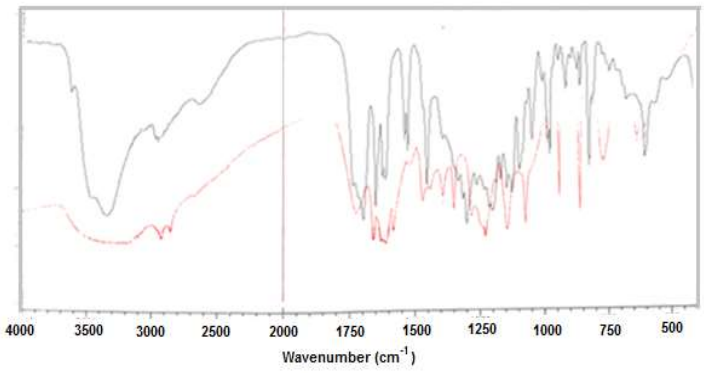

Figure 5 Overlaid IR spectra of M_5 (red) and chlorogenic acid (black) (AIST)

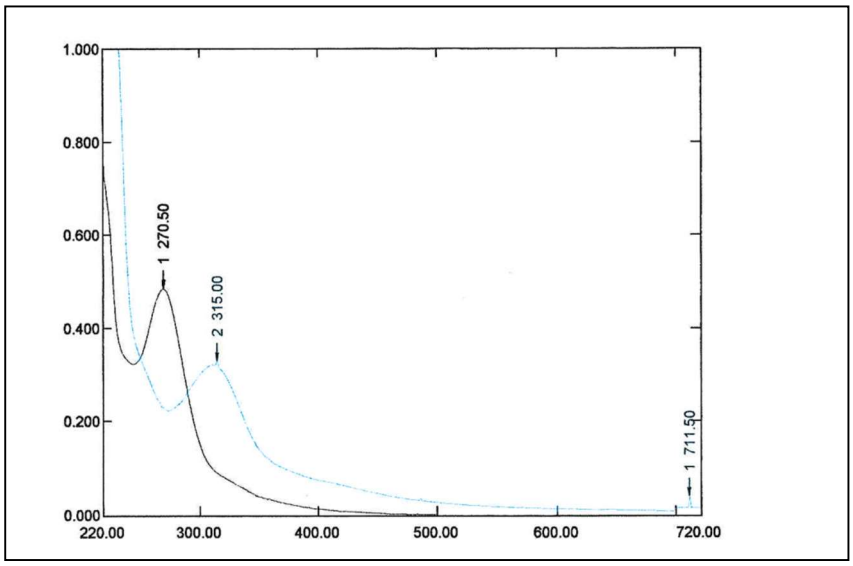

Figure 6 UV spectra of isolated compound M_5 (chlorogenic acid) from yacon tuber

Compound M_6

The isolated compound **M_6** (R_f 0.34, Silica gel GF_{254}, EtOAc) was also invisible under UV short and long wavelengths on TLC plate, but could be visualized as violet spot upon heating with anisaldehyde-sulphuric acid reagent, suggesting a steroid/terpenoid compound. But its higher polarity suggested by its TLC solvent system and intense IR absorption bands for O-H and C-O groups (Figure 7) indicate a glycoside. Apart from these two absorption bands, the remaining bands are very similar to β-sitosterol. Furthermore, the observed bands are very similar to those reported for β-sitosterol β-D-glucoside. Assignment of bands for **M_6** compared with the reported bands (Arunachalam *et al.*, 2009) for β-sitosterol β-D-glucoside is given in Tables 2 and 3.Therefore **M_6** should be β-sitosterol β-D-glucoside.

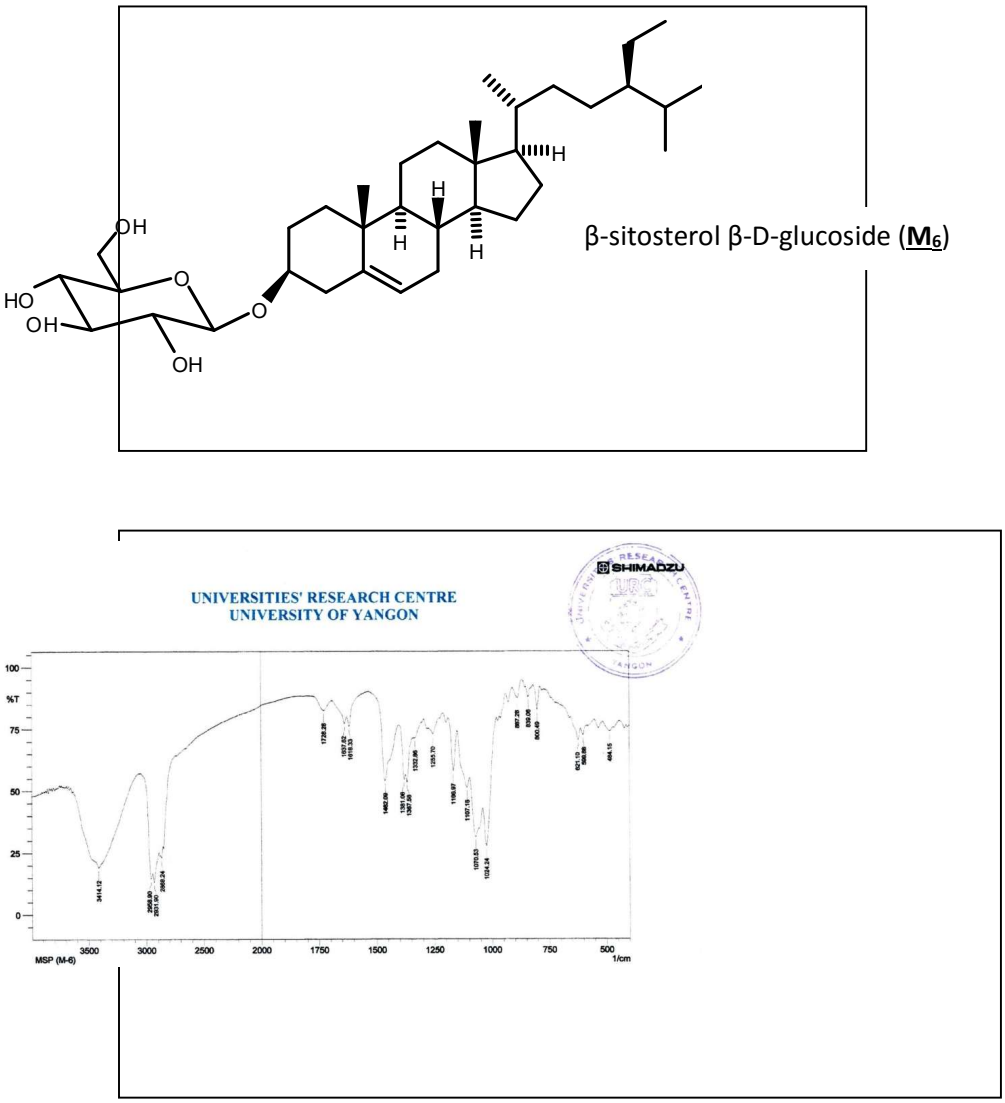

Figure 7 FTIR spectrum of isolated compound M_6 (β-sitosterol β-D-glucoside) from yacon tubers

Table 2 FTIR Spectral Data of The Isolated Compounds from Ethyl Acetate Extraction of Yacon Tuber

Sample code	Wavenumber (cm^{-1})									
	v O-H	v=C-H	v C-H	First overtone of δ CH_2	v C=O	v C=C	δas C-H	δs C-H	v C-O	δoop=C-H
M_1	-	-	2957, 2926, 2855	-	1739	-	1464	1383	1261	804, 723, 702
M_2	-	-	2960, 2926, 2855	-	1738	-	1464	1379	1287	800
M_3	3550-2500	-	2970, 2840	2675	1697	-	1466, 1412	1350	1296, 1229, 1207	939, 723
M_4	3447	-	2980, 2850	-	-	-	1464	1381, 1370	1064, 1074	839, 800
M_5	3550-2500	3100	2970, 2850	-	1726, 1659	1613, 1580, 1520, 1470	1470	-	1144, 1074	943, 864
M_6	3414	-	2960, 2850	-	-	-	1462	1381,1368	1167, 1107 1070, 1024	839, 800

Table 3 UV Spectral Data Assignment of Compound M_5

Reagents	Observed λ_{max}(nm)	Assignment
Sample + MeOH	270.50	$\pi \rightarrow \pi^*$ transition
Sample + MeOH + NaOH	315.00	$n \rightarrow \pi^*$ transition

Table 4 Comparison of FT IR Spectral Data of Compound M_6 and β-sitosterol β-D-glucoside

Wavenumber (cm^{-1})		Vibrational mode	Group assignment
Isolated Compound	β-sitosterol β-D-glucoside*		
3414	3395	ν O-H	$-OH$
2960-2850	2934, 2870	ν C-H	$-CH_3$, $>CH_2$, $\geq CH$
1462	1461	δCH_2 & δ_{as} CH_3	$>CH_2$, $-CH_3$
1381, 1368	1373	δ_{sy} CH_3	$-CH_3$
1167, 1107, 1070, 1024	1072, 1024	ν C-O	2° alcohol & ether
839, 800	-	δ_{oop} = C-H	trisubstituted double bond

*Arunachalam *et al.*, 2009

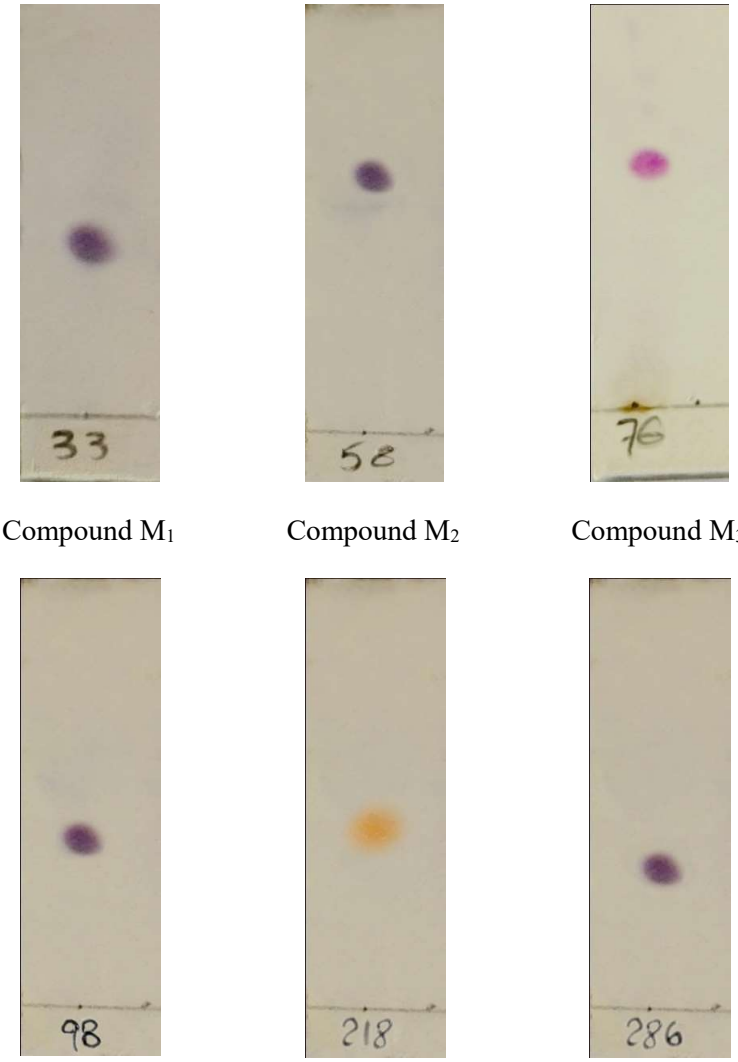

Compound M_1 Compound M_2 Compound M_3

Compound M_4 Compound M_5 Compound M_6

Spraying regent – Anisaldehyde – conc:H_2SO_4 and 10% $FeCl_3$
Solvent system – PE : EA – 99:1, 99:1, 9:1, 5:1, 1:4, EA only
R_f value of M_1, M_2, M_3, M_4, M_5, M_6 – 0.43, 0.63, 0.65, 0.44, 0.42, 0.34

Figure 8 Thin layer chromatograms of six isolated compounds from EA extract of yacon tuber

Conclusion

The results of the present study established the presence of phytochemicals in the yacon tuber extract. Qualitative phytochemical screening was carried out to establish the presence of alkaloids, flavonoids, polyphenols, α-amino acids, glycosides, steroids, terpenoids, phenolic compounds, carbohydrate, saponins, tannins, protein and reducing sugars in the yacon tuber. Starch and cyanogenic glycosides were not detected.The experimental data also suggested the presence of significant amounts of stigmasteryl acetate (0.003%), β-sitosteryl acetate (0.005 %), hexadecanoic acid (0.009%), β-sitosterol (0.02%), chlorogenic acid (0.12 %) and β-sitosterol β-D-glucoside (0.8%) in the ethyl acetate fraction of the 70 % ethanol extract of the yacon tuber. Thus yacon, *i.e.Smallanthus sonchifolius* tubers has great potential for the human health.

Acknowledgements

The authors would like to thank the Myanmar Academy of Arts and Science for allowing to present this paper and Professor and Head Dr DawKhin Than Htay, Department of Chemistry, University of Taunggyi, for her kind encouragement.

References

AIST: *Spectral Database for Organic Compounds*, http:// sdbs.db.aist. go.jp/sdbs/cgi- bin/cre-index.cg. (Accessed12 November 2016)

Arunachalam, G., Paromita, B. and Chattopadhyay,D. (2009). "Phytochemical and Phytotherapeutic Evaluation of *Mallotuspeltatus*(Geist.)" . *Journal of Pharmacognosy and Phytotherapy*, vol. 1(1), pp.001-013.

Nakanishi, T.(1997). "Cultivation of Yacon" . *Nogyonoyobi Engei*,vol. 72, pp. 44-50.

Mayer, A. M. (1987). "Polyphenol Oxidases in Plants- Recent Progress" .*Phytochemistry*, vol. 26, pp. 11-20.

Stuardxchange. (2016). *Philippine Medicinal Plants,* http:// www.stuartxcharge.org/ Yacon, (Accessed 12 November 2016)

William, P. J, and Douglas,K. (2006). *Extraction of Plant Secondary Metabolites in Natural Products Isolation*. New Jersey: 2nd edn. Humana Press, vol. 20, pp. 323-351.

Yabuta, G., Koizumi, Y.,Namiki, K., Hida,M. and Namiki,M. (2001). "Structure of Green Pigment Formed by the Reaction of Caffeic Acid Esters (or ChlogenicAcid) with a Primary Amino Compound." *Biosci. Biotechnol.Biochem*, vol. 65, pp. 2121- 2130.

Yan, X., Suzulei, M.O, Kameyama, M., Sada, Y. and Nakanishi,T. (1999). "Extraction and Identification of Antioxidants in the Roots of Yacon (*Smallanthus sonchifolius*)"*J. Agric. Food Chem*,.vol. 47, pp. 4711-4713.

STUDY ON CONSTITUENTS IN MYANMAR TRADITIONAL MEDICINAL PLANT, *Holoptelea integrifolia* (ROXB.) PLANCH

Arnt Win[1], Aye Mon Thida Nyo[2], Yoshiaki Takaya[3], Masatake Niwa[4], Than Than Aye[5]

Abstract

Holoptelea integrifolia (Roxb.) Planch (Ulmaceae) is a tree widely distributed on the Myanmar, India, Indochina and Asia, and it is locally called in Myanmar as "Pyauk-seik". The various extracts of stem bark of *H.integrifolia* were analyzed by Thin Layer and Column Chromatography method. The stem barks of *H. integrifolia* were collected from Chaik Village, Pakokku Township, Magway Region, Myanmar. They were washed, driedin shade, weighed and cut into small pieces and extracted in methanol. The fractionation of crude extract, followed by the addition of distilled water, n-hexane , ethyl acetate and n-butanol to an aqueous portion of each solvent, to obtain the dried masses of each four layers. Three pure compounds such as new 2-(2-hydroxyethylamino)-1,4 -naphthoquinone (**1**),(-)-syringaresinol (**2**), and(+) (4S)-4-hydroxy-α-tetralone (**3**) are isolated from ethyl acetate portion of this plant. The structures of these compounds were elucidated by analysis of NMR spectroscopic and mass spectrometric data. Although compound (**1**) is synthetically known, to the best of our knowledge, there is no previous report of its natural occurrence. The compounds (**2** and **3**) are described for first time from *H. integrifolia* species. Moreover, the antioxidant activity of compound**3**was evaluated by measuring the half inhibition concentration (IC_{50}) using chemiluminescent method. This isolated compound was found to exhibit significant antioxidant property which is comparable to standard ascorbic acid, at a specific concentration.

Keywords: *Holoptelea integrifolia* (Roxb.) Planch, 2-(2-hydroxyethyl amino)-1,4-naphthoquinone, (-)-syringaresinol, (+)(4S)-4-hydroxy- α-tetralone, chemiluminescent method, antioxidant activity

---

[1] Associate Professor, Dr, Department of Chemistry, Kyaukse University

[2] Associate Professor, Dr, Department of Chemistry,University of Mandalay

[3] Associate Professor, Dr, Department of Chemistry(Shigen), Meijo University,Japan

[4] Professor, Dr, Department of Chemistry(Shigen), Meijo University,Japan

[5] Professor and Head, Dr, Department of Chemistry, Kyaukse University

Introduction

Holoptelea integrifolia(Roxb.) Planch belongs to the family Ulmaceae, having 15 genera and about 200 species,commonly known as Myanmar name "Pyauk-seik". The native distribution of the plant can be seen in Asia-Tropical region including India, Nepal, Sri Lanka, Indo-China, Cambodia, Laos, Myanmar, Vietnam and China (Bamhole and Jiddewar, 1985).

H. integrifolia is used traditionally for the treatment of inflammation, gastritis, dyspepsia, colic, intestinal worms, vomiting, wound healing, leprosy, diabetes, hemorrhoids, dysmenorrhoea and rheumatism. Bark and leaves are used as bitter, astringent, thermogenic, anti-inflammatory digestive, carminative, laxative, anthelmintic, depurative, repulsive, urinary astringent and in rheumatism. Bark and leaf paste of the plant are applied externally on the white patches or leucoderma (Kumar *et al*., 2012).

The stem bark of *H.integrifolia* consists of the β-sitosterol, lupeol, ellagic acid and β-sitosterol-glucoside. 2-aminonaphthoquinone, Friedlin, β-sitosterol, and β-D-glucose are also isolated from stem bark (Sharma *et al*., 2005). 1,4-Naphthalenedione has been isolated from leaves of *H.integrifolia* and is reported to possess antibacterial activity against *Staphylococcus aureus* (Vinod *et al*., 2010). Hexacosanol, octacosanol, β-sitosterol, β-amyrin are isolated from leaves. β-sitosterol, 2",3"-dihydroxyoelan-12-en-28 oic acid and hederagenin are isolated from heartwood (Rastogi and Mehrotra., 1991).

H.integrifolia has been reported that various parts and different kinds of extracts of this plant showed the several biological activities, such as, anti-inflammatory activity, antioxidant activity, antimicrobial activity, antiviral activity, wound-healing activity, anthelminitic activity, antidiabetic activity, antidiarhoeal activity, adaptogenic activity, antitumor activity, and cross reactivity(Kumar *et al*., 2012).Althoughvarious parts and different kinds of extracts of this plant have been measured on the many biological activities, a very little test has been done on the biological activity and plausible medicinal applications of isolated compounds. A drug development programme should be undertaken to develop modern drugs with the compounds isolated from *H. integrifolia*. Hence, extensive investigation is needed to exploit their therapeutic utilities to combat diseases. And *H. integrifolia*, the versatile

medicinal plant is the unique source of various types of bioactive compounds having diverse chemical structures. Therefore, extensive research is needed to get more bioactive and interesting new compounds from this versatile medicinal plant,*H. integrifolia*.

In this paper, we report a simple and rapid antioxidant assay by chemiluminescence. The method is based on antioxidant-dependent quenching of chemiluminescence generated from lipid hydroperoxide and isoluminol/microperoxidase reagent. This method was used to evaluate the antioxidant ability of various antioxidants by measuring half inhibition concentration (IC_{50}). When an antioxidant is present in the assay mixture, it scavenges the oxyradical and quenches the production of light. Thus, by using a constant amount of lipid hydroperoxide (oxyradical donor) the ability of antioxidants can be estimated as the decrease in chemiluminescence. We employed cumene hydroperoxide as the oxyradical donor and improved the assay conditions to ensure reproducibility. The method was used effectively to evaluate the antioxidative ability of a wide range of natural and synthetic components and the results were compared to the half inhibition concentration (IC_{50}) of standard ascorbic acid (Osamu *et al*., 1997).

The aim of this paper is to study the more affective and new chemical constituents of*H. integrifolia*.In the present investigation, we report the isolation and structural elucidation of one new 2-(2-hydroxyethylamino)-1,4-naphthoquinone (**1**),(-)-syringaresinol (**2**),and(+) (4S)-4-hydroxy-α-tetralone (**3**) from the ethyl acetate extract of bark of *H.integrifolia*. Compounds(**2** and **3)**have not been previously isolated or reported from the bark of this variety.

Materials and Methods

IR spectrum was recorded on FT-IR-410 spectrophotometre.^{1}H- and ^{13}C-NMR spectra were recorded on a JEOL ECA-500 (^{1}H: 500 MHz and ^{13}C: 125 MHz). Chemical shifts for^{1}H- and ^{13}C-NMR are given in parts per million (δ) relative to solvent signal (Chloroform-D: δH 7.24 and δC 76.9) as internal standard. EI-Mass spectrum was obtained with a JEOL JMSMS-700 and HX-110, respectively. Optical rotation was recorded on a JASCO P-1020 polarimeter (cell length 100 mm).Analytical TLC was performed on Silica gel 60 F254 (Merck). Column chromatography was carried out on silica gel BW-

820MH (Fuji Silysia Chemicals, Co. Ltd, Seto, Japan). Isoluminol (6-amino-2,3-dihydro-1,4-phthazinedione), microperoxidase, ascorbic acid and cumene hydroperoxide were purchased from Wako Pure Chemical Industries (Osaka Japan).

Plant Material

The stem bark of *Holoptelea integrifolia* (Roxb.) Planch (Ulmaceae) (Figure 1), Myanmar name Pyauk-seik was collected from Chaik Village, Pakokku Township, Magway Region, Myanmar, in April 2012.

Figure 1 *Holoptelea integrifolia* (Roxb.) Planch (Ulmaceae)

Extraction and Isolation

The air-dried stem bark of *H.integrifolia* was extracted with MeOH at room temperature for one month. The MeOH extract was concentrated and the residue (30.0 g) was suspended in water. This suspension was successively extracted with n-hexane, ethyl acetate, and *n*-butanol. The ethyl acetate soluble extract was concentrated by rotary evaporator to produce a residue (2.85 g). The extract was fractionated on a silica gel column using *n*-hexane and ethyl acetate gradient to afford seven fractions (frs. 2.1 - 2.7). Fraction 2.2was rechromatographed over silica gel eluted with n-hexane and ethyl acetate (4:1) to yield compound **3** (116.1 mg). Fraction 2.5 was subjected to column chromatography over silica gel using chloroform and methanol and the eluate was separated into fractions (2.5.1 – 2.5.3). Fraction 2.5.1 was rechromatographedover silica gel eluted with same solvent mixtures followed by preparative TLC (MeOH−$CHCl_3$, 1:19) to yield compound **1** (1.6 mg). Fraction 2.5.2 was further subjected to column chromatography on silica gel using same eluent mixtures of increasing polarity followed by preparative TLC (MeOH−$CHCl_3$, 1:19) to give compound **2** (3.6 mg).

Determination of Antioxidant Activity

Preparation of chemiluminescent reagent and oxyradical donor

Aqueous sodium borate solution (0.5 M) containing 0.2 mM EDTA was prepared, and its pH was adjusted to 10 with sodium hydroxide. Isoluminol (18 mg) was dissolved in 70 mL of methanol and 30 mL of the above described borate solution, and microperoxidase (10 mg) was dissolved in 10 mL of 70% methanol. Both solutions were stored at -20°C. The isoluminol and microperoxidase solution were mixed in a volume ratio of 100:1 before use, and used as the chemiluminescent reagent.

Cumene hydroperoxide [30 μL, corresponding to 160 μmol, which was determined by idometry] was dissolved in 50 mL of ethanol containing 5 mM EDTA and stored at -20°C. The solution was diluted 200 times with methanol before use, and used as the oxyradical donor (16 μM).

Preparation of sample

The pure compound was prepared inmethanol with various concentrations such as 0.02 $mgmL^{-1}$, 0.04 $mgmL^{-1}$, 0.06 $mgmL^{-1}$, 0.08 $mgmL^{-1}$, and 0.1 $mgmL^{-1}$,respectively.

Standard assay for antioxidant activity

A photo counter (Model AB-2200/-R Luminescence PSN, Japan) was used for the determination of chemiluminescence. 130 μL cumene hydroperoxide solution and 25 μL sample were placed in a 0.8 mL glass tube, and the tube was set in the instrument. The chemiluminescent reagent (200 μL) was put into the vial. The chemiluminescence produced was measured for 3 min. The control was performed in the same manner in the mixture, replacing the sample solution with methanol.

Results and Discussion

The concentrated methanolic extract of the stem bark of *H.integrifolia* was fractionated with distilled water, n-hexane, ethyl acetate and n-butanol. The ethyl acetate crude extract was separated by chromatography on a

silica gel column using hexane-ethyl acetate and chloroform-methanol from non-polar to polar with various ratios to obtain one new compound, 2-(2-hydroxyethylamino)-1,4-naphthoquinone, (-)-syringaresinol,and(+) (4S)-4-hydroxy-α tetralone compounds.

2-(2-hydroxyethylamino)-1,4-naphthoquinone (**1**) was obtained as orangecrystal. The molecular formula of **1** was determined to be $C_{12}H_{11}O_3N$ from the observation of a molecular ion peak at m/z 217 [M^+] on EI mass spectrometry. The FT IR spectrum exhibited absorption bands at 3600-3200, 3066.26, 2932.23, 2863.77, 1682.59, 1600.63, 1561.09, 1518.67, 1367.28, and 1082.83 cm^{-1}, ascribable to hydroxyl, amine, sp^2 H/C, sp^3 H/C, carbonyl, aromatic ring, and C-N amine functional groups, respectively. The ^{1}H- and ^{13}C-NMR(DMSO, Table-1) spectra of **1** showed the presence of four aromatic protons coupled with each other[δH 7.98 (1H, dd, J= 7.6,1.3 Hz; H-8), 7.93 (1H, dd, J= 7.6,1.3 Hz; H-5), 7.83 (1H, td, J= 7.6,1.3 Hz; H-6) and 7.72 (1H, td, J= 7.6,1.3 Hz; H-7],one singlet sp^2 methine proton bearinga carbonyl group[δH5.73 (1H, s; H-3)], oneoxygenated methylene [δH3.59 (2H, t, *J* = 5.7 Hz; H-2′)], another one nitrogen bearing methylene [δH 3.25 (2H, t, *J* = 5.7 Hz; H-1′)] , three quaternary carbons [148.7 (C-2),130.3 (C- 9), 133.2 (C- 10)], and two carbonyl groups [181.5 (C- 1), 181.4 (C- 4)]. All above data indicated that **1** is 1,4-naphthoquinone derivative. Moreover, the ^{1}H–^{1}H COSY experiment on **1**indicated the presence of two partial structures which are ortho-disubstituted benzene ring andethyl alcohol group (-CH_2-CH_2-OH).In the^{1}H and ^{13}C -NMR and ^{1}H–^{1}H COSY spectra, the proton signals due to an ortho-disubstituted aromatic ring, singlet methane proton and two carbonyl carbons suggested the 2-amino-1,4-naphthoquinone moiety in **1**. The two fragments, 1,4-naphthoquinone and ethyl group could be connected by NH group flank between these two groups in which the downfield chemical shift methylene group [δH 3.25 (2H, t, *J* = 5.7 Hz; H-1′)] and downfield chemical shift sp^2 quaternary carbon, [148.7 (C-2)]are observed in ^{1}H NMR and ^{13}C NMR spectra respectively (Table 1). It was confirmed by NOESY experiment. On the basis of the above evidence, the structure of **1** was determined to be 2-(2-hydroxyethylamino)-1,4-naphthoquinone **1**,as shown in

Figure 2. In addition, the spectral data of **1** were identical to the previously reported for synthesized 2-(2-hydroxyethylamino)-1,4-naphthoquinone (Cao *et al.,* 2009).

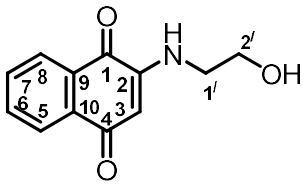

Figure 2 Structure of Compound **1**

(-)-Syringaresinol**2** isolated as colorless crystal, possessed the molecular formula $C_{22}H_{26}O_8$ as assigned by EI-MS ion at m/z 418 $[M]^+$ which is stable base peak, calculating ten degrees of unsaturation. In EIMS spectrum, the observation of molecular ion peak m/z at 418 indicated that this pure compound is dimmer (lignan). The ^{1}H NMR spectral data(Table 2) revealed the four typical singlet with same chemical shift of methoxy groups at δ_H 3.90, two same chemical shift of ether bearing methylene groups at δ_H 4.28 and 3.91, two same chemical shift of methine protons at δ_H4.73 (oxygenated and benzylic), another two same chemical shift methine protons at δ_H 3.07 and two same tetrasubstituted benzene rings which contain two equivalent singlet protons at δ_H 6.58. The ^{13}C NMR, HMQC and DEPT spectral data displayed the presence of eight quaternary carbons (six ether bearing and two phenolic), four sp^2 methine carbons (same chemical shift), four sp^3 methine carbons (two oxyganated and benzylic), two methylene carbons (same chemical shift), and four methoxy carbons (same chemical shift). In DQF-COSY spectrum, the observation of medium graphic area of methine proton (H-1 and H-5) with other ones (H-2 and H-6) and methylene protons (H-4a, H-4b, H-8a and H-8b) indicated the CH-2– CH-1– CH_2-8 and CH-4– CH-5– CH_2-6 fragments. Moreover, the connectivity of these fragments to C-1′, and C-1″ was established by HMBC correlations H-1′/C-2, H-6′/C-2, H-1″/C-6, H-6″/C-6, H-2/C-1′, H-2/C-6′, H-6/C-2″, and H-6/C-6″. Since two aromatic rings of **2** accounted for eight out of ten units of unsaturation, the remaining two units indicated two pentacyclic systems. The above all spectral data strongly

suggested that **2** was a syringaresinol lignan. Moreover, these spectral values were in good agreement with values previously reported for syringaresinol (Abulajiang *et al*., 2012).

The relative configuration (+)-syringaresinol (Reference compound)at H-1 and H-2 could be determined by the3J1,2, H-C-C-H (12.4 Hz) coupling constant which indicated that the two protons were located opposite side with dihedral angle 180° and H-2 and H-6 were both axial (Figure 3).By comparing the ^{1}H-NMR data of (-)-syringaresinol (Reference compound) [3J1,2, H-C-C-H (4.3 Hz)] with those of compound **2**, the relative configuration of compound **2**at H-1 and H-2 could be assigned by the3J1,2, H-C-C-H (4.5 Hz) coupling constant which revealed that the two protons were located axial-equatorial like position. According to the above previously reported data and NMR data of **2** showed that in the isolated compound, H-2 (d, 4.5 Hz) and H-6 (d, 4.5 Hz) were both in equatorial position (Figure 4). Moreover, the relative configurations between H-2 (δ_H4.73) with H-8b (δ_H 3.91) and H-1 (δ_H3.07) with H-2'(δ_H6.58) were also established as cis-configuration by an NOE experiment. Hence, **2** was detected to be (-) syringaresinol (Figure 4).

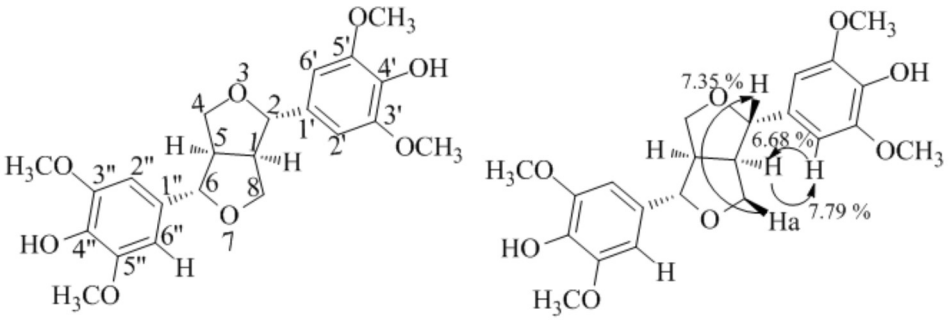

Figure 3 Structure of (+)-syringaresinol (reference compound) and NOE experiment

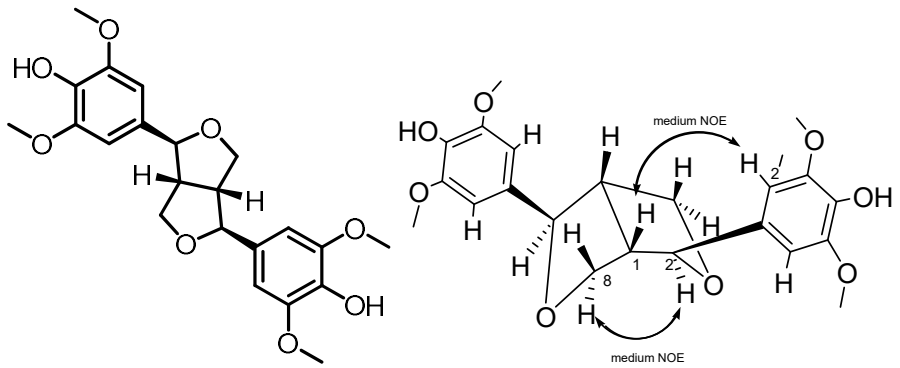

Figure 4 Structure of Compound **2** and NOE experiment

The molecular formula of compound **3** was assigned as $C_{10}H_{10}O_2$based on the FT IR,^{1}H and ^{13}C NMR, HMQC, DEPT and EIMS [M^+] (*m*/*z* 162). Its mass spectrum exhibited a molecular ion at *m*/*z* 162 which is its molecular mass. The stable ion of *m*/*z* 105 which is base peak was formed by the liberation of CH_2=CH-CHO molecule and hydrogen radical ($H^{\bullet}$) from the molecular ion (m/z 162). In the ^{1}H NMR(500 MHz) (Table 3),the observation of proton signals at δ 8.03 (1H, d, J= 7.7 Hz), 7.60 (2H, m), and 7.43 (1H, m) and proton coupling with each other in DQF-COSY experiment, led to the ortho-disubstituted benzene moiety. The^{1}H NMR(500 MHz)also represented a set of proton signals due to two methylenes at *δ*2.95 (1H, ddd, *J* = 17.3, 7.4, 4.5 Hz) and 2.62 (1H, ddd, *J* = 17.3, 9.7, 4.9 Hz), and 2.42 (1H, m), 2.19 (1H, m), a carbinol methine at *δ* 4.99 (1H, dd, J= 8.0, 3.9 Hz). In addition,^{13}C NMR(125 MHz), and HMQC spectra displayed signals for two methylene carbons at *δ* 35.1 and 32.1, a carbinylic carbon at *δ*67.9, and a carbonyl carbon at *δ*197.3. These above data indicated that **3** is4-hydroxy-α-tetralone.More detailed analysis of DQF-COSY, HMQC and HMBC supported a 4-hydroxy-α-tetralone structure. The carbinol methine proton (*δ* 4.99) at C-4 could be deduced to be equatorial from its coupling constant value of 3.9 Hz with H_{ax}-3 (*δ* 2.42).By comparing the spectroscopic data, such as MS, NMR and $[\alpha]_D^{25}$ of **3**with those of reported reference compound, compound **3**was identified to be (4S)-4-hydroxy-α-tetralone (**3)** (Joyl and Nair, 2001).Based on the above

evidence, the structure of compound **3** was assigned as(+) (4S)-4-hydroxy-α-tetralone (Figure 5).

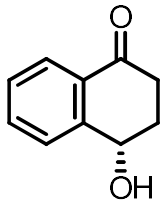

Figure 5 Structure of Compound **3**

Table 1 ^{13}C, ^{1}H NMR Data of 2-(2-hydroxyethylamino) -1,4-naphthoquinone and ^{1}H-^{13}C, ^{1}H-^{1}H Correlations Exhibited in the 2D NMR Spectra in $CDCl_3$

Carbon	$\delta^{13}C$ (DEPT)	Proton	Proton $\delta^{1}H$ (J Hz)	HMBC correlation	COSY correlation
1	181.5(C=O)	-	-	-	-
2	148.7	-	-	-	-
3	99.6 (CH)	3	5.73 (s)	C-1, C-4, C-10	-
4	181.4(C=O)	-	-	-	-
5	125.3 (CH)	5	7.93(dd, 7.6 and 1.3)	C-7, C-9	H-6, H-7
6	134.9 (CH)	6	7.83(td, 7.6 and 1.3)	C-8	H-5, H-7,H-8
7	132.2 (CH)	7	7.72(td, 7.6 and 1.3)	-	H-5, H-6, H-8
8	125.9 (CH)	8	7.98(dd, 7.6 and 1.3)	-	H-6,H-7
9	130.3	-	-	-	-
10	133.2		-	-	-
1′	44.6 (CH_2)	1′	3.25(t, 5.7)	-	H-2′
2′	58.4 (CH_2)	2′	3.59(t, 5.7)	-	H-1′

Table 2 ^{13}C, ^{1}H NMR Data of (-)-syringaresinol and ^{1}H-^{13}C, ^{1}H-^{1}H Correlations Exhibited in the 2D NMR Spectra in $CDCl_3$

Carbon	$\delta^{13}C$ (DEPT)	Proton	Proton $\delta^{1}H$ (*J* Hz)	HMBC correlation	COSY correlation
1	54.4(CH)	1	3.07 (m)	-	H-2, H-8a, H-8b
2	86.1(CH)	2	4.73(d, 4.5)	C-4,C-8,C-2′,C-6′	H-1
3	-	-	-	-	-
4	71.8(CH_2)	4a 4b	4.28(dd, *J* = 9.1, 6.8) 3.91(m)	C-2, C-6 C-2, C-6	H-4b, H-5 H-4a, H-5
5	54.4(CH)	5	3.07(m)	-	H-4a, H-4b, H-6
6	86.1(CH)	6	4.73(d, 4.5)	C-4,C-8,C-2′,C-6′	H-5
7	-	-	-	-	-
8	71.8(CH_2)	8a 8b	4.28(dd, *J* = 9.1, 6.8) 3.91(m)	C-2, C-6 C-2, C-6	H-8b, H-1 H-8a, H-1
1′	132.1	-	-	-	-
2′	102.8(CH)	2′	6.58(s)	C-2,C-1′,C-3′,C-4′,C-6′	-
3′	147.2	-	-	-	-
4′	134.4	-	-	-	-
5′	147.2	-	-	-	-
6′	102.8(CH)	6′	6.58(s)	C-2,C-1′,C-2′,C-4′,C-5′	-
1″	132.1	-	-		
2″	102.8(CH)	2″	6.58(s)	C-6,C-1′,C-3′,C-4′,C-6′	-
3″	147.2	-	-	-	-
4″	134.4	-	-	-	-
5″	147.2	-	-	-	-
6″	102.8(CH)	6″	6.58(s)	C-6,C-1″,C-2″,C-4″,C-5″	-
3′-O$\underline{C}H_3$	56.4	3′-O$\underline{C}H_3$	3.90(s)	C-3′	-
5′-O$\underline{C}H_3$	56.4	5′-O$\underline{C}H_3$	3.90(s)	C-5′	-
3″-O$\underline{C}H_3$	56.4	3″-O$\underline{C}H_3$	3.90(s)	C-3″	-
5″-O$\underline{C}H_3$	56.4	5″-O$\underline{C}H_3$	3.90(s)	C-5″	-

Table 3 ^{13}C, ^{1}H NMR Data of (4S)-4-hydroxy-1-tetralone and ^{1}H-^{13}C, ^{1}H-^{1}H Correlations Exhibited in the 2D NMR Spectra in $CDCl_3$

Carbon	$\delta^{13}C$ (DEPT)	Proton	Proton $\delta^{1}H$ (*J* Hz)	HMBC correlation	COSY correlation
1	197.3(C=O)	-	-	-	-
2	35.1(CH_2)	2a	2.95(ddd, 17.3,7.4,4.5)	C-1, C-3, C-4	H-2b, H-3a, H-3b
		2b	2.62(ddd, 17.3,9.7,4.9)	C-1, C-3, C-4	H-2a, H-3a, H-3b
3	32.1(CH_2)	3a	2.42(m)	C-1, C-2, C-4	H-2a, H-2b, H-3b
		3b	2.19(m)	C-1, C-2, C-4	H-2a, H-2b, H-3a
4	67.9(CH)	4	4.99(dd, *J* = 8.0, 3.9)	-	H-3a, H-3b
5	126.9(CH)	5	7.60(m)	C-7, C-8, C-9,C-10	H-7
6	134.1(CH)	6	7.60(m)	C-7, C-8, C-9,C-10	H-7
7	128.4(CH)	7	7.43(m)	C-5, C-6, C-8,C-9	H-5, H-6, H-8
8	127.2(CH)	8	8.03(d, *J* = 7.7)	C-1, C-6, C-10	H-7
9	131.2	-	-	-	-
10	145.3	-	-	-	-

Compound 1: Orange crystal.FT IR (KBr): (cm^{-1}) 3600-3200 (-OH and -NH), 3066.26 (=C-H), 2932.23, 2863.77 (Sat-H/C), 1682.59 (C=O), 1600.63, 1561.09, 1518.67, (ArH and NH), 1367.28 (C-OH): ^{1}H-NMR (500 MHz, DMSO) δ: 7.98 (1H, dd, J= 7.6,1.3 Hz; H-8), 7.93 (1H, dd,J= 7.6,1.3 Hz; H-5), 7.83 (1H, td,J=7.6,1.3 Hz; H-6), 7.72 (1H, td,J= 7.6,1.3 Hz; H-7), 5.73 (1H, s; H-3), 3.59 (2H, t, *J* = 5.7 Hz; H-2′), 3.25 (2H, t, *J* = 5.7 Hz; H-1′), ^{13}C-NMR (125 MHz, DMSO) δ: 181.5 (C- 1), 181.4 (C- 4), 148.7 (C-2), 134.9 (C-6), 133.2 (C- 10), 132.2 (C- 7), 130.3 (C- 9), 125.9 (C- 8), 125.3 (C - 5), 99.6 (C-3), 58.4 (C-2′), 44.6 (C-1′), . EIMS *m*/*z* (rel. int.): 231 [M^+] ($C_{12}H_{11}O_3N$).

Compound 2: colourless crystal. $[\alpha]_D^{25}$= - 8.4° (*c* 0.058, $CHCl_3$).FT IR (KBr): (cm^{-1})3421.1(-OH), 3084.58 (=C-H), 2935.13, 2862.81 (Sat-H/C), 1614.13, 1518.67, 1459.85 (ArH), 1215.9, 1113.69 (C-O-C): ^{1}H-NMR (500 MHz, $CDCl_3$) δ: 6.58 (1H, s ; H-2′), 6.58 (1H,s ; H-6′), 6.58 (1H, s ; H-2″), 6.58 (1H, s ; H-6″), 4.73 (1H, d, *J* = 4.5 Hz; H-2), 4.73 (1H, d, *J* = 4.5 Hz; H-6), 4.28 (1H, dd, *J* = 9.1, 6.8 Hz; H-4a), 4.28 (1H, dd, *J*= 9.1, 6.8 Hz; H-8a), 3.91 (1H, m ; H-4b), 3.91 (1H, m ; H-8b), 3.90 (3H, s ; C-3′-OC<u>H</u>$_3$), 3.90 (3H, s ; C-5″-OC<u>H</u>$_3$), 3.90 (3H, s ; C-3′-OC<u>H</u>$_3$), 3.90 (3H, s ; C-5′-OC<u>H</u>$_3$), 3.09 (1H, m ; H-1), 3.09 (1H, m ; H-5), ^{13}C-NMR (125 MHz,$CDCl_3$) δ: 147.2 (C- 3′), 147.2 (C- 5′), 147.2 (C- 3″), 147.2 (C- 5″), 134.4 (C- 4′), 134.4 (C- 4″), 132.1 (C- 1′), 132.1 (C - 1″), 102.8 (C- 2′), 102.8 (C- 6′), 102.8 (C- 2″), 102.8 (C- 6″), 86.1 (C- 2), 86.1 (C- 6), 71.8 (C- 4), 71.8 (C- 5), 56.4 (C-3′-O<u>C</u>H$_3$), 56.4 (C-5′-O<u>C</u>H$_3$), 56.4 (C-3″-O<u>C</u>H$_3$), 56.4 (C-5″-O<u>C</u>H$_3$), 54.4 (C-1), 54.4 (C-5). EIMS *m*/*z* (rel. int.): 418 [M^+] ($C_{22}H_{26}O_8$).

Compound 3:yellowish amorphous solid. $[\alpha]_D^{25}$= + 13.5° (*c* 0.066, $CHCl_3$). FT-IR(KBr): (cm^{-1}) 3408.57(-OH), 3062.41 (=C-H), 2926.45, 2869.56 (Sat-H/C), 1684.52 (C=O), 1600.63, 1455.99, 1415.49 (ArH), 1287.25 (C- C -O): ^{1}H-NMR (500 MHz, $CDCl_3$) δ: 8.03 (1H, d, J= 7.7 Hz; H-8), 7.60 (2H, m ; H-5 and H-6), 7.43 (1H, m ; H-7), 4.99 (1H, dd, J= 8.0, 3.9 Hz ; H-4), 2.95 (1H, ddd, *J* = 17.3, 7.4, 4.5 Hz; H-2a), 2.62 (1H, ddd, *J* = 17.3, 9.7, 4.9 Hz; H-2b), 2.42 (1H, m ; H-3a), 2.19 (1H, m ; H-3b), ^{13}C-NMR (125 MHz,$CDCl_3$) δ: 197.3 (C- 1), 145.3 (C-10), 134.1 (C-6), 131.2 (C- 9), 128.4 (C- 7), 127.2 (C- 8), 126.9 (C- 5), 67.9 (C - 4), 35.1 (C-2), 32.1 (C-3). EIMS *m*/*z* (rel. int.): 162 [M^+] ($C_{10}H_{10}O_2$).

Evaluation of Antioxidant Activity

This pure yellowish amorphous solid compound, (+)(4S)-4-hydroxy-α-tetralone isolated from the stem bark of*H. integrifolia*. traditionally used in Myanmar system of medicine was screened for its antioxidant activity using ascorbic acid as standard antioxidant. The free radical scavenging potential of this compound was evaluated by a sensitive and simple chemiluminescent method. By using the resulted number of photon data from the printed graph, the % inhibition of isolated compound was calculated with the following equation.

$$\% \text{ inhibition of sample} = 1 - \frac{number\ of\ photo\ \ of\ the\ sample}{number\ of\ phot\ \ \ of\ blank} \text{x } 100$$

The calculated data of pure compound are described in the following Table 4.

Table 4 % Inhibition of (+)(4S)-4-hydroxy-1-tetralone

Cocentratiom (mg/mL)	0.02	0.04	0.06	0.08	0.1
% Inhibition (%)	17.34	38.9	48.54	61.85	70.85

In accordance with graph (Figure 6), the half inhibition concentration (IC_{50}) of this compound was determined as 0.065 mg mL^{-1}. The pure compound was found to show significant antioxidant property which is comparable to IC_{50}value of standard ascorbic acid, at a specific concentration.

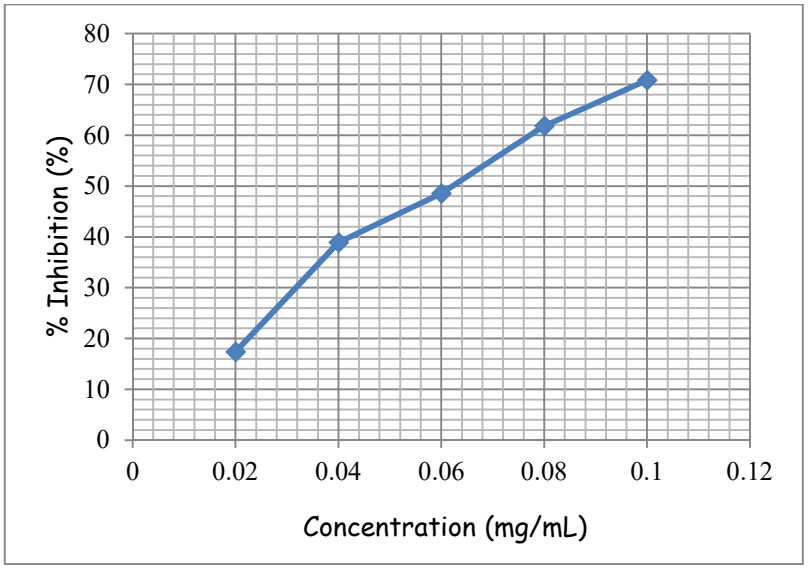

Figure 6 The graph of % inhibition (%) Vs concentration (mg/mL) of (+)(4S)-4-hydroxy-1-tetralone

Conclusion

In the present investigation, we describe the isolation of one new compound (**1**) and other two interesting compounds (**2** and **3**)from the stem bark of *H. integrifolia* (Pyauk-seik). Moreover,the elucidated pure yellowish amorphous solid compound which is described for first time, (+)(4S)-4-hydroxy-α-tetralone isolated from the EtOAc extract of stem bark of *H. integrifolia* (Pyauk-seik) traditionally used in Myanmar system of medicine, responds significant antioxidant activity by comparing the half inhibition concentration (IC_{50}) of ascorbic acid as standard antioxidant using a sensitive and simple chemiluminescent method. Further studies are required and are in progress here.

Acknowledgements

We are extremely grateful to Dr Myint Lwin, Rector, Dr Si Si Khin, Pro-Rector, and Dr Kyae Mon Lwin, Professor, Department of Chemistry, Kyaukse University, Myanmar for their permission, understanding, kind helps and good guidance on our study. We are thankful to the fellowship of International Exchange Center from Meijo University, Japan for providing financial support for our research.

References

Abulajiang, T., Yong, J. and Peng-Fei, T. (2012). "Nine Lignans from *Arteisia absinthim* L.". *Journal of Chinese Pharmaceutical Sciences.*vol. 21 (4),pp.360-364.

Bamhole, V.D. and Jiddewar, G.G. (1985). "Antiobesty Effect of *Iris versicolor* and *Holoptelea integrifoliain* Rats". *Scahitra Ayurveda,* vol.37,pp.557-561.

Cao, S., Murphy, B.T, Foster, C., Lazo, J.S. and Kingeston, D.G.I. (2009)."Bioactivities of Simplified Adociquinone and Naphthoquinone Derivatives against Cdc25B, MKP-1, and MKP-3 Phosphatases". *Bioorg Med Chem* vol.14:2276–2281

Jyol, S. and Nair, M.S. (2001). "Efficient Enzymatic Kinetic Resolution of 4-Hydroxytetralone and 3- Hydroxyindanone".*Tetrahedron: Asymmetry,* vol.12, pp.2283-2287.

Kumar, D., Kumar, K., Gupta, J., Bishnoi, N. and Kumar, S. (2012). "A Mini Review on Chemistry and Biology of *Holoptelea integrifolia* Roxb. Planch (Ulmaceae)". *Asian Pacific Journal of Tropical Biomedicine,* vol.2(2), pp.S1200-S1205.

Osamu, H., Masako, T., Kazuyo, H. and Saori, K.(1997)."Evaluation of Antioxidant Activity by Chemiluminecence Method". *Analytical Chemistry*,vol.247,pp.237-241.

Rastogi, R. P. and Mehrotra, B.N. (1991). *Compendium of Indian Medicinal Plants*. New Delhi:1st Edn., CDRI Lucknow,vol.2, pp.375.

Sharma, P. C., Yelene, M.B. and Dennis,T.J. (2005)."Database on Medicinal Plants Used in Ayuveda". Central Council for Research in Ayuvedar and, Gov. of India, vol. 2,pp. 171-173.

Vinod, N. V., Shijina,R., Dileep,K.V.and Sadasivan, C. (2010)."Inhibition of Beta-Lactamase by 1,4- Naphthalenedione from *Holoptelea integrifolia* Roxb. Planch (Ulmaceae)".*Applied Biochemistry and Biotechnology,* vol.160, pp.1752-1759.

BIOSYNTHESIS OF ZINC OXIDE NANOPARTICLESUSING *CALOTROPIS GIGANTEA*L. (MA-YO-GYI),CHARACTERIZATION AND ANTIMICROBIAL ACTIVITIES

Khin Mar Cho[1], Aye Thet Khaing[2]

ABSTRACT

This research deals with biosynthesis of zinc oxide nanoparticles using *Calotropis gigantea*L. (ma-yo-gyi), characterization and antimicrobial activities. The aim of this research is to synthesize, characterize and study the antimicrobial activities of biosynthesized zinc oxide nanoparticles. Leaves of *Calotropis gigantea* L. (Ma-yo-gyi) were collected from Kathitkan village in Aung Lan Township, Magway Region and identified in Department of Botany, Pyay University. The phytochemical screening of aqueous leaves extract of *Calotropis gigantea* L. was carried out by test tube method and aqueous leaves extract was also characterized by FT IR technique. Zinc oxide nanoparticles were biosynthesized fromzinc nitrate by method Iand method II using aqueous leaves extract of *Calotropis gigantea* L. as a reducing agent. Thermal stability of green synthesized zinc oxide nanoparticles by method I was studied by Thermogravimetric-Differential Thermal Analyzer (TG-DTA). The effects of calcination temperature on crystallize sizes of biosynthesized ZnO nanoparticles by method I was also studied. The crystallinity and purity of biosynthesized zinc oxide nanoparticles by methods I and II werestudied by X-ray Diffraction (XRD) technique. The biosynthesized ZnO nanoparticles by both methods were found to be crystalline in nature and which has hexagonal structure. The average crystallize sizes were calculated by using Debye-Scherrer equation and found to be in the range of (25-33) nm. The antimicrobial activities of biosynthesized ZnO nanoparticles on six microorganisms such as *B. subtilis, B. pumilus, C. albicans, S. aureus, E. coli* and *P. aeruginosa* were studied by ager well diffusion method. It was found that the high antimicrobial activities of biosynthesized ZnO NPs (23-26 mm) on gram positive and negative bacteria strain except *P. Aeruginosa* and also high activity on fungus like *Candida albicans.* For the investigation of the storage time of guava and tomato fruits at room temperature, biosynthesized ZnO nanoparticles coated on surface of these fruits and found to be fresh without any moltuntilone month.

[1] Associate Professor, Department of Chemistry, Pyay University
[2] MRes Candidate, Department of Chemistry, Pyay University

Keywords ZnO nanoparticles, biosynthesis, *Calotropis gigantea*L., antimicrobial activity

Introduction

Nowadays, nanotechnology has grown to be an important research field in all areas. For several years, scientists have constantly explored different synthetic methods to synthesize nanoparticles (Sridhara *et al*., 2013).Because of their unique physicochemical and optoelectronic properties, nanoparticles are of particular interest for a number of applications as catalysts, chemical sensors, electronic components, medical diagnostic imaging, pharmaceutical products, and medical treatment protocols. Conventional synthesis of nanoparticles can involve expensive chemical and physical processes that often use toxic materials with potential hazards such as environmental toxicity, cytotoxicity and carcinogenicity(Alagumuthu and Kirubha, 2012). Use of biological organisms such as microorganisms, plant extract or plant biomass could be an alternative to chemical and physical methods for the production of nanoparticles (Sridhara *et al*., 2013). In comparison with microorganisms, the plant approach is more advantageous since it does not need any special, complex and multi-step structures. Furthermore, synthesis in plants tends to be faster than microorganisms, is more cost-effective and is relatively easy to scale up for the production of large quantities of nanoparticles. Plant extracts containing bioactive alkaloids, phenolic acids, polyphenols, proteins, sugars and terpenoids are believed to have an important role in first reducing the metallic ions and then stabilizing them (Shah *et al*., 2015). Zinc oxide nanoparticles stand out as one of the most versatile materials, due to their diverse properties, functionalities and applications. They also possess antimicrobial actions against some bacteria and fungi. As far as synthesis of zinc oxide nanoparticles is concerned they can be synthesized by chemical methods but in recent times due to evolution of green chemistry, biogenic synthesis of ZnO nanoparticles is also possible by using different plant extracts. The biosynthesis of ZnO nanoparticles is much safer and environment friendly compared to chemical synthesis because it does not lead to formation of toxic byproduct (Sabir *et al.*, 2014). The aim of this research is to

synthesize, characterize and study the antimicrobial activities ofbiosynthesized zinc oxide nanoparticles using plants extracts.

Scientific Classificationof *Calotropisgigantea L.* (Chandrabhan *et al.*, 2011)

Kingdom	:	Plantae
Order	:	Gentianales
Family	:	Apocynaceae
Subfamily	:	Asclepiadoideae
Genus	:	*Calotropis*
Species	:	*C. gigantean*
Botanical name	:	*Calotropisgigantea*L.
Myanmar name	:	Ma-yo-gyi

Materials And Methods

Preparation and Characterization of Aqueous Leaves Extract of *C.gigantea*

The extract of *C.gigantea* leaves was prepared by placing 20 g of clean and driedcrushed leaves in 250 mL glass beaker along with 200 mL of distilled water. The mixture was then boiled for 20 min until the color of aqueous solution changed from watery to brown-yellow. Then, the mixture was cooled to room temperature and filtered with Whatman No. 1 filter paper. The presence of functional groups in the aqueous leaves extract sample was investigated by test tube method and characterized by FT IR technique.

Preparation and Characterization of Zinc Oxide Nanoparticles

For the synthesis of zinc oxide nanoparticles by (Method I) 50 mL of *C.gigantea* leaves extract was taken and heated to 60-80ºC using a magnetic stirrer heater. 5 g of zinc nitrate was added to the above solution and maintained the temperatures at about 80ºC. This mixture was continue heated until it reduced to a deep yellow colored paste and then collected in a ceramic crucible and a light yellow colored powder was obtained by calcination at

200ºC, 300ºC, 400ºC, 500ºC and 600ºC for 2 h in muffle furnace (Sabir *et al*., 2014).

Method II was also used for biosynthesis of zinc oxide nanoparticles. A 50 mL of *C.gigantea* leaves extract was heated to 60-80ºC using a magnetic stirrer heater. 5 g of zinc nitrate was added and this mixture is then stirred and heated to achieve good homogeneity. The mixture was heated without stirring to obtain gel and then heated to obtain finally the desired product ZnO in the form of ash powder. A pale yellow colored powder was calcined in muffle furnace at 500ºC for 2 h and finally white powder ZnO was obtained. The biosynthesized zinc oxide nanoparticles were characterized by TG-DTA and XRD techniques.

Study on Antimicrobial Activities of Zinc Oxide Nanoparticles

One mL each of the bacterial suspension of 24 h of nutrient agar was added in each of the petri-dishes. Immediately after hardening of the agar well were made with a 10 mm sterile cork borer from each seeded agar. After removing the agar disks, the wells were incubated at 37°C for 18-24 h. The diameters of the inhibition zone were measured and recorded in mm.The well plate diffusion method was used to test the antibacterial action of the zinc oxide nanoparticles on 24 h broth culture of the organisms used.

Determination of Storage Time of Fruits at Room Temperature by Coating withZnO Nanoparticles

Storage time of guava and tomato fruits at room temperature were investigated by coating the solution of biosynthesized ZnO nanoparticles (0.01 g in 100 mL distilled water) on surface of fruits by layer coating method. The test samples were marked as control for non-coating and S and S_1 for coating with nanoparticles synthesized by methods I and II, respectively. All samples were kept at normal room temperature for observation of results.

Results and Discussion

PhytochemicalsPresent in Aqueous Extracts of *C. gigantea*Leaves and Characterization

The aqueous extract of *C.gigantea* leaves was screened for the presence of various bioactive phytochemicals. The analysis revealed the presence of glycosides, alkaloids, polyphenols, flavonoids, tannins, saponins and α-amino acids in these aqueous leaves extract (Table 1). The functional groups present in aqueous extract of *C.gigantea* leaves were determined by FT IR techniqueas shown in Table 2 and Figure 1. The broaden peaks at 3342 cm^{-1} corresponds to the stretching vibration of OH group. The band at 2941 cm^{-1}corresponds to stretching vibrations of CH group. The bands at 1599 cm^{-1} can be attributed to C=C stretching vibrations of aromatic compounds. The spectrum showed bands at 1394 cm^{-1} corresponding to the sp^3 C–H bending of alkanes. The bands at 1192 and 1109cm^{-1} can be attributed to C-O stretching vibration. The spectrum showed bands at 655 and 617cm^{-1} corresponding to C-H bending for H-bond to sp^2 carbon (Coates, 2000). These are tabulated in Table 2.

Table 1 Phytochemicals Screening in Aqueous Leaves Extracts of *C. gigantea*

No.	Tests	Test Reagents	Observations	Remark
1	Glycosides	10% Lead acetate solution	White ppt.	+
2	Carbohydrates	10% α-naphthol, conc: H_2SO_4	Red ring not form	ND
3	Alkaloids	Mayer's reagent	Orange colour	+
4	Polyphenols	10%$FeCl_3$, 5%$[K_3Fe(CN)_6]$	Blue black colour	+
5	Flavonoids	Conc:HCl, Conc:H_2SO_4, Mg ribbon	Yellow colour	+
6	Tannins	Gelatin, 1%$FeCl_3$	White ppt.	+
7	Saponins	Distilled water	Frothing	+
8	Steroids	Acetic anhydride, Conc: H_2SO_4	No greenish blue colour	ND
9	α-Amino acids	Ninhydrin	Purple spot	+

10	Reducing sugars	Benedict's solution	No brick-red ppt.	ND

(+) present (ND) Not Detected

Table 2 FT IR Data of Leaves Extract of *C.gigantea*

No.	Wavenumber (cm^{-1})		Band Assignment
	Observed Values	Literature Values*	
1	3342	3650-3200	-OH stretching
2	2941	2960-2850	-CH stretching
3	1599	1650-1550	C=Cstretching
4	1394	1400-1393	C-H bending
5	1192, 1109	1250-1050	C-O stretching
6	655, 617	1000-600	C-H bending

*Coates, 2000

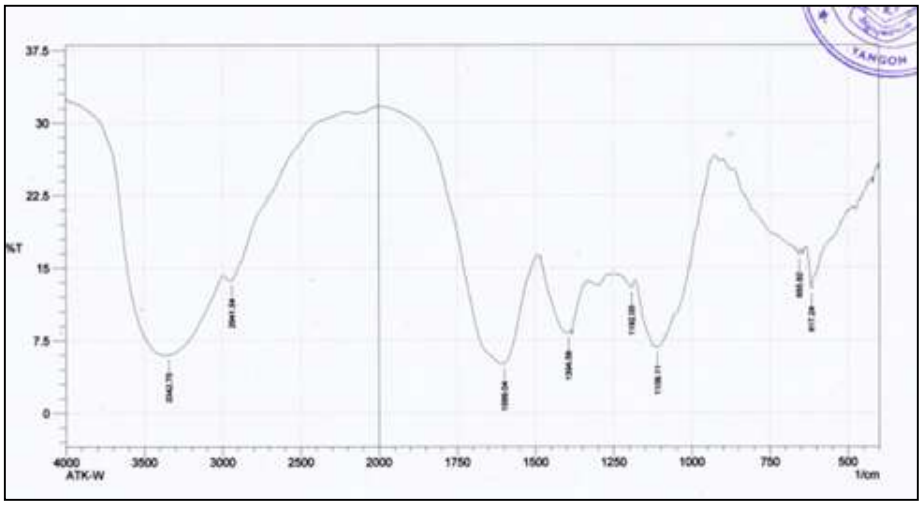

Figure1 FT IR spectrum of aqueous leaves extract of *C.gigantea*

Characterization of Biosynthesized Zinc Oxide Nanoparticles before

Calcination TG-DTA analysis

Thermal stability of biosynthesizedzinc oxide by method I was investigated by TG-DTA technique and the resultant TG-DTA thermogram is shown in Figure 2. TG-DTA data of the prepared zinc oxide nanoparticles before calcinations showed the total weight loss 52.98% in the temperature range of 38.59-601.76°C. This is attributed to the evaporation of trapped water in the crystal, decomposition of organic residue and zinc nitrate to zinc oxide in the preparation of biosynthesized zinc oxide. The TG-DTA thermogram indicated the two endothermic peaks at 139.56°C and 198.98°C corresponding to the loss of trapped water anddecomposition of organic matter in sample, respectively. The exothermic peak at 369.97°C was related with complete transition of zinc nitrate to crystalline zinc oxide nanoparticles.TG-DTA data indicated that the biosynthesized zinc oxide was found to be thermally stable in the temperature range of 460-500°C.

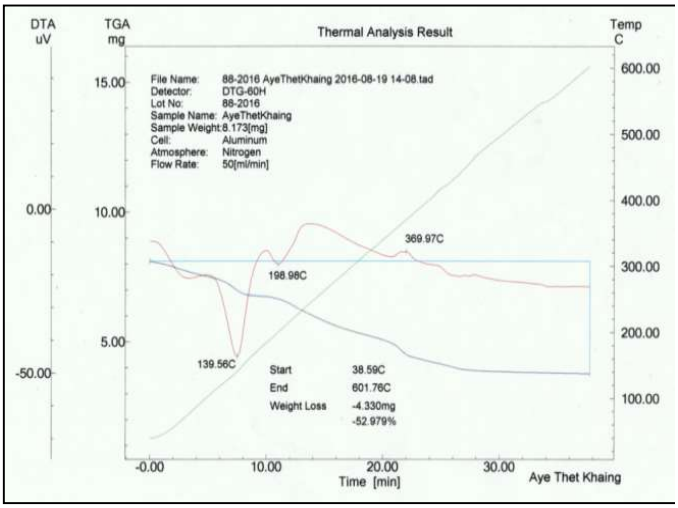

Figure 2 TG-DTA thermogram of biosynthesized ZnO nanoparticles by method I before calcination

XRD analysis

The structures of the zinc oxide nanoparticles biosynthesized by methods I and II before calcination were studied by XRD technique (Figures 3 and 4). In Figure 3, the XRD pattern of zinc oxide nanoparticles is matched with PDF file of 89-0138 of zinc hydroxide, $Zn(OH)_2$. It can be seen that some noise peaks, other peaks and broadness of the peak which indicated the amorphous nature and the presence of phytochemical and impurities in the prepared ZnO nanoparticles. Figure 4 shows the XRD pattern of zinc oxide nanoparticles biosynthesized by method II. It can be seen that in addition to characteristic peaks of ZnO, the presence of impurity peaks were observed because of the presence of phytochemicals and impurities in the prepared ZnO nanoparticles.

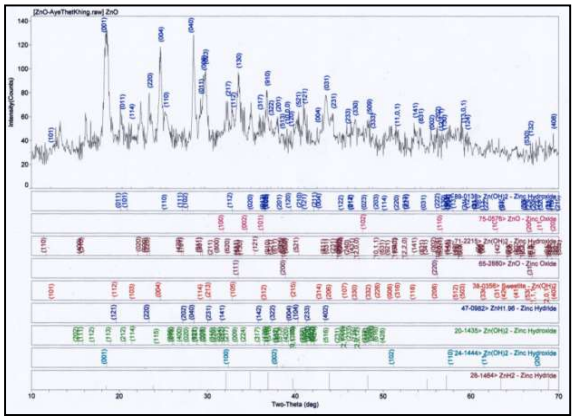

Figure 3 XRD diffractogram of biosynthesized ZnO particles by method I before calcination

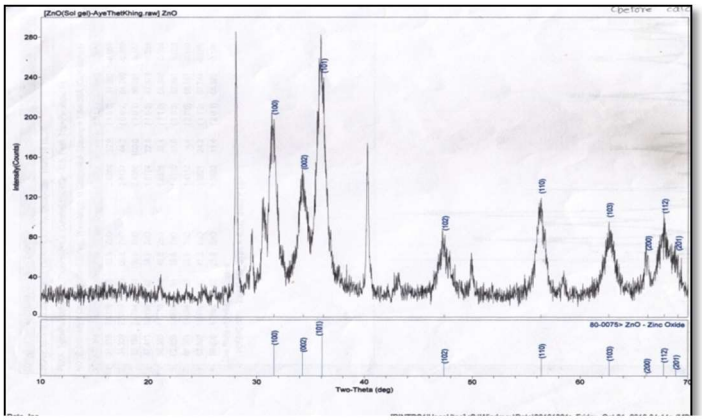

Figure 4 XRD diffractogram of biosynthesized ZnOparticles by method II before calcination

Characterization of Biosynthesized Zinc Oxide Nanoparticles after Calcination XRD analysis

The Powder XRD patterns of the ZnO samples calcined at different temperatures are shown in Figure 5. When the temperature was increased, decomposition began and hexagonal ZnO started to appear. The hexagonal ZnO crystal was initially detected at 300°C and broad diffraction peaks became nice and sharp at both 500 and 600°C. The average lattice constant of ZnO nanoparticles calcined at 500 °C and 600 °C were found to be a, b=3.2534Å, c=5.2118Å and a, b=3.2736Å, c=5.2255Å, respectively. The average lattice constants of ZnO nanoparticles calcined at 500 °C are close to literature value of a, b=3.2475 to 3.2501 Å, c=5.2042 to 5.2075 Å. This result is consistent with DTA data. In DTA curve, the phase transition temperature was found to be 369.97°C. Therefore, it can be seen that ZnO nanoparticles with well-developed crystal structures appeared at the calcination temperature between 400 and 500°C. From these studies, in order to get pure crystal of hexagonal ZnO, the calcination temperature of about 500°C was chosen.

The effect of calcination on crystalized structure of biosynthesized zinc oxide nanoparticles by method II was also studied at the calcination temperature of 500°C. crystalized structure of the zinc oxide nanoparticles biosynthesized by method II at 500°C were analysed by X-ray diffractometer (Figure 6). There are nine typical diffraction peaks, (100) at 31.557°, (002) at 34.227°, (101) at 36.051°, (102) at 47.344°, (110) at 56.365°,(103) at 62.662°, (200) at 66.272°,(112) at 67.680° and (201) at 68.933° which may be assigned to the characteristic peaks of hexagonal ZnO crystal and are matched with library card number89-1397 ZnO. High purity and crystallinity of ZnO nanoparticles was obtained at that temperature.

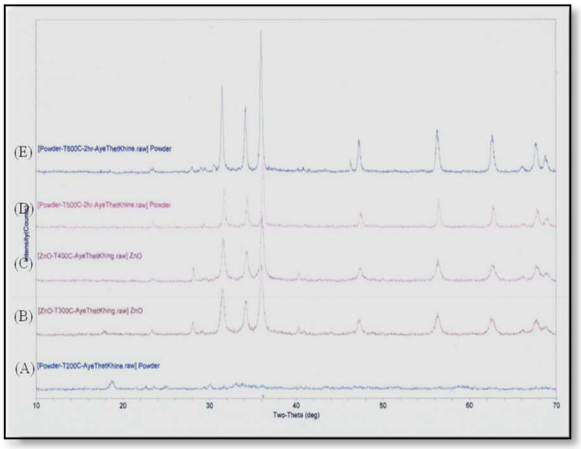

Figure 5 XRD diffractograms of biosynthesized ZnO nanoparticles by methodI calcined at (A) 200°C (B) at 300°C (C) at 400°C (D) at 500°C (E) at 600°C for 2 h

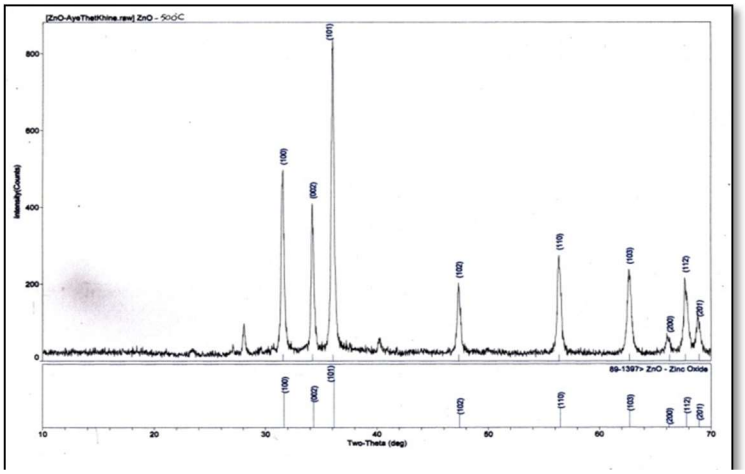

Figure 6 XRD diffractogram of biosynthesized ZnO nanoparticlesprepared by method II calcined at 500 °C for 2 h

Average Crystallite Sizes of Biosynthesized Zinc Oxide Nanoparticles

The average crystallite sizes of biosynthesized zinc oxide particles were calculated by using Debye-Scherrer equation, $t=0{\cdot}9\lambda/\beta\cos\theta$, where t is the crystallite size, λ the wavelength of the X-ray used, β is the full width at half maximum (FWHM) of the peak inradians and θ is the diffraction angle or the Bragg angle of the peak (Jenkins and Snyder, 1996). After calcined at 400°C, amorphous nature disappeared and crystalline nature of ZnO appeared but its crystal structure has some impurities peaks. When the calcination temperature was higher than 500°C, the XRD patterns showed the strong diffraction peaks of ZnO. Moreover, the characteristic peaks of ZnO became sharper and stronger when the calcination temperatures change from 300 °C to 400°C, 500°C and 600°C, indicating that ZnO are getting better nanocrystalline size. The data revealed that the crystallite size increased with the increase in the final calcination temperature. Their difference in crystallization and crystallite size could be mainly attributed to the relative calcination temperature. The average crystallite sizes of biosynthesized zinc oxide nanoparticles by method I at different calcination temperatures were calculated to be 24.82 nm at 300°C, 25.99 nm at 400°C, 31.26 nm at 500°C and 30.31 nm at 600°C. It was found that average crystallite size increased with increase in calcination temperature up to 500°C but decreased in calcination temperature of 600°C which may be due to agglomeration in the calcinations process. However, the average crystallite size of biosynthesized zinc oxide nanoparticles by method II after calcination at 500°C found to be 27.00 nm. Similarly, the lattice parameters of ZnO nanoparticles were much closed to literature value at calcination temperature of 500°C. The data are shown in Table 3. In order to obtain smaller ZnO particles with well-developed crystal structures, calcination

temperature of 500°C was chosen for the study of the application of ZnO nanoparticles.

Table 3 Average Crystallite Size and Lattice Parameters of Biosynthesized Zinc Oxide Nanoparticles at Different Calcination Temperatures

Method	Calcination temperature (°C)	Average crystallite size (nm)	Lattice Parameters(Å)	
			a=b	c
Method I	300	24.82	3.2709	5.2215
	400	25.99	3.2636	5.2116
	500	31.26	3.2534	5.2118
	600	30.31	3.2736	5.2255
Method II	500	27.00	3.2692	5.2200

Antimicrobial Activities of Zinc Oxide Nanoparticles

Antimicrobial activities of biosynthesized zinc oxide nanoparticles using aqueous leaves extract of *C. gigantean* prepared by methods I and II against bacteria like *Bacillus subtilis*, *Staphylococcus aureus*, *Pseudomonas aeruginosa*, *Bacillus pumilus*, *E. coli* and fungi like *Candida albicans* were quantitatively evaluated in culture media by using Agar well diffusion method. It was observed that the growth of inhibition zones of all bacteria and fungi were solely high in both biologically synthesized zinc oxide nanoparticles except *Pseudomonas aeruginosa*. High antimicrobial activities was observed against *Bacillus subtilis* (25 mm), *Staphylococcus aureus* (24 mm), *Bacillus*

pumilus (23 mm), *E. coli* (25 mm), *Candida albicans* (23 mm) and low activity was shown against *Pseudomonas aeruginosa* (16 mm) by using zinc oxide nanoparticles biosynthesized by method I. Similarly, high antimicrobial activity was observed against *Bacillus subtilis* (26 mm), *Staphylococcus aureus* (24 mm), *Bacillus pumilus* (25 mm), *E.coli* (24 mm), *Candida albicans* (26 mm) and low activity was shown against *Pseudomonas aeruginosa* (14 mm) by using zinc oxide nanoparticles biosynthesized by method II. The results are shown in Table 4 and Figure 7. Antimicrobial effects of zinc oxide nanoparticles obeyed a dual action mechanism of antimicrobial activity i.e, the bacterial and fungicidal effect of zinc ions membrane disrupting effect of the polymer subunits. The microbial activity of particles depends on the stability in the cultured medium too. The result confirmed that the treated microbial cells were damaged showing leakage of proteins and nucleic acid into nutrient agar media. These particles which can be prepared in a simple, rapid and cost effective manner are suitable for the formulation of new types of microbial materials.

Basically the detected active oxygen species generated by these metal oxide particles could be the main mechanism of their antibacterial activity. The antibacterial mechanism of ZnONPs involves the direct interaction between ZnO nanoparticles and cell surfaces affecting cell membrane permeability; afterwards these nanoparticles enter and induce oxidative stress in bacterial cells, which results in thein hibition of cell growth and eventually cell death; the demonstrated antibacterial activity of ZnONP recommends its possible application in the food preservation field. It can be applied as a potent sanitizing agent for disinfecting and sterilizing food industry equipment and containers against the attack and contamination with foodborne pathogenic bacteria. The NPs of ZnO showed both toxicity on pathogenic bacteria and beneficial effects on microbes, which has bioremediation potential and is a strong root colonizer (Molina *et al*., 2006).

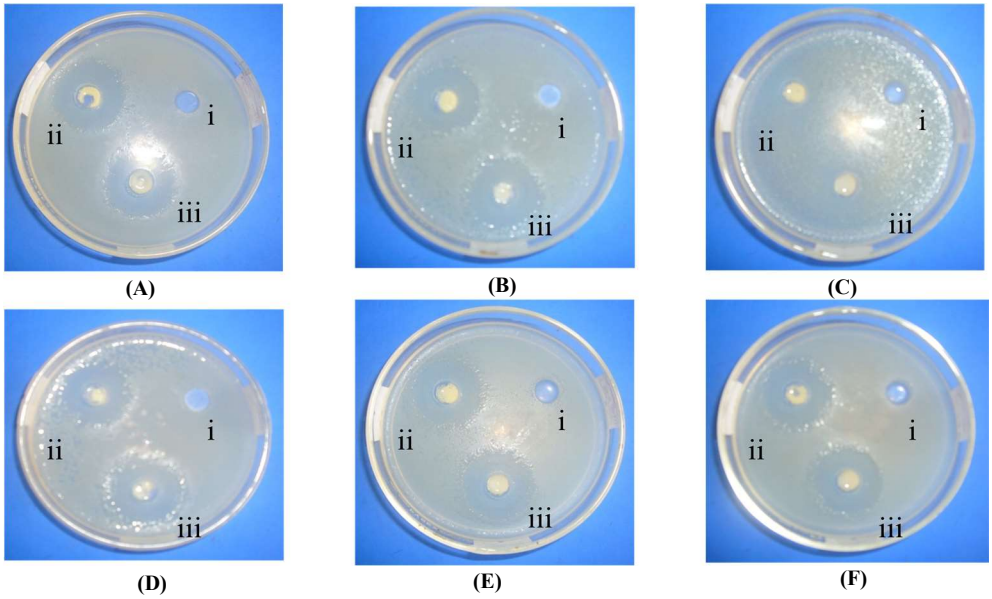

Figure7 Antimicrobial activitivies of biosynthesized zinc oxide nanoparticles on six microorganisms (A) *Bacillus subtilis* (B) *Staphylococcus aureus* (C) *Pseudomonas aeruginosa* (D) *Bacillus pumilus* (E) *Candida albicans* (F) *E. coli*
(i) Control, (ii) ZnO NPs (method I), (iii) ZnO NPs (method II)

Table 4 Antimicrobial Activity of Biosynthesized Zinc Oxide Nanoparticles on Different Species of Microorganism (Agar Well Diffusion Method)

Microorganisms	**Diameter of inhibition zone (mm)**	
	Method I	**Method II**
Bacillus subtilis	25(+++)	26(+++)
Staphylococcus aureus	24(+++)	24(+++)

Pseudomonas aeruginosa	16(++)	14(+)
Bacillus pumilus	23(+++)	25(+++)
Candida albicans	23(+++)	24(+++)

Agar well - 10 mm, 10 mm ~ 14 mm (+), 15 mm ~ 19 mm (++), 20 mm above (+++)

Coating of Biosynthesized Zinc Oxide Nanoparticles on Fruits

Storage time of guava and tomato fruits at room temperature were investigated by coating ZnO nanoparticles on surface of fruits by layer coating method. The test samples were marked as control for non-coating and S and S_1 for coating with zinc oxide nanoparticles biosynthesized by methods I and II as shown in Figure 8. All samples were kept at normal room temperature for observation of results. Although the control sample keeping after tomato for 15 days and guava for 20 days at room temperature start to rot, the tested samples without any molt were found to be fresher than the controlled until one monthstorage. It can be deduced that coating the fruits with biosynthesized ZnO nanoparticles have highly resistant to oxidation (Jeong *et al.,* 2005).

Storage time of guava and tomato fruits at room temperature were investigated by coating ZnO nanoparticles on surface of fruits by layer coating method. The test samples were marked as control for non-coating and S and S_1 for coating with zinc oxide nanoparticles biosynthesized by methods I and II as shown in Figure 8. All samples were kept at normal room temperature for observation of results. Although the control sample keeping after tomato for 15 days and guava for 20 days at room temperature start to rot, the tested samples without any molt were found to be fresher than the controlled until one monthstorage. It can be deduced that coating the fruits with biosynthesized ZnO nanoparticles have highly resistant to oxidation (Jeong *et al.,* 2005).

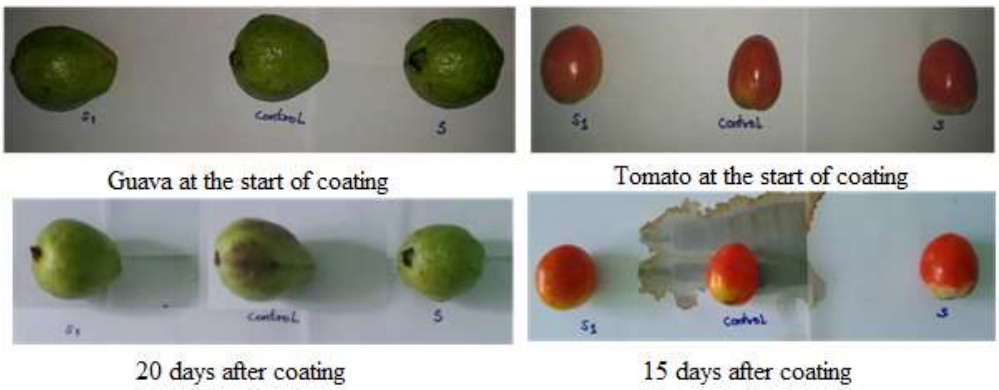

Figure 8 Coating of biosynthesized ZnO nanoparticles on guava and tomato S and S_1 = fruits coating of ZnO NPs biosynthesized by methodsI and II respectively

Conclusion

ZnO nanoparticles were successfully biosynthesized from zinc nitrate by methods I and II. Aqueous leaves extract of *C. gigantean* (Ma-yo-gyi) was used as reducing and stabilizing agents. Phytochemical screening of aqueous leaves extracts of *C.gigantea* (Ma-yo-gyi) indicated the presence of phytochemicals such as α-amino acids, glycoides, polyphenols, saponins, alkaloids and flavonoids. FT IR confirms the presence of above phytochemicals in aqueous leaves extracts of *C.gigantea* which can stabilized the nanoparticles. From TG-DTA data, decomposition of $Zn(NO)_3$ to ZnO start at 369.9ºC andcomplete formation of ZnO was temperature between 400-500ºC. XRD data confirm complete formation of pure ZnO at 500ºC with hexagonal phase and consistent with literature value of lattice parameters. From study on antimicrobial activities of biosynthesized ZnO nanoparticles, high antimicrobial activities of ZnO nanoparticles on six microorganisms proved to a pronounced influence on inhibiting the growth of both gram positive, gram negative bacteria strain except *P. aeruginosa* and also high activity on fungus like *Candida albicans.* Thus, it is concluded that the reported biosynthesized ZnO nanoparticles can act as an effective antimicrobial agent. Coating of the guava and tomato fruits with biosynthesized zinc oxide nanoparticles (Methods I and II) by layer coating method at room temperature had benefits for the ability to retard fruit pathogens and highly resistant to oxidation, increase the storage time of guava

and tomato at room temperature. From these results, the biosynthesis of zinc oxide nanoparticles by methods I and II are much safer and environment friendly compared to chemical synthesis because it does not lead to formation of toxic by-product chemicals.

Acknowledgements

The authors wish to express gratitude to Dr Tun Cho, Professor and Head, Department of Chemistry, Pyay University, for his kind encouragement and Myanmar Academy of Arts and Science Association for submission of this research paper.

References

Alagumuthu, G. and Kirubha,R. (2012). "Green Synthesis of Silver Nanoparticles using Cissus Quadrangularis Plant Extract and Their Antibacterial Activity". *International Journal of Nanomaterials and Biostructures*, vol. 2(3), pp. 30-33

Chandrabhan, S., Sumint, S. T. and Santosh, K. V. (2011). "Antibacterial Efficacy and Phytochemical Analysis of Organic Solvent Extracts of *Calotropis gigantea*" . *J. Chem. Pharm. Res*., vol. 3(6), pp. 330-336

Coates, J. (2000). *Interpretation of Infrared Spectra, A Practical Approach*, *Encyclopedia of Analytical Chemistry*.Chichester: John Wiley & Sons Ltd., pp. 10815-10837

Jenkins, R. and Snyder, R. (1996). *Introduction to X-ray Powder Diffractometry*. New York: John Wiley & Sons, Inc.

Jeong, S.H, Yeo,S.Y. and Yi, S.C. (2005). "The Effect of Filler Particles Size on The Antibacterial Properties of Compounded Polymer/ Silver Fibers". *J. Mat. Sci,*vol.,40,pp. 5407-5411

Molina, M. A., Ramos, J. L. and Espinosa-Urgel, M. (2006). "A Two-partner Secretion System is Involved in Seed and Root Colonization and Iron Uptake By *Pseudomonas Putida* KT 2440"..*Environmental Microbiology*, vol. 8, pp. 639-647

Sabir, S., Arshad, M. and Chaudhari, S. K. (2014). "Zinc Oxide Nanoparticles for Revolutionizing Agriculture: Synthesis and Applications", *The Sci. World J.* vol. 2014, pp.1-8

Shah, M., Fawcett, D., Sharma, S., Tripathy, S. K., and Poinern,G. E. J. (2015). "Green Synthesis of Metallic Nanoparticles via Biological Entities", *Materials*, vol. 8, pp.7278-7308

Sridhara, V., Pratima, K., Krishnamurthy,G. and Sreekanth,B. (2013). "Vegetable Assisted Synthesis of Silver Nanoparticles and Its AntibacterialActivity Against Two Human Pathogens". *Asian Journal of Pharmaceutical and Clinical Research,*vol. 6, (2), pp. 53-57

MOLECULAR FORMULA DETERMINATION AND STRUCTURE ELUCIDATION OF BIOACTIVE PORPHYRIN DERIVATIVE COMPOUND ISOLATED FROM THE WHOLE PLANT OF *Corallodiscus lanuginosus* (WALL. ex R.Br.) BURTT

Thinn Myat Nwe[1], Myoe Myoe[2]

Abstract

In this research paper, *Corallodiscus lanuginosus* (Wall. ex R.Br.) Burtt which is one of the Myanmar indigenous medicinal plants known as Pan ma o` was selected for chemical analysis. The preliminary phytochemical screening of the whole plant of Pan ma o` was carried out, which indicated the presence of alkaloid, steroid, terpenoid, glycoside, lipophilic, polyphenol, saponin, phenolic and tannin, respectively. Antimicrobial activities of the crude extract of the whole plant of Pan ma o` were tested in various solvents system by using agar well diffusion method on six selected organisms. The ethyl acetate crude extract of Pan ma o` gives rise to high activities on all selected organisms such as *Bacillus subtilis, Staphylococcus aureus, Pseudomonas aeruginosa, Bacillus pumilus, Candida albicans and E.coli.* Moreover, porphyrin derivative compound was isolated from the whole plant of Pan ma o` as indigo crystal (19.6 mg) by thin layer and column chromatography separation methods. The yield percent was found to be (0.529%) based upon the EtOAc crude extract. Moreover, antimicrobial activities of this compound were rechecked by using agar well diffusion method. The ethyl acetate extract of this compound responds high activities on all selected organisms except *Staphylococcus aureus*. In addition, the molecular formula of this compound could be determined as $C_{30}H_{35}N_9O_4$ (Hydrogen Deficiency Index = 18), applying some spectroscopic methods such as FT IR, ^{1}H NMR (500 MHz), ^{13}C NMR (125 MHz), DEPT and FAB-mass spectral data respectively. The complete structure of this porphyrin derivative compound could be elucidated by

[1] Associate Professor,Dr, Department of Chemistry, Mandalay University of Distance Education.

[2] Lecturer, Department of Chemistry, Taunggyi University.

DQF-COSY, HMQC, HMBC and DEPT spectroscopic methods. The elucidated compound could be described as below.

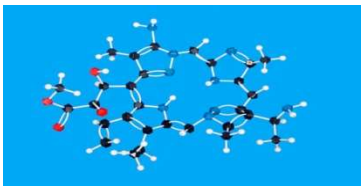

Methyl-3-((1E, 4Z, 6Z, 10Z, 14E, 16E) -18- amino-7- (1-aminoethyl) -12-ethyl-3, 8, 17-trimethyl-13-vinyl-2, 9, 19-triazaporphyrin-15-yl) -3-hydroxy-2-oxopropano-ate

Keywords: Pan ma o`, *Corallodiscus lanuginosus,* porphyrin derivative compound, antimicrobial activities

Introduction

Traditional medicine has existed in Myanmar long long ago (WHO). At present day the image of traditional medicine differs from that of olden day image. Traditional medicine is always taking vital role in the most essential part of humanity for their survival and longevity. Over the years, traditional medicine has been instrumental in maintaining physical and mental strength of people of Myanmar.

Plants have been used in treating human diseases for thousands of years and nowadays many currently used medicines are derived from natural sources. For thousands of years medicine and natural products have been closely linked through the use of traditional medicines and natural poisons (Grabley and Thiericke, 2000). In most areas of the world, herbals medicine has remained the mainstay of the therapy because of the cause and availability and perhaps cultural preference.

Herbal medicine is a major remedy in traditional medicine system, which is largely based on the use of roots, leaves, barks, seeds and flowers of the plants. They are free from side effects, adverse effects and they are economical, easily available and beneficial for the mankind over a century (Genapathy *et al*., 2013). Medicinal plants are rich source of bioactive compounds and thus serve as important raw materials for drug production. Nowadays the potent formulation of traditional medicines are extensively used to complete with that of the western medicines in fight against various dreadful

diseases such as heart diseases, AIDS, tuberculosis, cancer, liver diseases and malaria. In this research work, a porphyrin derivative compound was isolated from the whole plant of *Corallodiscus lanuginosus* (Wall. ex R.Br.) Burtt, locally known as Pan- ma- o` ( Figure 1), which is one of the indigenous medicinal plant. It was chemically analyzed for new source of compound in this field (Harborne, J.B, 1984). The plant of Pan ma o` is widely distributed in Lwe Tan Mountain, Paung Lin, Pa Lè Tint village, Hopone Township, Taunggyi Region. It is medicinally used as liver diseases, disorders of kidney, to cure poisoning, diarrhoea caused by hot diseases.

Botanical Description

Family name	: Gesneriaceae
Botanical name	: *Corallodiscus lanuginosus* (Wall. ex R.Br.) Burtt
Local name	: Pan ma o`
Common name	: Blue stone flower
Part used	: The whole plant
Medicinal uses	: To cure poisoning, diarrhoea caused by hot diseases, liver diseases, kidney problems and wounds

Figure 1 The plant of *Corallodisus lanuginosus* (Wall. ex R.Br.) Burtt

Materials and Methods

The sophisticated instruments used in the isolation and structure elucidation of pure compound were UV-lamp (Lambda-40, Perkin-Elmer Co., England), FT IR spectrophotometer (Shimadzu, Japan), ^{1}H NMR spectrometer (500 MHz),^{13}C NMR spectrometer (125 MHz), FAB-mass spectrometer, electric balance (Shimadzu, Japan) and melting point apparatus.

Materials

Commercial grade solvents were used after distillation. Analytical preparative thin layer chromatography was performed by using percolated silica gel (Merk Co. Inc, Kiesel gel 60 F_{254}). Silica gel Merk Co.Inc, Kiesel gel 70-230 Mesh ASTM) was used for column chromatography. Iodine vapor and UV detector were used for visualizing the compound on TLC plates.

Preliminary Phytochemical Screening

Phytochemical analysis for alkaloids, flavonoids, steroids, terpenoid, glycosides, reducing sugars, lipophilic, polyphenols, saponins , phenolic compounds and tannin were carried out according to reported methods (Harborne, 1993; Yadav and Munin, 2011).

Extraction and Isolation of Porphyrin Derivative Compound

Air dried sample (625 g) was percolated with ethanol (4.3 L) for about two months. Percolated solution was filtered and concentrated to yield residue. It was extracted with ethyl acetate (150 mL) and evaporated. The ethyl acetate crude sample (3.7 g) was obtained. It was fractionated by column chromatography over silica gel (70-230 mesh) eluted by various solvent ratio of n-hexane and ethyl acetate from non- polar to polar. Totally (333) fractions were obtained. These fractions were combined according to same R_f values under UV lamp and iodine detector. Ten combined fractions were obtained. The combined fraction (VIII) was checked by TLC for purity amount. It gave one spot on TLC in (R_f = 0.37) with n-hexane : EtOAc (7 : 3 v/v) and UV

active. The pure compound indigo crystal (19.6 mg) was obtained. The yield percent was found to be (0.529%) based upon the EtOAc crude extract.

Investigation of Antimicrobial Activities of the Crude Extract of the Whole plant of *Corallodisus lanuginosus* and Isolated Porphyrin Derivative Compound

Antimicrobial activities of the crude extract of the whole plant of *C. lanuginosus* (Pan ma o`) and isolated porphyrin derivative compound were tested in various solvents system by using agar well diffusion method on six selected organisms, such as *Bacillus subtilis, Staphylococcus aureus, Pseudomonas aeruginosa, Bacillus pumilus, Candida albicans and E.coli* at Pharmaceutical Research Department (PRD) in Insein, Yangon.

Structure Elucidation of the Isolated Compound

The molecular formula determination of isolated compound was done by spectroscopic methods such as ^{1}H NMR, ^{13}C NMR, DQF-COSY, HMQC, DEPT, FAB-mass and HMBC respectively (Breitmaier, 2002; Crews *et al*., 1998; Hesse *et al*., 1997; Nakanishi, 1962; Silverstein *et al*., 2005).

Results and Discussion

Preliminary Phytochemical Screening of the Whole Plant of *C. lanuginosus* (Wall. ex R.Br.) Burtt

Phytochemical screening was carried out by general methods to indicate the presence of general classes of phytochemical constituents. Table 1 shows the results of the phytochemical tests.

Table 1 Result of Preliminary Phytochemical Tests

No.	Constituents	Reagents used	Observation	Results
1	Alkaloid	Wagner's reagent Dragendorff's reagent	Reddish brown Orange ppt	+
2	Flavonoid	Mg coil, Conc:HCl	No pink color solution	-
3	Steroid	Pet ether, Conc:H_2SO_4, acetic anhydride	Green color solution	+
4	Terpenoid	Ethanol, $(CH_3CO)_2O$, Conc: H_2SO_4,$CHCl_3$	Red color solution	+
5	Glycoside	10% Lead acetate	White ppt	+
6	Sugar	Benedict's solution	No orange ppt	-
7	Lipophilic	0.5 M KOH, NaOH, distilled water	Deep color solution	+
8	Polyphenol	1% $FeCl_3$, $K_3Fe(CN)_6$	Deep green blue solution	+
9	Saponin	distilled water	Frothing	+
10	Phenolic	10% $FeCl_3$	Green blue solution	+
11	Tannin	10% $FeCl_3$, dil H_2SO_4	Yellowish brown	+

(+) = Present (-) = Absent

According to this Table 1, the sample consists of alkaloid, steroid, terpenoid, glycoside, lipophilic, polyphenol, saponin, phenolic and tannin, respectively.

Antimicrobial Activity of the Whole plant of *C. lanuginosus* (Wall. ex R.Br.) Burtt

The results of the antimicrobial activities of the crude extract of the whole plant of *C. lanuginosus* are shown in Figure 2 and Table 2. According to this table, ethyl acetate crude extract of *C. lanuginosus* showed high activities on all selected organisms such as *Bacillus subtilis, Staphylococcus aureus, Pseudomonas aeruginosa, Bacillus pumilus, Candida albicans and E.coli.* Moreover, ethanol extract responded high activity on *Bacillus pumilus*.

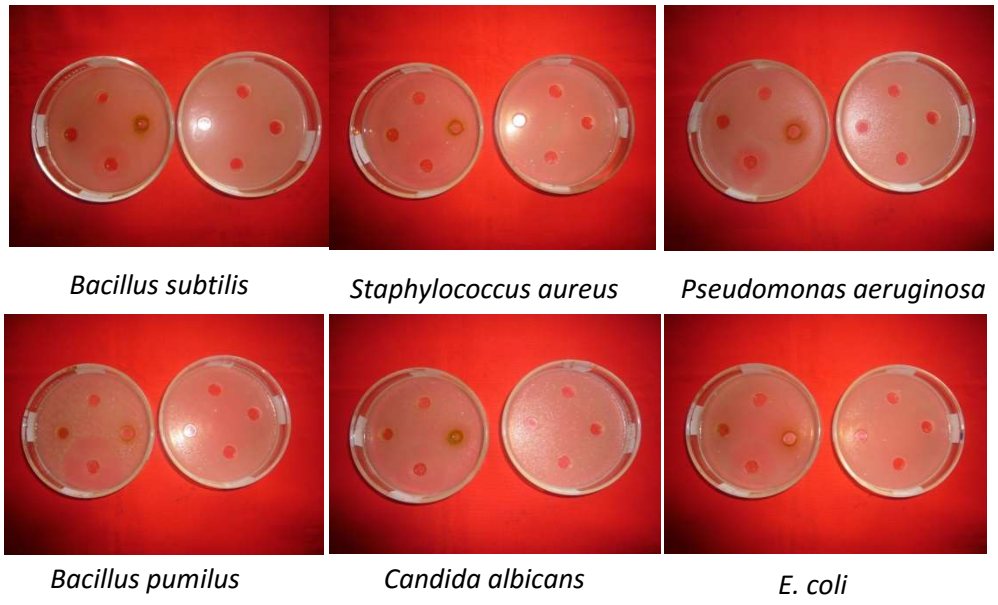

Figure 2 Antimicrobial activities of the whole plant of *C. lanuginosus* (Wall. ex R.Br.) Burtt

Table 2 Results of Antimicrobial Activities of the whole plant of *C. lanuginosus* (Wall. ex R.Br.) Burtt

No	Solvent	Inhibition Zone Diameter (mm)					
		I	II	III	IV	V	VI
1	n-hexane	-	-	-	-	-	-
2	$CHCl_3$	13 (+)	12 (+)	12 (+)	15 (++)	12 (+)	-
3`	EtOAc	22 (+++)	34 (+++)	29 (+++)	40 (+++)	32 (+++)	34 (+++)
4	EtOH	16 (++)	13 (+)	15 (++)	20 (+++)	15 (++)	18 (++)

agar well ~ 10mm
10 mm ~ 14 mm (+)
15 mm ~ 19 mm (++)
20 mm above (+++)

Organisms
I. *Bacillus subtilis*
II *Staphylococcus aureus*
III *Pseudomonas aeruginosa*
IV *Bacillus pumilus*
V *Candida albicans*
VI *E. coli*

Antimicrobial Activities of the Porphyrin Derivative Compound

Antimicrobial activities of isolated compound were rechecked by using agar well diffusion method on six selected organisms. The results are described in Figure 3 and Table 3.

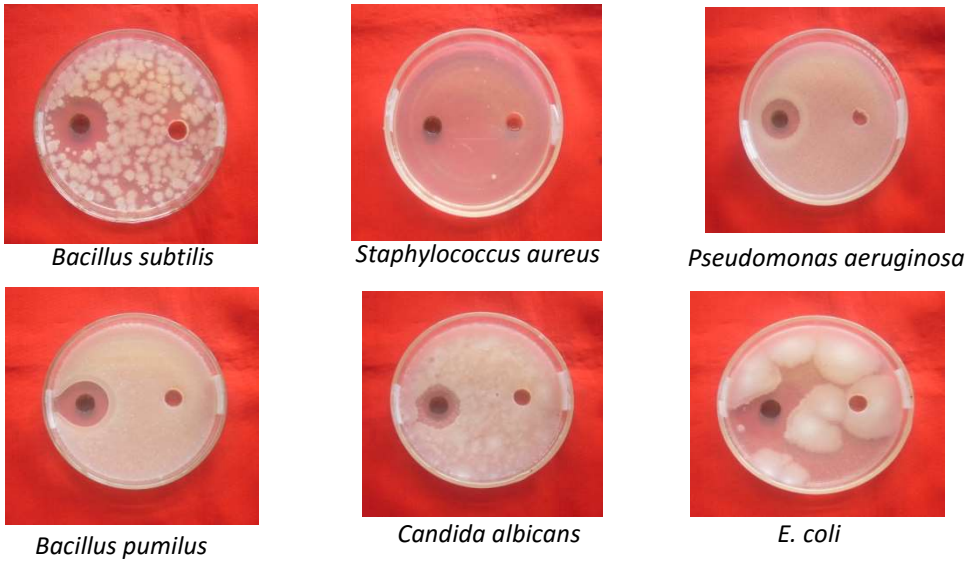

Figure 3 Antimicrobial activities of porphyrin derivative compound

Table 3 Results of Antimicrobial Activities of Porphyrin Derivative Compound

Sample	Solvent	Inhibition Zone Diameter (mm)					
		I	II	III	IV	V	VI
Pure compound	EtOAc	+++	–	+++	+++	+++	+++
Control	EtOAc	–	–	–	–	–	–

agar well ~ 10mm		Organisms	
10 mm ~ 14 mm	(+)	I.	*Bacillus subtilis*
15 mm ~ 19 mm	(++)	II	*Staphylococcus aureus*
20 mm above	(+++)	III	*Pseudomonas aeruginosa*
		IV	*Bacillus pumilus*
		V	*Candida albicans*
		VI	*E. coli*

According to this table, the ethyl acetate extract of isolated compound gives rise to high activities on all selected organisms except *Staphylococcus aureus*.

Molecular Formula Determination of Isolated Compound

The molecular formula of isolated compound could be determined by spectral data of some spectroscopic methods, such as FT IR (Figure 4), ^{1}H NMR (500 MHz)(Figure 5), ^{13}C NMR(125 MHz) (Figure 6), HMQC (Figure 7), DEPT(Figure 8) and FAB-mass (Figure 9).

According to ^{1}H NMR and ^{13}C NMR spectral data, the partial molecular formula could be assigned as $C_{30}H_{28}$. In ^{13}C NMR spectrum, down field chemical shift of sp^2 quaternary carbons (δ 169.57 ppm, and δ 189.89 ppm) should be 2 carbonyl carbons. Therefore, the partial molecular formula is $C_{30}H_{28}O_2$. According to the FT IR spectrum, this compound should consist of at least one –OH and one $–NH_2$ groups due to the presence of the bands at 3392.99 cm^{-1} and 3291.05 cm^{-1}. On the other hand, 1735.99 cm^{-1} and 1219.05 cm^{-1} indicate the presence of one ester group. Therefore, the partial

molecular formula and partial molecular mass are $C_{30}H_{31}NO_4$ and 469 respectively.

Moreover, in FAB mass spectrum, the $[M^+ + Na]$ ion peak shows at m/z 608. Therefore, the molecular ion peak of isolated compound is m/z 585 which indicates the molecular mass of this compound. According to the nitrogen rule, the odd number of molecular mass indicates the containing of odd number of nitrogen atoms. Hence, the partial molecular formula becomes $C_{30}H_{31}N_3O_4$. And so, the partial molecular mass is 497. Therefore, the remaining partial molecular mass is 585 - 497 = 88. The remaining partial molecular mass (88) may be one $–NH_2$ group, 2 –NH groups and 3 nitrogen atoms. Consequently, the real molecular formula of this compound could be assigned as $C_{30}H_{35}N_9O_4$. The hydrogen deficiency index of isolated compound is 18.

Structure Elucidation of Isolated Compound

According to the DEPT, HMQC and DQF-COSY (Figure 10) spectral data, the exomethylene fragment could be assigned.

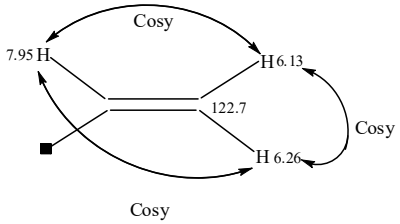

This monosubstituted alkenic fragment could be confirmed by their splitting patterns and coupling constant (J values) of these protons in ^{1}HNMR spectrum. In which the sp^2 methine proton (δ 7.95 ppm, dd, J=11.4Hz and 17.9Hz) one of the sp^2 exomethylene protons (δ 6.13 ppm, dd, J=1.2Hz and 11.4Hz) and one of the sp^2 exomethylene protons (δ 6.26 ppm, dd, J=1.2Hz and 17.9Hz) are shown below.

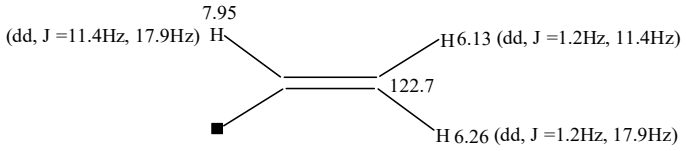

In addition, the observation of α, β and γ ^{1}H-C long range signal in HMBC spectrum (Figure 11) produces the following fragments **a**, **b** and **c**.

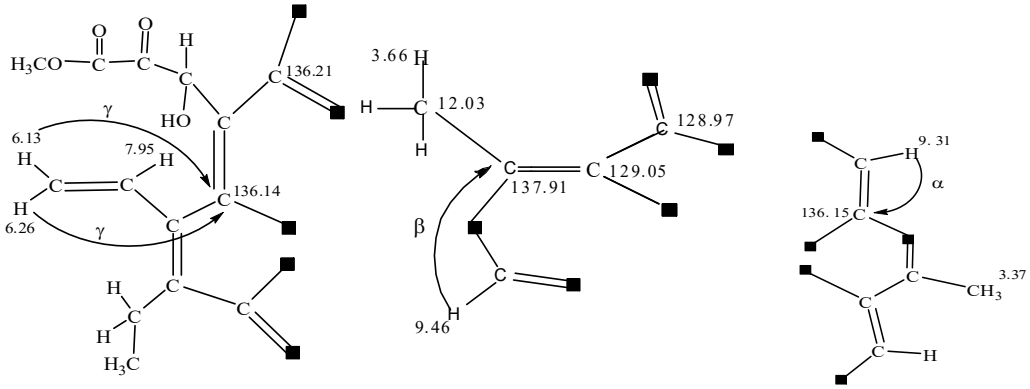

fragment **a** fragment **b** fragment **c**

These fragments could be connected due to the existence of ^{1}H-C long range signal in HMBC spectrum. It gives rise to the following fragment **d.**

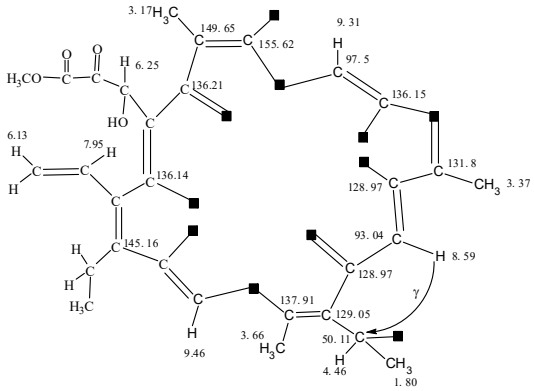

fragment **d**

According to the FT IR spectrum, this compound should consist of at least one $–NH_2$ group due to the presence of the absorption band at 3291.05 cm^{-1}. Hence, this $–NH_2$ group must be connected to the down field chemical shift of sp^2 quaternary carbon (δ 155.62 ppm) due to the logical connection. Therefore, the following extended fragment could be observed.

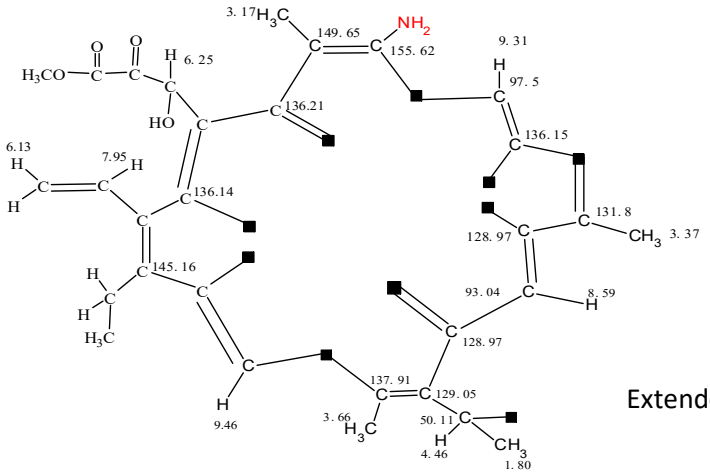

Extended fragment

Furthermore, the existence of α ^{1}H – C long range signal between more high field chemical shift two –NH protons (δ – 1.65 ppm) and two sp^2 quaternary carbons (δ 136.14 ppm, δ 136.15 ppm) in HMBC spectrum, informs the following fragment **e**.

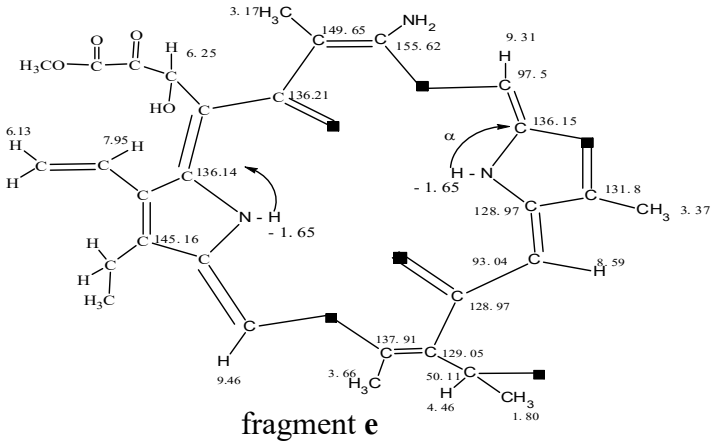

fragment **e**

Consequently, the partial molecular formula of fragment **e** could be assigned as $C_{30}H_{33}N_3O_4$. The real molecular formula is $C_{30}H_{35}N_9O_4$. Therefore, the remaining partial molecular formula is H_2N_6. It should be one $–NH_2$ group and five N atoms.

The five trivalent nitrogen atoms are logically connected to the three sets of down field chemical shift of sp^2 quaternary carbons (δ 104.37 ppm, δ 137.91 ppm, δ 128.97 ppm), (δ 131.8 ppm, δ 136.15 ppm) and (δ 136.21 ppm, δ 155.62 ppm, δ 97.5 ppm). Therefore, the following fragment **f** is displayed.

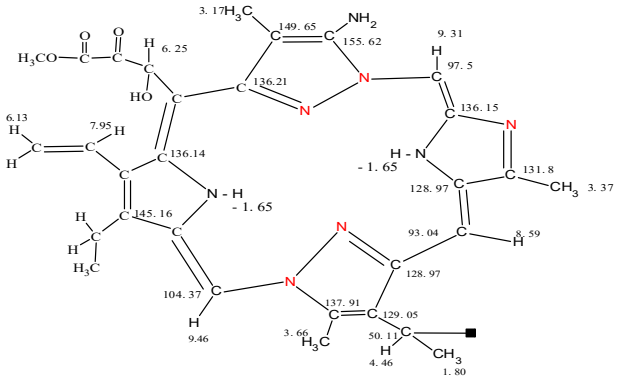

fragment **f**

Finally, the complete structure of porphyrin derivative compound could be assigned by the connection of the remaining $–NH_2$ group to the sp^3 methine carbon (δ 50.11 ppm).

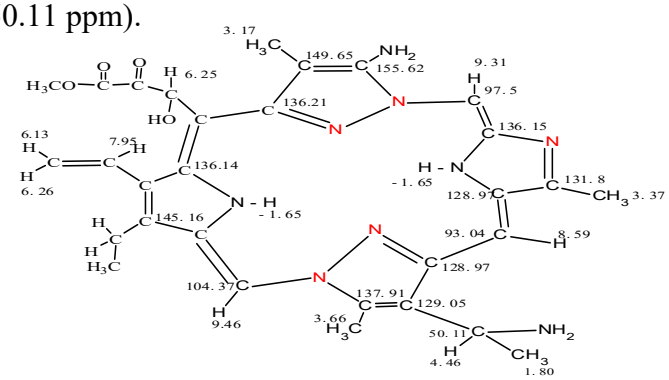

The planar structure of elucidated porphyrin derivative compound could be described as follows.

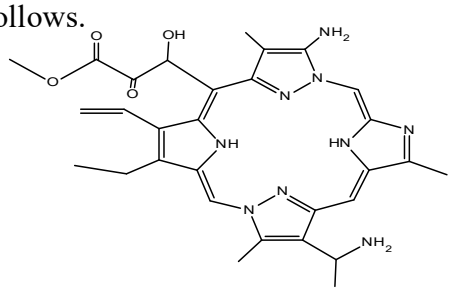

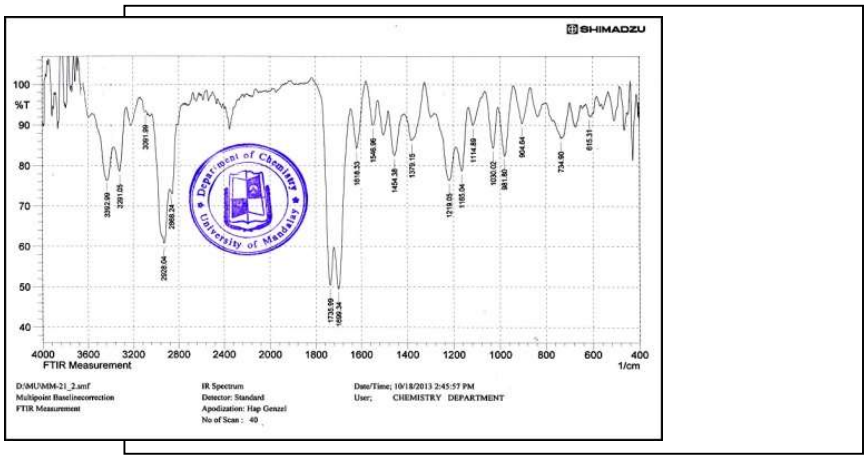

Figure 4 FT IR spectrum of isolated compound

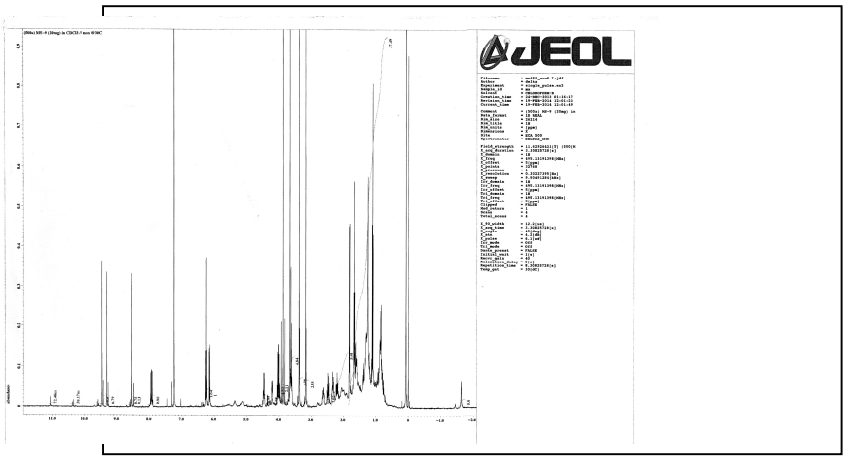

Figure 5 ^{1}H NMR spectrum of isolated compound

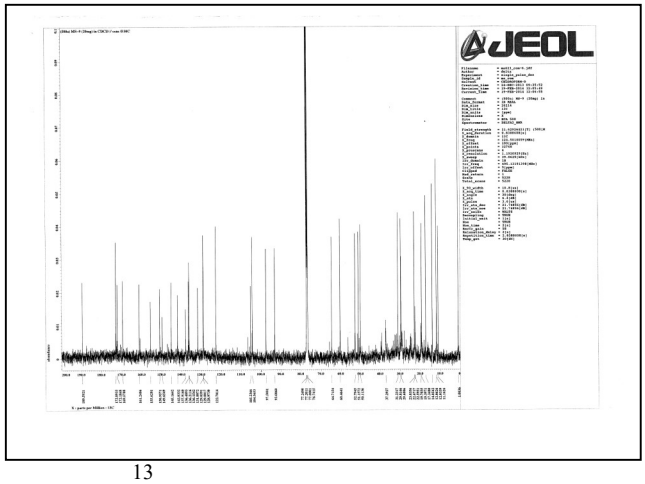

Figure 6 ^{13}C NMR spectrum of isolated compound

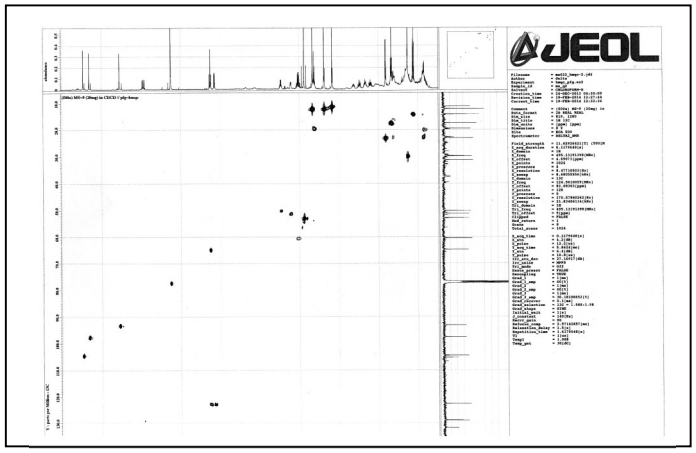

Figure 7 HMQC spectrum of isolated compound

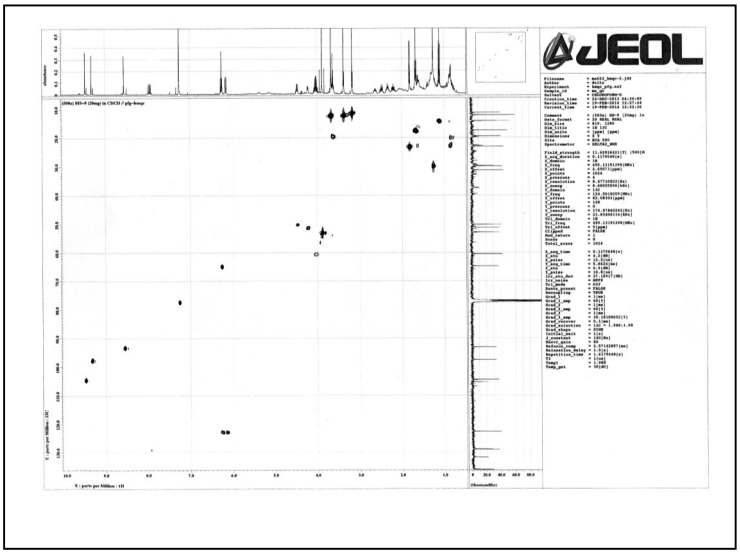

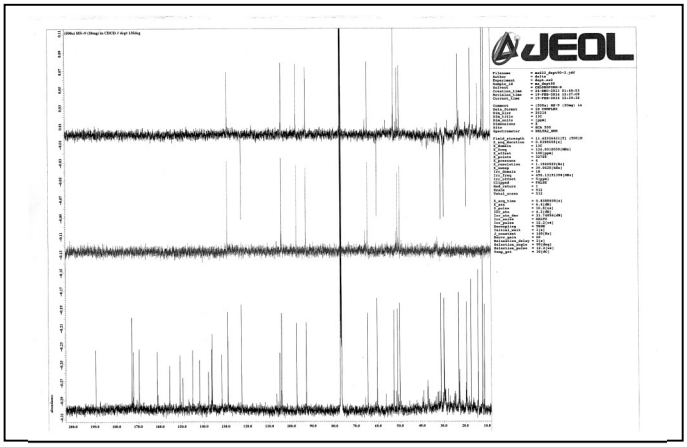

Figure 8 DEPT spectrum of isolated compound

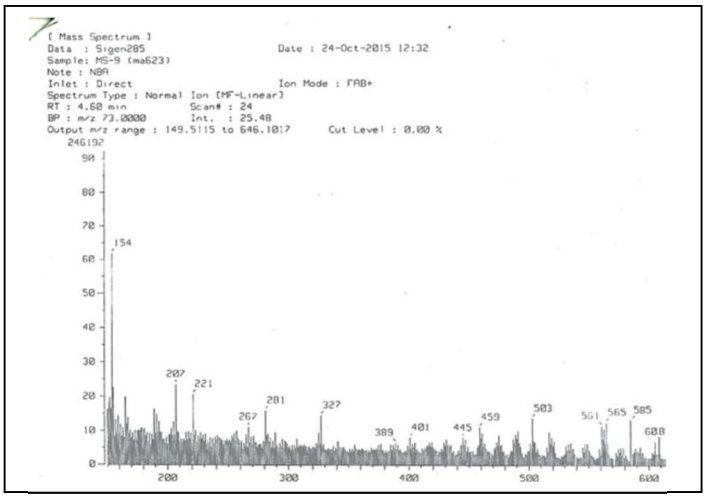

Figure 9 FAB –mass spectrum of isolated compound

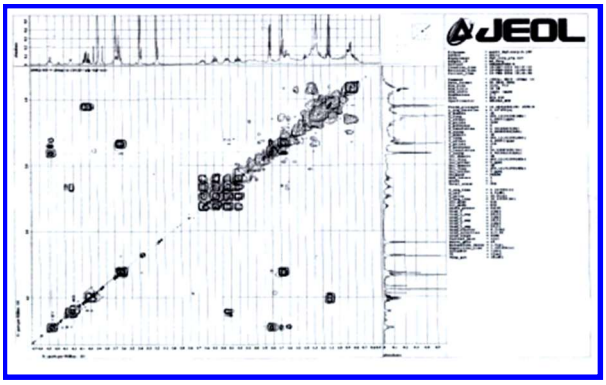

Figure 10 DQF-COSY spectrum of isolated compound

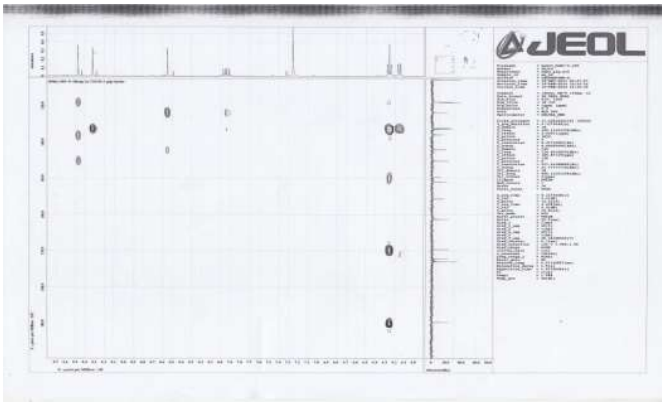

Figure 11 HMBC spectrum of isolated

Conclusion

In this research work, one of Myanmar indigenous medicinal plants, *C. lanuginosus*, locally known as Pan ma o` was selected for preliminary phytochemical screening, antimicrobial activities and isolation of organic compound were carried out. The research systematically focused on the complete structure elucidation of porphyrin derivative compound.

The preliminary phytochemical screening of the whole plant of *C. lanuginosus* was done by usual method which responded a variety of constituents, such as alkaloid, steroid, terpenoid, glycoside, lipophilic, polyphenol, saponin, phenolic and tannin, respectively. Moreover, antimicrobial activities of crude extracts in four solvent systems were tested by agar well diffusion method on six selected organisms. Among four solvents systems, the ethyl acetate extract responded high activity on all selected organisms. In addition, the antimicrobial activities of isolated compound were rechecked by agar well diffusion method on the same microorganisms. The ethyl acetate extract of isolated compound showed high antimicrobial activities on all selected organisms except *Staphylococcus aureus*.

The molecular formula of this isolated compound could be determined as $C_{30}H_{35}N_{92}O_4$. by using some sophisticated spectroscopic methods such as FT-IR, ^{1}H NMR, ^{13}C NMR, DEPT, HMQC and FAB-mass spectral data. The complete structure of this isolated compound was elucidated by DQF-COSY, HMQC and HMBC spectral data. The IUPAC name of this compound is methyl-3-((1E, 4Z, 6Z, 10Z, 14E, 16E)-18-amino-7-(1-aminoethyl)-12-ethyl-3, 8,17-trimethyl-13-vinyl-2,9,19-triazaporphyrin-15-yl)-3-hydroxy-2-oxopropanoate.

Acknowledgements

The authors would like to thank Professor and Head, Dr Daw Khin Aye Tint Nwe and Professor Dr Khin Mar Yee, Department of Chemistry, Mandalay University of Distance Education, Myanmar, for their valuable advice and permission. The authors are also thankful to Dr Yoshiaki Takaya, Associate Professor, Meijo University, Nagora, Japan, for giving me opportunity to have valuable spectra.

References

Breitmaier, E. (2002). *Structure Elucidation by NMR in Organic Chemistry- A Practical Guide*. West Sussex : 3rd Edn, John Wiley and Sons Ltd.

Crews, P., Jaime, R. and Marcel, J., (1998). *Organic Structure Analysis*: *Solutions Manual.* New York: Oxford University Press

Ganapthy, S., Ramaiah,M.,Sarala,S. Babu,P.M. (2013). " Enthobotanical Literature Survey of Three Indian Medicinal Plants for Hepatoprotective Activity". *Int. J.Res. Aryuveda Pharm* , vol.4(3), pp. 378-381

Grabley, S. and Thiericke, R.(2000). *Drug Discovery from Nature*. Berlin : Springer , pp 3-37.

Harborne, J.B. (1993). *Phytochemical Methods: A Guide to Modem Techniques of Plant Analysis*. New York: Chapman and Hall Ltd., pp.40-249

Hesse, M., Meier. H., and Zeeh, B. (1997). *Spectroscopic Methods in Organic Chemistry* . New York: George Thieme Verlag Stuttgart

Nakanishi, K., (1962). *Infrared Absorption Spectroscopy - Practical*. San Francisco: Holden-Day Inc.

Silverstein, R. M., Webster, F. X. and Kiemle, D. J. (2005). *Spectrometric Identification of Organic Compounds.* New York: 7th edition, John Wiley and Sons, Inc.

Yadav, R.N.S. and Munin, A.(2011). "Phytochemical Analysis of Some MedicinalPlants". *Journal of Phytology*, vol3 (12), pp. 10-14.

INVESTIGATION ON SOME PHYTOCHEMICAL CONSTITUENTS AND BIOACTIVITIES OF SEED EXTRACTS OF *Mucuna Pruriens* L.(KHWE-LEYA)

Myint Myin Khine[1] , Kyaw Thu[2], Aye Aye Aung[3]

Abstract

The research focused on the investigation of some phytochemical constituents of *Mucuna pruriens* (L.) seed and some of its biological activities. The sample was collected from Ingapu Township, Ayeyawady Region and it was identified at Department of Botany, Hinthada University. Preliminary phytochemical tests have revealed the presence of alkaloids, carbohydrates, flavonoids, α-amino acids, starch, organic acids, phenolic compounds, saponins, glycosides, reducing sugars, steroids and terpenoids in the sample according to test tube methods and TLC profile. The seed sample was found to contain 14.39 % of moisture, 3.43 % ash, 23.22 % of protein, 8.98 % of dietary fiber, 1.68 % of crude fat, 48.30 % of carbohydrate, and 302 kcal /100 g of energy value based on dried sample. The seed sample was found to have relatively highest content of K and P whereas minor components of S, Ca, Fe, Zn, Cu and Mn according to EDXRF analysis. The *in vitro* antimicrobial activities of PE, EtOAc, $CHCl_3$, 95 % EtOH and H_2O extracts from *M. pruriens*seed were screened by agar well diffusion method on six species of microorganisms, namely *Bacillus pumilus*, *Bacillus subtilis*, *Candida albicans*, *Escherichia coli*, *Pseudomonas aeruginosa* and *Staphylococcus aureus*. All extracts of seed sample were observed to possess antimicrobial activity. Among the tested crude extracts, EtOH extract was found to possess the most potent antimicrobial activity (inhibition zone diameter ranged between 14~16 mm). *In vitro* antioxidant activities of 95 % EtOH and watery extracts from *M. pruriens* seed were assessed by DPPH radical scavenging activity assay. The antioxidant activity of watery extract (IC_{50}= 3.62 µg/mL) was found to be higher than ethanol extract (IC_{50}= 4.49 µg/mL). From the results of phytochemical constituents, antioxidant and antimicrobial activities of the *M. pruriens* seed observed in the present study, the seed could be applied as the local health remedy for the local indigenous communities of our country.

Keywords: *Mucuna pruriens* (L.) (Khwe-leya), phytoconstituents, TLC profile, antimicrobial activity, antioxidant activity

---

[1] Associate Professor, Dr, Department of Chemistry, Hinthada University

[2] Lecturer, Dr, Department of Chemistry, Hinthada University

[3] MSc candidate, Department of Chemistry, Hinthada University

Introduction

Traditional Medicine and Medicinal Plants

Pharmacognosy is the first step in deciding the status of a plant organ as a crude medicine, hence the current study was done. The present study comprises macroscopy, microscopy, histochemistry, physicochemical parameters, fluorescence analysis and preliminary phytochemistry. The use of traditional medicine and medicinal plants in most developing countries, as a normative basis for the maintenance of good health, has been widely observed.

Traditional medicine is the sum total of the knowledge, skill and practices based on the theories, beliefs, and experiences, indigenous to different cultures, whether explicable or not, used in maintenance of health as well as in the prevention, diagnosis, improvement or treatment of physical and mental illness. It refers to health practices, approaches, knowledge and beliefs incorporating plants, animal and mineral based medicines, spiritual therapies, manual techniques and exercises, applied singularly or in combination to treat, diagnose and prevent illnesses or maintain well-being.

The diseases as described and defined in Modern medicine were in existence globally since long times and were named differently in various civilizations. Ayurveda, considered as the oldest "Science of Life" describes various diseases and its treatment with herbs, minerals, and parts of animals. The Ayurveda describes various neurological diseases such as kampavat (Parkinson's disease), apasmar (epilepsy), Unmad (schizophrenia), smrutinash (dementia), avsaada (depression), manas mandata (mental retardation), etc. Kampavata, (meaning tremors caused by excess of vata), is characterized in Ayurveda by tremors, rigidity, akinesia, dyskinesia, loss of olfaction, uncontrollable body movements, difficulty in step initiation, difficulty in maintenance of posture, etc. *Mucuna pruriens* is the most commonly used herb in treatment of Parkinson's disease, either alone or with other herbs.

The incidence of Parkinson's disease (PD) is very high in aged population and levodopa is still the gold standard in management of PD. Prolonged use of levodopa leads to dyskinesias, toxicity, and diminishing efficacy (Cenci, 2007). Despite of several advancements in drug development, the control over progression of neurological damage is inadequate. Before the

introduction of modern medicine, every civilization had it own traditional system of medicine. Several plants, minerals, and biochemical substances were used in almost every traditional system of medicine. The diseases, as defined by the modern system of medicine, were described along with their symptoms in the traditional system of medicine also.

Houghton and Howes (2005) and have reviewed plants having neuroprotective activity in rat model of PD. The Ayurvedic physicians treat PD disease using seeds of *Mucuna pruriens* and some other medicinal plants such as *Celastrus paniculatus, Withania somnifera* and *Tinospora cordifolia, Nardostachys jatamansi*, etc. depending on the symptoms. There are pharmacological studies supporting therapeutic practice of using the above mentioned plants.

Mucuna pruriens L.(Khwe-Leya)

It is mainly distributed in Asia, Africa, Pacific Islands and the United States. *M. pruriens* has been of keen interest in phytochemical and Ayurvedic research due to its excellent medicinal values. Medicinal herbs are moving from fringe to main stream use with a great number of people speaking remedies and health approaches free from side effects caused by synthetic chemicals. *M. pruriens* is highly regarded as an universal panacea in the ayurvedic medicine. It is one of the universal plant having medicinal activities.

Botanical aspects of *Mucuna pruriens*

Family - Fabaceae

Botanical Name - *Mucuna pruriens*

Myanmar Name - Khwe-Leya

English name - Velvet beans, Cowharge, Cowitch, Lacuna bean, Lyon bean

Parts used - Seed

Chemical constituents of *Mucuna pruriens*

The seeds of *M. pruriens* (Figure 1) in addition to the levodopa also contained protein, lipid, dietary fiber and carbohydrates, minerals such as sodium, potassium, calcium, magnesium, iron, zinc, copper, manganese, and phosphorus. The seeds also contain phenolics, tannins and phytic acid. The fatty acids found in the seeds were palmitic acid, stearic acid, oleic acid, linoleic acid, linolenic acid and behenic acid. The seeds also contained niacin and ascorbic acid. The amino acids found in seeds were glutamic acid, aspartic acid, serine, threonine, proline, alanine, glycine, valine, cystine, methionine, isoleucine, leucine, tyrosine, phenylalanine, lysine, histidine, tryptophan, and arginine. Sridhar and Bhat (2007) have reported a number of value-added phytochemicals of *Mucuna* seeds of medicinal importance (e.g. alkaloids, alkylamines, arachidic acid, beta-carboline, harmine, bufotenin, dopamine, flavones, galactose, gallic acid, genistein, glutathione, hydroxygenistein, 5-hydroxytryptamine, N,N-dimethyltryptamine (DMT), 5-methoxy-dimethyltriptamine(5-MeO-DMT), 6-methoxyharman, mucunadine, mucunain, mucunine, myristic acid, nicotine, prurienidine, prurienine, riboflavin, saponins, serotonin, stizolamine, trypsin, tryptamine, vernolic acid (Figure 2). Mucunadine, prurienine and pruricininine are the additional alkaloids isolated from seed extracts (Mehta and Majumdar, 1994).

Medicinal uses of *Mucuna pruriens*

The root is used as a blood purifier, diuretic, emmenagogue, for asthma, cholera, dropsy, delirium, elephantiasis, fevers, gout, kidney stones rheumatism, to relieve dysmenorrhea, in catarrh and dropsy. The leaf is used as an aphrodisiac, diuretic, nerve tonic, uterine stimulant, for scorpion stings and in dysentery. The infusion of the pods is also good for dropsy. The seed cure night dreams and impotency and to promote fertility, for sexual debility, seminal weakness and spermatorrhea, as an aphrodisiac to increase seminal fluid and manly vigour, antivenin, diarrhea, diabetes.

(a)

(b)

Figure 1 Photographs of (a) *Mucuna pruriens* seeds in pod (b) seeds

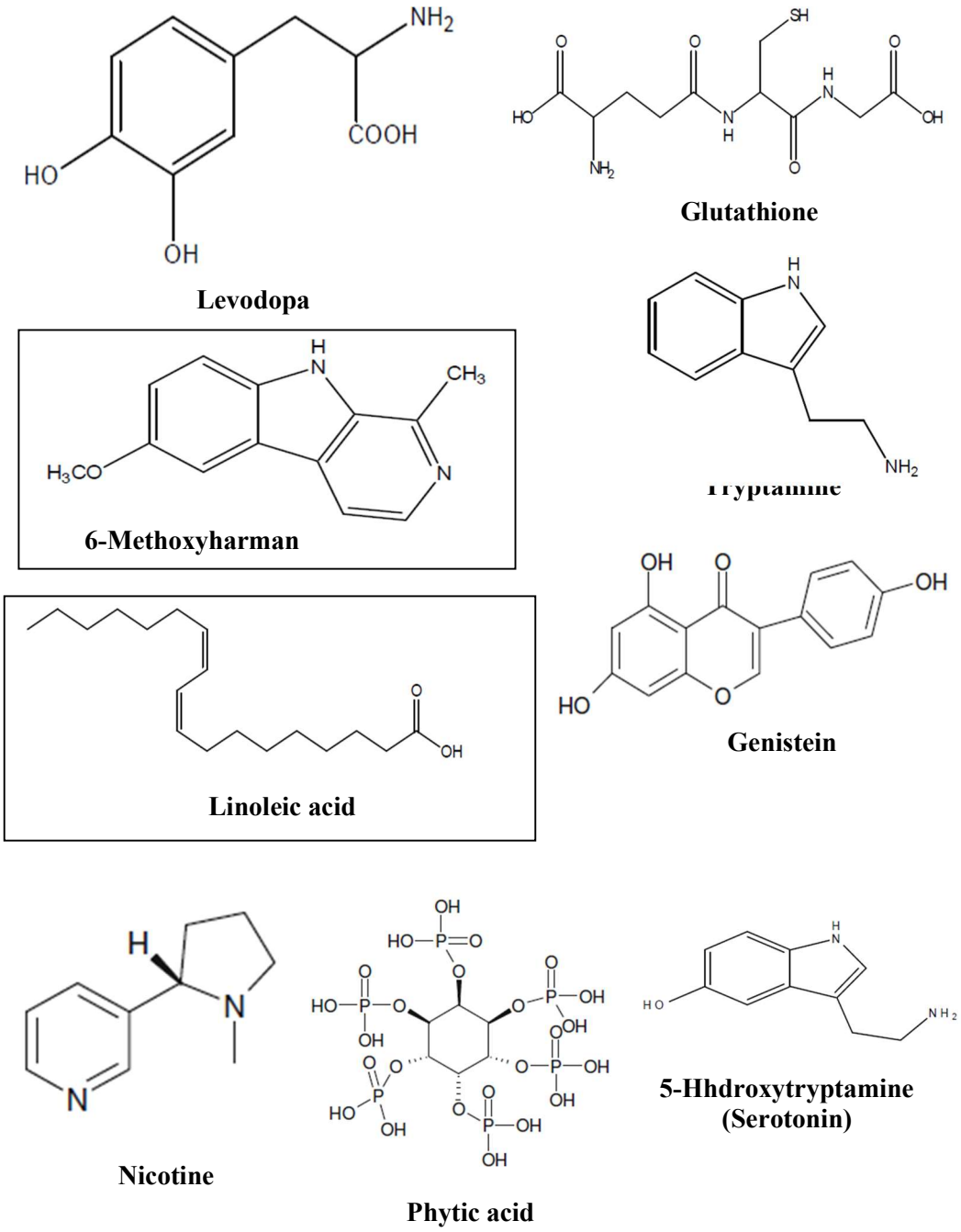

Figure 2 Structures of some chemical constituents of *Mucuna pruriens* seed

The main aim of this study was to investigate some phytochemical constituents from the seed of *Mucuna pruriens* L. (Khwe-Leya) and to study some of its biological activities such as antimicrobial activity and antioxidant activity.

Materials and Methods

Sample Collection

The seed sample of *Mucuna pruriens* (L.) (Khwe-leya) was collected from Ingapu Township, Ayeyawady Region in October, 2016. After being collected, the scientific name of the sample was identified by authorized botanists at Botany Department, Hinthada University.

Sample Preparation

The fresh sample was cleaned by washing with water and air-dried. The dried sample was ground using grinding machine. And then this powdered sample was kept in the sealed air-tight container to prevent moisture changes and other contamination. It was then used without further purification or refining.

Qualitative Screening of the Phytochemicals

In order to classify the types of organic constituents present in seed samples, preliminary phytochemical tests on samples were carried out according to the series of test tube methods.

Elemental Analysis of the Seed of *Mucuna pruriens* L. by Energy Dispersive X-ray Fluorescence (EDXRF) Spectrometry

Relative abundances of elements in the seed were determined by Energy Dispersive X-Ray Fluorescence (EDXRF) Spectrometer.

Determination of Some Nutrient Values of the Samples

Determinations of some nutritional values present in seed samples such as moisture, ash, fiber, protein, fat and carbohydrate contents were carried out by Association of Official Analytical Chemists method (AOAC,1990).

Separation of some Organic Constituents from Crude Extracts of *Mucuna pruriens* L. (Khweleya) Seed

Thin layer chromatographic examinations on methanol, ethyl acetate and petroleum ether extracts were performed by using silica gel GF_{254} precoated plate and a variety of solvent systems. TLC plates used in the laboratory were purchased as 20 cm x 20 cm sheets. Each large sheet cut into plate was measured. Using a pencil, a line was drawn across the plate at the 0.5 cm mark. About 1 mg of petroleum or ethyl acetate or methanol extracts was dissolved in 1 mL of a respective solvent. The tip of the capillary tubes was dipped into the solution and then gently touches the end of it into the proper location on the TLC plate.

The developing container for TLC was designed as chamber, a beaker with a watch glass on the top. Each solvent (various ratio of petroleum ether or ethyl acetate or MeOH) was poured into the chamber to a depth of just less than 0.5 cm. The beaker was covered with a watch glass, swirled gently, and it was allowed to stand for 5 minutes.

The prepared TLC plate was placed in the developing beaker; the beaker was covered with the watch glass. The solvent was raised up the TLC plate by capillary action. The plate was allowed to develop until the solvent was about half a centimeter below the top of the plate. The plate was removed from the beaker and immediately marked the solvent front with a pencil. The plate was allowed to dry. After developing the chromatograms, these were viewed with the various spraying agents such as Liebermann Burchard reagent, 5 % H_2SO_4 solution, $AlCl_3$ solution, Dragendorff's reagent and 5 % $FeCl_3$ solution to develop colour and classify the seed constituents .

Screening of Antioxidant Activity of Crude Extracts from *M. pruriens* Seed by DPPH Assay

DPPH (1,1-diphenyl-2-picryl-hydrazyl) radical scavenging assay was chosen to assess the antioxidant activity of seed materials. This assay has been widely used to evaluate the free radical scavenging effectiveness of various flavonoids and polyphenols in food system.

In this experiment, the antioxidant activity was studied on 95% ethanol extract and watery extract from selected seed sample by DPPH free radical scavenging assay.

Antimicrobial Activity Screening by Agar Well Diffusion Method

The antimicrobial activities of different crude extracts such as pet ether, ethyl acetate, chloroform, 95% ethanol and water extracts were determined against six microorganisms such as *Bacillus subtilis, Staphylococcus aureus, Pseudomonas aeruginosa, Bacillus pumilus, Candida albicans* and *E. coli* species by employing agar well diffusion method at Pharmaceutical Research Department, Ministry of Industry, Yangon, Myanmar.

Results and Discussion

The phytochemical investigation was carried out according to the test tube method. In Table 1, α-amino acids, alkaloids, carbohydrate, flavonoids, glycosides, phenolic compounds, reducing sugars, starch, saponins, steroids, terpenoids, oganic acids were found to be present in *M. pruriens* seed.

Table 1 Results of Phytochemical Investigation on *M. pruriens* Seed

Sr.No.	Tests	Extract	Test Reagents	Observation	Remark
1.	α-amino acids	H_2O	Ninhydrin reagent	pink colour	+
2.	Alkaloids	1% HCl	Mayer's reagent	white ppt	+
			Dragendorff's reagent	orange ppt	+
				brown ppt	+
			Wagner's reagent	yellow ppt	+
			Sodium picrate		
3.	Cyanogenic glycosides	H_2O	Sodium picrate solution	no brick red	-
4.	Carbohydrate	H_2O	10% α-naphthol & H_2SO_4	red ring	+
5.	Flavonoids	EtOH	Mg ribbon & conc.HCl	pink colour	+
6.	Glycosides	EtOH	10% lead acetate	white ppt	+
7.	Phenolic	EtOH	1% $[K_3Fe(CN)_6]$ &	Deep blue	+

Sr.No.	Tests	Extract	Test Reagents	Observation	Remark
	compounds		5% $FeCl_3$	colour	
8.	Reducing sugars	H_2O	Benedict's solution	brick-red ppt	+
9.	Starch	H_2O	Iodine solution	Blue colour	+
10.	Saponins	H_2O	Distilled water	frothing	+
11.	Steroids	Toluene	Acetic anhydride & conc. H_2SO_4	green colour	+
12.	Tannins	H_2O	Gelatin & 1% $FeCl_3$	no white ppt	-
13.	Terpenoids	$CHCl_3$	Acetic ahydride & conc. H_2SO_4	pink colour	+
14.	Organic acids	H_2O	Bromocresol green	blue colour	+

(+) presence ; (-) absence

The relative abundances of elements present in *M. pruriens* seed were determined by EDXRF spectrometer. In Table 2 K was found to be the most abundant element followed by P,S,Ca,Fe,Zn,Cu,Mn.

Table 2 Relative Abundances of Some Elements in *M. pruriens* Seed (By EDXRF)

No.	Elements	Relative Abundance (%)
1.	K	1.294
2.	P	0.353
3.	S	0.236
4.	Ca	0.102
5.	Fe	0.011
6.	Zn	0.04
7.	Cu	0.002
8.	Mn	0.002

The nutrient values such as moisture, ash, proteins, fiber, fat and carbohydrate contents were determined and by AOAC method and energy value was found and seed sample. The results are described in Table 3.

Table 3 Some Nutritional Values of *M. pruriens* (Khwe-Leya) Seed

No.	Parameters	Contents (%)
1.	Carbohydrate	48.30
2.	Crude Protein	23.22
3.	Moistures	14.39
4.	Crude Fiber	8.98
5.	Ash	3.43
6.	Crude Fat	1.68
7.	Energy value	302 (kcal/100g)

The antioxidant activity of the seed sample was determined by DPPH assay. The results obtained are shown in Table 4 and illustrated with Figures 3 and 4. From these observations the activity of aqueous extract (IC_{50} = 3.62 μg/mL) was more potent than ethanol extract (IC_{50} = 4.49 μg/mL)

Table 4 % Oxidative Inhibition and IC_{50} Values of 95 % EtOH and Aqueous Extracts of *M. pruriens* Seed and Standard Ascorbic Acid

Extracts	% Inhibition (mean ±SD) in different concentrations (μg/mL)						IC_{50} (μg/mL)
	0.625	1.25	2.5	5	10	20	
Ethanol	13.98 ± 2.35	17.06 ±1.34	41.00 ±0.84	53.08 ±0.84	57.35 ±0.84	61.61 ±1.01	4.49
Aqueous	14.95 ±1.15	26.63 ±2.31	43.21 ±0.96	57.34 ±2.69	61.96 ±1.54	64.13 ±1.15	3.62
Ascorbic acid	14.04 ±2.09	54.83 ±2.48	72.44 ±3.83	81.13 ±1.47	87.40 ±2.23	91.21 ±0.48	1.17

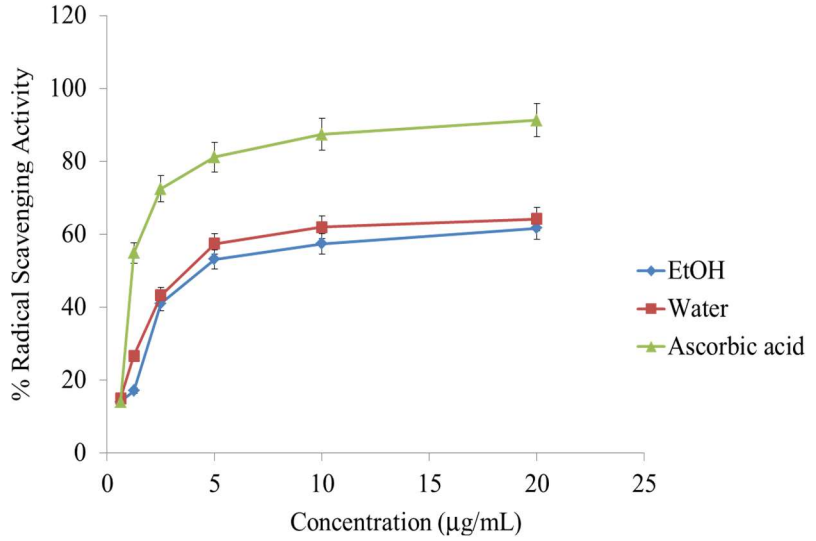

Figure 3 Plot of % oxidative inhibition Vs concentrations (µg/mL) of ethanol and aqueous crude extracts of *M. pruriens* seed in comparison with ascorbic acid

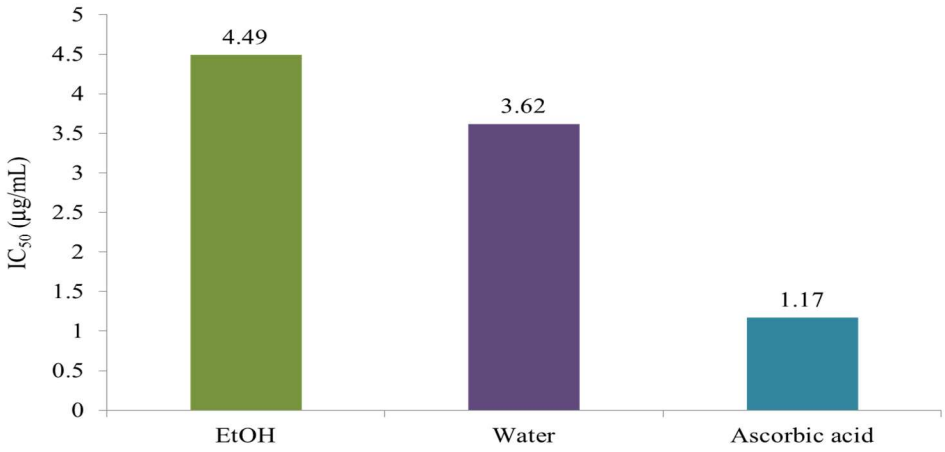

Figure 4 A bar graph of IC_{50} values of 95 % EtOH and aqueous extracts of *M. pruriens* seed in comparison with ascorbic acid

In vitro antimicrobial activity of various crude extracts such as PE, EtOAc, EtOH and H_2O extracts was investigated by employing agar well diffusion method against *Bacillus pumilus, Bacillus subtilis, Candida albicans, Escherichia coli, Pseudomonas aeruginosa, Staphylococcus aureus* microorganisms. The inhibition zone diameter (ID) showed the degree of the antimicrobial activity. The larger the inhibition zone diameters, the higher the antimicrobial activity. Inhibition zone diameters of crude extracts of *M. pruriens* seed against six microorganisms are shown in Table 5 and Figure 6.

Table 5 Inhibition Zone Diameters of Crude Extracts of *M. pruriens* seed against Six Microorganisms

Microorganisms	**Types of Microorganisms**	**Inhibition Zone Diameters (mm)**				
		PE	**$CHCl_3$**	**EtOAc**	**EtOH**	**H_2O**
Bacillus pumilus	Gram (+) ve	-	13	13	15	-
Bacillus subtilis	Gram (+) ve	12	13	12	15	-
Candida albicans	Fungi	13	15	13	14	11
Escherichia coli	Gram (–) ve	12	14	13	16	-
Pseudomonas aeruginosa	Gram (–) ve	-	11	13	14	15
Staphylococcus aureus	Gram (+) ve	12	14	13	15	-

Agar well diameter = 10 mm

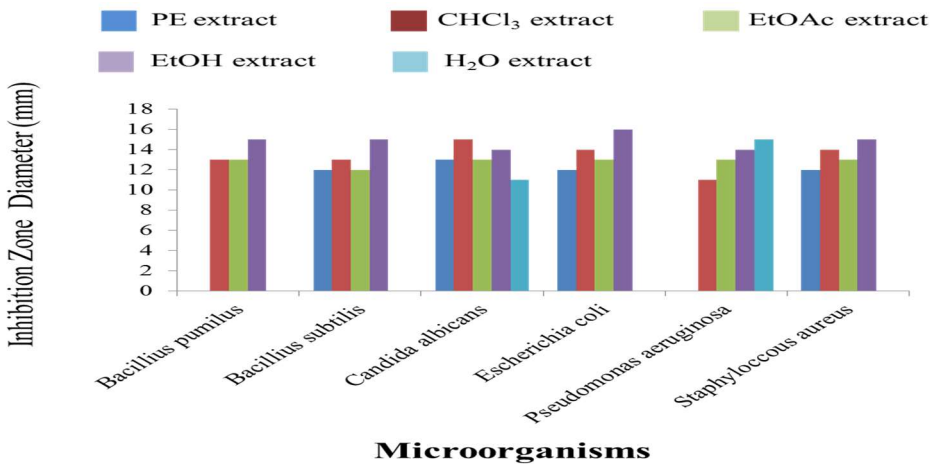

Figure 6 Comparison of inhibition zone diameters for various crude extracts against six microorganisms

Conclusion

From the overall assessment of the present work, the following inferences could be deduced.

(i) The preliminary phytochemical tests on *M. pruriens* (Khwe-leya) seed revealed the presence of α-amino acids, alkaloids, carbohydrates, flavonoids, glycosides, phenolic compounds, reducing sugars, starch, saponins, steroids, terpenoids and organic acids but the absence of cyanogenic glycosides and tannins.

(ii) From EDXRF spectrum, K, P, S, Ca, Fe, Zn, Cu and Mn were found in the seed of *M. pruriens* (Khwe-leya).

(iii) The nutritional values for *M. pruriens* (Khwe-Leya) seed were found to be 14.39 % of moisture, 1.68 % of crude fat, 8.98 % of dietary fiber, 23.22 % of protein and 3.43 % ash. 48.30 % of carbohydrate was observed to be present in the seed sample and thus *M. pruriens* seed can be utilized as good source of carbohydrate and protein.

(iv) According to the antioxidant activity screening of two crude extracts such as ethanol and aqueous extracts from *M. pruriens* seed using DPPH assay, the order of antioxidant activity was as aqueous extract (IC_{50}= 3.62 μg/mL) > ethanol extract (IC_{50}= 4.49 μg/mL). From these observations, the radical scavenging activity of aqueous extract of *M. pruriens* seed was found to be more effective than that of ethanol extract.

(v) Screening of antimicrobial activity of various crude extracts showed that $CHCl_3$, EtOAc, and EtOH extracts of *M. pruriens* seed responded antimicrobial activity against all tested microorganisms ranging the inhibition zone diameter 11-16 mm. Among these, EtOH extract of *M. pruriens* seed possessed more potent activity, exhibiting the inhibition zone diameters ranging 14-16 mm against all six tested organisms. PE, H_2O extracts of *M. pruriens* seed showed inactive against *Bacillus pumilus.* All extracts except PE extract exhibited inhibition zone within the range between 11-15 mm against *Pseudomonas aeruginosa*. H_2O extract showed activity against *Candida albicans* and *Pseudomonas aeruginosa*.

Acknowledgement

We would like to express my profound gratitude to Rector, Dr Tin Htwe, and Pro-rector Dr Theigi Shwe, Hinthada University for their encouragement throughout the course of research work. We wish to express our sincere thanks to Dr Theingi Nyo (Professor & Head) and Dr Cho Cho Than (Professor), Department of Chemistry, Hinthada University, for their kind help with very effective suggestions, advices, comments and encouragement.

References

AOAC. (1990). *Official and Tentative Methods of Analysis, Association of Official Analytical Chemists*. Washington DC: 15th Ed.

Cenci, M.A. (2007). "Dopamine Dysraregulation of Movement Control LDOPA-induced Dyskinesia". *J. Trends Neurosci.,* vol.30(5), pp.236-243

Houghton, P. J.,and Howes.M. J, (2005). "Natural Products and Derivatives Affecting Neurotransmission Relevant to Alzheimer's and Parkinson's Diesases". *J of Neurosignal*, vol.14, pp.6-22

Mehta, J. C., and Majumdar, D. N., (1994). "Indian Medicinal Plants V- *Mucona pruriens* Bark (Papilionaceae)". *Indian J. of Pharmacol*, vol.6, pp. 92-94

Sridhar, K. R. and Bhat, R., (2007). "Agrobotanical, Nutritional and Bioactive Potential of Unconventional Legume - Mucona". *Livestock Res. Rural Dev*., vol.19(9), pp.126-130

ISOLATION OF ASARONE FROM THE RHIZOME OF *Acorus calamus* L. (LIN-NE) AND ANTIBACTERIAL SCREENING OF THE CRUDE EXTRACTS AND ASARONE

Ei Ei Khaing[1]

ABSTRACT

The rhizome of *Acorus calamus* L. (Lin-ne) used in the treatment of diarrhoea and dysentery in traditional Myanmar medicinal system was chosen for present study. The aim of the study is to isolate asarone from the rhizome of *Acorus calamus* L. (Lin-ne) and antibacterial screening of its crude extracts and asarone. At first, four crude extracts of this plant were prepared by using various solvents; petroleum ether, ethyl acetate, 96 % ethanol and 50 % ethanol. *In vitro* antibacterial activity of four crude extracts was investigated against 19 bacterial strains by using agar disc diffusion method. Among the four crude extracts, the most active ethyl acetate extract was selected for isolation of active compound by using column chromatographic method. The isolated compound, asarone (0.712 %) was identified by TLC and spectroscopic methods; UV, FT IR, GC-MS and then tested on 11 bacteria; *Klebsiella* species, *Salmonella paratyphi* A, *Citrobacter* species, *Escherichia coli* ATCC, *Pseudomonas aeruginosa, Salmonella typhi, Escherichia coli* YCH 149, *Shigella flexneri, Proteus* species, *Staphylococcus aureus* and *Vibrio cholerae* O1 by agar disc diffusion method. In addition minimum inhibitory concentration (MIC) of asarone was determined by microtitre plate dilution method and the MIC value 0.06 mg/mL of asarone on tested bacteria, *E. coli* LT and *S. aureus* was found.

Keywords: *Acorus calamus* L., asarone, antibacterial activity, MIC

Introduction

Diarrhoea and dysentery are important health problems in worldwide especially developing countries. So the Government of Myanmar has initiated a national programme for the development of Traditional Medicine System in

[1] Associate Professor, Dr, Department of Chemistry, Sagaing University of Education

combating six major types of diseases: namely; malaria, tuberculosis, diarrhoea, dysentery, diabetes and hypertension.

Diarrhoea is the host response to infection of the gastrointestinal tract by a variety of viruses, bacteria and parasites. There are three types of diarrhoea, namely acute diarrhoea, persistent diarrhoea and chronic diarrhoea. Acute diarrhoea is usually defined as the passage of 3 (or) more liquid motions within 7 days. Persistent diarrhoea have a usually long duration, more than 2 weeks, but usually less than 2 weeks duration. Chronic diarrhoea lasts for more than three weeks (Khan, 2001).

Dysentery is an inflammatory disorder of the lower intestinal tract, usually caused by bacteria, parasitic, or protozoa infection and resulting in pain, fever, and severe diarrhoea, often accompanied by the passage of blood and mucous. Dysentery is caused by an *Amoeba* or *Bacillus* that infects the colon (Boyd and Marr, 1980).

In this study, Myanmar medicinal plant, *Acorus calamus* L. (Lin - ne or Lin - lay) (Figure 1) was selected to find out of active principle for the treatment of dysentery and diarrhoea. *A. calamus* plants are found in the north temperate regions and South East Asia. These plants are found wild or cultivated throughout India and Srilanka, ascending to 6000 ft. *A. calamus* L. is indigenous and grows wild and extensively in Myanmar, especially in "Myitkyina". It can be also found in Pan Ta Naw Township in Ayeyarwady Region and Shan State. The rhizome in this study was collected from Ywa Thar Gyi, Yangon Region. The yellow oil, asarone is major constituent responsible for peculiar warm and spicy odour of *A. calamus* L. (Bose *et al*., 1960; Fluck, 1976). In Myanmar, *A. calamus* L. is used in treating dyspepsia, chronic diarrhoea, dysentery of children, fever, bronchitis and insecticide (Mar Mar Nyein *et al*., 2006).

In *A. calamus* L., essential oil mainly contains cis or trans asarone and it shows antioxidant, antibacterial activity as well as antimicrobial activity. The rhizome of *A. calamus* L. has been also used in the treatment of gastrointestinal (GI) problems, anorexia, flatulence and then used as spice, perfume in food and industry (Bruno *et al*.,2005; Devi and Ganjewala, 2011; Raina *et al*., 2003). Therefore, antibacterial activity investigation on four crude extracts (PE, EtOAc, 96% EtOH, 50% EtOH) and some isolated phytoconstituents

from the rhizome of *A. calamus* L. were carried out by using agar disc diffusion method. Minimum inhibitory concentration (MIC) of major constituent was also determined by microtitre plate dilution method in this study.

Botanical Aspects of *Acorus calamus* L.

Name : Lin-ne (or) Lin-lay (in Myanmar),
The Sweet-Flag (in English)

Botanical Name : *Acorus calamus* L.

Family : Acoraceae
(Kress *et al*., 2003)

Genus : *Acorus*

Rhizome : Root-stock creeping wit
5 feet long horizontal and
much branched aromatic rhizome

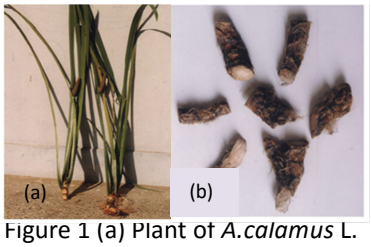

Figure 1 (a) Plant of *A.calamus* L.
(b) Rhizome of *A.calamus* L.

Distribution

A. calamus L. (Lin-ne) is widely distributed in Myanmar and often planted for its medicinal properties.

Chemical Constituents

The rhizome of *A. calamus* L. (Lin-ne) contained volatile oil, α-pinene, camphene, calamene, calamenol, calamenone, asarone, aromatic glucoside (acorin), a strong base calamine, a soft resin, tannin, mucilage, starch and calcium oxalate.

Materials and Methods

Plant Materials

The rhizome of *A. calamus* L. was collected from Ywa Thar Gyi, Yangon Region. The plant was identified at Department of Botany, Yangon University. The rhizome of *A. calamus* L. was washed, cleaned and dried at room temperature for two weeks. Then the dried sample powdered and stored in air- tight container.

Instruments: Shimadzu UV-240, (MeOH), Shimadzu FT IR- 8400, GC-MS; Turbo Mass Perkin Elmer, URC and University of Goettingen, Germany,

Chemicals : CC; Merck Silica gel 60 (70-230) mesh, eluents; Petroleum - ether (PE)-ethyl acetate(EtOAc), only ethyl acetate, TLC; precoated silica gel 60 (F_{254}, Merck)

Extraction and Isolation of Asarone from Rhizome of *Acorus calamus* L.

Preparation of extracts from rhizome of *Acorus calamus* L.

The air-dried powder (1kg) was cold extracted with (2500 mL) of various solvent; petroleum-ether (60-80°C), ethyl acetate, 96% ethanol and 50% ethanol, respectively for 7 days and then filtered. The filtrate was evaporated to dryness at normal pressure on a water bath and dessicated. The yield % of petroleum-ether extract, ethyl acetate extract, 96% ethanol extract and 50% ethanol extract were determined.

Isolation of phytoconstituents from EtOAc extract of rhizome of *Acorus calamus* L.

The EtOAc extract was subjected to isolate the active phytoconstituents from Lin-ne rhizome by column chromatography. The column was packed with silica gel (400g) by the wet method using petroleum-ether the column was eluted consecutively with the solvent system (v/v) (PE : EtOAc) (30:1, 19:1, 9:1, 2:1, 1:1) and only ethyl acetate according to their increasing polarity. The column was completely filled with the solvent system and fractionation was started. Flow rate was adjusted to about 1 drop per second. Fractions were monitored by thin layer chromatography (TLC). The fractions

that gave similar spots on thin layer chromatography (TLC) plates were combined together and the solvent was removed. Finally, isolated compound (yellow oil, 0.712 %) was characterized as asarone by spectroscopic methods.

In vitro Studies on the Antibacterial Activity of Rhizome of *A. calamus* L. by Agar Disc Diffusion Method

Screening of antibacterial activity of crude extracts against 19 tested bacterial strains

Agar disc diffusion method was used for the detection of antibacterial activity for four crude extracts from *A. calamus* L. rhizome. The test procedure was as follows: the extracts (1g each for testing 19 cultural bacterial strains) were introduced into sterile petridishes and dissolved in 1 mL of their respective solvents, petroleum ether, ethyl acetate, 96 % ethanol and 50% ethanol. Discs obtained by filter paper (Toyo No.26, Japan) punched to 6 mm diameter, were used to impregnate the extracts. To obtain approximately 20 μg/disc and prior to adherence on the culture plates the discs were allowed to dry at 42° C in incubator.

The bacterial suspension from trypticase soy broth was streaked evenly into three places on the surface of the trypticase soy agar plates with sterile cotton swab (Puritan, USA). After the inoculums had dried for 5 min, the dried disc impregnated with extracts were placed on the agar with flamed forceps and gently pressed down to ensure proper contact. A disc impregnated with solvent only was placed alongside the test discs for control and comparing purposes known antibiotics tetracycline was also used as positive control.

The plates were incubated immediately (or) within 30 min after inoculation. After overnight incubation at 37°C, the zones of inhibition diameter including 6 mm discs were measured, by means of a thin transparent ruler or by a divider. The most active extract (EtOAc) was selected for isolation of active compound and MIC determination.

Screening of Antibacterial Activity of EtOAc Extract and Iolated Asarone from Active EtOAc extract of rhizome (*A. calamus* L.) against 11 tested bacterial strains

The selected most active EtOAc extract and isolated compound asarone (0.712 %) were subjected to study antibacterial activity against 11 tested bacteria from clinical sources, National Health Laboratory (NHL), Yangon; related to acute diarrhoea (cholera), dysentery, abscess, pneumonia and typhoid.

Determination of Minimum Inhibitory Concentration (MIC) by Microtitre Plate Dilution Method

The isolated compound, asarone, from *A. calamus* L. was tested with 5 strains; *Escherichia coli* ATCC, *Escherichia coli* LT, *Escherichia coli* STLT, *Staphylococcus aureus* ATCC, *Staphylococcus aureus* by microtitre plate dilution method.

Microtitre plate dilution method was done by using trypticase soy broth by dissolving with appropriate soluble compound, asarone in 2-fold dilutions. First, an inoculum of pure culture of respective bacteria was seeded in 5 mL of trypticase soy broth (TSB) and incubated at 37˚C for 3-4 h to obtain a turbidity of 0.05 by MacFarland nephelometer which corresponded to a bacterial suspension of 10^6 organisms per mL. Prior to the experiment, 50 L of TSB was introduced into all wells of 96-well microtitre plate. The compound (asarone) was dissolved in ethyl acetate and diluted with trypticase soy broth to obtain the following concentration: 5 mg/mL, 2.5 mg/mL, 1.25 mg/mL, 0.625 mg/mL, 0.32 mg/mL, 0.16 mg/mL, 0.08 mg/mL, 0.04 mg/mL, 0.02 mg/mL, 0.01 mg/mL, 0.005 mg/mL, 0.0025 mg/mL in 96 - well microtitre plates.

Then 0.02 µL of the prepared inoculum was introduced to its respective wells and the microtitre plates were incubated at 37°C for 18 h. Prior to taking spectrophotometer readings, contents of all wells were thoroughly mixed with a multi-channel pipetter to resuspend clamped cells at the bottom of the wells in a solution. Growth of the bacteria was determined by automated microplate reader (Bio Rad) at a wavelength of 450 nm as well as confirmed by the growth of culturing onto trypticase soy agar to incubate at

37°C for overnight. The last well with no growth of bacteria was taken to represent the minimum inhibitory concentration (MIC) of the compound.

Results and Discussion

Isolation of Asarone from Ethyl Acetate Extract of *A.calamus* L. Rhizome

The dried rhizome powder collected from Ywa Thar Gyi, Yangon Region was extracted using various solvents and the yield % of petroleum-ether extract (1.1%), ethyl acetate extract (1.5%), 96% ethanol extract (2.0%) and 50% ethanol extract (3.2%) were obtained respectively. Asarone (0.712%) has been isolated from ethyl acetate extract of *A. calamus* L. by column chromatographic separation method. The structure of isolated compound as asarone have been identified by TLC determination, UV(Figure 2), FT IR (Figure 3), and GC - MS (Figure 4 a, b) spectrometry. Isolated compound gave R_f value 0.43 with petroleum ether - ethyl acetate (4:1) system and red purple colour was observed with vanillin-conc. H_2SO_4 in TLC chromatogram.

Asarone : Yellow oil (1.78 g, 0.712 % yield); λ_{max}^{MeOH} 250, 300 (nm) (Obs. value), λ_{max}^{EtOH} 252, 302 (nm) (Lit. value) ; FT IR $(CHCl_3)/cm^{-1}$ 2995.2, 2933.5, 2829.4 (ν_{CH} for asym & sym of – CH_3), 1604.7, 1506.3 ($\nu_{C=C}$ of aro-), 1458.1(δ_{asym} – CH_3) , 1392.5, 1321.1 (δ_{sym} – CH_3), 1201.6, 1126.3 ($\nu_{asym\ C\text{-}O\text{-}C}$ of aro-), 1039.6 ($\nu_{sym\ C\text{-}O\text{-}C}$) , 981.7 ($\delta_{CH}$ of trans double bond), 850.5, 763.8 (δ_{CH} of aro - system); GC-MS (m/z) 208 (M^{+o}), 209 $(M + H)^+$, 193 $(M – CH_3)^+$ [C_{12} H_{16} O_3] (Figures 2,3 and 4) (Silverstein *et al*., 1991)

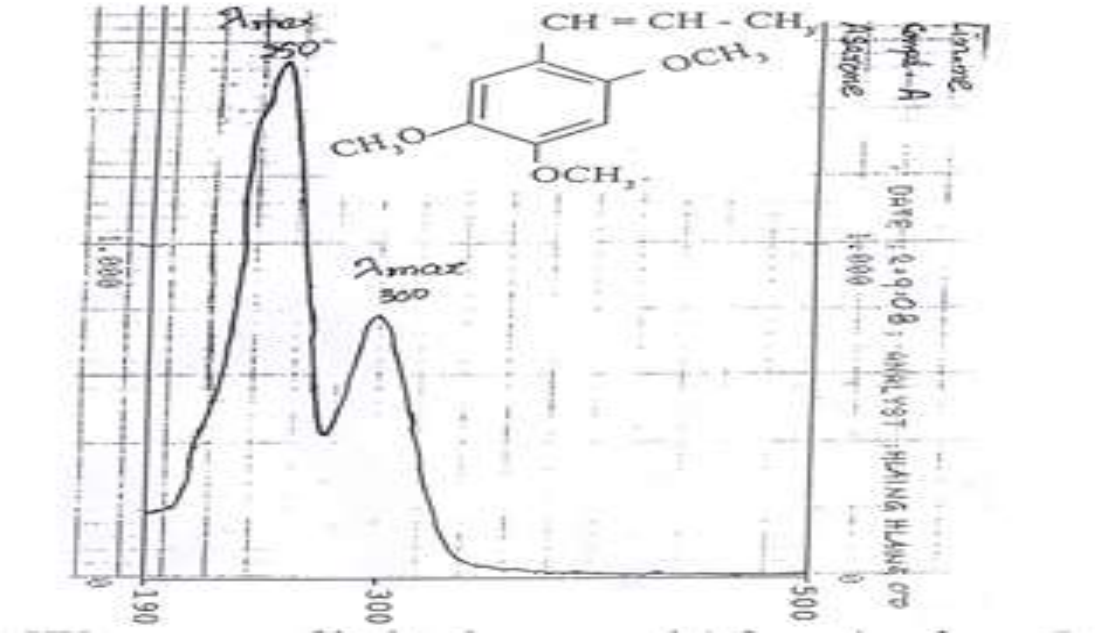

Figure 2 Ultraviolet spectrum of isolated compound from *Acorus calamus* L.

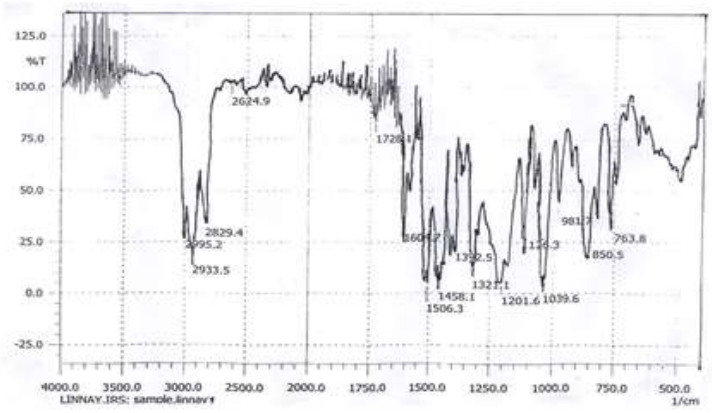

Figure 3 FT IR spectrum of isolated compound from *Acorus calamus* L.

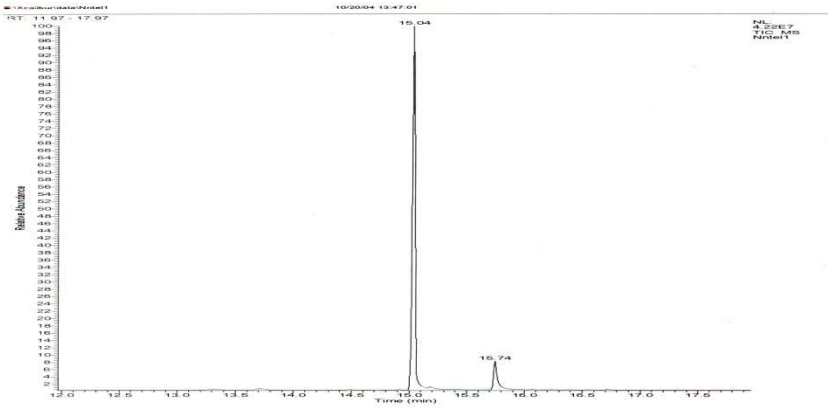

(a)

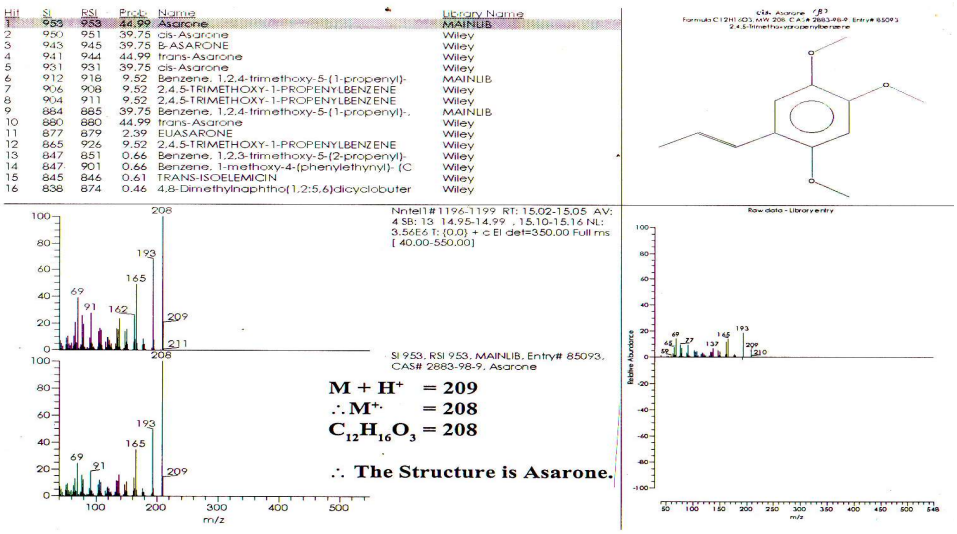

(b)

Figure 4 GC-MS spectrum of isolated compound from *Acorus calamus* L.
(a) GC spectrum of isolated compound from *Acorus calamus* L.
(b) MS spectrum of isolated compound from *Acorus calamus* L.

Screening of Antibacterial Activity of Crude Extracts and Isolated Asarone

Screening of antibacterial activity of 4 crude extracts has been done by agar disc diffusion method. The inhibition zone diameters of extracts tested with 19 strains of bacteria from clinical sources are shown in Table 1. The most active ethyl acetate extract with the range of inhibition zone diameter (12-22) mm against 7 strains, namely *Escherichia coli* LT, *Escherichia coli* EHEC, *Salmonella paratyphi, Vibrio chlolerae* Inaba, *Pseudomonas pyocyanea, Salmonella typhi* and *Staphylococcus aureus* was selected for isolation of active compound. Antibacterial activity of ethyl acetate extract and isolated asarone were being compared on 11 tested bacteria shown in Figure 5. In Table 2 it was found that the isolated asarone showed more potent activity with inhibition zone diameters (12-33) mm of all strains except *Proteus* species but ethyl acetate extract exhibited less potent to 8 out of 11 strains with inhibition zone diameter (7-11) mm. According to these zone diameters, the antibacterial activity of asarone against *Klebsiella* species, *Salmonella paratyphi* A, *Citrobacter* species, *Escherichia coli* ATCC, *Salmonella typhi, Escherichia coli* YCH 149 and *Shigella flexneri* are more potent than tetracycline, the control except *Pseudomonas aeruginosa, Staphylococcus aureus,* and *Vibrio cholerae* O1. From the screening results, it can be generally deduced as follows. The EtOAc extract and isolated asarone from *A. calamus* L. were found to inhibit the tested bacteria with regard to acute diarrhoea (cholera), dysentery, pneumonia, typhoid, urinary tract infection, sepsis and abscess. In addition, asarone, major constituent yielded (0.712%) from *A. calamus* L. was employed by microtitre plate dilution method for minimum inhibitory concentration (MIC) determination with 3 strains of *Escherichia coli* and 2 strains of *Staphylococcus aureus* obtained from clinical sources at Bacteriology Research Division, DMR (LM) are shown in Table 3. The microtitre plate dilution method also elaborates the specificity, sensitivity and the least amount required for media, reagents and glassware. It also saves time and working space in conducting the experiments. The lowest minimum inhibitory concentration (MIC), 0.06 mg/mL of asarone with *Escherichia coli* LT and *Staphylococcus aureus* showed the plant possess bactericidal activity on them. From the MIC elucidation, asarone isolated from the rhizome of Linne would be more effective for the treatment in diarrhoea and abscess. Since it

has bacterial action against *E. coli* responsible for diarrhoea and *Staphylococcus aureus* responsible for abscess occurred in skin, mouth and nose.

Table 1. Results of Antibacterial Activity of Four Extracts of *A. calamus* L. on 19 Species of Bacteria

No.	Type of bacteria	Inhibition zone diameter (mm)			
		EtOAc extract	96%EtOH extract	50%EtOH extract	PE extract
1	*Salmonella derby*	-	-	-	-
2	*Escherichia coli* LT	14	12	-	-
3	*Escherichia coli* O128	-	-	-	-
4	*Escherichia coli* EHEC	13	-	-	11
5	*Staphylococcus aureus* ATCC	-	18	12	12
6	*Salmonella paratyphi*	20	15	12	20
7	*Salmonella stanley*	-	-	-	-
8	*Shigella boydii*	-	-	-	-
9	*Salmonella pollorum*	-	-	-	-
10	*Shigella dysenteriae*	-	-	-	-
11	*Vibrio cholerae* Inaba	12	-	10	-
12	*Escherichia coli* ATCC	-	-	-	-
13	*Pseudomonas pyocyanea*	12	-	10	-
14	*Vibrio cholerae* O1	-	-	-	-
15	*Salmonella typhi*	12	-	-	-
16	*Vibrio cholerae* O139	-	-	-	-
17	*Shigella flexneri*	-	-	-	-
18	*Bacillus subtilis*	-	-	-	-
19	*Staphylococcus aureus*	22	20	15	20

(-) = no activity

Disc diameter = 6 mm

Table 2. Antibacterial Activity of EtOAc Crude Extract and Asarone, Isolated from Lin- ne or Lin - lay Rhizome

Sample	Inhibition zone diameter (mm) against test bacteria										
	1	2	3	4	5	6	7	8	9	10	11
Crude (Lin-ne)	8	7	-	7	-	7	11	10	7	7	-
Asarone	20	33	31	27	12	22	33	24	-	28	22
Blank disc	-	-	-	-	-	-	-	-	-	-	-
EtOAc solvent (-) control	-	-	-	-	-	-	-	-	-	-	-
Tetracycline (+) control	13	25	25	25	15	10	25	12	-	29	29

Tested Bacteria (From Clinical Sources*)

1 = *Klebsiella* species
2 = *Salmonella paratyphi* A
3 = *Citrobacter* species
4 = *Escherichia coli* ATCC
5 = *Pseudomonas aeruginosa*
6 = *Salmonella typhi*
7 = *Escherichia coli* YCH 149
8 = *Shigella flexneri*
9 = *Proteus* species
10 = *Staphylococcus aureus*
11 = *Vibrio cholerae* O1

Disc diameter = 6 mm
- = no activity

* National Health Laboratory (NHL), Yangon

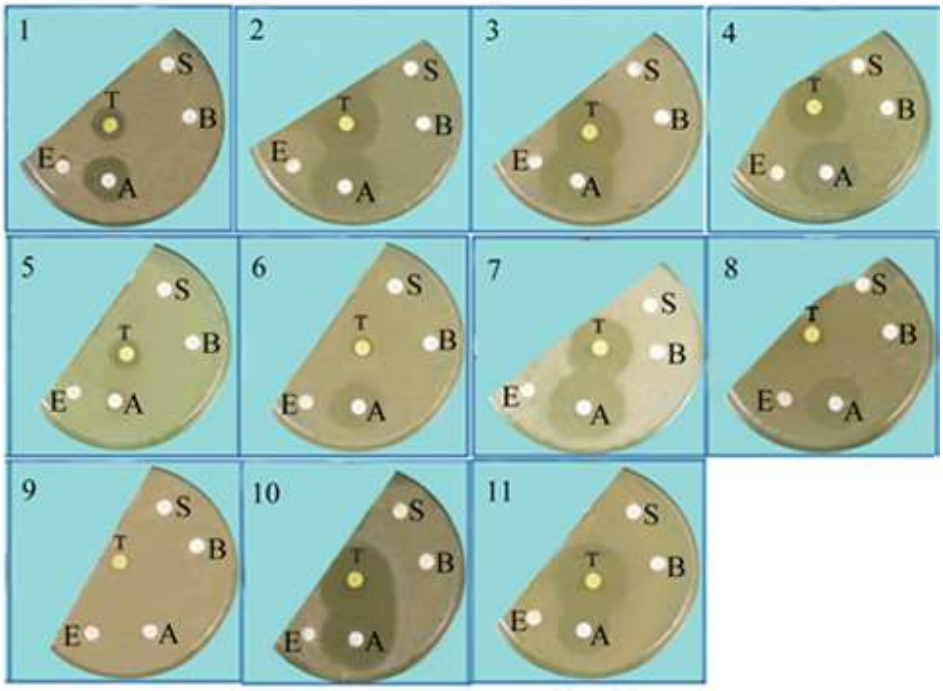

1 = *Klebsiella* species

2 = *Salmonella paratyphi* A

3 = *Citrobacter* species

4 = *Escherichia coli* ATCC

5 = *Pseudomonas aeruginosa*

6 = *Salmonella typhi*

7 = *Escherichia coli* YCH 149

8 = *Shigella flexneri*

9 = *Proteus* species

10 = *Staphylococcus aureus*

11 = *Vibrio cholerae* O1

E = EtOAc crude extract (Lin – ne or Lin - lay)

A= Asarone

S = EtOAc solvent (-) control

B = Blank

S = EtOAc solvent (-) control

T = Tetracycline (+) control

Figure 5 Antibacterial activity of EtOAc crude extract and asarone, isolated from Lin - ne or Lin – lay

Table 3. Minimum Inhibitory Concentration (MIC) of Active Isolated Compound Asarone (mg/mL) of *Acorus calamus* L.

No.	Bacteria	MIC(mg/mL)
1	*Escherichia coli* ATCC	0.12
2	*Escherichia coli* LT	0.06
3	*Escherichia coli* STLT	0.63
4	*Staphylococcus aureus* ATCC	0.12
5	*Staphylococcus aureus*	0.06

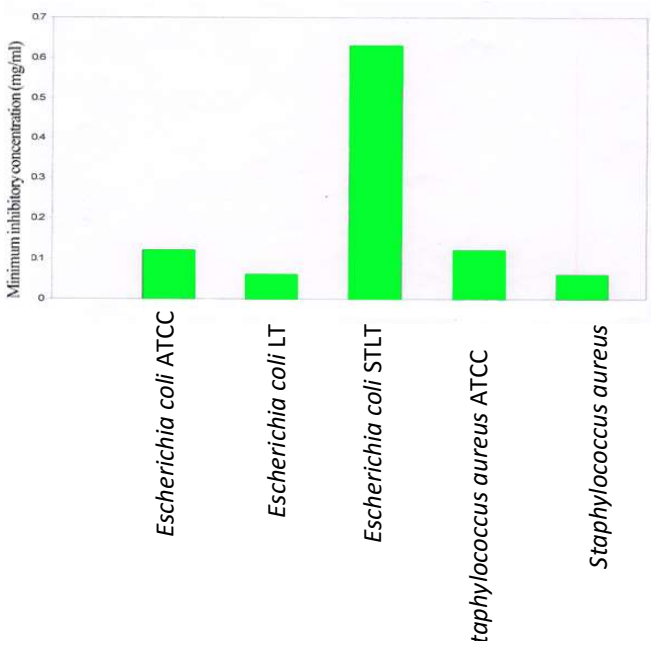

Figure 6 Minimum inhibitory concentration (MIC) of asarone from EtOAc extract of *Acorus calamus* L. rhizome against different bacteria by microtitre plate dilution method

CONCLUSION

From the rhizome of *A. calamus* L., four crude extracts: PE extract (1.1 %), EtOAc extract (1.5 %), 96 % EtOH extract (2.0 %) and 50 % EtOH extract (3.2 %) were obtained and screened antibacterial activity against 19 tested bacteria by agar disc diffusion method. Among the four crude extracts of Lin-ne, only EtOAc extract showed the most potent antibacterial activity with the related larger zone diameter (12-22) mm on *Escherichia coli* LT, *Escherichia coli* EHEC, *Salmonella paratyphi, Vibrio cholerae* Inaba, *Pseudomonas pyocyanea, Salmonella typhi* and *Staphylococcus aureus* out of 19 bacterial strains. Using column chromatographic separation, yellow oil (1.78 g, 0.712 %) was isolated from the most active EtOAc extract of *A. calamus* L. (Lin-ne) and identified as asarone by UV, FTIR and GC-MS spectrometry.

In vitro antibacterial activity of ethyl acetate crude extract and asarone were also investigated and it was found that asarone showed the range of inhibition zone diameter (12-33) mm whereas inhibition zone diameter of EtOAc extract ranged between (7-11) mm. It was concluded that asarone, pure compound was more effective on 10 out of 11 tested bacteria than that of the crude EtOAc extract and tetracycline for the treatment of dysentery, abscess and diarrhoea.

Acknowledgements

I would like to express my thanks to Dr Saw Pyone Naing, Rector and Dr. Myo Thant, Pro-Rector, Sagaing University of Education, for giving the permission to report this research work. I would also like to extend my gratitude to Dr. Kathy Myint Thu, Professor (Head), Department of Chemistry, Sagaing University of Education, for her enthusiastic guidance in this research work. I am also grateful to Dr Than Soe, Rector, University of Myitkyina and Dr Mar Mar Nyein, Director (Retired), Bacteriology Research Division, Department of Medical Research (Lower Myanmar) for their valuable suggestions.

References

Bose, B.C., Vijayvargiya, R., Saifi, A.Q. and Sharma, S.K. (1960). "Some Aspects of Chemical and Pharmacological Studies of *A. calamus* Linn.". *J. of the American Pharmaceutical Asso*, vol. 49 (1), pp. 32-34

Boyd, R.F. and Marr, J. J. (1980). *Medical Microbiology.* Boston: 1st Ed., Little Brown and Company, p. 597

Bruno, M., Alessandra, P., Silvia, P. and Andrea, S. (2005). "Chemical Composition of the Essential Oil and Supercritical CO_2 Extract of *C. myrrha* N. and *A. calamus* L.". *Journal of Agricultural and Food Chemistry,* vol. 53 (20), pp. 7939-7943

Devi, A.S. and Ganjewala, D. (2011). "Antioxidant Activities of Methanolic Extracts of Sweet- Flag (*A. calamus* L.) Leaves and Rhizomes". *Journal of Herbs Species & Medicinal Plants,* vol. 17, pp. 1-11

Fluck, H. (1976). *Medicinal Plants and their Uses*. London: 2nd Ed., W. Foulsham & Co. Ltd., pp. 101-110

Khan, M.R. (2001). "Antibacterial Activity of Some Tanzanian Medical Plants". *Pharmaceutical Biology*, vol. 39 (3), pp. 206-212

Kress, W.J., Defilipps, R.A., Farr, E. and Daw Yin Yin Kyi. (2003). *A Checklist of the Trees, Shrubs, Herbs and Climbers of Myanmar.* Washington, DC: 1st Ed., Department of Systematic Biology-Botany, National Museum of Natural History, p. 37

Mar Mar Nyein, Mi Mi Htwe, Ba Han and Ei Ei Khine. (2006). "Antibacterial Activity of Some Plants and Formulations and Determination of Minimum Inhibitory Concentration (MIC) by Microtitre Plate Dilution Method". *The Myanmar Health Sciences Research Journal,* vol. 18 (1), pp. 26-30

Raina, V.K., Srivastava, S.K. and Syamasunder, K.V. (2003). "Essential Oil Composition of *A. calamus* L. from the Lower Region of the Himalayas". *Flavour and Fragrance Journal,* vol. 18 (1), pp. 18-20

Silverstein, R.M., Bassler, G.C. and Terence, C.M. (1991). *Spectrometric Identification of Organic compounds*, Singapore: 5th Ed., John Wiley and Sons, Inc., pp. 289-315

ISOLATION OF ASARONE FROM THE RHIZOME OF *ACORUS CALAMUS* L. (LIN-NE) AND ANTIBACTERIAL SCREENING OF THE CRUDE EXTRACTS AND ASARONE

A Research Paper Submitted to the Myanmar Academy of Arts and Science

By

Ei Ei Khaing
BSc (Hons.), MSc, PhD
Associate Professor
Department of Chemistry
Sagaing University of Education

June, 2017

STUDY ON THE PREPARATION OF BIOCHARS FROM SOME PLANT MATERIALS

Maung Maung Khin[1],Khin Hnin Mon[2], Saw Hla Myint[3], Daw Hla Ngwe[4]

Abstract

This research concerns with the study on the preparation of biochar from some plant materials. Baw-za-gaing (*Leucaena leucocephela* (Lam.) De Wit), Kathit-su (*Zanthoxylum budrunga* Wall), Htiyo-wa (*Thyrsostachys siamensis* (Kurz ex Munro) Gamble), Pan-mezali (*Peltophorum pterocarpum* (DC.) Back. ex K.), and rice husk (*Oryza sativa* L.) were collected for preparation of biochars. Different amounts of biochar were 18.75 % from Baw-za-gaing, 10.0% from Kathit-su, 19.04% from Htiyo-wa, 10.0 % from Pan-mezali and10.0 % from rice husk. In the biochar preparation process, the effectiveness of TLUD (Top-Lit UpDraft) furnace was studied by using various chimney height (1′-3′). The highest yield % of biochar from different plant materials was acquired with the chimney height in the range of 1′ 6″ - 2′ 6″. Among the five different samples, Htiyo-wa gave the highest yield % of biochar (19.04 %). Furthermore, ash content (1.2 % from baw-za-gaing, 0.13 % from htiyo-wa, 0.2 %,from kathit-su, 0.18 % from pan –mezali, and 0.62 % from rice husk), moisture content (2.65 % from baw-za-gaing, 1.75 % from htiyo-wa,2.32 % from kathit-su, 0.18 % from pan-mezali, and 3.251 % from rice husk), and bulk density (84.78 g/100 mL from baw-za-gaing, 79.12 g/100 mL from kathit-su, 82.21 g/100 mL from pan-mezali, 80.12 g/100 mL from rice husk, and 75.12 g/100 mL from htiyo-wa) were also determined in the laboratory.Similarily, the volatile matter contents of biochars were determined 2.12%, 2.00%, 2.10 %, 2.50%, and 2.15%, respectively, from Pan-mezali, Baw-za-gaing, Htiyo-wa, Kathit-su, and Rice- husk .The fixed carbon contents were 95.775 % from Baw-zagaing, 98.72 % from Htiyo-wa, 97.23 % from Kathit-su, 97.718 % from Pan-mezali, and 96.015 % from Rice Husk.Nitrogen content (3.1% from baw-za-gaing, 2.5 % from kathit-su, 3.0 % from pan-mezali, 2.1 % from rice husk, and 2.4 % from htiyo-wa), potassium content (0.1814 % from baw-za-gaing, 0.8459 % from kathit-su, 0.8457 % from pan-mezali, 0.8471 % from rice husk, and 1.802 % from htiyo-wa) and phosphorous contents (0.032% from baw-za-gaing, 0.023 % from kathit-su, 0.026 % from pan-mezali, 0.018 % from rice husk, and 0.027 % from htiyo-wa) were observed in biochar, which can be used as soil amendment for plant growth.

Keywords: Biochar, TLUD furnance,ash contents, bulk density, fixed carbon

[1]Lecturer, Dr,Department of Chemistry, University of Yangon
[2]Associate Professor, Dr,Department of Chemistry, PanglongUniversity
[3]Part-time Professor, Dr,Department of Chemistry, University of Yangon
[4]Professor and Head, Dr,Department of Chemistry, University of Yangon

Introduction

Biochar is the carbon-rich product when biomass (such as wood, manure or crop residues) is heated in a closed container with little or no available air. It can be used to improve agriculture and the environment in several ways, and its stability in soil and superior nutrient-retention properties make it an ideal soil amendment to increase crop yields (Lehmann and Joseph, 2009). .Biochar is a form of charcoal produced by super-heating biomass. It is found naturally in soils around the world as a result of vegetation fires. Biochar has also been created and used by humans in traditional agricultural practices in the Amazon Basin of South America for more than 2,500 years. Addition of BC to agriculture soils has been projected as a means to improve soil fertility and mitigate climate change(Rondon *et al.,* 2007 ; Wardle *et al.,* 2008 ;Amutio *et al.,* 2013). Dark, charcoal-rich soil (known as *Terra preta* or black earth) supported productive farms in areas that previously had poor, and in some places toxic, soils. *Terra preta* was discovered in the 1950's by Dutch soil scientist Wim Sombroek in the Amazon rainforest. Terra preta still covers 10 % of the Amazon Basin. Similar sites have been found in Ecuador, Peru, Benin and Liberia in West Africa.Todaybiochar can be produced in an environmentally friendly way - and it needs to be; Pyrolysis, burning with limited oxygen in a closed system, allow material to be burned at high temperatures and all the emissions captured.

Materials and Methods

Collection and Preparation of Samples

The selected samples such as Htiyo-wa, Kathit-su, Pan-mezali, Rice-husk and Baw-za-gaing were collected from an area of 20-Quarter, Shwepyithar Township, Yangon Region. The samples were especially cultivated.The collected samples were cut into many pieces of nearly equal size, which is 1.5 cm in length and 0.4 cm in width. And then, the samples were kept in air to dry at room temperature for a few weeks. Futhermore, the samples were dried in an oven at 99 ºC for 4 h because of its moisture content.

Determination of Some Parameters of Plant Materials

Determination of bulk density of samples

A clean dry 100 mL graduated cylinder was weighed. It was then filled with the dry sample to the 100 mL mark and reweighed. The graduated cylinder was placed in a tapping box and the cylinder was gently tapped until there was no more reduction in volume. The minimum volume was recorded and the bulk density was calculated (Antal and Gronli,2003). The results are illustrated in Table 1.

Determination of moisture content (Oven Drying Method)

Into a flat–bottom metallic dish, finely divided asbestos were spreaded in a thin layer. It was firstly dried at 110 ºC for 1 h, the dish was covered, cooled and weighed. Sample (20 g) was uniformly spread over the asbestos layer. It was weighed as quickly as possible to avoid loss of moisture. The cover was removed and dried in a hot air oven at atmospheric pressure. A temperature of 100 ºC was maintained in the case of plant tissue. The duration of heating will vary with the type of tissues; 16 – 18 h is sufficient for most tissues. After drying, the lid was replaced, the sample was cooled in a desiccator, and it was reweighed. The sample was reheated, if necessary, until the consecutive weighings do not vary by more than 3 – 5 mg. Tissues which contain volatile organic constituents or high percentage of sugars cannot be brought to a constant weight. In such cases, a compromise procedure must be adopted. A standard technique should be employed. Drying at 55 ºC for four days is generally suitable. The sample after determination of moisture content– could be used for ashing and estimation of minerals (Buzarbarua, 2000). The results are shown in Table 2

Determination of ash contents of plant materials

Accurately weighed about 10 g of some plant materials such as Htiyo-war, Kathit-su, Pan-mezali, Rice-husk, and Baw-za-gaing were added to the five tared porcelain crucibles and the organic matter was dried and burnt off without flaming and finally heated in a muffle furnace at 823 K (550 ºC). Heating was continued until the resultant ashes were white in color and free from particles of unburnt carbon and fused 12 mps. Then, the crucibles

containing the residues were cooled to room temperature in a desiccator and weighed. Heating, cooling and weighing were repeated until a constant weight was obtained. The ash contents were then calculated (Buzarbarua, 2000). The results are shown in Table 3.

Preparation of Biochars from Some Plant Materials

Accurately 600 g wood chips of sample (Pan-mezali) was put into top-lit up draft (TLUD) Furnace. Three nails, which were triangle in position, were placed under a TLUD can. One–third of sample was mixed with fuel such as absolute ethyl alcohol (25 mL) and it was put into a TLUD-can as a top-layer. Then, they were started to burn with a candle flame. As burning continues, the crown was set up at the top of TLUD – can and then chimney , two feet height, was kept over the crown. After complete burning, a blue colored smoke comes out, it was stopped to prevent-ventilation, because air enters from bottom to top during burning which rise in temperature 252 ºC by using two feet chimney height for 26 min and it was allowed for cooling. And then, the weight of biochar was determined. Furthermore, biochars were prepared from 600 g wood chips of Pan-mezali by varying the chimney height (Antal and Gronli, 2003).

Similarly, biochars were prepared frombaw-za-gaing,kathit-su,htiyo-wa, and rice-husk by using above the same procedure.

Determination of Plant Nutrients in Biochars

Determination of nitrogen contents in biochars

0.1 g of finely ground biochar was transferred to a Kjeldahl flask. 1 mL of salicylic acid sulphuric acid mixture was added and thoroughly mixed. After 20 min, approximately 0.3 g sodium thiosulphate was added and gently heated until fumes are evolved. The mixture was cooled and 0.06 g of catalyst (a mixture of $CuSO_4$ and K_2SO_4 with the ratio of 1:2) and 0.75 mL nitrogen free H_2SO_4 were added. The mixture was heated on a digestion rack (electric) over a small flame for about an hour until the solution became apple green in colour. The digested sample was cooled and diluted with about 10 – 15 mL of distilled water to dissolve the sample.

The digest was transferred to the flask of the distillation unit through the side tube. The digestion flask was repeatedly washed with 2 – 3 mL of distilled water so that no digest is left in the flask. Excess of 40 % NaOH was added to the flask and the distillation process was continued. A conical flask containing 5 mL of 2 % boric acid solutionwas placed below the condenser. The distillation process was continued until 20 mL of distillate was collected in the receiving flask.

Two drops of Conway's indicator (mixed indicator of methyl red and bromocresol green) was added to the conical flask containing boric acid and it was titrated against 0.01 N HCl until a faint pink colour is obtained. Blank determination (without sample) using all the reagents as in the case of sample was also made (Buzarbarua, 2000) .

Determination of phosphorus content in biochars (Colorimetric Method)

2 mL of digested sample extract was transferred into 25 mL volumetric flask. A few drops of 2,4-dinitrophenol indicator was added and the contents was neutralized with 4 N ammonia. Any excess of ammonia was neutralized with 2 N H_2SO_4 and the volume to about two third of the flask was made with water. Sulphomolybdate solution (1 mL) was dispensed into it. The neck of the volumetric flask was washed with distilled water, and 0.5 mL of freshly prepared stannous chloride solution was added. The contents were thoroughly mixed and the volume was made to 25 mL. Then, within 4 to 20 mins the absorbance was recorded at 660 nm using a spectrophotometer. Following the above procedure prepare a standard curve containing 0.2 – 1.0 ppm phosphorous. The amount of phosphorous in the sample was found out from the standard cure and the results were expressed as mg /100 g dry weight of the sample after taking into account the dilution factors.

Determination of potassium content in biochars

The sample mineral extract to be analysed was aspirated into the instrument and the observation was recorded after compensation for the blanks. Readings of the standard solutions were periodically taken in between the samples to ensure proper functioning and reproducibility of the instrument response.

Determination of Volatile Matter Contents in Biochars

Accurately 5 g of the sample was weighed into a tared dish which had been previously dried and cooled in a desiccator. It was dried in an oven at 105 ºC (AOCS, recommendation 101 ºC ± 1ºC), and it was removed from the oven. And then,it was cooled in a desiccator and weighed. The procedure was repeated until the loss in weight does not exceed 0.05 % per 30 min drying period.

Results and Dicussion

Some Parameters of Plant Materials

Bulk density

Bulk density is an important property of biomass that directly affects the costs of distribution and storage. The bulk density as the physical characteristic depends on material composition, shape and dimensions of particles, orientation of particles, their density and size distribution, moisture content, pressure, contamination degree, rate and kind of deposit formation. The bulk densities of some plant materials such as Pan-mezali, Baw-zagaing, Kathit-su, Htiyo-wa, and Rice husk were determined. The results are shown in Table 1and Figure 1.

Table 1 Bulk Density of Plant Samples for Preparation of Biochars

Parameter	Baw-za-gaing	Htiyo-wa	Kathit-su	Panmezali	Rice husk
Density (g cm^{-3})	84.78	80.12	79.12	82.21	75.12
Moisture content (%)	2.65	1.75	2.32	1.89	3.25
Ash content (%)	1.2	0.13	0.20	0.18	0.62

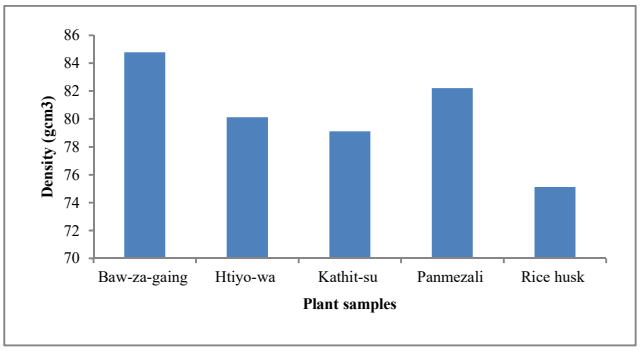

Figure 1 Bar graph showing bulk densities of plant samples for biochar preparation

Moisture content

Moisture content was determined by drying in an oven. This method consists in measuring the weight loss by plant materials due to the evaporation of waters. Drying methods are generally used as they give accurate results. The moisture content of rice-husk is the highest and the yield percent is the least as well as the moisture content of htiyo-wa is the least and the yield percent is the highest (Table 1 and Figures 2 and 3).

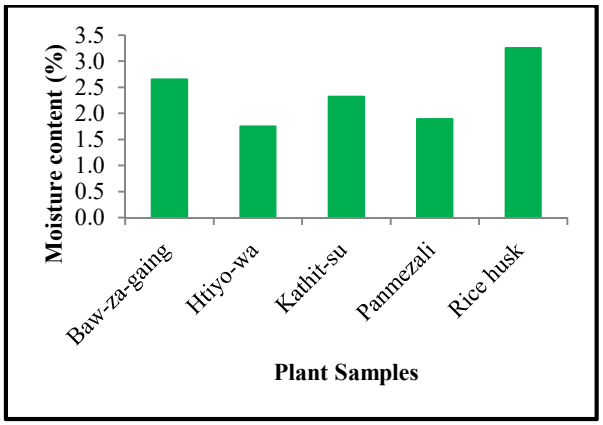

Figure 2 Bar graph showing moisture contents for plant samples used to prepare biochars

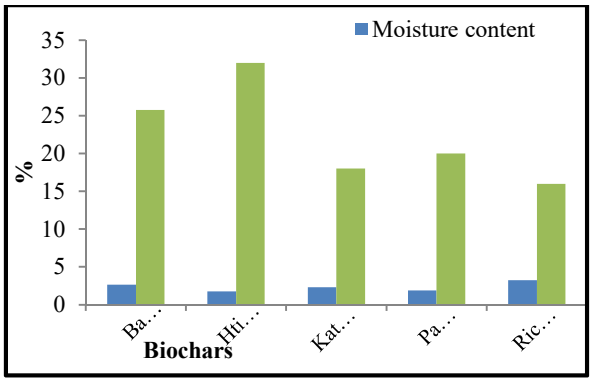

Figure 3 Bar graph for comparison of moisture content and yield percent of biochars

Ash content

Ash content of plant materials represents inorganic residues remaining after destruction of organic matter. It may not necessarily be exactly equivalent to the mineral matter as some changes may occur due to volatilization or some interaction between constituents. High ash content and / or a low alkalinity of the ash may in some cases be suggestive of the presence of adulterants. The acid insoluble ash is a measure of sand and other silicious matter present. Difficulty of effecting complete combustion in some sample, and the possible loss by volatilization on ignition may be overcome by moistening the substance to be ignited or the carbonaceous residue therefrom with concentrated sulphuric acid. In the determination of ash content in the collected plant materials, it was observed in Figure 4 that the ash content in Baw-zagaing was the highest and that of Htiyo-wa was the lowest. The results are shown in Table 1 and Figure 4.

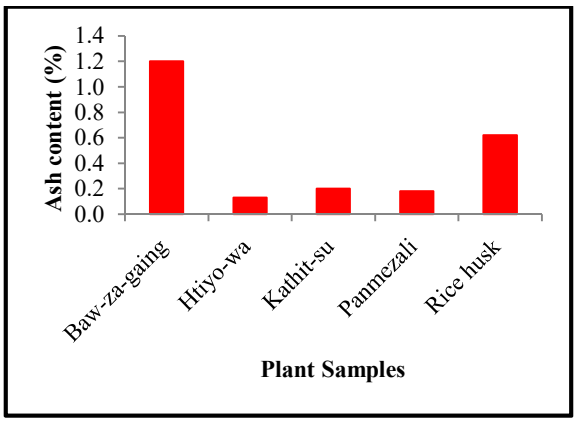

Figure 4 Bar graph showing ash contents of plant samples

Biochar from pan-mezali

Many methods can be used to produce biochar. Even with the same equipment process parameters can vary. It is generally known that the yield of products from pyrolysis varies heavily with temperature. The lower the temperature the more char is created per unit biomass. But TLUD method gave the yield percent between 10 and 19.04. Biochar was prepared from pan-mezali by using two feet chimney height and the rise of temperature was recorded. Furthermore, biochar was prepared by changing different chimney heights (1 feet – 3 feet) and the rise in temperature was recorded. In the preparation of biochar by changing the chimney height, the yield percent gave the highest at two feet-six inches. The results are shown in Table 2.With one feet chimney height rise in temperature to248 °C within 29 mins, with one and half feet chimney height rise in temperature to 250 °C within 30 mins, with two and half feet chimney height rise in temperature to 275 °C within 28 min and with three feet chimney height rise in temperature to272 °C within 22 min. were observed (Antal and Gronli, 2003).

Table 2 Biochar from Pan-mezali Wood at Different Chimney Heights

No.	Chimney height	Sample wt (g)	Time taken (min)	Temperature (ºC)	Product wt (g)	Yield (%)
I	1′ 0″	600	29	248	60	10.00
II	1′ 6″	600	30	250	60	10.00
III	2′ 0″	600	26	252	60	10.00
IV	2′ 6″	600	28	275	100	16.70
V	3′ 0″	600	22	272	60	10.00

Biochar from baw-za-gaing

Biochar was prepared from baw-zagaing by using two feet chimney height and the rise in temperature was recorded. Furthermore, biochar was prepared at different chimney heights and the rise in temperatures was recorded. In the preparation of biochar by changing the chimney height, the yield percent was the highest at two feet and one feet-six inches heights. The results are shown in Table 3.

Table 3 Biochar from Baw-za-gaing Wood at Different Chimney Heights

Sample No.	Chimney height	Sample wt (g)	Time taken (min)	Temperature (ºC)	Product wt (g)	Yield (%)
I	1′ 0″	400	18	280	50	12.50
II	1′ 6″	400	18	289	75	18.75
III	2′ 0″	400	18	300	75	18.75
IV	2′ 6″	400	20	320	50	12.50
V	3′ 0″	400	17	300	50	12.50

Biochar from kathit-su

Biochar was prepared from kathit-su by using two feet chimney height and the rise in temperature was recorded. Furthermore, biochar was prepared by changing different chimney heights and the rise in temperature was also recorded. In the preparation of biocharby changing the chimney height, the yield percent of the char was highest at one feet-six inches. The results are shown in Table 4.

Table 4 Biochar from Kathit-su Wood at Different Chimney Heights

Sample No.	Chimney height	Sample wt (g)	Time taken (min)	Temperature (ºC)	Product wt (g)	Yield (%)
I	1′ 0″	300	15	130	30	10.00
II	1′ 6″	300	16	128	50	16.69
III	2′ 0″	300	13	152	30	10.00
IV	2′ 6″	300	17	238	30	10.00
V	3′ 0″	300	13	200	30	10.00

Biochar from htiyo-wa

Biochar was prepared from htiyo-wa by using two feet chimney height and the rise in temperature was recorded. Furthermore, biochar was prepared by changing different chimney heights and the rise in temperature was recorded. In the preparation of biochar by changing the chimney height, the yield percent was the highest at two feet and two feet-six inches. The results are shown in Table 5.

Table 5 Biochar from Htiyo-wa Stem at Different Chimney Heights

Sample No.	Cheminey height	Sample wt (g)	Time taken (min)	Temperature (°C)	Product wt (g)	Yield (%)
I	1′ 0″	1050	50	280	180	17.14
II	1′ 6″	1050	53	279	180	17.14
III	2′ 0″	1050	56	296	200	19.04
IV	2′ 6″	1050	55	280	200	19.04
V	3′ 0″	1050	53	295	180	17.14

Biochar from rice-husk

Biochar was prepared from rice-husk by using two feet chimney height and the rise in temperature was recorded. Furthermore, biochar was prepared by changing different chimney heights and the rise in temperature was recorded but, it was observed that it did not give the complete combustion as the above samples.

Plant Nutrients in Biochars

Nitrogen content in biochars

Nitrogen content was estimated by the Kjeldahl method which is based on the determination of the amount of reduced nitrogen (NH_2 and NH) present in the sample (char). The various nitrogen compounds are converted into ammonium sulphate by boiling with concentrated H_2SO_4. The ammonium sulphate formed is decomposed with an alkali (NaOH), and the ammonium liberated is absorbed in excess of neutral boric acid solution and then titrated with standard acid. The results are shown in Table 6.

Table 6 Nitrogen Contents inBiochars

Parameter	Baw-za-gaing	Htiyo-wa	Kathit-su	Panmezali	Rice husk
Nitrogen content (%)	3.1	2.4	2.5	3.0	2.1

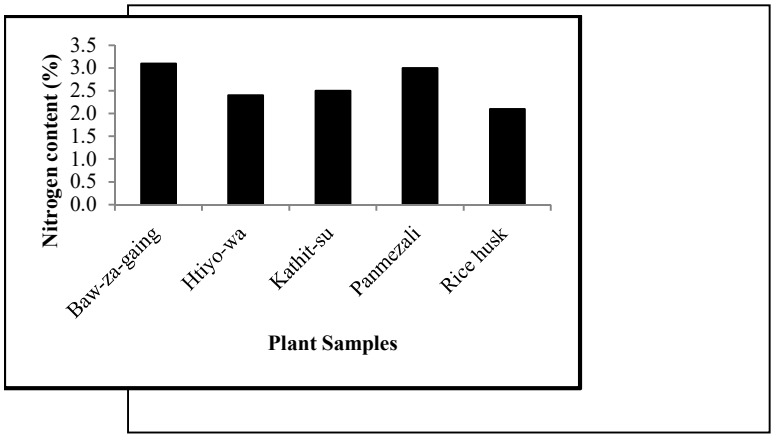

Figure 5 Bar graph showing nitrogen contents of biochars

Phosphorous content in biochars

For the determination of total phosphorous, the sample in which organic matter has been destroyed by tri-acid mixture is used. The phosphate containing solution is treated with sulphomolybdic acid to produce phosphomolybdic acid. This is then reduced by stannous chloride giving a blue coloured complex whose colour intensity is proportional to the amount of phosphate in the preparation. The results are shown in Table 7.

Table 7 Phosphorous Contents inBiochars

Parameter	Baw-za-gaing	Htiyo-wa	Kathit-su	Panmezali	Rice husk
Nitrogen content (%)	3.1	2.4	2.5	3.0	2.1

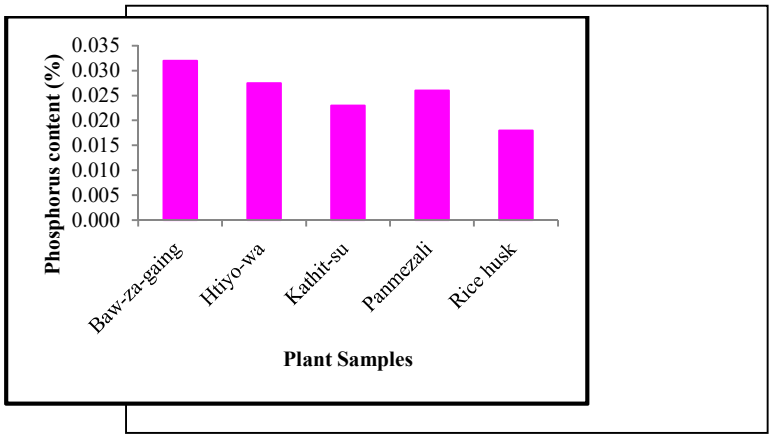

Figure 6 Bar graph showing phosphorous content of biochars

Potassium content in biochars

The atomic absorption spectrophotometry was used for the determination of potassium content. The plant tissue must first be properly processed before its introduction into the atomic absorption spectrophotometer (AAS). Dry ashing can effectively be used for determination of potassium in plant tissue. The results are shown in Table 8.

Table 8 Potassium Contents in Biochars

Parameter	Baw-za-gaing	Htiyo-wa	Kathit-su	Panmezali	Rice husk
Potassium contents (%)	0.1814	1.807	0.8459	0.8457	0.8471

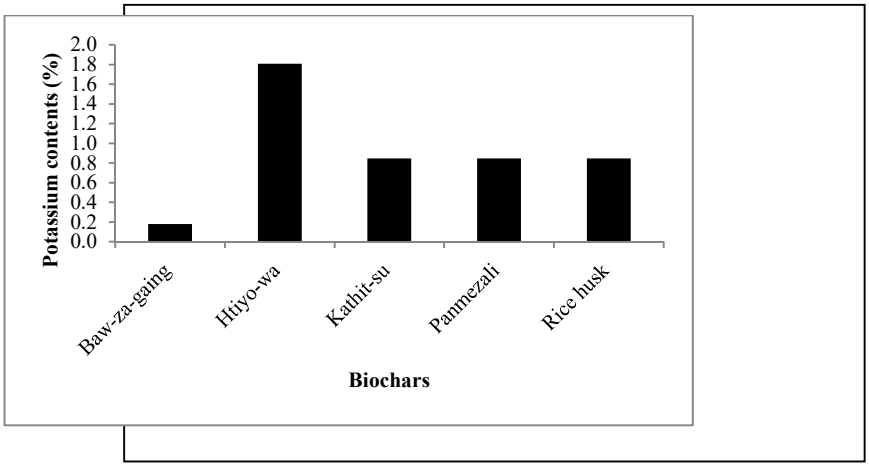

Figure 7 Bar graph showing potassium contents of biochars

Volatile Matter Contents in Biochars

The volatile matter other than water in biochar comprises all those liquid and tarry residues not fully driven-off in the process of carbonisation. If the carbonisation is prolonged and at a high temperature, then the content of volatiles is low. When the carbonisation temperature is low and time in the retort is short, then the volatile matter content increases. The volatile matter in biochar can vary from a the highest of 40% or the lowest to 5% or less. It is measured by heating away from air, a weighed sample of dry biochar at 900°C to constant weight. The weight loss is the volatile matter. Volatile matter is usually specified free of the moisture content, i.e. volatile matter - moisture or (V.M. - moisture). High volatile biochar is easy to ignite but may burn with a

smoky flame. Low volatile biochar is difficult to light and burns very cleanly. A good commercial biochar can have a net volatile matter content - (moisture free) of about 30%. High volatile matter biochar is less friable than ordinary hard burned low volatile biochar and so produces less fines during transport and handling. It is also more hygroscopic and thus has a higher natural moisture content.Volatile matter content in biochars was determined by using muffle furnance at 950 ºC. At this temperature some elements in biomass decomposed and changed into volatile gases. The results are shown in Table 9.

Table 9 Volatile Matter Contents of Biochars

Parameter	Baw-za-gaing	Htiyo-wa	Kathit-su	Panmezali	Rice husk
Potassium contents (%)	0.1814	1.807	0.8459	0.8457	0.8471

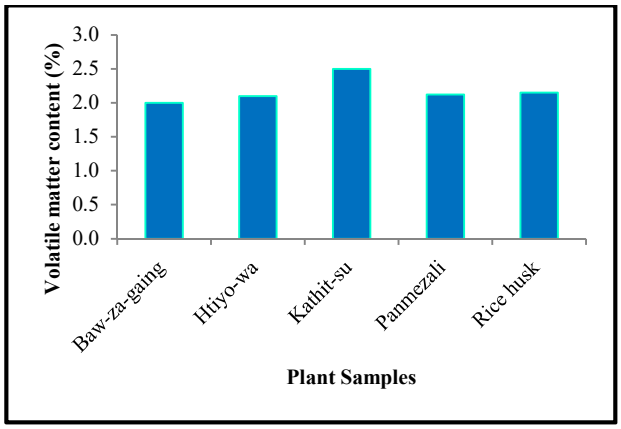

Figure 8 Bar graph showing volatile matter contents in biochars

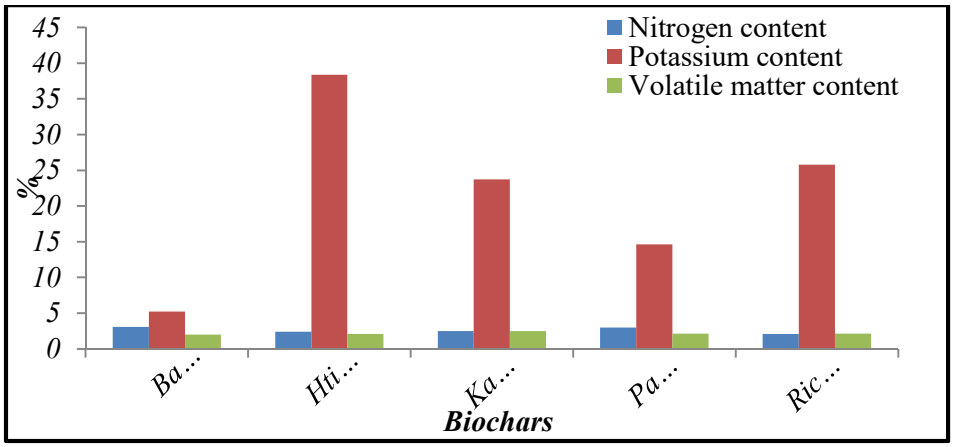

Figure 9 Bar graph for comparison of nitrogen, potassium and volatile matter contents of biochars

Fixed Carbon Content of Biochars

The fixed carbon content of biochars ranges Low between 95.775 % and around 98.72 %. Thus biochars consist mainly of carbon. The carbon content is usually estimated as a "difference", that is to say, all the other constituents are deducted from 100 as percentages and the remainder is assumed to be the per cent of "pure" or "fixed" carbon. The fixed carbon content is the most important constituent in metallurgy since it is the fixed carbon which is responsible for reducing the iron oxides of the iron ore to produce metal. But the industrial user must strike a balance between the friable nature of high fixed carbon biochar and the greater strength of biochar with a lower fixed carbon and higher volatile matter content to obtain optimum blast furnace operation. Figure 10 shows the comparison of fixed carbon content of some plant materials. It was observed that Baw-zagaing had the lowest content and Htiyo-wa had the highest content. The results are shown in Table 10.

Table 10 Fixed Carbon Contents of Biochars

Parameter	Baw-za-gaing	Htiyo-wa	Kathit-su	Panmezali	Rice husk
Fixed carbon content (%)	95.775	98.720	97.230	97.718	96.015

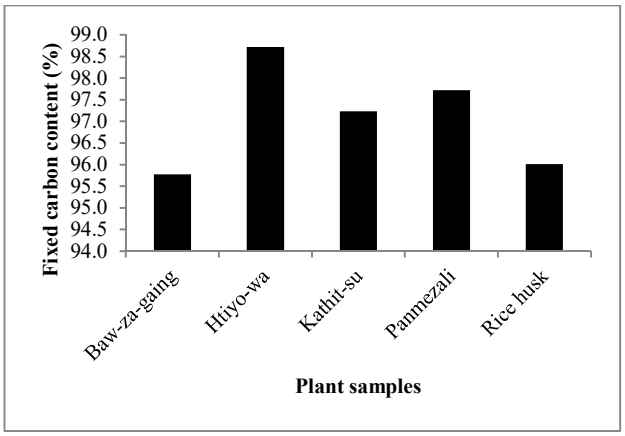

Figure 10 Bar graph showing fixed carbon contents in biochars

Conclusion

In the preparation of biocharsfrom some plant materials, it could be concluded as follows.The prepared biochars were obtained 10.0 %, 18.75 %, 10.0 %, 19.04 %, and 10.0 % yields from some plant materials: namely Pan-mezali, Baw-za-gaing, Kathit-su, Htiyo-wa and Rice-husk, respectively. In the process of biochar preparation, the effectiveness of chimney height in TLUD furnance was studied by using various chimney heights (1-3). The highest yield % of biochar from different plants materials was acquired in the range of 1’ 6’’- 2’ 6’’ chimney height. Among the five different samples, Htiyo-wa gave the highest yield % of biochar (19.04 %). Bulk densities of plant samples such as Pan-mezali 82.21 g/100 cm^3,

Baw-zagaing 84.78 g/100 cm^3 , Htiyo-wa 80.12 g/100 cm^3 , Kathit-su 79.12 g/100 cm^3, and Rice husk 75.12 g/100 cm^3 were determined . Moisture contents of plant materials were found out to be, Pan-mezali 1.89 %, Baw-za-gaing 2.65%, Htiyo-wa 1.75%, Kathit-su 2.32 %, and Rick husk 3.25 %. Ash contents of plant materials were found to be, Baw-za-gaing 1.20 % , Htiyo-wa 0.13%, Kathit-su 0.20 %, Panmezali 0.18% and Rick husk 0.62 %. The plant nutrients such as nitrogen , phosphorus , and potassium contents in biochars of some plant materials were also determined. The nitrogen contents of biochars from Pan-mezali, Baw-za-gaing, Htiyo-wa, Kathit-su, and Rice- husk were determined to be 3.0% , 3.1% , 2.4% , 2.5%, and 2.1%, respectively. The phosphorus contents of biochars from Pan-mezali, Baw-za-gaing , Htiyo-wa, Kathit-su, and Rick- husk were 0.026%,0.032% , 0.027%, 0.023%, and 0.018%, respectively. The potassium contents in biochars of Pan-mezali, Baw-za-gaing, Htiyo-wa, Kathit-su, and Rice- husk were also determined as, 0.8457 %, 0.1814 %, 1.807 %, 0.8459 %, and 0.8471 %, respectively. Similarly, the volatile matter contents of biochars were found to be 2.12%, 2.00%, 2.10 %, 2.50%, and 2.15%, respectively, from Pan-mezali, Baw-za-gaing, Htiyo-wa, Kathit-su, and Rice- husk. The fixed carbon contents were obtained 95.775 % from Baw-za-gaing, 98.72 % from Htiyo-wa, 97.23 % from Kathit-su, 97.718 % from Pan-mezali, and 96.015 % from Rice Husk, respectively. Further Study is to be made for the biochars for useful and as soil amendment in agriculture.

Acknowledgement

The authors would like to express their profound gratitude to the Department of Higher Education, Ministry of Education, Yangon, Myanmar, for giving the opportunity to do this research and Myanmar Academy of Arts and Science for allowing to present this paper.

.

References

Amutio ,M., Lopez , G., Alvarez ,J., Moreira ,R., Duarte ,G., Nunes ,J., Olazar ,M. and Bilbao, J.(2013). "Flash Pyrolysis of Forestry Residues from the Portuguese Central Inland Region within the Framework of the BioREFINA-Ter Project." vol.129, pp.512-518

Antal Jr., M.J. and Gronli, M. (2003). "The Art, Science, and Technology of Charcoal Production." *Industrial and Engineering Chemistry Research*, vol. 42(8), pp.1619-1640

Buzarbarua, A. (2000). *A Textbook of Practical Plant Chemistry*. New Delhi: S. Chang & Co. Ltd., pp.70-72

Lehmann, J. and Joseph, S. (Editor) (2009). *Biochar for Environmental Management: Science and Technology*. London: Earthscan, p.1

Rondon,M.A., Lehmann, J., Ramirez, J. and Hurtudo, M. (2007). "Biological Nitrogen Fixation by Common Beans (*Phaseolus vulgaris* L.) Increases with Bio-char Additions." *Biology and Fertility of Soils*, vol. 43(6), pp. 699–708

Wardle, D.A., Nilsson, M. and Zackrisson, O. (2008). "Fire-derived Charcoal Causes Loss of Forest Humus." *Science*, vol. 320 (5876),p. 629

SYNTHESIS AND CHARACTERIZATION OF RICE HUSK SILICA FROM RICE HUSK ASH AND It's UTILIZATION FOR POROUS CERAMIC CANDLE FILTER

Naw Mu Htoo[1], Mya Kay Thi Aung[2], Kyi San Aye[3]

Abstract

This work concerns with the synthesis and characterization of rice husk silica (RHS) from rice husk ash (RHA) and its utilization for porous ceramic candle filter. Ma Naw Thukha rice husk was used to prepare RHA, by calcinations of rice husk (RH) at 700 ºC for 6 h. Preparation of silica powder was carried out from RHA by using precipitation method. The silica from RHA was extracted by 2.4 M NaOH for 3 h and then precipitated by adding concentrated H_2SO_4.The characterization of sample was carried out by modern techniques (SEM, FT IR, XRD, EDXRF) and determination of physicochemical properties using conventional methods. SEM micrograph indicates sponge like nature. XRD diffractogram exhibits an indication of amorphous silica. From FT IR spectral assignment, the band at 1150 to 1000 cm^{-1} indicates the stretching vibration of Si-O (asym) band in Si-O-Si group. From EDXRF analysis, the highest relative abundance of silica was found to be 99.33 % in RHS. The yield percent of RHS was found to be 52.7 %. Ceramic candle filter (CCF) was prepared by using the raw materials such as RHS, sand, char and clay. The physicochemical properties of CCF were also determined by conventional methods. The performance of ceramic candle filter (CCF) made from a mixture of sand, char, natural clay and RHS in removing chloride from sodium chloride solution was investigated. Removal of chloride ion from sodium chloride solution was studied with different parameters (flow rate for 100 mL fraction: 5, 10, 15, 20, 30, 40, 60 min; different concentrations: 100,200 and 400 ppm). Determination of chloride ion in sodium chloride solution was determined by argentometric method. From the results, the optimum condition for ceramic filter was found to be 69.58 mgg^{-1} of sorption capacity at a flow rate of 20 min for 100 mL fraction. Removal of chloride ion from lakes of Naung Bo Village (NB) and San Pyaw Village (SP), Naung Bo Group, Ka Wa Township, Bago Region was carried out. From the results, ceramic candle filter (CCF) was found relatirly as an effective adsorbent for saline water treatment.

Keywords : Rice Husk Ash (RHA), Rice Husk Silica (RHS), calcination, precipitation method, argentometric method, ceramic candle filter (CCF)

[1]Lecturer, Department of Chemistry, Military Institute of Nursing and Paramedical Science
[2] Lecturer, Dr, Department of Chemistry, University of Yangon
[3]Associate Professor, Dr, Department of Chemistry, Bago University

Introduction

Paddy rice is grown on every continent except Antarctica and the extent of paddy cultivation covers about 1 percent of the earth's surface. More than half of the world's population depends on rice as a staple food and it ranks second to wheat in terms of cultivation area and production. Production of rice is dominated by Asia, where rice is the only food crop that can be grown during the rainy season in the waterlogged tropical areas. Asia generates over 90 percent of world rice production (Noor and Rohasliney, 2012).

Rice husk, as one of the most trifling agricultural products, can act as a good absorbent by absorbing heavy metals and removal of colour. Rice husk ash (RHA) was obtained after burning. The beneficiation of rice husk ash has been used in many applications. RHA can be an economically variable raw material for production of silica gels and powders. The amorphous nature of RHA silica makes it extractable at lower temperature, and hence provides a low energy method. Rice husk ash contains over 80% of silica. (Abedi-Kopai and Mohri-Esfahani, 2012; Rafiee *et al.,*2012 ; Thudaij and Nuntiya,2008).

The most important aspect in improving the health of the people is to provide communities with safe and clean water. In this modern age, the 21st century, an estimated 1.1 billion people worldwide still do not have access to safe potable water. A large percentage of these people are from the developing world, especially in the rural areas and low-income communities (WHO, 2007).

Safe drinking water is also an immediate priority in most emergencies. When normal water supplies areinterrupted or compromised due to natural disasters, complex emergencies, or outbreaks, responders often encourage affected populations to boil or disinfect their drinking water to ensure its microbiological integrity. Recently, point-of-use water treatment (PoUWT) options verified in the development context have been recommended for use in emergencies (Lantagne and Clasen, 2009).

Point-of-use or household water treatment methods can be used to improve the quality and safety of water for drinking in situations where there is no safe centrally treated water supply or where the treated water supply system has been compromised. Some studies have shown that simple and relatively

inexpensive home water treatment and storage methods can result in substantial improvements in the microbial quality of drinking water and reduced risks of illness and death, even in the absence of improved sanitation. There are four household water treatment systems (HWTS) in removing bacterial and chemical contaminants: the biosand filter (BSF), the bucket filter (BF), the ceramic candle filter (CCF) and the silver-impregnated porous pot filter (SIPP) (Mwabi,2011).

In this study, RHS from RHA will be prepared and characterized by conventional and modern techniques. Ceramic candle filter (CCF) was made with RHS as raw material. Sorption capacity of CCF for the removal of chloride ion from sodium chloride solution were also be investigated.

Materials and Methods

Collection of Rice Husk (RH)Sample

Ma Naw Thukha rice husk was collected from Aung Thuka Rice Mill, Bago Region, Bago Township. The locally available rice husk RH was washed with water and dried at room temperature as shown in Figure 1. The sample was stored in air tight plastic bags.

Figure 1 Rice husk

Collection of Water Samples

Water samples were collected from lakes of Naung Bo and lake of San Pyaw, Naung Bo group, Ka Wa Township, Bago Region. CCF was prepared by using the raw materials such as RHS, sand, char and clay.

Preparation and Characterization of RHS

Preparation of Rice Husk Ash (RHA) from RH

RH (380g) was preheated on electrical hot plate until to obtain char. This rice husk char (RHC) was burnt in porcelain crucible using muffle furnace about 6 h at 700 ºC until to obtain a grey ash. After burning, the ash was cooled at room temperature and then passed through the 180 mesh size sieve. The sample was stored in the desiccators at room temperature.

Preparation of Rice Husk Silica (RHS)

10 gram of RHA sample was stirred in 80mL of 2.4 M sodium hydroxide solution. RHA was boiled in a 250 mL beaker with covering at 90-100 °C for 3h. The solution was filtered and the residue was washed with 20mL distilled water. The filtrate was allowed to cool to room temperature and 5 M $H_2SO_4$was added until pH 2 and then NH_4OH was added until pH 8 was reached and allowed to cool to room temperature. The filtrate was then dried at 120 °C for 12 h and refluxed with 6 M HCl for 4 h and then washed repeatedly using deionized water to make it acid free. It was dissolved in 2.4 M NaOH solution by continuous stirring for 10 h on a magnetic stirrer and then concentrated H_2SO_4 was added to adjust pH in the range of 7–8. The precipitated silica was washed repeatedly with warm deionized water until the filtrate became completely alkali free and it was dried at 50 °C for 48 h in the oven.

Characterization of prepared samples

Determination of physicochemical properties of prepared sample was done by conventional methods. The results are shown in Table 1.RHS was characterized by modern techniques (SEM, FT IR, EDXRF, XRD).

Preparation of Ceramic Candle Filter and its Sorption Study

Preparation of ceramic candle filter (CCF)

Ceramic Candle Filter (CCF) was prepared by using the raw materials such as RHS, sand, char and clay. The processfor making of ceramic candle

were grinding, screening, mixing, modeling drying and firing. The filter was equipped with a flow rate controller as shown in Figure 2 (a) and (b).

Determination of physicochemical properties of CCF

Determination of physicochemical properties of CCF was carried out using conventional methods. The results are shown in Table 3.

Determination of sorption study of prepared CCF

Removal of chloride ion from sodium chloride solution was studied with different parameters (flow rate for 100 mL fraction : 5, 10, 15, 20, 30, 40, 60 min, different concentrations : 100, 200, 400 ppm). Concentration of chloride ion in sodium chloride solution was determined by Argentometric method. The results were shown in Tables 4,5 and Figures 7 (a, b, c, d, e, f, g), Figure 8.

Removal of Chloride Ion from Lakes of Naung Bo and San Pyaw by CCF

The saline water collected from lakes ofNaung Bo and San Pyaw were treated for the removal of chloride ion by CCF at a flow rate of 20 min for 100 mL fraction. The results are shown in Table 6 and Figure 9.

(a)

(b)

Figure 2. (a) Ceramic
(b) Ceramic Candle Filter

Results and Discussion

Physicochemical Analysis of Prepared Samples

Rice husk ash (RHA) was obtained by heating rice husk in muffle furnace for 6 h at 700˚C. RHS was prepared from RHA using precipitation method.

The characteristic of the physicochemical properties of prepared samples were determined. Table 1 showsthe physicochemical properties of prepared samples. It was found that pH value is nearly neutral. Bulk density and moisture content of RHA were smaller than that of RHS.

Table 1 Physicochemical Properties of Prepared Samples

Sample	pH	Moisture content (%)	Bulk density (g mL^{-1})
RHA	6.5	4	0.29
RHS	7.5	8	0.45

Vogel, 1968

C**haracterization of RHS**

SEM analysis

Surface morphology of sample was observed by SEM analysis. SEM micrograph of RHS is shown in Figure 3. It indicated the sponge like nature of RHS.

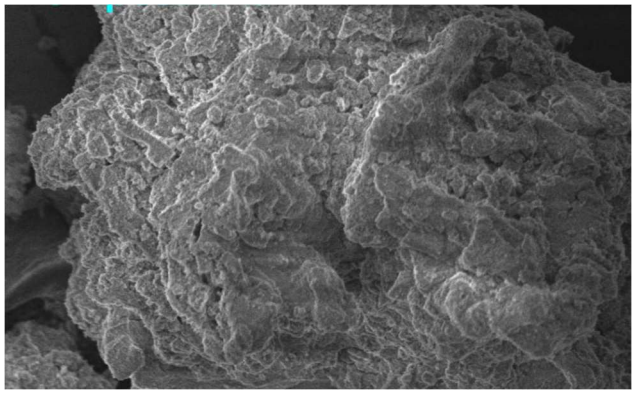

Figure 3 SEM microphotograph of RHS

FT IR analysis

FT IR analysis of silica is presented in Figure 4. The result is shown in Table2. From the FT IR spectral assignment, the strong bands at a range from 1150 cm^{-1} to 1000 cm^{-1} are due to asymmetric stretching mode of Si-O-Si group.

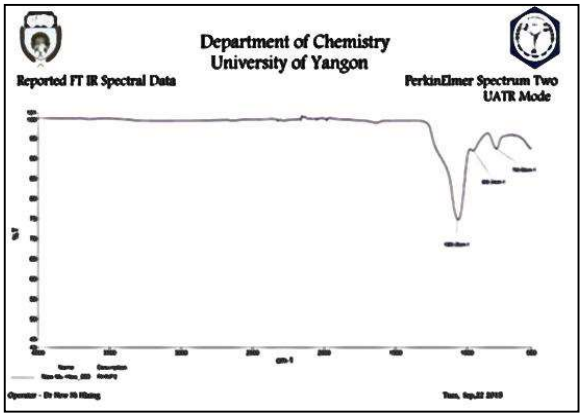

Figure 4 FT IR spectrum of RHS

Table 2 FT IR Spectral Assignment of RHS

Observed Frequency (cm^{-1})	*Literature Frequency (cm^{-1})	Band Assignment
1060	1150-1000	$\upsilon_{Si-O(asym)}$

*Nakamoto, 1986

XRD analysis

The X-ray diffraction pattern of RHS is shown in Figure5. The XRD pattern exhibits broad maximum, extending 2θ value from 19°to 25° for RHS which is an indication of amorphous silica.

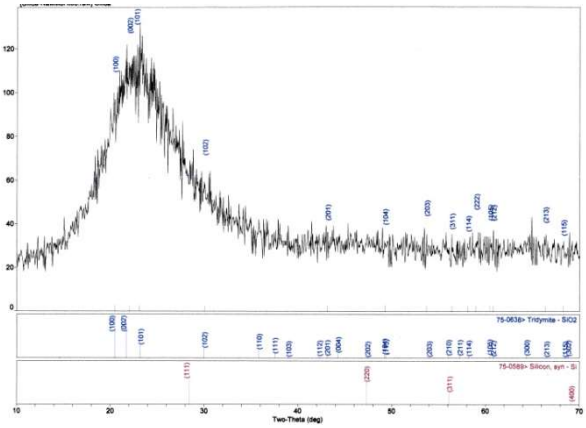

Figure 5 XRD spectrum of RHS

EDXRF analysis of prepared sample

The EDXRF spectra exhibited the relative abundance of silica in RHS described in Figure 4. From these results, it was obvious that the relative abundance of SiO_2 was high in RHS. Other compounds (K_2O, CaO,Fe_2O_3, MnO, ZnO, and CuO, etc) were also observed. The relative abundance of silica was 99.33 %.

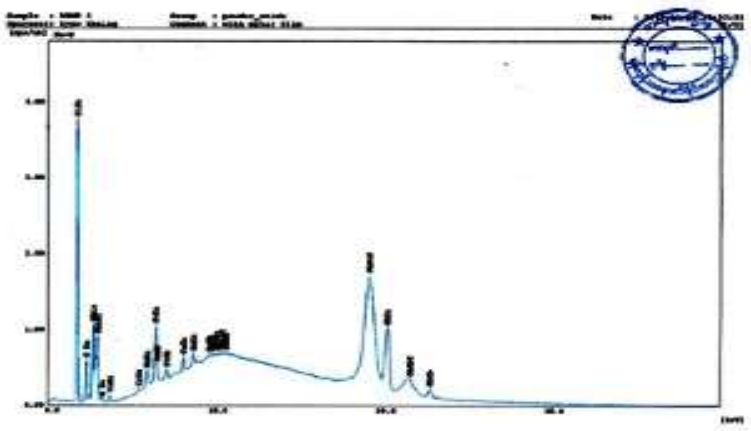

Figure 6 EDXRF spectrum of RHS

Characterization of Ceramic Candle filter (CCF)

Determination of Physicochemical Properties of CCF

The results of bulk density, porosity, water absorption and flow rate are shown in Table 3.

Table 3 Physicochemical Properties of CCF

Bulk Density ($g\ mL^{-1}$)	Porosity (%)	Water Absorption (%)	Flow rate (L/h)
0.71	53.39	67.63	1.4

ASTM (2010)

Removal of chloride ion from sodium chloride solution by CCF with different flow rates

Removal of chloride ion from sodium chloride solution with different flow rates for 100 ml fraction in 5,10,15,20,30,40,60 min can be seen in Figure 7 (a, b, c, d, e, f, g). The results are shown in Table 4. It can be observed that sorption capacity increased as the flow time increased but decreased after 20 min flow time was used.

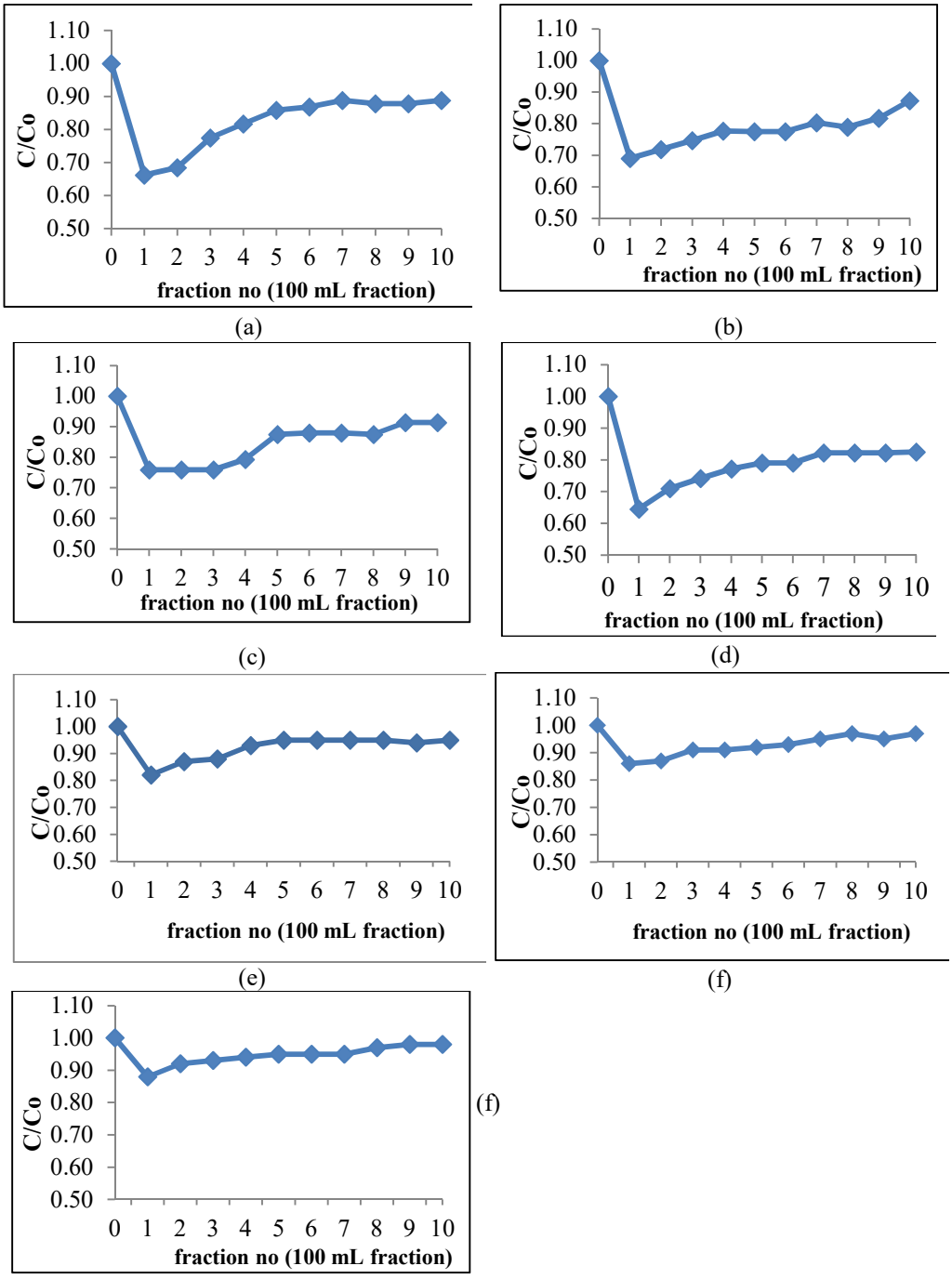

Figure 7 : Breakthrough curve for removal of chloride ion from 100 ppm NaCl solution by CCF with a flow rate of 100 mL fraction for (a) 5 min (b) 10 min (c) 15 min (d) 20 min (e) 30 min (f) 40 min (g) 60 min

Table 4 Removal of Chloride Ion with Different Flow Rates

Flow time for 100 ml fraction(min)	Sorption capacity of CCF (mg g^{-1})
5	29.82
10	39.96
15	49.70
20	69.58
30	49.70
40	29.82
60	19.88

Removal of chloride ion from sodium chloride solution by CCF with different concentrations

The effect of initial concentration of sodium chloride was studied using various concentrations such as 100, 200, 400 ppm. The removal percent of chloride ion by CCF decreased as the initial concentration was increased. The removal percent of chloride from 100 ppm sodium chloride solution was found to be the highest value (36%). The results are shown in Table 5 and Figure 8.

Table 5. Percent Removal of Chloride Ion from Sodium Chloride Solution by CCF

Initial concentration (ppm)	Final concentration of chloride ion (ppm)	Percent removal(%)
100	64	36
200	148	26
400	336	16

Flow rate for 100 ml faction = 20 min

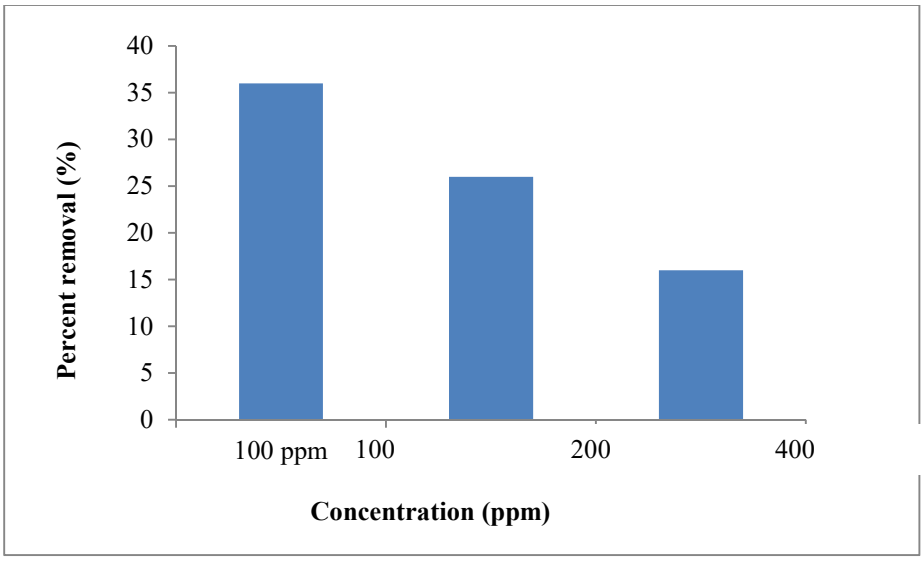

Figure 8 Percent removal of chloride ion in 100 ppm, 200 ppm and 400 ppm by CCF with a flow rate of 100 mL fraction for 20 min

Removal of Chloride Ion from Lakes of Naung Bo and San Pyaw by CCF

The saline water collected from lakes of Naung Bo and San Pyaw were treated for the removal of chloride ion by CCF. The results are shown in Table 6 and Figure 9.CCF is the effective and efficient adsorbent for removal of chloride ion in SP (2) compared to NB and SP (1).

Table 6 Percent Removal of Chloride ion by CCF

Sample	Initial concentration of chloride ion (ppm)	Final concentration of chloride ion (ppm)	Percent removal (%)
NB	55	38	31
SP (1)	527	476	10
SP (2)	69	46	33

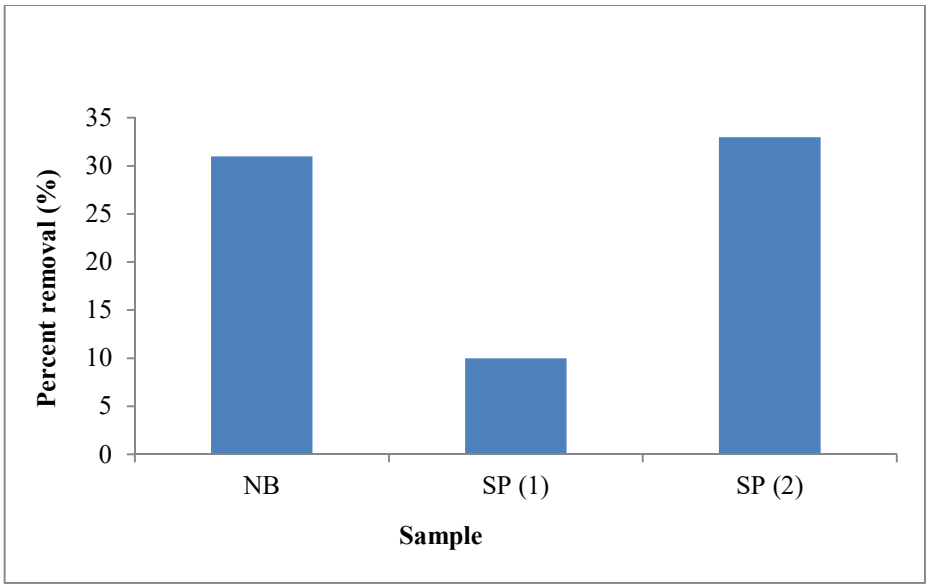

Figure 9 Percent removal of chloride ion in N B, SP (1) and SP (2) by CCF with a flow rate of 100 mL fraction for 20 min

Conclusion

Ma Naw Thu Kha rice husk was collected from Aung Thukha Rice Mill, Bago Township, Bago Region. Rice Husk Ash (RHA) was prepared from Rice Husk (RH) by calcinations at 700°C for 6 h in muffle furnace. Preparation of rice husk silica (RHS) was carried out from RHA using precipitation method. From the results of physicochemical properties determination, the pH of the samples were nearly 7. The bulk densities of RHA and RHS were 0.29 and 0.45 g mL^{-1} respectively. The moisture content of RHA and RHS were found to be 4 % and 8 % respectively. From SEM analysis, RHS was found to have sponge like nature. From FT IR spectral assignment, the frequency between 1150 to 1000 cm^{-1} indicates the stretching vibration of Si-O (asym) band indicating that silica is present in RHS. According to XRD diffractogram, RHS exhibited broad maximum extending 2θ values from 19° to 25°. An indication of amphorous silica was observed. From ED XRF spectrum, the

highest relative abundance of silica was found to be 99.33% in RHS.CCF was prepared by using the raw materials such as RHS, sand, char and clay. The bulk density of CCF was found to be 0.71 g mL^{-1}. The porosity, flow rate and water absorption of CCF was found to be 59.39 %, 1.4 L h^{-1} and 67.63 % respectively. The sorption capacity of CCF was observed the highest in the removal of chloride from 100 ppm sodium chloride solution with the flow rate of 20 min for 100 mL fraction. Moreover, CCF was studied for the removal of chloride ion from lakes of Naung Bo and San Pyaw. CCF is the effective and efficient adsorbent for removal of chloride ion in SP (2) compared to NB and SP (1).

Acknowledgements

The authors would like to express their profound gratitude to the Department of Higher Education, Ministry of Education, Myanmar, for giving opportunity to do this research and Myanmar Academy of Arts and Science for allowing to present this paper.

References

Abedi-Koupai, J. and Mohri-Esfahani.E. (2012).“Desalination of Water Using Nanoparticles of Husk Ashes in Sand Filter”. *Proceedings of the 4th International Conference on Nanostructures (ICNS4*) , pp. 1150-1152

ASTM. (2010). *Standard Test Method for Apparent Porosity, Water Absorption, Apparent Specific Gravity, and Bulk Density of Burned Refractory Brick and shapes by Boiling Water.* United States: ASTM International, pp. 6-8

Lantagne, D. S. and Clasen, T. (2009).“Point of Use Water Treatment in Emergency Response”. London: *London School of Hygiene and Tropical Medicine*, vol. 80(5), pp. 819–823

Mwabi, J. K., Adeyemoand, F. E. and Mahlangu, T. O. (2011) .“Household Water Treatment Systems: A Solution to the Production of Safe Drinking Water by the Low-income Communities of Southern Africa”. *Physics and Chemistry of the Earth,* vol. 36, pp. 1120–1128

Nakamoto, K. (1986). *Infrared and Ramann Spectra of Inorganic and Coordination Compounds.* New York: 2nd Edition, John Wiley and Sons, Inc., pp. 200-201

Noor, S. S. and Rohasliney, H. (2012).“Rice Husk as Biosorbent”. *Health and the Environmental Journal,* vol. 3(1), pp. 89-95.

Rafiee, E., Shahebrahimi, S., Feyzi, M. and Shaterzadeh, M. (2012). “Optimimzation of Synthesis and Characterization of Nano Silica Produced from Rice Husk (Common Waste Material)”. *International Nano Letters,* vol. 2(29), pp. 1-8

Thudaij, N. and Nuntiya, A. (2008).“Preparation of Nanosilica Powder from Rice Hask by Precipitation”.*Chiang Mai Journal Science,* vol. 35(1), pp. 266-211

Vogel, A.I. (1968). *Quantitative Inorganic Analysis.* London: 3rdEd., Longmans Co. Ltd., pp. 116-120

World Health Organization.(2007). *Desalination for Safe Water Supply.* Geneva: pp. 35-36

PREPARATION OF MALTODEXTRIN USING STARCH FROM *Musa Chilliocarpa* BACKER AND A-AMYLASE FROM *Phaseolus Vulgaris* L.

Latt Latt Chaw[1], Ni Ni Sein[2], Thida Win[3]

ABSTRACT

Banana maltodextrin was prepared by enzymatic hydrolysis of banana starch by using α-amylase from immature *Phaseolus vulgaris* L. (White Kidney bean) seeds. α-Amylase from immature *Phaseolus vulgaris* L. (White Kidney bean) seeds was isolated by ammonium sulphate precipitation (20-60 %) followed by Sephadex G- 100 gel filtration chromatography. The optimum pH and optimum temperature of α-amylase were 5.6 and 50 ^{o}C, respectively. Starch was isolated from unripe *Musa chilliocarpa* Backer cv. Pheegyan (Banana) and yield percent was 43.6 %. Banana starch was characterized by SEM, XRD and TG-DTA methods. Banana maltodextrin (yield percent of 5.5 %) was found to have a dextrose equivalent of 6 by phenol-sulphuric assay method. Low dextrose equivalent maltodextrin was characterized by SEM and some of its chemical properties were also determined.

Keywords: banana maltodextrin, *Musa chilliocarpa* Backer,*Phaseolus vulgaris* L., α-amylase , banana starch, dextrose equivalent

Introduction

The white kidney bean (*Phaseolus vulgaris* L.) (Figure 1) is a warm season annual plant, with quick growth, weak stems usually climbing and alternate compound leaves, composed of three large leaflets; the flower vary in color from white to purple. The tender pods are used as vegetable. The seeds are rich in protein. White kidney beans are extensively cultivated in all parts of Myanmar. So the white kidney beans can be a cheaper source for the alpha

[1] Lecturer , Dr., Department of Chemistry, Kyaukse University
[2] Professor (Retired), Dr., Department of Chemistry, University of Yangon
[3] Rector, Dr., University of Mandalay

amylase which is extensively used in food, textiles and pharma industries (Nerkar *et al*., 2011). Scientific classification of white kidney bean (Kress *et al*., 2003) is described as follows:

Family	:	Fabaceae
Genus	:	*Phaseolus*
Binominal Name	:	*Phaseolus vulgaris* L.
English Name	:	Common bean, Kidney bean, Bush bean, French bean
Myanmar Name	:	Bo-sa-pe

(a) (b) (c)

Figure 1. White kidney bean (*Phaseolus vulgaris* L.)
(a) flower (b) plant (c) pods and seeds

Banana belongs to the family *Musaceae*, genus *Musa* and is a general term embracing a number of species or hybrids in this genus. Bananas are an important foodcrop in many countries and grown extensively in the tropical and subtropical regions. Banana is one of the vegetable fruits that grow well in the tropics (Ihekoronye and Nogddy, 1985). Banana though generally consumed as a dessert fruit, also contains high content of starch when unripe and could be exploited as a starch source. Green bananas have a large amount of starch during its unripe stage (Cordenunsi and Lajolo, 1995).

Amylases are important enzymes employed in the starch processing industries for the hydrolysis of polysaccharides such as starch into simple sugar constituents (Adu *et al*., 2005). α-Amylase (1,4-D-glucan

glucanohydrolase, E.C.3.2.1.1) catalyzes the random hydrolysis of amylose, amylopectin and related polysaccharides to smaller oligosaccharides and glucose. α-Amylases are hydrolytic enzymes that are widespread in nature, being found in animals, microorganisms and plants (Franco *et al.*, 2000). Amylases (α- amylase) are among the most important enzymes in present-day biotechnology. α -Amylase was used as the raw material in various industries, such as food industry, detergent industry, textile industry and pharmacy industry. α - Amylase was widely used in the food industry such as baking, brewing, fruit juices, starch syrups.

Maltodextrin $(C_6H_{10}O_5)_n.H_2O$ is a mixture of saccharides with a molecular weight between polysaccharides and oligosaccharides with dextrose equivalent lower than 20 (not sweet), which is available as white powders mostly or concentrated solution (Alexander, 1992). Maltodextrin is more soluble in water than native starches, also is cheaper in comparison with other major edible hydrocolloids and its solutions have a bland flavour and smooth mouthfeel (Dokic-Baucal *et al*., 2004).

In Myanmar, banana is abundant because it can grow all year long. Therefore, this research focuses on the use of low cost banana to prepare maltodextrin using α- amylase from white kidney bean seeds as a route to improve the value - added raw material.

Materials and Methods

Sample Collection

Immature white kidney bean (*Phaseolus vulgaris* L.) seeds and unripe banana fruits (*Musa chilliocarpa*), locally known as phee–gyan– nget–pyaw, were collected from Tawma Village, Sint Kaing Township, Mandalay Region.

Extraction of α-Amylase from Immature White Kidney Bean Seeds

Immature white kidney bean seeds (200 g) were ground in a mortar to obtain a homogeneous mixture. Into it, 500 mL of acetate buffer (pH 5.6) was added and stirred for 30 min. The mixture was filtered through two layers of muslin and the filtrate was collected. Then it was centrifuged at 3000 rpm for

15 min to obtain crude enzyme extract. The crude α- amylase enzyme extract was first brought to 20 % saturation with solid ammonium sulphate (analar) (66.24 g). After centrifugation for 15 min at 3000 rpm the supernatant was applied again with ammonium sulphate (143.4 g) to achieve 60 % saturation. The resulting enzyme precipitate was collected by centrifugation at 3000 rpm for 15 min.

Crude α-amylase (0.382 g) was dissolved in 5 mL of 0.1 M acetate buffer (pH 5.6). This solution was applied to a Sephadex G-100 gel filtration column previously equilibrated with the same buffer. The flow rate was adjusted to 12 mL/h by a mini pump and 1.5 mL fractions were collected per tube using a fraction collector. After collection, the protein content of each tube was checked by measuring the absorbance at 280 nm wavelength using a UV-visible spectrophotometer. Each tube was also measured for α-amylase enzyme activity by Nelson-Somogyi method.The fraction that had the highest activity of α-amylase enzyme was pooled. The protein content and α-amylase activity of pooled enzyme fraction were analyzed by the Biuret method and α-amylase activity was measured by Nelson-Somogyi method (Nelson and Somogyi, 1973). The pooled fraction showing the highest α-amylase activity was concentrated with acetone 1:9 ratio.

Determination of Optimum pH of α- Amylase- catalyzed Reaction

A 0.1 mL of 2 % (w/v) starch solution was added into a test tube containing 0.1 mL of hydrochloric acid–sodium chloride buffer solution (pH 1) and the contents were mixed well. Into another test tube 0.1 mL of enzyme solution was added. Both test tubes were kept at 30 ^{o}C for 10 min to reach the thermal equilibrium. The former solution mixture was poured into a test tube containing 0.1 mL of enzyme solution and the contents were mixed well. Then the solution mixture was kept at 30^{o}C. After 10 min , the reaction was interrupted by adding 1 mL of alkaline copper reagent solution. The contents were then mixed thoroughly. The test tube was heated on a vigorously boiling water bath for 10 min. Next, the test tube was cooled under running tap water for 1 min and 1 mL of arsenomolybdate colour reagent solution was added into the test tube. After shaking vigorously, this solution was diluted to 10 mL with distilled water and mixed by inversion. The absorbance was measured at

750 nm. For blank solution, 0.1 mL of distilled water was used instead of 0.1 mL of prepared enzyme solution.

The whole of the above procedure was repeated with hydrochloric acid–sodium chloride buffers (pH 1.6 and 2.2), acetate buffers (pH 3.6, 4.6, and 5.6), phosphate buffers (pH 6.2, 7.0, and 8.0) and sodium carbonate–bicarbonate buffers (pH 9.6 and 10.6).

Determination of Optimum Temperature of α-Amylase-Catalysed Reaction

A 0.1 mL of 2 % (w/v) starch solution was added into a test tube containing 0.1 mL of acetate buffer (pH 5.6) solution and the contents were mixed well. Into another test tube 0.1 mL of enzyme solution was added. Both test tubes were kept at 20 ºC for 10 min to reach the thermal equilibrium. The former solution mixture was poured into a test tube containing 0.1 mL of enzyme solution and the contents were mixed well. Then, the solution mixture was kept at 20ºC. After 10 min incubation, 1 mL of alkaline copper reagent solution was added to stop the reaction. The test tube was heated in a vigorously boiling water bath for 10 min. Next, the test tube was cooled under running tap water for 1 min and 1 mL of arsenomolybdate colour reagent solution was added into the test tube. After shaking vigorously, this solution was diluted to 10 mL with distilled water and mixed by inversion. The absorbance was measured at 750 nm. For blank solution 0.1 mL of distilled water was used instead of 0.1 mL of enzyme solution.

The whole of the above procedure was repeated except that the temperature was fixed variously at 30ºC, 40ºC, 45ºC, 50ºC, 55ºC, 60ºC, 65ºC, 70ºC and 75ºC.

Extraction of Starch from Banana

Banana starch was isolated using the procedure of Kim*et al* (1995) with some modification. The fruits were peeled and cut into 5 to 6 cm cubes (500 g total weight), immediately rinsed in sodium sulphite solution (1.22 g / L) and macerated with the sulphite solution (1:1 ratio) for 2 min at low speed in a blender. The homogenate was consecutively sieved through 50 and

100 meshes until the washing water was clear. The solution was centrifuged at 3000 rpm for 30 min and the sediment dried in air for 48 h, and finally ground with a mortar and pestle until passing through a 100 mesh sieve. Yield percent of banana starch was 43.6 %.The resulting banana starch was stored at room temperature in a sealed container.

Preparation of Maltodextrin by Enzymatic Hydrolysis of Banana Starch using α-Amylase

Maltodextrin was prepared from banana starch according to the procedure of Bello- Perez *et al* (2002).

A banana starch (20 g) was mixed with 100 mL of distilled water. The suspension in distilled water was adjusted to pH 6.5 and then gelatinized in a boiling water bath for 10 min. After cooling to 60°C, α-amylase from white kidney bean seeds was added to achieve a concentration of 0.01 % (w/v). The flask was tightly covered and the hydrolysis reaction was allowed to proceed at 60°C for 15 min under mild agitation. After that, the sample was cooled down to 4°C in water-ice bath and then centrifuged at 3000 rpm for 30 min. The supernatant was recovered and the enzyme inactivated by heating in a boiling water bath for 10 min after addition of 0.1 M hydrochloric acid to reach a pH value of 4.02. After freeze drying, the maltodextrin was collected.

Characterization of Banana Starch and Maltodextrin

Surface morphology of prepared banana starch was investigated by a scanning electron microscope model (Jeol-JSM-5610 LV, Japan) operating at 15 kV and 550 x magnification and that of prepared maltodextrin by 15kV and 1000 x magnification at Universities' Research Center. X-ray diffraction (XRD) analysis of banana starch was carried out using X-ray diffractometer (Rigaku, Tokyo, Japan). The banana starch powder was scanned using Cu K_α radiation (λ = 1.54056 Å) at 40 kV and 40 mA. The scanning region of the angles (2θ) was from 10º to 70º. Thermogravimetric–Differential Thermal Analysis (TG-DTA) of banana starch was done by using Simultaneous TG-DTA (DTG-60H), Thermal Analyzer (Shimadzu, Japan)at Universities' Research Center.

Determination of Dextrose Equivalent of Prepared Maltodextrin by Phenol – Sulphuric Assay Method

Standard glucose (0.2 g) was dissolved in 20 mL of distilled water in a 100 mL volumetric flask and the volume of the solution was made up to the mark with distilled water to obtain 2000 μg/ mL of solution. From this stock solution 1, 2, 3, 4, 5, 6, 7, 8, 9 and 10 mL of solutions were drawn out and placed in each 100 mL volumetric flask and diluted to the mark with distilled water to give 20, 40, 60, 80, 100, 120, 140, 160, 180 and 200 μg/ mL of glucose solutions, respectively.

Into ten separate test tubes, 1 mL each standard solutions (20, 40, 60, 80, 100, 120, 140, 160, 180 and 200 μg/ mL) were added. Next, 1 mL of 5% phenol solution was added to each test tube and mixed. A blank and sample solutions were prepared with 1 mL each of distilled water and sample solution (0.1 % w/v), respectively, instead of standard glucose solution. Concentrated sulphuric acid (5 mL) was again added to each test tube so that the steam hit the liquid surface directly to produce good mixing and homogeneously. Each tube was agitated during addition of acid. After about 10min, the tubes were shaken again and placed in water- bath at 30°C for 20 min. The yellowish brown colour was stable for several hours. Calibration curve was constructed by employing 10 different concentrations of standard glucose at 490 nm. From the calibration curve the reducing sugar content in maltodextrin was calculated. Dextrose equivalent (DE) was determined by the following equation.

$$DE = \frac{\text{Reducing sugar content as dextrose}}{\text{Total solid}} \times 100$$

Determination of pH, Moisture and Protein of Prepared Maltodextrin

pH of banana maltodextrin was determined by a pH meter (Oyster- 15) which was previously calibrated with pH 4 and 7 buffer solutions.Moisture content was determined by oven drying method and protein content was determined by Kjeldahl digestion method**.**

Results and Discussion

Purification of α-Amylase

Various organic solvents (e.g., acetone, alcohol, and diethyl ether) and salt (e.g., ammonium sulphate, ammonium carbonate, etc.,) can be used to make partial purification of enzyme. In this study α - amylase was isolated from immature white kidney bean seeds by ammonium sulphate precipitation method followed by Sephadex G-100 gel filtration chromatography. Ammonium sulphate precipitation method was chosen for salt fractionation because of its high solubility in water, lack of toxicity, cheapness and lack of harmful effects on enzyme activity. It is the most commonly used reagent for salting out the proteins because of its high solubility that permits the achievement of the solutions with higher ionic strength (Voet *et al.,* 1999). Sephadex G-100 (superfine) is a new kind of gel filtration medium which combines a highly porous gel structure with excellent chemical and physical stability. It fractionates proteins in the molecular weight range of 3000 to 60,000.

α-Amylase activities, protein contents and specific activities of the enzyme solutions in each purification step are shown in Table 1. The crude extract having specific activity of 0.10 was subjected to ammonium sulphate precipitation and resulted in specific activity of 1.20 μmol min^{-1} mg^{-1} at the final purification step. So 12.0 fold purification was achieved. Michelena and Castillo (1984) purified α- amylase from *Aspergillus foetidus* by $(NH_4)_2SO_4$ precipitation and achieved 11fold purification.

Table 1. Enzyme Activity and Specific Activity at Different Purification Steps

Purification steps	Total activity (μmol min^{-1})	Total protein (mg)	Specific activity (μmol min^{-1} mg^{-1})	Purification (fold)
Crude extract	781.2	7937.6	0.10	1
After 20% ammonim sulphate precipitation	778.5	2412.0	0.32	3.2
After 60% ammoium sulphate *precipitation*	149.5	243.3	0.61	6.1
Sephadex G-100	204.4	171	1.20	12.0

Optimum pH of α-Amylase – Catalyzed Reaction

The effect of pH on the activity of immature white kidney bean α-amylase is shown in Figure 2. The enzyme activity increased steadily from pH 1 to 5.6 and then decreased with increasing pH. Enzyme showed the optimum activity at pH 5.6 with activity of 0.5807 μmol min^{-1} mL^{-1}. A decline in the enzyme activity was recorded on either side of pH 5.6. It was reported that optimum pH of mango α- amylase was 5.5(Yasin and Chaudhary, 1981). Khoo *et al* (1994) reported that the α-amylase enzyme was found to have maximum activity at pH 6.0. α-Amylase from apple showed the optimum activity at pH 6.8 (Kanwal *et al* 2004).

Optimum Temperature of α-Amylase – Catalyzed Reaction

The effect of temperature on the activity of immature white kidney bean α-amylase is shown in Figure 3. Initially the activity increased with increase in temperature and then decreased after reaching a maximum. The

results showed that the temperature optimum of the amylase enzyme was found to be 50˚Cin acetate buffer (pH 5.6). It was observed that α-amylase lost 40.44% of its activity at 75ºC. Mohamed (2009) reported that the optimum temperature for partially purified α-amylase from Wheat *Triticum aestivum* was 50˚C. Khoo *et al* (1994) reported that the optimum temperature for purified α-amylase was 55˚C. Plant amylases (Wheat alpha -1, Pearl millet alpha-1, and Safflower seeds, mat beans) were found to have optimum temperature of 55ºC (Nerkar *et al*., 2011).

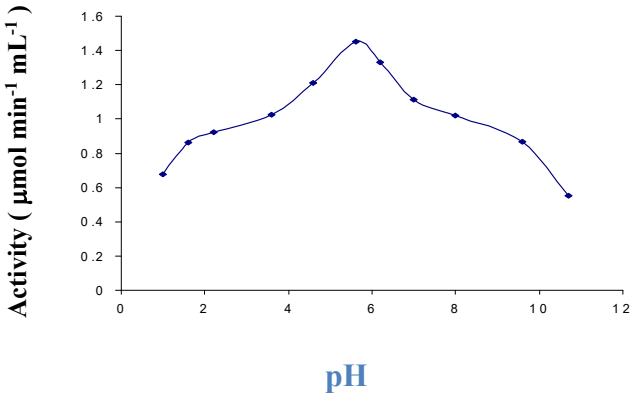

Figure 2. Plot of α–amylase activity as a function of pH of the solution

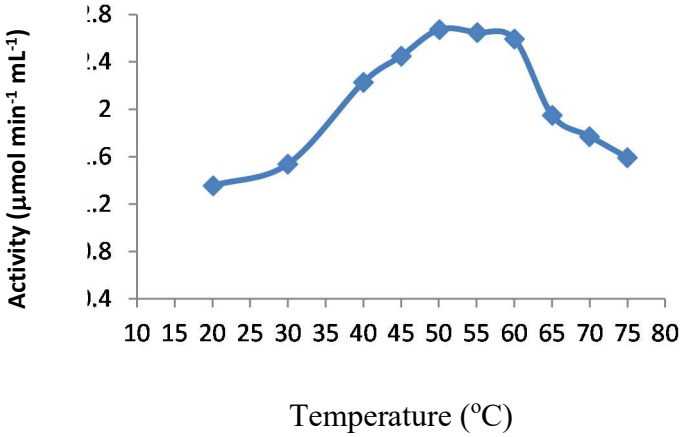

Figure 3. Plot of α–amylase activity as a function of temperature of the solution

Surface Morphology of Prepared Banana Starch

The morphology of banana starch is shown in SEM image (Figure 4). Banana starch granules were found to have irregular shapes and appeared as elongated oval. Its shape ranged from oval to irregular with the size varying from 5 to 45μm, the average size being in the range of 21 to 24 μm. The surface of the banana starch granules was found to be very smooth. So it could be indicated that isolation process was efficient and it did not cause damage to starch granules.

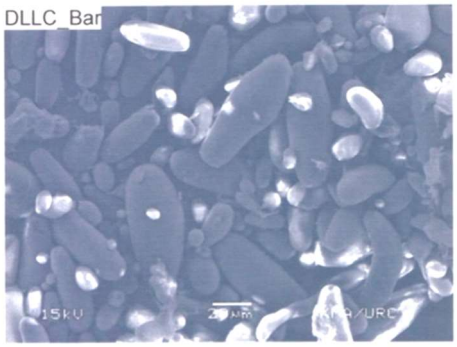

Figure4. SEM image of banana starch granules (550× magnification)

X-Ray Powder Diffraction Pattern of Prepared Banana Starch

Semi-crystalline nature of banana starch was observed in X-ray diffractogram (Figure 5) because of the presence of both sharp and diffuse diffraction peaks. Banana starch showed strong diffraction peaks at 15.3°, 17.2°, 22.1°and23.4° of 2θ. Parallel double amylopectin molecules result in the formation of crystalline regions, while amylose molecules result in the formation of amorphous regions in the starch structure.

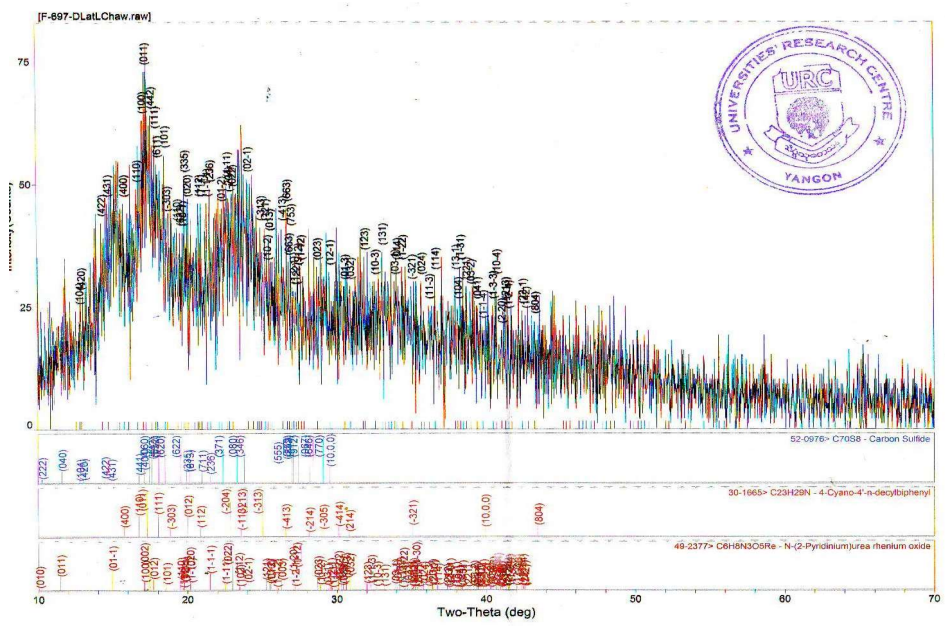

Figure 5. X ray diffractogram of banana starch

Thermal Properties of Banana Starch

TG- DTA thermogram of banana starch is shown in Figure 6. It was noted that initial weight loss began at approximately 50°C and reached a constant weight plateau after losing about 16% of its initial weight. The weight loss corresponds to the loss of moisture content from the banana starch. DTA curve shows a small endothermic peak at 65.56 °C. Between 120 °C and 307 °C, banana starch was found to be thermally stable. Moreover, another weight loss was started at approximately 308°C. At this temperature the banana starch began to degrade. This temperature is the degradation temperature of banana starch. Aht-Ong and Charoenkongthum (2002) reported that the degradation temperature of banana starch was 315 °C. DTA curve shows two exothermic peaks at 357.42 °C and 482.31 °C due to degradation of starch. At the end of the experiment (503.46 °C), weight loss % was 96.945 % and thus 3.055 % residue was left.

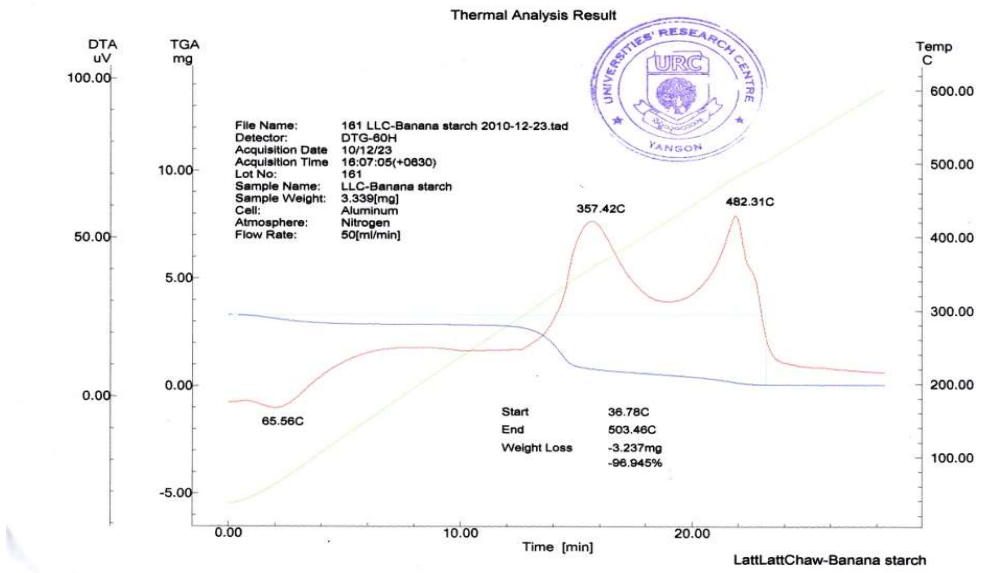

Figure 6. TG-DTA thermogram of banana starch

Maltodextrin Preparation by Using α–Amylase

Nowadays, acid hydrolysis of starch is limited for maltodextrin production and particularly recommended for production of glucose syrups . Enzymatic hydrolysis of starch has distinct advantages compared to acid process. There is no need to remove salts formed during acid neutralization and due to wider pH range and lower temperatures this process is more economic and control of process is easier too (Haki and Rakshit, 2003). The action of α- amylase on granular starch consists of the following three steps:

(1) diffusion of the enzyme toward the substrate,

(2) the adsorption of the enzyme on the substrate surface and possible pores, and

(3) the catalytic event .

In this study enzyme-catalyzed conversion with α-amylase from immature white kidney bean seeds was used for the preparation of maltodextrin from banana starch. The yield percent of maltodextrins was

5.5 %. The banana maltodextrin prepared in this study was found to have white colour.

Morphology of Banana Maltodextrin

Scanning electron micrograph of banana maltodextrin is depicted in Figure 7. It was observed that banana maltodextrin showed particles with irregular shapes and rough surface compared to elongated oval shape and smooth surface of banana starch. The change in granular surface is due to the attack of α-amylase. The amylase either erodes the granule surface or digests channels from selected points on the surface toward the center of the granule. Five patterns of attack have been identified: pin-holes/ pepper-potting, sponge-like erosion, many medium- sized holes, distinct loci leading to single holes individual granules and surface erosion (Evers, 1979). In this study two patterns of attack were observed, *i.e,* sponge- like erosion and surface erosion.

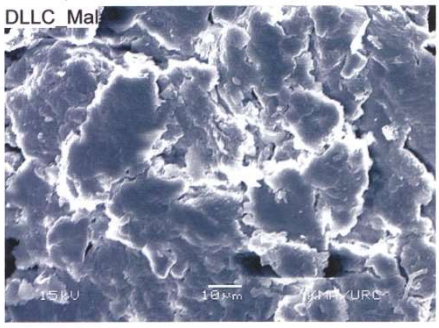

Figure 7. SEM image of banana maltodextrin (1000 x magnification)

Dextrose Equivalent of Banana Maltodextrin

Dextrose equivalent of maltodextrin was obtained by determining the reducing sugar content employing phenol-sulphuric assay method. The reaction of carbohydrate with phenol and sulphuric acid in aqueous solution gives a brown colour. This reaction can be used for the quantitative

colorimetric microdetermination of monosaccharides and their polymerization products, such as oligosaccharides and polysacchairdes (Handa,1966).

The calibration curve was constructed using different concentrations of standard glucose (20, 40, 60, 80, 100, 120, 140, 160, 180 and 200 μg mL^{-1}) at 490 nm. A straight line (R^2 = 0.9984) passed through the origin implying Beer's law was obeyed (Figure 8). Dextrose equivalent was calculated from glucose content of banana maltodextrin. The dextrose equivalent was found to be 6.

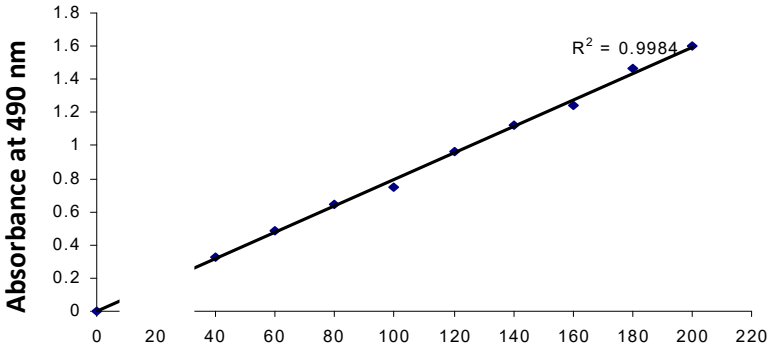

Figure 8. Calibration curve for standard glucose solution

Chemical Characteristics of Maltodextrin

Table 2 shows the chemical characteristics of prepared banana maltodextrin together with the reported values (Bello-Perez *et al*., 2002). Dextrose equivalent of prepared maltodextrin was determined as 6.00. Moisture percent was 5.00 % and pH was found to be acidic, i.e., 4.02. Protein content was 0.83%. Moisture percent and pH of present work was not much different with the reported values. However, dextrose equivalent was less than reported value of 9.0. In literature, dextrose equivalent of maltodextrin is in the range of 3 to 20 (Chronakis,1998). Protein content in prepared maltodextrin

was greater than the reported value. Regulated protein residue in maltodextrin is in the range of ≤ 0.5 to 1 % (Food Safety Information Papers, 2009).

Table 2. Chemical Characteristics of Maltodextrin

	Banana maltodextrin (Present Work)	*Reported Values
Dextrose equivalent	6.00	9.00
Moisture%	5.00	5.90
pH	4.02	4.00
Protein(%)	0.83	0.10

*Bello-Perez *et al*., (2002)

Conclusion

This study revealed the simple method for preparation of maltodextrin from banana starch by hydrolysis of α- amylase from immature white kidney bean seeds. α-Amylase from immature white kidney bean seeds was isolated and purified by ammonium sulphate fractionation (20 – 60 %) followed by gel filtration chromatography. α-Amylase was purified 12 fold compared to the crude extract. The specific activity of α-amylase was found to be 1.20 μmol min^{-1} mg^{-1} of protein at final purification step. Surface morphology of prepared banana starch was elongated oval shape with smooth surface. Banana starch started to degrade at 315°C and two exothermic peaks appeared in TG-DTA thermogram indicating that degradation of banana starch. Semi-crystalline nature of banana starch was indicated by X ray diffraction analysis. Surface morphology of prepared maltodextrin was irregular shape with sponge-like erosion and surface erosion. Dextrose equivalent of prepared maltodextrin was found to be 6 indicating low dextrose maltodextrin.

Acknowledgement

The authors would like to thank the Myanmar Academy of Arts and Science for allowing to present this paper and Professor and Head Dr DawThan Than Aye and Professor Dr Kyae Mon Lwin , Department of Chemistry,Kyaukse University for their kind encouragement.

References

Adu, E.A., Ado S. A. and James, D. B. (2005) . "Raw Starch Degrading Amylases Production by Mixed Culture of *Aspergillus niger* and *Saccharomyces cerevisae* Grown on *Sorghum pomace* ". *African. J. Biotechnol*., vol.4(8) , pp. 785 - 790.

Aht-Ong, D. and Charoenkongthum, K. (2002). "Thermal Properties and Moisture Absorption of LDPE/ Banana Starch Biocomposite Films ". *Journal of Materials, Metals and Minerals*, vol.12(1), pp. 1-10.

Alexander, R.J. (1992). *Maltodextrins : Production, Properties and Applications.* In: *Starch Hydrolysis Products*. Schenck, E.W. and Hebeda, R.E. (Eds.). New York: VCH Publishers, pp.233-276

Bello- Perez, L.A., Sanchez- Hernandez, L. Moreno-Damian, E. and Toro – Vazquez, J.F. (2002). " Laboratory Scale Production of Maltodextrins and Glucose Syrup from Banana Starch". *Acta Cient Venez* , vol.53 (1) pp.44-48

Chronakis, I.S. (1998). " On the Molecular Characteristics, Compositional Properties, and Structural – Functional Mechanisms of Maltodextrin: A Review". *Crit. Rev.Food Sci. Nutr.,* vol.38 (7) pp.599-637.

Cordenunsi, B.R. and Lajolo, F.M. (1995). " Starch Breakdown during Banana Ripening: Sucrose Synthase and Sucrose Phosphate Synthase". *J. Agric. Food Chem*., vol. 43 , pp. 347 - 351.

Dokic-Baucal, L., Dokic, P. and Jakovlijevic, J. (2004). " Influence of Different Maltodextrins on Properties of O/W Emulsions". *Food Hydrocolloids,* vol.18 , pp.233 - 239.

Evers, A.D. (1979). *Cereal Starches and Proteins*. In : *Food Microscopy* . Vaughan, J.G.(ed.), London: Academic Press, pp. 139-191.

Food Safety Information Papers. (2009). *Chemical Residues*. Washington DC: Corn Refiners Association, Inc., pp. 1-8.

Franco, O.L., Rigden, D.J.,Melo, F.R., Bloch, Jr, CC. Silva, P. and Grossi de Sa, M. F.(2000). "Activity of Wheat α-Amylase Inhibitors towards Burchid α-Amylases and Structural Explanation of Observed Specificities". *Eur.J.Biochem*, vol.267,pp 2166-2173.

Haki, G.D., and Rakshit , S.K. (2003). " Developments in Industrially Important Thermostable Enzymes: A Review". *Bioresource Technology*, vol.89, pp.17 – 34.

Handa, N. (1966) . " Examination on the Applicability of the Phenol Sulfuric Acid Method to the Determination of Dissolved Carbohydrate in Sea Water ". *Jour. Oceanogr. Soc.Japan*, vol. 22(3), pp. 79 - 86.

Ihekoronye, A.I., and Nogddy, P.O. (1985) . *Integrated Food Science and Technology for the Tropics*. London: 1st edn., Macmillan Publishers Ltd., pp. 301 – 302.

Kanwal, B., Zia, M.A., Yasin, M., Rahman, K. and Sheikh, M. A . (2004). "Purification and Characterization of α–Amylase from Apple (*Malus pumila*". *Int. J. Agri.Biol*.,vol. 6(2), pp. 233-236.

Khoo, S.L., Amirul, A.A., Kamaruzaman, M., Nazalan, N. and Azizan, M.N. (1994). "Purification and Characterization of α-Amylase from *Aspergillus flavus*". *Folia Microbial (Praha),* vol.39(5), pp. 392-398.

Kim, Y.S., Wiesenborn, D.P., Orr, P.H. and Grant, L.A. (1995). "Screening Potato Starch for Novel Properties using Differential Scanning Calorimetry". *J. Food Sci*. vol.60, pp. 1060 - 1065.

Kress, W.J., De Fillipps, R.A., Farr, E. and Daw Yin Yin Kyi. (2003). *A Checklist of the Trees, Shrubs, Herbs, and Climbers of Myanmar*. Washington D.C: Department of Systematic Biology-Botany National Museum of National History, p.243.

Michelena, V. V. and Castillo, F. J. (1984). " Purification and Characterization of Amylase by *Aspergillus foetidus* on Rice Flavor Medium". *J. Appl. Bacteriol*., vol.56, pp. 395-407

Mohamed, S. A., Al-Malki, A. L. and Kumasani, T. A. (2009). " Partial Purification and Characterization of Five α-Amylases from a Wheat Local Variety (Balady) During Germination". *Aust. J. Basic and Appl. Sci.,* vol.3 (3),pp. 1740-1748.

Nelson, N. and Somogyi, M. (1973). "A Reagent for the Copper Iodometric Determination of Very Small Amounts of Sugar".*J. Biol. Chem*., vol. 117, p. 779.

Nerkar,G. S., Chaudhari, Y. A. and Khutle, N. M. (2011)."Extraction and Characterization of Alpha Amylase from *Phaseolus aconitifolius* ". *Current Pharma Research*, vol.1(2), pp. 115-122.

Voet, D., Voet, J. G. and Pratt, C. W. (1999) . *Fundamentals of Biochemistry*. New York: John Wiley and Sons, pp 687-689.

Yasin, M., S. and Chaudhary, A. H. (1981). "Characterization of Amylase from Mango". *Pakistan J. Agric. Res*., vol. 2, pp.20-23.

SPECTROSCOPIC DETERMINATION OF A PURE ORGANIC COMPOUND ISOLATED FROM THE STEM BARK OF *Butea monosperma* (LAM.) KUNTZE

Soe Tun Myaing[1], Thein Tun Aung[2], Arnt Win[3]

Abstract

One of Myanmar indigenous medicinal plants, *Butea monosperma* (Lam.) Kuntze, Myanmar name (Pouk) was chosen for chemical analysis. A pure organic compound, pale yellow needle shape compound was isolated from the stem bark of Pouk by applying advanced separation methods such as, Thin-Layer and Column Chromatographic methods. This pure compound was checked by phytochemical test which gave rise to positive for flavonoid test. The yield percent of this pure compound was found to be 0.63 % based upon the ethyl acetate crude extract. The molecular formula of the pure compound was determined as $C_{31}H_{20}O_{10}$ by using some spectroscopic techniques, such as FT-IR, ^{1}H NMR (500 MHz), ^{13}C NMR (125 MHz), DEPT, HMQC and FAB-mass spectral data respectively. Hydrogen deficiency index of this compound is 22. Finally, the complete structure of pure compound was elucidated by applying DQF-COSY, ^{1}H NMR splitting patterns, coupling constant (J values) and HMBC spectroscopic studies.

Keywords : *Butea monosperma* (Lam.) Kuntze, thin-layer and column chromatographic methods, spectroscopic techniques

Introduction

Medicinal plants constitute an important natural wealth of a country. They play a significant role in providing primary health care services to rural people. They serve as therapeutic agents as well as raw materials for the manufacture of traditional and modern medicine. Substantial amount of foreign exchange can be earned by exporting medicinal plants to other countries. In

[1] Lecturer, Dr.,Department of Chemistry, Magway University
[2] Lecturer, Dr.,Department of Chemistry, Mandalay University of Distance Education
[3] Associate Professor, Dr.,Department of Chemistry, Kyaukse University

this way indigenous medicinal plants play significant role of an economy of a country (Sofowora, 1982).

People living in rural areas from their personal experience know that these traditional remedies are valuable source of natural products to maintain human health, but they may not understand the science behind these medicines, but know some medicinal plants are highly effective only when used at therapeutic doses. Traditional use of medicine is recognized as a way to learn about potential future medicines. Researchers have identified number of compounds used in mainstream medicine which were derived from ′ ethnomedical′ plant sources(Elezabeth and Subramanian, 2013).

Butea monosperma (Pouk) is a medium-sized deciduous tree belonging to family Fabaceae . They comprise one of the largest families of flowering plants numbering 630 genera and 18000 species (The Wealth of India, 1988) . This tree grows up to 50 ft high ,with clusters of flowers. *Butea monosperma* is used as tonic, astringent , aphrodisiac and diuretics . All parts of plant have been used as crude drug for the treatment of tumors, piles, skin diseases, wounds and ulcers. The stem bark is used for the treatment of dyspepsia, diarrhoea and dysentery. Stem bark powder is used to apply on injury caused due to axe. Paste of stem bark is applied in case of body swelling (Patil *et al*., 2006). It is also used for the cure of ulcer, sore throat and snake bite (Fageria and Rao,2015**).**

This study aimed to isolate a pure organic compound from stem bark of *Butea monosperma* (Lam.) Kuntze , locally known as Pouk and to elucidate its structure.

Materials and Methods

Commercial grade reagents from; BDH, MERCK, etc, were used in this research work. Analytical and preparative TLC was performed by using precoated silica gel plates (Merck Co Inc., Kiesel gel $60F_{254}$). Silica gel (70 to 230 Mesh ASTM) was used for column chromatography.

The following advanced instruments were used in the characterization of the samples and elucidation of the pure compound.

1. UV-lamp (Lambda-40, Perkin Elmer Co. England)
2. FT IR Spectrophotometer, Shimadzu, Japan
3. ^{1}H NMR Spectrometer, 500 MHz, Japan
4. ^{13}C NMR Spectrometer, 125 MHz, Japan
5. FAB-mass Spectrometer

Sample Collection

The stem barks of Pouk (Figure1) were collected from Khone Su village, Minbu (Sagu) Township, Magway Region. The samples were cut into small pieces and allowed to dry in air. Then the dried pieces were stored in a well-stoppered bottle and used throughout the experiment.

Figure 1. The plant and stem bark of *Butea monosperma* (Lam.) Kuntze

Extraction and Isolation of a Pure Compound

The air dried stem bark sample (1150 g) was percolated with 5 L of 95 % ethanol for two months. The percolated solution was evaporated and then extracted with (350 mL) of ethyl acetate. When ethyl acetate extract was

concentrated, the crude sample (5.87 g) was obtained. This extract (2.94 g) was taken and chromatographed on a silica gel column, eluting with n-hexane and ethyl acetate with various ratios from non-polar to polar to produce (324) fractions. Each and every fractions were checked by TLC. The same R_f value fractions were combined. Thirteen combined fractions were obtained. Then, the combined fraction (X) was found to be main fraction which showed only one spot on TLC and UV active. It was recrystallized by 30 % EtOAc in n-hexane. The yield percent of this pale yellow needle shape pure compound is found to be 0.63 % (18.5 mg) based upon the crude ethyl acetate extract.

The molecular formula and the structure of this isolated compound were assigned by using advanced spectroscopic methods such as FT IR, ^{1}H NMR (500 MHz), ^{13}C NMR (125 MHz), DEPT, HMQC, DQF-COSY, HMBC and FAB-mass spectral data (Breitmaier, 2002; Crews *et al*., 1998; Hesse *et al*., 1997; Nakanishi, 1962; Silverstein *et al*., 2005).

Results and Discussion

The ethyl acetate crude extract was separated on a silica gel column using gradient elution with n-hexane and ethyl acetate from non-polar to polar to obtain one pure bioactive bi-isoflavonoid compound, 3-(2,4-dihydroxyphenyl)-5-hydroxy-7-((3-(4-hydroxyphenyl)-7-methoxy-4-oxo-4*H*-chromen-5-yl) oxy)-4*H*-chromen-4-one.

Molecular Formula Determination of the Isolated Pure Compound

This isolated compound was obtained as pale yellow needle shape crystal.The FT IR spectrum exhibited absorption bands at 3392.90, 3041.84, 2928.04, 2854.74, 1684.98, 1614.47, 1579.75, 1253.77, 1188.19, 1037.74, 916.22, 835.21 and 779.27 cm^{-1} ascribable to hydroxyl, sp^2 H/C, sp^3 H/C, ether, carbonyl and aromatic ring functional groups respectively (Figure 2). The ^{1}H NMR spectrum (Figure 3 and Table 1) revealed one methoxy singlet at δ_H 3.87 ppm, two same chemical shift of aromatic protons at δ_H 6.82 ppm, another two same chemical shift aromatic protons δ_H 7.37 ppm and two down field chemical shift singlet methine protons δ_H 8.22 ppm and δ_H 8.30 ppm. The DEPT and FT-IR spectral data displayed the presence of one sp^3 methoxy

carbon, thirteen sp^2 methine carbons, fifteen sp^2 quaternary carbons, two carbonyl carbons, OH group and ether group. The molecular formula was determined to be $C_{31}H_{20}O_{10}$ from the observation of ^1H NMR spectrum, ^{13}C NMR (Figure 4) and FAB mass spectrometry (Figure 5).

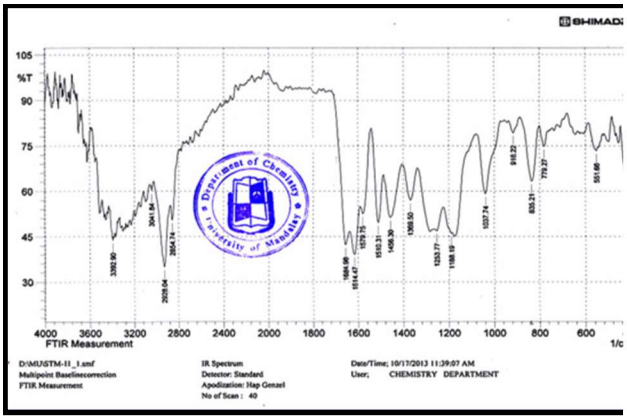

Figure 2. FT IR Spectrum of Pure Compound (KBr)

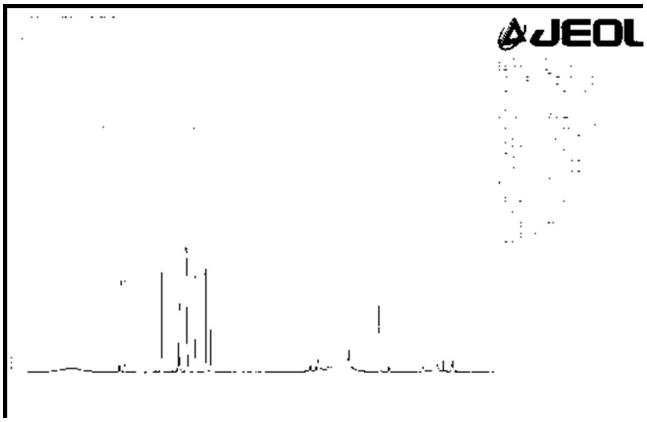

Figure 3. ^1H NMR Spectrum of Pure Compound

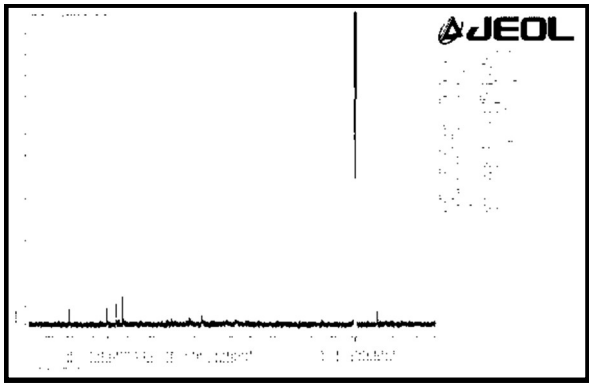

Figure 4. ^{13}C NMR Spectrum of Pure Compound

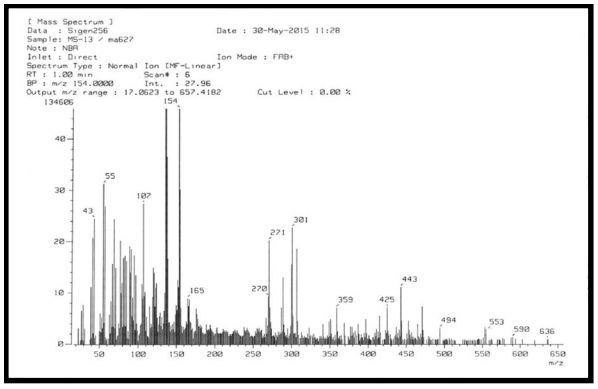

Figure 5. FAB-Mass Spectrum of Pure Compound

Table 1. ^{1}H NMR Spectral Data of Isolated Pure Compound

No.	Chemical shift (δ/ppm)	No. of protons	Splitting pattern	Coupling constant (J value Hz)	Proton assignment
1.	3.87	3H	s	–	sp^3methoxy proton
2.	6.22	1H	d	2.1	sp^2methine proton
3.	6.28	1H	dd	2.1, 8.2	sp^2methine proton
4.	6.37	1H	d	2.3	sp^2methine proton
5.	6.38	1H	d	2.3	sp^2methine proton
6.	6.40	1H	d	2.2	sp^2methine proton
7.	6.63	1H	d	2.2	sp^2methine proton
8.	6.82	1H	d	8.5	sp^2methine proton
9.	6.82	1H	d	8.5	sp^2methine proton
10.	6.99	1H	d	8.2	sp^2methine proton
11.	7.37	1H	d	8.5	sp^2methine proton
12.	7.37	1H	d	8.5	sp^2methine proton
13.	8.22	1H	s	–	sp^2methine proton
14.	8.30	1H	s	–	sp^2methine proton
Total number of protons					16

Structure Elucidation of Pure Compound

The structure elucidation of pure compound could be determined by ^{1}H NMR, DQF-COSY, HMQC and HMBC spectral data, respectively.

In the structure elucidation, the tri-substituted benzene ring fragments $\underset{\sim}{a}$, $\underset{\sim}{b}$ and $\underset{\sim}{c}$ could be assigned by DQF-COSY, ^{1}H NMR, splitting pattern, coupling constant (J-values), HMQC and HMBC spectra.

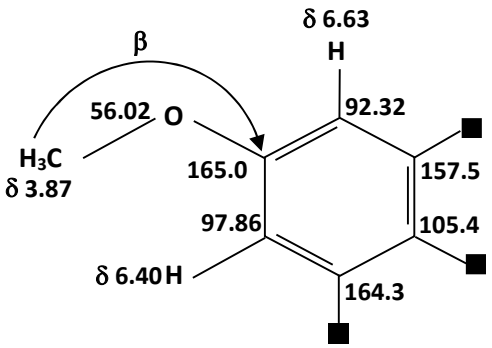

a

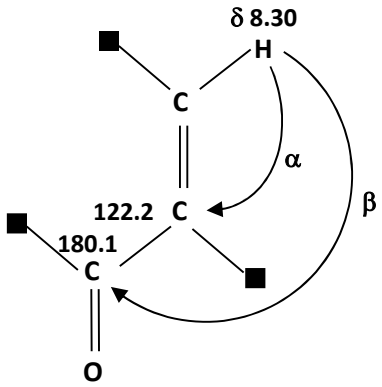

b

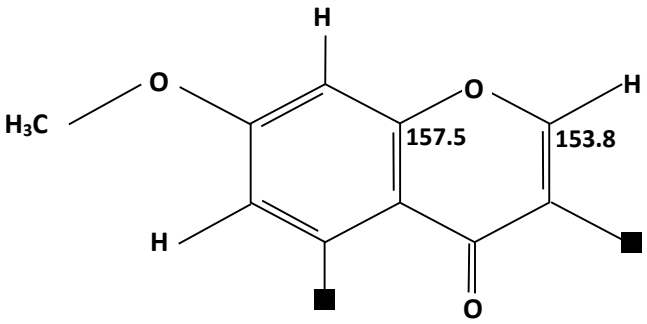

c

Moreover, another symmetrical disubstituted benzene ring fragment d could also be assigned by DQF-COSY, ^{1}H NMR, HMQC and HMBC spectral data.

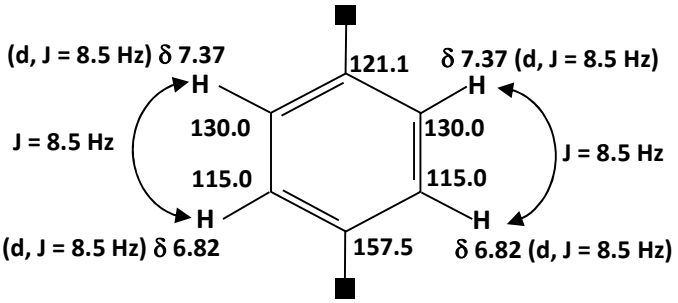

d

Furthermore, the fragments c and d were connected by using HMBC spectrum which produced the extended isoflavonoid partial structure e.

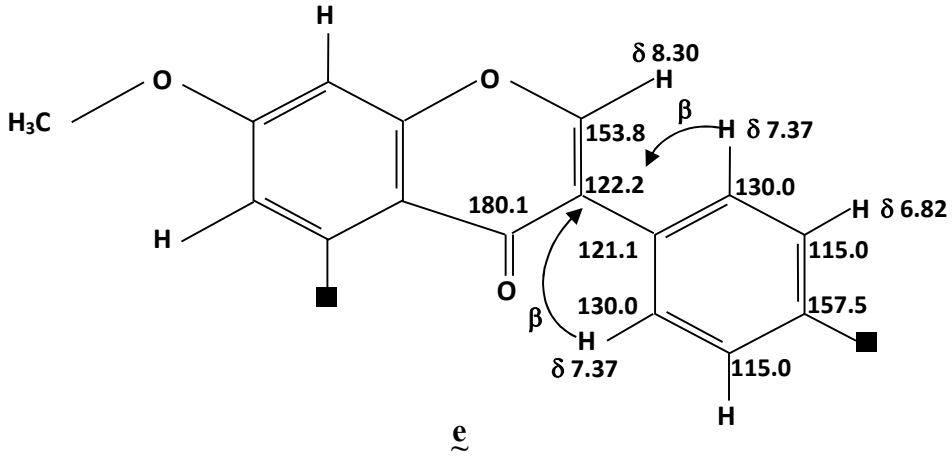

e

In addition, another isoflavonoid skeleton type fragment f with different substituent groups from the former one could be assigned by using spectroscopic data as described below.

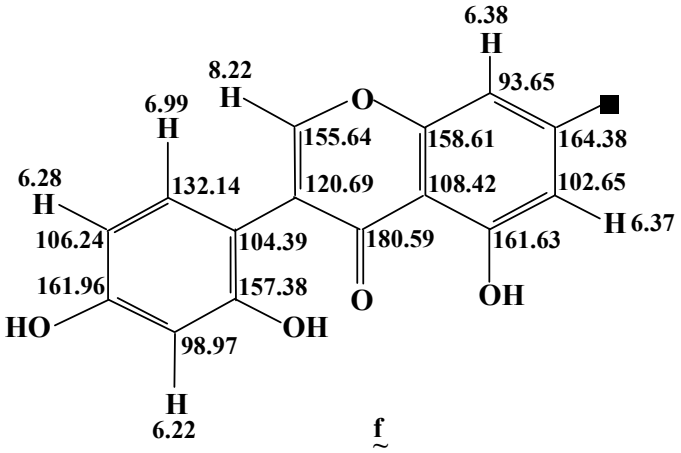

f
~

The connection between two different isoflavonoid moiety (e and f) by applying the only HMBC signal leads to the following biflavonoid skeleton type fragment g .

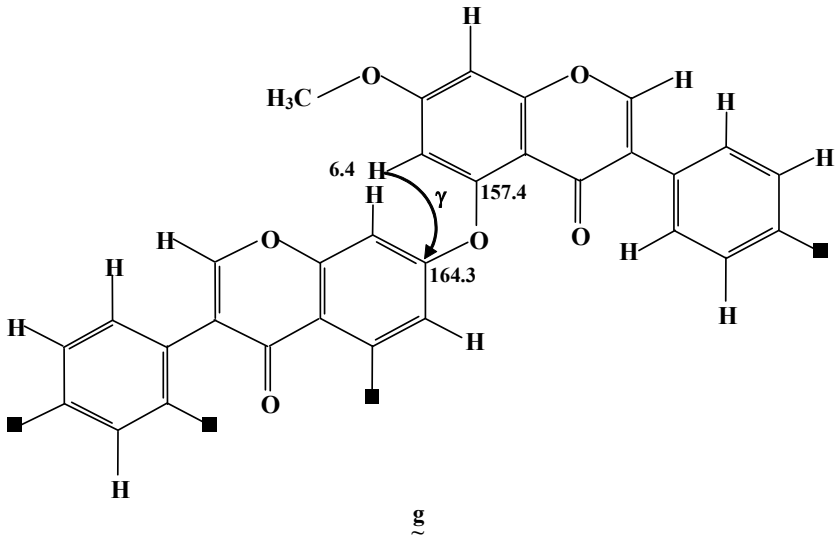

g
~

In this stage, the elucidated partial molecular formula is $C_{31}H_{16}O_6$ and remaining molecular formula is ($C_{31}H_{20}O_{10} - C_{31}H_{16}O_6 = H_4O_4$). It must be four hydroxy groups.

Finally, the remaining four hydroxy groups attached to reasonable four downfield chemical shift carbons (161.96 ppm, 157.38 ppm, 161.63 ppm and 157.50 ppm) could be established the complete planar structure of pure compound.

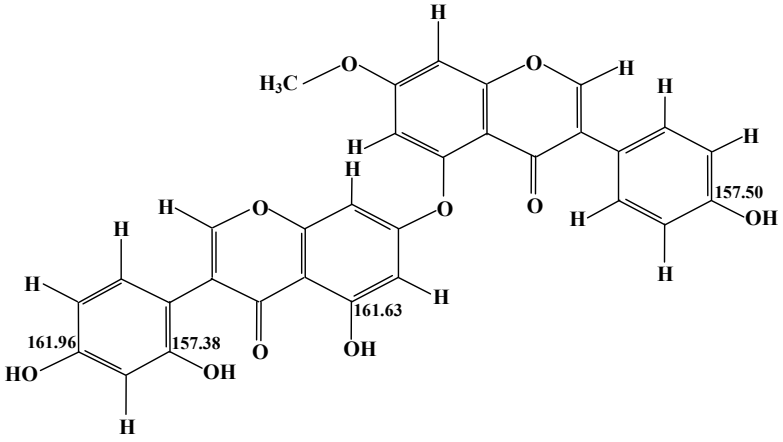

The elucidated structure of pure compound could be confirmed by FAB-mass fragmentation behaviour. The IUPAC name of pure compound is 3-(2,4-dihydroxyphenyl)-5-hydroxy-7-((3-(4-hydroxyphenyl)-7-methoxy-4-oxo-4*H*-chromen-5-yl) oxy)-4*H*-chromen-4-one.

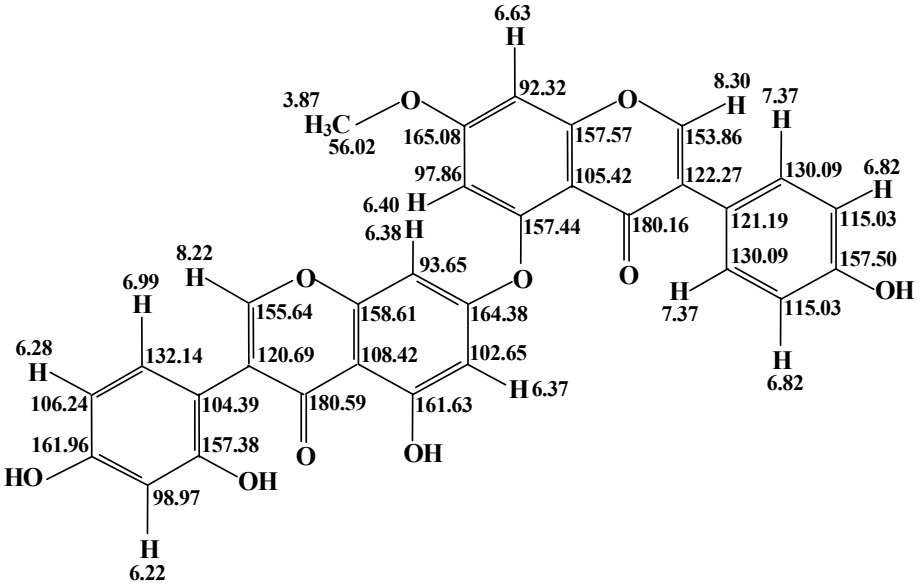

Conclusion

In the present investigation, was described the isolation of pure bioactive bi-isoflavonoid compound which possessed many biological activities, especially anti-inflammatory activity from the stem bark of *Butea monosperma* (Lam.) Kuntze (Pouk). Moreover, the fractionated pure pale yellow needle shape compound could be illustrated by using sophisticated spectroscopic method and confirmed by FAB mass fragmentation behaviour. Further studies are required and are in progress.

Acknowledgements

The authors are extremely grateful to Dr Khin Maung Oo, Rector, Dr Win Soe, Pro-Rector, Professor Dr Chaw Khin, Head of Department of Chemistry and Dr Thida Aung, Professor, Department of Chemistry, Magway University, for their permission, understanding, kind help and good guidance.

References

Breitmaier, E. (2002). *Structure Elucidation by NMR in Organic Chemistry- A Practical Guide*. West Sussex : 3rd Edn, John Wiley and Sons Ltd.

Crews, P., Jaime, R. and Marcel, J., (1998). *Organic Structure Analysis*: *Solutions Manual.* New York: Oxford University Press

Elezabeth, D. V. and Subramanian, A., (2013), "Identification of Phytochemical Constituents and Antimicrobial Activity of *Indigotera suffruticosa* Leaves". *International Journal of current Biotechnology*, ISSN: 2321-8371

Fageria, D. and Rao , D.V. (2015) . "A Review on *Butea monosperma* (Lam.) Kuntze: A Great Therapeutic Valuable Leguminous Plant ". *International Journal of Scientific and Research Publications*, vol. 5 (6), pp.1-8

Hesse, M., Meier. H., and Zeeh, B. (1997). *Spectroscopic Methods in Organic Chemistry* . New York: George Thieme Verlag Stuttgart

Nakanishi, K., (1962). *Infrared Absorption Spectroscopy - Practical*. San Francisco: Holden-Day Inc.

Patil, M. V., Pawar, S. and Patil, D. A. (2006). "Enthobotany of in North Maharashtra, India". *Natural Product Radiance* ,vol. 5(4) pp. 323-325

Silverstein, R. M., Webster, F. X. and Kiemle, D. J. (2005). *Spectrometric Identification of Organic Compounds.* New York: 7th edition, John Wiley and Sons, Inc.

Sofowora, A. (1982), *Medicinal Plant and Traditional Medicine in Africa*. New York: John Wiley and Sons Ltd. The Wealth of India.(1998). *Raw Materials*. New Delhi: CSIR, pp. 341-346.

STRUCTURE ELUCIDATION AND SOME BIOACTIVITIES OF PURE ORGANIC COMPOUNDS ISOLATED FROM THE STEM BARK OF *Polyalthia cerasoides*(ROXB.) BEDD. (THAYET-THAMON)

Mi Mi Latt[1], HninThanda Aung[2], Myint Myint Sein[3]

Abstract

In this research work, one of the Myanmar indigenous medicinal plants, *Polyalthia cerasoides* (Roxb.) Bedd. (thayet-thamon) was chosen for chemical analysis and pharmacological investigation of the stem bark. The acute toxicity test of 95 % ethanol extract of the stem bark of *P. cerasoides* was carried out in this study. The ethyl acetate extract was chromatographed by various chromatographic techniques to give pale yellow powder of pure compound (MML-1) and brown oily form of pure compound (MML-2). The antimicrobial activities of three different solvent extracts of crude sample and pure compounds (MML-1) and (MML-2) were tested by agar well diffusion method on six selected organisms; *Bacillus subtilis, Staphylococcus aureus, Bacillus pumilus, Pseudomonas aeruginosa, Candida albicans* and *Escherichia coli*. Then, the antioxidant activity of ethanol crude extract and pure compounds (MML-1) and (MML-2) was evaluated by using DPPH radical scavenging assay. The molecular structures and conformational analyses of compounds (MML-1) and (MML-2) were determined by high resolution spectrometric techniques such as ^{1}HNMR, ^{13}CNMR, DEPT, DQF-COSY, HMQC, HMBC, EI MS spectral data and molecular modeling. The pure compounds (MML-1) and (MML-2) possess the types of flavonoid and lignan compounds.

Keywords: *Polyalthia cerasoides*(Roxb.) Bedd., the acute toxicity test, antimicrobial activities, antioxidant activity

[1] Lecturer, Dr., Department of Chemistry, Monywa University
[2] Lecturer, Dr., Department of Chemistry, University of Mandalay
[3] Professor, Head of Department (Retd.), Dr., Department of Chemistry, University of Mandalay

Introduction

For thousands of years, natural products have played a very important role in health care and prevention of diseases. The use of natural products as medicines has been described throughout history in the form of traditional medicines, remedies, lotions and oils with many of these bioactive natural products still being unidentified. According to recent studies conducted by the World Health Organization (WHO), about 80 % of the world's population relies on traditional medicine (Butler, 2004).

Flavonoids are polyphenolic compounds that are ubiquitous in nature and are categorized, according to chemical structure, into flavonols, flavones, flavanones, isoflavones, catechins, anthocyanidins and chalcones. Over 4,000 flavonoids have been identified, many of which occur in fruits, vegetables and beverages (tea, coffee, beer, wine and fruit drinks). The flavonoids have aroused considerable interest recently because of their potential beneficial effects on human health they have been antiplatelet, anti-inflammatory, reported to have antiviral, anti-allergic, antitumor and antioxidant activities (Marais *et al*., 2006).

The lignans are a group of chemical compounds found in plants. Plant lignans are polyphenolic substances derived from phenylalanine via dimerization of substituted cinnamic alcohols, known as monolignols, to a dibenzylbutane skeleton. Lignans serve an antioxidant role in the plant's defenses against biotic and abiotic factors, and have shown anti-inflammatory and antioxidant activity in basic research models of human diseases. Lignans may also have anticarcinogenic activities. Some epidemiological studies have shown that lignin exposure associates with lower risk of breast cancer.

In this study, one of Myanmar traditional medicinal plants namely, *Polyalthia cerasoides* (Roxb.) Bedd. (Figure1), belonging to the family Annonaceae was used for isolation and structural elucidation of pure organic compounds. Plants belonging to the family Annonaceae have long been used as a major source of medicines for the prevention and treatment of a variety of diseases in India and many Asian countries. To date, ethnopharmacological claims for Annonaceae include the use of its bark to control blood pressure, diabetes and its use as a febrifuge. In this research work, screening of phytochemical constituents, determination of antimicrobial activities were

carried on the crude extracts from the bark of*P. cerasoides*. Moreover, evaluation of the antioxidant activities, determination of acute toxicity of ethanol crude extracts were also carried out. In addition, pure compounds were isolated from the bark of *P.cerasoides* by applying advanced separation techniques such as thin layer, preparative thin layer chromatography and column chromatography. The chemically isolated pure compounds (MML-1 and MML-2) were used for examination of antimicrobial and antioxidant activities, and structural elucidation.

Scientific Classification

Family name	Annonaceae
Botanical name	*Polyalthiacerasoides* (Roxb.) Bedd.
Myanmar name	Thayet-thamon
Common name	Cherry Ashok
Parts of plant used	Bark
Medicinal uses	Hypertension, tonic to combat stress and pain, anti-inflammatory, anti-analgesic

(a) **(b)** **(c)**

Figure 1 (a)Plant, (b) flowers and (c) fruits of *Polyalthia cerasoides* (Roxb.) Bedd.

Materials And Methods

General Experimental Procedures

IR spectra were recorded on FT IR-8400 spectrophotometre. ^{1}H and ^{13}C NMR spectra were recorded on a JEOL ECA-500 (^{1}H: 500 MHz and ^{13}C: 125 MHz). Chemical shifts for ^{1}H and ^{13}C NMR are given in parts per million (δ) relative to solvent signal (chloroform-*d*: δ_H 7.26 and δ_C 77.0) as internal standard. EI mass was obtained with a JEOL JMS MS-700. The melting point of the pure compound in crystal form was measured by Stuart SMP 30 melting point apparatus. Commercial grade reagents and solvents were purchased from Chemico Co. Ltd, Yangon. Column chromatography was carried out on silica gel (BW – 820 MH, Fuji Silysia, Aichi, Japan). Analytical preparative thin layer chromatography was conducted on Kieselgel 60 (F_{254}, Merck).

Plant Material

Bark of *P. cerasoides* was collected from Ye-kyi-su village, Pa-thein-gyi Township, Mandalay Region.

Solvent Extraction and Partition of *P. cerasoides*

The air dried powder of the stem bark of Thayet-thamon (1000 g) was percolated with methanol (3000 mL) for about two months. Then the percolated solution was filtered and evaporated to concentrate at room temperature. The residue was extracted with ethyl acetate and water. The ethyl acetate fraction was concentrated to dryness in vacuum, to give 3.2 g of dried extract.

Isolation and Purification of Pure Compounds

The ethyl acetate extract (2.5 g) was chromatographed over a silica gel column, eluted with a gradient solvent system of increasing polarity (n-hexane, 19:1-1:4, then ethyl acetate only) to give 544 fractions (Figure 2),. Each fraction was checked by TLC, iodine vapour and UV lamp. Then, the fractions of the same R_f values were combined and (19) combined fractions were

obtained. The sub-fraction 18-4 was subjected to preparative thin layer chromatography (PTLC) using n-hexane : ethyl acetate (6:4) as eluents to afford brown oily form of pure compound MML-2 (8.2 mg).The combined fraction (19) was rechromatographed by silica gel column chromatography using n-hexane : ethyl acetate as eluents to give nine sub-fractions. The sub fraction 19-8 was also subjected to PTLC using
n-hexane : ethyl acetate (1:1) as eluents to give pale yellow crystals of pure compound MML-1 (6.4 mg).

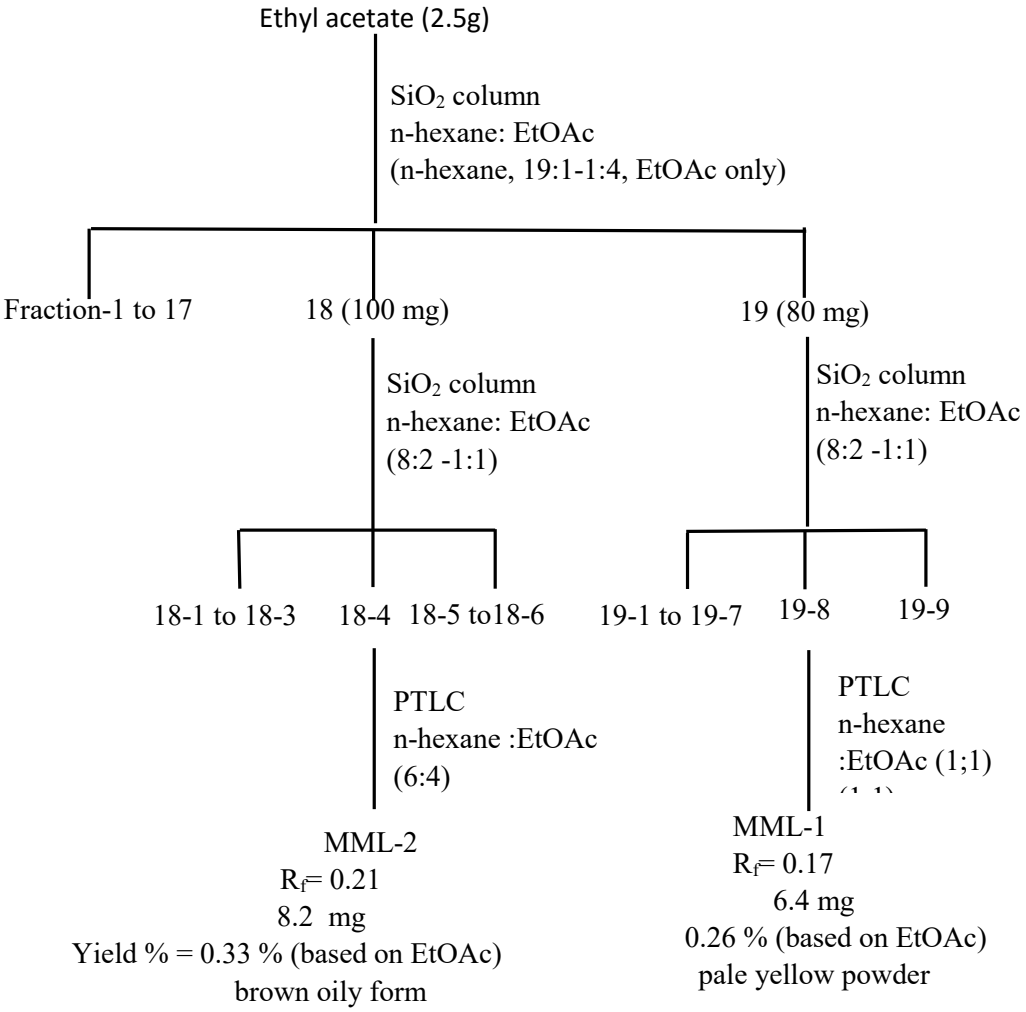

Figure 2 Flow diagram for isolation and purification of pure compounds MML-1 and MML-2 from the bark of *P. cerasoides*

Phytochemical Analysis

Phytochemical analysis for alkaloids, flavonoids, terpenes, steroids, glycosides, reducing sugars, lipophilic, polyphenols, tannins, saponins and phenolic compounds were carried out according to general methods mentioned in phytochemical methods (Harborne, 1993; Yadav and Munin, 2011).

Investigation of Antimicrobial Activities of the Barks of *P. cerasoides*

The bark was extracted with three solvents n-hexane, ethyl acetate and ethanol. Antimicrobial activities of the bark extracts were tested by using agar-well diffusion method on six selected organisms; *Bacillus subtilis, Staphylococcus aureus, Bacillus pumilus, Pseudomonas aeruginosa, Candida albicans* and *Escherichia coli* at Pharmaceutical Research Department (PRD), Insein, Yangon.

Acute Toxicity Study of Plant Crude Extract of *P. cerasoides*

An acute toxicity study was carried out on 95 % ethanol extract of the stem bark of *P.cerasoides* using mice as the experimental model. Both sexes of healthy Albino ICR (Institute of Cancer Research) Strain mice (25g to 30g) were randomly selected and kept in their cages for at least 5 days prior to the experiment to allow for acclimatization for Laboratory conditions. Before the experiment, the animals were kept fasting overnight for 18 h but were allowed with free access to water. Following period of fasting, mice were weighed and dose was calculated according to the body weight. The doses were selected from the sequence 500mg/kg, 1000 mg/kg, 1500 mg/kg, 2000mg/kg and 2500 mg/kg respectively for specific regulatory needs. Then, the test substance was dissolved in ethanol for required concentration and administered orally in a single dose by using cannula. One group was served as the control and only distilled water was given orally.

Each dose of (500 mg/kg, 1000 mg/kg, 1500 mg/kg, 2000 mg/kg and 2500 mg/kg) was administered orally to each of five group of mice. Mice were observed after dosing at least once during the first 30 min, periodically during the first 24 h with special attention given during the first 4 h and daily up to 10 days. Signs of toxicity and mortality of the mice were recorded. Observations

included changes in fur, eyes, mucous membranes, respiratory rate, autonomic central nervous systems and behavioral pattern. The time of death if any was recorded. Individual body weights of mice were measured and recorded shortly before the test substance was administered and once weekly thereafter. At the end of the test (i.e. 10 days) the mice were weighed.

Determination of Antioxidant Activities of Crude Extract and Isolated Compounds by DPPH Assay

DPPH radical scavenging activity was determined by using UV-visible spectrophotometer. The sample solution was also prepared by mixing 1.5 mL of 0.002 % DPPH solution and 1.5 mL of test sample solution. These bottles were incubated at room temperature and were shaken on shaker for 30 min. After 30 min, the absorbance values of these solutions were measured at 517 nm and the percentage of radical scavenging activity (% RSA) was calculated by the following equation.

$$\% \text{ RSA} = [(A_{DPPH} - A_{Sample}) - A_{Blank} / A_{DPPH}] \times 100$$

The antioxidant power is expressed as IC_{50} (50 % inhibitory concentration). It is the test substances concentration (μg/ mL) that result in a 50 percent reduction of initial absorbance of DPPH solution. IC_{50} values were calculated by linear regressive excel program (Marinova and Batchvarov, 2011).

Structure Elucidation of Pure Compounds MML-1 and MML-2

The structures of two pure compounds MML-1 and MML-2 were elucidated by high resolution spectrometric techniques such as ^{1}H NMR, ^{13}C NMR, DEPT, DQF-COSY, NMQC, HMBC, EI MS spectral data and molecular modeling (Silverstein *et al*., 2005).

Results and Discussion

Phytochemicals Present in the Bark of *P. cerasoides*

The results of the phytochemical screening tests from the bark of *P. cerasoides* are shown in Table 1. The presence of alkaloids, flavonoids, terpenes, sterols, glycosides, reducing sugars, lipophilic, polyphenols, saponins and phenolic compounds was detected in the extract of bark of *P. cerasoides.*

Table 1 Results of Phytochemical Analysis of the Stem Bark of *P. cerasoides*

No.	Constituents	Test Reagent	Observation	Results
1	Alkaloids	1%HCl, Dragendorff's reagent	Orange ppt	+
2	Flavonoids	EtOH, Mg turning, Conc:HCl	Pink color solution	+
3	Terpenes	Pet ether, Conc:H_2SO_4, Acetic anhydride	Pink color solution	+
4	Steroids	$CHCl_3$, Conc:H_2SO_4, Acetic anhydride	Blue color solution	+
5	Glycosides	H_2O, 10% Lead acetate	White ppt	+
6	Reducing sugars	H_2O, Benedict's solution	Bricked red color ppt	+
7	Lipophilic	H_2O, 0.5 M KOH	Deep color solution	+
8	Polyphenols	EtOH, 10% $FeCl_3$, 1% $K_3Fe(CN)_6$	Greenish blue color solution	+
9	Saponins	H_2O, Shake	Frothing	+
10	Phenolic compounds	H_2O, 10% $FeCl_3$	Purplish color solution	+
11	Tannins	H_2O, 10% $FeCl_3$, H_2SO_4	No yellowish brown color	-

Plus sign indicates the presence and minus sign indicates the absence.

Antimicrobial Activities of Extracts of *P. cerasoides*

The antimicrobial activities of crude extract in various solvents from the bark of *P. cerasoides* were tested by using agar-well diffusion method on six selected organisms. The results are tabulated in Table 2.

Table 2 Antimicrobial Activities of the Different Extracts of *P. cerasoides*

Samples	Solvents	Diameter of Inhibition Zone(mm)					
		1	**2**	**3**	**4**	**5**	**6**
P. cerasoides	n-hexane	-	-	-	-	-	-
	ethyl acetate	-	-	19 (++)	26 (+++)	22 (+++)	24 (+++)
	ethanol	11(+)	-	12 (+)	-	11 (+)	-
Control	n-hexane	-	-	-	-	-	-
	ethyl acetate	-	-	-	-	-	-
	ethanol	-	-	-	-	-	-

agar well -10 mm organisms
10 mm ~ 14 mm (+)
15 mm ~ 19 mm (+ +)
20 mm above (+ + +)

1. *Bacillus subtilis* (N.C.T.C-8236)
2. *Staphylococcus aureus* (N.C.P.C-6371)
3. *Pseudomonas aeruginosa* (6749)
4. *Bacillus pumilus* (N.C.I.B-8982)
5. *Candida albicans*
6. *Escherichia coli* (N.C.I.B-8134)

According to Table 2, n-hexane extracts of the bark of *P. cerasoides* did not show any activity on all tested organisms. Ethanol extract showed low activities on *Bacillus subtilis*, *Pseudomonas aeruginosa* and *Candida albicans*. Ethyl acetate extract gave rise to medium activity on *Pseudomonas aeruginosa* and high activities against three tested organisms such as *Bacillus pumilus, Candida albicans* and *Escherichia coli.* That is why ethyl acetate extract was selected for further analysis. All of the tested extracts did not show any activity against *Staphylococcus aureus*.

Antimicrobial Activities of Pure Compounds (MML-1 and MML-2)

The antimicrobial activities of pure compounds (MMl-1) were investigated by agar well diffusion method against six selected organisms. The results are shown in Table 3.

Table 3 Antimicrobial Activities of Pure Compounds (MML-1 and MML -2)

Samples	Solvents	Diameter of Inhibition Zone(mm)					
		1	**2**	**3**	**4**	**5**	**6**
Pure Compound MML-1	EtOAc	12(+)	14 (+)	12 (+)	14 (+)	12 (+)	14 (+)
Pure Compound MML-2	EtOAc	-	12 (+)	-	13 (+)	11 (+)	11 (+)

According to Table 3, pure compounds (MML-1 and MML-2) showed low activities on all tested organisms and pure compound (MML-2) showed low activities on four tested organisms such as *Staphylococcus aureus***,** *Bacillus pumilus, Candida albicans* and *Escherichia coli*.

Acute Toxicity of 95% Ethanol Extract of the Bark of *P. cerasoides*

The mice administered with 500 mg/kg, 1000 mg/kg, 1500 mg/kg, 2000 mg/kg and 2500 mg/kg doses of ethanol extract of *P. cerasoides* were kept under observation for 10 days. The observation parameters used in this experiment were cage side observations, daily body weight and mortality record. The results obtained from this experiment are shown in the following Table 4 .

Table 4 Acute Toxicity Study on the Ethanol Extract of the Bark of *P. cerasoides* Based on Cage Side Observations

No.	Parameters	Observations
1.	Condition of the fur	Normal
2.	Skin	Normal
3.	Subcutaneous swellings	Nil
4.	Abdominal distension	Nil
5.	Eyes-dullness	Nil
6.	Eyes-opacities	Nil
7.	Pupil diameter	Normal
8.	Ptosis	Nil
9.	Color and consistency of the feces	Normal
10.	Wetness or soiling of the perineum	Nil
11.	Condition of teeth	Normal
12.	Breathing abnormalities	Nil
13.	Gait	Normal

In this experiment, five mice were used for each group. At the end of observation period, all the mice were alive, did not show any toxic symptoms such as diarrhea, inactivity, restlessness, aggressiveness, eye-dullness, breathing, abnormalities, etc. and did not exhibit loss and obvious changes of body weight. Thus, the lethal dose LD_{50} was more than 2500 mg/kg body weight. Hence, the ethanol extract of this plant is practically nontoxic and may be relatively harmless.

Antioxidant Activity of Crude Extract, MML-1 and MML-2by Using DPPH Assay

In the present work, investigation of radical scavenging activity of pure compounds, MML-1,MML-2 and ethanol extract from the stem bark of*P. cerasoides* was performed by using DPPH assay. Figure 3 shows the percent radical scavenging activities of pure compounds, MML-1, MML-2 and ethanol extract together with that of standard ascorbic acid versus concentrations (µg/mL). The antioxidant power is expressed as IC_{50} (50% inhibitory concentration).

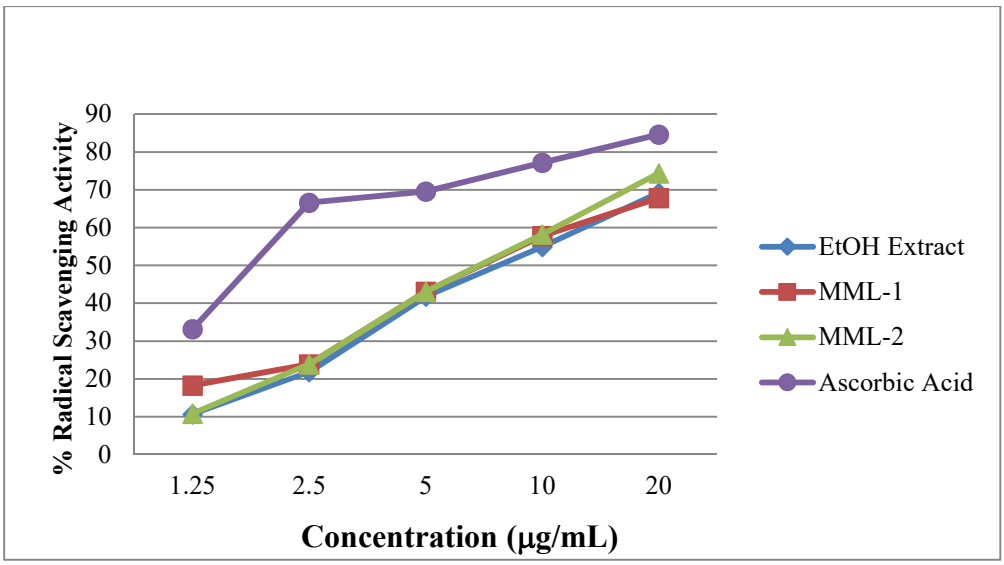

Figure 3 Percent radical scavenging activities versus concentration (µg/mL) of ascorbic acid, ethanol extract, MML-1 and MML-2

The antioxidant activity of the ethanol extract, pure compounds MML-1 and MML-2 exhibited IC_{50} value of 8.14 µg/mL, 7.29 µg/mL and 7.29 µg/mL respectively (Figure 4).

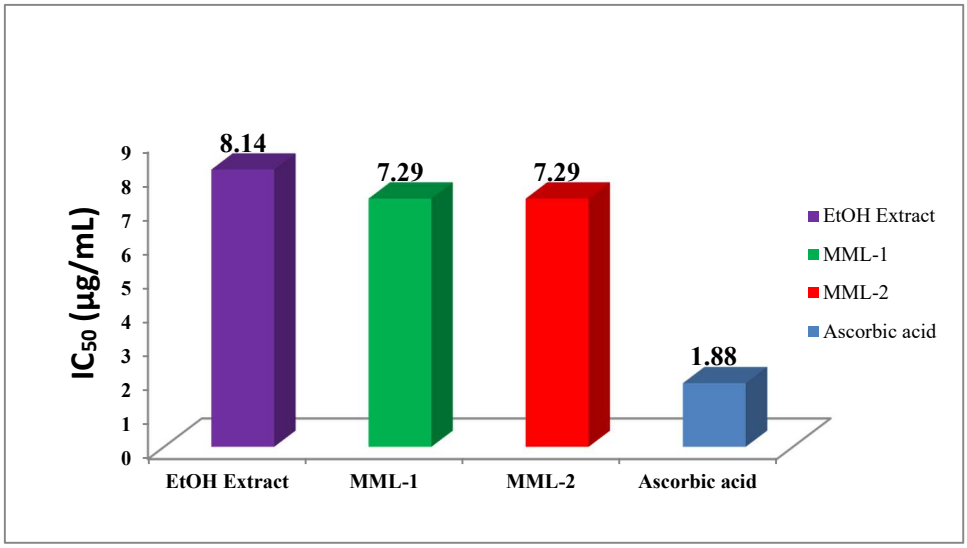

Figure 4 IC_{50} values of ethanol extract, MML-1, MML-2 and ascorbic acid

Isolation of Some Bioactive Compounds from the Bark of *Polyalthia cerasoides* (Roxb.) Bedd.

The ethyl acetate extract (2.5 g) was chromatographed over a silica gel column, eluted with a gradient solvent system of increasing polarity (n-hexane, 19:1-1:4, then ethyl acetate only) to give two pure compounds of MML-1 and MML-2.

Structure Elucidation of Pure Compounds MML-1 and MML-2

Pure compound MML-1 was identified (Silverstein *et al*., 2005) as [(2R, 3R)-3,5,7-trihydroxy-2-(4-hydroxyphenyl)chroman-4-one] by using FT IR (Figure 5a), ^{1}HNMR (Figure 5 b), ^{13}C NMR (Figure 5 c), DEPT (Figure 5 d), DQF COSY (Figure 5 e), HMQC (Figure 5 f), HMBC (Figure 5 g), NOESY (Figure 5 h) and EI Mass (Figure 5 i) spectra and then MML-2 was identified as [4, 4' (1R,3aS,4R, 6aS) –hexahydrofuro [3,4-c] furan-1,4-diyl) bis (2,6-dimethoxy phenol)]by using FT IR (Figure 6 a), ^{1}HNMR (Figure 6 b), ^{13}C NMR (Figure 6 c), DEPT (Figure 6 d), DQF COSY (Figure 6 e), HMQC

(Figure 6 f), HMBC (Figure 6 g), NOESY (Figure 6 h) and EI Mass (Figure 6 i) spectra. .

The molecular formula of pure compounds (MML-1) and (MML-2) were found to be $C_{15}H_{12}O_6$ and $C_{22}H_{26}O_8$. The molecular mass of pure compound (MML-1) and (MML-2) are 288 and 418, in good agreement with molecular ion peak at (m/z 288) and (m/z 418) in EI mass spectrum. They were also confirmed by the mass fragmentation peaks at (259, 153, 134 and 107 for MML-1) and (193, 181, 167 and 154 for MML-2) in EI mass spectrum.

(2R, 3R)-3,5,7-trihydroxy-2-(4-hydroxyphenyl) chroman-4-one (MML-1)

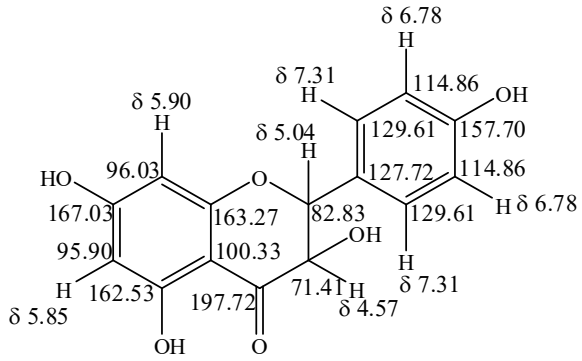

Complete structure of pure compound MML-1

molecular weight: 288(m/z = 288 in EI mass spectrum)

melting point : 177 - 179˚C

physical form :pale yellow powder

R_f value : 0.17 (n-hexane :EtOAc(1:1)

molecular formula : $C_{15}H_{12}O_6$

FT IR : (KBr), $\nu_{max}(cm^{-1})$

3433.41and 3383.26(ν_{OH}), 3039.91($\nu_{C=CH2}$),2924.18 and 2834.31(ν_{asym} and ν_{sym} of CH), 1639.55($\nu_{C=O}$), 1518.03($\nu_{C=C}$),

1458.23(δ_{C-H} of CH_2 and CH_3), 1359.68(ν_{OH} of phenol),

1273.06(ν_{C-O} of phenol), 1166.97and1035.81(ν_{C-O-C} of ether),

819.77(δ_{C-H} out of plane bending)

^{1}H NMR: 600MHz,DMSO,δ_H(ppm)

4.57(dd, J=4.8Hz, 11.34Hz, 1H), 5.04(d, J=11.34Hz, 1H),

5.85(d,J=2.62Hz, 1H), 5.90(d, J=2.39Hz, 1H),

6.78(d,J=9.08Hz,2H),7.31(d, J=9.0Hz, 2H)

^{13}C NMR : 150MHz, DMSO, δ_C(ppm)

71.41(CH-3), 82.83(CH-2), 95.90(CH-6), 96.03(CH-8),

100.33(Cq-10), 114.86(CH-3'), 127.72(Cq-1'), 129.61

(CH-2'),157.70(Cq-4'),162.53(Cq- 6), 163.27(Cq-9),167.03

(Cq-7), 197.72 (Cq- C=O)

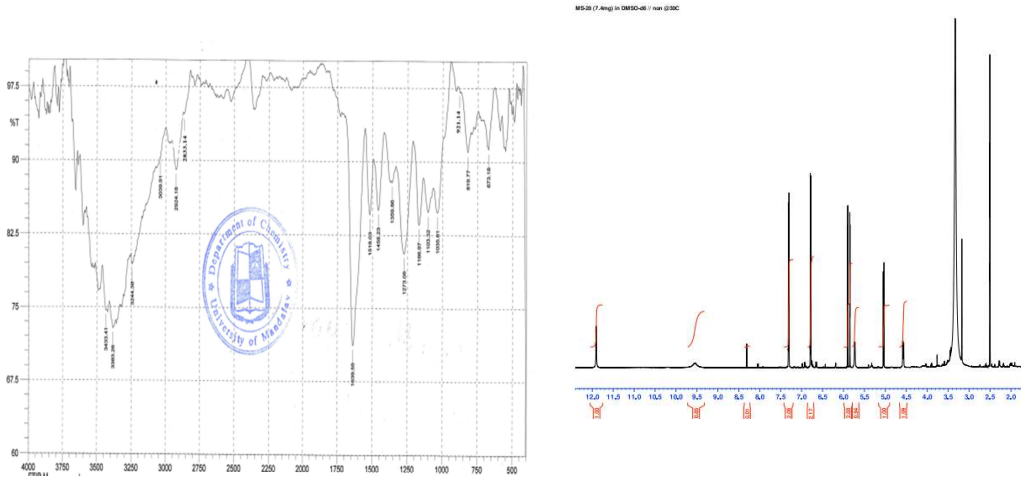

(a) (b)

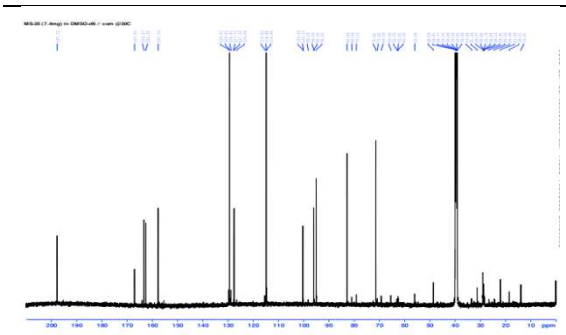

(c)

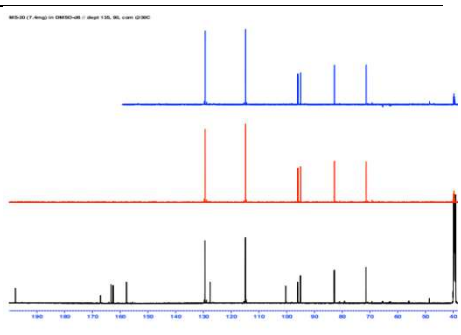

(d)

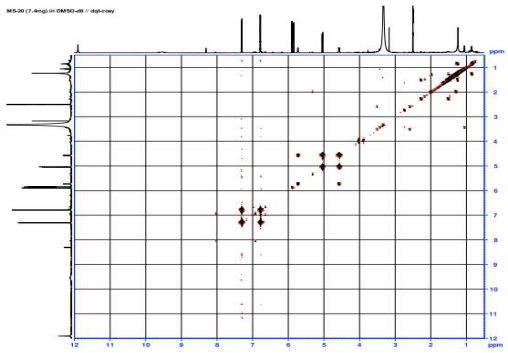

(e)

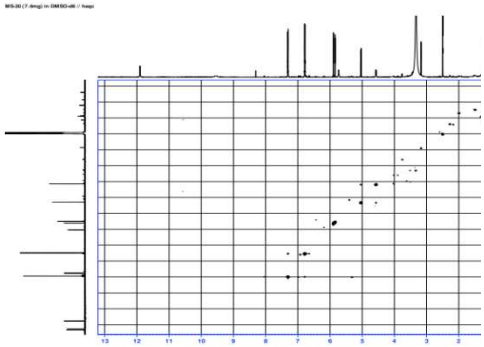

(f)

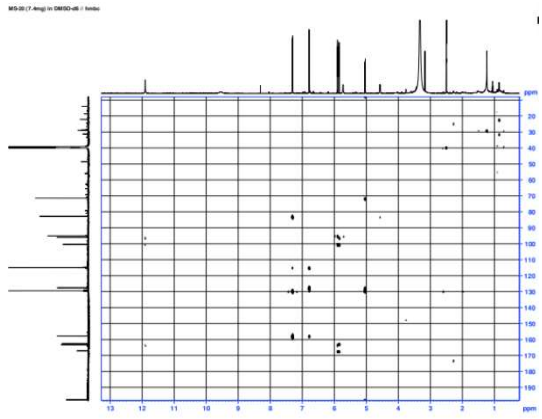

(g)

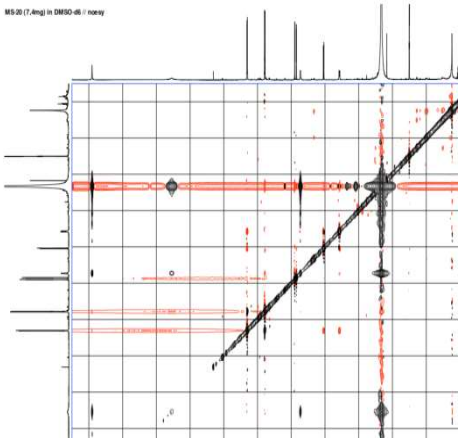

(h)

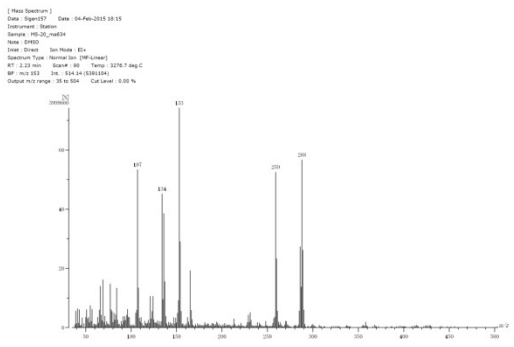

(i)

Figure 5 (a) FT IR, (b) ^{1}HNMR, (c) ^{13}C NMR, (d) DEPT, (e) DQF COSY, (f) HMQC, (g) HMBC, (h) NOESY and (i) EI Mass Spectra of Pure Organic Compound (MML-1)

4, 4' (1R,3aS,4R, 6aS) –hexahydrofuro [3,4-c] furan-1,4-diyl) bis (2,6-dimethoxy phenol)(MML-2)

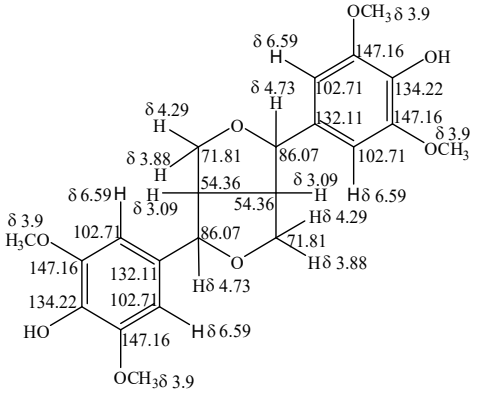

Complete structure of pure compound MML-2

molecular weight	:	418 (m/z = 418 in EI mass spectrum)
physical form	:	brown oily form
R_f value	:	0.12 [n-hexane :EtOAc (6:4)]
molecular formula	:	$C_{22}H_{26}O_8$

FT IR : (KBr), $\nu_{max}(cm^{-1})$
3400.62(ν_{OH}), 3082.35($\nu_{C=CH2}$), 2960.83 and 2854.74(ν_{asym} and ν_{sym} of CH), 1610.61 and 1518.03($\nu_{C=C}$), 1460.16(δ_{C-H} of CH_2 and CH_3), 1371.43(ν_{OH} of phenol), 1259.56 and 1026.16(ν_{C-O-C} of ether), 1215.19(ν_{C-O} of phenol), 804.34(δ_{C-H} out of planebending)

^{1}H NMR : 600MHz, $CDCl_3$,δ_H(ppm)
3.09(ddd, J=4.8Hz, 5.28Hz, 6.39Hz, 1H), 3.90(s,6H) ,
3.88(dd,J=5.28Hz, 9.16Hz, 1H), 4.29(dd, J=6.9Hz, 9.16Hz,
1H), 4.73(d, J=4.8Hz, 1H), 6.59(s,2H)

^{13}C NMR : 150MHz, $CDCl_3$,δ_C(ppm)
54.36(CH-3a), 56.38(CH_3-7'), 71.81(CH_2-2), 86.07(CH-1), 102.71(CH-5'), 132.11 (Cq-4'), 134.22(Cq-1'), 147.16(Cq-2')

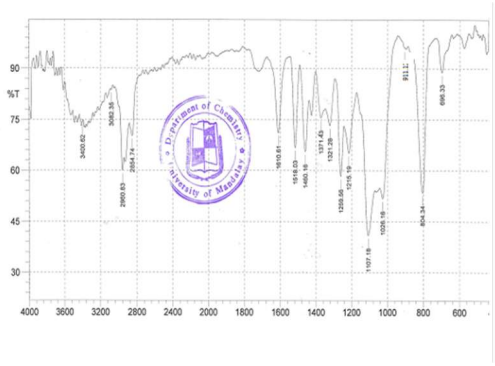

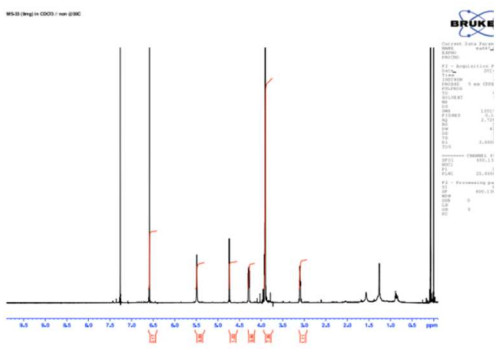

(a) (b)

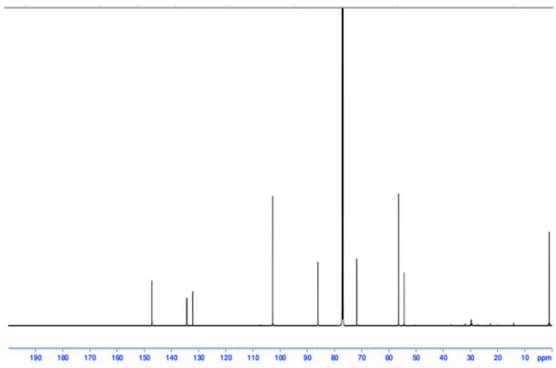

(c)

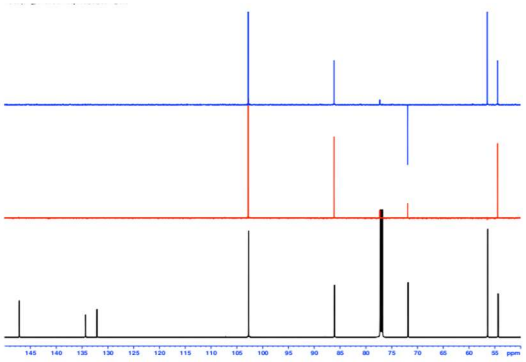

(d)

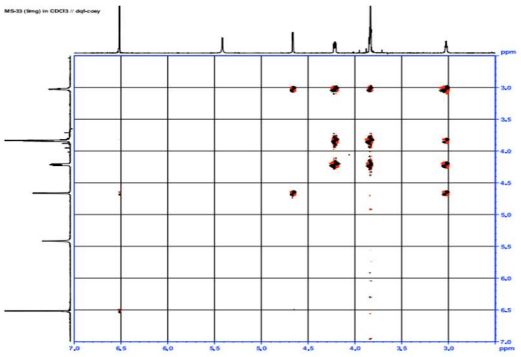

(e)

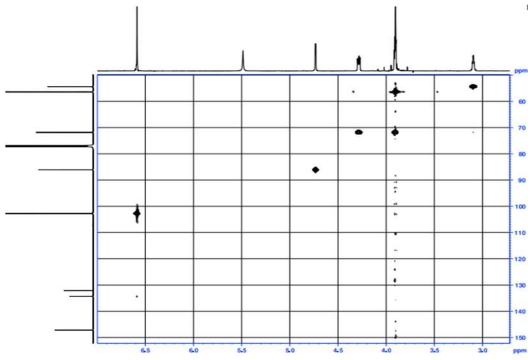

(f)

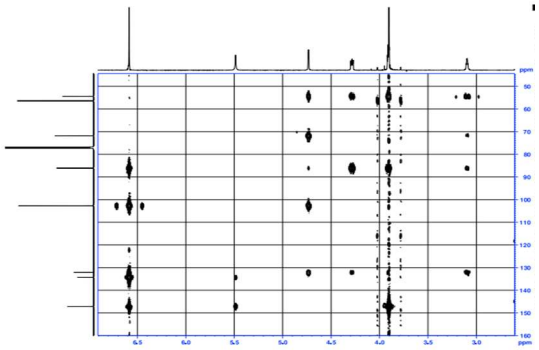

(g)

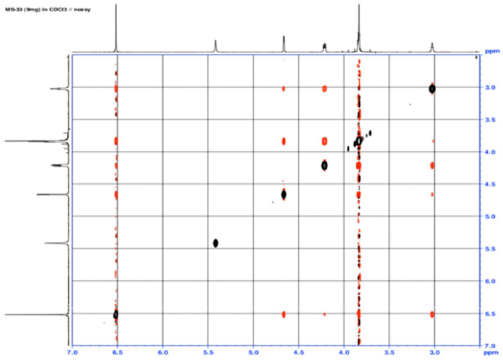

(h)

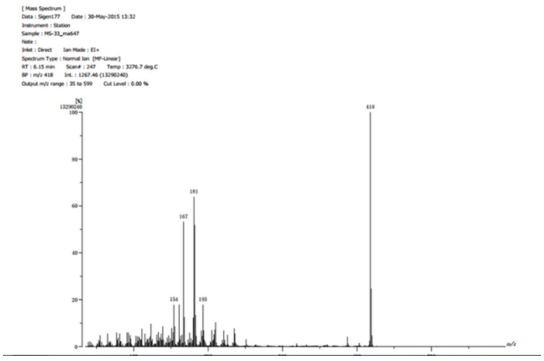

(i)

Figure 6 **(**a) FT IR, (b)[1]HNMR, (c) [13]C NMR, (d) DEPT, (e) DQF COSY, (f) HMQC, (g) HMBC, (h) NOESY and (i) EI Mass Spectra of Pure Organic Compound (MML-2)

Conclusion

In this study, one of Myanmar medicinal plants, *P. cerasoides* was used for isolation and structural elucidation of pure organic compounds. The results of the phytochemical analysis revealed that glycosides, phenolic compounds, reducing sugars, saponins, steroids, flavonoids, alkaloids, terpenes and polyphenols were present in the extract of *P. cerasoides*. The ethyl acetate extract was chromatographed by various chromatographic techniques to give pale yellow powder of pure compound(MML-1) and brown oily form of pure compound (MML-2). The melting point of pure compound (MML-1) was found to be 177-179°C. The Structurer of those pure compounds were elucidated by modern technique

According to the results of the antimicrobial activity, the ethyl acetate extract of *P. cerasoides* showed the high activity on all tested microorganisms except on *Bacillus subtilis* and *Staphylococcus aureus*. The isolated pure

compound (MML-1) showed low antimicrobial activity on all tested organisms. The isolated pure compound (MML-2) showed low antimicrobial activity on four tested organisms such as *Staphylococcus aureus***,** *Bacillus pumilus, Candida albicans* and *Escherichia coli*.

The, antioxidant activity of the crude ethanol extract and pure compounds (MML-1) and (MML-2) were evaluated using DPPH radical scavenging assay. MML-1 andMML-2 showed the antioxidant activity with the IC_{50} values of 8.14 µg/mL and 7.29 µg/ml respectively.

Moreover, the acute toxicity study on 95% ethanol extract of the stem bark of *P. cerasoides* was observed to show no toxic effect up to dose level of 2500 mg/kg. Therefore, the medium lethal dose (LD_{50}) was expected to be more than 2500 mg/kg. The molecular structures and conformational analysis of compounds (MML-1) and (MML-2) were determined by high resolution spectrometric techniques and molecular modeling. The pure compounds (MML-1) and (MML-2) possess the types of flavonoid and lignan compounds. The IUPAC names of the pure compounds (MML-1 and MML-2) are **(**2R, 3R)-3,5,7-trihydroxy-2-(4-hydroxyphenyl) chroman-4-one and 4, 4' (1R,3aS,4R, 6aS) –hexahydrofuro [3,4-c] furan-1,4-diyl) bis (2,6-dimethoxy phenol) respectively.

Acknowledgments

The author would like to thank the Myanmar Academy of Arts and Science for allowing to present this paper.

References

Boyd, E.M. (1959). "The Acute Oral Toxicity of Acetylsalicylic Acid" . *Appl, Pharmacol*, vol 1 p.229

Butler, M.S. (2004). "The Role of Natural Product Chemistry in Drug Discovery". *J. Nat. Prod*, vol. 67, pp. 2141-2153

Harborne, J.B. (1993). *Phytochemical Methods: A Guide to Modem Techniques of Plant Analysis*. New York: Chapman and Hall Ltd., pp.40-249

Marais, J.P.J., Deavours, B., Dixon, R.A. and Ferreira, D. (2006). *The Stereo Chemistry of Flavonoids*. New York: Springer Science, Inc., pp. 1-4

Marinova, G. and Batchvarov, V. (2011). "Evaluation of the Methods for Determination of the Free Radical Scavenging Activity by DPPH". *Bulgarian Journal of Agricultural Science*, vol. 17 (1), 11-24

Silverstein, R. M., Webster, F. X. and Kiemle, D. J. (2005). *Spectrometric Identification of Organic Compounds.* New York: 7th edition, John Wiley and Sons, Inc.

Yadav, R.N.S. and Munin, A. (2011). "Phytochemical Analysis of Some Medicinal Plants ". *Journal of Phytology*, vol3 (12), pp. 10-14.

ACUTE TOXICITY OF THE ETHANOLIC PLANT EXTRACT AND STRUCTURE ELUCIDATION OF PURE ORGANIC COMPOUND FROM THE BARK OF *Cordia wallichii* G.DON. (THANAT-GYI)

Win Htay[1], Myint Myint Khaing[2], Aye Mon Thida Nyo[3]

Abstract

In this research work, one Myanmar indigenous medicinal plant, *Cordia wallichii* G.Don. (Thanat-gyi) was selected for chemical analysis. It was collected in Pyin Oo Lwin Township, Mandalay Region in Myanmar. The phytochemical screening of this plant was determined which gave positive tests for flavonoids, terpenes, glycosides, reducing sugars, polyphenols, tannins, saponins, lipophilic and phenolic compounds. The antimicrobial activities of crude extract of this plant were tested in various solvent systems by Agar well diffusion method on six selected microorganisms: *Bacillus subtilis, Staphylococcus aureus, Bacillus pumilus, Pseudomonas aeruginosa, Candida albicans* and *E. coli*. In addition, the acute toxicity test of 95 % ethanolic extract of the bark of *Cordia wallichii* G.Don. was done by Organization of Economic Cooperation and Development (OECD) guideline 425 (2008) on albino mice. The pure organic compound (WH-1) was next isolated from the bark of Thanat-gyi by Thin Layer and Column Chromatographic methods. The pure yellowish brown crystal (0.62 %) was obtained based upon the ethyl acetate crude extract. Furthermore, the molecular formula ($C_{16}H_{12}O_7$), molecular mass (316) and complete structure of this pure compound was determined by FT-IR, ^{1}H NMR, ^{13}C NMR, DEPT, HSQC, DQF-COSY, HMBC and EI-MS spectral data respectively. The IUPAC name of pure organic compound (WH-1) is (E)-4-(4-(2-carboxyvinyl)-2-hydroxyphenoxy)-3-hydroxy benzoic acid.

Keywords :*Cordia wallichii* G.Don., Thanat-gyi, acute toxicity, Chromatographic methods, NMR, EI-MS

[1] Lecturer, Dr,Department of Chemistry, Monywa University
[2] Associate Professor, Dr, Department of Chemistry, Mandalay University of Distance Education
[3] Associate Professor, Dr,Department of Chemistry, University of Mandalay

Introduction

Medicinal plants and plant derived medicine are widely used in traditional cultures all over the world and they are becoming increasingly popular in modern society. Plants have the ability to synthesize a wide variety of chemical compounds that are used to perform important biological functions and to defend against attack from predators such as insects, fungi and herbivorous mammals (Lemmens *et al*., 1999). The drugs are derived either from the whole plant or from different organs, like leaves, stem, bark, root, flower and seed, etc. Some drugs are prepared from excretory plant product such as gum, resins and latex (Merck Index, 1983). Some important chemical intermediates needed for manufacturing the modern drugs are also obtained from plants. Not only, that plant-derived drug offers a stable market world wide, but also plants continue to be an important source for new drugs (Khare, 2007).

In Myanmar, most of the people prefer on traditional medicinal plants and tested medicines rather than modern medicines for the treatment of various human diseases. There is still many medicinal plants that are not well known for their medicinal values in our country. In future, biologically active plant derived chemicals can be expected to play an increasingly significant role in the commercial development of new agrochemicals and pharmaceuticals (Aye Than, 1996).

Before the medicinal plant could be used as medicines, it must be ensured to be safe. The Organization for Economic Cooperation and Development (OECD) defines acute toxicity as "the adverse effects occurring within a short time of (oral) administration of a single dose of a substance or multiple doses given within 24 h. The median lethal dose (LD_{50}) test is used to determine the acute toxicity of a substance. A key stage in ensuring the safety of drugs is to conduct toxicity tests in appropriate animal models. In Myanmar, most of the acute toxicity data comes from animals testing.

Fruits and barks of *Cordia wallichii* G.Don (Thanat-gyi) (Figure 1) were medicinally used in India and Myanmar. The fruits were used as an expectorant, astringent and demulcent. The fruits are also useful in treating coughs, the diseases of the chest and chronic fever (Parmar, and Kaushal., 1982). They remove pain from the joints and the burning of the throat and are

also effective in treating the diseases of the spleen. The bark is used in toothache and to expel bladder and kidney stones (Ah Shin Nagathein, 1967).

In this research, the acute toxicity of 95 % ethanolic extract of the bark of *Cordia wallichii* G.Don. was carried out based on the OECD guideline 425 on albino mice. A pure organic compound (WH-1) was isolated from the bark of *Cordia wallichii* G.Don. by applying Thin Layer and Column Chromatography. The complete structure of pure organic compound (WH-1) could be elucidated by using advanced spectroscopic methods such as FT IR, ^{1}H NMR (500 MHz), ^{13}C NMR (125 MHz), DEPT, DQF-COSY, HSQC,

(a) (b) (c) (d)

Figure 1. (a)Plant, (b)fruits,(c) flowers and (d) barks of *Cordia wallichii* G.Don.

Materials and Methods

Sample Collection

The barks of *Cordia wallichii* G.Don. were collected from Pyin Sar Village, Pyin Oo Lwin Township, Mandalay Region. The samples were cut into small pieces and allowed to air dry. Then the dry samples were stored in a well-stoppered bottle and used throughout the experiment.

Study on Acute Toxicity of the Bark of *Cordia wallichii* G.Don.

Method for Acute Toxicity Study

Acute oral toxicity test on 95 % ethanolic extract of the bark of *Cordia wallichii* G.Don. was carried out according to OECD 425 guideline (2008). Therefore, the limit test at 5000 mg/kg was performed. Total number of adult albino mice, weighing (20-30 g) were selected. Since the route of administration selected should be the intended route for administration of the tested drug given to the human during therapy, the oral route was chosen for this test.

Figure 2. Administration of test substance suspension to the mice

Extraction and Isolation of Pure Compound (WH-1) from the Bark of *Cordia wallichii* G.Don.

Air dried sample (950 g) was percolated with 95 % ethanol (3.5 L) for two months. The extracted solution was filtered and evaporated in air. Then it was re-extracted with ethyl acetate (300 mL) and evaporated. The ethyl acetate crude extract (2.03 g) was obtained. Ethyl acetate crude extract was checked by TLC with n-hexane : EtOAc various ratios.

Column size	(1.5 × 40) cm
Adsorbent	SiO_2 (Silica Gel)
Flow rate	0.4 mL/min

The ethyl acetate crude extract (2.03 g) was fractionated by column chromatography over silica gel with various ratios of n-hexane and ethyl acetate from non-polar to polar. Totally (192) fractions were obtained. Each fraction was checked by TLC. The same R_f value fractions were combined and 6 combined fractions were obtained. Major combined fraction (V) gave only one spot on TLC and UV active. The pure yellowish brown crystal (12.6 mg)

was obtained. The yield percent of this pure compound (WH-1) was found to be 0.62 % based upon the ethyl acetate crude extract.

The molecular formula and the structure of this isolated compound were assigned by using advanced spectroscopic methods such as FT IR, ^{1}H NMR (500 MHz), ^{13}C NMR (125 MHz), DEPT, DQF-COSY, HSQC, HMBC and EI-MS spectral data.

Results and Discussion

Phytochemical Tests for the Bark of *Cordia wallichii* G.Don.

The phytochemical screenings of the bark of *Cordia wallichii* G.Don. are carried out and these results are shown in Table 1.

Table 1. Phytochemical Test for the Bark of *Cordia wallichii* G.Don.

No.	Constituents	Reagent used	Observation	Results
1.	Alkaloid	Dragendorff's reagent	No orange ppt	–
2.	Flavonoid	EtOH, Mg ribbon, Conc: HCl	Pink colour solution	+
3.	Steroid	Petether, acetic anhydride, $CHCl_3$, Conc: H_2SO_4	No greenish blue colour solution	–
4.	Terpene	EtOH, acetic anhydride, $CHCl_3$, Conc: H_2SO_4	Reddish brown colour solution	+
5.	Glycoside	10 % lead acetate	Yellow ppt	+
6.	Reducing sugar	Benedict's solution	Red ppt	+
7.	Polyphenol	1 % $FeCl_3$, 1 % $K_3[Fe(CN)_6]$	Greenish blue colour solution	+
8.	Tannin	10 % $FeCl_3$, dil H_2SO_4	Yellowish brown ppt	+
9.	Saponin	Distilled H_2O shaken	Frothing	+
10.	Lipophilic	0.5 N KOH solution	Deep yellow colour solution	+
11.	Phenolic	H_2O, Δ, 10 min, 10 % $FeCl_3$	Greenish blue colour solution	+

(+) = presence of constituents, (–) = absence of constituents

According to this table, the bark of *Cordia wallichii* G.Don. contains flavonoid, terpene, glycoside, reducing sugar, polyphenol, tannin, saponin, lipophilic and phenolic compound.

Antimicrobial Activities of the Bark of *Cordia wallichii* G.Don.

The antimicrobial activities of the bark of *Cordia wallichii* G.Don. were tested in various solvent systems by using Agar well diffusion method. The results are tabulated in Table 2.

Table 2. Antimicrobial Activities of Crude Extract of Bark of *Cordia wallichii* G.Don.

Sample	Solvent	Diameter of Inhibition Zone (mm)					
		I	II	III	IV	V	VI
Thanat-gyi	n-hexane	–	–	–	–	–	–
	EtOAc	30 (+++)	50 (+++)	28 (+++)	–	35 (+++)	43 (+++)
	EtOH	–	–	12 (+)	–	30 (+++)	–

Agar Well – 10 mm
(+) ~ 10 mm – 14 mm
(++) ~ 15 mm – 19 mm
(+++) ~ 20 mm above

I = *Bacillus subtilis*
II = *Staphylococcus aureus*
III = *Pseudomonas aeruginosa*
IV = *Bacillus pumilus*
V = *Candida albicans*
VI = *E. coli*

According to this table, the ethyl acetate extract of Thanat-gyi responds high activities on *Bacillus subtilis, Staphylococcus aureus, Pseudomonas aeruginosa, Candida albicans* and *E. coli*. The ethanol extract of Thanat-gyi shows high activity on *Candida albicans* and low activities on *Pseudomonas aeruginosa*.

Result of Acute Toxicity Study for *Cordia wallichii* G.Don.

Acute toxicity test was done by using limit test according to OECD 425 guideline (2008). The test substance was non-toxic at the test dose 5000 mg/kg. There was no lethality of the mices up to 14 days observation period. Therefore, median lethal dose (LD_{50}) of the ethanolic extract of bark of *Cordia wallichii* G.Don. was supposed to be greater than 5000 mg/kg.

Clinical observations

For evaluation of toxicity, no significant changes were observed in toxic parameters. Skin and fur changes, eyes, mucous membrane, respiratory rate, motor activity and behavioral pattern were found to be normal. Salivation, convulsion, cyanosis, tremors and diarrhoea did not occur in all mices. There was no abnormality detected (Table 3).

Table 3. Acute Toxicity Study of the Bark of *Cordia wallichii* G.Don. Based on Mortality Record

Extracts	Groups	No: of mice/ group	Diet	Dose of extract (mg/kg)	Final volume given (mL/kg)	Observed Period (week)	Ratio of dead and tested	Death %
Extract of Bark of *Cordia wallichii* G.Don.	I	3	Stock diet and DW	175	10	2	0/3	0
	II	3	Stock diet and DW	550	10	2	0/3	0
	III	3	Stock diet and DW	2000	10	2	0/3	0
	IV	3	Stock diet and DW	5000	10	2	0/3	0
	Control	3	DW	0	10	2	0/3	0

After two weeks, all the mice were alive and did not show any toxic symptoms such as body weight loss, diarrhoea, inactivity, aggressiveness, restlessness, etc. and no death when compared with that of the control group.

Body Weight

According to this table, four different groups of mices were administered with four different doses. Individual mice was weighed daily thereafter for 14 days. There was no significant change in body weight before and after administration of the test drug (Table 4).

Table 4. Acute Toxicity Study of the Bark of *Cordia wallichii* G.Don. Based on Daily Body Weight Record

Groups	Marking	Sex	Dose in mg/kg Body Weight	Weight of mice (g) 1st day	7th day	14th day
I	Head	Female	175	26.1	27.0	27.8
	Head	Male		18.5	24.5	27.7
	Bark	Male		20.8	26.4	28.9
		Mean value		**21.8**	**26.0**	**28.1**
II	Bark	Female	550	24.3	25.2	25.2
	Tail	Male		21.2	27.0	29.5
	R-Hand	Male		19.8	23.1	27.4
		Mean value		**21.8**	**25.1**	**27.4**
III	Tail	Female	2000	27.4	28.1	28.9
	R-Hand	Female		30.8	28.3	28.8
	L-Hand	Male		26.6	25.7	28.1
		Mean value		**28.3**	**27.4**	**28.6**
IV	Head	Female	5000	24.0	26.7	27.4
	Bark	Female		22.4	24.6	25.2
	Tail	Female		23.0	25.2	24.2
		Mean value		**23.1**	**25.5**	**25.6**
Control	R-Hand	Female	Distilled Water	25.1	25.9	26.4
	R-Leg	Male		20.1	23.6	26.1
	L-Hand and L-Leg	Male		25.8	27.8	28.6
		Mean value		**23.7**	**25.8**	**27.0**

In accordance with the results summarized in Tables 3 and 4 this plant extract can be labeled unclassified in the hazard category according to Globally Harmonized System and can be considered relatively safe.

Molecular Formula Determination of Pure Compound (WH-1)

The molecular formula of the isolated compound (WH-1) was determined by FT IR, ^{1}H NMR (500 MHz), ^{13}C NMR (125 MHz), DEPT, HSQC and EI-mass spectral data (Silverstein *et al*., 2005)

FT IR assignment of compound (WH-1)

FT IR spectrum of isolated compound (WH-1) was measured at the Department of Chemistry, University of Mandalay. It is described in Figure 3 a.

According to FT IR spectral data, compound consists of carboxylic acid group, sp^2 hydrocarbon, carbonyl group, aromatic benzene ring, C – C – O stretching vibration of alcohol group, C – O – C stretching vibration of ether group and trans or E and cis or Z alkenic group respectively. The assignments of FT IR spectral data are shown in Table 5.

Table 5. FT IR Assignment of Pure Compound (WH-1)

Frequencies (cm^{-1})	Assignment
3300-2750	O – H stretching vibration of carboxylic acid group
3078.68	= C – H stretching vibration of sp^2 hydrocarbon
1707.06	C = O stretching vibration of carbonyl group
1604.83, 1516.10	C ---- C stretching vibration of aromatic benzene ring
1276.92	C – C – O stretching vibration of alcohol group
1192.05, 1031.95	C – O – C stretching vibration of ether group
985.66	= C – H out of plane bending vibration of trans or E alkenic group
819.77, 767.69	= C – H out of plane bending vibration of cis or Z alkenic group

^{1}H NMR spectral data of compound (WH-1)

^{1}H NMR spectrum (CD_3OD, 500 MHz) of this isolated compound is indicated in Figure 3b. According to this spectrum, compound (WH-1) contains (8) protons.

^{13}C NMR spectral data of compound (WH-1)

^{13}C NMR (125 MHz) spectrum, Figure 3c , indicates the total number of carbons (16) in this compound.

According to ^{1}H NMR, ^{13}C NMR, HSQC (Figure 3d) and DEPT (Figure 3 e) spectral data, the partial molecular formula of compound (WH-1) is $C_{16}H_8$ and partial molecular mass is 200. From the FT-IR assignments, compound (WH-1) should consist of at least one – OH group, one carbonyl group and one ether oxygen atom. Therefore, the partial molecular formula becomes $C_{16}H_9O_3$ and extended partial molecular mass is 249. In the ^{13}C NMR spectral data, two carbonyl carbons could be observed at (δ 170.27 ppm and δ 171.15 ppm). Thus, the extended partial molecular formula is $C_{16}H_9O_4$ and its molecular mass is 265. In accordance with EI-mass spectrum (Figure 3 f), molecular ion peak m/z is 316 which indicates the molecular mass of compound. The remaining molecular mass is (316 – 265 = 51). It must be three – OH groups. Therefore, the real molecular formula of compound (WH-1) is $C_{16}H_{12}O_7$.

$$\text{Hydrogen Deficiency Index (HDI)} = C - \frac{H}{2} + 1$$

$$= 16 - \frac{12}{2} + 1 = 11$$

Confirmation of molecular formula of compound (WH-1)

Molecular formula of compound (WH-1) could be confirmed by FT IR spectrum (Figure 3 a) and DEPT spectrum (Figure 3e) as shown in Table 6.

Table 6. Results Given by FT-IR and DEPT Spectral Data of Compound (WH-1)

Assignments	No. of Carbon	No. of Proton	No. of Oxygen
DEPT Spectrum			
- Eight sp^2 methine carbons	8	8	–
- Six sp^2 quaternary carbons	6	–	–
- Two sp^2 carbonyl carbons	2	–	2
FT-IR Spectrum			
- One –OH group	–	1	1
- One ether functional group	–	–	1
Partial molecular formula	C_{16}	H_9	O_4

Partial molecular mass = 265

Molecular ion peak m/z = 316

Remaining molecular mass = 316 – 265 = 51

It must be three –OH groups.

∴ Real molecular formula = $C_{16}H_{12}O_7$

Structure Elucidation of Pure Organic Compound (WH-1)

The structure of pure organic compound (WH-1) could be elucidated by applying DQF-COSY, ^{1}H NMR, HSQC and HMBC spectra respectively. The occurrence of medium graphic area in DQF-COSY spectrum (Figure 3 g) and HMBC spectrum (Figure 3h) lead to the following fragments.

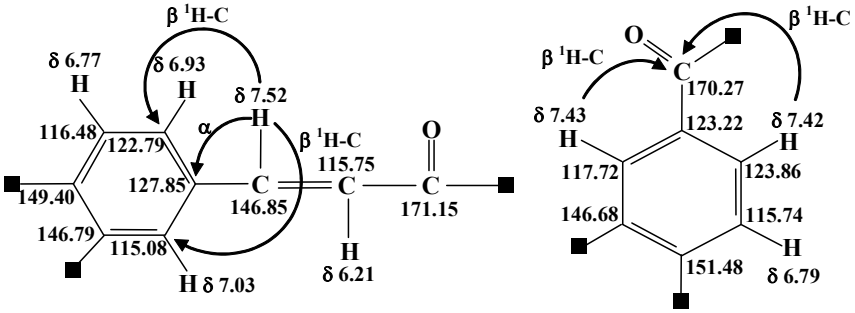

In accordance with HMBC spectral data, the complete structure of (WH-1) can be assigned.

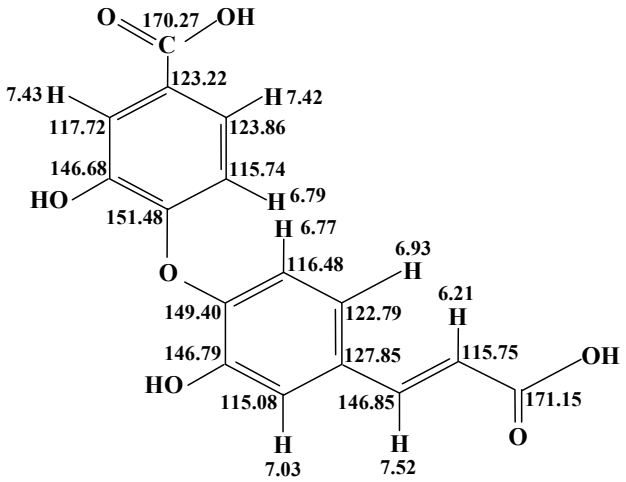

Mass Fragmentation Behaviour of Pure Compound (WH-1)

The elucidated structure of pure compound (WH-1) could be confirmed by EI-mass fragmentation behaviour. The proposed mechanisms for the fragmentation pattern in EI-mass spectrum (Figure 3f) are shown as follows.

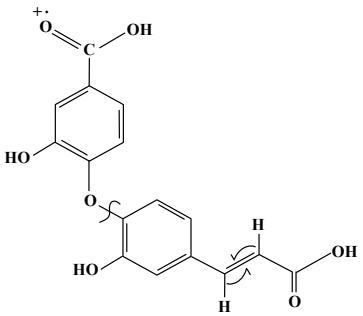

m/z – 316

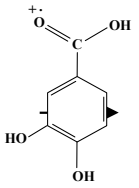

fragment a

m/z – 154 (54 %)

+

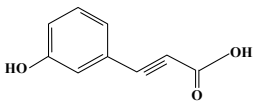

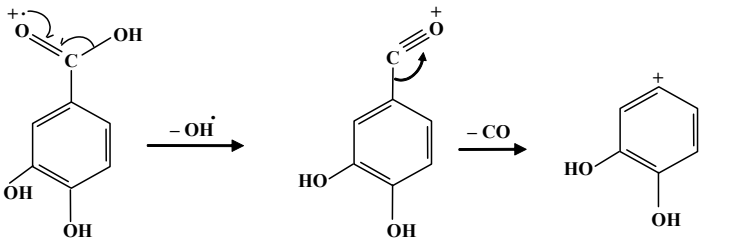

fragment a

fragment b
m/z – 137 (100 %)
(base peak)

fragment c
m/z – 109 (33 %)

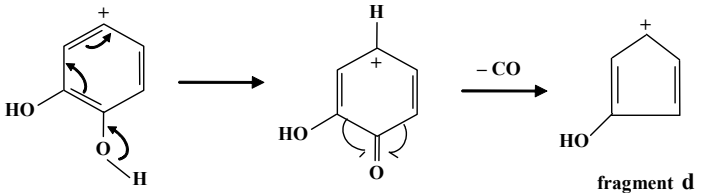

fragment c
m/z – 109

fragment d
m/z – 81 (37 %)

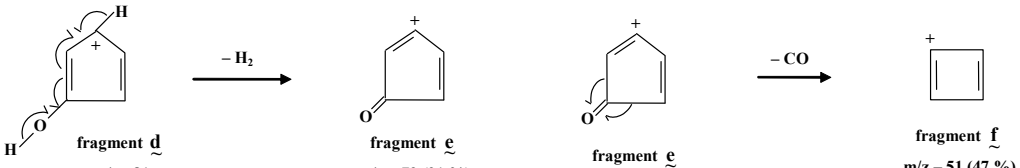

fragment d
m/z - 81

fragment e
m/z – 79 (21 %)

fragment e
m/z – 79

fragment f
m/z – 51 (47 %)

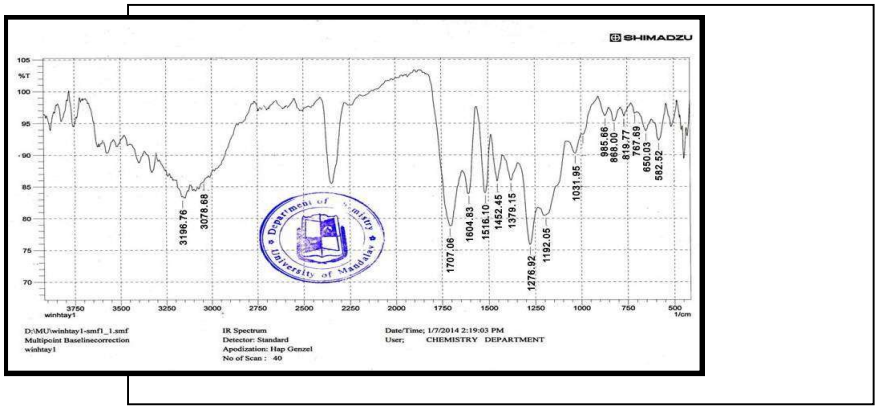

(a)

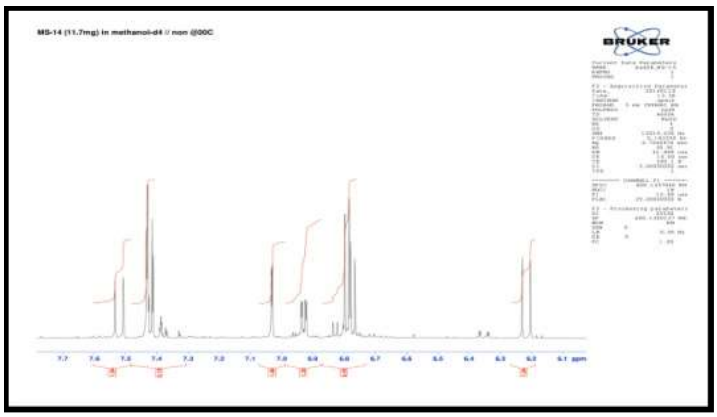
MS-14 (11.7mg) in methanol-d4 // non @00C
BRUKER

(b)

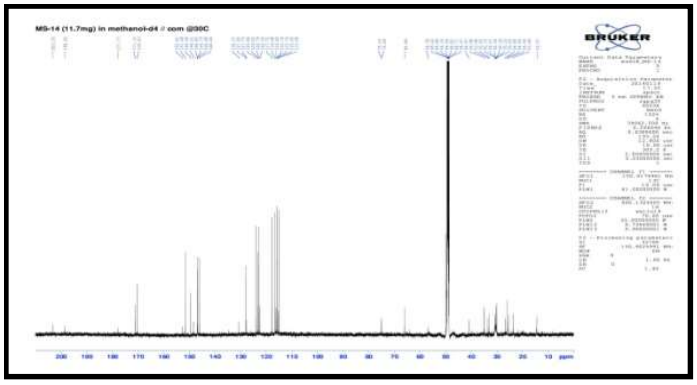
MS-14 (11.7mg) in methanol-d4 // com @00C
BRUKER

(c)

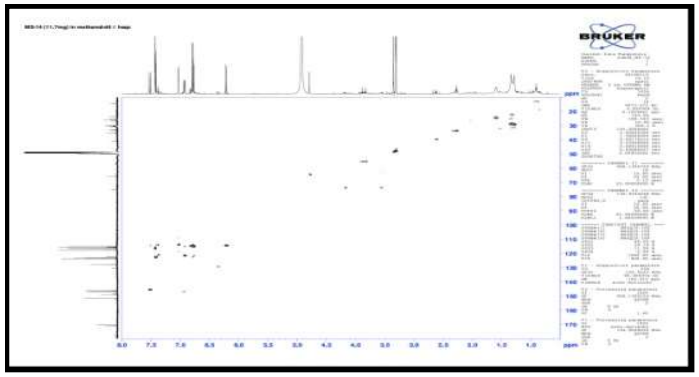
BRUKER

(d)

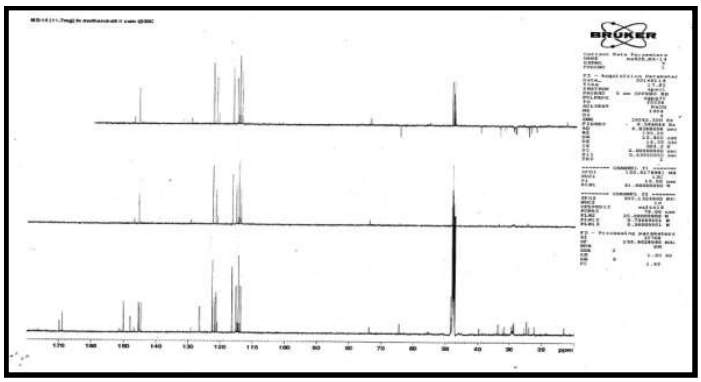

(e)

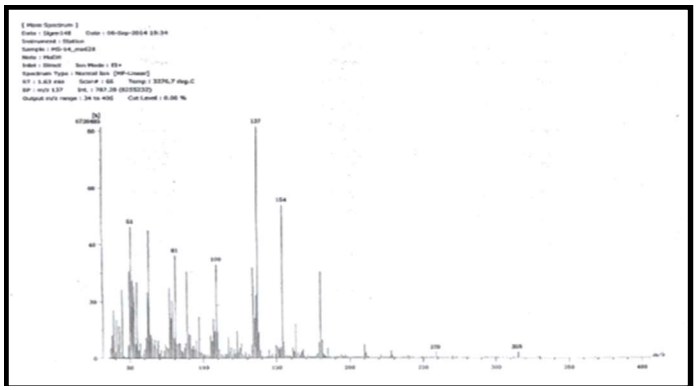

(f)

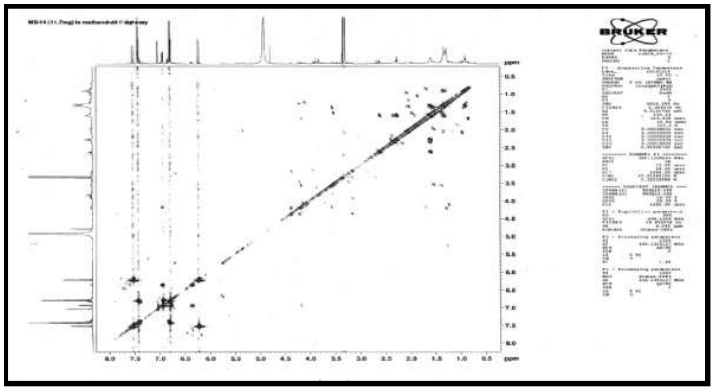

(g)

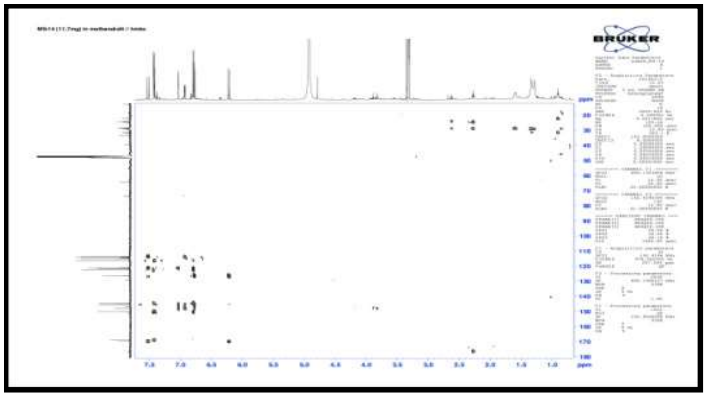

(h)

Figure 3. (a) FT- IR, (b) ^{1}HNMR, (c) ^{13}C NMR, (d) HSQC, (e) DEPT, (f) EI- Mass, (g) DQF-COSYand (h) HMBC-Spectra of Pure Organic Compound (WH-1)

Conclusion

In this research work, one Myanmar indigenous medicinal plant, *Cordia wallichii* G.Don. was selected for chemical idextification.

Firstly, phytochemical tests were examined and according to these results, the bark of Thanat-gyi contains flavonoids, terpenes, glycosides, reducing sugars, polyphenols, tannins, saponins, lipophilic and phenolic compounds.

Moreover, the antimicrobial activities of various plant extracts were tested by Agar well diffusion method on six selected organisms. Ethyl acetate extract of Thanat-gyi responds high activities on five selected organisms such as *Bacillus subtilis, Staphylococcus aureus, Pseudomonas aeruginosa, Candida albicans* and *E. coli*.

Regarding with the evaluation of toxicity, no significant change was observed in toxic parameters during 14 days. There was no significant change in body weight before and after administration of the test drug. After two weeks, all the mice survived no toxicity sign was observed up to the dose level

of 5000 mg/kg body weight. Hence, the tested substance (95 % ethanolic extract of the bark of *Cordia wallichii* G.Don.) can be labeled unclassified in the hazard category according to Globally Harmonized System and can be considered relatively safe.

Furthermore, pure compound (WH-1) was isolated from the bark of Thanat-gyi by using Thin Layer and Column Chromatographic techniques. The pure yellowish brown crystal (12.6 mg, 0.62 % yield) was obtained. The molecular formula of isolated pure compound was determined as ($C_{16}H_{12}O_7$) by applying spectroscopic methods such as FT-IR, ^{1}H NMR (500 MHz), ^{13}C NMR (125 MHz), DEPT, HSQC and EI-mass spectra. The structure of this isolated compound was elucidated by DQF-COSY, ^{1}H NMR, splitting patterns, coupling constant (J-values) and HMBC spectroscopic studies. Finally, the elucidated structure of isolated compound was confirmed by the fragmentation behavior of EI-mass spectrum.

The IUPAC name of isolated pure compound (WH-1) is (E)-4-(4-(2-carboxyvinyl)-2-hydroxyphenoxy)-3-hydroxy benzoic acid.

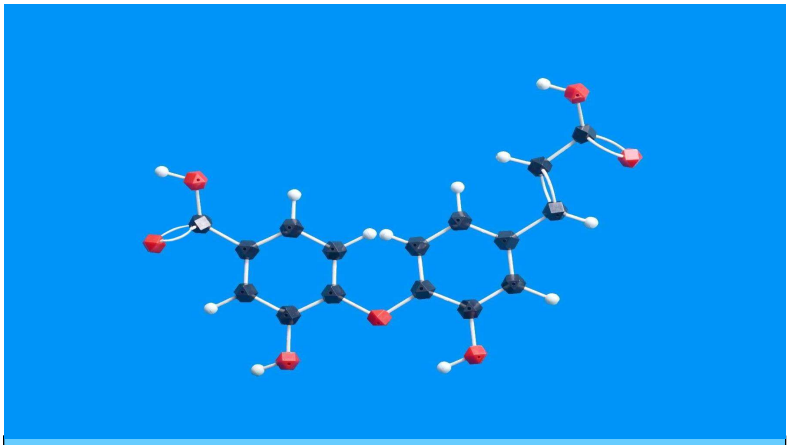

(E)-4-(4-(2-carboxyvinyl)-2-hydroxyphenoxy)-3-hydroxy benzoic acid

Acknowledgements

The author would like to thank Dr Than Than Win, Professor, Department of Chemistry, Monywa University for her constant encouragement.

References

Ah Shin Nagathein, (1967). "Pon Pya Say Abidan", Rangoon: 3rd Edition, Mingala Press, vol. 4.pp.289-295.

Aye Than, (1996). "Scientific Studies on Myanmar Medicinal Plants", *DMR Bulletin*, vol. 10(1)p.3.

Khare, C.P. (2007). *Indian Medicinal Plants. An Illustrated Dictionary*. New Delhi: Springer-Verlag

Lemmens, R.H.M.J.] de Padau, L.S. and Bunyapraphatsara, N. (1999). "Medicinal and Poisonous Plants 3." *Plant Resources of South-East Asia*, vol. 12(1),pp12-19

Merck Index. (1983). *An Encyclopedia of Chemical, Drugs, and Biologicals*. New York: 10th Edition, Merck & Co. Inc.

Organization of Economic Co-operation and Development (OECD). (2008). *Acute Oral Toxicity Up and Down Procedure*. In:. OECD Guideline for Testing of Chemicals, 425.

Parmar, C. and Kaushal, M.K. (1982). *Cordia obliqua* In: Wild Fruits,. New Delhi:Kalyani Publishers, P. 19-22.

Silverstein, R. M., Webster, F. X. and Kiemle, D. J. (2005). *Spectrometric Identification of Organic Compounds.* New York: 7th edition, John Wiley and Sons, Inc.

ACKNOWLEDGEMENTS

The author would like to thank Dr Than Than Win, Professor, Department of Chemistry, Monywa University for her constant encouragement.

IDENTIFICATION OF SOME BIOACTIVE ORGANIC CONSTITUENTS FROM THE AERIAL PARTS OF *Clerodendrum indicum* (L.)KUNTZE(NGA-YANT-PADU) USED IN THE TREATMENT OF ASTHMA

Myint Myint Kyi[1], Daw Hla Ngwe[2], Maung Maung Htay[3]

Abstract

The purpose of this research work was to study bioactive phytochemical constituents from aerial parts of the selected medicinal plant: *C. indicum* (L.) Kuntze (Nga-yant-padu) which are widely used in Myanmar for the treatment of diseases such as asthma, cough, typhoid, vermifuge, diarrhea and urinary complaint. By silica gel column chromatographic separation method, 0.002% of palmitic acid (A) (m.pt 63-64°C), 0.24% of stigmasta-5, 22, 25-triene-3ol (B) (m.pt 151-152°C) was isolated from PE extract of *C. indicum* whereas separation of defatted EtOAc extract of this plant provided hispidulin (C) (0.36%, m.pt 287-288°C), pectolinarigenin (D) (0.064%, m.pt 208-210°C) and stigmasterolglucoside (E) (0.05%, m.pt 283-284°C). The isolated compounds were identified by determination of melting point, some color tests and modern spectroscopic methods. As part of the work on the bioactivity investigation of selected plant, the antiasthmatic action was studied on histamine induced guinea pig trachea *in vitro*. All selected compounds (except palmitic acid) such as stigmasta-5, 22, 25-triene-3ol, hispidulin, pectolinarigenin and stigmasterolglucoside were observed to possess 80.2% ($P<0.01$), 73.0% ($P<0.01$), 70.2% ($P<0.01$) and 63.0% ($P<0.01$) of relaxation response on histamine induced guinea pig trachea. Therefore, it can be inferred that selected plant may be useful as a remedy for the treatment of bronchial asthma.

Keywords : *Clerodendrum indicum* (L.) Kuntze, stigmasta-5,22,25-triene-3ol, hispidulin, pectolinarigenin, stigmasterolglucoside, antiasthmatic activity

[1] Lecturer, Dr,Department of Chemistry, Myingyan Degree College

[2] Professor and Head, Dr,Department of Chemistry, University of Yangon

[3] Professor and Head (Rtd), Dr,Department of Chemistry, University of Yangon

Introduction

Clerodendrum indicum (L.)Kuntze (Nga-yant-padu) belongs to the family *Verbenaceae*, which is distributed in tropical and sub-tropical zones including Hawaii, India, Java, Indo-China and Myanmar. Most *C. indicum* are found in Southern and Eastern India and cultivated for medicinal uses as well as for ornamental purposes. In Myanmar, it is widely cultivated throughout the country and readily available (Hundley and Chit KoKo, 1987).

The roots and leaves of *C. indicum* have been used to treat asthma in Myanmar and Java. In Myanmar, the leaves are also used as a remedy for the treatment of cough, scrofulous affections, vermifuge and bitter tonic. The juice of the leaves and tender branches are employed syphilitic rheumatism, herpetic eruptions and diarrhea. The extract of the whole plant is also used as an anthelmintic, pemphigus and for certain types of mental disorders. Assays realized in India, with alcoholic extract of the whole plant, displayed muscle relaxing effect, anti-inflammatory, confirming its popular use as an antispasmotic. In addition, significant anti-inflammatory activity has been reported to show in the total benzene extract of *C. indicum* against acute, sub-acute and chronic models of inflammation (Aye Than *et al*., 1995).

A hydroquinone diterpenoid – uncinatone, six cleroindicins A – F, stigmasta-5, 22, 25-triene-3ol, β-sitosterol, scutellarein, hispidulin, pectolinarigenin, iridoid glycoside are the chemical constituents of the aerial parts of *C. indicum* (Tian and Zhang, 1997). The aerial parts of that also contain numerous flavonoids and steroidal compounds, possess controllers or anti-inflammatory effects for asthmatic patients (Rang and Moore, 2003).

A diterpene hydroquinone – uncinatone has antitubercular and HIV inhibitory activity. In Dai nationality, there was a report that clerosterolsie., cleroindicins have antimalarial and antirheumatic effects (Tian and Zhang, 1997). One of the major sterol derivative, stigmasta-5,22,25-triene-3ol showed anti-inflammatory and antispasmotic activity (Patrick, 1995). Scutellarein, hispidulin and pectolinarigenin are a class of flavonoids that showed biological activities including antimutagen, antiviral, antioxidant, anti-inflammatory, antihistaminic, cytostatic and antibacterial activity. Airidoid glycoside was reported to exhibit the antimicrobial activity of Streptomyces species (Tian and Zhang , 1997). In the present work, five organic compounds: palmitic acid,

stigmasta-5, 22, 25 triene-3ol, hispidulin, pectolinarigenin and stigmasterolglucoside were isolated from the aerial parts of *C.indicum*. And the anti-asthmatic property of the four isolated compounds (except palmitic acid) were investigated.

Bronchial asthma is a disease of the lungs in which an obstructive ventilation disturbance of the respiratory passages evokes a feeling of shortness of breath. It has also become a major health problem especially in industrialized countries (Aung Htay Oo, 1996). As the number of asthmatics has increased during the last decades, mainly due to air pollution and improper ventilation. Non-allergic bronchial asthma is a genetic predisposition. Nonspecific stimuli such as cigarette smoke, air pollution, medications, emotional factors such as shock, career or family problems, disturbed parent-child relationships and also viral, bacterial or fungal infections can trigger asthma attacks. The pathogenesis of non-allergic asthma causes the release histamine from the mast cell of the bronchial wall. Asthma cannot be cured, but it can be controlled with proper asthma management (Barnes *et al.,*1998).

Materials and Methods

The experimental works were conducted at the Department of Chemistry, University of Yangon (UY). Aerial parts of Nga-yant-padu (*C. indicum*, family *Verbenaceae*) were collected from Hlaing Township, Yangon Region during November to December in 2003. The selected plant was identified by authorized botanist at Botany Department, Yangon University. After cleaning the sample, they were air-dried at room temperature. Then, they were ground into powder by a motar and pestle and stored in air-tight container to prevent contamination and kept for isolation of organic compounds. The following instruments were used for structure elucidation of isolated compounds: Gallenkamp melting point apparatus (Organic Lab, UY), UV spectrophotometer (URC, Lower Myanmar), FTIR spectrophotometer (URC, Lower Myanmar), ^{1}HNMR ($CDCl_3$, 400MHz, BrukerAvance 400 Spectrometer) (University of Gottingen, Germany), ^{13}C NMR (DMSO, 75MHz, BrukerAvance 400 Spectrometer) (University of Gottingen, Germany), ESI-MS (JEOL JMS-DX 300 Mass Spectrometer) (University of Gottingen, Germany) and EI-MS (URC, Lower Myanmar). Column

chromatography was performed using Silica gel (40-60 μm, Wakogel) and precoated TLC plates (GF_{254}Aluminium plates, Merck) were applied for thin layer chromatographic separation. All of the solvents used were purified by distillation at their boiling point ranges.

Preparation of Crude Extracts

The dried powdered sample (ca. 300 g) were percolated in 95% ethanol (1L) for one week and filtered. This procedure was repeated three times. The combined filtrate was concentrated under vacuum rotatory evaporator to obtain ethanol crude extract. The ethanol crude extract was then successively extracted by partition with pet-ether (60-80°C) and ethyl acetate. The condensed pet-ether and ethyl acetate extracts were kept for isolation of organic constituents.

Isolation of Compounds from Pet-ether Extract

Pet-ether crude extract of *C. indicum* (5 g) was mixed with a little amount of silica gel in a motar. This mixture was separated by silica gel column chromatographic method using solvent system of PE and EtOAc (19:1 to 9:1 v/v). The eluent was collected with 3mL/fraction to provide 25 fractions (f_1- f_{25}) that were monitored by TLC to obtain two main fractions: F – I (f_1 – f_9) and F – II (f_{10} – f_{25}) resulting compound **A** (0.18 mg, 0.002%) and compound **B** (12 mg, 0.24%), respectively. The compound A was purified by recrystallization using PE and EtOAc and compound B was recrystallized from PE and EtOAc giving colourless needle shaped crystal.

Isolation of Compounds from Ethyl Acetate Extract

The ethyl acetate crude extract of *C. indicum*(5 g) was fractionated by using silica gel column chromatography, successively eluting with toluene : ethyl acetate (4 : 1, 1 : 1 v/v) and ethyl acetate and methanol (98 : 2, 95 : 5 v/v) to give 87 fractions (3mL/fraction). After combining the fractions giving the similar appearance on TLC chromatograms, three main fractions were finally collected. From these three main fractions, three compounds (**C**, **D** and **E**) were obtained in the yield of 0.36%, 0.064% and 0.05%, respectively.

Structural Elucidation of Isolated Compounds

The structures of isolated compounds A, B, C, D and E were elucidated by using modern spectroscopic techniques such as UV, FT IR, ^{1}H NMR, ^{13}C NMR, ESI-MS and EI-MS spectroscopies.

Determination of Antiasthmatic Activity of Isolated Compounds

The antiasthmatic activity of four isolated compounds (B, C, D and E) was studied on normal and histamine induced contraction on isolated guinea pig trachea in *in vitro*. The relaxation response (%) of the four isolated compounds from Nga-yant-padu on histamine induced tracheal chain was determined at different doses : 0.1 mg, 0.2 mg, 0.3 mg, 0.4 mg and 0.5 mg/mL bath concentration.

Results and Discussion

Isolated Compounds from Nga-yant-padu

Column chromatographic separation of pet-ether extract provided two compounds: compound A (Palmitic acid, 0.002% yield) and compound B (Stigmasta- 5, 22, 25 triene – 3ol, 0.24% yield). From active ethyl acetate extract, two flavonoids (C, Hispidulin, 0.36% yield), (D, Pectolinarigenin, 0.064% yield) and one steroidal glycoside (E, stigmasterolglucoside, 0.05% yield) were obtained.

Structural Identification of Isolated compounds

Stigmasta-5,22,25-triene-3ol (B) : $C_{29}H_{46}O$, colourless needle shaped, R_f 0.40, PE:EtOAc 5:1; violet colour by heating with 5% H_2SO_4, m.pt151-152°C ; UV λ_{max} (MeOH) (Figure 1) : 225 nm and 270 nm ; FT IR νcm^{-1}(KBr) (Figure 2): 3451 (ν_{O-H}), 2937, 2891, 2862 (asym&symν_{C-H}), 1641($\nu_{C=C}$),1450(δ_{CH} of CH_3& CH_2), 1380(δ_{CH} of dimethyl gp),1060(asymν_{C-OH}); ^{1}H NMR δ ppm($CDCl_3$, 300 MHz) (Figures 3 and 4): 0.7(s, 3H, H-18), 0.8(t, J=7.5 Hz, 3H, H-29), 1.0(d, J=7.5 Hz, 3H, H-21), 1.02(s, 3H, H-19), 1.2-1.5(m, 15H), 1.64 (s, 3H, H-27), 1.8-2.5(m, 10H), 3.5(m, 1H, H-3), 4.7(m, 2H, H-26), 5.2(m, 2H, H-22,23), 5.35(m, 1H, H-6) (Silverstein and Webster, 1998); EI-MS(m/z): 410$[M]^+$ (Figure 5).

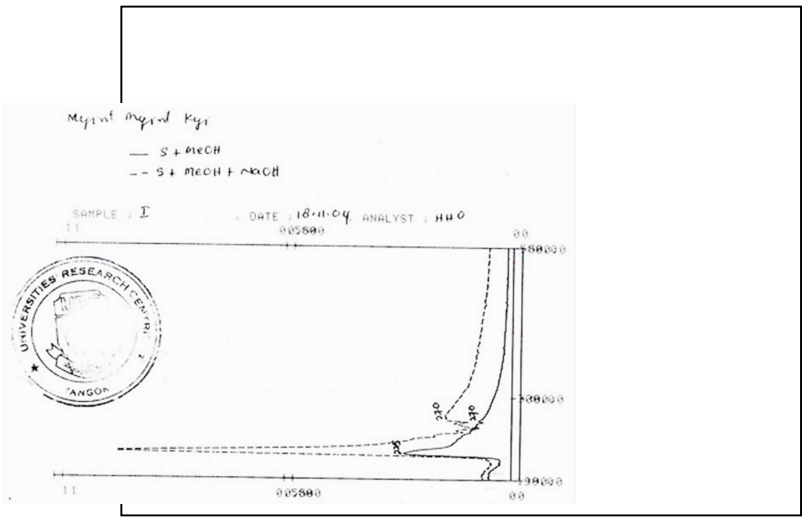

Figure 1 UV spectrum of compound B

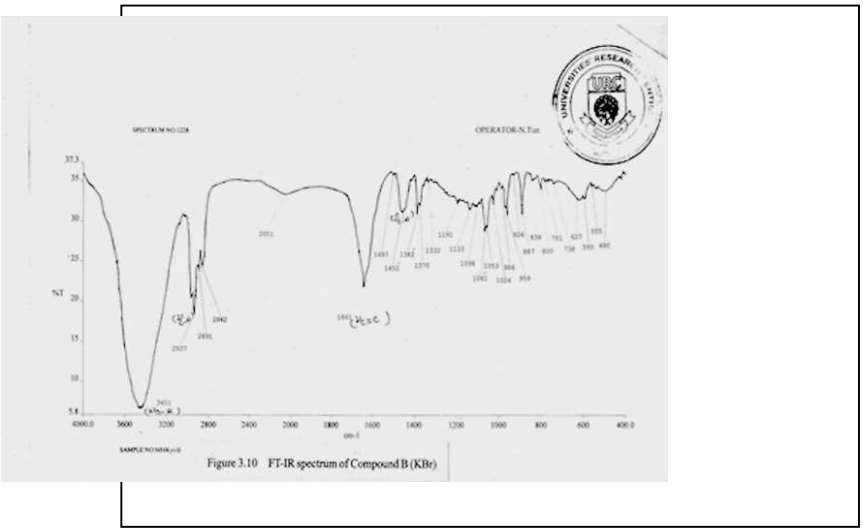

Figure 2 FT IR spectrum of compound B

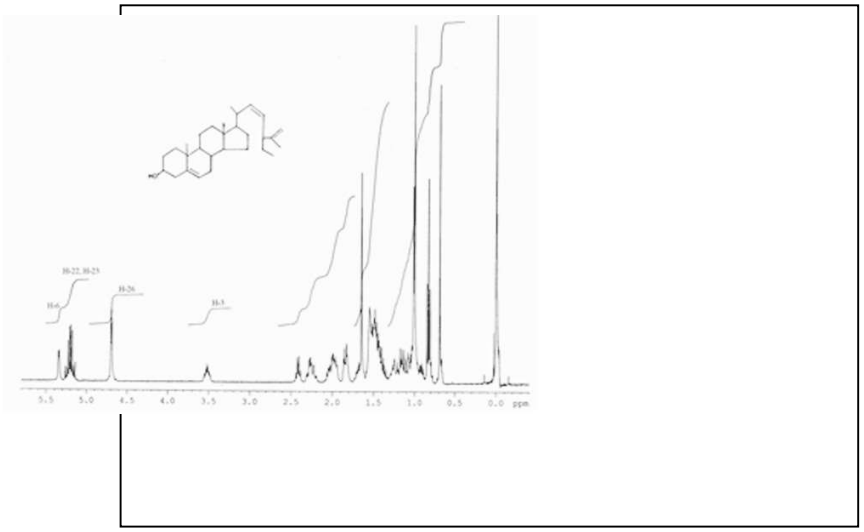

Figure 3 ^{1}HNMR ($CDCl_3$, 300 MHz) spectrum of compound B

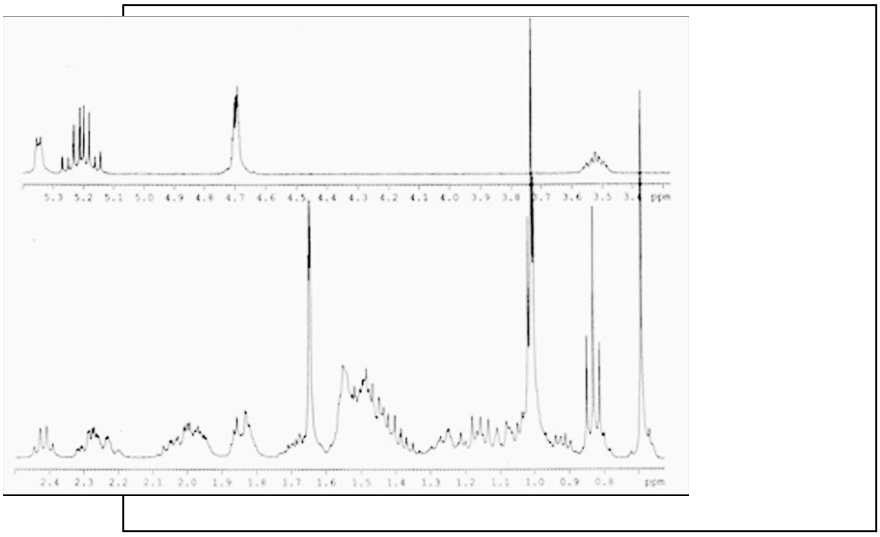

Figure 4 ^{1}HNMR spectra expended of compound B

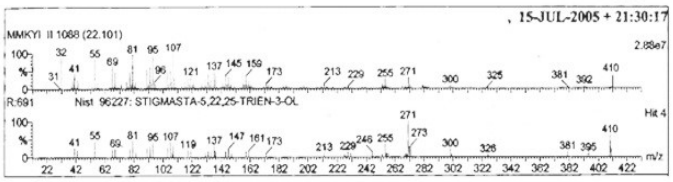

Figure 5 EI-MS spectrum of compound B

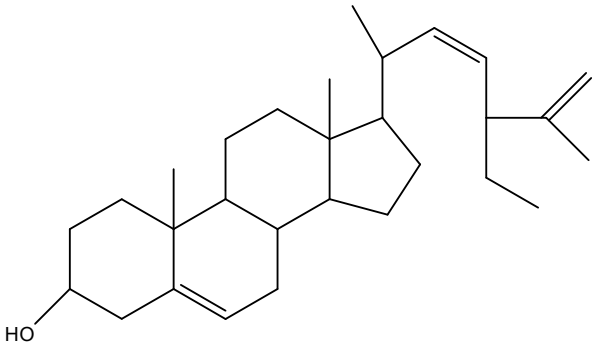

Stigmasta-5,22,25-triene-3ol($C_{29}H_{46}O$)

Hispidulin(C): $C_{16}H_{12}O_6$, pale yellow plate, R_f 0.31, Tol : EtOAc 2:1 ; dark yellow colour by heating with 5% H_2SO_4, m.pt 287-288°C ; UV λ_{max}(MeOH and MeOH/NaOH) (Figure 6) : 270, 340 nm and 270(sh), 325, 396 nm ; FT IR νcm^{-1} (KBr) (Figure 7): 3439(ν_{O-H}), 2943(ν_{C-H} of CH_3gp), 1651($\nu_{C=O}$ of α, β unsat'd carbonyl), 1615, 1583, 1492($\nu_{C=C}$ of aromatic),1439(δ_{CH} of CH_3gp), 1372(δ_{O-H}), 1252, 1178(ν_{C-O-C}), 1097(ν_{C-OH}), 827(δ_{oopC-H} of aromatic); ^{1}H NMR δ ppm(DMSO, 300 MHz) (Figure 8): 2.5(s, 1H, 4′-OH), 3.67(s, 3H, O-CH_3), 6.6(s, 1H, H-8), 6.75(s, 1H, H-3), 6.95(d, J=9.52 Hz, 2H, H-3′,5′), 7.9(d, J=9.52 Hz, 2H, H-2′,6′), 10.4(s, 1H, 7-OH), 13.05(s, 1H, 5-OH); ^{13}C NMR δ

ppm (DMSO, 75 MHz) (Figure 9): 163.72, 102.32, 182.01, 152.69, 131.28, 157.13, 94.14, 152.31, 104.00(C-2 to C-10), 121.19, 128.34, 115.85, 161.02(C-1′to C-6′), 59.9(6-OMe) (Takeshi *et al*., 1995) ; ESI-MS(m/z) : 300$[M]^+$ (Figure 10).

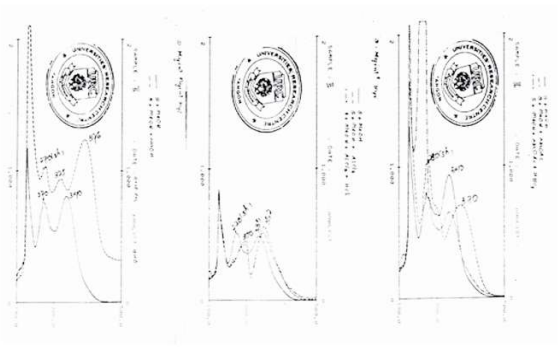

Figure 6 UV-Visible spectra of compound C

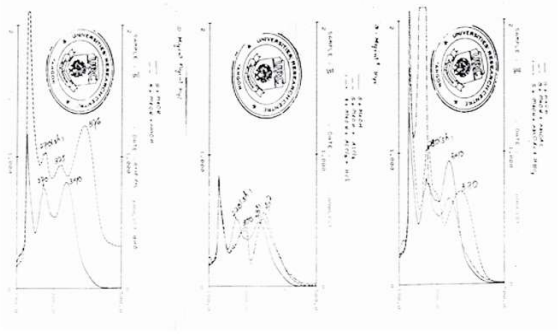

Figure 7 FT IR spectrum of compound C (KBr)

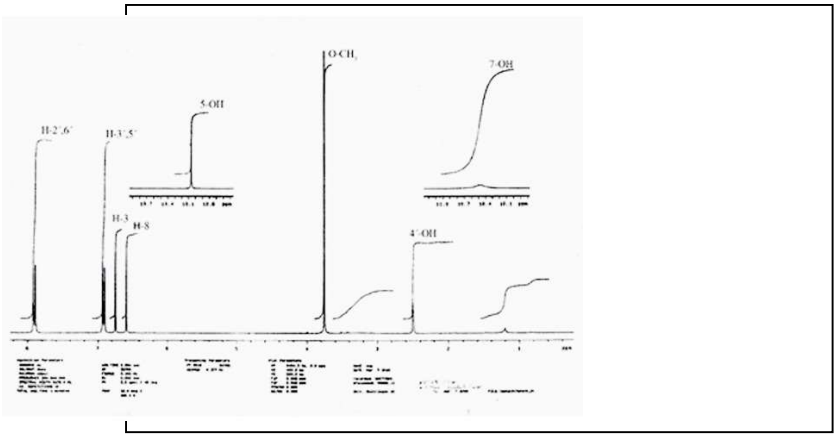

Figure 8 ^{1}HNMR (DMSO, 300 MHz) spectrum of compound C

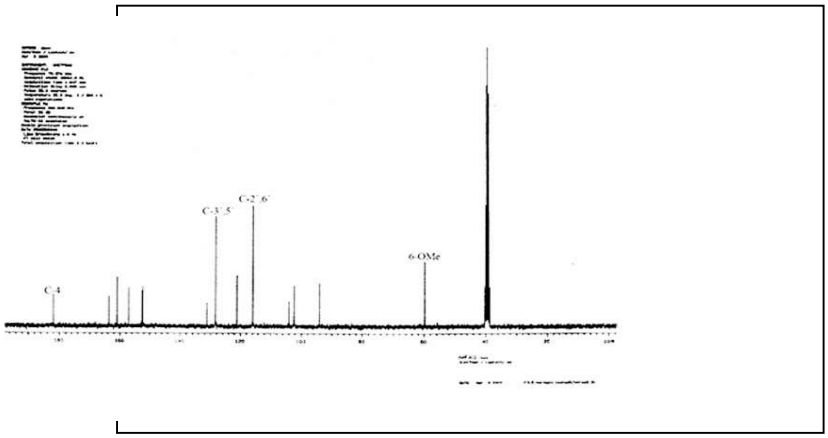

Figure 9 ^{13}CNMR (DMSO, 75 MHz) spectrum of compound C

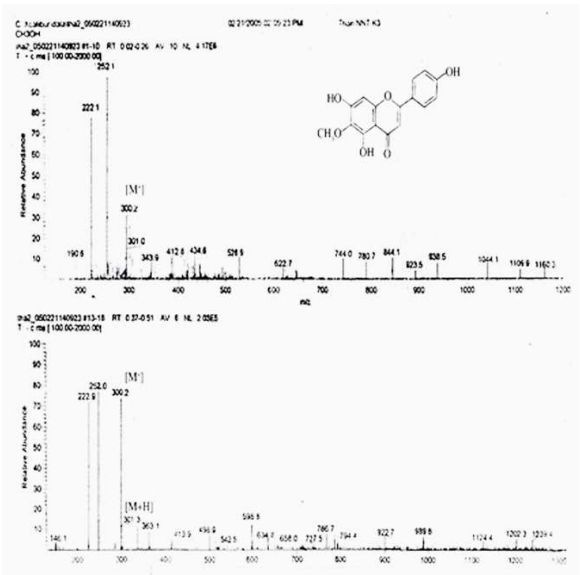

Figure 10 ESI-MS spectrum of compound C

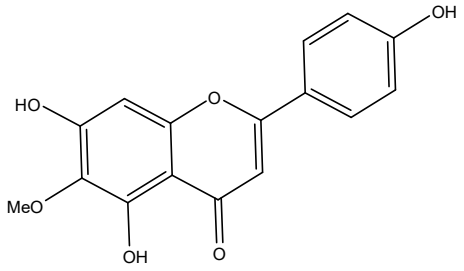

Hispidulin ($C_{16}H_{12}O_6$)

(6-methoxy-4′,5,7-trihydroxy flavones

Pectolinarigenin (D):$C_{17}H_{14}O_6$, pale yellow needles, R_f 0.45, EtOAc : MeOH 98:2 ; yellow colour by heating with 5% H_2SO_4, m.pt 208-210°C ; VU λ_{max}(MeOH and MeOH/NaOH) (Figure 11): 270, 330 nm and 270, 310(sh),

360, 380 nm ; FT IR νcm^{-1} (KBr) (Figure 12): 3420(ν_{O-H}), 1728($\nu_{C=O}$ of carbonyl gp), 1609($\nu_{C=C}$), 1488, 1465(δ_{CH-OH}), 1356(δ_{C-OH} in phenol), 1250, 1177(δ_{CH} of benzene), 1094, 1077(ν_{C-O-C}), 831(δ_{oopC-H} of aromatic) ; ^{1}H NMR δ ppm (Acetone+D_2O, 300 MHz) (Figure 13): 3.62(s, 3H, 4′-OMe), 3.8(s, 3H, 6-OMe), 6.6(s, 1H, H-8), 6.83(s, 1H, H-3), 6.9(d, 2H, H-3′,5′), 7.8(d, 2H, H-2′,6′); ^{13}C NMR δ ppm (Acetone-D_6/D_2O, 75 MHz) (Figure 14): 183.22(C-4), 169.56(C-2), 165.78(C-4′), 161.4s8(C-7), 156.22(C-5), 153.07(C-9), 132.91(C-6), 128.99(C-2′,6′), 121.87(C-1′), 116.48(C-3′,5′), 103.00(C-10), 100.34(C-3), 94.79(C-8), 62.47(6-OMe), 61.23(4′-OMe) (Takeshi *et al*., 1995) ; ESI-MS(m/z)(Figure 15): 314$[M]^+$.

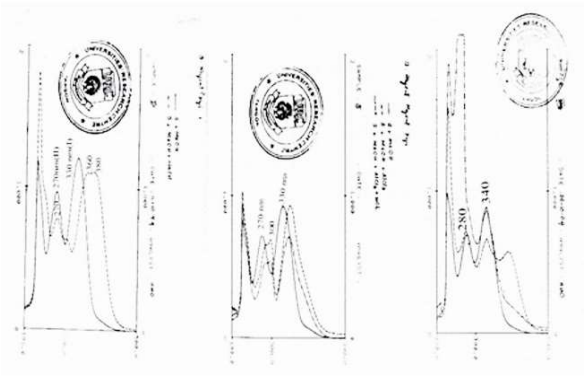

Figure 11 UV-Visible spectra of compound D

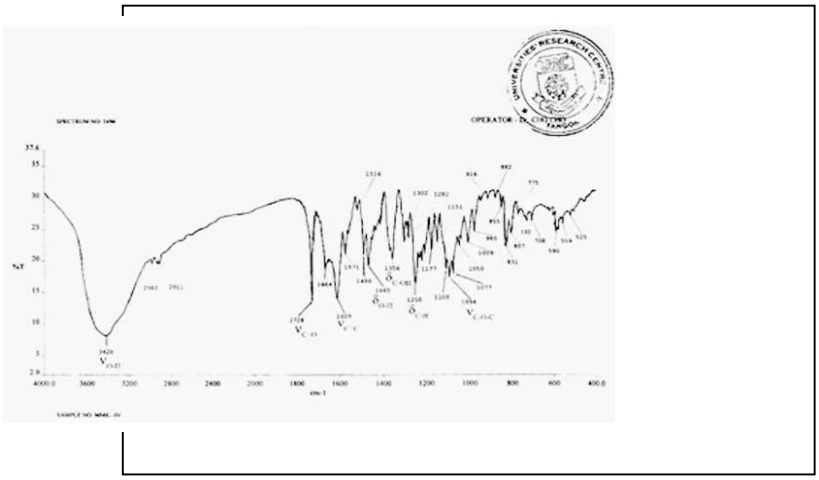

Figure 12 FT IR spectrum of compound D (KBr)

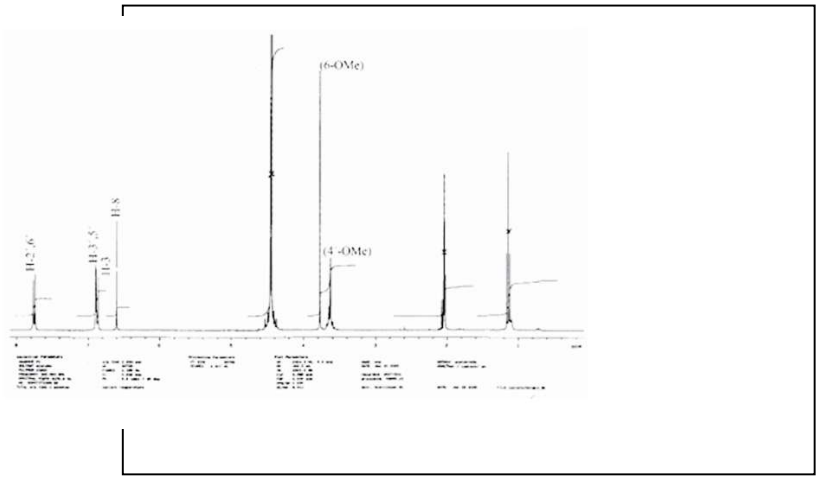

Figure 13 ^{1}HNMR (Acetone+D_2O, 300 MHz)

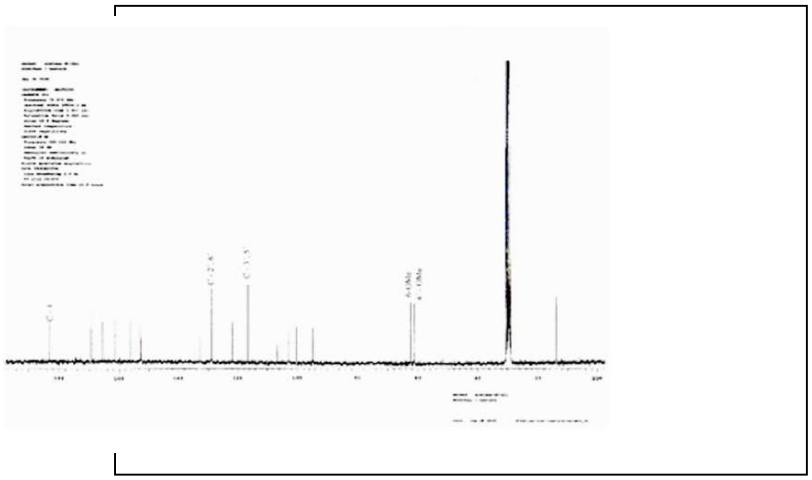

Figure 14 ^{13}CNMR(Acetone-d_6/d_2O, 75 MHz) spectrum of compound D

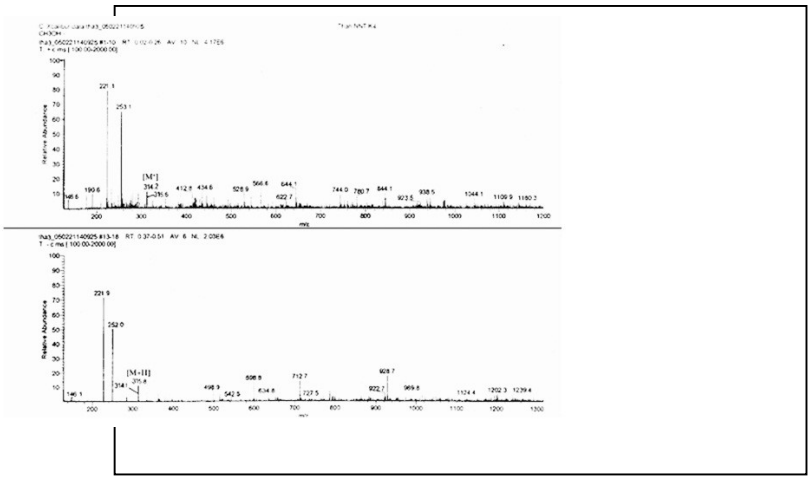

Figure 15 ESI-MS spectrum of compound D

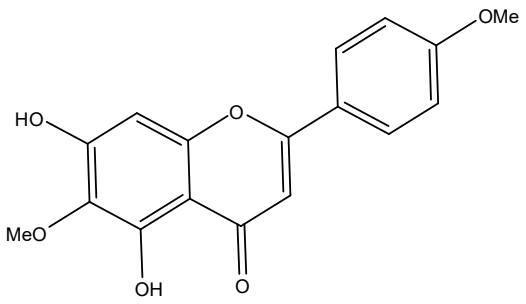

Pectolinarigenin ($C_{17}H_{14}O_6$)

(5,7-dihydroxy-6,4′-dimethoxy flavone

Stigmasterolglucoside(E) :$C_{35}H_{58}O_6$, fine colourless crystals, R_f 0.36, EtOAc : MeOH 95:5 ; purple colour by heating with 5% H_2SO_4, m.pt 283-284°C ; FT IR νcm^{-1}(KBr) is shown in (Figure 16): 3450(ν_{O-H}), 2961, 2933(asymν_{C-H}), 2869(symν_{C-H}), 1638($\nu_{C=C}$), 1463(δ_{CH}), 1383, 1367(δ_{OH}), 1165(ν_{C-O-C}), 1073-1024(asymν_{C-OH} in sugar), 891(δ_{CH} of sugar), 621, 600(δ_{oopOH}) ; ^{1}H NMR δ ppm (DMSO, 300 MHz) is shown in (Figure 17) : 5.39(t, 1H, H-6), 5.20(t, 1H, H-22), 5.10(d, 1H, H-23), 4.80(d, 1H, H-1′), 4.40(t, 1H, H-6′a), 4.23(d, 1H, H-6′b), 4.12(m, 1H, H-3′), 3.85(m, 1H, H-4′), 3.70(t, 1H, H-2′), 3.4(m, 1H, H-5′), 2.5(s, 1H, H-7a), 2.0(m, 1H, H-8), 1.6(m, 1H, H-7b), 1.2(d, 3H, Me-21), 1.0(s, 3H, Me-19), 0.85(d, 3H, Me-26), 0.65(s, 3H, Me-18) ; ^{13}C NMR δ ppm (DMSO, 75 MHz) is shown in (Figure 18): 139.7(C-5), 136.9(C-22), 127.8(C-23), 121.9(C-6), 102.3(C-1′), 78.5(C-3′), 78.1(C-3), 77.9(C-5′), 74.6(C-2′), 71.0(C-4′), 62.7(C-6′), 58.1(C-14), 56.9(C-17), 51.1(C-9), 46.0(C-24), 43.2(C-13), 39.9(C-12), 38.5(C-4), 37.4(C-1), 36.9(C-10), 35.1(C-20), 32.9(C-7), 32.0(C-8), 30.1(C-28), 29.4(C-16),28.5(C-2), 26.5(C-25), 23.8(C-15), 21.2(C-11), 20.0(C-26), 19.5(C-19), 19.2(C-27), 19.0(C-21), 13.1(C-29), 11.7(C-18)(El -Askary, 2005).

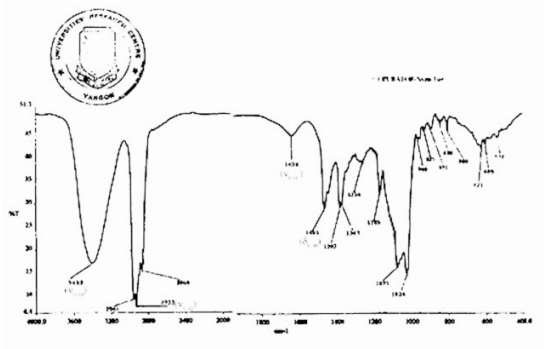

Figure 16 FT IR spectrum of compound E (KBr)

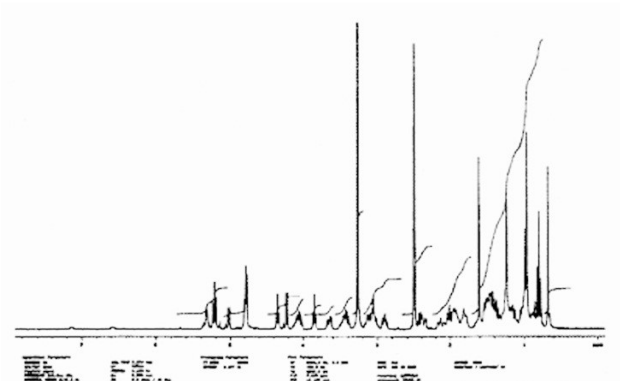

Figure 17 ^{1}HNMR (DMSO, 300 MHz) spectrum of compound E

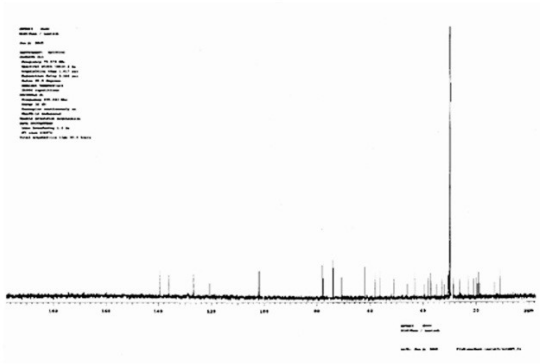

Figure 18 ^{13}CNMR (DMSO, 75MHz) spectrum of compound E

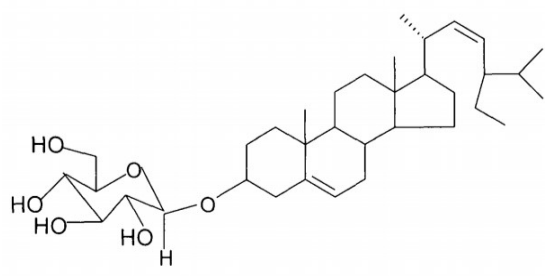

Sigmasterolglucoside ($C_{35}H_{58}O_6$)

Anti-asthmatic Activity of Isolated Compounds on Guinea pig Trachea

Among five compounds isolated from pet-ether and ethyl acetate extract of Nga-yant-padu, the anti-asthmatic activity of compounds B, C, D and E were subjected to study on histamine induced contraction in tracheal chain isolated from guinea pig. The relaxation response (%) of isolated compounds: B, C, D and E as well as 70 % EtOH and watery extracts of Nga-yant-padu on histamine induced tracheal chain are shown in Figure 19 and given in Table 1. When the isolated compounds were added to the organ bath,

the compounds (B, C, D and E) were found to exhibit direct relaxation effects of 80.2% (P<0.01), 73.0% (P<0.01), 70.2% (P<0.01) and 63.0% (P<0.01) of smooth muscle relaxation effect. Out of four isolated compounds tested, compound B is the most effective than the others. Compound B is a steroidal compound, stigmasta- 5, 22, 25 triene-3ol and compound E is also a steroidal glycoside, stigmasterolglucoside. Most steroidal compounds are used as controller or anti-inflammatory agents for asthmatic patients. Steroids are the most effective compounds of controlling inflammation in lungs. Compound C and D are flavonoids: hispidulin and pectolinarigenin. Flavonoids has been reported as H_2 – receptor blocking drug that can reduce histamine to have an antihistaminic effect. The anti-asthmatic activity of isolated compounds (at 0.1 mg/mL bath conc.) on histamine induced guinea pig trachea were found in the order of B > C > D > E.

Table 1 Relaxation Effect of Four Isolated Compounds and Different Extracts on Histamine Induced Tracheal Chain

Isolated Compounds and Extracts (n = 5)	Relaxation Response (%)	P – value
Stigmasta-5,22,25-triene-3ol (0.1mg/mL)	80.2 ± 0.84	< 0.01
Hispidulin (0.1mg/ mL)	73.0 ± 1.6	< 0.01
Pectolinarigenin (0.1mg/ mL)	70.2 ± 1.52	< 0.01
Stigmasterolglucoside (0.1mg/ mL)	63.0 ± 3.2	< 0.01
70% EtOH (NYP) (1.0mg/ mL)	77.8 ± 1.3	< 0.01
Watery (NYP) (1.0mg/ mL)	68.0 ± 1.4	< 0.01

Student's t – test NYP = Nga-yant-padu

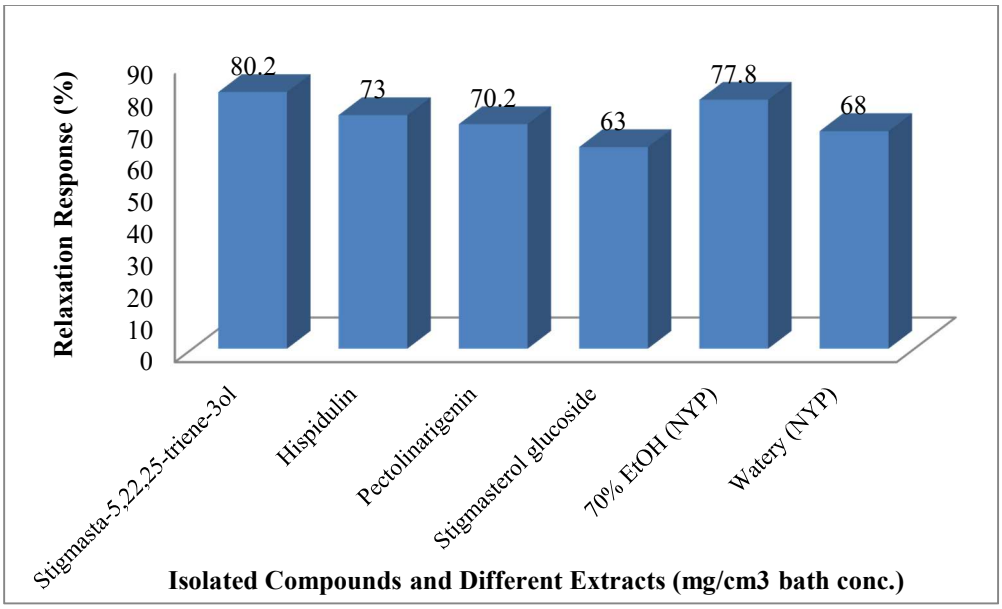

Figure 19 Relaxation effect of isolated compounds and different extracts on histamine induced tracheal chain

Conclusion

From the overall assessment of the present work, the following inferences could be deduced. By silica gel column chromatographic separation, palmitic acid (A, 0.002%), stigmasta-5, 22, 25-triene-3ol (B, 0.24%), hispidulin (C, 0.36%), pectolinarigenin (D, 0.064%) and stigmasterolglucoside (E, 0.05%) were isolated from Nga-yant-padu. *In vitro* screening of anti-asthmatic activity showed that all isolated compounds (except palmitic acid) from Nga-yant-padu possessed the anti-asthmatic property and the muscle relaxation effects of these compounds were found to be in the order of B (80.2%, $P<0.01$) > C (73.0%, $P<0.01$) > D (70.2%, $P<0.01$) > E (63.0%, $P<0.01$) on histamine induced guinea pig trachea. Therefore, it could be suggested that Nga-yant-padu might be used as a remedy for the treatment of asthma.

Acknowledgement

The authors would like to express their profound gratitude to the Ministry of Education, Department of Higher Education (Yangon Office), for giving the opportunity to do this research and Myanmar Academy of Arts and Science for allowing to present this paper.

References

Aung Htay Oo. (1996). *Study of Anti-asthmatic Action of CoelusaromaticusBenth. (Ziyar-ywet-htu)*,M.Med.Sc.(Pharmacology) Thesis, Institute of Medicine I, Yangon

Aye Than, Win Myint, Tin Myint, Mu Mu Sein Myint and Mya Bwin.(1995).“Direct Relaxant Effect of Some Plant Extracts on Isolated Tissue Models”. *Myan.Hlth. Sci. Res. J*., vol. 7(1), pp. 18-25

Barnes, P.J., Chung , K.F. and Page, C.P.(1998). “Inflammatory Mediators of Asthma: An Update”. *Pharmacol Rev*., vol. 50(4), pp. 515-596

El -Askary, H.I. (2005). “Terpenoids from *Cleome droserifolia* (Forssk) Del. ” *Molecules*, vol. 10(8), pp. 971-977

Hundley, H.G. and Chit Ko Ko. (1987). *Trees, Shrubs, Herbs and Principal Climbers* etc. Yangon: 4th Ed., Union of Burma Government Printing and Stationary

Patrick, G. L. (1995). *An Introduction to Medicinal Chemistry*. New York: Oxford University Press Inc.

Rang, H. and Moore,P. (2003). *Pharmacology, Drugs Affecting Major Organ System*. London: Academic Press, p. 341

Silverstein, R.M. and Webster, F.X., (1998). *Spectrometric Identification of Organic Compounds.* New York: 6th Ed., John Wiley and Sons Inc.

Takeshi, H., Kazuhiro, O. and Ryoji, K. (1995).“Revised Structure for Hortensin, A Flavonoid from *Millingtonia hortensis*”. *Phytochemistry*, vol. 40, pp. 287-290

Tian, J. and Zhang, X. (1997).*Monographs on Selected Medicinal Plants*.WHO, vol. 3, p. 7

ACKNOWLEDGEMENTS

The author would like to thank Dr Than Than Win, Professor, Department of Chemistry, Monywa University for her constant encouragement.

CHARACTERIZATION AND APPLICATION OF MAGNETITE AND GOETHITE FOR WASTEWATER TREATMENT

Aye Aye Mar[1], Thida Win[2], Thida Maw[3], Myat Myat Thaw[4],Kyaw Naing[5]

Abstract

In this research work, two different types of iron oxides (magnetite and goethite) were synthesized by co-precipitation method. These iron oxides were characterized by using some modern techniques (XRD, SEM, EDXRF and FT IR). According to XRD data, eight Miller indices [(111), (220), (311), (222), (400), (422), (511), (440)] of the magnetite samples were found. Three Miller indices [(130), (110), (200)] of the goethite sample were observed. SEM micrograph of magnetite and goethite samples indicated the porous nature of iron oxide samples. According to EDXRF data, the prepared iron oxides showed the presence of iron (100 %) and no other elements were present. According to FT IR data, the magnetite and goethite samples showed the presence of iron-metal oxide bonds. The bands at 894.9 cm^{-1} be possible due to the iron oxide for magnetite samples and the band located at 891.1 cm^{-1}may be Fe-O groups for goethite sample. Application of magnetite and goethite iron oxide samples were carried out by using model solutions for wastewater treatment. Sorption capacity on magnetite and goethite were measured for contact time and effect of dosage. The efficiency of iron oxide samples for the removal of dyes in wastewater samples were also studied.

Keywords: Magnetite, goethite, iron oxide, dyes, sorption capacity

Introduction

There is an ever-increasing world demand for fabrics due to population growth. In order to meet demand for fabrics more textile industries are being started daily. Not only the textile sector, but also other industries, use dyes and

[1] Assistant Lecture, Dr, Department of Chemistry, University of Yangon
[2] Associate Professor, Dr, Department of Chemistry, Yadanabon University
[3] Associate Professor, Dr, Department of Chemistry, Lashio University
[4] Professor, Dr, Department of Chemistry, University of Yangon
[5] Deputy Director General, Dr, Department of Higher Education (Yangon Office)

pigments to colour their products and to increase the market of their product (Popoola *et al.,* 1994). Other industries that discharge their wastewater into natural streams include producers of carpets, wool, and paint also the pigment paper and pulp mills, tanneries, electroplating industries, distrilleries, food companies and the printing industry (Guinot *et al.*, 2006). These industries discharge effluents bearing dyes, surfactants salts and heavy metals. Such discharge has created significant concern, as dyes impart toxicity and visibility. Dyes are almost invariably toxic and additionally a visible pollutant. So their removal from effluent stream is ecologically essential. The American Dye Manufacturing Institute showed that the basic dyes are generally more toxic than acid or direct dyes (Mathur and Bhandari, 2001).

Recent estimates indicate that approximately 12% of synthetic dyes used each year are lost during manufacture and processing operates and that 20-35% of these input dyes (Allen and Koumanova, 2005).The textile effluents composition is complex since it contains diverse dyes and other products such as dispersants, acids, alkalis, salts and some heavy metals. In general the effluent is highly colored, with a high biological (BOD) and chemistry demands of oxygen (COD) (Boyjoo, 1987).

Dyes are present in the textile effluent in concentrations of 10 to 50 mg/L. Approximately 1,000,000 kg/year of dyes are discharged in effluents by the textile industries, because approximately a 15% of the total dye used in the process is lost during the dying process. Color removal from textile effluents has been the target of great attention in the last few years, not only because of its potential toxicity, but mainly due to the potential environmental impact. Different treatments for the removal of dyes have been used such as special processes of filtration, activated mud, chemical coagulation, adsorption on activated carbon and processes of photodegradation. The solution to the problem depends on the use of different technological process.

One of the methods used to eliminate dyes of the effluents is the adsorption on a solid material. The most common adsorbent is the activated carbon, effective in the removal of organic components and not effective in the removal of inorganic compound. Due to its high cost, the use of alternative and efficient adsorbents for the removal of dyes and metals is been increasingly studied. Oxides and metal hydroxides have also been used as adsorbents in the

textile industry. The adsorption of cationic and anionic dyes on hydrated zirconium oxide or iron oxides has been reported. These materials are common as adsorbents by their limited solubility and their amphoteric properties. However, sometimes these oxides present low surface area and this aspect is a problem to resolve.

Goethite (FeO(OH)), is an iron bearing oxide mineral found in soil and other low-temperature environments. Goethite has been well known since prehistoric times for its use as a pigment. Evidence has been found of its use in paint pigment samples taken from the caves of Lascaux in France. It was first described in 1806 for occurrences in the Mesabi iron ore district of Minnesota. Recently, nanoparticulate authigenic goethite was shown to be the most common diagenetic iron hydroxide in both marine and lake sediments.

Magnetite is one of the most common oxide minerals and also one of the most common iron minerals. It is an important ore of iron and is found in igneous, metamorphic and sedimentary rocks (Forsling and Samshog, 1998). It can also be abundant in sediments. Magnetite is easy to identify. It is a black opaque, submetallic to metallic mineral with a hardness between 5.5 and 6.5. It is often found in the form of isometric crystals. However, its magnetic properties are distinctive. It is one of just a few minerals that are attracted to a work magnet. It is the most magnetic mineral found in nature. Sometimes it is automagnetized and attracts metal objects (Schwertmann and Cornell, 1964).

Materials And Methods

The following analytical grade reagents:$FeSO_4.7H_2O$,NaOH,$NaNO_3$ and $Fe(NO_3)_3.9H_2O$ were obtained from Analytical Laboratory Department of Chemistry, University of Yangon. The chemicals used in this research work were purchased from British Drug House (BDH) chemicals Ltd. Magnetite is prepared by slow adding the iron (II) sulphate solution into the beaker containing the solution of sodium nitrate and sodium hydroxide. The black precipitate was obtained and the sample was aged at room temperature for 16 days. Goethite was prepared by adding ferric nitrate in to a beaker containing sodium hydroxide solution .The precipitate obtained was aged at room temperature for 48 h and then in an oven at 65°C for 72 h.

The sample were characterized by SEM, EDXRF, FTIR and XRD. Sorption properties of these samples were determined with eriochrome blue black B and alizarin red S dyes. In the contact time effect 0.2 g of sample was placed into separated glass stoppered bottles and treated in 20 mL 20 ppm dye solution at pH 7.The bottles containing dye and iron oxide as absorbents were placed in the thermostatic shaker at room temperature. The contact time setting were 10,20,30,40,60,120 and 180 min. After shaking the sample solutions were filtered off and the filtrates were spectrophotometrically measured at maximum wavelengths. The removal percent of dyes with the iron oxides were calculated by the equation $R\,(\%) = \frac{C_0 - C_e}{C_0} \times 100$ .The dosage effect were carried out by the similar procedure.

Furthermore application of prepared iron oxide samples for the removal of dyes in wastewater sample (collected from south Dagon Myothit) were determined. In this research absorption spectrum of wastewater samples were recorded by using UV-visible spectrophotometer. In this study a 50mL of wastewater was mixed with 2.5g of magnetite powder in a bottle. The bottle was agitated in thermostatic shaker at temperature of 30 °C for 1h. Then the solution was filtered off and the absorbance of resultant filtrate was measured. The same procedure was carried out for the goethite sample.

Results and Discussion

Preparation of Magnetite and Goethite Samples

Magnetite and Goethite were prepared in the laboratory by co-precipitation method. Figures 1 and 2 show photographs of Magnetite and Goethite.

Characterization of Prepared Iron Oxide Samples (magnetite and goethite) by SEM, EDXRF, FT IR and XRD

Surface morphology of the prepared iron oxide samples

Surface morphology of the prepared iron oxide samples were studied, by using SEM. Figures 3 and 4 show the SEM micrographs of magnetite and goethite samples respectively. The SEM microphotographs indicated the porous nature of the surface. Therefore dyes can enter the porous of the iron oxide samples.

EDXRF data of the prepared iron oxide samples

EDXRF measurements were carried out on prepared iron oxide samples. Figures 5 and 6 show the EDXRF spectra of magnetite and goethite samples respectively. According to the EDXRF data the prepared iron oxide samples were pure and free from impurities.100% of iron are present in these samples.

FTIR data of the prepared iron oxide samples

FT IR measurements were carried out on the prepared iron oxide samples. Figures 7 and 8 show the FT IR spectra of prepared iron oxides. FT IR data indicated the presence of functional groups in the samples. Tables1 and 2 showed the FT IR data of magnetite and goethite samples. In the magnetite sample O-H stretching vibration was found at 3448.5cm^{-1}, O-H in plane bending vibration was found at 1357.8 cm^{-1} and Fe-O group vibration was found at 894.9cm^{-1}.In the goethite sample O-H stretching vibration was found at 3132.2cm^{-1},O-H in plane bending vibration was found at 1380.9cm^{-1} and Fe-O group vibration was found at 891.1cm^{-1} respectively.

X**RD Data of the Prepared Iron Oxide Sample**

XRD measurements were carried out on the prepared iron oxide samples. Figures 9 and 10 depicted the XRD pattern of magnetite and goethite samples respectively.XRD pattern can be used to examine the phase purity and phase structure. The XRD pattern of magnetite sample clearly matched with the standard library data of PDF-19-0629-magnetite. Eight Miller indices [(111),(220), (311),(222), (400),(422), (511),(440)] of the magnetite sample

matched with the standard data(Fe_3O4).XRD pattern of goethite sample matched with the standard library data of PDF-81-0464-FeO(OH). Three Miller indices [(130),(111),(200)] of the goethite sample matched with the standard data.

Sorption Study of Magnetite and Goethite using Modern Dye Solutions

Effect of contact time on sorption of eriochrome blue black B

Sorption capacity of magnetite and goethite samples onto eriochrome blue black B were studied. Tables 3 and 4 described the relationship between contact time and percent of eriochrome blue black B on magnetite and goethite samples. Figure 11 show plot of eriochrome blue black B sorbed percent as a function of contact time on magnetite and goethite samples. For the contact time of 180 min 70.34 % and 77.50 % of eriochrome blue black B were sorbed on magnetite and goethite samples, respectively.

Effect of dosage on sorption of eriochrome blue black B

Effect of dosage of the prepared iron oxide samples on eriochrome blue black B dye was studied by choosing the dosage of the prepared iron oxide samples from 0.1 to 1.4 g. Tables 5 and 6 show the relationship between dosage of magnetite and goethite, respectively, with the percent sorption of eriochrome blue black B.

Figure 12depicted the histogram of percent sorption of eriochrome blue black B with dosage of the prepared iron oxide samples.By using 1.4 g of magnetite and goethite samples, sorption percent of eriochrome blue black B were 88.40 % and 89.10% respectively.

Effect of contact time on sorption of alizarin red S

Sorption capacity of magnetite and goethite samples onto alizarin red S were studied. Tables 7 and 8 shows the relationship between contact time and percent sorption of alizarin red S on magnetite and goethite samples respectively. Figure 13 shows plot of sorption percent of alizarin red S as a function of contact time on magnetite and goethite samples. For the contact

time of 180 min, sorption of alizarin red S on magnetite and goethite samples were 83.56%and 89.00% respectively.

Effect of dosage on sorption of alizarin red S

Effect of dosage of the prepared iron oxide samples on sorption of alizarin red S dye was studied by choosing the dosage of the prepared iron oxide samples from 0.1 to 1.4 g. Tables 9 and 10 show the relationship between dosage of magnetite and goethite, respectively with the percent sorption of alizarin red S.

Figure 14 shows the histogram of sorption percent of alizarin red S with dosage of the prepared iron oxide samples. By using 1.4 g of magnetite and goethite samples, sorption percent of alizarin red S were 90.25% and 90.65% respectively.

Application of iron oxide samples for the removal of dyes in wastewater samples

Applications of the prepared iron oxide samples were studied for the treatment of dyes in wastewater. Wastewater samples were collected from pulp and paper industry, South Dagon MyoThit. The wavelength of maximum absorption of wastewater sample was found to be 414.24nm. After treatment the results show that sorption percent of dye on magnetite and goethite were 87.32%, 99.41% respectively. Table 11 shows the percent removal of dyes from wastewater sample by magnetite and goethite samples. Figure 15 shows the wastewater samples after treatment with magnetite and goethite samples.

Figure 1. The photograph of prepared magnetite

Figure 2. The photograph of a prepared goethite

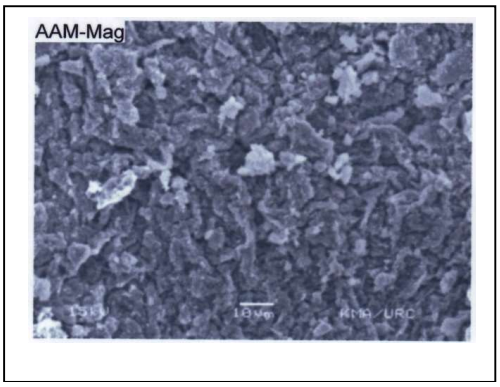

Figure 3. SEM micrograph of magnetite (X 1000)

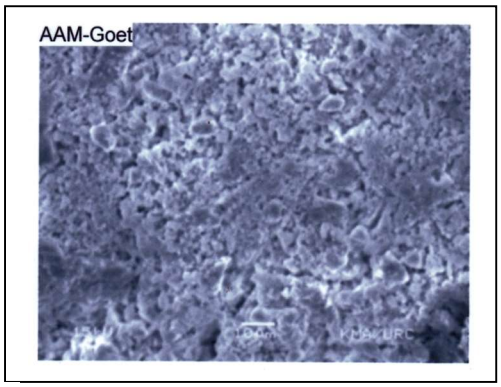

Figure 4. SEM micrograph of goethite (X 1000)

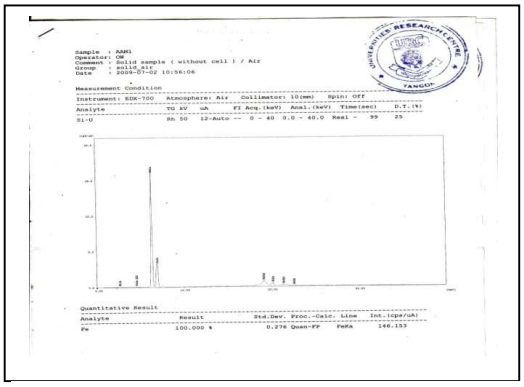

Figure 5. EDXRF spectrum of prepared magnetite

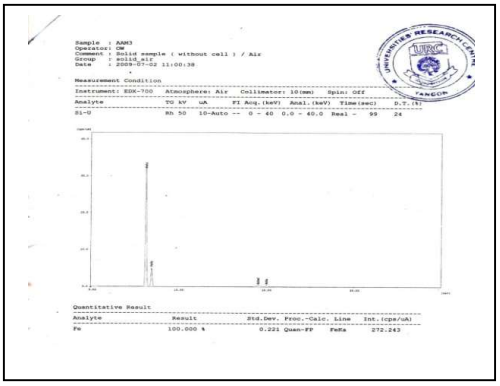

Figure 6. EDXRF spectrum of prepared goethite

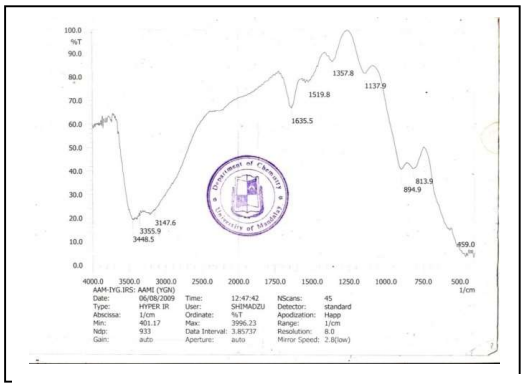

Figure 7. The FT IR spectrum of prepared magnetite sample

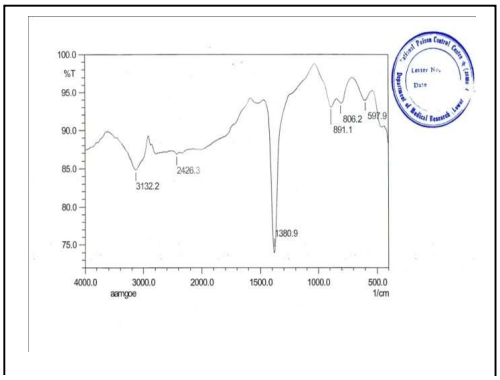

Figure 8. The FT IR spectrum of prepared goethite sample

Table 1. FT IR Data of Prepared Magnetite Sample

No.	Wave number (cm^{-1})	Functional group
1	3448.5	ν_{O-H} stretching
2	1357.8	ν_{O-H} in plane bending
3	894.9	$\nu_{Fe-O,}$Fe-O group

Table 2. FT IR Data of Prepared Goethite Sample

No.	Wave number (cm^{-1})	Functional group
1	3132.2	ν_{O-H} stretching, - OH group
2	1380.9	ν_{O-H} in plane bending, -OH group
3	891.1	$\nu_{Fe-O,}$Fe-O group

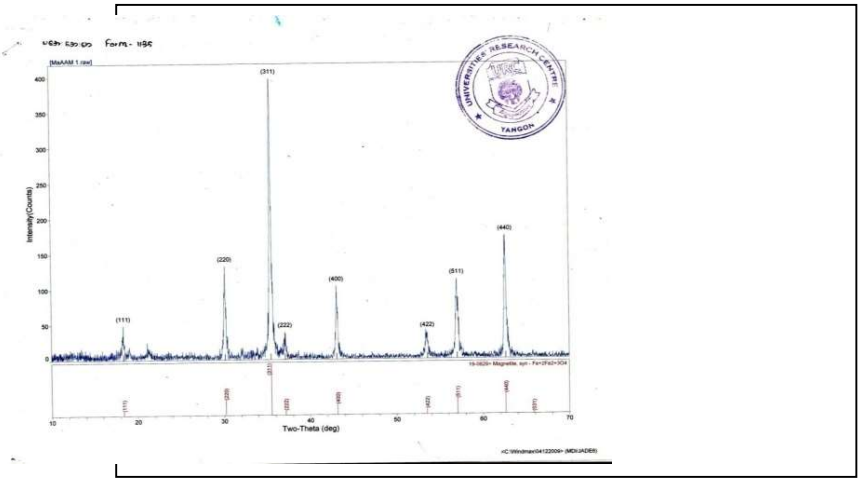

Figure 9. XRD pattern of the prepared magnetite

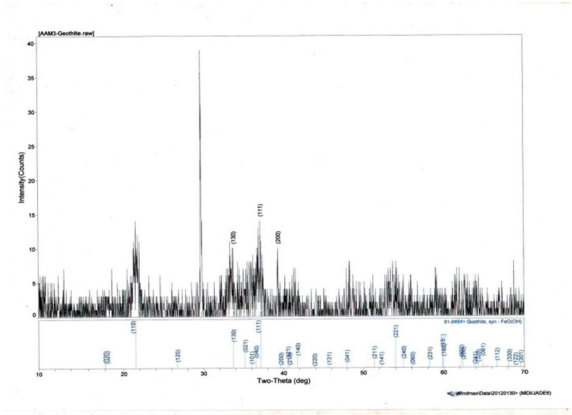

Figure 10. XRD pattern of the prepared goethite

Table 3. Relationship between Contact time and Percent Sorption of Eriochrome Blue Black B on Magnetite

Contact time (min)	**Percent sorption of EBBB (%)**
0	0
10	25.00
20	41.34
30	52.54
40	60.49
60	63.97
120	69.80
180	70.34

Experimental condition pH=7
Amount of magnetite =0.2 g
Concentration of dye = 20 ppm
Volume of EBBB solution=20mL

Table 4. Relationship between Contact Time and Percent Sorption of Eriochrome Blue Black B on Goethite

Contact time (min)	Percent sorption of EBBB (%)
0	0
10	27.95
20	33.80
30	43.40
40	53.70
60	67.65
120	77.50
180	77.50

Experimental condition
pH=7
Amount of magnetite =0.2 g
Concentration of dye = 20 ppm
Volume of EBBB solution=20mL

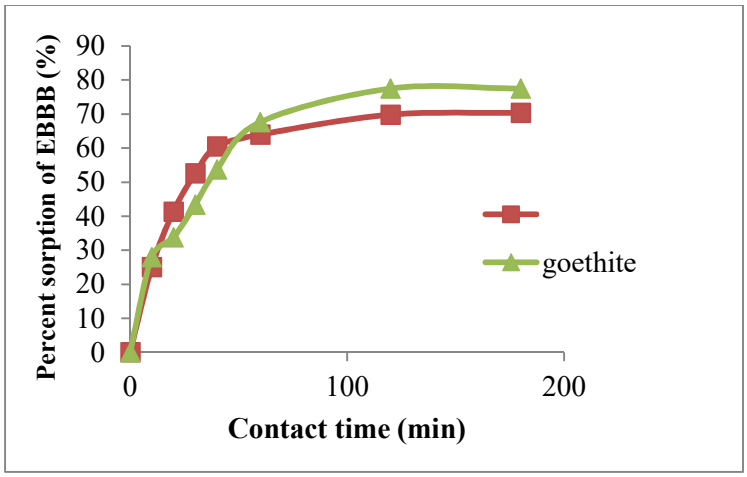

Figure 11. Plot of percent sorption of eriochrome blue black B as a function of contact time on magnetite and goethite

Table 5. Relationship between Dosage of Magnetite and Percent sorption of EBBB

Weight of Magnetite (g)	Percent sorption of EBBB (%)
0.1	33.65
0.2	63.81
0.4	73.74
0.6	77.56
1.0	85.37
1.4	88.40

Experimental condition pH=7
Concentration of dye=20 ppm
Contact time=1hr
Volume of EBBB solution=20 mL

Table 6. Relationship between Dosage of Goethite and Percent sorption of EBBB

Weight of Goethite (g)	Percent sorption of EBBB (%)
0.1	46.56
0.2	76.25
0.4	80.45
0.6	85.7
1.0	89.05
1.4	89.10

Experimental condition pH=7
Contact time =1hr
Concentration of dye=20 ppm
Volume of EBBB solution=20mL

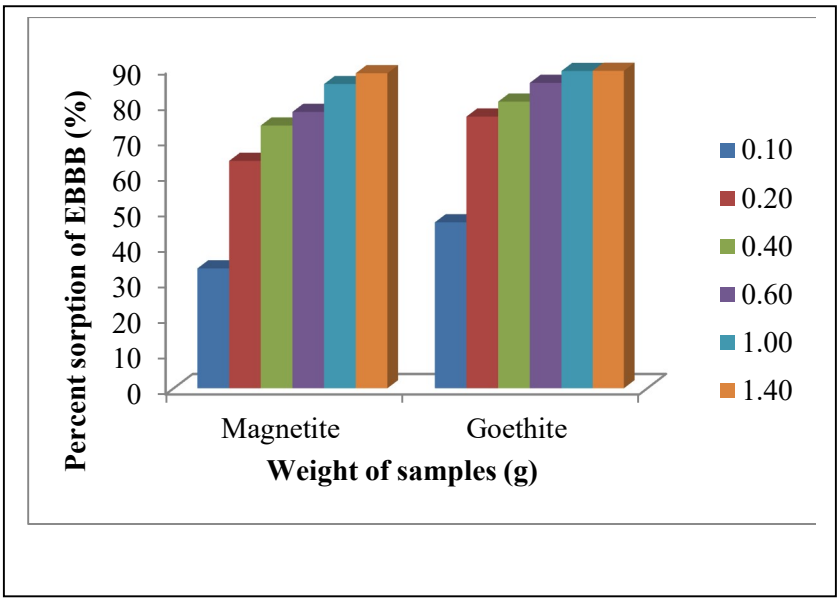

Figure 12. Histogram of percent sorption of EBBB with dosage of the prepared iron oxide samples

Table 7. Relationship between Contact Time and Percent sorption of Alizarin red S on Magnetite

contact time(min)	Percent sorption of Alizarin red S (%)
10	28.75
20	34.25
30	52.05
40	64.35
60	78.08
120	82.19
180	83.56

Experimental condition
pH=7
Concentration of dye=20 ppm
Amount of magnetite=0.2g
Volume of alizarin red S solution=20 mL

Table 8. Relationship between Contact Time and Percent sorption of Alizarin red S on Goethite

Contact time(min)	Percent sorption of Alizarin red S (%)
10	33.05
20	45.25
30	60.05
40	79.35
60	88.95
120	89.00
180	89.00

Experimental condition pH=7
Concentration of dye = 20 ppm
Amount of Goethite = 0.2 g
Volume of alizarin red S solution = 20 mL

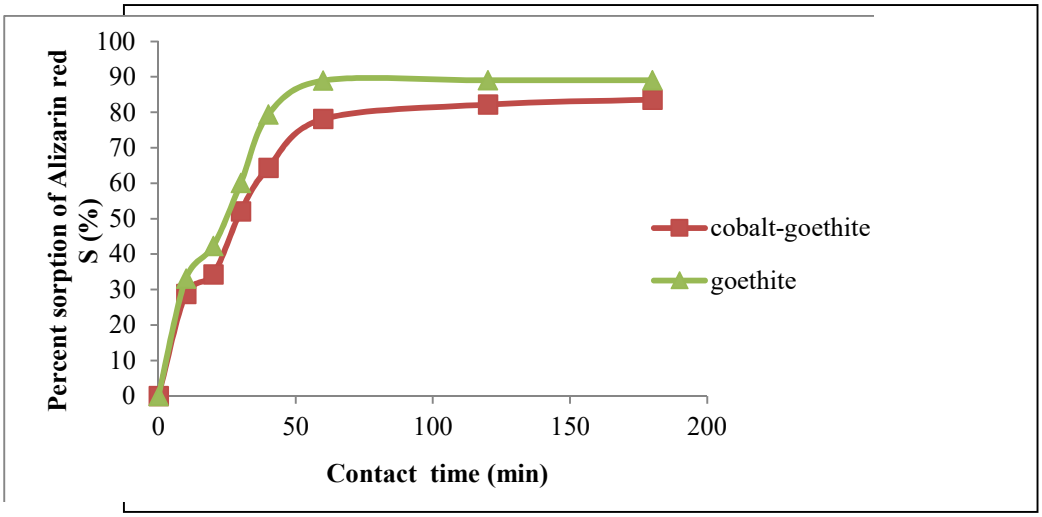

Figure 13. Plot of sorption percent of alizarin red S as a function of contact time on magnetite and goethite

Table 9. Relationship between Dosage of Magnetite and Percent Sorption of Alizarin red S

Weight of Magnetite (g)	Percent sorption of Alizarin red S (%)
0.1	48.45
0.2	76.25
0.4	83.55
0.6	88.85
1.0	89.75
1.4	90.25

Experimental condition pH=7
Contact time=1 h
Concentration of dye=20 ppm
Volume of alizarin red S solution=20 mL

Table 10. Relationship between Dosage of Goethite and Percent Sorption of Alizarin red S

Weight of Goethite (g)	Percent sorption of Alizarin red S (%)
0.1	56.45
0.2	89.00
0.4	90.05
0.6	90.10
1.0	90.60
1.4	90.65

Experimental condition pH=7
Contact time = 1 h
Concentration of dye = 20 ppm
Volume of alizarin red S solution = 20 mL

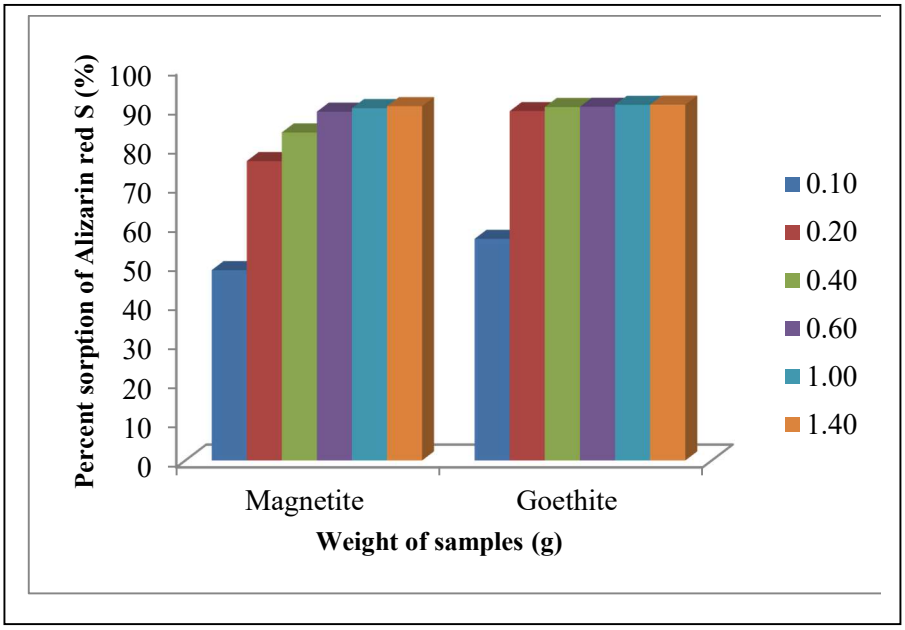

Figure 14. Histogram of percent sorption of alizarin red S with dosage of the prepared iron oxide samples

Table 11. Treatment of Wastewater Samples by the Prepared Iron Oxides

Iron Oxide Sample	Dye removal %
Magnetite	87.32
Goethite	99.41

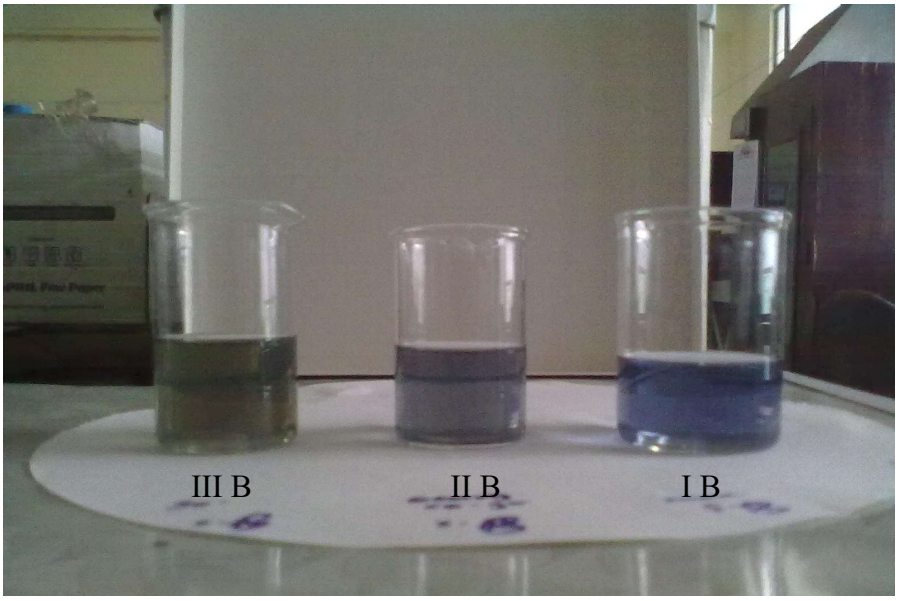

Figure 15. Photograph of wastewater sample

I B = Sample before treatment
II B = Sample after treatment with goethite
III B = Sample after treatment with magnetite

Conclusion

In this research, iron oxides were synthesized by co-precipitation method. Characterization of the prepared iron oxides were carried out by using SEM, EDXRF, FT IR and XRD. The SEM micrographs indicated the porous nature of the surface. Therefore dyes can enter the pores of iron oxide samples. From EDXRF patterns it was found that the prepared magnetite and goethite were pure and free from impurities. The FT IR data of magnetite and goethite showed the presence of Fe-OH and Fe-O groups. The XRD diffractogram of the magnetite sample well matched with the standard XRD data of Fe_3O_4 and goethite well matched with the standard XRD data of FeO(OH) in software library. Sorption properties of goethite is a little higher than that of magnetite,

this is because the formula of goethite is FeO(OH), magnetite is Fe_3O_4. OH groups in the goethite have strong attractive interaction with functional groups in the dyes. From the wastewater treatment it can be seen clearly that colours of wastewater decreased significantly after treatment. According to the results, it can be concluded that the prepared iron oxides (magnetite and goethite) can be used effectively for the removal of dyes from wastewater.

Acknowledgements

The authors would like to express their profound gratitude to the Department of Higher Education (Yangon Office), Ministry of Education, Yangon, Myanmar, for giving the opportunity to do this research and Myanmar Academy of Arts and Science for allowing to present this paper.

References

Allen, S.J. and Koumanova, B.(2005)."Decolourization of Water/Wastewater Using Adsorption". *J.Univ. Chem. Technol. Metal,* vol.40, pp. 175-215

Boyjoo, A.C. (1987)."Removal of Dyes from Aqueous Solution".*J. Water Research*, vol.30, pp. 129-138

Forsling, W. and Samshog, P.O. (1998). "Surface Characteristics of Magnetite in Aqueous Suspension", *J. Colloid Interface Sci.*, vol. 197, pp. 151-160

Guinot, P., Roge,A. and Argadennec, A. (2006)."Convention of Natural Dyes". *J. Colour Technol.*, vol. 41, pp. 93-122

Mathur, J. P. and Bhandari, C. S. (2001)."Natural Dyes and their Application to Textile". *Indian J. Fibre Text Res*., vol. 26, pp. 313-401

Popoola, A. V., Ipinmoroti, K. O. and Adetuyi, A. O. (1994). "Application of Natural Dyes on Textiles".*J. Sci Industrial Res.,*pp. 37-217

Schwertmann, U. and Cornell, R.M. (1964).*Preparation and Characterization of Iron Oxides in the Laboratory.* New York: 4th Ed., VCH, pp. 225-253

INVESTIGATION OF SOME BIOLOGICAL ACTIVITIES OF WATER SOLUBLE CHITOSAN

Hnin Wuit Yee[1], Daw Hla Ngwe[2]

Abstract

The main aim of the research is to study the deacetylation of chitin extracted from prawn shell by enzymatic method and to evaluate scientifically on some biological activities. The isolation of chitin deacetylase producing *Bacillus thermoleovorans* from soil and bioconversion of chitin to chitosan and water soluble chitosan (WS-chitosan) was converted from the prepared E-chitosan by oxidative depolymerization method. Some pharmacological activities such as antimicrobial activity, antitumor activity, antioxidant activity, acute toxicity, weight loss activity and antilipidemic activity of water soluble chitosan (WS-chitosan) were currently assayed. The antimicrobial activity of WS-chitosan was more effective on gram positive bacteria than gram negative bacteria. The antitumor activity of WS-chitosan was assayed by potato crown gall (PCG) method. It was found that, the different concentration ranges of chitosan have different inhibited tumor growth manner. In the determination of antioxidant activity of WS-chitosan, the IC_{50} was found to be 4.20 µg/mL. The acute toxicity test of WS-chitosan on albino mice done by the method of the Litchfield and Wilcoxon indicated no toxic effect. According to the study on the weight loss activity of WS-chitosan on albino mice carried out by the method of Han *et al*., 1999, the 600 mg/kg b. wt dose of WS-chitosan is the most eligible dose to reduce the body weight of male and female albino mice. In the investigation of antilipidemic activity of WS-chitosan on albino rats, it was observed the significantly decrease in the "bad" cholesterol: LDL cholesterol and increase in "good"cholesterol : HDL cholesterol. Treatment with WS-chitosan (600mg/kg b.wt) significantly decreased in levels at TC by 59 % , TG by 62 % and LDL by 40 % and 26 % increased in HDL levels at 21 days.

Keywords : water soluble chitosan, antimicrobial, antitumor, antioxidant, weight loss activity, antilipidemic activity

Introduction

Chitosan is a natural linear polysaccharides comprising copolymers of glucosamine and N-acetyl glucosamine and can be obtained by the partial deacetylation of chitin. Nowadays, chitosan is used in versatile applications

[1] Assistant Lecturer, Dr, Department of Chemistry, Bago University

[2] Professor and Head, Dr, Department of Chemistry, University of Yangon

(Choi *et al*., 2004). Chitosan has been widely used in vastly diverse fields ranging from waste management to food processing, medicine and biotechnology. It becomes an interesting material in pharmaceutical applications due to its biodegradability and biocompatibility, and low toxicity.

Water soluble chitosan (WS-chitosan) was prepared from enzymatically prepared chitosan (E-chitosan) that was produced by using chitin deacetylase enzyme (CDA) extracted from *B. thermoleovorans* that was isolated from soil sample (Hnin Wuit Yee *et al.,* 2016). In the present study, some biological activities such as antimicrobial, antioxidant, antitumor, weight loss and antilipidemic activities of the water soluble chitosan were investigated.

Antimicrobial activity: Chitosan is effective in inhibiting growth of bacteria but lower toxicity towards mammalian cells (Takemone *et al*., 1989). The antimicrobial properties of chitosan depend on its molecular weight and the type of bacterium, chitosan generally showed stronger bacterial effects for gram-positive bacteria, (*Listeria monocytogenes, Lactobacillus plantarum, L.brevis, Bacillus cereus, Staphylococcus aureus, Bacillus subtilis and Bacillus pumilus*) than for gram-negative bacteria (*Pseudomonas aeruginosa, Pseudomonas fluorescens, E. coli, Salmonella typhymurium and Vibrio parahaemolyticus*) in the presence of 0.1 % chitosan (No *et al*., 2002).

Antitumor activity: The use of highly specific, quantitative bioassays which require only a short period of time to obtain results is available for studying crown gall tumor formation (Anand and Heberlein, 1977). The crown gall tumor assay (CGTA) is one of several bench top bioassays recommended for the rapid screening of plants with anti-cancer activity (Galsky *et al*., 1980 and Srirama *et al*., 2008).

Antioxidant activity: Antioxidant activity is one of the well-known functions of chitosan. Many studies have shown that chitosan inhibit the reactive oxygen species (ROS) and prevent the lipid oxidation in food and biological systems (Kim and Thomas, 2007). Chitosan can scavenge free radicals or chelate metal ions from the donation of a hydrogen or the lone pairs of electrons (Xie *et al*., 2001). The interaction of chitosan with metal ions could involve several complex actions including adsorption, ion-exchange and chelation (Onsosyen and Skaugrud, 1990). The hydroxyl group (OH) and amino groups (NH_2) in

chitosan are the key functional groups for its antioxidant activity but can be difficult to be dissociated due to the semi-crystalline structure of chitosan with strong hydrogen bonds (Xie *et al*., 2001). There has been increasing interest in finding natural antioxidants, since they can protect the human body from free radicals and retard the progress of many chronic diseases.

Weight loss activity: Chitosan is viewed as potentially useful for increase fecal fat excretion. This effect has been demonstrated in animal studies. Several studies have examined whether chitosan consumption will reduce adiposity in animal models, as might be expected, based on the increase in fecal fat. None the less, in human studies, the chitosan with low molecular weight can accelerate the weight loss when subjects are on a weight reduction diet, but that when food intake is not restricted, no weight loss should be expected.

Antilipidemic activity: Chitosan is believed to affect cholesterol levels and weight because it has positively charged amino groups at the same pH as the gastrointestinal tract. These amino groups are believed to bind to negatively charged molecules, such as lipids and bile, preventing their absorption and storage by the body. The action of chitosan in cholesterol management may be explained by the theory that ingested chitosan salts react with fatty acids and bind lipids because of hydrophobic interactions; these bound lipids are extracted rather than absorbed (Gallaher *et al*., 2000).

Materials and Methods

Screening of Pharmacological Activities of Prepared Water Soluble Chitosan

The isolation of chitin deacetylase producing *Bacillus thermoleovorans* from soil and bioconversion of chitin and chitosan and water soluble chitosan (WS-chitosan) was converted form the enzymatically prepared chitosan (E-chitosan) by oxidative depolymerization method were previously described (Hnin Wuit Yee *et al.,* 2016). Some pharmacological activities of water soluble chitosan chitosan such as antimicrobial activity, antitumor activity, antioxidant activity, acute toxicity, weight loss activity and antilipidemic activity were presently studied.

Screening of antimicrobial activity by agar well diffusion method

Antimicrobial activity of various concentration of prepared water soluble chitosan (WS-chitosan) was studied by agar well diffusion method at Pharmaceutical Research Department, Insein, Yangon Region. The agar well plate diffusion method was used to test the antibacterial action of the extracts on 24 h broth culture of the organisms used. The prepared water soluble chitosan (WS-chitosan) in various concentrations such as 1.0 mg, 2.0 mg and 3.0 mg were dissolved in 1mL of sterile distilled water. 1 mL each of the bacterial suspension of 24 h of nutrient agar was streaked evenly onto the surface of trypticase soy agar plates with sterile cotton swab. Immediately after hardening the agar, the wells were made with a 10 mm sterile cork borer from each seeded agar. After removing the agar, the wells were filled with the WS-chitosan to be tested. The plates were incubated at 37 °C for 18 - 24 h. The diameters of the inhibition zone were measured and recorded in mm.

Screening of antitumor activity by potato crown gall test

Isolated *Agrobacterium tumefacien* has been maintained as solid slants under refrigeration. For inoculation into the potato discs, 48 h broth cultures containing 5×10^7-5×10^9 cell/mL were used. Fresh, disease free potatoes were purchased from a local market. Tubers of moderate size were surface sterilized by immersion in 0.1 % sodium hypochlorite for 20 min. Ends were removed and the potatoes were soaked an additional 10 minutes. A core of the tissue was extracted from each end and discarded. The remainder of the cylinder was cut into 0.5 cm thick discs with a surface sterilized scalpel. The discs were then transferred to agar plates (1.5 g of agar dissolved in 100 mL sterile distilled water (DW), autoclaved for 20 min at 121°C, 20 mL poured into each petri-dish). Each plate contained four potato discs and 4 plates were used for each sample dilution.

Each sample of 2.50, 1.25 and 0.625 mg was separately dissolved in 2 mL of Hexodeutrodimethyl sulphoxide (DMSO) and filtered through millipore filters (0.22 μm) into sterile tube. This solution (0.5 mL) was added to sterile DW (1.5 mL), and broth culture of *A. tumefaciens* in 2 mL of phosphate buffer saline (PBS) was added. Control was made in this way; DMSO (0.5 mL) and sterile DW (1.5 mL) were added to the tube containing 2 mL of broth culture

of *A. tumefaciens*. Using a sterile disposable pipette, 1 drop (0.05 mL) from these tube was used to inoculate each potato disc, spreading it over the disc surface. After inoculation, Petri dishes were sealed by para film and incubated at 27 - 30 °C for 3 weeks. Tumors were observed on potato discs after 21 days under stereo-microscope followed by staining with Lugol's iodine (10 % KI and 5 % I_2) after 30 minutes and compared with control. The antitumor activity was examined by observation of tumor produced or not. The steps involved in the preparation of potato discs for PCG test were shown in Figure 1.

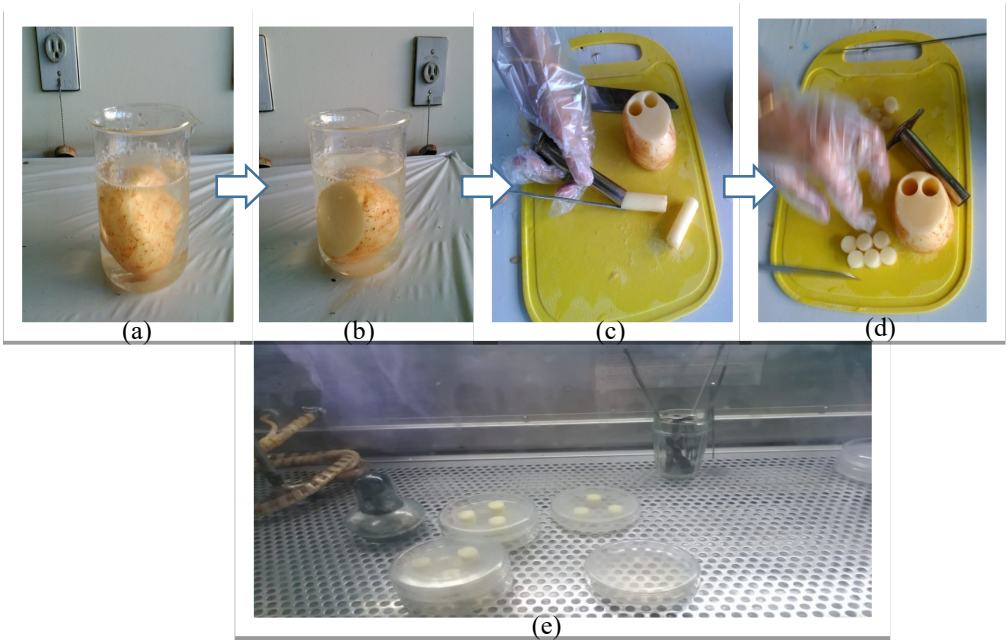

Figure 1. Photographs showing the steps involved in the preparation of potato discs for PCG test

(a) Sterilized potato tuber surface by immersion in 0.1 % sodium hypochlorite solution
(b) Removed both ends of potato tuber surface by sterilized cutter and soaked in another 0.1 % sodium hypochlorite solution
(c) Extracted the core of potato with sterilized cork borer
(d) Cut the core of potato into 0.5 cum thick discs with a sterilized scalpel
(e) Transferred the potato discs to petridish containing agar medium

Determination of antioxidant activity by using DPPH assay

DPPH radical scavenging activity was determined by UV visible spectrophotometric method. Control solution was prepared by mixing 60 μM DPPH solution (1.5 mL) and 70 % ethanol (1.5 mL). The sample solution was prepared by thoroughly mixing 60 μM DPPH solution (1.5 mL) and test sample solutions (1.5 mL). The solution was then allowed to stand at room temperature for 30 minutes. Absorbance of these solutions was measured at 517 nm by using spectrophotometer and % inhibition was calculated by using the following equation. The 50 % inhibition concentration (IC_{50}) value for each test sample was determined by linear regressive excel programme from a plot of % inhibition values versus the concentration of each test sample.

$$\% \text{ Inhibition} = \frac{A_{Control} - A_{Sample}}{A_{Control}} \times 100$$

Where, $A_{Control}$ = absorbance of control solution

A_{Sample} = absorbance of tested sample solution.

Study on acute toxicity of water soluble chitosan

The acute toxicity test on prepared water soluble chitosan was done according to the method of Litchfield and Wilcoxon (1949). Fifty healthy albino mice (ddy strain) of both sexes (30-35) g were used for this study. They were separated into 6 groups, each group containing of 10 mice. On the experiment day, all groups of mice were fasted overnight and only water was taken. Four doses (1 g/kg, 2 g/kg, 3 g/kg, 4 g/kg and 5 g/kg) of prepared water soluble chitosan were administered orally. The mice of control group were given distilled water only. The general signs and symptoms of toxicity were recorded hourly up to 6 hours and daily up to two weeks (Litchfield and Wilcoxon, 1949). The procedure steps of acute toxicity test on albino mice are illustrated in Figure 2.

(a) **(b)**

Figure 2. Acute toxicity test on albino mice (DDY strain)

(a) Mice were put in laboratory condition: standardized boxes, natural light and ambient temperature, allowed free access to both water and animal feed

(b) Administration of the prepared WS-chitosan by oral route using intragastric syringe

Weight loss effect of prepared water soluble chitosan (WS-chitosan) in mice

The weight loss activity of WS-chitosan tested on albino mice was carried out according to the method of Han *et al*., (1999). Eighty healthy albino mice (ddy strain) of male and female (32-35 g) were used for this study. They were separated into 4 groups, each group containing of 10 mice. Group I was given distilled water only and served as control group. Groups II, III and IV were orally given with three different doses (400, 600 and 800 mg/kg) of prepared sample respectively and orally administered once a day for 4 weeks as shown in Figure 3.

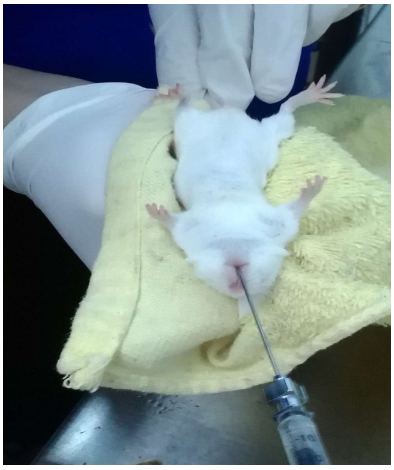

(a) Administration of the prepared WS-chitosan in different concentrations by oral route using intragastric syringe

(b) Checking the weight of tested mice by using animal balance

Figure 3. Weight loss test on albino mice (DDY strain)

Antilipidemic effect of prepared water soluble chitosan

All rats were weighed before the experiment. The dosages were calculated on the body weight basis for each tested rat. Thirty female albino rats were divided into five groups, each group containing of 6 animals. Hyperlipidemia was induced in rats by single intraperitoneal injection of freshly prepared solution of triton WR-1339 (400 mg/kg) in physiological saline solution after the animals were kept fasting for 24 h (Sikarwar and Patil, 2012).

Each animal was given single dose of triton 400 mg/kg intraperitoneally shown in Figure 4 (a). The Group I was given distilled water only and served as control group. After 48 h of triton injection, Group II was orally treated with atorvastatin 10 mg/kg and served as a standard drug treated group. Groups III, IV and V were orally given with three different doses (400, 500, 600 mg/kg) of prepared WS-chitosan respectively after 48 hours of triton

injection. Atorvastatin and three different doses of WS-chitosan were orally administered once a day for 4 weeks (Figure 4). The plasma lipid levels (TC, TG, HDL, LDL) of each rat were measured at the start of the study i.e., before triton injection (For base line plasma lipid level) 48 hours after triton injection (to confirm triton induced hyperlipidemia), 2 days, 7 days, 14 days and 21 days after orally administered by samples and standard drug for all respective groups. The photographs showing the measurement steps of plasma lipid level are shown in Figure 5.

(a)

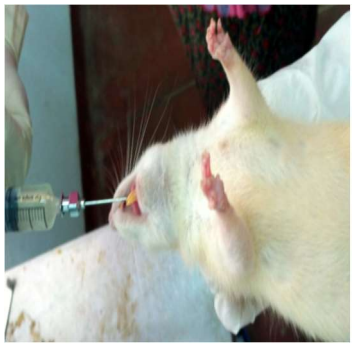

(b)

(c)

Figure 4. Steps involved in the antilipidemic test on albino rats (Wistar strain)

(a) Intraperitoneal injection of triton (400mg/kg) to albino rats

(b) Administered the Atorvastatin (10mg/kg) to albino rats by oral route using intragastric syringe

(c) Administered the prepared WS-chitosan to albino rats by oral route using intragastric syringe

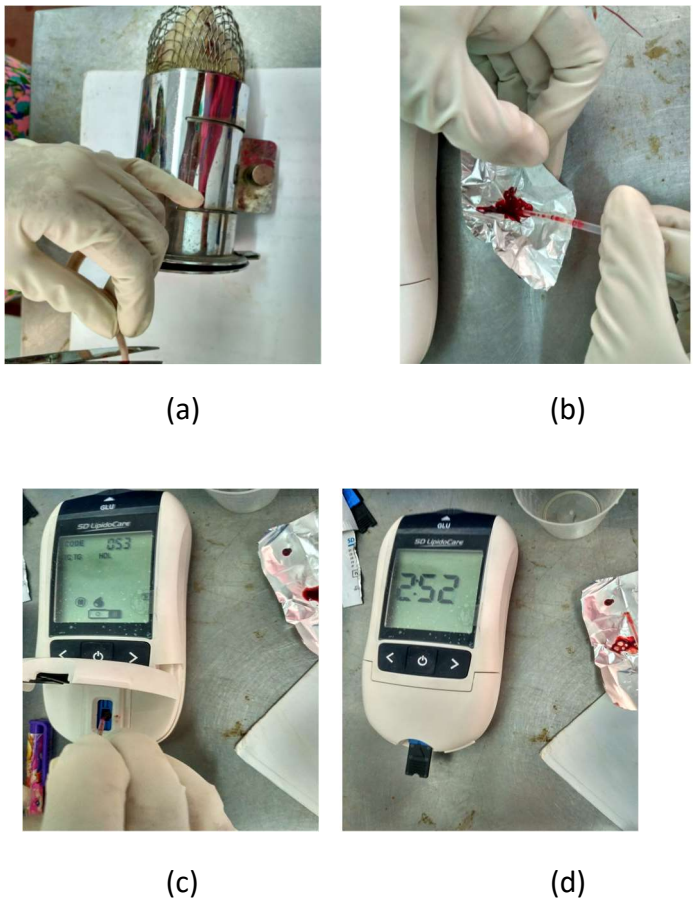

Figure 5. Photographs showing the steps involved in the measurement of plasma lipid levels (TC, TG, HDL, LDL) of each rat by using "SD Lipidocare" device

(a) Cut the rat tail to collect the blood by sterilized scissors

(b) Take the rat blood about 30 µL with capillary tube

(c) Plugged the test strip in the SD Lipidocare device and put the rat blood sufficiently on the sensor of this device

(d) Read the data of plasma lipid levels (TC, TG, HDL, LDL) by choosing the mode

RESULTS AND DISCUSSION

Pharmacological Activity of Prepared Water Soluble Chitosan

In vitro screening of antimicrobial activity of prepared WS-chitosan by agar well diffusion method

From the results shown in Figure 6, it was observed that 2.0 mg concentration showed slightly higher activity than other (1 mg and 3.0 mg) in 1 mL of sterile distilled water. According to the investigation of antimicrobial activities on tested microorganisms, the prepared water soluble chitosan showed stronger antimicrobial effects for gram positive bacteria such as *B.subtilis, Staphylococcus aureus* and *B.pumilus* than others. Diameters of inhibition zone (mm) for tested samples are summarized in Table 1. The inhibition zone diameters of tested samples against seven microorganisms were found in the range of 15-18 mm.

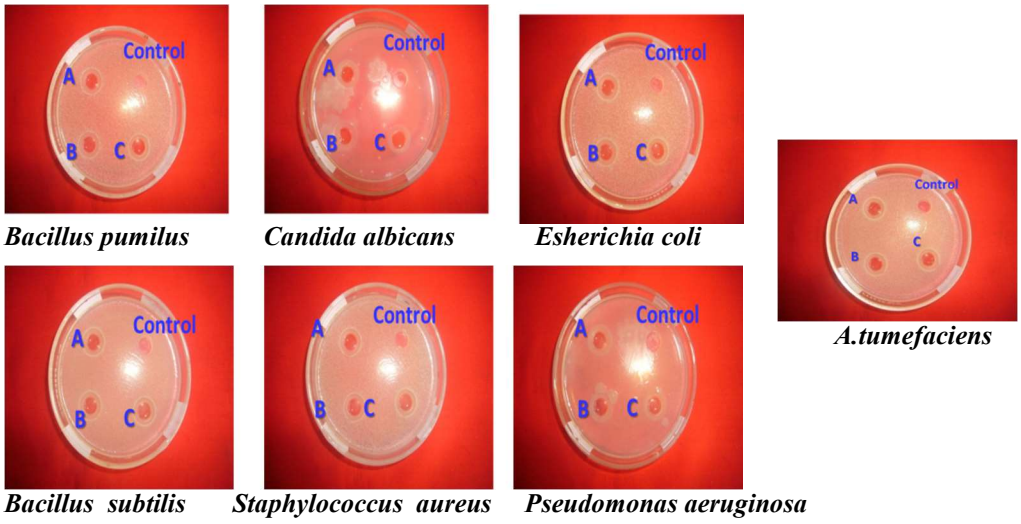

Figure 6. Screening of antimicrobial activity of prepared WS-chitosan against six microorganisms and *A. tumefaciens*

Table 1. Inhibition Zone Diameters of Prepared WS-chitosan in Different Concentrations

Samples	Concentration (mg/mL)	Diameters of inhibition zone (mm) against different microorganisms						
		I	**II**	**III**	**IV**	**V**	**VI**	**VII**
WS – chitosan in distilled water	1.0	17 (++)	16 (++)	15 (++)	16 (++)	16 (++)	16 (++)	16 (++)
	2.0	18 (++)	18 (++)	15 (++)	18 (++)	15 (++)	16 (++)	17 (++)
	3.0	17 (++)	17 (++)	15 (++)	16 (++)	15 (++)	15 (++)	17 (++)
Control (D/W)	-	-	-	-	-	-	-	-

I	*Bacillus subtilis*	Agar Well – 10 mm
II	*Staphylococcus aureus*	10 mm ~ 14 mm (+)- lower activity
III	*Pseudomonas aeruginosa*	15 mm ~ 19 mm (++) - higher activity
IV	*Bacillus pumilus*	20 mm ~ above (+++) - highest activity
V	*Candida albicans*	
VI	*Escherichia coli*	
VII	*A. tumefaciens*	

Antitumor activity of prepared water soluble chitosan (WS-chitosan)

It could be seen from the Figure 7 that the low molecular weight water soluble chitosan (WS-chitosan) inhibited tumor growth in concentration dependent manner. Significant tumor inhibition was observed at 7.81 µg/disc and slightly inhibited on tumor growth at 3.90 µg/disc, but not at 1.95 µg/disc. Hussian *et al* (2007) have also shown that inhibition rate on potato discs are dependent on concentration of chitosan and also tumor producing *A. tumefaciens* strains. It was noticed that tumor formation was observed when *Agrobacterium* strains alive on potato disc. The potato discs were often

damaged due to the contamination and other physiological factors when there was no tumor formation. Thus successful attachment of *Agrobacterium* on living potato disc is needed for antitumor test. The results of antitumor activity are presented in Table 2.

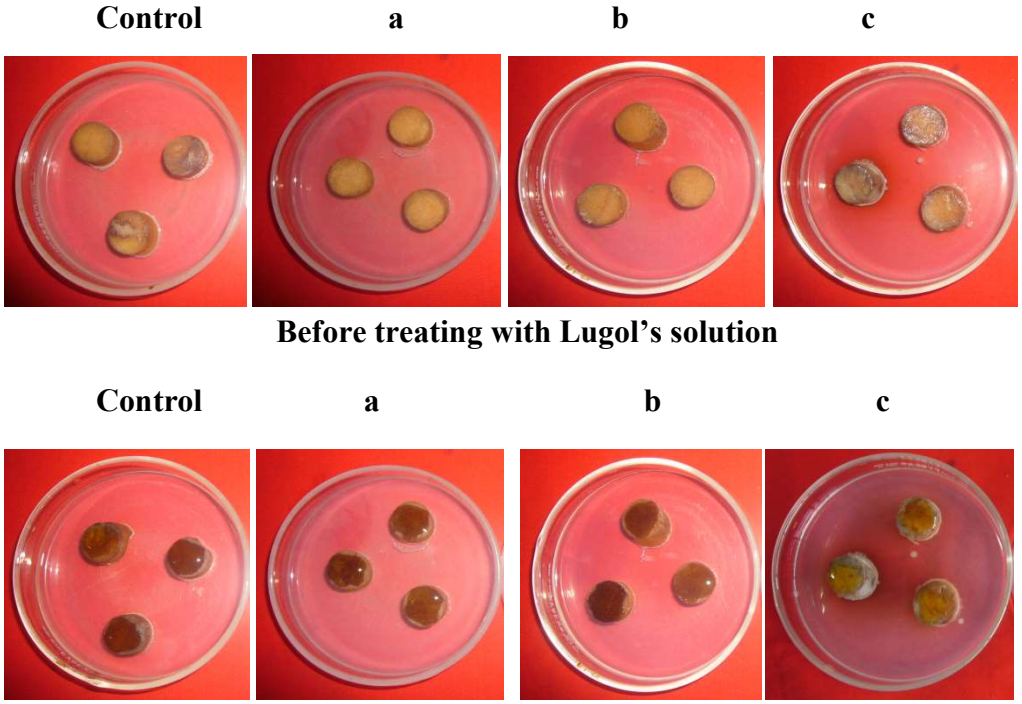

a = 7.81 µg/disc **b** = 3.90 µg/disc **c** = 1.95 µg/disc

Figure 7. Screening of tumor inhibition of WS-chitosan on potato discs in different concentrations

Table 2. Tumor Inhibition by the WS- chitosan through *A. tumefaciens* Infection using Potato Disc Bioassay

Test Sample	**Concentration (µg/disc)**	**Tumor**
WS-Chitosan	7.81	-
	3.90	-
	1.95	+
Control (D/W)	-	+

(+) tumor appeared (-) no tumor appeared

Antioxidant activity of low molecular weight water soluble chitosan (WS-chitosan)

DPPH (2, 2-diphenyl -1, picryl hydrazyl) method is the most widely reported method for screening of antioxidant activity on many organic drugs. This method is based on the reduction of color of free radical DPPH in ethanol solution by different concentrations of the samples. The antioxidant activity was expressed as 50 % oxidative inhibitory concentration (IC_{50}). In this study, ten different concentrations (0.195, 0.39, 0.78, 1.56, 3.125, 6.25, 12.5, 25, 50, 100 µg/mL) of prepared WS-chitosan were used. Determination of absorbance was carried out at wavelengths 517 nm using UV visible spectrophotometer. Each experiment was done triplicate. The lower the IC_{50} showed the higher the free radical scavenging activity. The IC_{50} values was found to be 4.20 µg/mL for water soluble chitosan which was lower than standard ascorbic acid (IC_{50} =1.43 µg/mL) in antioxidant activity presented in Figure 8.

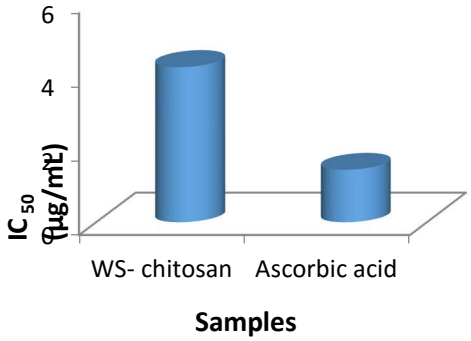

Figure 8. A bar graph representing IC_{50} values of water soluble chitosan and standard ascorbic acid

Acute toxicity study of water soluble chitosan (WS-chitosan)

In this research work, the acute toxicity of water soluble chitosan (WS-chitosan) was determined by Litchfield and Wilcoxon method (1949). Since the route of administration selected should be intended route for administration of tested drugs to human during therapy, the oral route was chosen and different doses were administered orally in mice. The mice weighing 30-35 g were treated with 1, 2, 3, 4 and 5 g/kg body weight doses of each extract. They

were then kept under observation for two weeks. All of the animals were observed to be remained alive and did not show any visible symptom of toxicity like restlessness, respiratory disorders, convulsions, aggressive activities, coma and death at the dosages tested. According to the results as shown in Table 3, no lethality of the mice was observed up to two weeks, even with the maximum soluble dose of 5 g/kg body weight. From these results, it was found that the prepared WS-Chitosan was free from acute toxic effect under condition.

Table 3. Results of Acute Toxicity Test of Water Soluble Chitosan on Mice after Two Weeks Treatment

No	Groups	Drug Administration	Dosage g/kg (b. wt)	No. of death per tested mice	% of death
1.	Control	Distilled Water	-	0/10	0
2.	I	Water soluble chitosan	1	0/10	0
3.	II	Water soluble chitosan	2	0/10	0
4.	III	Water soluble chitosan	3	0/10	0
5.	IV	Water soluble chitosan	4	0/10	0
6.	V	Water soluble chitosan	5	0/10	0

Note : Each group contains 10 no: of mice

Medium lethal dose LD_{50}> 5 g/kg body weight

Weight loss effect of water soluble chitosan

In this research, the weight loss activity of WS-chitosan tested on albino mice by Han *et al.,* 1999. In this test, 80 healthy albino mice (32-40 g b.wt) of male and female were used. They are subdivided into four main groups. Each group contains10 male mice and 10 female mice. The group I was the control group and it was given distilled water only. Groups II, III, IV were test groups treated with three different doses (400 mg/kg, 600 mg/kg and

800 mg/kg) of water soluble chitosan, respectively. They were orally administered once a day for 4 weeks.

In Group II, water soluble chitosan (400 mg/kg body weight) treated group is slightly decreased in third week and in fourth week compared to "0" week. In fourth week, weight loss (29.0 g to 28.6 g) decreased in male albino mice and (29.7 g to 26.0 g) in female albino mice were observed. WS-chitosan possessed more weight loss effect on female albino mice than male albino mice by the above data (Figures 9 (a) and (b)). In the WS-chitosan (600 mg/kg b.wt) treated group III, the weight loss activity was significantly high at fourth week compared to "0" week, 31.4 g reduced to 29.1 g in male albino mice and 31.0 g reduced to 27.3 g in female albino mice. In the water soluble chitosan (WS-chitosan), 800 mg/kg body weight treated Group IV, the weight loss activity showed high at third week compared to "0" week, 36.0 g lowered to 34.6 g in male and 30.8 g lowered to 28.5 g in female albino mice. According to the data, (600 mg/kg body weight) dose of WS-chitosan showed the highest activity than others. Comparison of weight loss activity of different concentrations of WS-chitosan with control group of male and female albino mice is shown in Figure 9.

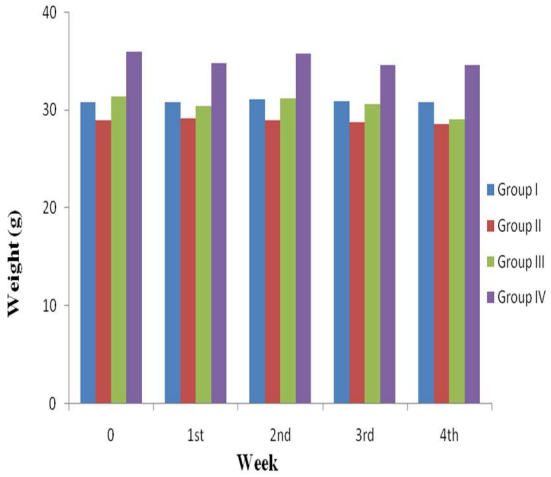

(a) Male

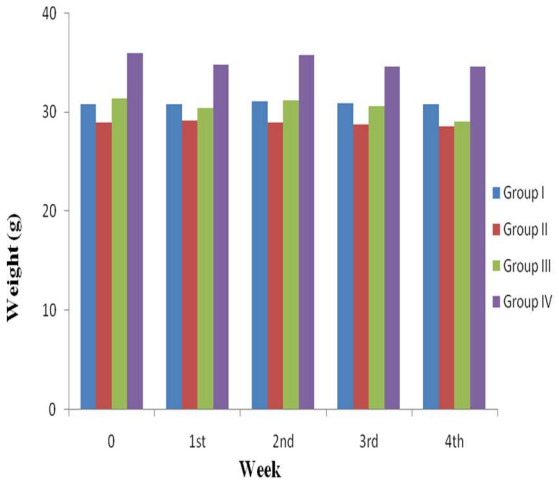

(b) Female

Group I = Control group treated with D/W only
Group II = The Group treated with 400 mg/kg body weight dose of WS-chitosan
Group III = The Group treated with 600 mg/kg body weight dose of WS-chitosan
Group IV = The Group treated with 800 mg/kg body weight dose of WS-chitosan

Figure 9. Comparison of weight loss activity treated with three different doses of WS-chitosan and control group of (a) male and (b) female albino mice in each week

Study on antilipidemic activity of prepared water soluble chitosan

In hyperlipidemic activity, 30 female albino rats in the weight range of 250-300 grams were used in which 18 rats treated with prepared water soluble chitosan. Thirty albino rats were divided into five groups, each group

containing of 6 animals. Each animal was given a single dose of a triton at a dose of 400 mg/kg b.wt intraperitoneally. The Group I animals were injected triton only and served as control group. After 48 h of triton injection, Group II was orally treated with standard drug (Atorvastain) 10 mg/kg b.wt daily and served orally doses of (400, 500, 600 mg/kg b. wt) of the prepared water soluble chitosan powders, respectively, orally after 48 h of triton injection in Groups III, IV, V. The plasma lipid levels (TC, TG, HDL and LDL ratio) of each rat were measured by SD "Lipidocare" lipid profile at the start of the study i.e., before triton injection (for base line plasma lipid level), 2 days, 7 days, 14 days and 21 days after triton injection (to confirm induced hyperlipidemia) for all groups.

The mean serum levels of base line lipid profiles at "0" hour

The mean serum levels of total cholesterol at 0 h in Groups I, II, III, IV and V were 121.1 ± 27.99 mg/dL, 124.1 ± 28.11 mg/dL, 123.7 ± 30.94 mg/dL, 115.0 ± 17.10 mg/dL and 107.0 ± 31.11 mg/dL respectively. The mean serum levels of triglycerides at 0 h in Groups I, II, III, IV and V were 81.3 ± 11.31, 104.8 ± 21.87, 114.0 ± 11.32, 94.0 ± 21.11 and 75.4 ± 31.50 mg/dL, respectively. The mean serum levels of HDL at 0 hour in Groups I, II, III, IV and V were 57.8 ± 11.20, 70.8 ± 17.10, 75.8 ± 20.81, 77.0 ± 15.99 and 63.5 ± 15.28 mg/dL, respectively. The mean serum levels of LDL at 0 hour in Groups I, II, III, IV and V were 46.6 ± 12.27, 33.0 ± 11.27, 25.5 ± 15.81, 19.3 ± 11.10 and 27.7 ± 6.11 mg/dL, respectively. The resultant lipid profile status of all group of rats at 0 hour of observation were not significantly different ($P< 0.05$). Therefore, the baseline values were same and comparable.

Effect of triton on lipid profiles of triton induced albino rats

The lipid profile observed at 0 h before administration of triton (400 mg/kg b.wt) in Group I were found to be TC: 121.12 ± 27.9 mg/dL, TG: 81.3 ± 11.31 mg/dL, HDL: 57.8 ± 11.2 mg/dL and LDL: 46.6 ± 12.2 mg/dL. The lipid profiles found at 2 days after administration with triton (400 mg/kg b.wt) dose in Group I were increased in TC: 223%, TG: 390 %, LDL: 207 % and HDL: 7 %. The lipid profiles found at 7 days after administration with triton (400 mg/kg b.wt) dose in Group I were increased in TC: 214 %, TG: 377 %, LDL: 199 % and HDL: 3 %. The lipid profiles found at 14 days after administration

with triton (400 mg/kg b.wt) dose in Group I were increased in TC: 134 %, TG: 312 %, LDL: 178 % and HDL: 3 %. The lipid profiles found at 21 days after administration with triton (400 mg/kg b.wt) dose in Group I were increased in TC: 89 %, TG: 303 %, LDL: 163 % and HDL: 2 %. The mean serum levels of TC, TG and LDL observed at 7 days were significantly increased from those observed at 0 hour in the same group ($p<0.05$). Therefore, triton 400 mg/kg can be successfully induced hyperlipidemia in albino rats. These results are presented in Table 4.

Table 4. Mean Plasma Lipid Levels of Group I Receiving Triton 400 mg/kg b.wt dose as Control Group after 2 days, 7 days, 14 days and 21 days

Mean Plasma Lipid Levels (mg/dL)	**Lipid Profile (mean ± SD)**			
	TC	**TG**	**HDL**	**LDL**
0 hour before triton	121.1 ± 27.9	81.0 ± 11.31	57.8 ± 11.2	46.6 ± 12.2
2 days after triton	391.2 ± 31.2	398.1 ± 51.7	61.7 ± 11.3	143.1 ± 22.8
Difference (%)	223	390	7	207
7 days after triton	379.8 ± 42.8	388.1 ± 58.5	59.8 ± 12.4	139.6 ± 14.9
Difference (%)	214	377	3	199
14 days after triton	283.4 ± 26.5	334.7 ± 11.4	59.3 ± 12.1	129.7 ± 14.6
Difference (%)	134	312	3	178
21 days after triton	228.7 ± 12.1	327.4 ± 16.7	59.1 ± 11.3	122.7 ± 16.4
Difference (%)	89	303	2	163

Effect of standard drug (Atorvastain) on lipid profile status in triton induced hypercholesterolemia albino rats

In this research work, the Group II experimental data of mean plasma levels of albino rats in 2 days after administration of triton WR-1339 (400 mg/kg b. wt) and in 7 days, 14 days and 21 days after treatment with Atorvastain (10 mg/kg b.wt) as standard drug are shown in Table 5. After administration of triton WR-1339 (400 mg/kg b. wt) obviously increased in levels of TC by 181 %, TG by 184 % and LDL by 308 % and decreased in HDL level by 7 % within 2 days. Treatment with Atorvastain (10 mg/kg b.wt) significantly decreased in levels of 59 % TC, 65 % TG and 42 % LDL and increased in 21 % HDL level of cholesterol within 21 days.

Table 5. Mean Plasma Lipid Levels of Group II Receiving Atorvastatin 10 mg/kg b.wt dose as Standard Drug Group for Water Soluble Chitosan after 2 days, 7 days, 14 days and 21 days

Mean Plasma Lipid Levels (mg/dL)	**Lipid Profile (mean ± SD)**			
	TC	**TG**	**HDL**	**LDL**
0 hour before triton	124.1 ± 28.1	104.8 ± 21.8	70.8 ± 17.1	33 ± 11.2
2 days after triton	348.2 ± 11.5	298.1 ± 41.3	65.9 ± 14.5	134.6 ± 23.7
Difference (%)	181	184	7	308
7 days after triton + Atorvastatin	276.8 ± 11.9	213.4 ± 34.1	67.1 ± 11.6	118.6 ± 23.4
Difference (%)	21	28	2	12
14 days after triton + Atorvastatin	211.7 ± 19.4	181.4 ± 31.8	73.7 ± 14.8	107.1 ± 17.9
Difference (%)	39	39	12	20
21 days after triton + Atorvastatin	144.1 ± 11.2	103.8 ± 6.4	79.4 ± 4.8	48.1 ± 14.1
Difference (%)	59	65	21	42

Effect of water soluble chitosan on lipid profile status in triton induced hypercholesterolemia albino rats

The test Group III, 2 days after administration of triton WR-1339 (400 mg/kg body weight) significantly increased in levels of TC by 169%, TG by 249 % and LDL by 297 % and decreased in HDL level by 8 %. Treatment with WS-chitosan at a dose of (400 mg/kg body weight) not significantly decreased in levels of TC by 64 %, TG by 77 % and LDL by 49 % and increased in HDL by 14 % at 21 days. These data are shown in Table 6. In Group IV, 2 days after administration of triton WR-1339 (400 mg/kg) significantly increased in levels of TC by 188 %, TG by 203 % and LDL by 349 % and decreased in level of HDL by 14 %. Treatment with WS-chitosan samples (500 mg/kg) evidently decreased in levels of TC by 67%, TG by 71% and LDL by 40% and increased in level of HDL by 24 % in 21 days (Table 7). In Group V, 2 days after administration of triton WR-1339 (400 mg/kg) significantly increased in levels of TC by 195 %, TG by 258 % and LDL by 351 % and increased in level of HDL by 9 %. After treatment with WS-chitosan (600 mg/kg b.wt) evidently decreased in levels of TC by 59 %, TG by 62 % and LDL by 40 % but increased in HDL level by 26 % at 21 days shown in Table 8.

According to the data of Groups III, IV and V, the Group V (WS-chitosan 600 mg/kg) showed the highest antilipidemic activity than others.

Table 6. Mean Plasma Lipid Levels of Group III Receiving Water Soluble Chitosan (400 mg/kg b.wt) after 2 days, 7 days, 14 days and 21 days

Mean Plasma Lipid Levels (mg/dL)	**Lipid Profile (mean ± SD)**			
	TC	**TG**	**HDL**	**LDL**
0 hour before triton	123.7 ± 30.9	114 ± 11.3	75.8 ± 20.8	25.5 ± 15.8
2 days after triton	332.3 ± 12.7	397.8 ± 27.1	69.9 ± 6.7	101.3 ± 11.4
Difference (%)	169	249	8	297
7 days after triton + WS-chitosan (400 mg/kg)	252.1 ± 11.7	181.7 ± 19.6	71.9 ± 21.3	85.6 ± 19.4
Difference (%)	32	54	3	15
14 days after triton + WS-chitosan (400 mg/kg)	209.6 ± 28.3	179.8 ± 31.4	78.1 ± 11.7	73.8 ± 17.6
Difference (%)	37	55	12	27
21 days after triton + WS-chitosan (400 mg/kg)	118.3 ± 13.6	89.4 ± 14.8	78.8 ± 21.3	62.1 ± 31.7
Difference (%)	64	77	14	39

Table 7. Mean Plasma Lipid Levels of Group IV Receiving Water Soluble Chitosan (500 mg/kg b.wt) after 2 days, 7 days, 14 days and 21 days

Mean Plasma Lipid Levels (mg/dL)	**Lipid Profile (mean ± SD)**			
	TC	**TG**	**HDL**	**LDL**
0 hour before triton	115 ± 17.1	94 ± 21.1	77 ± 15.9	19.3 ± 11.1
2 days after triton	331.6 ± 12.8	284.8 ± 71.9	66.1 ± 11.3	86.8 ± 15.4
Difference (%)	188	203	14	349
7 days after triton + WS-chitosan (500 mg/kg)	208.9 ± 17.6	174.3 ± 23.4	70.6 ± 11.2	68.9 ± 7.3
Difference (%)	37	39	7	21
14 days after triton + WS-chitosan (500 mg/kg)	178.6 ± 24.6	87.4 ± 31.7	75.8 ± 11.4	63.1 ± 6.6
Difference (%)	46	69	15	27
21 days after triton + WS-chitosan (500 mg/kg)	109.8 ± 11.7	83.4 ± 6.1	81.9 ± 23.1	51.8 ± 16.4
Difference (%)	67	71	24	40

Table 8. Mean Plasma Lipid Levels of Group V Receiving Water Soluble Chitosan (600 mg/kg b.wt) after 2 days, 7 days, 14 days and 21 days

Mean Plasma Lipid Levels (mg/dL)	Lipid Profile (mean ± SD)			
	TC	TG	HDL	LDL
0 hour before triton	107.0 ± 31.1	75.4 ± 31.5	63.5 ± 15.2	27.7 ± 6.1
2 days after triton	315.6 ± 27.8	288.9 ± 34.1	69.4 ± 14.4	124.9 ± 13.8
Difference (%)	195	258	9	351
7 days after triton + WS-chitosan (600 mg/kg)	208.9 ± 31.6	154.3 ± 11.3	72.8 ± 6.5	93.7 ± 21.6
Difference (%)	34	47	5	25
14 days after triton + WS-chitosan (600 mg/kg)	183.1 ± 11.7	153.1 ± 16.4	81.4 ± 21.2	81.6 ± 24.6
Difference (%)	42	47	17	35
21 days after triton + WS-chitosan (600 mg/kg)	128.5 ± 14.6	110.6 ± 20.8	87.7 ± 11.7	74.9 ± 19.6
Difference (%)	59	62	26	40

Conclusion

From the assessment of the antimicrobial activity, the water soluble chitosan was more effective on gram positive bacteria namely *Bacillus subtilis, Bacillus pumilus* and *Staphylococcus aureus* than others. By the investigation of the antitumor activity, the minimum inhibitory concentration of WS-chitosan was found to be 3.90 µg/disc. Antioxidant activity test was assessed by DPPH assay revealed by mild radical scavenging activity of water soluble chitosan. According to the investigation of antioxidant activity, the value of the IC_{50} of the water soluble chitosan was 4.20 µg/mL was evidently comparable with standard ascorbic acid (IC_{50} = 1.43 µg/mL). From acute toxicity test, it

was observed that the water soluble chitosan was free from toxic effect in the range of 1-5 g/kg body weight of albino mice. The concentration (600 mg/kg) of WS-chitosan showed the highest activity and more weight loss effect on female albino mice than male albino mice. The hypocholesterolemic or antilipidemic activity of the water soluble chitosan was determined on albino rat model using triton WR-1339 injection method. In this study, it indicated that water soluble chitosan has the ability to reduce "bad" cholesterol (TC, TG and LDL) and it also could significantly promote the "good" blood cholesterol (HDL) level especially the concentration of WS-chitosan at (600 mg/kg body weight) within 21 days. Thus, water soluble chitosan can be suitable for some applications particularly in health care products, nutrition, pharmacology and cosmetic additive process.

Acknowledgements

The authors would like to express their profound gratitude to the Department of Higher Education (Lower Myanmar), Ministry of Education, Yangon, Myanmar, for provision of opportunity to do this research and Myanmar Academy of Arts and Science for allowing to present this paper.

References

Anand, V. K. and Heberlein, G. T. (1977). "Crown Gall Tumor Genesis in Potato Tumor Tissue". *Am J Bot*, vol. 64(2), pp. 153-158

Choi, Y. J., Kim, E. J. Piao, Z. Yun, Y. C. and Shin, Y. C. (2004). "Purification and Characterization of Chitosanase from *Bacillus sp*. Strain KCTC0377BP and Its Application for the Production of Chitosan Oligosaccharides". *Applied and Environmental Microbiology,* vol. 70 (8), pp. 4522-4531

Gallaher, C. M., Munion, J. Hesslink, R. J. Wise, J. and Gallaher, D. D. (2000). "Cholesterol Reduction by Glucomannan and Chitosan is Mediated by Changes in Cholesterol Absorption and Bile Acid and Fat Excretion in Rats". *J. Nutr*., vol. 130, pp. 2753-2759

Galsky, A. B., Wilsey, J. P. and Powell, R. G. (1980). "Crown Gall Tumor Disc Bioassay: A Possible Aid in the Detection of Compound with Antitumor Activity". *Plant Physiol*, vol. 65(2), pp. 184-185

Han, L. K., Kimura, Y. and Okuda, H. (1999). "Reduction in Fat Storage during Chitin-Chitosan Treatment in Mice Fed A High Fat Diet". *Int J Obes Relat Metab Disord,* vol. 23, pp. 174-179

Hirano, S. (1996). "Chitin biotechnology application". *Biotechnol. Annu*. Rev, vol.2,pp.237-258

Hnin Wuit Yee, Nyan Tun and Daw Hla Ngwe. (2016). "Isolation of Bacterial Strain (*Bacillus thermoleovorans*) from Soil and Bioconversion of Chitin to Chitosan". *Jour. Myan. Acad. Arts & Sc.,* vol. XV, No. 1, press

Hussian, A., Zia, M. and Mirza, B. (2007). "Cytotoxic and Antitumor Potential of *Fagonia certica* L.". *Turkish J. Bial.,* vol. 31, pp. 19-24

Kim, K. W. and Thomas, R. L. (2000). "Antioxidative Activity of Chitosans with Varying Molecular Weights". *Food Chemistry*, vol. 101 (1), pp. 308-313

Litchfield, J. T. and Wilcoxon, F. (1949). "A Simplified Method of Evaluating Dose Effect Experiments". *Journal of Pharmacology Experimental Therapy,* vol. 96, pp. 99-113

No, H. K., Park, N. Y. Lee, S. H. and Meyers, S. P. (2002). "Antibacterial Activity of Chitosans and Chitosan Oligomers with Different Molecular Weights". *International Journal of Food Microbiology*, vol. 74, pp. 65-72

Onsosyen, E. and Skaugrud, O. (1990). "Metal Recovery using Chitosan". *Journal of Chemical Technolgy and Biotechnology*, vol. 49 (4), pp. 395-404

Sikarwar, M. S. and Patil, M. B. (2012). "Antihyperlipidemic Activity of *Salacia Chinensis* Root Extracts in Triton-induced and Atherogen Diet-induced Hyperlipidemic Rats". *Indian Pharmacol*, vol. 44 (1), pp. 88-92

Srirama, R., Ramesha, B. T. Ravikanth, G. Shaanker, R. U. and Ganeshaiah, K. N. (2008). "Are Plants with Anti-Cancer Activity Resistant to Crown Gall? A Test of Hypothesis". *Current Science*, vol. 95 (10), pp. 117-119

Takemono, K., Sunamoto, J. and Akasi, M. (1989). "Polymers and Medical Care". *Applied and Environmental Microbiology*, vol. 44 (6), pp. 1466-1470

Xie, W., Xu, P. and Liu, Q. (2001). "Antioxidant Activity of Water Soluble Chitosan Derivatives". *Bioorganic and Medicinal Chemistry Letters*, vol. 11(13), pp. 1699-1701

INVESTIGATION OF PHYTOCONSTITUENTS AND SOME BIOACTIVITIES OF LEAVES AND BARKS OF *Aquilaria agallocha* ROXB. (THIT-MHWAE)

May Myint Thu[1],Khin Hnin Mon[2], Hnin Hnin Aye[3], Daw Hla Ngwe[4]

Abstract

The research deals with phytochemical and medico-chemical investigation of *Aquilaria agallocha* Roxb. (Thit-mhwae) (*A. agallocha*) leaves and barks. The samples were collected from Katawe village, Thayatchaung Township, Tanintharyi Region. Antimicrobial activity of three different extracts (PE, EtOAc, EtOH) of *A. Agallocha* leaves and barks were determined by agar well diffusion method. Test microorganisms were *B. subtilis, S. aureus, P. aeruginosa, B. pumilus, C. Albicans* and *E. coli.* EtOAc extracts of leaves and barks of *A. Agallocha* showed the higher antimicrobial activity than other extracts. The cytotoxicity of Thit-mhwae leaves and barks of EtOH and water extract were tested by brine shrimp cytotoxicity bioassay. According to results, the ethanol extract of leaves showed strong cytotoxic effect at LD_{50} = 23.56 μg/mL whereas other extracts (ethanol bark, watery leaves and bark) showed cytotoxic to brine shrimp at LD_{50} = 33.34, 58.50, 60.70 μg/mL respectively. Therefore, the EtOH extract of leaves was the most potent than other extracts because of the lowest LD_{50} value and strong cytotoxic. But all of these samples were lower activity than standards $K_2Cr_2O_7$ (LD_{50} = 4.38 μg/mL) and greater activity than caffeine (LD_{50} = 1000 μg/mL) in cytotoxicity.

Keywords : *Aquilaria agallocha* Roxb., cytotoxicity, EtOAc extracts, EtOH extract

Introduction

During the past decade, traditional system of medicine has become a topic of global interest (WHO, 1998). It is estimated that 80 % of world's population utilize traditional medicines for the treatment of diseases. Herbal

[1]Assistant Lecturer, Dr, Department of Chemistry, Dawei University
[2]Associate Professor, Dr, Department of Chemistry, Panglong University
[3]Professor, Dr, Department of Chemistry, University of Yangon
[4] Professor and Head, Dr, Department of Chemistry, University of Yangon

medicine based on the use of roots, leaves, barks, seeds and flowers of the plants. Depending on the localities or geographic regions with different temperatures, climates, rainfall, altitude and radiations characteristics, the herbal plants may have different chemical composition and different efficacy of biological activities.

Myanmar is rich in varieties of medicinal as well as aromatic plants due to presence of different climate zone in the country. In Myanmar, most of the people depend on traditional medicinal plants and herbal medicines rather than modern medicines for the treatment of various disorders. The study of traditional medicinal plants and their therapeutics play a very important role in health care system of Myanmar because 80% of its population is in the rural area and have been using traditional medicine for centuries.

In this paper Agar wood (Figure 1), a plant drug of controversial identity is taken for investigation. A wood known as Eagle wood (Trade name), Agaru (Hindi), Agil, Akil (Tamil) is credited with several pharmacological properties as per the literature claims; it is also a highly priced incense wood of much popular antiquity.

This plant have been rich sources of medicine because they produce a host of bioactive molecules, most of which probably evolved as chemical defenses against infection. Bioassays are adaptable for screening and testing plant extracts. The aim of the present work is to investigate the isolation of bioactive compounds from leaves and bark of agar wood and also studied some biological activities such as antimicrobial activity, antioxidant activity, cytotoxicity and antitumour activity. Farther work on isolation and characterization of bioactive compound will be published in the future.

Selected Myanmar Medicinal Plant*Aquilaria agallocha* Roxb.
Botanical aspect

Botanical Name	-	*Aquilaria agallocha*
Family	-	Thymelaeaceae
Genus	-	*Aquilaria*
Species	-	*agallocha*
Myanmar Name	-	Thit-mhwae
Common Name	-	Agar wood, eagle wood, Gaharu
Plant Part Used	-	Leaves and barks

(a) Plant

(b) Leaves

(c) Flowers

(d) Fruits

Figure 1. Photographs of *Aquilaria agallocha*. (Thit- mhwae)

Materials And Methods

Collection and Preparation of Samples

The selected medicinal plant used in this study was *Aquilaria agallocha* Roxb. (Thit- Mhwae, TM). The leaves and bark of Thit-mhwae were collected from Katawe village, Thayetchaung Township, Tanintharyi Region on February to May 2013. After collection, the scientific name of *Aquilaria agallocha* was identified by Botanist at Department of Botany, Dawei University. The collected fresh samples were washed with water and dried in an oven at 50 °C. The air dried samples were cut into small pieces and made powder by using grinding machine. And then, the leaves and barks powdered samples were separately stored in the air-tight container to prevent moisture and other contamination. The dried powdered samples were tested for biological activities and isolation of organic compounds.

Screening of Antimicrobial Activity of Leaves and Barks of *Aquilaria agallocha Roxb.*(Thit-mhwae) by Agar Well Diffusion Method

The screening of antimicrobial activity of various crude extracts such as PE, EtOAc and 70 % EtOH extracts of leave and bark of *Aquilaria agallocha* Roxb. (Thit-mhwae) was carried out by agar well diffusion method at Fermentation Laboratory, Pharmaceutial Research Department, Ministry of Industry, Yangon, Myanmar. Six microorganisms namely *Bacillus subtilis*(JAP-022/215), *Staphylococcus aureus* (ATCC-12277*), Pseudomonas aeruginosa* (IFO-3080), *Bacillus pumilus* (IFO-12102), *Candida albicans* (IFO- 1060) and *Escherichia coli* (ACCT-25922) were used for this test.

Meat extract (0.5 g), peptone (0.5 g) and sodium chloride (0.25 g) were mixed with distilled water and the solution made up to 100 mL with distilled water. The pH of this solution was adjusted at 7.2 with 0.1 M sodium hydroxide solution and 1.5 g of agar was then added. The nutrient agar medium was put into sterilized conical flask and plugged with cotton wool and then autoclaved at 121 ºC for 15 min. After cooled down to 40 ºC, one drop of

suspended strain was inoculated to the nutrient agar medium near the burner. About 20 mL of medium was poured into the sterilized Petri dish and left for 10-15 min in order to set the agar. After that the agar wells were made with a 10 mm sterilized cork borer and the wells filled with 0.1 mL of extracts to be tested. Then, the plates were incubated at 27 ºC for 24 h. After incubation, the diameters of inhibition zones including 10 mm wells were measured.

Screening of Anti-Tumor Activity

Anti-tumor activity of ethanol and ethyl acetate extracts and some isolated compounds was examined by Potato disc Assay (PDA) method (Ferrigni *et al.,* 1982) at Fermentation Laboratory, Pharmaceutical Research Department, Ministry of Industry, Yangon, Myanmar.

Potato Crown Gall Test or Potato Assay

Fresh, disease-free potatoes were purchased from a local market. Tubers of moderate size were surface sterilized by immersion in 0.1 % sodium hypochlorite for 20 min. Ends were removed and the potatoes were soaked an additional10 min. A core of the tissue was extracted from each end and discarded. The remainder of the cylinder was cut into 0.5 cm thick discs with a surface sterilized scalpel. The discs were then transferred to agar plates (1.5 g of agar dissolved in 100 mL DDW, autoclaved for 20 min at 121 ˚C , 20 mL poured into each Petridish). Each plate contained four potato discs and 4 plates were used for each sample dilution.

Samples (2.0, 0.1 and 0.5 mg) were respectively dissolved in DMSO (2 mL) and filtered through Millipore filters (0.22 μm) into sterile tube. This solution (0.5 mL) was added to sterile DW (1.5 mL), and broth culture of *A. tumefaciens* in PBS (2 mL) was added. Controls were made in this way; DMSO (0.5 mL) and sterile DW (1.5 mL) were added to the tube containing 2 mL of broth culture of *A. tumefaciens*. Using a sterile disposable pipette, 1 drops (0.05 mL) from these tubes was used to inoculate each potato disc, spreading it over the disc surface. After inoculation, Petri dishes were sealed

by par film and incubated at 27-30 ˚C for3 weeks. Tumors were observed on potato discs after 21 days under stereo-microscope followed by staining with Lugol's iodine (10 % KI and 5 % I_2) after 30 min and compared with control. The antitumor activity was examined by observation of tumor produced or not.

Screening of Antioxidant Activity of Crude Extracts and Isolated Compound from *Aquilaria agallocha* Roxb. (Thit-mhwae) Leaves and Barks

DPPH (2, 2-diphenyl-1-picry-hydrazyl) radical scavenging assay was chosen the antioxidant activity of plant materials. This assay has been widely used to evaluate the free radical scavenging effectiveness of various flavonoids and polyphenols in food system.

The effect on DPPH radical was determined using the method by Marinova and Batchvarov (2011). The control solution was prepared by mixing 1.5 mL of 60 M DPPH solution and 1.5 mL of EtOH using shaker. The test sample solution was also prepared by mixing thoroughly 1.5 mL of 60 μM DPPH solution and 1.5 mL of each sample solution. The mixture solutions were allowed to stand at room temperature for 30 min. Then, the absorbance of these solutions was measured at 517 nm by using UV-7504 spectrophotometer. Absorbance measurements were done in triplicate for each concentration and then mean values so obtained were used to calculate percent inhibition of oxidation and the capability to scavenge the DPPH radical was calculated using the following equation:

$$\% \text{ oxidative inhibition} = \frac{A_{Control} - (A_{Sample} - A_{Blank})}{A_{Control}} \times 100\ \%$$

where, $A_{Control}$ = absorbance of control solution

A_{Sample} = absorbance of sample solution

A_{Blank} = absorbance of the blank (EtOH solution)

Investigation of Cytotoxicity by Brine Shrimp Bioassay

Cytotoxicity of leaves and barks of *Aquilaria agallocha Roxb.*(Thit-mhwae) were investigated by brine shrimp bioassay according to the procedure described by Dockery and Tomkins (2000).Test solution (1 mL) was mixed with 9 mL of artificial sea water and placed in the chamber of ice cup. Alive brine shrimp (10 napulli) was taken with Pasteur pipette and placed into each chamber which was kept at room temperature for about 24 h. After 24 h incubation, the number of survival brine shrimp was counted and 50 % lethality dose (LD_{50}) was calculated (Dockery and Tomkins, 2000). The control solution was prepared as the above procedure by using distilled water instead of sample solution.

Results And Discussion

Antimicrobial Activity of Crude Extracts by Agar Well Diffusion Method

Screening of antimicrobial activity of various crude extracts such as PE, EtOAc and 70 % EtOH extracts of TM leaves and barks were done by employing agar well diffusion method (Table 1 and 2). In this study, the samples were tested on six pathogenic microorganisms such as *Bacillus subtilis, Staphylococus aureus, Pseudomonas aeruginosa, Bacillus pumilus, Candida albicans* and *Escherichia coli* .

From these results, it was found that PE extract of TM leaves and barks did not exhibit any antimicrobial activity against all tested microorganisms whereas EtOAc and EtOH extracts from TM leave and bark exhibited inhibition zone diameters ranged between in 12 mm ~ 50 mm respectively against all tested microorganisms. The TM leaves and barks of EtOH extract showed less activity and EtOAc extract was observed to be most effective in antimicrobial activity.

Therefore all the crude extracts of two samples, except PE extract of TM exhibited antimicrobial activity against all microorganisms tested. Among the crude extract, EtOAc extract of two samples showed the most pronounced antimicrobial activity against all microorganisms tested. Thus, TM leaves and barks, might be effective in the formulation of medicine for the treatment of

diseases infected by the microorganisms, such as diarrhea, skin disease, aphrodisiac and vomiting.

Table 1. Inhibition Zone Diameters of Crude Extracts of *Aquilaria agallocha* Roxb. (Thit-mhwae) Leaves against Test Microorganisms

Sample	**Extracts**	**Inhibition zone diameters (mm) of various crude extracts against different microorganisms**					
		B.subtilis	***S.aureus***	***P.aeruginosa***	***B.pumilus***	***C.albicans***	***E.coli***
Leave	Pet-ether	-	-	-	-	-	-
	EtOAc	29 (+++)	42 (+++)	32 (+++)	45 (+++)	33 (+++)	34 (+++)
	EtOH	12 (+)	12 (+)	14 (+)	13 (+)	12 (+)	-

Agar well-10mm

10 mm ~ 14 mm (+)

15 mm ~ 19 mm (++)

20 mm above (+++)

Table 2. Inhibition Zone Diameters of Crude Extracts of *Aquilaria agallocha* Roxb. (Thit-mhwae) Bark against Test Microorganisms

Sample	Extracts	Inhibition zone diameters (mm) of various crude extracts against different microorganisms					
		B.subtilis	***S.aureus***	***P.aeruginosa***	***B.pumilus***	***C.albicans***	***E.coli***
Bark	Pet-ether	-	-	-	-	-	-
	EtOAc	32 (+++)	49 (+++)	30 (+++)	40 (+++)	35 (+++)	42 (+++)
	EtOH	16 (+)	12 (+)	15 (+)	16 (+)	12 (+)	12 (+)

Agar well-10 mm

10 mm ~ 14 mm (+)

15 mm ~ 19 mm (+) (+)

20 mm above (+++)

Antitumor Activity of *Aquilaria agallocha* Roxb. (Thit-mhwae) Leaves, Bark and isolated compounds

Screening of antitumor activity of crude extracts such as ethanol and watery extracts from *Aquilacia agallocha Roxb.*was done by agar well diffusion method (Ghanney and Rhouma, 2015). In this investigation, the extracts and some isolated compounds were tested against *Agrobacterium tumefaciens* (Table 3).

According to the result, the ethanol extracts of TM bark do not show strong antitumor activity against *A. tumefaciens* at the (concentration of 0.1 - 0.3 g/mL). But, watery extracts of TM leave showed strong antitumor activity against *A. tumefaciens* at the (concentration 0.1 - 0.3 g/mL).The watery extract of leave exhibited the antitumor activity significantly at a concentration at (0.1 - 0.3) g/mL. So, the MIC value is 0.1 g/mL.

Table 3. Tumor Inhibition of the Crude Extracts and Isolated Compounds of *Aquilaria agallocha* Roxb. (Thit-mhwae)

Test Sample		**Concentration (g** /mL**)**	**Tumor**
	Control	++	-
***Aquilaria agallocha* Leave**	EtOH extract	0.1	-
		0.2	-
		0.3	-
***Aquilaria agallocha* Bark**	EtOH extract	0.1	+
		0.2	+
		0.3	+
***Aquilaria agallocha* Leave**	H_2O extract	0.1	-
		0.2	-
		0.3	-
***Aquilaria agallocha* Bark**	H_2O extract	0.1	+
		0.2	+
		0.3	+

(+) = tumor appeared
(-) = no tumor appeared
ND = not detected

Antioxidant Activity of Crude Extracts and Isolated Compound of Thit-mhwae

The antioxidant activity of 70 % EtOH and water extracts of two samples, one isolated compound (*p*-hydroxy benzoic acid) and standard vitamin C was studied by DPPH (2, 2 - diphenyl - 1 - picryl - hydrazyl) free radical scavenging assay method. This method is the most widely reported method for screening of antioxidant activity on many plant drugs. It is based on the reduction of color of free radical DPPH in ethanolic solution by different concentrations (6.25, 12.5, 25, 50, 100, 200 μg/mL) of each crude extract, one isolated compound and standard vitamin C in ethanol solvent were used. The absorbance of each solution (control, sample) was measured at λ_{max}517 nm using UV-visible spectrophotometer.

It was found that as the concentrations increased, the absorbance values decreased. The radical scavenging activity of crude extracts were expressed in terms of % inhibition and IC_{50} (50 % inhibition concentration) values and calculated by linear regressive excel program. The results were summarized in Table 4. In the antioxidant activity screening, IC_{50} values of 16.53 μg/mL for H_2O extract and 144.7 μg/mL for EtOH extract in leaves and 90.76 μg/mL for H_2O extract and 57.86 μg/mL for EtOH extract in bark samples were found isolated parahydroxy benzoic acid showed antioxidant activity at (IC_{50} = 59.77 μg/mL). Among the tested crude extracts and isolated compound, watery extract of TM leaves and p-hydroxy benzoic acid compound were found to be more effective than that of ethanol crude extract of leaves and H_2O barks of in free radical scavenging activity. According to this observation water extract of leaves (16.53 μg/mL) was higher activity than others but lower than standard vitamin C (IC_{50} = 7.99 μg/mL).

Table 4. % Free Radical Scavenging Activity of Crude Extracts and Isolated Compounds from *Aquilaria agallocha* Roxb. (Thit-mhwae) Leaves and Bark

Sample	% Inhibition (mean ± SD) in different concentrations (μg/mL)						
	6.25	**12.5**	**25**	**50**	**100**	**200**	**IC_{50} (μg/mL)**
Thit-mhwae leave (H_2O)	13.51 ± 1.96	44.97 ± 1.96	60.57 ± 0.75	71.47 ± 0.74	73.07 ± 1.20	76.81 ± 0.45	16.53
Thit-mhwae bark (H_2O)	10.96 ± 1.09	22.61 ± 1.56	26.57 ± 1.86	35.69 ± 1.01	53.33 ± 0.24	60.78 ± 1.15	90.76
Thit-mhwae leave (EtOH)	10.21 ± 1.49	11.10 ± 1.48	11.84 ± 1.72	22.54 ± 1.60	37.66 ± 1.49	65.27 ± 1.73	144.7
Thit-mhwae bark (EtOH)	18.04 ± 1.73	19.05 ± 1.50	32.16 ± 1.50	48.35 ± 1.20	58.11 ± 1.01	73.96 ± 1.49	57.86

Cytotoxicity of Ethanol and Water Crude Extracts of *Aquilaria agallocha* Roxb. (Thit-mhwae)

The cytoxicity of *Aquilaria agallocha Roxb.* leave and bark were investigated by brine shrimp cytoxicity bioassay (Dockery and Tomkins, 2000). The tested organisms used were brine shrimp (*Artemia salina*). The cytotoxic effect was expressed at LD_{50} values (50 % lethality dose). The cytotoxicity of ethanol and water crude extracts of leave and bark evaluated in this study are reported in Table 5 . All of four tested extracts were found to possess cytotoxic in the brine shrimp bioassay. As shown in Table 5, the most cytotoxic extract was found to be the ethanol leave extract (LD_{50} = 23.56 μg/mL) whereas other extracts (ethanol barks, watery leaves and barks) were 33.34, 58.50 and 60.70 μg/mL respectively.

These result suggested that the EtOH extract of leave is the most potent, and the other extracts were less cytotoxic to brine shrimp. All of these samples are lower than standards $K_2Cr_2O_7$ (LD_{50} 4.38 μg/mL) and greater than caffeine (LD_{50} 1000 μg/mL) in cytotoxicity.

Table 5. Cytotoxicity of Different Doses of Watery and Ethanol Crude Extracts of *Aquilaria agallocha* Roxb. (Thit-mhwae)

Tested	Sample	Numbers of Death Brine Shrimp (Mean± SEM) in Various Concentration (µg/mL)				
		1	**10**	**100**	**1000**	**LD_{50} (µg/mL)**
1	Watery Extract(L)	1.33 ± 0.58	4.33 ± 0.58	5.67 ± 0.58	8.00 ± 1.00	58.50
2	EtOH Extract(L)	1.67 ± 0.58	4.67 ± 0.58	7.00 ± 0.00	7.67 ± 0.58	**23.56**
3	Watery Extract(B)	1.00 ± 0.00	3.33 ± 0.58	6.33 ± 0.58	7.33 ± 0.58	60.70
4	EtOH Extract(B)	3.33 ± 0.58	4.33 ± 0.58	7.00 ± 1.00	8.33 ± 0.58	33.34
5	$K_2Cr_2O_7$	4.00 ± 1.00	6.67 ± 0.58	8.33 ± 0.58	9.33 ± 0.58	4.38
6	Caffeine	0	2.33 ± 1.20	3.00 ± 0.58	5.00 ± 1.16	1000

Conclusion

Investigation of Myanmar indigenous plant, leaves and barks of *Aquilaria agallocha* Roxb. used to be ingredient for traditional medicine was systematically carried out. Antimicrobial activity of three different extracts (PE, EtOAc, EtOH) of *Aquilaria agallocha* Roxb. leaves and barks were determined by agar well diffusion method. Test microorganisms were *B. subtilis, S. aureus, P. aeruginosa, B. pumilus, C. albicans* and *E. coli.* EtOAc extracts of leaves and barks of *Aquilaria agallocha* Roxb. showed the higher

antimicrobial activity than other extracts. Antitumor activity investigated by potato crown gall (PCG) assay revealed that EtOH and H_2O extracts and isolated compounds hydroquinone (benzene 1,4-diol) and *p*-hydroxy benzoic acid inhibited tumor growth in a concentration dependent manner. Significant tumor inhibition was observed at 0.1 g/mL of the leaves EtOH extracts and 0.01 g/mL bark H_2O for the isolated compounds. The antioxidant activity screening of EtOH and water extracts and isolated compounds were determined by using DPPH assay. According to this observation water extract of leave (16.53 µg/mL) was higher activity than others but lower than standard vitamin C (IC_{50} = 7.99 µg/mL).The cytotoxicity of *Aquilaria agallocha* Roxb. leaves and barks of EtOH and water extract were tested by brine shrimp cytotoxicity bioassay. From the results, the leave EtOH extract was the most potent in other extracts because it possessed the lowest LD_{50} value in cytotoxic to brine shrimp. ID_{50} values of these samples were lower than standards $K_2Cr_2O_7$ (LD_{50} = 4.38 µg/mL) and caffeine (LD_{50} = 1000 µg/mL) in cytotoxicity.

Acknowledgements

The authors would like to express their profound gratitude to the Department of Higher Education (Yangon Office), Ministry of Education, Yangon, Myanmar, for provision of opportunity to do this research and Myanmar Academy of Arts and Science for allowing to present this paper.

References

Dockery, M. and Tomkins,S. (2000). *Brine Shrimp Ecology*. London : 1st Ed., The British Ecology Society, pp. 92-93

Ferrigni, N.R, Putnan, J.E., Anderson, B., Jacobsen, L.B., Nichols, D.E., Moore, D.S. and Mellaughlin, J.L. (1982).“Modification and Evaluation of the Potato Disc Assay and Antitumor Screening of Euphorbiaceae Seeds”. *J. Nat. Prod.,*vol. 45 (6), pp. 679-686

Marinova, G. and Batchvarov, V. (2011).“Evaluation of the Methods for Determination of the Free Radical Scavenging Activity by DPPH”. *Bulgarian Journal of Agricultural Science*, vol. 17,pp.11-24

WHO.(1998). *Determination of Extractable Matter.* In: *Quality Control Method for Medicinal Plant Materials.* Geneva, p. 35

Ghanney, N. and Rhouma, A.(2015). "*Schinus terebinthifolius* Raddi (Anacardiaceae) Leaf Extracts:

Antibacterial Activity against Two *Agrobacterium tumefaciens* Strains." *J. Crop Prot.* vol. 4 (1), pp.85-96

INVESTIGATION ON ANTIDIARRHOEAL ACTIVITY OF SOME PHYTOCONSTITUENTS OF *Gardenia coronaria* BUCH-HAM. (YIN-GAT-GYI)

Mi Cho[1], Tet Tun[2], Hnin Hnin Aye[3], Daw Hla Ngwe[4]

Abstract

The present work concerns with the investigation of some bioactive constituents and anti-diarrhoeal activity of flower and bark of *Gardenia coronaria* Buch-Ham. (Yin-gat-gyi). The preliminary phytochemical investigation reveals the presence of α–amino acids, carbohydrates, flavonoids, glycosides, organic acids, phenolic compounds, reducing sugars, saponins, steroids and terpenoids in flower while observing alkaloids, carbohydrates, glycosides, organic acids, phenolic compounds, saponins, starch, steroids, tannins and terpenoids in barks. Three organic constituents: benzoic acid (compound I) (0.004%, colourless needle shape), kaempferol (compound II) (0.002%, yellow amorphous form, m.pt = 275-280°C) from EtOAc crude extracts of flower and stigmasterol (compound III) (0.0003%, colourless crystals, m.pt = 167-170°C) from EtOAc crude extract of bark of YGG have been isolated by using thin layer chromatography and column chromatographic separation methods. *In vivo* antidiarrhoeal activity of compound I, compound II, 95 % ethanol and aqueous extracts of YGG were carried out by using castor oil–induced mice models. The mean frequency of defecation in four hours was found to be significantly decreased by both extracts, compound I, compound II and standard drug loperamide compared with that of control in castor oil – induced diarrhoeal in mice ($p<0.005$-$p<0.001$). The percent inhibitions of defecation within four hours for 95 % ethanol extract (1g/kg bw), aqueous extract (4g/kg bw), compound I (5mg/kg bw), compound II (6mg/kg bw) and standard drug loperamide (6mg/kg bw) were 74.41 %, 69.61 %, 57.61 %, 84.78 % and 69.61 %, respectively. It was found that the percent inhibitions of defecation for 95 % ethanol extract (1g/kg bw) and compound II (6mg/kg bw) were higher than that of the standard drug loperamide. Aqueous extract (4g/kg bw), 95 % ethanol extract (1g/kg), compound I and compound II were found to be significantly reduced both volumes and weights of the intestinal fluids secretion, comparable to the

[1] Assistant Lecturer, Dr, Department of Chemistry, Mawlamyine University
[2] Associate Professor, Dr, Department of Chemistry, Hpa-an University
[3] Professor, Dr, Department of Chemistry, University of Yangon
[4] Professor and Head, Dr, Department of Chemistry, University of Yangon

effect of the standard drug loperamide in castor oil induced enteropooling test ($p < 0.05 – p < 0.001$). In the investigation of the intestinal transit test, the percent inhibition of all aqueous extracts and 95 % ethanol extracts (1 g/kg bw and 0.5 g/kg bw), compound I (5 mg/kg bw) and compound II (6 mg/kg bw) on intestinal transits were higher than that of standard drug loperamide ($p < 0.001$). From these results, the anti-diarrhoeal index in percents for aqueous extracts (4g/kg bw, 2g/kg bw, 1g/kg bw), 95% ethanol extract (1g/kg bw), compound I (5mg/kg bw), compound II (6mg/kg bw) and standard drug loperamide (6mg/kg bw) were found to be 175.82 %, 168.01 %, 115.44 %, 238.53 %, 146.17 % and 285.99 % and 104.3 % respectively. It indicated that both extracts, compound I and compound II were more effective than standard drug loperamide in antidiarrhoeal activity since the higher the anti-diarrhoeal index (%), the more potent in antidiarrhoeal activity. It may be inferred that aqueous and ethanolic extracts of flower of YGG and isolated kaempferol may be used in the formulation of antidiarrhoeal medicine.

Keywords : *Gardenia coronaria* Buch-Ham., Yin-gat-gyi, anti-diarrhoeal activity

Introduction

Diarrhoea is one of the most popular disease in all over the world and it caused several millions of deaths in the world annually. In developing countries, they are the most common causes of morbidity and mortality. Some medicinal plants possess the property to cure diarrhoeal disease. The present work deals with the evaluation of anti-diarrhoeal activity of the selected medicinal plant.

Gardenia coronaria Buch-Ham., (Rubiaceae family) locally known as Yin-gat-gyi in Myanmar is a small to medium-sized but tall, deciduous tree, 7.6-9 m high. Leaves are subsessile, 15-30 cm long, obovate, shortly acuminate, shining on both surfaces. Flower are large, subsessile, terminal, white, changing to yellow, fragrant. Fruit is 2.5 cm long, ellipsoid, 5-ribbed (Uddin, 2013). Flowering period is January to April and fruiting period is February to August (Kyaw Soe and Tin Myo Ngwe, 2004). It is naturalized or cultivated throughout Myanmar for its fragrant flower (Silva and Gol, 1997).

It is used for haemoptysis, haematemesis and melena, diarrhoeal diseases, skin disorders, as antiseptic and oedema (Medicinal Plants of

Myanmar, 2010). Flower is used for pyrexia due to either biliary or chest infections or blood dyscrasia and diseases related to microorganisms. Fruit is used for cough; mucolytic (Kyaw Soe and Tin Myo Ngwe, 2004).

Materials And Methods

Sample collection

The flower and bark of *Gardenia coronaria* Buch-Ham. (Yin-gat-gyi, YGG) were collected from Chaungzone Township, Mon State. After washing with water, the collected samples were dried at room temperature. The dried samples were cut into small pieces and ground into powder by a grinding machine. These powdered samples were stored separately in air-tight containers.

Preparation of various crude extracts from YGG

The various crude extracts (PE, 95%EtOH, EtOAc and H_2O) were prepared by successive soxhlet extraction method. The extracts were concentrated by vacuum rotatory evaporator under reduced pressure to yield PE, 95% EtOH, EtOAc and H_2O extracts. The crude extracts were used to test antimicrobial and antidiarrhoeal activities and to isolate some bioactive organic constituents.

Isolation and characterization of phytochemical constituents

The EtOAc extract (5 g) of flower of YGG was separated by silica gel column chromatography with PE:EtOAc gradient elutions (9:1 to EtOAc only) to give two compounds: (I, 0.004 %, colourless needle shape and II, 0.002 %, yellow amorphous form). From the separation of EtOAc extract (5 g) of bark of YGG, one steroid compound: (III, 0.0003%, white powder form) was isolated with PE:EtOAc solvent systems (9:1 to 1:1). Then the isolated compounds were characterized by melting points, R_f values, solubilities and some chemical tests such as treating with 5% H_2SO_4, vanillin-H_2SO_4, anisaldehyde-H_2SO_4, Liebermann-Burchard reagent on TLC chromatogram followed by treating with 1% $FeCl_3$ solution.

Identification of some phytochemical constituents

The structures of isolated compounds were identified by modern spectroscopic techniques such as UV, FT IR, and ^{1}H NMR.

Screening of Antidiarrhoeal Activity

Materials

Ethanolic extract of flower of YGG, 90 albino mice of both sexes (body weight 20-30 g), mice cages, castor oil (MPF), loperamide HCl (Picco Pharma Co.Ltd), 0.9 % NaCl (normal saline, Euro-med laboratories PHIL., INC), 10 % charcoal powder, syringes and needles, intragastric dosing cannula (18 gauge) were used.

Method

Castor oil-induced diarrhea

According to the method of Awounters, 1978, mice were divided into ten groups of six animals each. Group 1 received saline (10 mL/kg bw orally) served as control group, group 2 received loperamide (6 mg/kg bw orally) served as standard group, served as group 3, 4 and 5 received aqueous extracts (4, 2, 1 g/kg bw, orally), groups 6, 7 and 8 received 95 % ethanol extracts (2, 1, 0.5 g/kg bw, orally), group 9 received compound I (5 mg/kg bw, orally) and group 10 received compound II (6 mg/kg bw, orally) respectively 1 h before castor oil administration. Diarrhoea was induced by administering 10 mL/kg body weight of castor oil orally. The onset of diarrhea, number of diarrhoeal droppings were counted hourly for 4 h, mean of the dropping passed by the treated groups were compared with that of the control group consisted of animals given an oral administration of saline (10 mL/kg bw).

Castor oil-induced enteropooling

Intraluminal fluid accumulation was determined by the method of Robert *et al*., 1976. Overnight fasted mice were divided into ten groups of six animals each. Group 1 received normal saline, orally (10 mL/kg bw), served as a control, group 2 received loperamide (6 mg/kg bw) and groups 3, 4 and 5 received aqueous extracts (4, 2, 1 g/kg bw, orally), groups 6, 7 and 8 received 95 % ethanol extracts (2, 1, 0.5 g/kg bw, orally), group 9 received compound I (5 mg/kg bw, orally) and group 10 received compound II (6 mg/kg bw, orally)

respectively, 1 h before the oral administration of castor oil. Thirty minutes after administration of castor oil, the mice were sacrificed and the small intestine was removed after tying both ends with thread, and weighed. The intestinal contents from each intestine were collected by milking into a beaker and their volume was measured. The intestine was reweighted and the difference between full and empty intestine was calculated as the weight of fecal matter.

Castor oil-induced small intestinal transit

According to the method of Mascolo *et al*., 1994, mice were fasted for 18 h, and divided into ten groups of six animals each. Group 1 received normal saline (10 mL/kg bw, orally), group 2 received loperamide (6 mg/kg bw, orally), groups 3, 4 and 5 received aqueous extracts (4, 2, 1 g/kg bw, orally), groups 6, 7 and 8 received 95 % ethanol extracts (2, 1, 0.5 g/kg bw, orally), group 9 received compound I (5 mg/kg bw, orally) and group 10 received compound II (6 mg/kg bw, orally) respectively, 1 hour before administration of castor oil. The maker (10 mg/kg body weight of 10 % charcoal suspension in 5% gum acacia) was administered orally 1 h after castor oil treatment. The mice was sacrificed 30 min after maker administration and the distance travelled by charcoal meal from the pylorus was measured and expressed as percentage of the total length of the intestine from the pylorus to caecum (i.e., % intestinal transit).

$$\% \text{ intestinal transit} = \frac{\text{Distance travelled by charcoal mea}}{\text{Total length of small intestine}}$$

***In vivo* antidiarrhoeal index of *Gardenia coronaria* Buch-Ham.**

The *in vivo* antidiarrhoeal index of YGG was expressed according to the following formula.

$$\text{ADI } in\ vivo = \sqrt{D_{freq} x\ G_{mag} x\ P_{freq}}$$

where, D_{freq} = delaying defecation time of diarrhoea onset, in percent of control

G_{mag} = gut meal travel distance reduction, in percent of control

P_{freq} = purging frequency as number of stool reduction, in percent of control (Aye Than *et al*., 1989)

Results and Discussion

Preparation of Crude Extracts

The various crude extracts by using successive solvent extraction method were prepared as PE (3.21 %), EtOH (25.07 %), EtOAc (10.08 %) and H_2O (11.89 %) in flower as well as PE (0.29 %), EtOH (11.13 %), EtOAc (3.48 %) and H_2O (4.68 %) in bark.

Identification of Isolated compounds

Compound I from flower of YGG

Benzoic acid (7.5 mg, 0.004 %), ^{1}H NMR (400 MHz, $CDCl_3$), δ = 8.12 (d, J = 7.2 Hz), 7.62 (t, J = 7.2 Hz), 7.48 (t, J = 7.6 Hz)

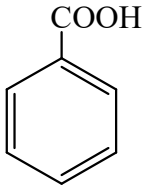

Compound II from flower of YGG

Kaempferol (4.6 mg, 0.002 %, 275-280°C), UV: (MeOH), λ_{max} = 269,322, 367 nm (MeOH/NaOMe), λ_{max} = 277,320,409 nm, (MeOH/$AlCl_3$), λ_{max} = 269,340,424 nm, (MeOH/$AlCl_3$/HCl), λ_{max} = 265,304,359,425 nm, (MeOH/NaOAc), λ_{max} = 269,305,370 nm, (MeOH/NaOAc/H_3BO_3), λ_{max} = 266,324,364 nm, FT IR : (KBr), ν_{max} = 3450 (broad) (ν_{OH}), 3017($\nu_{=CH}$), 1658 ($\nu_{C=O}$), 1612, 1507 ($\nu_{C=C}$), 1458 (δ_{CH}), 1381(δ_{OH}), 1255(ν_{C-O}), 1174 (ν_{C-O}), 885 cm^{-1}(δ_{CH}), ^{1}H NMR: (400MHz, $CDCl_3$), δ = δ_H 6.18 (1H, d, J = 2.0 Hz), δ_H 6.39 (1H, d, J = 2.0 Hz), δ_H 8.06 (1H, d, J = 8.9 Hz), δ_H 6.89 (1H, d, J = 8.9 Hz), δ_H 6.89 (1H, d, J = 8.9 Hz), δ_H 8.06 (1H, d, J = 8.9 Hz)

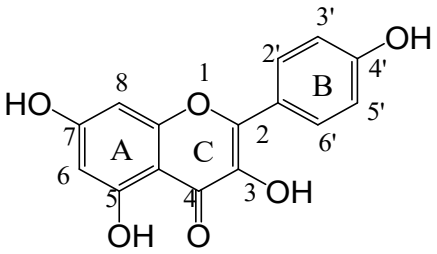

Compound III from bark of YGG

Stigmasterol (1.781 mg, 0.0003%, 167-170°C), FT IR: (KBr), ν_{max} = 3450-3050 (broad) (ν_{OH}), 2935 (ν_{CH}), 1650 ($\nu_{C=C}$), 1463 (δ_{CH}), 1377 (δ_{symCH}), 1049 (ν_{C-O}), 958 [δoop(=CH)], 839-800 cm^{-1}[δoop(=CH)]

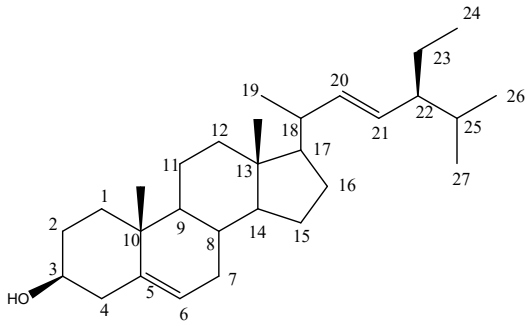

Antidiarrhoeal activity

Antidiarrhoeal activity of the isolated compounds, 95 % ethanol and watery extracts of flower of YGG were screened by using castor oil-induced mice models.

Castor oil-induced diarrhoea

In the investigation of castor oil-induced diarrhoea, it was found that the mean frequency of aqueous extract with 4 g/ kg bw dose (6.33 ± 0.80) is the lowest in all of the aqueous extracts (4 g/kg bw, 2 g/kg bw, 1 g/kg bw). The percent inhibition of defecation of aqueous extracts (1 g, 2 g, 4 g/kg bw) of YGG were 40.81 %, 46.37 %, 69.61 %, respectively (Table 1). When the dose is increased, the mean frequency of diarrhoea become reduced. These results showed reduction in dose dependent manner.

Similarly, it was found that the mean frequency of 95 % ethanol extract with 1 g/ kg bw dose (5.33 ± 0.85) is the lowest in all of the 95 % ethanol extracts (0.5 g/kg bw, 1 g/kg bw, 2 g/kg bw). The percent inhibition of defecation of aqueous extracts (0.5 g, 1 g, 2 g/kg bw) of YGG were 32.79 %, 74.41 %, 35.19 %, respectively (Table 1). Although there were more increase in dose, no reduction in frequencies of diarrhoea. These results showed reduction in dose independent manner. Therefore, it was deduced that the medium dose (1 g/kg bw) of 95 % ethanol extract was found to possess the best activity in all of the ethanol extracts.

The percent inhibitions of defecation of compound I (5 mg/kg bw) and compound II (6 mg/kg bw) of YGG were found to be 57.61 % and 84.78 %, respectively (Table 1). The mean frequency of defecation in 4 hour and percent inhibition are shown in Table 1 and Figure 1. Based on the results of all samples, it was also found that the mean frequency of diarrhoea increased with increase in time after drug adniaintration.

Table 1. Effect of Extracts and Isolated Compounds from Flower of YGG on Castor Oil-Induced Diarrhoea in Mice

Treatment	Mean defecation in 4 h	% Inhibition of defecation
Control	20.83 ± 1.51	
Loperamide 6 mg/kg	6.33± 2.59*	69.61
Aqueous extract 4 g/kg	6.33 ± 0.80	69.61
Aqueous extract 2 g/kg	11.17 ± 2.39*	46.37
Aqueous extract 1 g/kg	12.33 ± 1.31**	40.81
Ethanolic extract 2 g/kg	13.5 ± 0.76*	35.19
Ethanolic extract 1 g/kg	5.33 ± 0.84*	74.41
Ethanolic extract 0.5 g/kg	14.00 ± 0.58*	32.79
Compound I 5 mg/kg	8.83 ± 1.30	57.61
Compound II 6 mg/kg	3.17 ± 0.65*	84.78

*$P < 0.001$, **$P < 0.005$

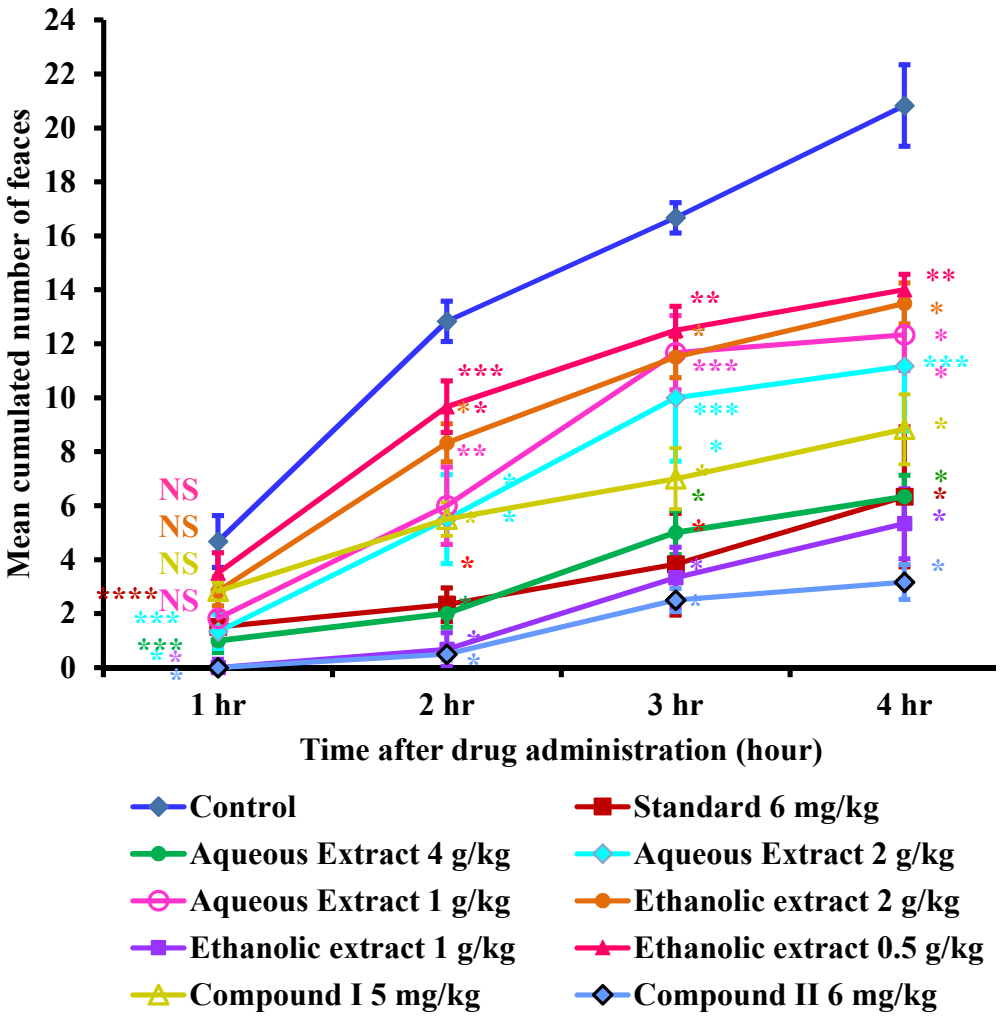

Figure 1. Comparative effects of aqueous extract of (4 g/kg bw, 2 g/kg bw, 1g/kg bw), 95 % ethanolic extract of (2 g/kg bw, 1g/kg bw, 0.5 g/kg bw), compound I, compound II of flower of YGG and standard drug loperamide on mice with castor oil-induced diarrhea at various time intervals $^{*}P<0.001$, $^{**}P<0.005$, $^{***}P<0.01$, $^{****}P<0.05$

Castor oil-induced enteropooling

In the study of castor oil-induced enteropooling, it was investigated that the mean weight (0.87 ± 0.11 g) and volume (0.37 ± 0.06 mL) of intestinal content in aqueous extract 4 g/kg bw treated group were reduced more than that of the remaining aqueous extracts (2 g/kg bw and 1 g/kg bw) (Table 2). There was dose dependent reduction in fecal weight and volume. It was found that the more increase in doses, the more reduction in the fecal weight and volume. So, the extract has negative relationship between dose and effect (Figures 2 and 3).

Similarly, it was investigated that the mean weight (0.79 ± 0.25g) and volume (0.40 ± 0.06 mL) of intestinal content in 95 % ethanol extract with 1 g/kg bw dose were reduced more than that of the remaining 95 % ethanol extracts (0.5 g/kg bw and 2 g/kg bw). There was dose independent reduction in fecal weight and volume. The more increase in doses, the less reduction in the fecal weight and volume (Figures 2 and 3).

The mean weight (g) and volume (mL) of intestinal content for compound I treated group were 0.87 ± 0.11 g ($p < 0.05$) and 0.32 ± 0.07 mL ($p< 0.01$) respectively and that of compound II treated group were 0.33 ± 0.06 g ($p < 0.001$) and 0.17 ± 0.04 mL ($p< 0.001$) respectively and the results were significantly when compared with the control group.

Comparative weight (g) and volume (mL) of intestinal content of the control, loperamide, compound I, compound II and different doses of aqueous and ethanol extracts of YGG on castor oil-induced enteropooling in mice are shown in Table 2 and Figures 2 and 3.

Table 2. Effect of Compound I, Compound II, 95% Ethanol and Watery Extract of flower of YGG on Castor Oil-induced Enteropooling in Individual Mice

Treatment	Weight of intestinal content (g)	Volume intestinal content (mL)
Control	1.43 ± 0.09	0.82 ± 0.07
Loperamide 6 mg/kg	0.39 ± 0.08*	0.18 ± 0.03*
Aqueous extract 4 g/kg	0.87 ± 0.11**	0.37 ± 0.06*
Aqueous extract 2 g/kg	1.06 ± 0.09***	0.53 ± 0.09***
Aqueous extract 1 g/kg	1.15 ± 0.09****	0.55 ± 0.05***
Ethanolic extract 2 g/kg	0.90 ± 0.10**	0.40 ± 0.07**
Ethanolic extract 1 g/kg	0.79 ± 0.25****	0.40 ± 0.06*
Ethanolic extract 0.5 g/kg	1.02 ± 0.07**	0.52 ± 0.06****
Compound I 5 mg/kg	0.87 ± 0.11****	0.32 ± 0.07***
Compound II 6 mg/kg	0.33 ± 0.06*	0.17 ± 0.04*

*P < 0.001, **P < 0.005, ***P < 0.01, ****P < 0.05

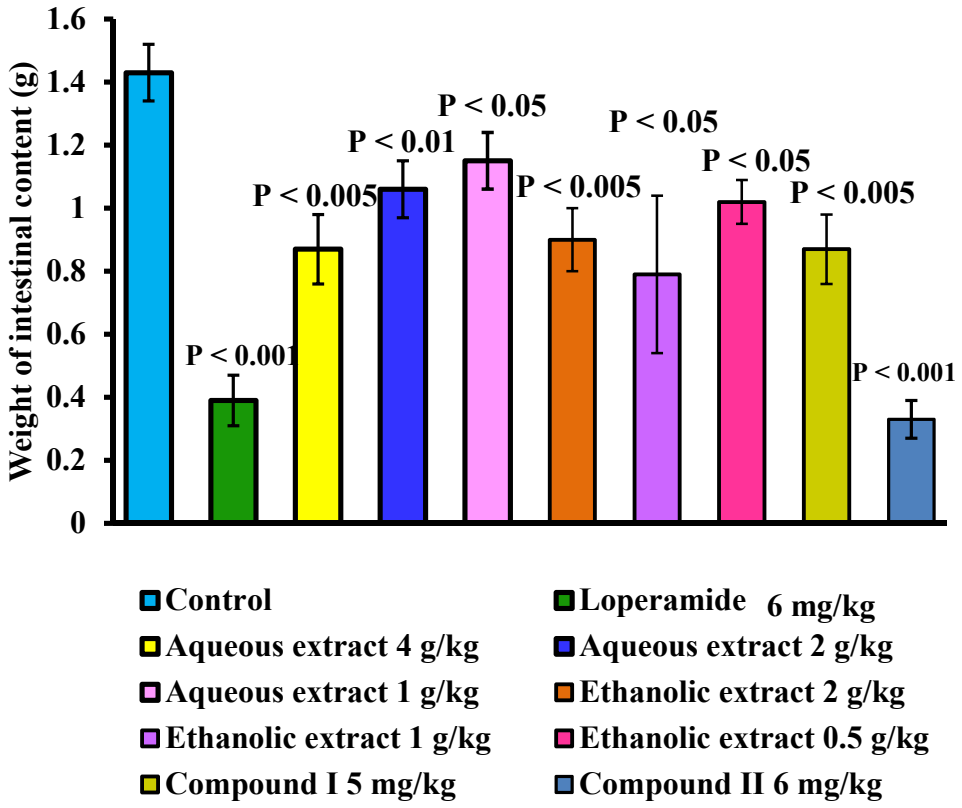

Figure 2. Comparative antidiarrhoeal effects (weight of intestinal content) of flower of YGG aqueous extract (4 g/kg bw, 2 g/kg bw, 1g/kg bw), 95 % ethanolic extract (2 g/kg bw, 1 g/kg bw, 0.5 g/kg bw), compound I (5 mg/kg bw), compound II (6 mg/kg bw) and standard drug loperamide (6 mg/kg bw) on castor oil-induced enteropooling in mice

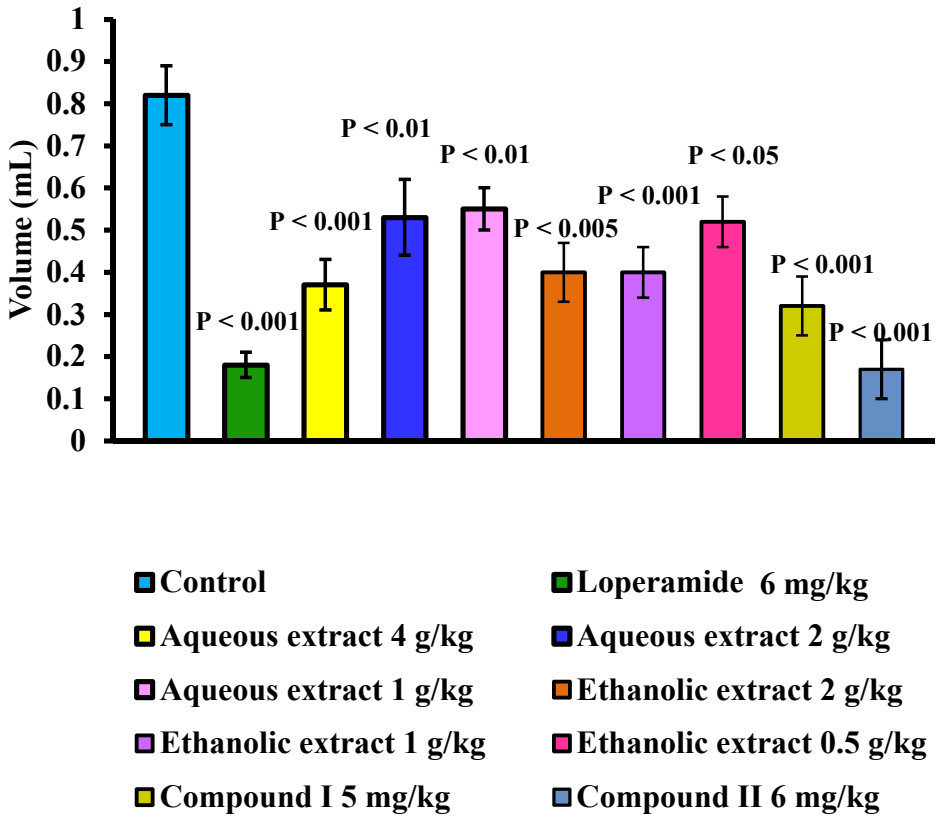

Figure 3. Comparative antidiarrhoeal effects (volume of intestinal content) of flower of YGG aqueous extract (4 g/kg bw, 2 g/kg bw, 1g/kg bw), 95 % ethanolic extract (2 g/kg bw, 1 g/kg bw, 0.5 g/kg bw), compound I (5 mg/ kg bw), compound II (6 mg/kg bw) and standard drug loperamide (6 mg/kg bw) on castor oil-induced enteropooling in mice

From the table and figure, it can be seen that the mean weight (0.33± 0.06 g) and volume (0.17± 0.04 mL) of intestinal content of compound II with 6 mg/kg bw dose the lowest in all of the samples tested. In addition, it was found to be more potent than that of the standard loperamide.

Castor oil-induced small intestinal transit

In the small intestinal transit test, it was found that the intestinal transit (25.29 ± 2.97 % ($p < 0.001$) of charcoal and inhibition of intestinal transit (74.71 ± 2.97 % ($p < 0.001$) of individual mice in aqueous extract 4 g/kg bw treated group) were better than that of the remaining samples (Table 3). The more increase in dose, the more reduction in percent intestinal transit. The results showed reduction in dose dependent manner (Figures 4 and 5).

It was also found that the intestinal transit 38.48 ± 5.29 % ($p < 0.001$) of charcoal and inhibition of intestinal transit 61.53 ± 5.29 % ($p < 0.001$) of individual mice in 95 % ethanol extract with 1 g/kg bw dose were better than that of the remaining samples. Although there was more increase in dose, no reduction in percent intestinal transit. The results showed reduction in dose independent manner (Figures 4 and 5).

Comparative intestinal transit (%) and inhibition of intestinal transit (%) of the control, loperamide, compound I, compound II, different doses of aqueous and ethanol extracts of YGG on castor oil-induced intestinal transit in mice are shown in Table 3, Figures 4 and 5. In the present work, the percent intestinal transit of compound I (5 mg/kg bw) was reduced more than the those of remaining samples. Therefore, the (%) inhibition of intestinal transit of compound I was the highest in all of the samples tested. According to castor oil-induced small intestinal transit test, it was found that the more decrease in intestinal transit (%) and the more increase in transit inhibition (%), the better is its antidiarrhoeal activity.

Table 3. Effect of Compound I, Compound II, 95 % Ethanol and Watery Extracts of flower of YGG On Castor Oil-induced Intestinal Transit in Individual Mice

Treatment	% Intestinal transit	% Inhibition
Control	71.77 ± 2.04	28.23 ±2.04
Loperamide 6 mg/kg	46.99 ± 5.31*	53.01 ±5.31*
Aqueous extract 4 g/kg	25.29 ± 2.97*	74.71 ± 2.97*
Aqueous extract 2 g/kg	36.07 ± 4.35*	63.93 ± 4.35*
Aqueous extract 1 g/kg	35.39 ± 3.21*	64.61 ± 3.21*
Ethanolic extract 2 g/kg	47.75 ±4.37*	52.25 ±4.37*
Ethanolic extract 1 g/kg	38.48 ±5.29*	61.53 ±5.29*
Ethanolic extract 0.5 g/kg	42.55 ±1.62*	57.45 ±1.62*
Compound I 5 mg/kg	16.47 ± 1.92*	83.53 ± 1.92*
Compound II 6 mg/kg	22.96 ± 4.89*	77.04 ± 4.89*

*$P < 0.001$

From Figures 4 and 5, it can be seen that the mean intestinal transit (16.47 ± 1.92 % ($p < 0.001$)) and the mean of transit inhibition (83.53 ± 1.92 % ($p < 0.001$)) of compound I were the best in all of the samples tested.

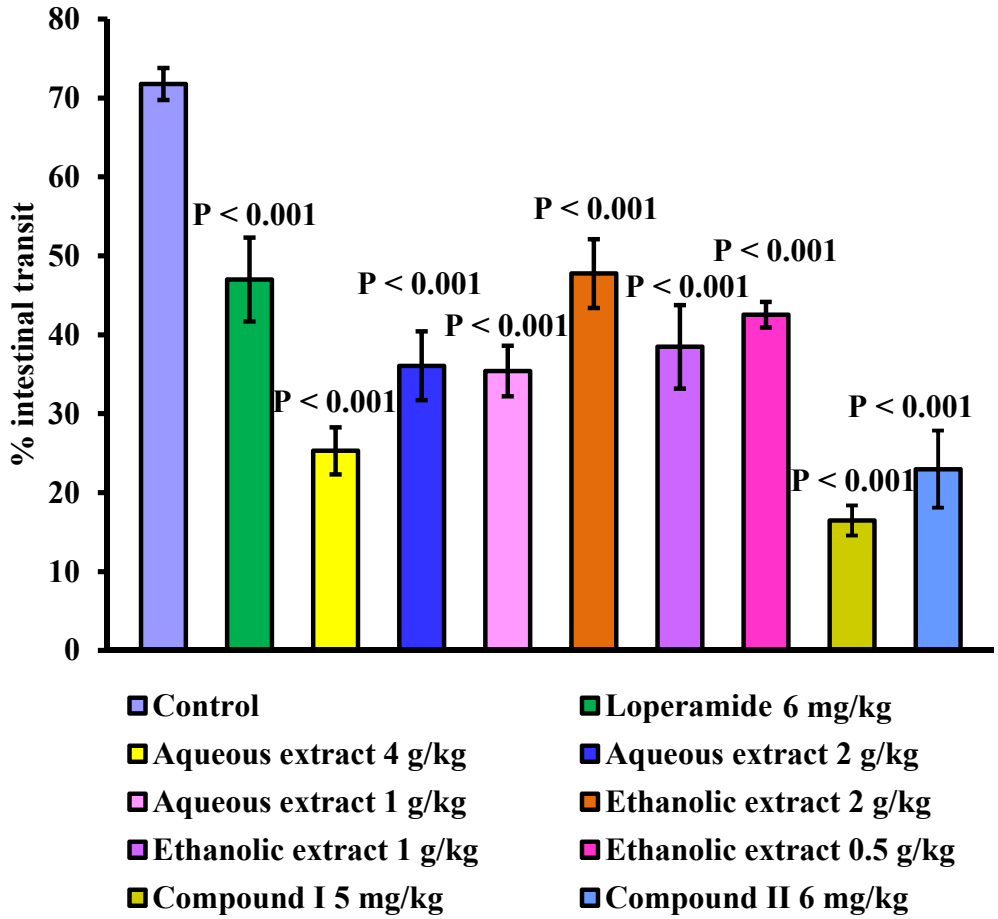

Figure 4. Percentage intestinal transit of aqueous extract (4 g/kg bw, 2 g/kg bw, 1g/kg bw), 95 % ethanolic extract (2 g/kg bw, 1 g/kg bw, 0.5 g/kg bw), compound I (5 mg/kg bw), compound II (6 mg/kg bw) of flower of YGG and standard drug loperamide (6 mg/kg bw) on castor oil-induced intestinal transit in mice

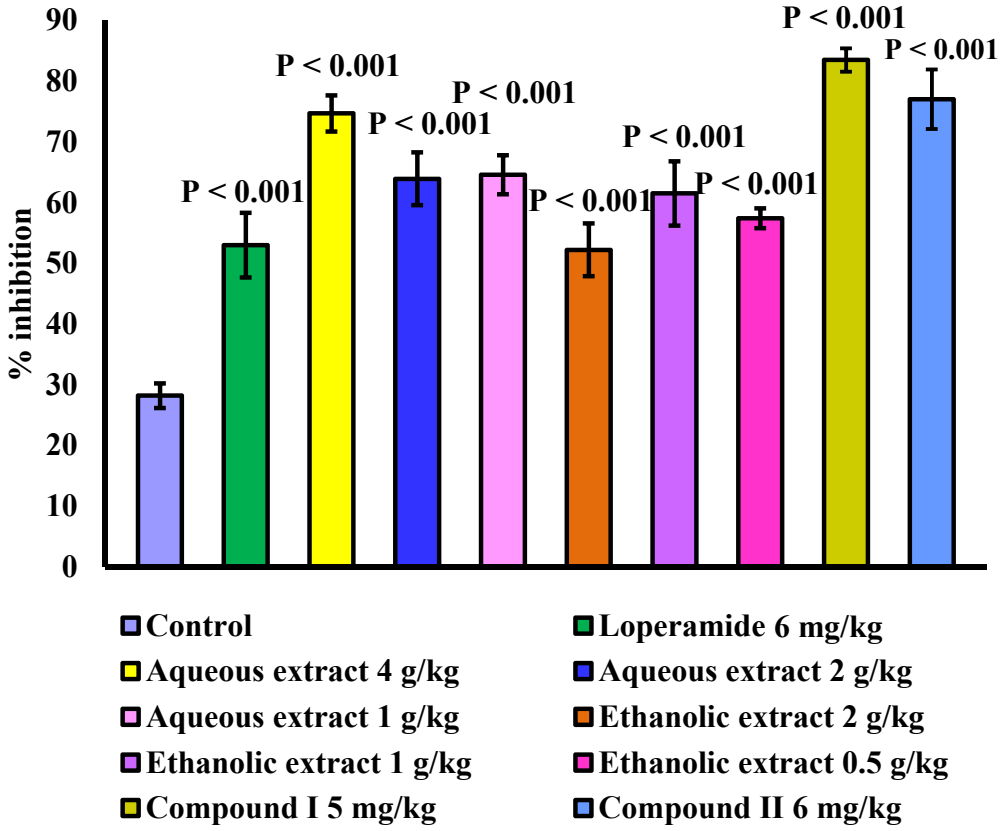

Figure 5. Percentage inhibition effect of aqueous extract (4 g/kg bw, 2 g/kg bw, 1g/kg bw), 95 % ethanolic extract (2 g/kg bw, 1 g/kg bw, 0.5 g/kg bw), compound I (5 mg/kg bw), compound II (6 mg/kg bw) of flower of YGG and standard drug loperamide (6 mg/kg bw) on castor oil-induced inhibition in mice

Table 4. Antidiarrhoeal efficacies of *Gardenia coronaria* Buch-Ham. on *in vivo* mouse models

Treatment	Delaying defaecation time of onset in mice, min	Gut meal travel distance in mice, cm	Purging frequency in mice, in number of stool	*In vivo* antidiarrhoeal index (%)
Control	3.50 ± 0.85	42.05 ± 1.39	20.83 ± 1.51	0
Loperamide 6 mg/kg	19.67 ± 10.75	27.33 ± 2.89*	6.33 ± 2.59*	104.30
Aqueous extract 4 g/kg	49.50 ± 25.34	17.07 ± 2.04****	6.33 ± 0.80	175.82
Aqueous extract 2 g/kg	68.17 ± 35.82	18.78 ± 2.51*	11.17 ± 2.39***	168.01
Aqueous extract 1 g/kg	30.17 ± 13.44	21.25 ± 2.20*	12.33 ± 1.31**	115.44
Ethanolic extract 2 g/kg	13.33 ± 7.23	27.88 ± 2.49*	13.5 ± 0.76**	69.32
Ethanolic extract 1 g/kg	130 ± 24.81*	20.83 ± 2.72*	5.33 ± 0.84*	238.53
Ethanolic extract 0.5 g/kg	19.5 ± 12.47	23.98 ± 1.59*	14 ± 0.58**	86.36
Compound I 5 mg/kg	29.5 ± 8.36***	11.37 ± 1.27*	8.83 ± 1.3*	146.17
Compound II 6 mg/kg	139.17 ± 14.27*	12.12 ± 2.51*	3.17 ± 0.65*	285.99

*$P < 0.001$, **$P < 0.005$, ***$P < 0.01$, ****$P < 0.05$

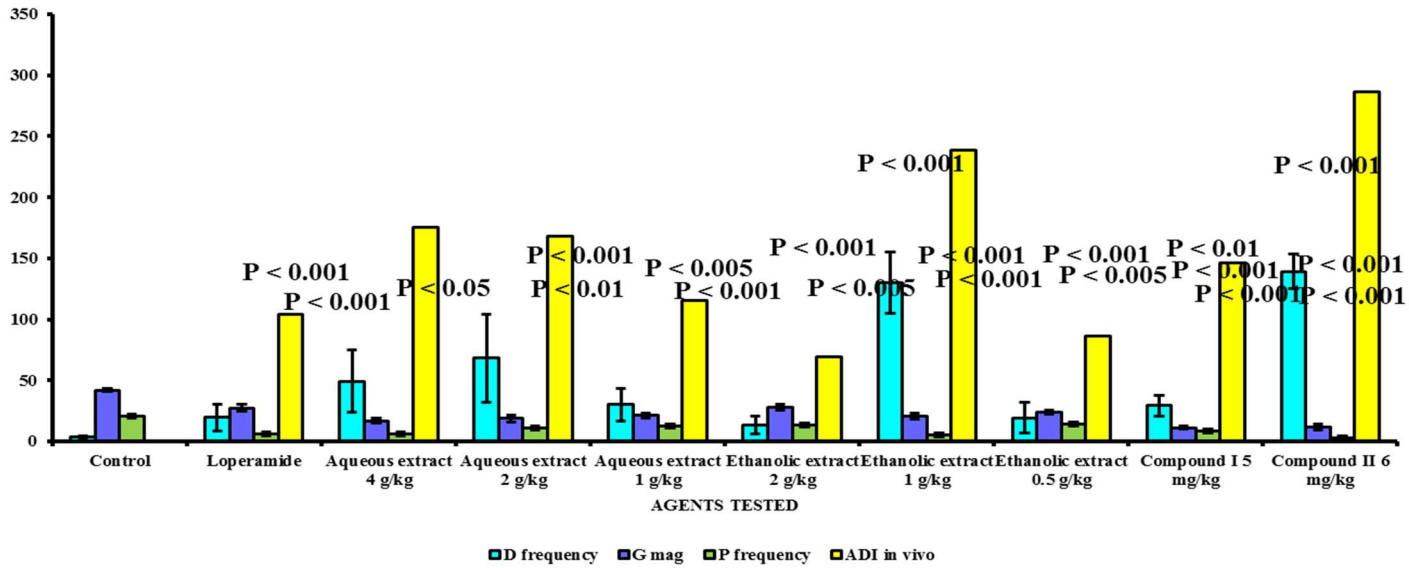

Figure 6. Comparative anti-diarrhoeal efficacies of flower of YGG aqueous extract (4 g/kg bw, 2 g/kg bw, 1g/kg bw), 95 % ethanolic extract (2 g/kg bw, 1 g/kg bw, 0.5 g/kg bw), Compound I (5 mg/kg bw), Compound II (6 mg/kg bw) and standard drug loperamide (6 mg/kg bw) on *in vivo* mouse model

D frequency = Delaying defecation time of onset in mice, in min

G mag = Gut meal travel distance in mice, in cm

P frequency = Purging frequency in mice, in number of stool

ADI *in vivo* = *In vivo* antidiarrhoeal index, in percent

Antidiarrhoeal index (ADI) was calculated by the method of Aye Than *et al*., 1989. ADI of aqueous extract (1, 2 and 4 g/kg bw) were 115.44 %, 168.01 % and 175.82 %, respectively (Table 4 and Figure 6). This means that when the dose was increased, the antidiarrhoeal index was also increased. However, ADI of 95 % ethanol extract (0.5, 1 and 2 g/kg bw) were 86.36 %, 238.53 % and 69.32 %, respectively (Table 4 and Figure 6). This means that when the dose was increased, the antidiarrhoeal index was decreased. Nevertheless, it was found that the higher the index, the better is the antidiarrhoeal activity. Therefore, it could be deduced that the antidiarrhoeal activity of compound II (6 mg/kg bw) with 285.99 % ADI value was the best in all of the samples tested and it was found to be considerably more potent than the standard loperamide (104.3 % ADI value).

The results of the present study showed that the flower of YGG produced significant frequency, enteropooling and intestinal transit. This also indicated showed that YGG has antisecretory and antimotility effects. So, *in vivo* test of this study revealed that the antidiarrhoeal activity of 6 mg/kg bw of compound II from flower of YGG was comparable with that of loperamide 6 mg/kg on counting number of stool, enteropooling and intestinal transit.

The flower of YGG is abundant in Mon State, Myanmar. The remarkable antidiarrhoeal effect of YGG against castor oil-induced diarrhoea showed its utility in a wide range of diarrhoea.

Conclusion

Therefore, it could be deduced that YGG flower may be used for the treatment of the diseases caused by some microorganisms. In addition, it may be effective for the diseases infected by bacteria causing diarrhoea such as haemoptysis, haematemesis, melena and diarrhoeal diseases Compound I (Benzoic acid), Compound II (Kaempferol) and Compound III (Stigmasterol) were extracted from the bark of YGG. It may be inferred that aqueous and ethanolic extracts of flower of YGG and isolated kaempferol may be used in the formulation of antidiarrhoeal medicine.

Acknowledgements

The authors would like to express their profound gratitude to the Department of Higher Education (Yangon Office), Ministry of Education, Yangon, Myanmar, for provision of opportunity to do this research and Myanmar Academy of Arts and Science for allowing to present this paper.

References

Awouters,F., Niemegeers, C.J.E., Lenaerts, F.M. and Janseen, P.A.J. (1978). "Delay of Castor Oil-Induced Diarrhoea in Rats, A New Way to Evaluate Inhibitors of Prostaglandin Biosynthesis". *Journal of Pharmacy and Pharmacology*, vol. 30, pp. 41-45

Aye Than, Kulkarni, H.J., Wut Hmone and Tha, S.J. (1989). "Antidiarrhoeal Efficacy of some Burmese Indigenous Drug Formulations in Experimental Diarrhoeal Test Models". *International Journal of Crude Drugs Research*, vol. 27(4), pp. 195-200

Kyaw Soe and Tin Myo Ngwe. (2004). *Medicinal Plants of Myanmar, Rubiaceae*. Forest Resource Environment Development and Conservation Association (FREDA), http://www.tuninist.net/ MMPD/ KSTMN/ Rubiaceae.htm (Accessed 7 November 2013)

Mascolo, N., Izzo, A.A., Avtore, G. and Barboto, F. (1994). "Nitric Oxide and Castor Oil Induced Diarrhea". *J. Pharmacol. Exp. Ther*, vol. 268, pp. 291-295

Medicinal Plants of Myanmar. (2010). http://www.moh.gov.nn, Department of Traditional Medicine, Ministry of Health, (Accessed 7 November 2013)

Robert, A., Nezamis, J.E., Lancaster, C., Hanchar, A.J. and Klepper , M.S. (1976). "Enteropooling Assay ; A Test for Diarrhea Produced by Prostaglandins". *Prostaglandins*, vol. 11(5), pp. 809-828

Silva, G.L. , Gil, R.R., Cui,B., Chai,H.,Suntisuk,T., Srisook, E. Reutrakul, V., Tuchinda,P., Sophansan, S. Sujarit, S. Upatham,S. ,Lynn,S.M., Farthing,J.E., Yang, S.L., Lewis,J.A., O'Neill,M.J.,Farnsworth,N.R., Cordell,G.A. and Kinghorn, A.D. (1997). "Novel Cytotoxic Ring-A *seco*-Cycloartane Triterpenes from *Gardenia coronaria* and *G. sootepensis*".*Tetrahedron*, vol.53 (2),pp.529-538

Uddin, B.S. (2013). *Gardenia coronaria*. http//www.mpbd.info/plants/gardeniacoronaria php (Accessed 15
August 2013)

APPLICATION OF STARCH AND ITS DERIVATIVE FROM CASSAVA (*Manihot esculenta* Crantz.) AS DISINTEGRANTS

IN PHARMACEUTICAL TABLETS FORMULATION

Theingi Win Naing[1], Nwet Nwet Win[2], Daw Hla Ngwe[3]

Abstract

The main aim of the research work focused on the application of the starch and its derivative prepared from cassava (*Manihot esculenta* Crantz.) and their application in pharmaceutical tablets formulation. The cytotoxicity of aqueous solution of local cassava starch (LCS) and its derivative carboxymethyl cassava starch (CMCS) were evaluated by brine shrimp cytotoxicity assay. According to the brine shrimp cytotoxicity assay, LCS and CMCS were observed to be free from cytotoxicity (LD_{50} > 1000 ppm), up to 1000 μg/mL concentration. The morphological characteristics of LCS and CMCS were recorded by using standard plate count method and Gram staining method indicating, the absence of *Escherichia coli* in both samples. LCS and CMCS were applied as disintegrants with different weights in chlorpheniramine maleate tablets formulation. 2.3 % (w/w) of LCS and 1.2 % (w/w) of CMCS were found to be most suitable for chlorpheniramine maleate tablets formulation determined by their physical properties such as moisture content, thickness, hardness, friability and disintegration times in distilled water as well as 0.1 M HCl solution.

Keywords: cytotoxicity, microbiological characteristics, tablets formulation, physical properties

Introduction

Carboxymethylation of polysaccharides is a widely studied conversion since it is simple and leads to products with a variety of promising properties. The polysaccharides (10 g) is activated with 80 mL of 40 % sodium monochloroacetic acid in the presence of 4 mL of 2 M NaOH solution.This

[1] Assistant Lecturer, Department of Chemistry, Bago University
[2] Associate Professor, Department of Chemistry, University of Yangon
[3] Professor and Head, Department of Chemistry, University of Yangon

first step is one mole of polysaccharides transformed into an alkoxide form. In the second step etherification occur to give synthesis yielding the carboxymethyl (CM) polysaccharide derivative. Not only cellulose and starch but also various polysaccharides from different sources are applied as starting materials (Ashok and Jitendra, 2012). Toxicology is the study of the adverse effects of chemicals, physical or biological agent on living organisms and the ecosystem. Brine shrimp lethality assay was applied for toxicity test since it is considered as a useful for preliminary assessment of toxicity. Its has been established as a safe, practical and economic method for determination of bioactivities of synthetic compound as well as plant products. Brine shrimp lethality bioassay is a rapid and comprehensive bioassay for the bioactive compounds of natural and synthetic origin. This method is attractive because it is very simple, inexpensive and low toxin amounts are sufficient to perform the test in the microwell scale. The assay is widely used in the evaluation of toxicity of fungal toxics, heavy metals, pesticides, and medicines etc. (Lee *et al.,* 1999). Reasons for microbial analysis are to meet certain set standards, to estimate the shelf-life of the product, to determine quality of the products and for public health purpose (Kiiyukia, 2003). Local cassava starch were used as binder and disintegrant in solid dosage form, but due to poor flow ability their utilization is restricted. So, starch can be modified by using chemical modification. Modified starches have been developed known as disintegrant, which are used to improve the efficiency of solid dosage forms. This is achieved by decreasing the disintegration time which in turn enhances drug dissolution rate. Disintegrants are an essential component in tablet formulation. A disintegrant is added to facilitate the rupture of bonds and subsequent disintegration of the tablets. This increases the surface area of the drug exposed to the gastrointestinal fluid. The oldest and still the most popular disintegrants are corn, potato starch that has been well dried and powdered. Nowadays cassava starches are the most widely used as disintegrant in pharmaceutical industry. Local starch has certain limitation and the concentration of starch in a conventional tablet formation is normally up to 10 % w/w. So, modified starches are now commonly used and it has specialized characteristics. Modified starch are used as disintegrants, it was found that the higher dissolution rates, find dispersion of particle form and disintegrant within two minutes. There are two methods of disintegrating agents into the tablet, (1)

Internal addition and (2) External addition. In external addition method, the disintegrant is added to the sized granulation with mixing prior to compression. In internal addition method the disintegrant is mixed with other powders before wetting the powder mixtures with the granulation fluid (Desia *et al.,* 2016). In this research, local cassava starch and carboxymethyl cassava starch were investigated the cytotoxicity of aqueous solution by brine shrimp cytotoxicity assay. It was indicated the microbiological analysis and to be used as potential pharmaceutical disintegrating agents for tablet formulation.

Materials And Methods

In the experiments, the chemicals used were procured from the British Drug House (BDH) Chemical Ltd., England. All specific chemicals used were cited in detail in each experimental section. In all investigation, the recommended methods and standard procedures involving both conventional and modern techniques were employed. Instruments employed in this work consists of conventional laboratory wares, glassware and other supporting facilities. Some of the instruments used in this study were balance (310 ± 0.1 mg) (LA 310 satorius AG, Gottingen, Germany), Granulating & Drying Machine (Model No. Strea-1 Fuji Sangyo. Co., Ltd., Japan), Mixer, Labo-Mill (Model No-OT 21, Yamato Co., Ltd., Japan), Stainless Steel Sieve (16 mesh, 32 mesh, 24 mesh, 100 mesh), Tableting Machine (Model No. Clean Press 19, Kyoto, Japan), Y-cone Blender (Model No-H 25, Yamato Co., Ltd., Japan). Infrared Moisture Meter (Kett) (Model No. F.1 A, Kyoto, Japan), Electronic Digital Caliper (Model No. E-23112, Peacock Co., Ltd), Hardness tester (Model No. D-63512 (Hainburg) Germany), Friabilator (Model No. D-63512 (Hainburg) Germany), Disintegration tester (Model No. D-63512 (Hainburg) Germany).

Preparation of Local Cassava Starch and Carboxymethyl Cassava Starch

The local cassava starch (LCS) was prepared by using conventional method. The local cassava starch (10.00 g) was dispersed in 200 mL of isopropanol/water (4:1, v/v) aqueous solution and 4 mL of 2 M NaOH solution was added with stirring. The mixture was stirred at room temperature for 10 min. 40 % sodium monochloroacetate (80 mL) was added and the mixture was

stirred for further 30 min. The pH of the mixture was then adjusted to about 5.0 by addition of 50 % glacial acetic acid. The carboxymethyl starch was filtered by Buchner funnel and washed with ethanol (95 %) until neutral condition was reached. The modified starch was dried at 50 °C for 6 h.

Study of Cytotoxicity and Microbiological Screening of the Local Cassava Starch and Carboxymethyl Cassava Starch

(a) Investigation of cytotoxicity by brine shrimp bioassay

The sample solution was prepared by dissolving 5 mg of respective sample in 5 mL of distilled water. The stock solution was tenfold diluted serially with distilled water to get the sample solution with the concentrations of 1000, 100, 10 and 1 μg/mL. Test solution (1 mL) was mixed with 9 mL of artificial sea water and placed in the chamber of ice cup. Alive brine shrimp (10 napulli) was taken with pasteur pipette and placed into each chamber which was kept at room temperature for about 24 h. After 24 h incubation, the number of survival brine shrimp was counted and 50 % lethality dose (LD_{50}) was calculated (Dockery and Tomkins, 2000). The control solution was prepared as the above procedure by using distilled water instead of sample solution. The cytotoxicity of different doses of tested samples are described (Table 1).

(b) Investigation of microorganisms by Agar Plates Count method

The agar plates count method was used to detect the microbiological action on local cassava starch and carboxymethyl cassava starch. Sample (0.1 mL) was spread into nutrient agar plates and potato dextrose agar plates, and then incubated in an incubator at 32 °C for 24 h. Single colony was transferred into EMB medium and incubated at 32 °C for 48 h.

Application of Local Cassava Starch and Carboxymethyl Cassava Starch in Tablet Manufacturing Process

Chlorpheniramine maleate tablets manufacturing

In this research work, chlorpheniramine maleate tablets were prepared by wet granulation method. Different weights of the disintegrants were used to

prepare tablets. Firstly, chlorpheniramine maleate (4 mg) was mixed with rate controlling polymers, calcium phosphate, calcium sulfate, colour in mixer granulator and then the filling agent lactose monohydrate powder added as compression aid. The mixture was wetted by addition of water and then granulated. Granules were dried in fluidizing, granulating and drying machine at 50 °C for 12 h and then passed through the 16 mesh sieve. The dried granules were mixed with local cassava starch (1.8 % and 2.3 %) or carboxymethyl cassava starch (1.2 %, 1.8 % and 2.3 %) powder in a motor mixer. The complete mixture was compressed into plain tablet by using 5 mm diameter, deep punches and dies in the rotary tablet press.

Quality Control and Measurement of Tablet Properties for Chlorpheniramine Maleate Tablets

(a) Determination of moisture contents of tablets

Sample (5 g) was placed in the pan of the Infrared Moisture Meter (Kett), which was measured under infrared lamp at 80 °C for 10 min. By direct reading from the infrared moisture meter, it indicated the loss of moisture in percentage from the samples. The test was repeated for three times and the average moisture content in percentage was calculated.

(b) Determination of thickness of tablets

The thickness of five tablets of chlorpheniramine maleate prepared with different weights of the LCS and CMCS was measured by Electronic digital caliper (Model No. E 23112, Peacock Co., Ltd). The means and standard deviation were also calculated for each sample.

(c) Determination of tablets hardness

Twenty tablets were randomly selected from each different weights of the tablet. Digital tablet hardness tester was employed to determine the mechanical strength of the tablets. A tablet is placed between two anvils, force is applied to the anvils and the crushing strength that just causes the tablet to

break is recorded, the average force required to crush the tablets sample was calculated.

(d) Determination of disintegration time of tablets

Six tablets from each different weights of sample were utilized for disintegration studies in distilled water and 0.1M hydrochloric acid at 37 °C ± 0.5 °C using a pharma test disintegration apparatus. Tablets were placed in each of the six tubes of the basket. The basket was mechanically raised and lowered in the immersion medium. The distintegration time of tablet was recorded when all particles from the tablet passed freely through the mesh of apparatus.

(e) Determination of tablets friability

To evaluate the degree of friability of the tablets from each tablet sample, ten tablets were randomly selected, dusted and weighed. These tablets were placed in a roche friabilator which rotated 100 times in 4 min. Afterwards the tablets were once again dusted and reweighed to determine the percentage loss of weight.

$$\% \text{ Friability} = \frac{W_1 - W_2}{W_1} \times 100$$

where,

W_1 = weight of tablets before operation

W_2 = weight of tablets after operation

Results and Discussion

Cytotoxicity of Local Cassava Starch and Carboxymethyl Cassava Starch

The cytotoxicity of different doses (1000 ppm, 100 ppm, 10 ppm, 1 ppm) of LCS and CMCS against *Artemia salina* (brine shrimp) is shown in Table 1. The cytotoxic effects were expressed in terms of mean ± SEM (standard error mean) and LD_{50} (50 % Lethality Dose). In this experiment,

potassium dichromate and caffeine were used as cytotoxic standard. As shown in (Table 1), LCS and CMCS were not cytotoxic to brine shrimp up to maximum dose of 1000 μg/mL. The LD_{50} standard $K_2Cr_2O_7$ and caffeine are 43.74 μg/mL and 1000 μg/mL respectively. According to the results, LCS and CMCS were found to be free from cytotoxicity.

Table 1. Cytotoxicity of Different Doses of Local Cassava Starch and Carboxymethyl Cassava Starch against *Artemia salina* (Brine Shrimp)

Sample	Brine Shrimp Survivals (Mean ± SEM) in Various Concentrations (μg/mL)				LD_{50} (μg/mL)
	1000	**100**	**10**	**1**	
LCS	10.00	10.00	10.00	10.00	>1000
CMCS	10.00	10.00	10.00	10.00	>1000
$K_2Cr_2O_7$*	0	0	8 ± 2.00	9.33 ± 0.67	44.19
Caffeine*	5 ± 1.15	7 ± 0.57	7.66 ± 1.20	10	1000

* Used as Cytotoxic Standards

SEM = Standard Error Means

The Morphological Characteristics of Local Cassava Starch and Carboxymethyl Cassava Starch

The morphological characteristics of LCS and CMCS were recorded by using standard plates count method and Gram staining method. The type of colonies on Nutrient Agar medium and Potato Dextrose Agar medium were observed. The stains have the morphology of coccus shape and Gram (-)ve in both samples and they may be in the same genus. These colonies are transferred to Eosin Methylene Blue (EMB) medium, on the EMB medium, the colour of colony is not red, therefore it was found to be confirmed that *Escherichia coli* are absent in the LCS and CMCS. For each stain, the type of colonies on Nutrient Agar medium, Potato Dextrose Agar medium and EMB medium are shown in Figure 1 and its morphological results are described (Table 2).

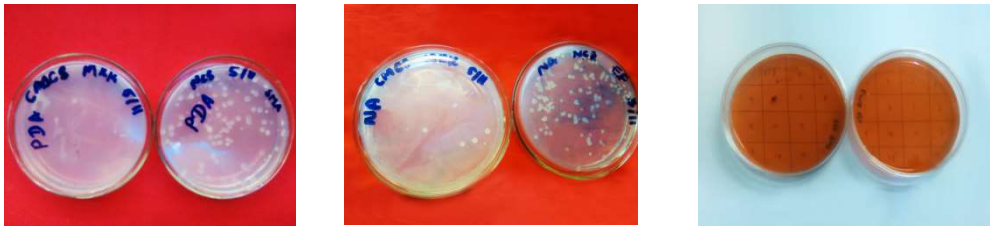

(a) **(b)** **(c)**

Figure 1. Types of colonies on (a) nutrient agar medium (b) potato dextrose agar medium (c) EMB medium

Table 2. The Morphological Characteristics of Microorganisms Observed in Local Cassava Starch and Carboxymethyl Cassava Starch

Stain	Morphology	Colony on N/A	Colony on PDA	Colony on EMB	Gram stain
LCS	Coccus with spore in long chain	Round and white colony grow on agar thickly	Small white colony grow on agar	Colony is not red	(-)ve
CMCS	Coccus with spore in long chain	Round and white colony grow on agar thickly	Small white colony grow on agar	Not grows	(-)ve

Application of Local Cassava Starch and Carboxymethyl Cassava Starch as Disintegrants in Tablet Manufacturing Process

Manufacture of tablet formulation

Chlorpheniramine maleate tablets were prepared in Credit Pharmaceutical Industry Co.Ltd. Different weights of local cassava starch (1.8 %, 2.3 %) and carboxymethyl cassava starch (1.2 %, 1.8 %, 2.3 %) were used as disintegrants in preparation of tablets. Prepared chlorpheniramine maleate tablets and procedure for tablet manufacturing process are shown in (Figure 2).

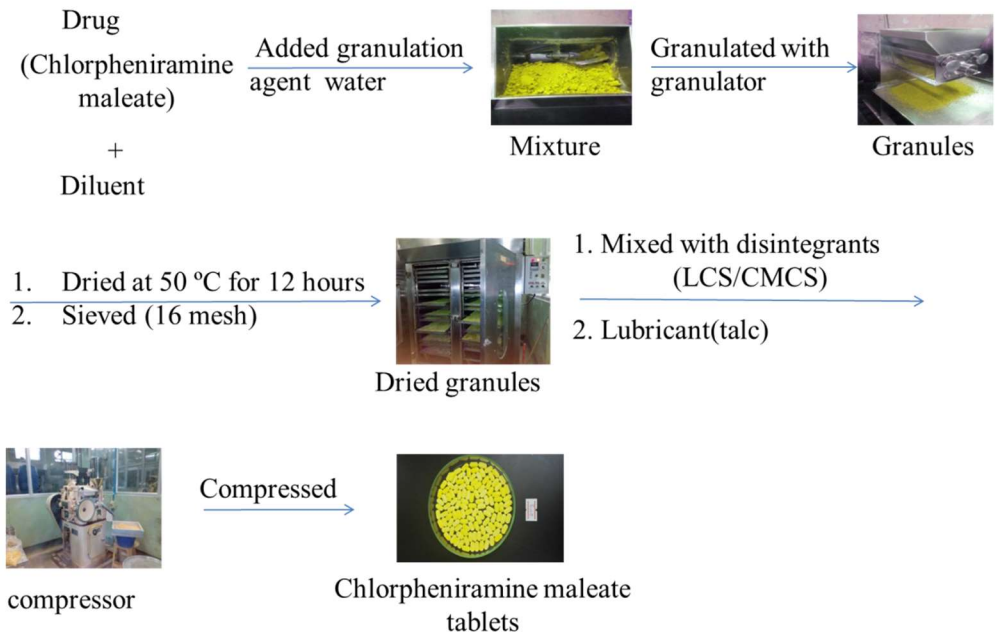

Figure 2. Determination of the Starch and its Derivative in Procedure for Tablet Manufacturing Process
LCS (1.8 %), (2.3 %)
CMCS (1.2 %), (1.8 %), (2.3 %)

Quality Control and Measurement of Tablet Properties for the Prepared Chlorpheniramine Maleate Tablets

(a) Moisture contents of the prepared chlorpheniramine maleate tablets

The moisture contents of prepared chlorpheniramine maleate tablets were measured by using the Infrared Moisture Meter (Kett) (Model No. F. 1 A, Kyoto, Japan) (Figure 3). Table 3 shows the moisture contents of chlorpheniramine maleate tablets prepared with different weights of LCS and that of CMCS used as disintegrants in tablets formulation. LCS used as disintegrant in different weight are in the range of 2.33 ~ 2.27 and CMCS used as disintegrant in different weights are in the range of 2.38 to 2.53, which are within the reported data range. Otherwise, it is important that the moisture contents be kept as low as possible during storage to prevent microbial

spoilage, hydrolysis and enzymatic decomposition. The resulting data are within the official limited (British Pharmaceutical Codex, 1994).

(b) Thickness of the prepared chlorpheniramine maleate tablets

The thickness of the prepared chlorpheniramine maleate tablets were measured by using the Electronic Digital Caliper (Model No. E-23112, Peacock Co., Ltd) (Figure 3). The thickness of chlorpheniramine maleate tablets data are described in Table 3. Chlorpheniramine maleate tablets were prepared by wet granulation method and by using 5 mm diameter, deep punches and dyed in the rotary tablet press. The thickness is generally less than half of the diameter. The thickness of tablets prepared with different weights (1.8 % and 2.3 %) of LCS used as disintegrants in tablet formulation was observed to be in the range of 2.74 ~ 2.89 mm and (1.2 %, 1.8 % and 2.3 %) CMCS used as disintegrant in tablets formulation was observed to be in the range of 2.75 ~ 3.02 mm, increased with increasing the weights of starches.

(c) Hardness (Crushing strength) of the prepared chlorpheniramine maleate tablets

The hardness of the prepared chlorpheniramine maleate tablets were measured by using the Hardness tester (Model No. D-63512 (Hainburg) Germany). The hardness of tablet with different weights (1.8 % and 2.3 %) of LCS and that of CMCS (1.2 %, 1.8 % and 2.3 %) used as disintegrants in tablets formulation are shown in Figure 3.

It was observed that, as the disintegrants weights increased, the hardness (crushing strength) increased. Therefore, hardness (crushing strength) is directly proportional to the weight of the disintegrant. The production of tablet with LCS (1.8 %) is complicated due to difficulties in tablet ejection, resulting in picking, sticking, capping and cracking of tablet high friability, lower hardness and disintegration time. The ejection of tablet has been found easier while using CMCS (1.2 %) as disintegrant, because this composition could minimize picking, sticking, capping, cracking etc., and subsequent of the tablet hardness and increased disintegration time and decreased the friability. Chlorpheniramine maleate tablets formulated with CMCS disintegrants exhibited higher values of hardness (crushing strength) then those formulated with LCS disintegrants. The hardness of the prepared tablets formulated with

both LCS (49 ~ 53 N) and CMCS (59 ~ 76 N) occurred in the range of the official limit of 50 ~ 300 N (British Pharmaceutical Codex, 1994).

(d) Friability of the chlorpheniramine maleate tablets prepared with local cassava starch and carboxymethyl cassava starch in different weights

The friability of the chlorpheniramine maleate tablets prepared with local cassava starch and carboxymethyl cassava starch in different weights were measured by using the friabiliator (Model No. D-63512 (Hainburg) Germany) (Figure 3).

The friability of the tablet with different weights of LCS and CMCS that used as disintegrants in tablets formulation are described in (Table 3). It was found that when the disintegrants weights increased, the values of friability of the tablet decreased. In tablet formulation, the higher values of hardness of tablets were observed with the lower values of friability of the tablets. The friability of the tablet is inversely proportional to the hardness of tablet.

The friability of the tablets was found to be higher in 1.8 % LCS than 2.3 % LCS used as disintegrants, and that of tablets formulated with CMCS was found in the order of 2.3 % < 1.8 % < 1.2 % CMCS used as disintegrants in the tablet formulation. The tablets that less than 1 % of their weights, friability of these tablets is good (Mohammad Saleem, 2014). But LCS has to be used in concentration above 2.3 %. Below 2.3 % there is insufficient, friability of the tablets ability is decreased, therefore transportation and packing is difficult. Above 2.3 %, the incompressibility of starch makes it difficult to compress tablets of sufficient hardness. CMCS has to be used in concentration is 1.2 %, there is sufficient, friability of the tablet ability is good therefore CMCS is more suitable used as disintegrant in tablets formulation.

(e) Disintegration time of the chlorpheniramine maleate tablets prepared with local cassava starch and carboxymethyl cassava starch in different weights

The disintegration time of the prepared chlorpheniramine maleate tablets formulated with local cassava starch and carboxymethyl cassava starch in different weights was measured by using Disintegration tester (Model No. D-63512 (Hainburg) Germany) (Figure 3).

Table 3 shows the resulted disintegration time of the tablets in distilled water and 0.1 M HCl solution. It was found that the disintegration time decreased with increasing the disintegrant weights of starches in the tablet formulation in distilled water as well as in 0.1 M HCl solution. When LCS was used as disintegrant in tablet formulation, the disintegration time were observed 2 to 3 min in distilled water and within 8 min in 0.1 M HCl solution. On the other hand, while CMCS was used as disintegrant in tablet formulation, the disintegration time was observed 4 to 5 min in distilled water and within 9 min in 0.1 M HCl solution.

Tablets containing disintegrants generally passed the official disintegration test for uncoated tablets within 5 to 15 min (Baker and Jaiyeoba, 2009). This may imply a faster onset of action and as such may be useful in immediate release formulations. Tablets containing disintegrants showed good olution profile.

The results show that CMCS is potentially useful as a disintegrant and may be suitable to use in various tablets formulation.

Table 3. Physical Properties of the Chlorpheniramine Maleate Tablets Prepared with Different Weights of Local Cassava Starch and Carboxymethyl Cassava Starch

Parameters	Properties of Tablets in Different weights of starch (%)						
	1.2		1.8		2.3		Official *
	I	II	III	IV	V	VI	Limited
Moisture	-	2.38	2.33	2.42	2.27	2.53	1-3 %
Thickness	-	2.75±0.04	2.74±0.03	2.83±0.02	2.89±0.05	3.02±0.06	-
Hardness (N)	-	59	49	69	53	76	50- 300
Friability (%)	-	0.1959	0.3611	0.1936	0.2229	0.1619	< 1**
Disintegration Time in water (s)	-	313	162	305	129	254	> 240
Disintegration Time in HCl (0.1 M) (s)	-	565	505	557	503	549	540-900

I, III, V = LCS
II, IV, VI = CMCS

*British Pharmaceutical Codex(1994)
**Mohammad *et al*.,(2014)

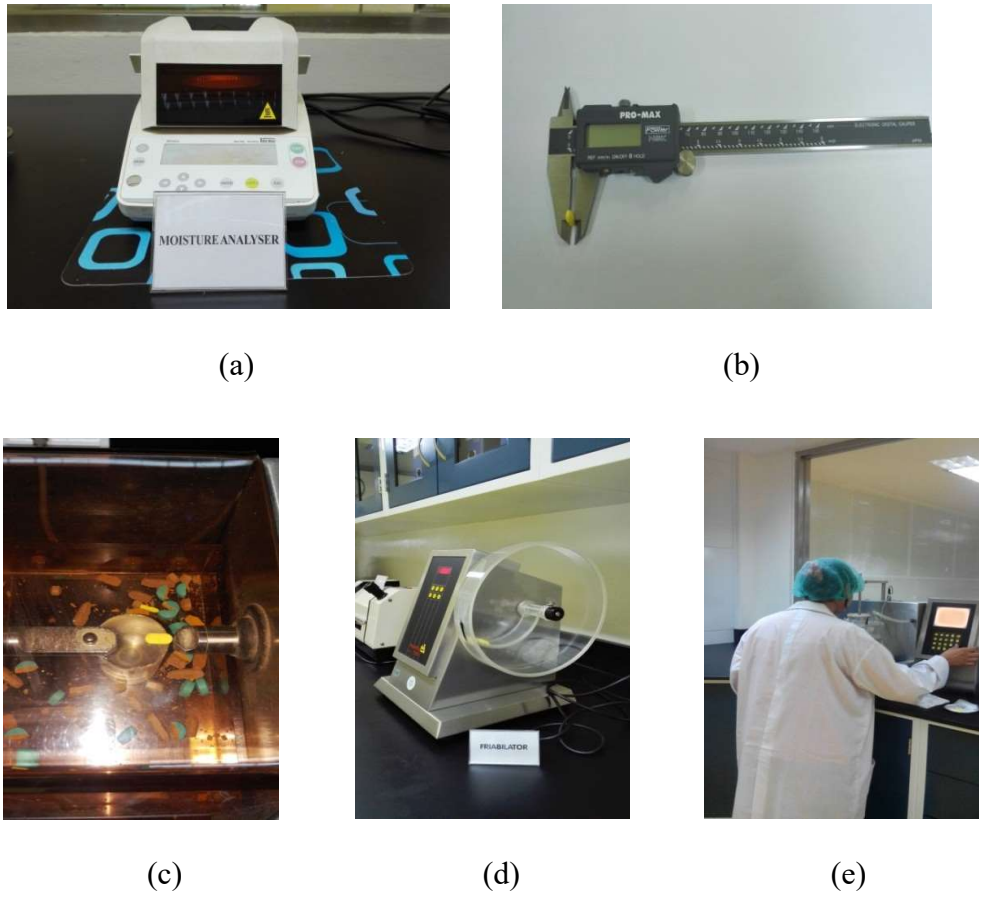

(a) (b)

(c) (d) (e)

Figure 3. Photographs of

(a) Infrared moisture meter (Kett) (Model No. F. 1 A, Kyoto, Japan)

(b) Electronic digital caliper (Model No. E-23112, Peacock Co., Ltd)

(c) Hardness tester (Model No. D-63512 (Hainburg) Germany)

(d) Friabilator (Model No. D-63512 (Hainburg) Germany)

(e) Disintegration tester (Model No. D-63512 (Hainburg) Germany)

Conclusion

From the overall assessment of the present work concerning with the starch and its derivative from cassava (*Manihot esculenta* Crantz.) and their application in pharmaceutical tablets formulation, the following inferences could be deduced. Both LCS and CMCS were observed to be free from cytotoxic effect and harmful bacteria *E. coli*. Consequently, LCS and CMCS were applied as disintegrants with different weights in chlorpheniramine maleate tablets formulation. LCS (2.3 % w/w) and CMCS (1.2 % w/w) were observed to be the best conditions as the disintegrants in the chlorpheniramin maleate tablets formulation according to their quality assessment of tablets such as moisture content, thickness, friability, hardness, disintegration time in distilled water as well as 0.1 M HCl solution. CMCS was found to be better than LCS in the tablet formulation as an alternative disintegrant. Therefore CMCS is so biodegradable and non-toxic product that the finding increases the number of application including the food and pharmaceutical area. According to these inferences, carboxymethylated polysaccharides in particular CMCS based on renewable resources are useful in many applications.

Acknowledgement

The authors would like to express their profound gratitude to the Department of Higher Education (Yangon Office), Ministry of Education, Yangon, Myanmar, for provision of opportunity to do this research and Myanmar Academy of Arts and Science for allowing to present this paper.

References

Ashok, D. S. and Jitendra, S. P. (2012). "Microwave Assisted Synthesis of Carboxymethyl Starch". *J.School of Chemical Sciences*, vol. 10, pp. 36-42

Baker, L. G. and Jaiyeoba, K. T. (2009). "Evaluation of a New Tablet Disintegrant from Dried Pods of *Abelmuscus esculentusl*(OKRA)". *Asia Journal of Pharmaceutical and Clinical Research,* vol. 2 (3), pp. 85-90

British Pharmaceutical Codex. (1994). *The Pharmaceutical Codex.* London: 12th Ed., pp. 1-16, 178-200, pp. 277,309

Desai, P. M., Liew, C. V. and Heng, W. S. (2016). "Review of Disintegrants and the Disintegration Phenomena". *Journal of Pharmaceutical Sciences*, vol. 105, pp. 2545-2555

Dockery, M. and Tomkins, S. (2002). *Brine Shrimp Ecology.* London: 1st Ed., The British Ecology Society, pp. 92-93

Kiiyukia, C. (2003). "Laboratory Manual Food Microbiology", Ethiopia health and Nutrition research institute, *Unido Project*, pp. 7-10, 50-55

Lee, T. H., Chen, Y. M. and Chou, H. N. (1994). "Toxicity Assay of Cyanobacterial Stains using *Artemai salina* in Comparison with the Mouse Bioassay." *Acta Zoological Taiwanica,* vol. 10 (1), pp. 1-8

Mohammad, N. A., Jusoh, N. A. Htike, Z. Z. and Win, S. L. (2014). "Bacteria Identification from Microscopic Morphology". *International Journal on soft computing, Artificial Intelligence and Applications* (IJSCAI), vol. 3 (2), pp. 1-12

SOME BIOACTIVITIESOF*CURCUMA AERUGINOSA* ROXB. (NA - NWIN–TAIN- PYAR) RHIZOMES

Zin Thu Khaing[1], Y-Mung San Aung[2], Daw Hla Ngwe[3]

Abstract

This research work has focused on the elucidation of chemical constituents and some biological activities of the fresh rhizome of *C. aeruginosa* Roxb. The phytochemical screening of *C. aeruginosa* Roxb. powder reveals the presence of several compounds. The main phytochemical constituents include alkaloids, carbohydrates, amino acid, flavonoids, phenolic compounds, glycosides, reducing sugars, starch, steroids, terpenoids, and tannins. However, cyanogenic glycoside and saponin were not detected at the assay conditions. In the screening of the antioxidant activity, ethanol extract (IC_{50}= 1.56 µg/mL) was found to be more potent than watery extract (IC_{50} =3.95 µg/mL). The total phenol contents (TPC) of ethanol extract (52.31 ±8.70 µg GAE/mg) was found to be higher than watery extract (16.92 ± 0.20 µg GAE/mg).The antimicrobial activities of (PE, EtOAc, EtOH and water) extracts from *C. aeruginosa* Roxb. sample were determined against seven strains of microorganisms (*B. subtilis, S. aureus, P. aeruginosa, B. pumilus, C. albicans, E.coli* and *A. tumefaciens*) by agar well diffusion method. The highest antimicrobial activity was observed in EtOH extract whereas H_2O extract showed minimum activity. Antitumor activity was carried out with EtOAc and EtOH extracts by PCG test. From this experiment, both extracts were found to prevent the tumor formation with the dose of 0.1 and 0.15 mg/disc. The rhizome of *C.aeruginosa* Roxb.could be applied not only as the local health remedy to the local indigenous but also for the treatment of some bacterial plant pathogen and diseases in agriculture of Myanmar.

Keywords: *Curcuma aeruginosa* Roxb., phytochemicals, antioxidant activity, antimicrobial activity, antitumor activity

[1] Lecturer, Department of Chemistry, University of Yangon
[2] Candidate, MSc. (2016-2017), Department of Chemistry, University of Yangon
[3]Professor and Head, Department of Chemistry, University of Yangon

Introduction

Many Plants have been the basis for medical treatments through much of human history, and such traditional medicine is still widely practiced today in Myanmar. Modern medicine recognizes herbalism as a form of alternative medicine. Herbal medicine has a great tradition of maintaining human health for centuries. A majority of the world's population living in the developing countries still relies on herbal medicine to meet its health care needs. Although modern medicine may be available in such countries herbal medicine have often maintained popularity for historical and cultural reasons. Currently, many people in developed countries have begun to turn to alternative or complementary therapies, including medicinal herbs. The use of herbal remedies is more prevalent in patients with chronic diseases such as cancer, diabetes, asthma and end-stage renal disease (WHO, 1991).

Traditional systems of medicine continue to be widely practiced on many accounts. In many of the developing countries the use of plant drugs is increasing because modern life saving drugs are beyond the reach of three quarters of the third world's population although many such countries spend 40-50% of their total wealth on drugs and health care (Thomas *et al.,*1998).

Curcuma is a herb with leaves and inflorescences rising to 18 inches from the ground. The rhizome is rather large, branched horizontal externally grey and polished, with white or pink tips, internally blue, greenish-blue or violet-blue and paler in the young parts. The rhizomes are carefully dug up with hand picks.*C.aeruginosa*Roxb.is found from Myanmar and Cambodia to Java (Newman *et al.,* 2004).In Myanmar it is cultivated in Kachin and Shan state.

Rhizome of *C. aeruginosa*Roxb.is used as medicine for rheumatic, cough, asthma and anthelmintic. The traditional medical practitioners in India have identified its usage in amebicdysentery, stomach ache, ulcer and indigestion.The rhizome of *C. aeruginosa*Roxb.isa promising source of potential anti-oxidants. It is employed for making various cosmetic items and for sprains and bruises. The other medicinal uses of rhizome include postcoital contraception, hepatoprotection, and reduced platelet-activation effects. Due to its high medicinal value and indiscriminate harvest from the wild, the natural population has come down and according to International Union for

Conservation of Nature (IUCN) report, the plant is in the critically endangered category (Srivastava *et al*.,2006).

Materialsandmethods

Sample Collection and Preparation of *Curcumaaeruginosa*Roxb.

The rhizomes of*C.aeruginosa*Roxb.(Figure 1)were collected from Mogaung Township, Kachin State. These samples were identified at Department of Botany, University of Yangon. The collected samples were cleaned and air-dried at room temperature. The dried samples were cut into small pieces and ground into powdered by a grinding machine(Figure 2). The dried powdered samples were used for further experiment.

Figure 1 Photographs of *C. aeruginosa*Roxb. Rhizomes

Figure 2 Preparation of dried powder sample (Na-Nwin-Tain-Pyar) Rhizomes

Preliminary Phytochemical Investigation of *Curcuma aeruginosa* Roxb.

In order to find out the types of phytoorganic constituents such as alkaloids, α-amino acids, carbohydrates, cyanogenic glycosides, flavonoids, glycosides, organic acids, phenolic compounds, reducing sugars, saponins, starch, steroids, tannins, and terpenoids in the sample, preliminary phytochemical tests were carried out according to the appropriate reported methods.

Various crude extracts (PE, EtOH, EtOAc) of *C.aeruginosa* Roxb. were prepared for TLC investigation. Extracts were loaded on the percolated TLC silica gel plate and the chromatography was carried out using an appropriate standard solvent system for *C. aeruginosa* Roxb. The developed chromatograms were first inspected under UV-254nm and 365 nm light and then sprayed with detecting reagents to classify the compounds present and their functional group.

Determination of Phenolic Contents in Crude Extracts of (Na-Nwin-Tain-Pyar) Rhizomes

The total phenolic content (TPC) assay was performed in accordance with modifications. A 0.2 mL of each sample solution was mixed with 1.5 mL of Folin-Ciocalteu Reagent in a test tube covered with aluminum foil. After 5 min, 1.5 mL of 10% Na_2CO_3 was added to each test tube. The sample was then incubated for 90 min at room temperature. The absorbance was measured at 765 nm spectophotometrically (KWF UV-7504). A standard curve of Gallic acid solutions (range from 0 - 250 μg mL^{-1}) was used for calibration. The experiment was done in triplicate. Concentrations of Gallic acid equivalent (GAE) in the plant extracts were calculated from the linear regression equation explored from standard curve construction for Gallic acid. TPC in the plant samples were expressed as (μg GAE/mg) (Reynertson, 2007).

Measurement of DPPH Radical Scavenging Activity by Spectrophotometric Method

Control solution was prepared by mixing (0.002 %) DPPH solutions (1.5 mL) and 95% ethanol (1.5 mL) using vortex mixer. Similarly, a blank solution was also prepared by mixing 95% ethanol (1.5 mL) and the sample solution (1.5 mL). The sample solution was also prepared by mixing the

sample solution (1.5 mL) with 0.002 % DPPH solution (1.5 mL). All these solution were allowed to stand at room temperature for30 min. Then, the absorbance was measured at λ_{max} 517 nm and recorded on spectrophotometer (KWF UV-7504), Shimadzu Corporation. Absorbance of individual solution was measured in triplicate and % inhibition of each sample solution was calculated by using the following formula:

$$\% \text{ RSA} = ([A_{DPPH} - (A_{Sample} - A_{Blank})] / A_{DPPH}) \times 100$$

where, % RSA = % radical scavenging activity

A_{DPPH} = absorbance of DPPH in EtOH solution

A_{Sample} = absorbance of sample + DPPH solution

A_{Blank} = absorbance of sample + EtOH solution

The antioxidant power (IC_{50}) is expressed as the test substances concentration (µg/mL) that result in a 50% reduction of initial absorbance of DPPH solution and that allows to determine the concentration. IC_{50} (50% inhibitory concentration) values were calculated by linear regressive excel program.

$$\text{Standard Deviation (SD)} = \sqrt{\frac{(\bar{x}-x_1)^2+(\bar{x}-x_2)^2+\ldots(\bar{x}-x_n)^2}{(n-1)}}$$

where, $A_{control}$ = Absorbance of control solution

A_{sample} = Absorbance of sample solution

A_{blank} = Absorbance of blank solution

$\overline{X}$ = Average % inhibition

$X_1, X_2 \ldots, Xn$ = % inhibition of test sample solution

n = number of times

Screening of Antimicrobial Activity of Crude Extracts of (Na-Nwin-Tain-Pyar) Rhizomes By Agar Well Diffusion Method

Antimicrobial activities of various crude extracts such as (PE, EtOAc, EtOH and water)extracts of Na-Nwin-Tain-Pyar were studied by agar well diffusion method at the Pharmaceutical Research Department, Ministry of Industry, Yangon. The test procedure is as follow, at first, the extracts (1 g each for 6 species of bacteria) were introduced into sterilized Petri-dishes and dissolved in 1mL of their respective solvents: PE, EtOAc, EtOH and H_2O. Four small holes of 10 mm diameter each were cut out in the inoculated agar to place samples to be tested. The volume of each sample placed in each hole was0.1 mL. The Petri-dishes were incubated of 37ºC for 24 hr and the inhibition zone diameter was measured the extent of antimicrobial activity.

Antitumor Activity Screening of Crude Extracts of(Na-Nwin-Tain-Pyar) Rhizomes by Potato Crown Gall Test or Potato Disc Assay Method

Tumor producing bacteria, *Agrobcterium tumefacien*, was used in this study. All of these strains have been maintained as solid slants under refrigeration. For inoculation of the potato discs, 48 hours broth cultures containing $5 \times 10^7 - 5 \times 10^9$ cell/mL were used.

Results and Discussion

Phytoconstituents of Various Crude Extracts of *C.aeruginosa*Roxb.(Na-Nwin-Tain-Pyar) Rhizomesby TLC Method

Preliminary phytochemical screening of *C.aeruginosa* Roxb. powder revealed the presence of several compounds. The main phytochemical constituents include alkaloids, carbohydrates, amino acid, flavonoids, phenolic compounds, glycosides, reducing sugars, starch, steroids, terpenoids, and tannins. However, cyanogenic glycoside and saponin were not detected at the assay conditions. Qualitative determination of phytoconstituents by thin layer chromatography indicated that essential oils, alkaloids, steroids, terpenoids, phenolic compounds and flavonoids were present in *C.aeruginosa* Roxb (Table 1).

Table 1 Results of Preliminary TLC Screening of *Curcuma aeruginosa* Roxb.

Type of compound	Spray reagent	Observation
Steroids &Terpenoids	10% H_2SO_4	Various color intensity
Steroids, Terpenoids& Essential oils	Vanilin	Bright Fluorescence color intensity
Phenolic compound	5% Ferric chloride	Black color
Flavonoids	1% Aluminium chloride	Formation of color zone
Alkaloids	Dragendorff	Black color intensity

Total Phenol Contents of Crude Extracts of *C.aeruginosa* Roxb. (Na-Nwin-Tain Pyar)Rhizomes By Folin-Ciocalteu Method

In this study, the total phenolic content of *C.aeruginosa* Roxb.was estimated by Folin-Ciocalteu method. Phenols react with an oxidizing agent phosphomolybdate in F-C reagent under alkaline conditions and result in the formation of blue coloured complex, the molybdenum blue which is measured at 765 nm colorimetrically. Total phenolic content (TPC) was expressed as micro gram of Gallic acid equivalent (GAE) per milligram of crude extract (µg GAE/mg).The total phenol content of ethanol extract (52.31 ±8.70 µg GAE/mg) was found to be higher than watery extract (16.92 ± 0.20 µg GAE/mg).

Table2 Total Phenol Content (TPC) of Ethanol and Watery Extracts of (Na-Nwin-Tain-Pyar) Rhizomes

No	Extracts	TPC (µg GAE/mg±SD)
1	Ethanol	52.31 ±8.70
2	Watery	16.92 ± 0.20

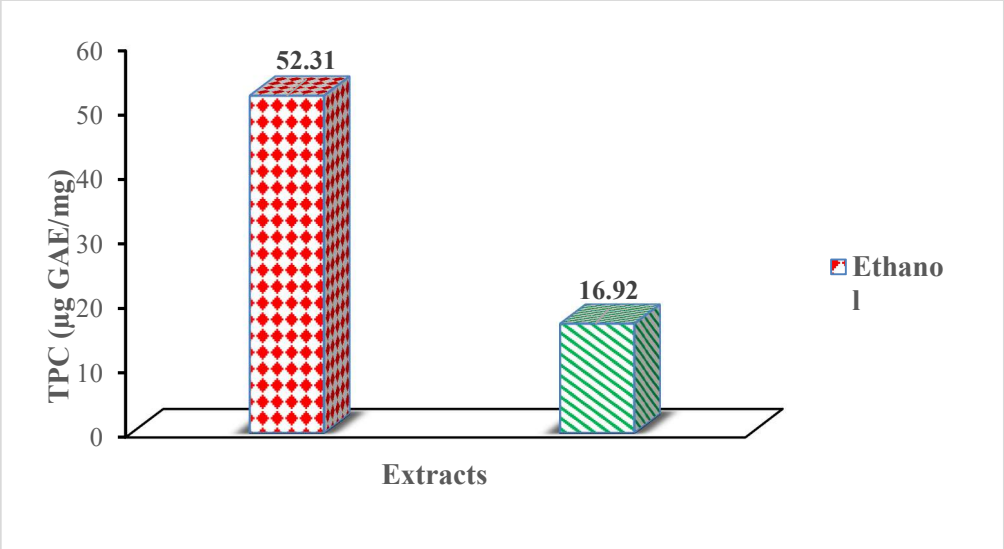

Figure 3 A bar graph of total phenolic contents of ethanol and watery extracts from (Na-Nwin-Tain-Pyar) rhizomes

Antioxidant Activity of Crude Extracts of (Na-Nwin-Tain-Pyar) Rhizomesby DPPH Radical Scavenging Assay

The antioxidant activity of EtOH and water extracts of *C.aeruginosa* Roxb.were studied by DPPH free radical scavenging assay method. DPPH free radical scavenging method is widely used to evaluate the free radical scavenging ability of various samples. DPPH radical is scavenged by antioxidant through the donation of electron forming the reduced DPPH. The color of the sample changes from purple to pale yellow which can be quantified by its decrease of absorbance at wavelength 517 nm (Maw *et al*., 2011).The radical scavenging activity and crude extracts were expressed in term of % RSA and IC_{50} (50 % inhibitory concentration).In this study, six different concentrations (20, 10, 5, 2.5, 1.25 and 0.625 µg /mL) of crude extracts were prepared by serial dilution. Ascorbic acid was used as standard and DPPH and ethanol without crude was employed as control. Absorbance was measured at λ_{max} 517 nm using UV-visible spectrophotometer (UV-1800, Shimadzu).From their average values of percent inhibition, IC_{50}(50 % inhibition concentration) values in µg/mL were calculated by linear regressive

excel program. The IC_{50}values of ethanol extract of Na-Nwin-Tain-Pyar rhizomes was1.56µg/mL and watery extract was 3.95µg/mL (Table 3 and Figure 4).The lower the IC_{50}values, the higher the free radical scavenging activity, the higher the antioxidative property. According to the results, the IC_{50}values of ethanol extract of *C. aeruginosa* Roxb. (IC_{50} = 1.56 µg/mL) was comparable to that of standard ascorbic acid (IC_{50} = 1.21 µg/mL), indicating that ethanol extract has potent antioxidant property than water extract.

Table 3 % Radical Scavenging Activity (% RSA) and IC_{50} Values of Ethanol and Watery Extracts of (Na-Nwin-Tain-Pyar) Rhizomes and Standard Ascorbic Acid

Samples	% Inhibition (Mean ± SD) in Different Concentration (µg/mL)						IC_{50}(µg/mL)
	0.625	1.250	2.500	5.000	10.000	20.000	
Ethanol Extract	42.01 ± 2.58	46.80 ± 0.32	51.14 ± 1.29	57.53 ± 1.93	62.78 ± 2.26	71.68 ± 1.29	1.56
Water Extract	36.11 ± 0.30	40.17 ± 1.21	44.66 ± 1.51	53.85 ± 0.60	57.91 ± 0.91	63.68 ± 1.21	3.95
Ascorbic acid	47.81 ± 0.88	57.18 ± 1.32	61.09 ± 0.22	67.50 ± 0.44	71.71 ± 1.54	79.21 ± 2.43	1.21

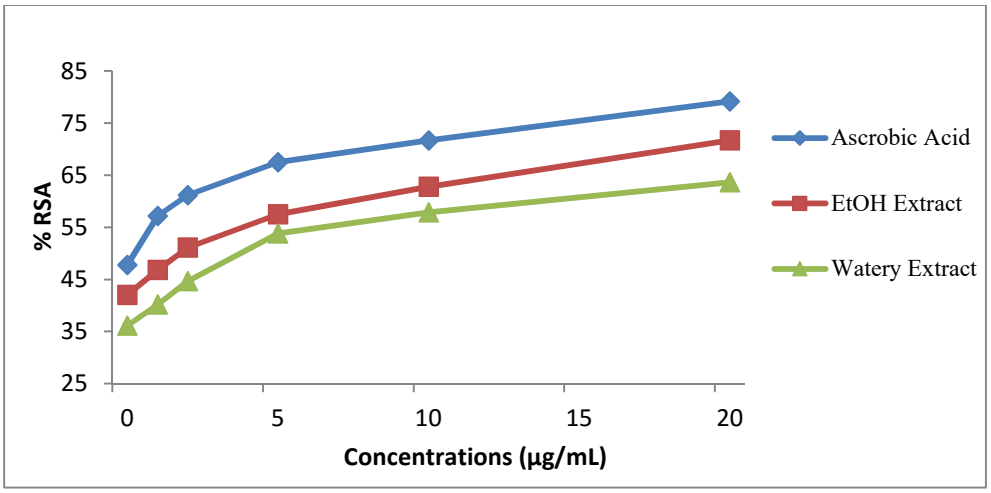

Figure 4 **% RSA vs. concentration of ethanol and watery extracts of (Na-Nwin-Tain-Pyar) rhizomes and standard ascorbic acid**

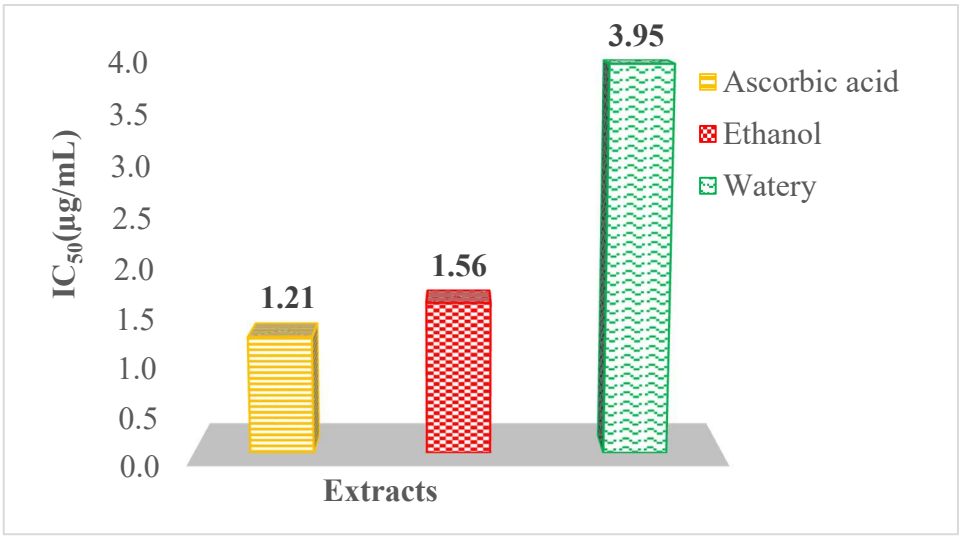

Figure 5 **IC_{50} values ofethanol and watery extracts of (Na-Nwin-Tain-Pyar) rhizomes and standard ascorbic acid**

Antimicrobial Activity of Crude Extracts of (Na-Nwin-Tain-Pyar) Rhizomes by Agar Well Diffusion Method

Screening of antimicrobial activity of crude extracts such as PE, EtOAc, 95 % EtOH and H_2O extracts from (Na-Nwin-Tain-Pyar) rhizomeswere done by agar well diffusion method. In this investigation, the various crude extracts was determined against seven species of microorganisms such as *B. subtilis, S. aureus, P. aeruginosa, B. pumilus, C. albicans* , *E. coli and A. tumefaciens* by using agar well diffusion method. The larger the inhibition zone diameters, the higher the antimicrobial activity.EtOH extract showed high potent antimicrobial activity with the inhibition zone diameter range between (16 ~ 25 mm) against seven microorganisms, whereas it could inhibit for *Agrobacterium* activity with the largest diameter 25 mm (Table 4 and Figure 7). In addition EtoAc extract inhibits all organisms with the same diameter 15 mm. Almost all of PE extract inhibited against all microorganisms except *P.aeruginosa*. However H_2O extract showed low activity on *B. subtilis, P.aeruginosa* and *B. pumilus* with the same diameter 11 mm and inactive against remaining microorganisms. From these findings, it could be concluded that (Na-Nwin-Tain-Pyar) rhizomes could be employed to cure ailment caused by such bacteria.

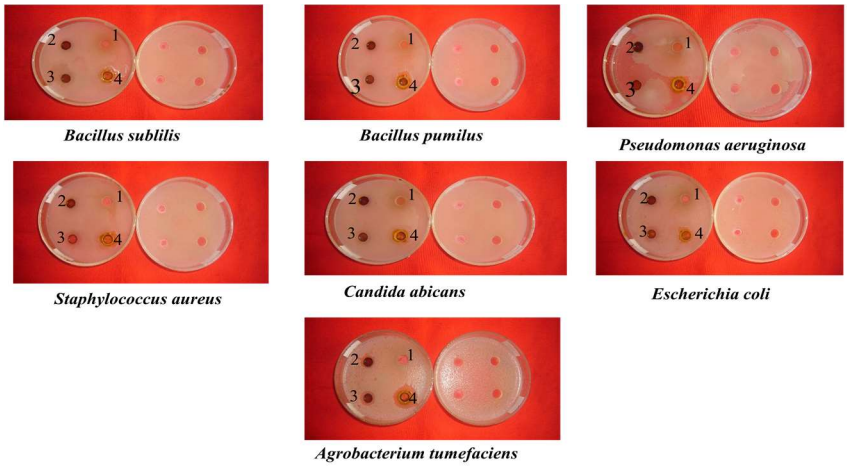

Figure 6 Effect of antimicrobial activity of (1) H_2O, (2) PE, (3) EtOAc, and (4) EtOH extracts from (Na-Nwin-Tain-Pyar) rhizomes on seven microorganisms

Table4 Antimicrobial Activity of Four Crude Extracts from(Na-Nwin-Tain-Pyar) Rhizomes by Agar Well Diffusion Method

No.	Microorganisms	Diameter of inhibition zone (mm)			
		PE extract	**EtOAc extract**	**EtOH extract**	**H_2O extract**
1.	*Bacillus subtilis*	13 (+)	15 (++)	20 (+++)	11 (+)
2.	*Staphylococcus aureus*	14 (+)	15 (++)	20 (+++)	_
3.	*Pseudomonas aeruginosa*	_	15 (++)	16 (++)	11 (+)
4.	*Bacillus pumilus*	14(++)	15 (++)	20 (+++)	11 (+)
5.	*Candida albicans*	14 (+)	15 (++)	18 (++)	_
6.	*Escherichia coli*	14 (+)	15 (++)	17 (++)	_
7.	*Agrobacterium tumefaciens*	14 (+)	15 (++)	25 (+++)	_

Agar Well – 10 mm

10 mm ~ 14 mm	(+)	low activity
15 mm ~ 19 mm	(++)	medium activity
20 mm ~ above	(+++)	highest activity

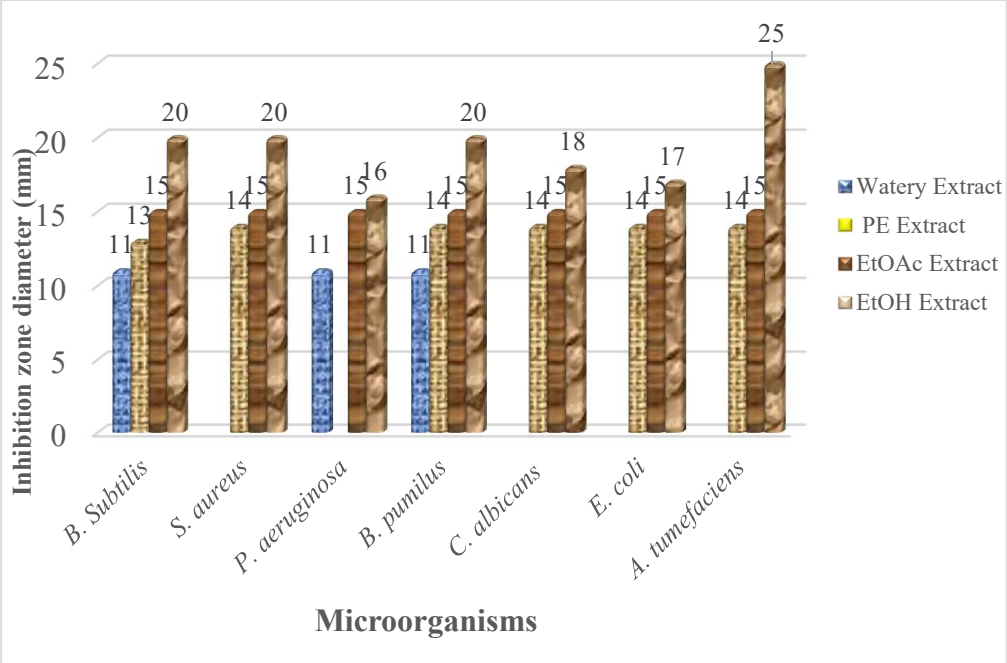

Figure 7 A bar graph of inhibition zone diameters of four crude extracts from (Na-Nwin-Tain-Pyar) rhizomes against seven microorganisms

Antitumor Activity of (Na-Nwin-Tain-Pyar) Rhizomes by Potato Crown Gall Test

The antitumor activity of EtOH and EtOAc extracts of (Na-Nwin-Tain-Pyar) rhizomes were investigated by using PCG test with bacterium *A. tumefaciens*. For inoculation of the potato disc, 48 hr broth cultures containing 5×10^9cells/mL were used. The tested samples were dissolved in DMSO, diluted and mixed with the bacterial culture for inoculated on the cleaned and sterilized potato discs, and incubated for 7 days, at room temperature. After that, the tumors were appeared on potato disc and checked by staining the knob with Lugol's(K_2-KI)solution. In the control, the formation of white knob on the blue background indicated the presence of tumors cells because there is no protein in tumor cells. The activities of test samples did not form any tumors on the potato discs and its surface remained blue. Tumors were counted with the aid of a dissecting scope after staining with Lugol's solution.

From this experiment, it was found that both EtOH and EtOAc extracts of *C. aeruginosa* Roxb. rhizomes were good for preventing the antitumor formation with the dose of 0.1 and 0.15 mg/discin *vitro* potato disc assays. In addition, both EtOH and EtOAc extracts were not significantly inhibited the formation of tumor with the dose of 0.05 mg/disc. The quantitative criteria and results are given as (-) for high inhibition, (+) for less activity and (++) for non inhibition of tumor growth after visual comparison with the control (Table 5 and Figure 8).

Table5 Antitumor Activity of EtOH and EtOAc Extracts of (Na-Nwin-Tain-Pyar) Rhizomes by PCG Test

No.	Test samples	Day	Concentration/disc (mg)		
			0.05	**0.1**	**0.15**
1.	Ethanol Extract	5 days	+	-	-
		7 days	+	-	-
2.	Ethylacetate Extract	5 days	+	-	-
		7 days	+	-	-
3.	Control		++		

Tumor Inhibition: (++) = non activity, (+) = less activity,(-) = high activity

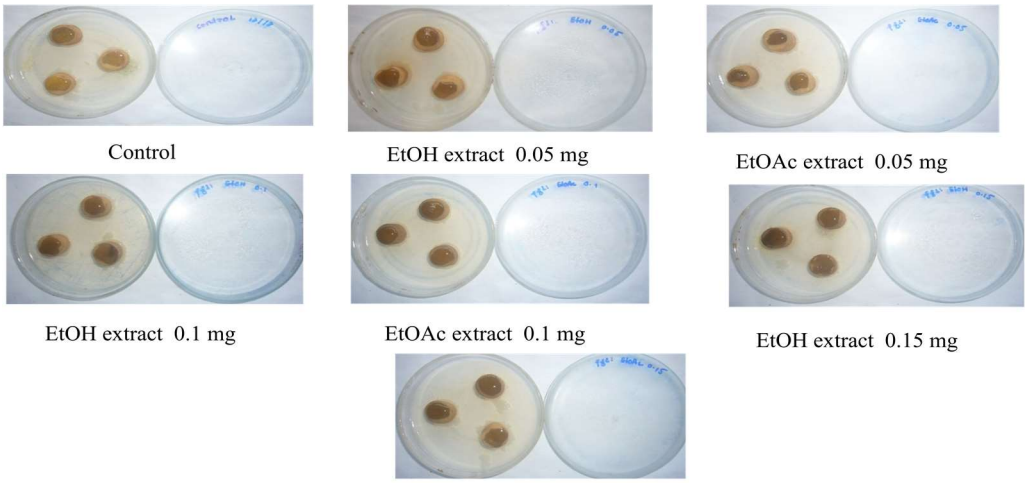

Figure 8 Antitumor screening of EtOH and EtOAc extracts of (Na-Nwin-Tain-Pyar) rhizomes incubated for7 days

CONCLUSION

By the biological activities investigations of *C.aeruginosa* Roxb. rhizome, the following inferences could be concluded.

Preliminary phytochemical screening of (Na-Nwin-Tain-Pyar) rhizomes powder indicated the presence of alkaloids, α-amino acid, carbohydrates, flavonoids, glycosides, phenolic compounds, reducing sugars, starch, steroids, terpenoids, and tannins. However, cyanogenic glycoside and saponin were not detected at the assay conditions. From the screening of the antioxidant activity, ethanol extract (IC_{50}= 1.56 µg/mL) was found to be more potent than watery extract (IC_{50} =3.95 µg/mL).For the determination of the total phenol contents (TPC) of watery and ethanol crude extracts, it was observed that ethanol extract (52.31 ±8.70 µg GAE/mg) was found to be higher than watery extract (16.92 ± 0.20 µg GAE/mg) of (Na-Nwin-Tain-Pyar) rhizomes. In addition, there was a positive correlation between the total phenolic content and antioxidant activity in the selected plant sample. The results indicated that high phenolic provided more potent antioxidant activity.

For the screening of antimicrobial activity of the various crude extracts(PE, EtOAc, EtOH and watery extracts) from (Na-Nwin-Tain-Pyar) rhizomes sample the highest antimicrobial activity was observed in EtOH extract whereas H_2O extract showed minimum activity. Antitumor activity was carried out with EtOAc and EtOH extracts by PCG test. From this experiment, both extracts were found to prevent the tumor formation with the dose of 0.1 and 0.15 mg/disc.

The rhizome of (Na-Nwin-Tain-Pyar) could be applied not only as the local health remedy to the local indigenous but also for the treatment of some bacterial plant pathogen and diseases in agriculture of our country.

ACKNOWLEDGMENT

The authors would like to thank the Department of Higher Education, Ministry of Education, Yangon, Myanmar, for the permission of doing this research and Myanmar Academy of Arts and Science for allowing the writing of this paper. I would like to express my sincere thanks to Dr Daw HlaNgwe (Professor and Head), Department of Chemistry, University of Yangon, for her kind advice, guidance and permission to allow this research work. The authors would like to thank for all from the Department of Chemistry.

REFERENCES

Maw, S. S., Mton M. M. and OoZ. K. (2011). "Study on Antioxidant Activities of Some Herbal Extracts". *World Academy of Science, Engineering and Technology*, vol**51**, pp 450 – 452

Newman, M.F., Lhuillier A., Poulsen A.D. (2004). "A Checklist of the Zingiberaceae of Malasia". *Blumea.,*vol **11**,pp 16-25

Reynertson, K. A. (2007). "*Phytochemical Analysis of Bioactive Constituents from Edible Myrtaceal Fruits*". PhD (Dissertation), New York, the City University

Srivastava S., Dan M.., Rawat A. (2006). "Pharmacognostic Evaluation of *Curcuma aeruginosa* Roxb.". *Nat Prod Sci.,vol* **12**,pp 162-165

Thomas, J., Joy P., sSkaria P. (1998). *Medical Plants*. India: 1st Ed., Kerala, 3-4

WHO. (1991). *Guidelines for the Assessment of Herbal Medicines, Programme on Traditional Medicine*.Geneva:1st Ed, World Health Organization,91-94

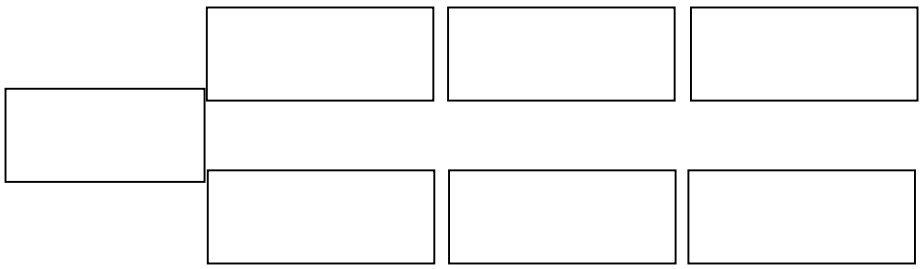

BIOSYNTHESIS OF SILVER NANOPARTICLES BY *SPIRULINA PLATENSIS* AND ITS UTILIZATIONS

Myat Myat Thaw[1], Khin Hla Mon[2], Hla Hla Win[3], Ohn Mar Kyi[4],New Nwe Aung[5]

Abstract

In Myanmar, the natural *Spirulina* is produced from the natural lake of Yae Khar lake. The aim of this research was to prepare silver nanoparticles from *Spirulina platensis* and to study its utilizations in biomedical, waste water treatment and some lotions for cosmetic products. Microalgae are microscopic photosynthesis organisms that are found in both marine and fresh environments. *Spirulina platensis* (blue green algae) plays very important role for health food. Silver nanoparticles were prepared by green synthesis of silver nitrate with spirulina at 50˚C for 3 h and characterized by XRD, SEM, AFM, UV visible spectrophotometer and FTIR techniques. Average crystallite size of silver nanoparticles from spirulina were found to be 23.93 nm by using Debye-Scherrer equation. The antimicrobial activity of silver nanoparticles against both gram positive bacteria (*Bacillus subtilis, Bacillus pumilus, Staphylococcus aureus and* gram negative bacteria *(Escherichia coli and Pseudomonas aeruginosa)* and *Candida albicans* , a fungus strain was done by agar well diffusion method. Among these strains, silver nanoparticles from *Spirulina platensis* on *Escherichia coli* and *Candida albicans* showed the highest antimicrobial activity. Silver nanoparticles were applied for the removal of textile dyes in waste water samples. Utilizations of *Spirulina platensis* and silver nanoparticles were performed for the formulation of face cream and body lotion and their sun protection factors (SPF) were observed to be 11.34 and 8.57. It was observed that these products can be used safely for face cream and body lotion because of the pH value and their characteristics of microbiological parameters (total plate count and yeast and mold count) for the cosmetic products compared with commercial products.

Keywords: Microalgae, *Spirulina platensis*, antimicrobial activity, cosmetic products, waste water

[1] Professor, Dr, Department of Chemistry, University of Yangon
[2] Professor and Head, Dr, Department of Industrial Chemistry, Dagon University
[3] Lecturer, Dr, Department of Chemistry, University of Yangon
[4] Assistant Lecturer, Department of Industrial Chemistry, Dagon University
[5] Lecturer, Dr, Department of Botany, University of Yangon

Introduction

Spirulina is microalgae and found in tropical and subtropical areas at high pH. Spirulina is one of the most important source of medical drugs and cosmetic products as well. It is used as medicine around the world. It contains vitamins especially vitamin A and vitamin C. The natural spirulina is also produced from the natural lake of Yae Khar which is located between Sagaing Hill and Min Wun Hill in Sagaing Region of central part of Myanmar. Yae Khar lake produces natural spirulina which is used in the production of medicines and consumer goods. Spirulina is a blue-green microalgae in alkaline water. It is highly nutritious and actually a total food for human nutrition. Human can survive with spirulina and water without taking any other food (Ghaeni and Roomiani, 2016). The spirulina can be found in the volcanic crater lakes and the natural lakes, having high pH level. Spirulina makes healthy, long life and free from diseases because nearly all vitamins are proportionately present in it.

Green Synthesis

Green chemistry is the designof chemical products and processes that reduce or eliminate the use and/or generation of hazardous substances. Green chemistry can also be described assustainable chemistry. This work aims to focus on development of more convenient methods by using green synthesis for production of eco-friendly, non toxic, and environmental nanoparticles (Mahdieh *et al*., 2012). Green synthesis methods include biological synthesis of nanoparticles by microorganisms and plants, irradiation, polysaccharide. Eco friendly bio-organics in plants extract contain proteins, which act as both reducing and capping agents forming stable and shape controlled silver nanoparticles. The green synthesis of silver nanoparticles involves three main criteria, which must be evaluated based on the green chemistry perspectives, including (1) selection of solvent medium (2) selection of environmentally reducing agent, and (3) selection of nontoxic substances for the silver nanoparticles stability (Mahdavi *et al*., 2013).

Cosmetics

Cosmetics include skin care creams, lotion, powders, perfumes, lipsticks, hair colours, hair sprays and gels, deodorants, hand sanitizers, baby products, bath oils, bubble baths, bath salts, shower cream and many other

types of products. Lotion is applied to external skin with bare hands, a brush, a clean cloth, cotton wool or gauze. While lotion may be used as a medicine delivery system, many lotions, especially hand lotions and body lotions are meant instead to simplify smooth, moisture and soften the skin. These may be used in anti-aging lotions, which can also be classified as a cosmetic in many cases and may contain fragrances. Face cream is applied to the skin to provide a smooth emollient base before the application of face powder and other make-up preparations. The original foundation creams were known as vanishing cream so called because they disappear when rubbed into the skin (Sathish *et al*., 2012).

They are based on stearic acid which is partially saponified with alkali, when the bulk of the acid is emulsified with the soap thus formed. The functions of lotion and cream are to protect the skin against harshness from the environment and any dry conditions of the skin. Manufacturing lotion and face cream can be completed in two cycles: (1) emollient and lubricants are dispersed in oil with blending and thickening agents and (2) perfume, colour and preservatives are dispersed in the water cycle. Active ingredients are broken up in both cycles depending on the raw materials involved and the desired properties of the lotion or cream.

Materials And Methods

Sample Collection of *Spirulina platensis*

The samples were collected from Sagaing June Pharmaceutical and Foodstuff Industry Ltd, Yae Khar Inn, Sagaing Region located at North Latitude 22˚ 02' 57.4" and East Longitude 95˚ 53'17.4". Yae Khar lake produces *Spirulina platesis* naturally (Figure 1).

All experiments and measurements were carried out at the Department of Chemistry, University of Yangon. *In vitro* screening of antibacterial activities of silver nanoparticles from *Spirulina platensis* were carried out by agar well diffusion method against six microorganisms (*Bacillus subtilis, Bacillus pumilus, Staphylococcus aureus, Escherichia coli, Pseudomonas aeruginosa* and *Candida albicans* fungus strain at Pharmaceutical Research Department (PRD), Ministry of Industry, Yangon, Myanmar.

Chemicals

Silver nitrate (BDH), cetyl alcohol, stearic acid, beeswax, olive oil, lanolin, titanium dioxide, triethanolamine, ethanol (HPLC grade) and deionized water were used.

Instruments used in the Characterization of Silver Nanoparticles from *Spirulina platensis*

The silver nanoparticles were characterized by using X-ray diffraction (XRD) (Rigaku Multiflex 2kW X ray diffractometer , Japan), Scanning electron microscopy (SEM) (ZEISS, (Germany), Fourier transform infrared spectrometer (FT IR) (Perkin Elmer 1600), EDXRF Energy dispersive X ray fluorescence Spectrometer Shimadzu EDX 700) and Double beam Shimadzu UV-Vis spectrophotometer (1800) equipped with 1cm quartz cell and computer, Atomic Force Microscope(AFM)(Bruker), N8 Rados (Germany).

Instruments used in the Determination of COD in Waste Water by using Silver Nanoparticles

Lovibond Photometer System MD 200 (Lovibond Water Testing) (Germany) was used to determine Chemical Oxygen Demand (COD).

Apparatus used in the Characterization of Silver Nano Body Lotion and Face Cream

Arsenic Test Kit by Lovibond Tintometer GmbH (Germany), Autoclave, Stomacher (Homogenizer), Colony counter (magnifier-illuminator), 3 M petrifilm aerobic count plate, 3 M yeast and mold count plate, Incubator, and Bunsen burner were used in this work**.** Incubator, and Bunsen burner.

Identification of *Spirulina platensis*

Botanical identification of spirulina sample was confirmed at the Department of Botany, University of Yangon.

Ye Kharr Lake

Figure 1 Location of *Spirylina platensis* in Myanmar

Synthesis and Characterization of Silver Nanoparticles

Dried powder *Spirulina platensis* (5 g) was extracted in 100 mL of deionized water in 250 mL beaker and mixed with 100mL of 1mM silver nitrate solution and adjusted to reach pH 7 and shaken and stirred for 30 minutes in a magnetic stirrer at 100 rpm at room temperature. Supernatant solution was removed and the pellet of this solution was taken and it was concentrated and heated in an oven (Tactical 308, Gallenkamp, England) for 3 hours at 50˚C (Ahmed et al.,2015).

Characterization of Silver Nanoparticles

The synthesized silver nanoparticles were characterized by UV visible spectrophotometer, XRD, SEM, AFM and FT IR analysis for detecting size, structure, shape and morphology.

UV Visible Spectrophotometry

0.01g silver nanoparticles was dissolved in deionized water and mixed with small amount of ethanol and added into the quartz cell and measure the wavelength of silver nanoparticles by UV visible spectrophotometer. The reduction of pure silver ions was recorded by measuring the UV–visible spectrum of the solution at room temperature with a Perkin Elmer Lambda 1234 UV–visible spectrophotometer at the wavelength of 200–800 nm.

Determination of Particle Size of Silver Nanoparticles from *Spirulina platensis* by Atomic Force Microscopy (AFM) and Scanning Electron Microscopy (SEM)

1mg of silver nanoparticles were dissolved in 90% ethanol and dispersed in a sonicator for 30 minutes and put in glass plate and measured the particles size of silver nanoparticles by AFM and SEM.

Antimicrobial Test by using Microorganisms for the Analysis

The *strains* of *Bacillus subtilis*(N.C.T.C-8236), *Bacillus pumilus* (N.C.I.B- 8982), *Candia albicans*, *Staphylococcus aureus* (N.C.P.C-6371), *Pseudomonas aeruginosa* (N.C.T.C-6749) and *Escherichia coli* (N.C.I.B-8134) from Pharmaceutical Research Department (PRD), Ministry of Industry were used in this work. Each strain was incubated in a temperature controlled shaker (1000 rpm) at 30˚C overnight. Antibiotic (amoxicillin) used for the analysis was purchased from Sigma Aldrich, India. Nutrient agar was prepared to culture theses microorganisms. Some plates for each organism were inoculated and four wells (10 mm diameter) were made by using cork borer. First well was made with 100 µL of distilled water. Second well was made with 100 µl of 1mg/mL concentration of silver nanoparticles. Third well was done with 100 µl of 1mg/mL of reference antibiotics (Amoxicillin).The fourth well was done with 100 µL of silver nanoparticles with equal amounts of antibiotics (0.5mg/mL). The plates were incubated for 24 h at 37˚C. The maximum zones of inhibition (in diameter) was determined (Sudha *et al*., 2011).

Determination of Chemical Oxygen Demand in Waste Water

Deionized water (2 mL) was used as a blank. 2 mL of waste water sample was taken and 0.1 g of silver nanoparticles was added into the tubes and mixed with COD reagents and closed tightly and mixed until became hot during mixing for several times and digested these tubes and heated in the reactor for 120 minutes at a temperature of 150˚C .The vials containing the sample tubes were removed from the reactor and allowed to cool down to 60˚C . Then the contents were mixed by inverting each vials for several times before

measuring. Then COD concentration was measured in waste water samples by Lovibond Photometer System MD 200 (Lovibond Water Testing)(Germany).

Preparation of Body Lotion on *Spirulina platensis* and Silver Nanoparticles

Beeswax (1g) was placed in a 250 mL beaker and heated at 50˚C. (2 g) of stearic acid, (10% V/V) of olive oil and 2 g of cetyl alcohol were added into the mixture and then the mixture was stirred at 80˚C for 20 minutes. The oil phase was obtained. Then, *Spirulina platensis* **(**5 g) was dissolved with 100 mL of distilled water and 2g of triethanolamine was added into a 250 mL beaker and stirred for 10 minutes. The water phase was obtained. The water phase was added into the oil phase at 80˚C. The mixture was continuously stirred and cooled to room temperature. After cooling, (2 mL) of fragrance oil was added into the mixture and stirred by using magnetic stirrer at a rate of 410 rpm. The body lotion was formed and filled into a bottle and then packed. Similarly, silver nanoparticles (0.1 g) were used for preparation of body lotion as mentioned above.

Preparation of Face Cream on *Spirulina platensis* and silver nanoparticles

Beeswax (1% wt) was placed in a 250 mL beaker and heated at 50˚C. (9 % wt) of stearic acid, (5% wt) of lanolin, (10% V/V) of olive oil and (0.1% wt) of titanium dioxide were added into the mixture and then the mixture was stirred at 80˚C for 20 minutes. The oil phase was obtained. Then *Spirulina platensis* **(**5 g) was dissolved in distilled water (60 mL), and (2 mL) of triethanolamine were added into a 250 mL beaker and stirred for 10 minutes the water phase was obtained. The water phase was added into the oil phase at 80˚C. The mixture was continuously stirred and cooled to room temperature. After cooling, (2% V/V) of fragrance oil was added into the mixture and stirred by using magnetic stirrer at the rate of 400 rpm. The spirulina face cream was filled into a bottle and then packed. Similarly, silver nanoparticles (0.1 g) for face cream was carried out as mentioned above.

Characteristics Properties of Prepared Body Lotion and FaceCream

Determination of pH

The pH of prepared body lotion and face cream were determined by using digital pH meter (Pen Type pH meter, Range: 0.0-14.0). The glass electrode was first standardized by using standard buffer solution of pH 4 and 7 and the electrode was adjusted to that value. Then, the values of prepared sample were measured with pH meter.

Determination of Some Metals

Ash sample (0.1)g was placed in a 250 mL beaker and 8 mL of concentrated nitric acid were slowly added. The solution was evaporated to dryness and the residue, after cooling, was dissolved in 6 mL of 25 % (v/v) nitric acid solution. The solution was transferred to a 100 mL volumetric flask and the volume was made up to the mark with distilled water. Lead and Arsenic content of these elements in the body and face lotion were determined by the atomic absorption spectrophotometer at Universities' Research Center.

Determination of Arsenic Test Kit by Lovibond Tintometer GmbH

Body lotion and face cream 10 % solution was made by using deionized water and one drops of arsenic reagent (1) , 2 mL of arsenic reagent (2) and 2 mL of arsenic reagent (3) were added in the reagent bottle and kept for 20 min and then arsenic test strips were kept on the reagent and grapped the gas. It did not show the yellow colour. It indicated the absence of arsenic content (Table 4).

Determination of Sun Protection Factor (SPF) of Face Cream by Ultraviolet Spectrophotometry

Sample Preparation for Determination of Sun Protection Factor

0.1g of sample was weighed, transferred to a 100 mL volumetric flask, diluted to volume with ethanol, followed by ultrasonication for 10 min and then filtered through Whatman No1 filter paper and collect the filtrate by rejecting the ten first mL of the filtrate. A 5.0 mL aliquot was taken to 50 mL

volumetric flask and diluted to volume with ethanol. Then a 5.0 mL of the diluted solution was transferred to a 25 mL volumetric flask and the volume made up with ethanol. The absorption spectra of samples in solution were obtained in the range of 290 to 320 nm for every 5 nm, and three determinations by using 1 cm quartz cell, and ethanol as a blank and calculated the SPF values by UV spectrophotometry. The Mansur equation was applied to calculate SPF values (Sudhahar *et al.,* 2013). The SPF of the samples were calculated using the equation (a mathematical expression derived by Mansur) below and the relationship between erythemogenic effect and radiation intensity at each wavelength, (EE X I) was determined as shown below.

$$SPF_{spectrophotometric} = CF \times \sum_{290}^{320} EE\ (\lambda) \times I(\lambda) \times Abs(\lambda)$$

EE – erythemal effect spectrum; I – solar intensity spectrum; Abs - absorbance of sunscreen product; CF – correction factor (= 10). The values of EE x I are constants.

Determination of Moisture Content

The sample (5) g was weighed accurately in a clean and dry moisture dish which was previously weighed. The dish was placed in an oven for 2 hours at 105˚C. The dish was removed from the oven, cooled in a dessicator at room temperature and weighed. The loss in weight of the sample was recorded. Drying, cooling and weighing were repeated until the loss in weight became constant. The moisture content of the sample was calculated as follows.

$$\text{Moisture \%} = \frac{\text{Loss in weight x 100 \%}}{Weigh\ \ of\ sample}$$

Determination of Emulsion Type

The type of emulsion was detected by dispersability of sample in water or oil. 1 g of sample was added into 10 mL of water and stirred. If the sample is oil in water emulsion type, the sample will be soluble in water. On the other hand, water in oil emulsion type is insoluble in oil.

Determination of Total Plate Count and Yeast and Mold Count

2.5g of sample was aspetically weighed into another sterile plastic bag. Each pieces of sample was aspetically cut into pieces in sterile plastic bag. 225mL of phosphate buffer was added and blended for 2 minutes at high speed. Dried film aerobic count plate was placed on flat surface. Top film was lifted and inoculated 1 mL test portion into center on film base.

Top film was carefully put down on inoculums. Test portion was distributed over prescribed growth area with downward pressure in center of plate spreader device. The plate was incubated for 24 hours for determination of total plate count and Coliform Plate for 48 hours at 35℃ was promptly counted after incubation and measured and counted by using colony counter.

Dermatological Test

The dermatological test of spirulina cream and lotion was determined using the open diagnostic patch test. The open patch test was best formed on the sensitive part of the skin like the bend of elbow, popliteal space, the skin behind ears in some instances, skin of the upper eyelid. The suspended cosmetic as actually was applied to 1 inch square of the skin and left uncovered. The subject was instructed not to wash it off or remove it in any other way. The site of the skin was inspected at the end of 6 h and if there was no reaction, the cosmetic may be applied to some sites of the skin. These tests were performed with persons and the results are tabulated in Table 6.

Results And Discussion

Characterization of Silver Nanoparticles by UV Visible Spectroscopy

UV–visible spectroscopy is one of the most widely used techniques for structural characterization of SNPs. Reduction of the silver ion to SNPs during exposure could be monitored by UV visible spectrophotometer. Silver nanoparticles was characterized by UV visible spectrophotometer within the range of 200–800 nm, Figure 3 shows the UV visible spectrum of the nano silver formation and the change in the colour of the reaction mixture turns

brown, indicating in the bio transformation of ionic silver to reduced silver. It is observed that the maximum absorbance was found at 426 nm.

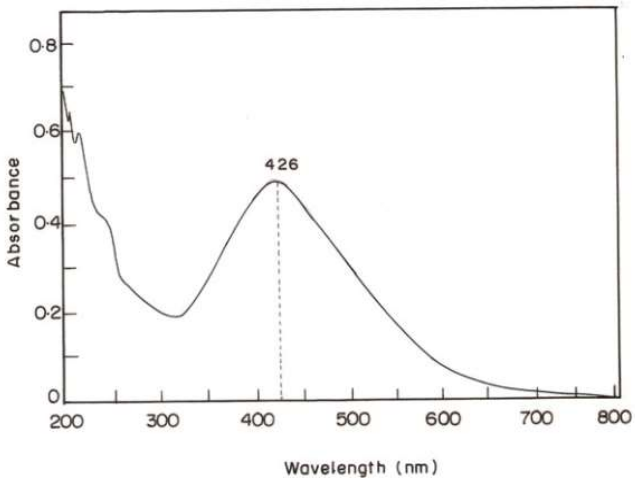

Figure 2 UV spectrum of silver nanoparticles from *Spirulina platensis*

Characterization of Spirulina by Energy Dispersive X-ray Fluorescence(EDXRF) Analysis

Figures 3 shows the EDXRF spectrum of the spirulina. The presence of K_2O, SO_3, P_2O_5, CaO, Fe_2O_3, MnO, ZnO, As_2O_3 and CuO were found in *Spirulina platensis* according to EDXRF data.

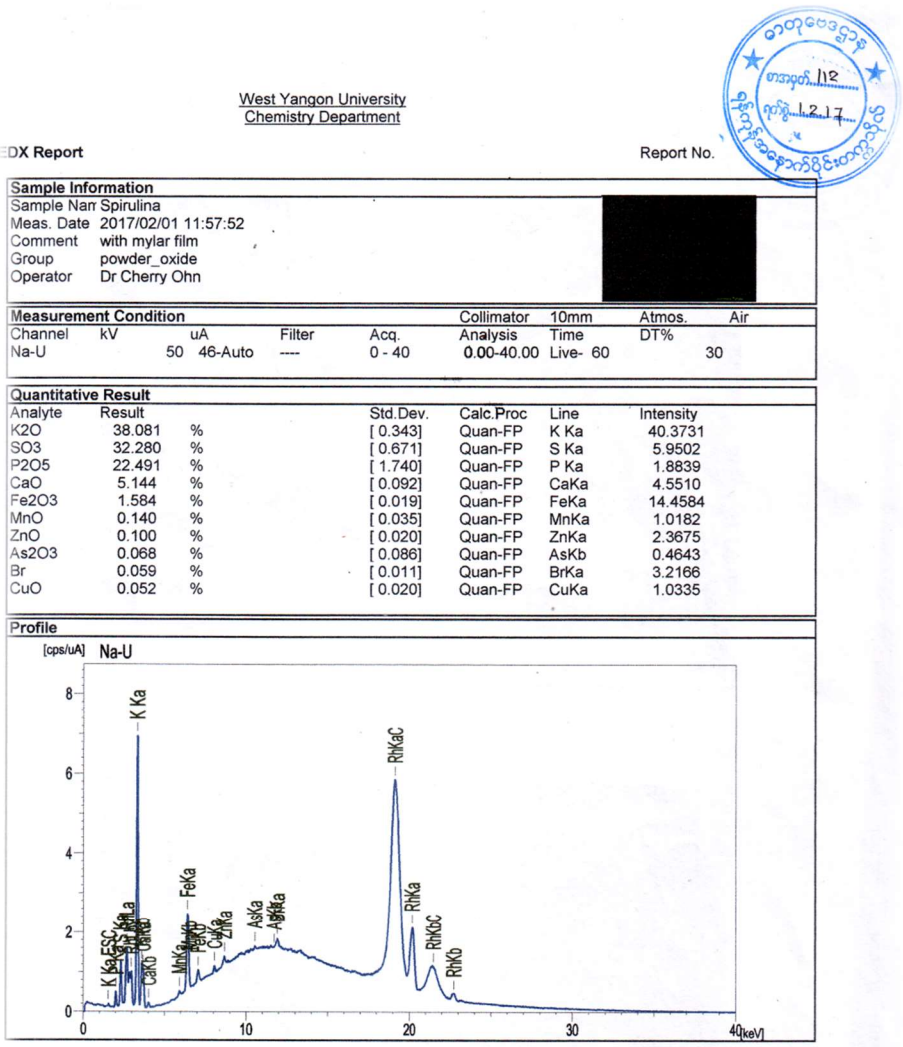

West Yangon University
Chemistry Department

DX Report Report No.

Sample Information

Sample Nam Spirulina
Meas. Date 2017/02/01 11:57:52
Comment with mylar film
Group powder_oxide
Operator Dr Cherry Ohn

Measurement Condition

Channel	kV	uA	Filter	Acq.	Collimator	10mm	Atmos.	Air
Na-U	50	46-Auto	----	0 - 40	Analysis 0.00-40.00	Time Live- 60	DT%	30

Quantitative Result

Analyte	Result		Std.Dev.	Calc.Proc	Line	Intensity
K2O	38.081	%	[0.343]	Quan-FP	K Ka	40.3731
SO3	32.280	%	[0.671]	Quan-FP	S Ka	5.9502
P2O5	22.491	%	[1.740]	Quan-FP	P Ka	1.8839
CaO	5.144	%	[0.092]	Quan-FP	CaKa	4.5510
Fe2O3	1.584	%	[0.019]	Quan-FP	FeKa	14.4584
MnO	0.140	%	[0.035]	Quan-FP	MnKa	1.0182
ZnO	0.100	%	[0.020]	Quan-FP	ZnKa	2.3675
As2O3	0.068	%	[0.086]	Quan-FP	AsKb	0.4643
Br	0.059	%	[0.011]	Quan-FP	BrKa	3.2166
CuO	0.052	%	[0.020]	Quan-FP	CuKa	1.0335

Profile

Figure 3 EDXRF spectrum of *Spirulina platensis*

Characterization of Silver Nanoparticles by X ray Diffraction Analysis (XRD)

Powder X-ray diffraction is one of the powerful techniques for the characterization of core-shell nanoparticles. . It could also be used for calculating mean particle size. It was observed that the sharp peaks of the silver nanoparticles indicated well-defined Miller indices of (111), (200), and (220), these peaks are well matched with standard library data of (PDS 04-0783), and shown in Figures 4 and 5. The required angle at specific counts was presented and scanned the sample with a start angle at 10 ˚C and a stop angle at 70˚C. From the results obtained, the average crystallite size of the nanoparticles was calculated using Debye-Scherrer's formula. The crystal structure of silver nanoparticles was found to be cubic according to lattice parameters (a= b= c= 4.11 Å) and two theta values 37.798, 43.96 and 64.120˚.

$$D = 0.9 \lambda / B \cos \theta$$

where λ is wavelength of copper Kα line (1.546 Å), θ is diffraction angle, Ḃ is full width at half maximum of peak (FWHM), and D is the average crystallite size. It was found that average crystallite size of silver nanoparticles was observed to be 23.93 nm.

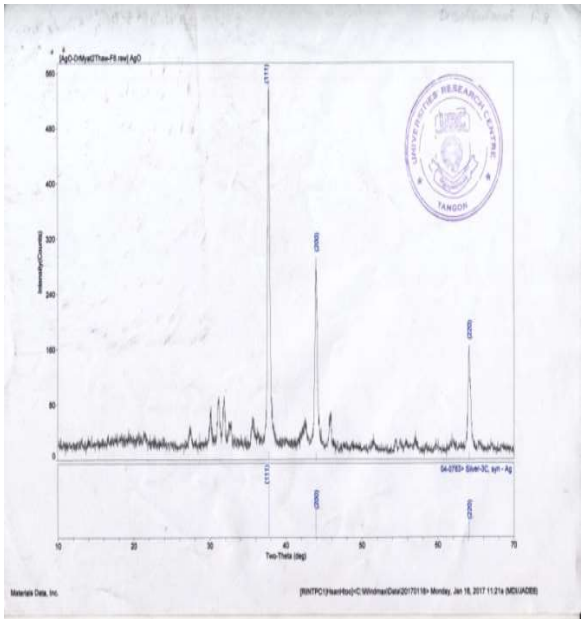

Figure 4 X ray diffractogram of prepared silver nanoparticles

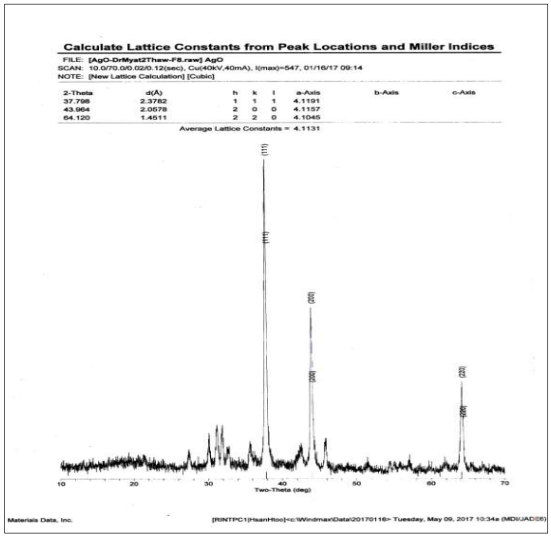

Figure 5 XRD data of silver nanoparticles

Characterization of Silver Nanoparticles by using Scanning Electron Microscope

SEM is important to know the dimensions of the structures fabricated and the materials prepared when characterizing device structures. The scanning electron microscopy results clearly indicate that the formation of spherical silver nanoparticles with its size ranging between 40 nm and 50 nm as shown in Figure 6.

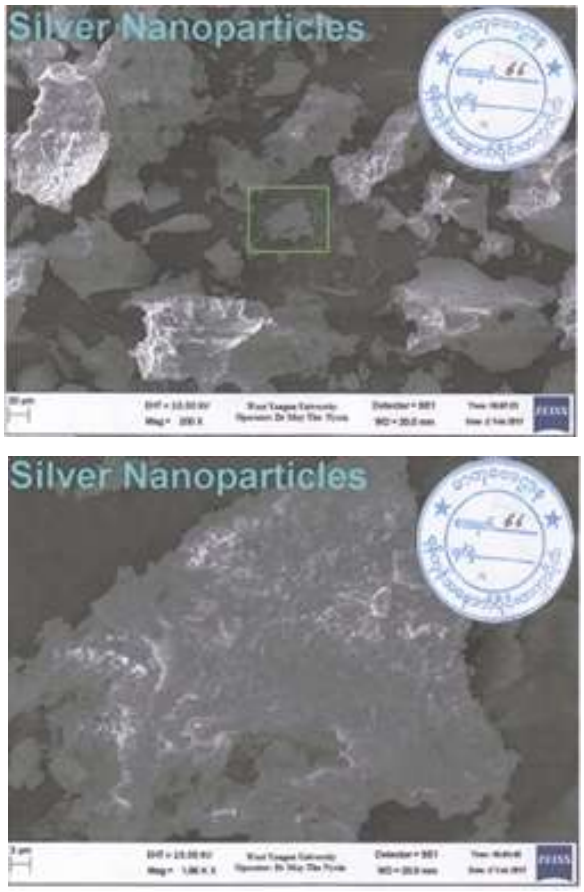

Figure 6 SEM images of silver nanoparticles

Characterization of Prepared Silver Nanoparticles by Atomic Force Microscopy (AFM)

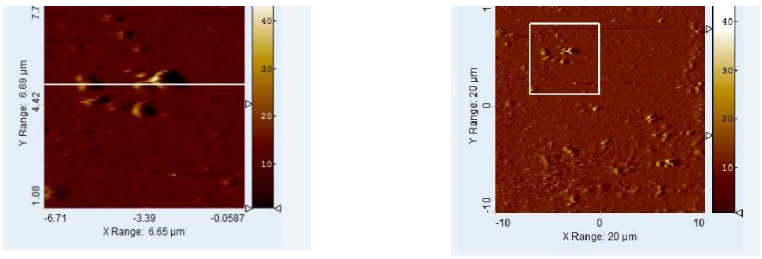

(a) 2 D structure of prepared silver nanoparticles

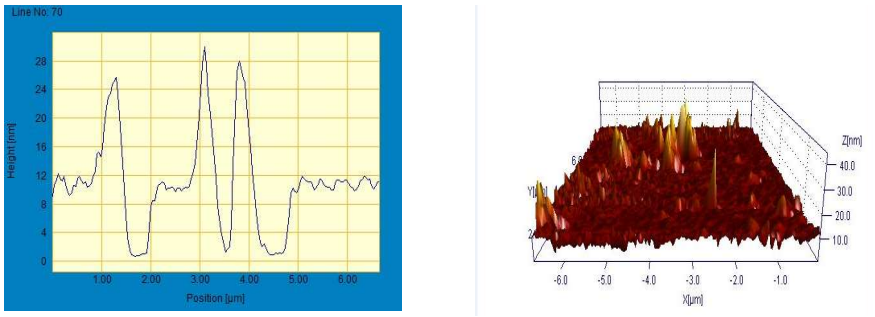

(b) Particle size of silver nanoparticles (c) 3Dstructure of silver nanoparticles

Figure 7 AFM images of prepared silver nanoparticles

In this work, the particle size of silver nanoparticles was determined by Atomic force microscopy. In the 2 D structure, there are some particles on the substrate. It was assessed that the highest particle size was approximately 30.5 nm by looking the colour scale bar as shown in Figure 7 (a). In the 3 D structure, the particles are very small and it was observed that the highest particle size is 30. 5 nm. It shows that the prepared silver nanoparticles was within the nano range by AFM(Figure 7 b and c). This method is capable of ultra-high resolution for particle size measurement by using AFM, quantitative

information regarding individual nanoparticles and groups of particles such as size (length, width, and height), morphology, and surface texture can be evaluated. The size and shape of metal nanoparticles are typically measured by analytical techniques atomic force microscopy (AFM). AFM is used to study the morphology of nanoparticles. Unlike SEM and TEM, AFM produces three-dimensional images so that particle size and height can be assessed.

Characterization of Silver Nanoparticles by using FT IR Analysis

In this work, the prepared silver nanoparticles from *Spirulina platensis* were characterized by FT IR technique**.** FT IR technique was used for evaluation the type of organic and inorganic complexes in plants. The infrared spectrum shows a frequency ranges from 3500-3200 cm^{-1} representing the O-H stretching vibration, presence of alcohol, phenol. The frequency ranges from 3000- 2800 cm^{-1} peaks are representing aliphatic C-H stretching vibration present in alkenes. The bands at 1634 and 1651cm^{-1} represent in the C=C stretching vibration present in the alkenes. The bands at 1084 and 1041cm^{-1} may be due to the C-N stretching due to, presence of C-H aliphatic amines. The bands at 447 and 410cm^{-1} may be assigned due to the metal oxygen bond and shown in Table 1 and Figure 8.

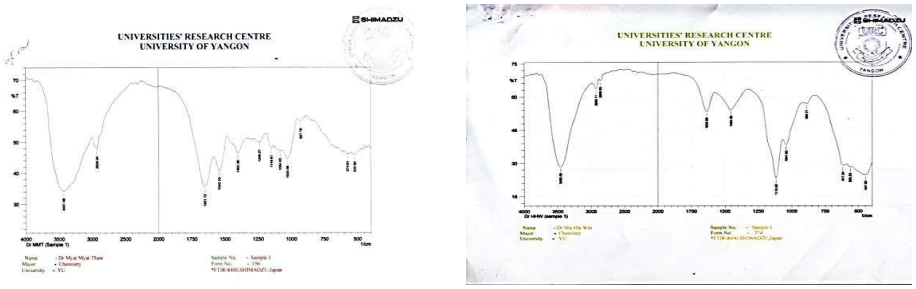

Figure 8 FT IR spectra of prepared silver nanoparticles

Table 1 FT IR Data of Prepared Silver Nanoparticles

Wave number			
Observed Value for spirulina(cm^{-1})	Observed Value for silver nanoparticles (cm^{-1})	Literature Value (cm^{-1})*,**	Assignments
3431	3458	3560-3500	OH Stretching vibration, presence of carbohydrate and amino acids
2928	2926	2925-2875	Aliphatic C-H stretching vibration (ester and amino acids)
1651	1634	1680-1640	C= C stretching vibration present in the alkenes
1084	1041	1020	C-N stretching, presence of C-H aliphatic amines
532	563	515	C-H stretching vibration presence of alkyl halides compounds
	447	410	Stretching vibration of Ag-O bond

* (Ali *et al*.,2015)
** (Ahmed *et al*., 2015)

Antimicrobial Activity of Spirulina Prepared Silver Nanoparticles

The antimicrobial activities of spirulina and silver nanoparticles were tested by using six microorganisms. Silver nanoparticles showed a characteristic inhibition zone of 23.06 mm and 28.19 mm diameter against *Bacillus subtilis*, 18.50 mm and 23.29 mm against *staphylococcus aureus*, 20.87 mm and 28.05 mm against *Pseudomonas aeruginosa*, 15.90 mm and 21.43 mm against *Bacillus pumilus*, 35.06 mm and 49.49 mm against *Candida albicans* and 31.70 mm and 38.98 mm against *E coli* respectively. Among

these strains, it was observed that *E coli* and *Candida albicans* are found the higher inhibition zone when silver nanoparticles . These results refer the sensitivity of the microbial species towards the nanoparticles for 100 µg MIC (minimum inhibitory concentration) and shown in Table 2 and Figures 9 and 10.

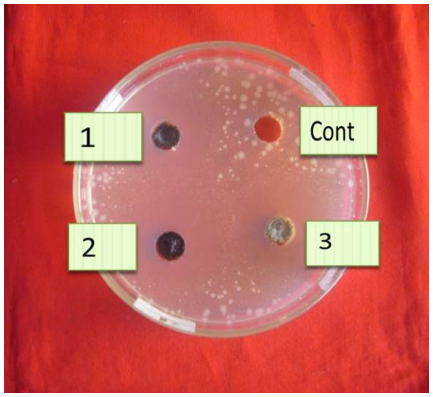

(a) *Bacillus subtilis*

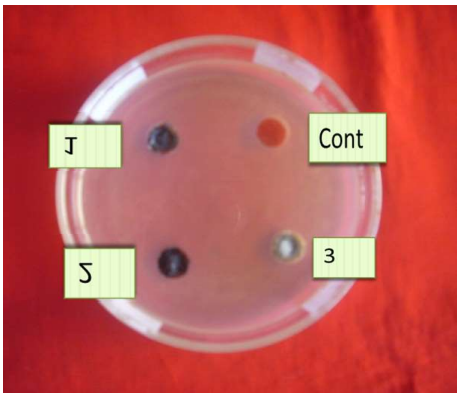

(b) *Staphylococcus aureus*

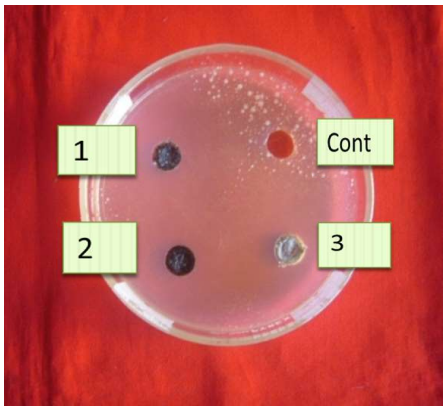

(c) *Pseudomonas aeruginosa*

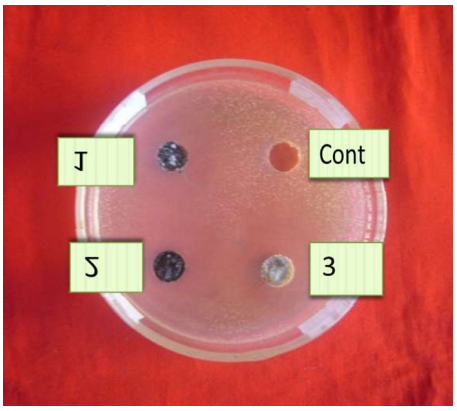

(d) *Bacillus pumilus*

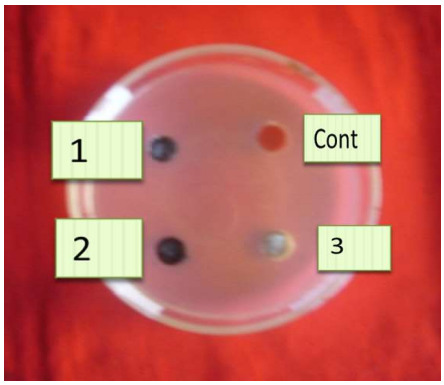

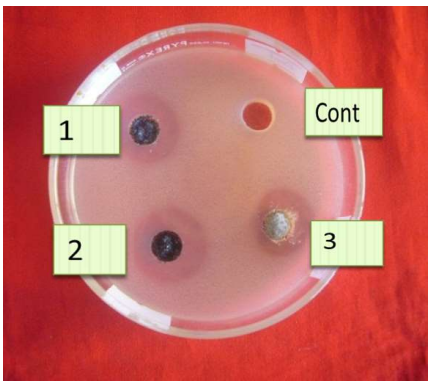

(e) *Candida albicans* (f) *Escherichia coli (E coli)*

Figure 9 Inhibition zone produced by (a), (b), (c), (d), (e) and (f)

Table 2 Comparison of Maximum Inhibition Zone Diameter of *Spirulina platensis* and Prepared Silver Nanoparticles against Six Microorganisms

Sample	**Diameter of inhibition zone (mm) against six microorganisms** *Bacillus subtilis*	*Staphylococcus aureus*	*Pseudomonas aeruginosa*	*Bacillus pumilus*	*Candida albicans*	*E coli*
Spirulina	23 (+++)	18 (+++)	20 (+++)	15 (++)	35 (+++)	31 (+++)
Silver nanoparticles from spirulina	28 (+++)	23 (++)	27 (+++)	21 (+++)	49 (+++)	38 (+++)
Control	10	10	10	10	10	10

Agar well- 10 mm
10 mm – 14 mm (+)
15 mm – 19 mm (++)
20 mm above (+++)

Organisms
1) *Bacillus subtilis* (N.C.T.C- 8236)
2) *Staphylococcus aureus* (N.C.P.C-6371)
3) *Pseudomonas aeruginosa* (N.C.T.C-6749)
4) *Bacillus pumilus* (N.C. I.B-8982)
5) *Candida albicans*
6) *E coli* (N.C.I.B-8134)

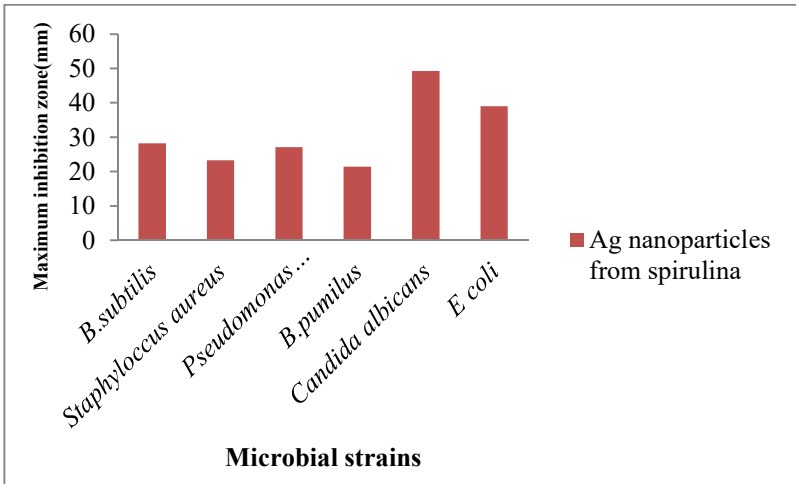

Figure 10 Maximum inhibition of silver nanoparticles from *Spirulina platensis*

Application of Silver Nanoparticles for the Colour Removal of Textile Dyes in Waste Water Samples

Figure 11 shows the presence of dye in waste water samples before and after treatment with silver nanoparticle. It can be seen clearly that colour of the dye solutions decreased gradually after treatment with silver nanoparticles. It was found that absorbance of these sample solutions decreased significantly after treatment with silver nanoparticles Figures 11 and 12.

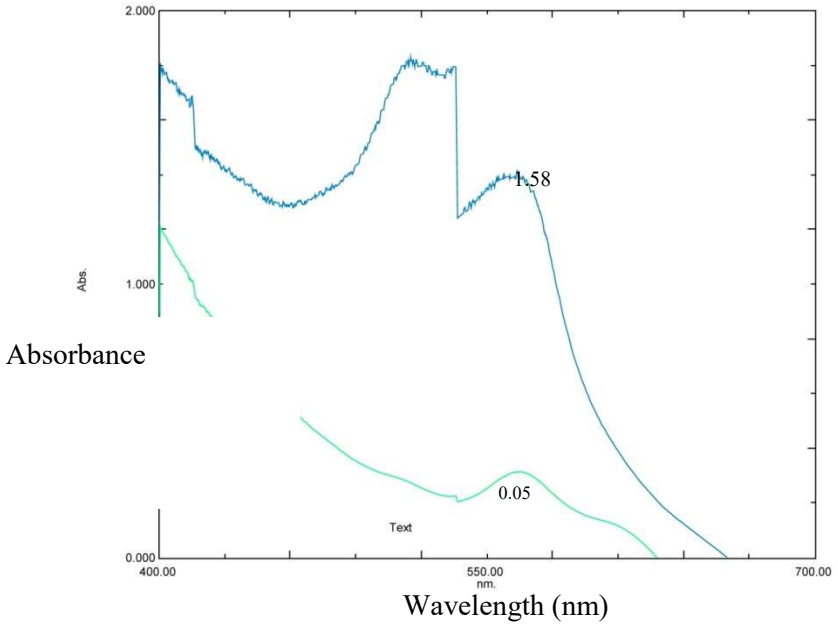

Figure 11 Absorption spectrum of dye waste water sample

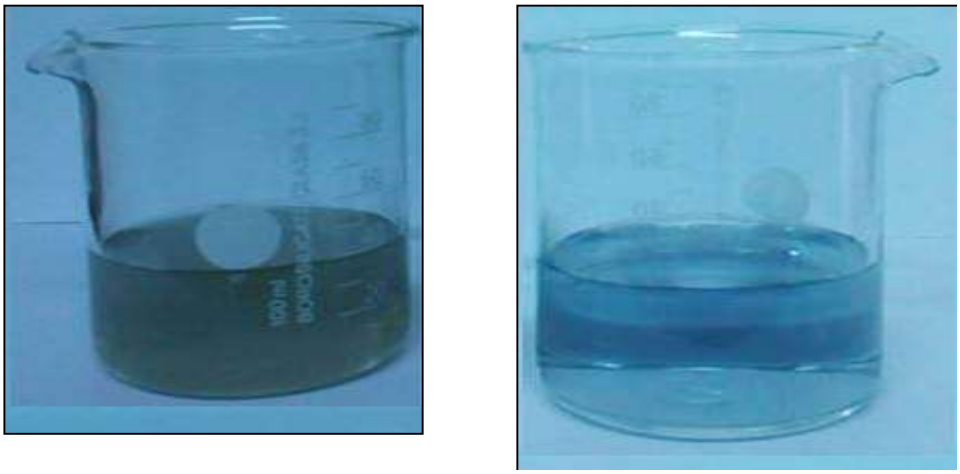

Figure 12 Photograph of dye waste water sample (a) before treatment (b)after treatment with silver nanoparticles for 2 hours

Treatment of Waste Water from Wundwin, Meiktila District by *Spirulina platensis* and Prepared Silver Nanoparticles

Table 3 shows the values and percentage of COD values in waste water treatment with *Spirulina platensis* and silver nanoparticles. It was found that chemical oxygen demand (COD) observed to be 55.5 mg/L by spirulina and 44.8 m/L by silver nanoparticles in the first day and increased to reach 74.35 % and 89.99 % in the 7 day. It showed good efficiency on the reduction of COD from waste water during the treatment period. Prevention and treatment of dyeing wastewater pollution are complementary. The higher the chemical oxygen demand, the higher the amount of pollutant in the water sample. However, COD is considered one of the important quality control parameter of an effluent in wastewater treatment.

Table 3 COD in Waste Water Samples from Wundwin Textile Factory

Sample		COD (mg/L)/Days				Treated with Spirulina and Silver nanoparticles Reduction after 7 days
		1	3	3	7	
Spirulina	85	55.5	42.30	30.8	21.80	74.35 %
Silver nanoparticles from spirulina	85	44.8	35.20	23.8	8.58	89.90 %

Application of Silver Nanoparticles by Body Lotion and Face Cream

The most favorable condition for the ingredients of prepared spirulina lotion and silver nano skin lotion were successfully achieved in this work. Quality and hazard of characteristics of spirulina and silver nano skin lotions were investigated by determining pH, moisture, total plate count, yeast and mold, emulsion type, lead and arsenic . These results are shown in Table 4.

Table 4 Characteristics of Body Lotion and Face Cream Prepared by Silver Nanoparticles

Sr. No.	Characteristics	Experimental Values	
		Silver nano body lotion	Silver nano face cream
1.	pH	6.8	7
2.	Moisture (%)	6	8
3.	Total Plate Count (cfu/g)	$<10^3$	$<10^3$
4.	Yeast and Mold (cfu/g)	$< 10^2$	1×10^3
5.	Emulsion	Water-in-oil	Water-in-oil
6.	Lead	ND	ND
7.	Arsenic	ND	ND
8	Free Alkali	ND	ND

ND = not detected
cfu = coliform unit

Sun Protection Factor (SPF) of Face Cream by Ultraviolet Spectrophotometry

In this research, two different commercial available sunscreen products (Nivea body lotion and Nivea face cream) were studied by UV spectrophotometry by using Mansur mathematical equation. The SPF labeled values were in the range of 8 to 30 according to literature values (Sudhahar and Balasubramaniam,2013). The prepared silver nanoparticles and commercial products are shown in Table 5. It can be observed that the SPF values found for the prepared silver nanoparticles are lower than labeled SPF in the commercial product. These data variations can be due to the various reasons like the type of emulsion used for the formulations, and the emulsion properties, for the use of different solvents in which the sunscreens are dissolved.

Table 5 Observed and Labeled SPF in the Prepared Silver Nanoparticles

Samples	SPF		
	Observed SPF	Labeled SPF	Literature values*(SPF)
Nivea body lotion (Germany)	20.114	30	(8- 30)
Plate snail body lotion (Thailand)	21.54	50	
Nivea face cream	39.11	30	
Silver Nanoparticles for face cream	*11.344*		
Silver nanoparticles for body lotion	*8.579*		

**(Abreu et al., 2004)*

The SPF is

Sample –Face Cream (SPF content) λ – (290~320nm)
Value of EE (λ) x 1(λ) x Abs (λ)
At 290nm
EE (290nm) x 1 (290nm) Abs (290nm) = 0.0150 x 0.926 = 0.0138
At 295 nm
EE (295 nm) x 1 (295 nm) x Abs (295 nm) = 0.0817 x 0.805 = 0.0657
At 300 nm
EE (300 nm) x 1 (300 nm) x Abs (300 nm) = 0.2874 x 0.664 = 0.1908
At 305 nm
EE (305 nm) x 1 (305 nm) x Abs (305 nm) = 0.3278 x 0.536 = 0.1757
At 310 nm
EE (310 nm) x 1 (310 nm) x Abs (310 nm) = 0.1864 x 0.420 = 0.0782
At 315 nm
EE (315 nm) x 1 (315 nm) x Abs (315 nm) = 0.0837 x 0.314 = 0.0262
At 320 nm
EE (320 nm) x 1 (320 nm) x Abs (320 nm) = 0.0180 x 0.229 = 0.0041
SPF = C x $\sum_{290}^{320} EE$ (λ) x 1 (λ) x Abs (λ)

= 10 (0.0537+.0.2214+0.1015+0.3966+0.2013+0.082+0.0144)
= 10 x 1.0826
= 11.3445

SPF of Face cream = 11.3445

Dermatological Test for body lotion was performed with 10 girls practically. It was observed that there is no irritation on these girls by using these lotions Table 6.

Table 6 Dermatological Test for Lotion on Spirulina and Silver Nanoparticles

Size of skin = 1 square inch
Testing time = 2 hours

Sr. No.	Males/ Females	Age (years)	Observation
1.	female	23	no irritation
2.	female	23	no irritation
3.	female	23	no irritation
4.	female	23	no irritation
5.	female	22	no irritation
6.	female	22	no irritation
7.	female	22	no irritation
8.	female	22	no irritation
9.	female	22	no irritation
10.	female	22	no irritation

Dermatological tests were performed with ten girls.

Conclusion

In this work, silver nanoparticles were synthesized by using method of green synthesis. This method provides an environmental friendly, simple, and efficient technique for the preparation of silver nanoparticles. From the technological point of view, silver nanoparticles have potential applications in the biomedical field and some advantages of cosmetic products for commercial production. *Spirulina platensis* was used as starting materials and capping agent. After the calcination at 500˚C for 3 hours, silver nanoparticles became the crystalline nature. Average crystallite size of silver nanoparticles was found to be 23.93 nm by using Debye-Scherrer equation. The highest antimicrobial activity of silver nanoparticles was observed on *Candida albicans* and *E coli* strains. Silver nanoparticles can reduce the COD content in waste water from Textile Factory. It can be clearly seen that colour of the textile dyes solution decreased significantly after treatment with silver nanoparticles for 2hours. The most suitable amounts of ingredients for preparation of face cream and body lotion by using spirulina platensis and silver nano body lotion and face cream were achieved and obtained as one of the cosmetic products (body lotion and face cream). Sun protection factor on face cream and body lotion was determined, and observed to be 11.34 and 8.579. The prepared face cream and body lotion have no skin irritation effect, and lead, free alkali and arsenic are in this product from for 2 months to till now. There is no hazard for human being according to the microbial profiles of all prepared skin lotion. Therefore, microbiological testing is essential to ensure the quality and integrity of the products. These applied research work shows that one of the cosmetic products (body lotion and face cream) by using silver nanoparticles was successfully achieved for applications.

Acknowledgements

The authors would like to thank deep appreciation to Rector Dr Pho Kaung, University of Yangon and Dr Hnin Hnin Aye, Professor and Head, Department of Chemistry, University of Yangon for allowing this paper and also special thanks to Department of Medical Research, Ministry of Health and Sports for giving this opportunity of external grant and the Myanmar Academy of Arts and Science for allowing to read at the 17th Research Conference, Yangon ,Myanmar.

References

Abreu,D.E., Oliveira,D.A, Hackmann, E.R and M.I.Santoro, (2004) " Determination of Sun Protection Factor (SPF) of Sunscreen by Ultraviolet Spectrophotometry." *Journal of Pharmaceutical Sciences*, Vol. 40, pp.381-385.

Ahmed, A.E., H. Ekhal Hafez Abdel, F. Amel M. Ismail, M.elsonbaty Sawsan, and S. Heba Abbas, A. Raw Heya, E.Salah Din, (2015) " Biosynthesis of Silver Nanopartilces by *Spirulina platensis* and Nostoc Sp." *Global Advanced Journal of Microbiology*, Vol. 4 (4), pp. 036-049.

Ali, M.I.,Sharma,G., Kumar, M. and Dut Jasuja,N. (2015) " Biological Approach of Zinc Oxide Nanoparticles Synthesis by Cell Free Extract of *Spirulina platensis*." *International Journal of Current Engineering and Technology*, Vol.4, pp. 35-39**.**

Ghaeni, M., and Roomiani, (2016) " Review for Application and Medicine Effect of Spirulina, *Spirulina platensis* Microalgae." *Journal of Advanced Agricultural Technologies*, Vol. 3, pp. 114-117.

Madhieh, M., A. Zolanvari and A.S. Azimee, (2012) " Green Biosynthesis of Silver Nanoparticles by *Spirulina platensis*." *Scientia Iranica* F. (1993), pp.926-929.

Mahdavi,M., Namvar.F, Ahmad. M.B, and Mohamad. R. (2013). "Green Biosynthesis and Characterization of Magnetic Iron Oxide (Fe3O4) Nanoparticles using Seaweed (Sargassummuticum) Aqueous Extract". *Journal of molecules*, Vol.18,pp.5954-5964.

Sathish.S., C. Mahesh, D.Saikat, D.S.B. Lavanyav, (2012) " Preparation and Evaluation of Salicylic Acid and Medicated Lipstick." *Journal of Advacned Pharmaceutical Sciences*, Vol. 2. pp. 254- 261.

Sudha. S. S., R. Karthic, J. Rengaramanujam and Athulya, (2011) " Antimicrobial Activity of *Spirulina platensis* and Aphanothece sp.on Selected Clinical Bacterial Isolate and its Antioxidant Activity." *South Ase. J.Biol. Sci.* Vol. 1(2), pp. 87-98.

Sudhahar,V., and V. Balasubramanian, (2013) " Sun Production Factor (SPF), Determination of Marketed Suncreen Formulation by *In- Vitro* Method using UV-Visible Spectrophotometer." *Archives of Applied Science Research*, Vol. 5(6), pp.119-122.

STRUCTURE ELUCIDATION OF BIOACTIVE ORGANIC COMPOUND ISOLATED FROM MYANMAR INDIGENOUS MEDICINAL PLANT, *Vitis latifolia* Roxb.

Khin San Win[1], Thinn Myat Nwe[2], Myint Myint Sein[3]

Abstract

In this research, *Vitis latifolia* Roxb., which is one of the Myanmar indigenous medicinal plants known as Chin taung mwe soke was selected for chemical analysis. Firstly, preliminary phytochemical screening of the tuber of Chin taung mwe soke was carried out, which indicated the presence of alkaloid, flavonoid, glycoside, phenol, polyphenol, sugar, saponin, sterol and terpene. The antimicrobial activity of crude extracts in various solvent systems of the tuber of Chin taung mwe soke was determined by agar well diffusion method on six selected organisms. Furthermore, a pure compound was isolated from the tuber of Chin taung mwe soke as needle shape crystal by Thin Layer and Column Chromatographic methods. The yield percent of this compound was found to be 0.61 % (21 mg) based upon the ethyl acetate crude extract and the melting point was (198-199°C). This pure compound gave positive for sterol test. Moreover, antimicrobial activity of this pure compound was rechecked by using agar well diffusion method. In addition, the molecular formula of pure compound could be determined as applying some spectroscopic methods such as FT IR, ^{1}H NMR, ^{13}C NMR and EI mass spectral data. The complete structure of steriodal derivative compound was elucidated by DQF-COSY, HMQC, HMBC and DEPT spectroscopic method. Finally, the conformational analysis of an organic compound was carried out by using ^{1}H NMR splitting patterns, coupling constant, NOESY spectral data and model studies. The structure of the isolated compound was elucidated as 10, 11, 15-trimethyl-17-(3-methylnona-2-yl)-2, 3, 4, 7, 8, 9, 10, 11, 12, 13, 14, 15, 16, 17-tetradecahydro-1H-cyclopenta [a] phenanthren-3-ol.

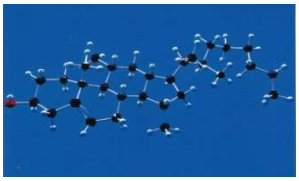

Keywords : *Vitis latifolia* Roxb., antimicrobial activity, agar well diffusion method, spectroscopic techniques

[1] Associate Professor, Dr, Department of Chemistry, Yadanabon University
[2] Associate Professor, Dr, Department of Chemistry, Mandalay University of Distance Education
[3] Professor and Head (Rtd), Dr, Department of Chemistry, University of Mandalay

Introduction

Medicinal plants are integral part of nature. Plants contain natural substances that can promote health. Plants produce a diverse range of bioactive molecules making them rich source of different types of medicine. Most of the drugs today are obtained from natural sources or semi synthetic derivatives of natural products. A medicinal plant is any plant which, in one or more of its organ, contains substance that can be used for therapeutic purpose or which is a precursor for synthesis of useful drugs.

Myanmar is rich in varieties of medicinal plants. Medicinal plants constitute an important natural wealth of a country. They play a significant role in providing primary health care services to rural people. They serve as therapeutic agent as well as important raw materials for the manufacture of traditional and modern medicine. Natural products are rich source of bioactive compounds and play an important role in the development of new drugs (Sofowara, 1982)

One Myanmar indigenous medicinal plant, *Vitis latifolia* Roxb. is widely distributed in Pyin Oo Lwin Township, Mandalay Region. According to Myanmar traditional medicine, it is medicinally used as tuberculosis, ulcer, breast cancer, bone fractures, antidote for snake poison (Ah Shin Nagathein, 1983).

Vitis latifolia Roxb may be a great natural source for the development of new drugs and may provide a cost-effective mean of treating cancers and other diseases in the developing world. So, *Vitis latifolia* Roxb. was selected for isolation of compound and its structure elucidation. The aim of the present research work is to elucidate the structure of bioactive pure organic compound isolated from the tuber of *Vitis latifotlia* Roxb.

Botanical Description

Botanical name - *Vitis latifolia* Roxb.
Family - Vitaceae
English name - Wild Grape
Myanmar name - Chin taung mwe soke
Habit - a large woody climber
Parts used - Tuber

Figure 1. The tuber of V. *latifolia*

Medicinal Uses

The tuber of V. *latifolia* is used to cure, tuberculosis, ulcers, breast cancer, bone fractures and antidote for snake poison. Root powder is boiled with mustard oil and used for massage in rheumatic pain. Infusion of the whole plant is taken in liver and renal complaints. Juice of crushed root is taken orally to stop excess urination mixed with blood.

Materials And Methods

Instrument

UV-lamp, FT IR Spectrophotometer, ^{1}H NMR Spectrophotometer (500 MHz), ^{13}C NMR Spectrophotometer (125 MHz) and EI-mass Spectrophotometer.

Materials

Commercial grade reagents and solvents were used after distillation. Analytical preparative thin layer chromatography was performed by using precoated silica gel (Merck Co. Inc, Kiesel gel 60 F_{254}). Silica gel (Merck Co. Inc, Kiesel gel 70-230 Mesh ASTM) was used for column chromatography. Iodine vapor and UV detector were used for visualizing the compound on TLC plates.

Collection and Preparation of Sample

Chin taung mwe soke, one of the effective medicinal plants was collected from Pyin Oo Lwin Township, Mandalay Region, Myanmar. The tuber of sample was cut into small pieces and allowed to air-dry for one month. The cut-dried pieces were stored in a well-stoppered bottle and used throughout the experiment.

Preliminary Phytochemical Screening of the Tuber of V. *latifolia*

Phytochemical screening on the tuber of V. *latifolia* was performed in order to know the presence of general classes of phytochemical constituents in the plant sample. (Harborne, 1984) The results are shown in Table (1).

Determination of Antimicrobial Activity on the Tuber of V. *latifolia*

Antimicrobial activity of the crude extract of the tuber of V. *latifolia* were tested in various solvent (n-hexane, ethyl acetate and ethanol) by using agar well diffusion method on six selected organisms at PFRD (Pharmaceutical and Food Research Department), Ministry of Industry, Yangon.

Extraction and Isolation of Pure Compound

Air dried sample (700 g) was percolated with ethanol (3 L) for about two months. The ethanol extract was filtered and concentrated. It was extracted with ethyl acetate (125 mL) and evaporated. The ethyl acetate crude sample (3.42 g) was obtained. It was fractionated by column chromatography over silica gel (70-230 mesh) eluting with various volume ratios of n-hexane and ethyl acetate from non-polar to polar. Totally 191 fractions were obtained. Each fraction was checked by TLC and combined the fractions with same R_f value. Finally, nine combined fractions were obtained.

The combined fraction (C) gave only one spot on TLC. The R_f value is 0.42 (7 : 3 v/v, n-hexane : EtOAc). Then this fraction was purified by recrystallization with n-hexane and ethyl acetate solution (4 : 1 v/v, n-hexane : EtOAc). After recrystallization, needle shape crystal (21 mg) was obtained. The yield percent of this pure compound was found to be 0.61 % based upon the ethyl acetate crude extract.

Determination of Melting Point of Pure Compound

The compound was inserted into the capillary tube and melting point was determined by using SMP 30 ADV melting point apparatus (UK) at Department of Chemistry, University of Mandalay.

Determination of Antimicrobial Activity of Pure Compound

Antimicrobial activity of pure compound was tested by using agar well diffusion method on six selected organisms at PFRD (Pharmaceutical and Food Research Department), Ministry of Industry, Yangon.

Results and Discussion

Preliminary Phytochemical Screening of the Tuber of V. *latifolia*

According to the results of phytochemical screening, the tuber of V. *latifolia* contained alkaloid, flavonoid, glycoside, phenol, polyphenol, sugar, saponin, sterol and terpene. (Table 1)

Table 1. Results of Phytochemical Screening of the Tuber of V. *latifolia*

No.	Constituents	Reagent used	Observation	Results
1	Alkaloid	Wagner's reagent	Brown ppt	+
2	Flavonoid	EtOH, Conc: HCl, Mg turning	Pink colour solution	+
3	Glycoside	10 % lead acetate	Yellow ppt	+
4	Phenol	10 % $FeCl_3$ solution	Brown colour solution	+
5	Polyphenol	EtOH, 1 % $FeCl_3$, K_3 [$Fe(CN)_6$]	Greenish blue colour solution	+
6	Sugar	Benedict's solution	Brick red ppt	+
7	Saponin	EtOH, Conc: H_2SO_4	Frothing	+
8	Sterol	Petether, acetic anhydride, Conc: H_2SO_4, $CHCl_3$	Greenish blue colour solution	+
9	Terpene	EtOH, acetic anhydride Conc: H_2SO_4, $CHCl_3$	Reddish brown colour solution	+

(+) = presence

(–) = absence

Antimicrobial Activity of the Tuber of V. *latifolia*

As the results of activity tests, the ethyl acetate crude extract of the tuber of V. *latifolia* responded to high activity on all selected organisms such as *Bacillus subtilis, Staphylococcus aureus, Pseudomonas aeruginosa, Bacillus pumilus, Candida albicans* and *E. coli*. Ethanol extract responded high activity on *Candida albicans* and medium activity on *Staphylococcus aureus, Pseudomonas aeruginosa, Bacillus pumilus* and *E. coli*. (Table 2)

Table 2. Results of Antimicrobial Activity of Tuber of V. *latifolia*

	Exliucli	Inhibition Zone Diameters (mm) of Different Exliucli against Six Microorganisms					
		I	II	III	IV	V	VI
	n-hexane	–	–	–	–	–	–
	EtOAc	28 (+++)	25 (+++)	25 (+++)	27 (+++)	26 (+++)	25 (+++)
	EtOH	14 (+)	18 (++)	18 (++)	19 (++)	20 (+++)	18 (++)
Control	n-hexane	–	–	–	–	–	–
	EtOAc	–	–	–	–	–	–
	EtOH	–	–	–	–	–	–

Agar well~10 mm
10 mm~14 mm(+)
15 mm~19 mm(++)
20 mm above (+++)

Organisms
I. *Bacillus subtilis*
II. *Staphylococcus aureus*
III. *Pseudomonas aeruginosa*
IV. *Bacillus pumilus*
V. *Candida albicans*
VI. *E. coli*

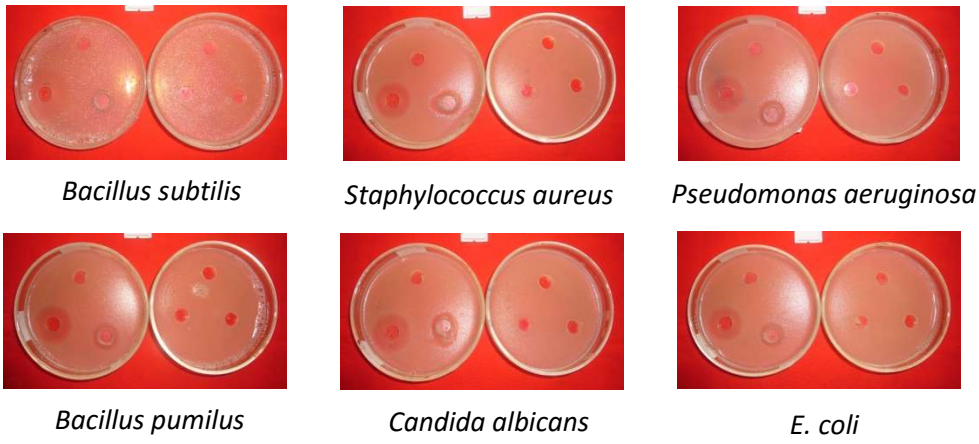

Figure 2. Antimicrobial activity of tuber of V. *latifolia* against six tested Microorganisms

Antimicrobial Activity of Pure Compound

The results in Table 3 and Figure 3 informed that the pure compound responded medium activity on *Candida albicans* and low activity on *Bacillus subtilis, Pseudomonas aeruginosa, Bacillus pumilus* and *E. coli*.

Table 3. Antimicrobial Activity of Pure Compound

Sample	Exliucli	Inhibition Zone Diameters (mm) of Pure Compound against Six Microorganisms					
		I	II	III	IV	V	VI
Compound	EtOH	12 (+)	–	13 (+)	14 (+)	19 (++)	11 (+)
Control	EtOH	–	–	–	–	–	–

Agar-well ~ 10 mm
10 mm ~ 14 mm (+)
15 mm ~ 19 mm (++)
20 mm above (+++)

Organisms
I. *Bacillus subtilis*
II. *Staphylococcus aureus*
III. *Pseudomonas aeruginosa*
IV. *Bacillus pumilus*
V. *Candida albicans*
VI. *E. coli*

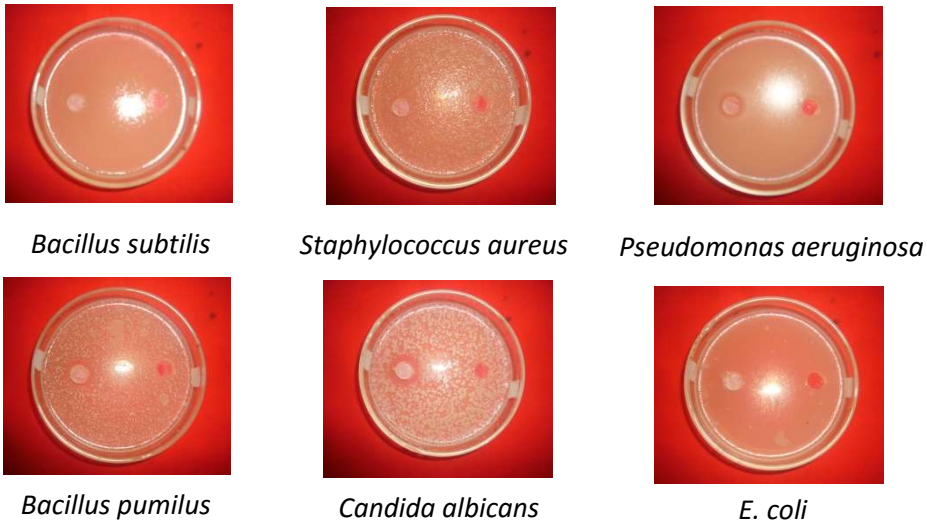

Figure 3. Antimicrobial activity of pure compound against six tested microorganisms

Molecular Formula Determination of Pure Compound

In Figure 4, the FT IR spectrum of pure compound informed that alcohol group (3409.9 cm–^{1}), sp^{2} hydrocarbon (3024.5 cm^{-1}), sp^{3} hydrocarbon (2931.6 cm^{-1}, 2858.3 cm^{-1}), alkenic group (1643.2 cm^{-1}), allylic hydrocarbon (1461.9 cm^{-1}) and methyl group (1373.2 cm^{-1}) could be assigned (Silverstein, Webster and Kiemle, 2005).

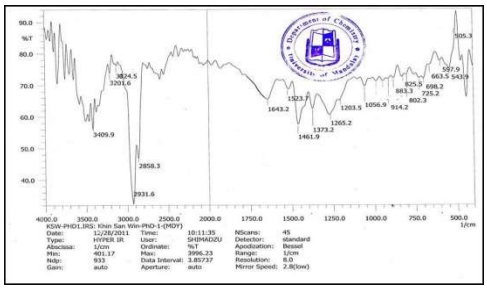

Figure 4. FT IR spectrum of pure compound isolated from V. *latifolia*

The ^{1}H NMR spectrum represents the chemical shift, splitting pattern and J value of the protons. According to the spectrum as shown in Figure 5, the isolated compound contained 51 protons (John, 2003).

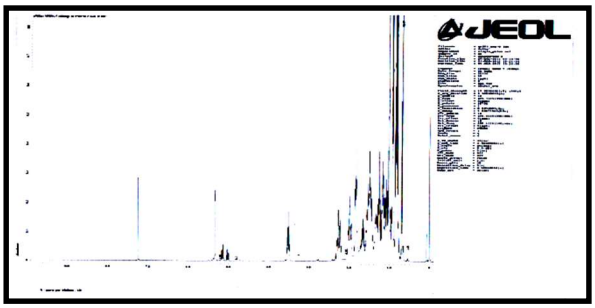

Figure 5. ^{1}H NMR spectrum of pure compound isolated from V. *latifolia*

The ^{13}C NMR spectrum in Figure 6 represents the totally 30 carbons in this compound (Le Roy and William, 1972).

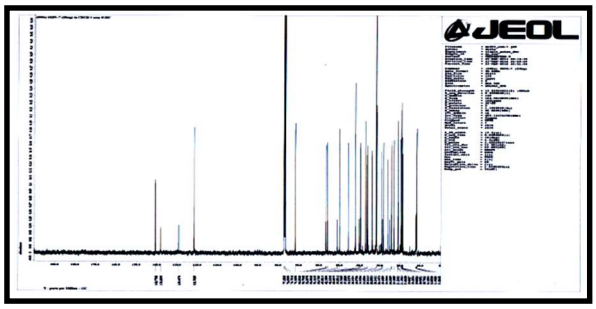

Figure 6. ^{13}C NMR spectrum of pure compound isolated from V. *latifolia*

The DEPT spectrum (Figure 7) confirms the number and kinds of carbon as well as protons (Silverstein, Webster and Kiemle, 2005).

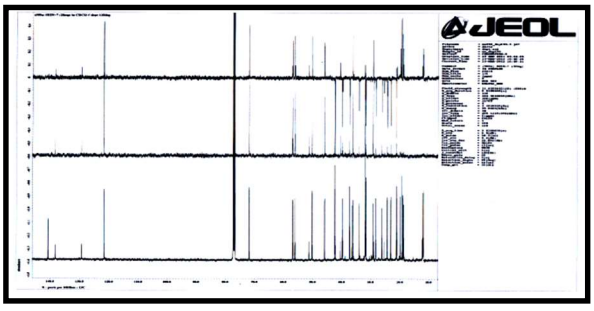

Figure 7. DEPT spectrum of pure compound isolated from V. *latifolia*

HMQC spectrum in Figure 8 of compound indicates the proton carbon direct correlation.

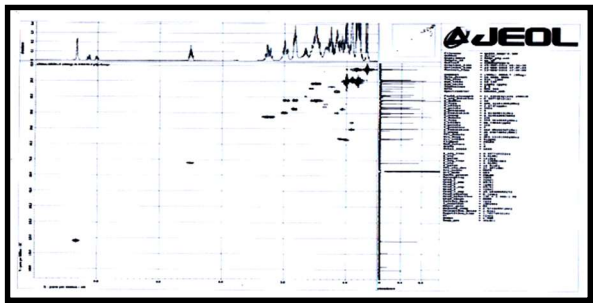

Figure 8. HMQC spectrum of pure compound isolated from V. *latifolia*

In EI-mass spectrum (Figure 9) of this pure compound, the molecular ion peak was m/z 428 which indicated the molecular mass of compound (Silverstein, Webster and Kiemle, 2005, Porter and Baldas, 1971).

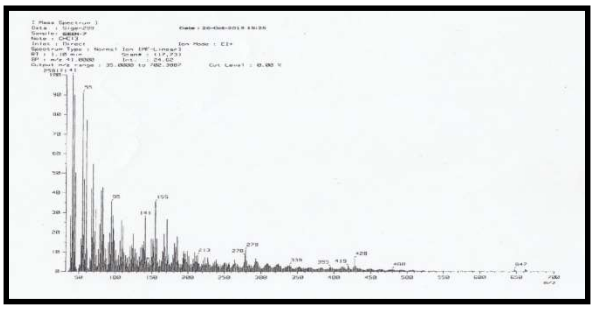

Figure 9. EI-Mass spectrum of pure compound isolated from V. *latifolia*

According to above spectrum, the molecular formula of pure compound could be assigned as $C_{30}H_{52}O$.

$$\text{Hydrogen deficiency index, HDI} = 30 - \frac{52}{2} + 1$$

$$= 5$$

Structure Elucidation of Pure Organic Compound

The structure of pure compound was elucidated by applying FT-IR, ^{1}H NNR, ^{13}C NMR, DEPT, DQF-COSY, HMBC, HMQC and EI-mass spectral data. According to these data, the following complete structure could be elucidated as 10, 11, 15-trimethyl-17-(3-methylnona-2-yl)-2, 3, 4, 7, 8, 9, 10, 11, 12, 13, 14, 15, 16, 17-tetradecahydro-1H-cyclopenta [a] phenanthren-3-ol.

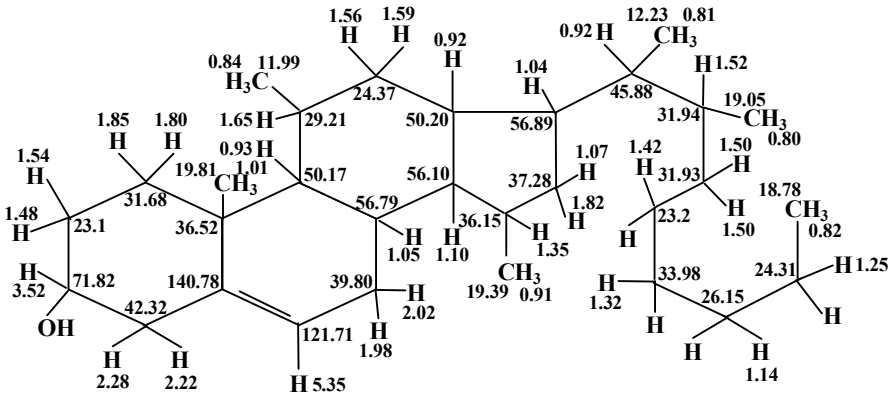

This structure was confirmed by EI-mass fragmentation behaviour. Calculated HDI 5 agreed with that values from the structure of this compound.

Conformational Analysis of Pure Compound

Conformational analysis of this compound was assigned by splitting patterns, J-values of some prominent protons in ^{1}H NMR, NOESY spectral data and model studies. (Figure 10)

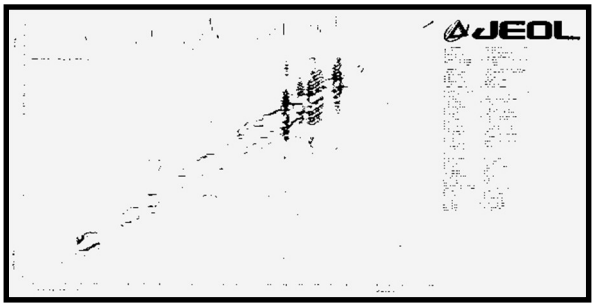

Figure 10. NOESY spectrum of pure compound isolated from V. *latifolia*

Conclusion

In this paper, the tuber of V. *latifolia* was selected for phytochemical screening, antimicrobial activity, isolation of organic compound and structure elucidation. Phytochemical screening of tuber of V. *latifolia* indicated the presence of alkaloid, flavonoid, glycoside, phenol, polyphenol, sugar, saponin, sterol and terpene. The yield percent of pure compound was found to be 0.61 % (21 mg) based upon the ethyl acetate crude extract and its melting point could be measured at (198-199°C). The ethyl acetate extract of the tuber of V. latifolia showed high potent activity (25-28mm) against six tested microorganisms. The antimicrobial activity of pure compound showed medium activity on *Candida albicans* and low activity on *Bacillus subtilis, Pseudomonas aeruginosa, Bacillus pumilus* and *E. coli*. The molecular formula as $C_{30}H_{52}O$ and the structure of this compound were determined by FTIR, ^{1}H NMR, ^{13}C NMR, DEPT, DQF-COSY, HMBC, HMQC and EI-mass spectral data. According to splitting patterns, coupling constant, NOESY spectral data and model studies, ring A and ring B were chair like and boat like conformers and ring C and ring D were chair and envelope conformers. Consequently, the absolute configuration of nine chiral carbons could be determined as C_3(S), C_8(S), C_9(S), C_{10}(R), C_{11}(R), C_{13}(R), C_{14}(R), C_{15}(S) and C_{17}(R) respectively. The isolated pure compound was elucidated as 10, 11, 15-trimethyl-17-(3-methylnona-2-yl)-2, 3, 4, 7, 8, 9, 10, 11, 12, 13, 14, 15, 16, 17-tetradecahydro-1H-cyclopenta [a] phenanthren-3-ol.

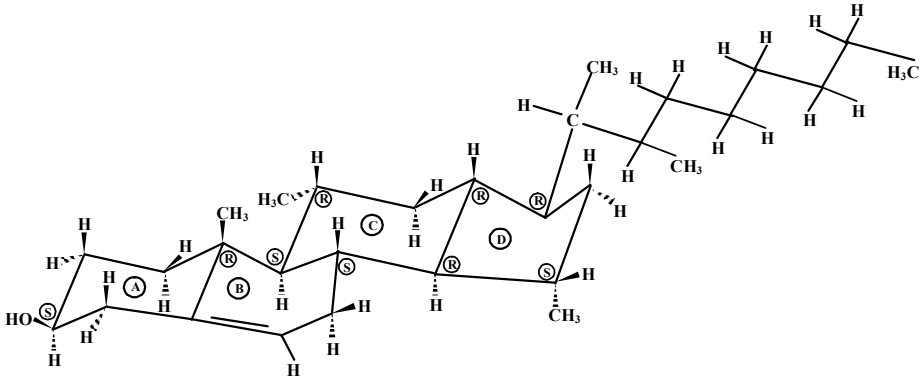

Acknowledgements

The authors acknowledge the Department of Higher Education (Lower Myanmar), Ministry of Education, Yangon, Myanmar for allowing us to carry out this research programme. Thanks are also extended to the Myanmar Academy of Arts and Science to accept this paper.

References

Ah Shin Nagathein, (1983). *Pon Pya Say Abidan*, Yangon. 3rd Edition, Mingala Printing Press.

Harborne, J.B. (1984). *Phytochemical Methods. A Guide to Modern Techniques of Plant Analysis*. New York. 2nd Edition. Chapman and Hall Ltd.

John, N.H. (2003). *Nuclear Magnetic Resonance Spectroscopy*, New Jersey. Pearson Education Inc., Upper Saddle River.

LeRoy F.J. and William, C.J. (1972). *Carbon 13 NMR Spectra*: A Collection of Assigned, Coded, and Indexed Spectra. A Wiley Interscience Publication.

Porter, Q.N. and Baldas, J. (1971). *Mass Spectrometry of Heterocyclic Compound*, New York. Wiley-Inter Science, A Division of John Wiley & Sons, Inc.

Silverstein, R.M., Webster, F.X. and Kiemle, D.J. (2005). *Spectrometric Identification of Organic Compound*, New York. 7th Edition, John Wiley & Sons, Inc.

Sofowara, E.A. (1982). *Medicinal Plant and Traditional Medicine in Africa*. Nigeria: John Wiley and Sons, Ltd.

STRUCTURE ELUCIDATION OF BIOACTIVE ORGANIC COMPOUND ISOLATED FROM MYANMAR INDIGENOUS MEDICINAL PLANT, *Vitis latifolia* Roxb.

A Research Paper Submitted to the Myanmar

Academy of Arts and Science

By

Khin San Win

Associate Professor

Department of Chemistry

Yadanabon University

June, 2017

STUDY ON THE UPTAKE OF ZINC(II) AND LEAD(II) BY DRY TARO (PEIN) *COLOCASIA ESCULENTA* L.

Khin Khin Wai[1], Su Myat Htwe[2]

Abstract

This researchis concerned with the study on the uptake of Pb(II) and Zn(II) metal cations by the dry taro (biomass) using batchwise system. The plant sample was collected from thePyay University Campus. The similar shape, size, weight and height of taro plant were selected and washed with tap water, distilled water and dried in air. The dried sample was made to powder by using grinder and sieved with 0.9-1 mm mesh. The determinations of the initial amounts of Pb(II) and Zn(II) metal cations in taro plant, soil and water from sample site were carried out. It was observed that the initial amounts of Zn(II) ion in plant, soil and water from sample site was greater than those of Pb(II) ion. In experiment I, 8.5 g of the dried powder sample was packed in a cotton bag and immersed in each of experimental buckets containing 3L of different metal cations with different concentrations separately to determine the uptake ofPb(II) and Zn(II) metal cations on daily up to 7 days.Moreover in experiment II, the amount of uptake of Pb(II) and Zn(II) metal cations were examined eight times at the interval of 15 min up to 120 min by adding (8.5 g) each of sample in 150 mL of solutions containing different concentrations of metal cations.The optimum contact time at 45 min for Pb(II) and 60 min for Zn(II).It could be seen clearly that the uptake capacity for Pb(II) was greater than Zn(II) in both experiments I and II. The effect of temperature on the uptake of Pb(II) and Zn(II) by the dry taro (biomass) was studied at the range between 20ºC and 70ºC based on 50, 25 and 10 ppm.The optimum temperature was at 40 °C. It was found that, the percent uptake of Pb(II) was higher than Zn(II) for the concentrations of 50, 25 and 10 ppm. The percent uptake of Zn(II) was investigated by the acidified biomass of drytaro at the interval of 15 min up to 120 minfor 50 ppm of Zn(II) solution. It was found that the optimum uptake of Zn(II) ion was reached at 60 min. The acidified biomass of dry taro was greater in uptake of Zn(II) ion than the non-acidified biomass of dry taro.

Keywords: dry taro, acidified dry taro, batchwise system, uptake of Pb(II) and Zn(II)

[1] Associate Professor, Department of Chemistry, Pyay University
[2] MRes Candiate, Department of Chemistry, Pyay University

Introduction

Taro plant is an aquatic plant and commonly seen in ponds, lakes, ditches and quiet streams. *Colocasiaesculenta* L.(Figure 1) is a tropical plant grown primarily for its edible corms, the root vegetables most commonly known as taro. It is believed to be one of the earliest cultivated plants. There are two major cultivars of taro. They are green stem (taro) and red stem (taro).Cooking of the taro will reduce the crystal chemicals to a safe level and improve the taste and texture of the plant. Taro is popular in many dishes worldwide. It is commonly prepared in stews and stir fries. Due to the crystal compounds it is considered a "last-resort" food in many regions and is only consumed if there is a food shortage (Hambali, 1979). A taro is basically a potato which has a thick, hairy skin. It is often called albi. It is used in making taro or albi plaster. Like potatoes, taro tubers can be baked, fried, steamed, boiled or mashed.

Most taro cultivars taste acrid and can cause swelling of lips, mouth and throat if they are eaten raw. The acridity of taro is thought to be concentrated in the outer layers of the corm and may be largely removed by peeling off a thick layer followed by prolonged boiling. This acridity is learned to be caused by calcium oxalate presents as fine needle-like crystals or raphides, which can penetrate soft skin. Thereafter an irritant presents on the raphides, probably a protease can cause discomfort in the tissue.Taro contains substantial quantities of oxalate (Wang, 1983), as do the majority of higher plants.

The two common toxic effect of oxalate poisonings are

(1) acute poisoning, resulting in hypocalcaemia after ingestion of high levels of soluble oxalates and

(2) (more commonly) chronic poisoning in which calcium oxalate crystals are deposited in the kidneys, resulting in renal disorder.

Figure 1 Photograph of Taro Plants (*Colocasiaesculenta* L.)

The oxalates are widely distributed in the plants in readily water soluble forms, such as potassium, ammonium and sodium oxalate and as insoluble needle like calcium oxalate crystal. Cooking can affect the soluble oxalate but not the insoluble oxalate content of the food. Boiling can reduce the soluble oxalate content of a food if the cooking water is discarded, while soaking, germination and fermentation will also reduce the content of soluble oxalates. Baking a food will reduce an effective concentration of oxalates in the food due to the loss of water from the baked food (Iwuoha and Kalu, 1995).

Sodium oxalate which presents in the plant can react with lead(II) nitrate by the metathesis reaction.

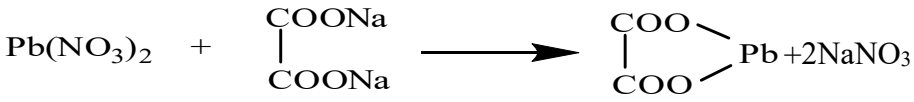

Lead(II) oxalate is sparingly soluble in water. Its solubility is increased in the presence of excess oxalate anions, due to the formation of $Pb(C_2O_4)_2^{2-}$ complex ion (Grases*et al*., 1993). But zinc oxalate is insoluble in water and converts to the oxide when heated.

Materials And Methods

Collection and preparation oftarosamples

All the tarosamples (green stem) used were of the long stem type, the botanical name being "*Colocasiaesculenta*L.".

Taro plants (green stem) were collected from a proliferated taro pond with dimensions roughly about 10 x15 feet and 2.5feet in depth. It was located beside the Chemistry Department inPyay UniversityCampus. The samples of all taro plants (green stem) have the nearly same condition of size, shape, height and weight. The selected sample (green stem) was washed thoroughly with tap water, distilled water and dried in air.

Determination of the amount of Zn(II) and Pb(II) in taro plant, soil and water sample

The taro plants, water and soil were collected from a proliferated taro pond with dimensions roughly about 10 x15 feet and 2.5feet in depth. It was located beside the ChemistryDepartment. Theconcentrations of Zn(II) and Pb(II) in Taro plant, soil and water sample were determined by AAS.

Preparation of dry taro plants for biosorbent

The biosorbent used in this study was the dry taro plants (*Colocasiaesculenta*L.). The collected samples weredried in air for about three weeks and then dried in an oven at 70°C. After being completely dried, the biomass was cut into pieces and ground by grinder. After this, the biomass was sieved to get particle size between 0.9-1 mm for use as biosorbent.

Uptake of Pb(II) and Zn(II) metal cations from model solution by the normal condition of dry taro (biomass) (batchwise of days and minutes)

(a) Preparation of model solutions

Model solutionsof Pb(II) and Zn(II) ions in 50,25 and 10 ppm concentrations were prepared by dissolving lead(II) nitrate and zinc nitrate in distilled water respectively. The fresh solutions were used for each study.

(b) Effect of contact time (day) on the uptake of Pb(II) ion and Zn(II) ion by the normal condition of drytaro (biomass) based on 50, 25 and 10 ppm(Experiment I)

Each of the prepared solution(Pb(II) ion, Zn(II) ion)was poured into the experimental bucket. 8.5 g of drytaro (biomass) were packed in the bag (diameter7 cm, height 11 cm) and then this bag was hanged by nylon thread as shown in Figure 2.

The prepared sample-bag was immersed in experimental bucket containing(3L±0.03 L) of the known metal cation solution. Whenever necessary the solution level was adjusted with the distilled water every morning.

Choosing the time frame of 1, 2, 3, days, an aliquot (40 mL) portion of Pb(II) solution was pipetted out by means of 20 mL glass syringe. Uptake of metal cations in thisprocedure was determined by AAS. The data of experimental work are shown in Tables 2, 3and 4 and Figures4, 5 and6.

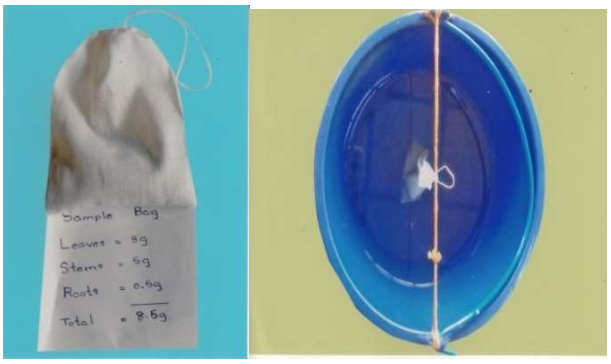

(a) (b)

Figure 2 Uptake of Pb(II) by the normal condition of dry taro (biomass) based on 50 ppm (a) sample bag (b) model bucket

-

(c)Effect of contact time (minute) on the uptake of Pb(II) ionand Zn(II) ion by thenormalcondition of dry taro (biomass) based on 50, 25 and 10 ppm(Experiment II)

Each standard lead(II) nitrate solution and zinc nitrate solution of 50, 25 and 10 ppm concentrationswas prepared. Accurately weighed sample (8.5 g) was added into a conical flask (250 mL) containing 150 mL of lead(II) nitrate solution at pH 5. The flask was placed in an orbital shaker bath at room temperature. The mixture of solution and biosorbent was agitated in 100 rpm. The amount of uptake was examined at the interval of 15, 30, 45, 60, 75, 90, 105 and 120 min. After this time, the sample solutions were separated by filtration.Aliquot (40 mL) of Pb(II) andZn(II) solutionswere pipetted out by means of 20 mL glass syringe. Uptake of metal cations in this procedure was determined by AAS. The resulting data are shown in Tables 5, 6 and7 and Figures 7, 8 and 9.

(d)Effect of temperature on the uptake ofPb(II) andZn(II) Ions by the normal condition of dry taro (biomass) based on 50, 25 and 10 ppm

Standard lead(II) nitrate andzinc nitrate solutionswere prepared. Accurately weighed sample (8.5 g) was added into a conical flask (250 mL) containing 150 mL of lead(II) nitrate solution at pH 5. The solution was shaken by a hot-plate magnetic stirrer. The mixture of solution and biosorbent was agitated at 100 rpm for 15 min at different temperatures of20°C, 30°C, 40°C, 50°C, 60°C and 70 °C by using thermometer.Then, the sample solutions were separated by filtration. The residual contents of lead(II) ion and zinc ion in the solution were determined by AAS. The resulting data are shown in Tables8, 9 and10 and Figures10,11 and 12.

Uptake of Zn(II) ion from model solution by the acidified condition of dry taro (biomass) based on 50 ppm (batchwise of minute)

(a)Preparation of acidified biosorbent

The biomass was subsequently loaded with H^+ in a solution of 0.1 M HCl (biomass concentration of 50 gL^{-1}) for 30 min under slow stirring for protonation, which eliminates interference of biosorption by other cations such as Na^+, K^+, Mg^{2+} and Ca^{2+}. Later the biomass was washed with deionized

water (1000 mL) up to four times to remove excess hydrogen ions for neutralization(pH 7). Then, the biosorbent was again dried at 70°C for 24 h until a stable weight was observed.

(b)Effect of contact time (minute) on the uptake of Zn(II) Ion by the acidified condition of dry taro (biomass) based on 50 ppm

Standard zinc nitrate solution of 50 ppm was prepared.Accurately weighed acidified sample (8.5 g) was added into a conical flask (250 mL) containing 150 mL of zinc nitrate solution at pH 5. The flask was placed in an orbital shaker bath at room temperature. The mixture of solution and biosorbent was agitated at 100 rpm. The amount of uptake was examined at the interval of 15, 30, 45, 60, 75, 90, 105 and 120 min.After this time, the sample solutions were separated by filtration. The residual content of Zn(II) ion in the solution was determined by AAS. The resulting data are shown in Tables 11 and 12 and Figures 13 and14.

Results And Discussion

Assay of metal contents in taro plant, water and soil sample

Table 1 and Figure 3 show the original contents of Zn(II) and Pb(II) ions in taro plant, water and soil sediment. The amount of Zn(II) ion was higher than Pb(II) ion in taro plant, water and soil sample (Figure 3).

Table 1 The contents of Zn(II) and Pb(II) ions in taro plant, water and soil samples

Sample	Zn(II) ion (ppm)	Pb(II) ion (ppm)
Plant	0.57	0.08
Water	0.57	0.43
Soil	3.84	0.69

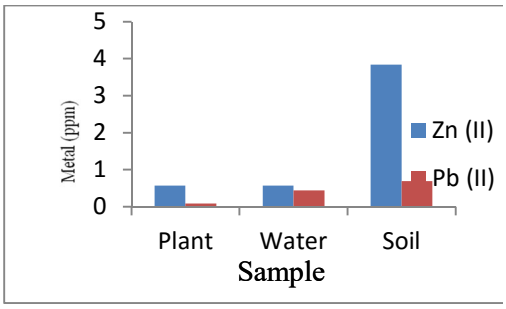

Figure 3 The contents of Zn(II) and Pb(II) ions in taro plant, water and soil sample

Effect of contact time (day) on the uptake of Pb(II) and Zn(II) ions by the normal condition of dry taro (biomass) based on 50, 25 and 10 ppm (Experiment I)

Tables 2, 3 and4 and Figures5,6 and7 show the uptake of metal cationsPb(II) and Zn(II) ions by the normal condition of drytaro (biomass).The uptake of the Pb(II) ion was found to be higherthan Zn(II) in the metal ion concentrationsof 50 ppm , 25 ppm and10 ppm.This is because sodium oxalate present in the of taro can react with lead(II)nitrate.Lead(II) oxalate is sparingly soluble in water. Its solubility increases in the presence of excess oxalate anions, due to the formation of $Pb(C_2O_4)_2^{2-}$ complex ion. But zinc oxalate is highly insoluble in water and converts to the oxide when heated.

The nature of uptake for each metal ion is quite different. The differential uptake of the drytaro (biomass) towards Pb(II) ion in first day was higher compared to Zn(II) ion at 50 ppm (i.e., the percent uptake of Pb(II) ion was 99.98%). It was observed that with the increases in concentration of heavy metal cations, the percent uptake increases and when the contact time increases percent uptake also increases.The uptake activity of the drytaro (biomass) towards Zn(II) ion was similar as Pb(II) ion. The increased differential still continued to uptake to the 6^{th} days (i.e., optimum percent uptake of Zn(II) ion was 98.08% based on 50 ppm).

Table 2 Effect of Contact Time (Day)on the Uptake of Pb(II) and Zn(II) ionsby the Normal Condition of dryTaro(Biomass) Based on 50 ppm (Batchwise)

Day	Percent uptake (%)	
	Pb(II)	Zn(II)
D_1	99.98	97.78
D_2	99.98	97.89
D_3	99.98	97.91
D_4	99.98	97.96
D_5	99.98	97.99
D_6	99.98	98.08
D_7	99.98	98.08

Each metal ion concentration = 50ppm
Weight of sample = 8.5g
pH = 5

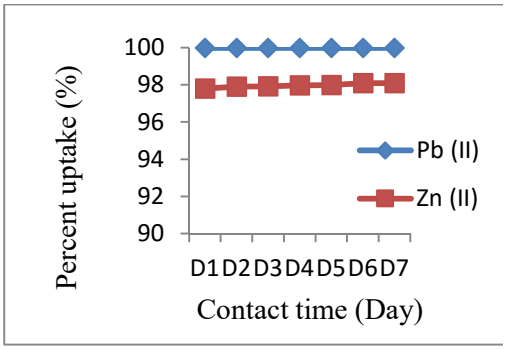

Figure 4 Uptake of metal cations by the normal condition of dry taro (Biomass) based on 50 ppm (Batchwise)

Table 3 Effect of Contact Time (Day) on the Uptake of Pb(II) and Zn(II) ions by the Normal condition of dry Taro (Biomass) Based on 25ppm (Batchwise)

Day	Percent uptake(%)	
	Pb(II)	Zn(II)
D_1	99.96	96.39
D_2	99.96	96.52
D_3	99.97	96.97
D_4	99.97	97.32
D_5	99.97	97.37
D_6	99.97	97.52
D_7	99.97	97.52

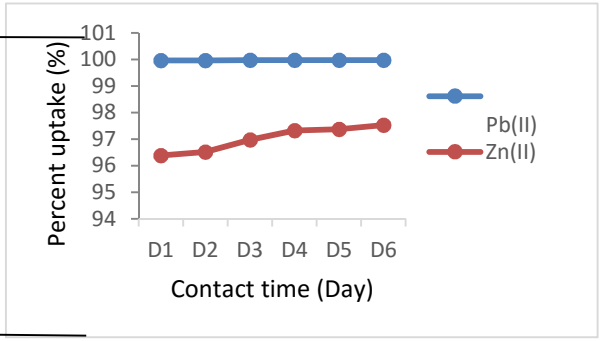

Each metal ion concentration = 25ppm
Weight of sample = 8.5g
pH = 5

Jptake of metal cations by the normal condition of dry taro (Biomass) based on 25 ppm

Table 4 Effect of Contact Time (Day) on the Uptake of Pb(II) and Zn(II) ions by theNormal Condition of dry Taro (Biomass)Based on 10 ppm (Batchwise)

Day	Percent uptake(%)	
	Pb(II)	Zn(II)
D_1	99.68	93.46
D_2	99.72	93.79
D_3	99.75	93.80
D_4	99.79	94.75
D_5	99.79	94.81
D_6	99.79	95.81
D_7	99.79	95.81

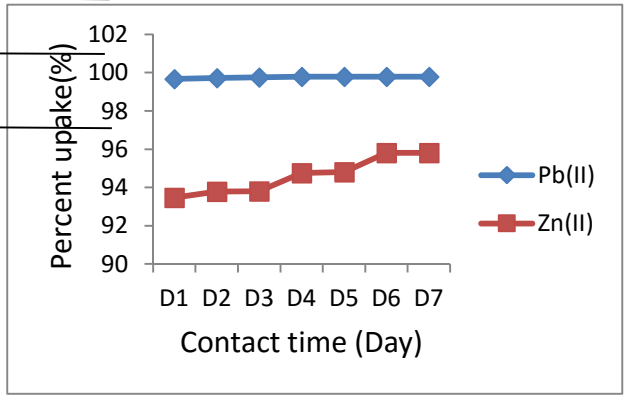

Figure 6 Uptake of metal cations by the normal condition of dry taro (Biomass) based on 10 ppm (Batchwise)

Effect of contact time (minute) on the uptake of Pb(II) and Zn(II) ions by the normal condition of dry taro (biomass) based on 50, 25 and 10 ppm(Experiment II)

Time dependency studies offered data about the change in metal removal related to time. In this study, the minimum time necessary for biomass to be in contact with the metal ion solutions was elucidated.The percent uptake of Pb(II) and Zn(II) ions with respect to contact time for 50, 25, and 10 ppm onto each dry biomass (8.5 g of powdered sample) at pH 5 werestudied by varying the contact time from 15 to 120 minutes. The results were presented in Tables, 5,6 and7 and Figures7,8 and 9.Tables and Figures show the uptake of Pb(II) ion by the drytaro (biomass) using initial concentration ranging from 50 to 10 ppm.The uptake of Pb(II) ion reached at 45 min (i.e., optimum percent uptake of Pb(II) ion was 99.98% based on 50 ppm).After the maximum contact time, it could be seen that the uptake of Pb(II) ion was decreased with increasing time and the stationary state was reached at 75 min attaining adsorption of 99.94%.The uptake activity ofbiomass towards Zn(II) ion was similar as Pb(II) ion. It was observed that the percent uptake of Zn(II) ionincreased with increasing time. The optimum percent uptake for Zn(II) ion was 97.96% at 60 min and the stationary state reached at 105 min attaining adsorption of 97.85% based on 50 ppm. This is because the higher biosorption at the initial contact time could be related to the driving force of heavy metal ions into the surfaces of drytaro (biomass) and the abundance of active sites on the adsorbent. The slow uptake capacity with the subsequent time may be due to the diffusion of heavy metal ions into the surface of thedrytaro (biomass) and fewer remaining binding sites.

Table 5 Effect of Contact Time (Minute) on the Uptake of Pb(II) and Zn(II)Ion by the Normal Condition of dry Taro (Biomass) Based on 50 ppm (Batchwise)

Minute (min)	Percent uptake (%)	
	Pb (II)	Zn (II)
15	99.94	97.76
30	99.94	97.77
45	99.98	97.79
60	99.96	97.96
75	99.94	97.90
90	99.94	97.87
105	99.94	97.85
120	99.94	97.85

Each metal ion concentration = 50 ppm
Weight of sample = 8.5 g
pH = 5

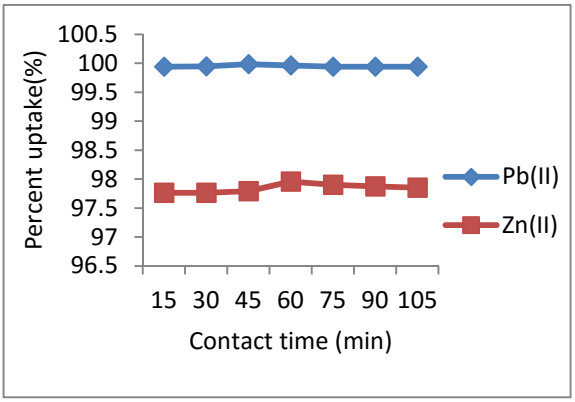

Figure 7 Uptake of metal cations by the normal condition of dry taro (Biomass) based on 50 ppm (Batchwise)

Table 6 Effect of Contact Time (Minute) on the Uptake of Pb(II) and Zn(II) ions by the Normal Condition of dry Taro (Biomass) Based on 25 ppm (Batchwise)

Minute (min)	Percent uptake (%)	
	Pb(II)	Zn(II)
15	99.92	95.78
30	99.92	95.80
45	99.98	95.94
60	99.97	96.26
75	99.96	95.91
90	99.96	95.79
105	99.96	95.76
120	99.94	95.76

Each metal ion concentration = 25 ppm
Weight of sample= 8.5 g, pH= 5

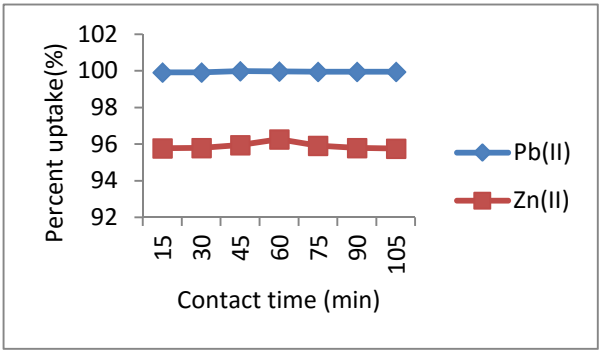

Figure 8 Uptake of metal cations by the normal condition of dry taro (Biomass) based on 25 ppm (Batchwise)

Table 7 Effect of Contact Time (Minute) on the Uptake of Pb(II) and Zn(II) ions by the Normal Condition of dry Taro (Biomass) Based on 10 ppm (Batchwise)

Minute (min)	Percent uptake (%)	
	Pb (II)	Zn (II)
15	99.91	89.74
30	99.97	89.81
45	100.00	89.82
60	99.96	89.90
75	99.96	89.81
90	99.96	89.73
105	99.96	88.92
120	99.96	88.92

Each metal ion concentration= 10 ppm
Weight of sample = 8.5 g
pH = 5

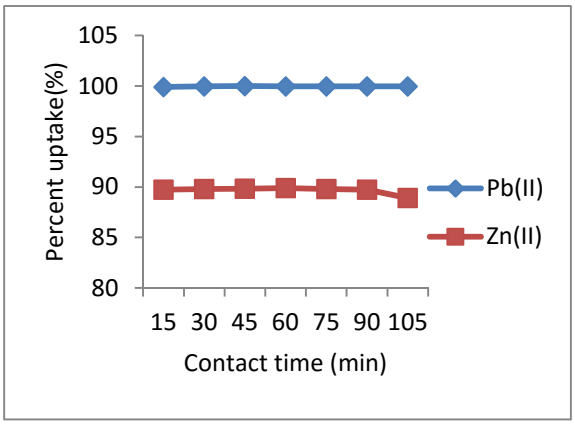

Figure 9 Uptake of metal cations by the normal condition of dry taro (Biomass) based on 10 ppm (Batchwise)

Effect of temperature on the uptake of Pb(II) and Zn(II) ions by the normal condition of dry taro (biomass) based on 50, 25 and 10 ppm

Results presented in Tables 8, 9, 10 and Figures 10,11,12 indicate the percent uptake for selected heavy metals by the drytaro (biomass) at different temperaturesof 20°C to 70°C, based on 50, 25 and 10 ppm.

From Tables and Figures, it was clear that the percent uptake of Pb(II) was higher than Zn(II) where each metal cations concentration used were 50 ppm, 25 ppm and10 ppm. The maximum uptake of 99.84% for Pb(II) and 97.93% for Zn(II) at 40°C based on 50 ppm were observed. There was a decrease in the uptake capacity after 40°C. The temperature profile indicates that as the temperature is increased the uptake capacity increased to a maximum value and then decreased. This is because the biosorbent loses its

properties at high temperature due to denaturation. So, the temperature increases above 40˚C the uptake capacity decreases.

Table 8 Effect of Temperature on the Uptake of Pb(II) and Zn(II) ions by the Normal Condition of dry Taro (Biomass) Based on 50 ppm (Batchwise)

Temperature (°C)	Percent uptake (%)	
	Pb (II)	Zn (II)
20	99.82	97.65
30	99.83	97.82
40	99.84	97.94
50	99.84	97.76
60	99.84	97.71
70	99.84	97.71

Each metal ion concentration= 50 ppm,
Weight of sample = 8.5 g
Contact time = 15 min,
pH = 5

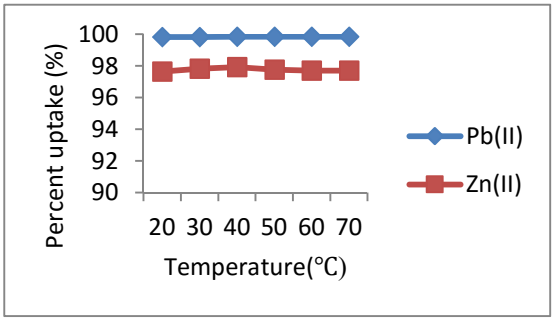

Figure 10 Uptake of metal cations by the normal condition of dry taro (Biomass) based on 50 ppm (Batchwise)

Table 9 Effect of Temperature on the Uptake ofPb(II) and Zn(II) ions by the NormalCondition of dry Taro (Biomass) Based on 25 ppm (Batchwise)

Temperature (°C)	Percent uptake (%)	
	Pb (II)	Zn (II)
20	99.72	95.68
30	99.72	95.72
40	99.78	95.80
50	99.73	95.74
60	99.73	95.72
70	99.73	95.72

Each metal ion concentration = 25 ppm
Weight of sample = 8.5 g
Contact time = 15 min, pH = 5

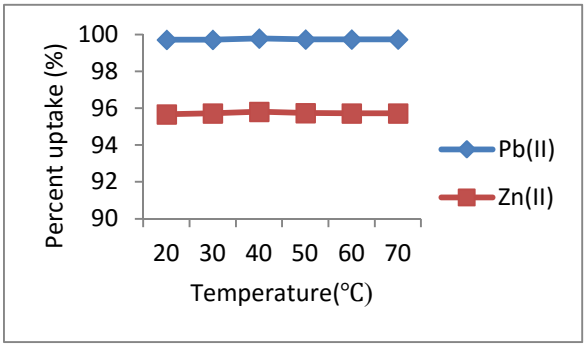

Figure 11 Uptake of metal cations by the normal condition of dry taro (Biomass) based on 25 ppm (Batchwise)

Table 10 Effect of Temperature on the Uptake of Pb(II) and Zn(II) ions by the Normal Condition of dry Taro (Biomass) Based on 10 ppm

Temperature (°C)	Percent uptake (%)	
	Pb (II)	Zn (II)
20	99.61	89.62
30	99.62	89.70
40	99.69	89.76
50	99.67	89.74
60	99.67	89.73
70	99.67	89.73

Each metal ion concentration = 10 ppm
Weight of sample = 8.5 g
Contact time = 15 min, pH = 5

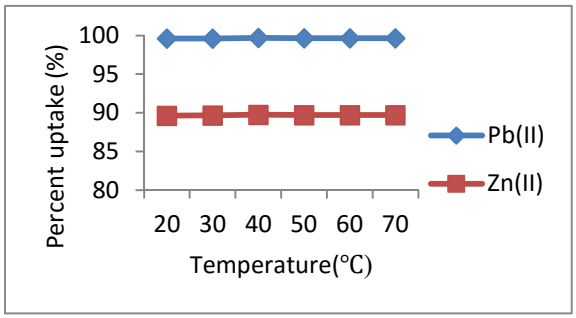

Figure 12 Uptake of metal cations by the normal condition of dry taro (Biomass) based on 10 ppm (Batchwise)

Effect of contact time (minute) on the uptake of Zn(II) ions by the acidified condition of dry taro (biomass) based on 50 ppm

The effect of contact time on the uptake of Zn(II) ion by the acidified condition of dry taro (biomass) based on 50 ppm were shown in Table 11 and Figure 13. According to the results, the time dependent behavior of adsorption was examined by varying the contact time between biosorbate and biosorbent in the range of 15-120 min. The uptake of Zn(II) ion increased with increasing contact time due to enough large surface area available of the adsorbent. The maximumpercent uptake was 99.18% at 60 min for Zn(II) based on 50 ppm. After the maximum contact time, it could be seen that the uptake of Zn(II) ion decreased with increasing time and the stationary state was reached at 105 min attaining adsorption of 99.15% based on 50 ppm.

Table 11 Effect of Contact Time (Minute) on the Uptake of Zn(II) ions by the Acidified Condition of dry Taro (Biomass) Based on 50 ppm (Batchwise)

Contact Time (min)	Zn(II) concentration (ppm)	
	Final	Percent uptake (%)
15	0.91	98.19
30	0.85	98.31
45	0.81	98.38
60	0.41	99.18
75	0.42	99.16
90	0.42	99.16
105	0.42	99.15
120	0.42	99.15

Each metal ion concentration = 25 ppm
Weight of sample = 8.5 g
pH = 3, Temperature = 15 ℃

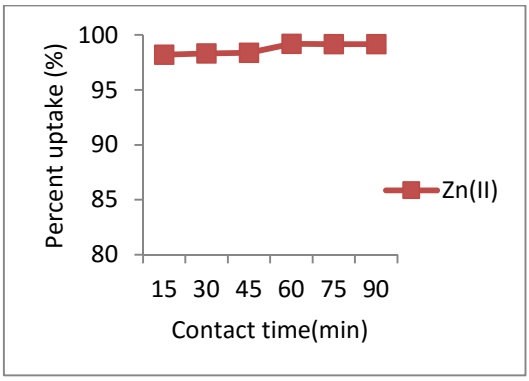

Uptake of metal cation by the acidified condition of non-living taro (Biomass) based on 50 ppm (Batchwise)

Comparative Study on the uptake of Zn(II) ion by the normal condition and acidified condition of dry taro (biomass) (batchwise) based on 50 ppm and contact time (minute)

Efficiency of drybiosorbent of normal biomass and acidified biomass were tested for the uptake of Zn(II) ion by varying the contact time from 15 to 120 min. Comparison of the results are presented in Table 12 and Figure 14. It was found that the uptake of Zn(II) ion by the acidified condition of drytaro (biomass) was more than that by the normal condition of dry taro (biomass). The maximum percent uptake of Zn(II) ion was 99.18% at 60 min for acidified biomass and 97.95% at 60 min for normal biomass respectively.

As the measurement of final pH represented the simultaneous release of H^+ with the uptake of heavy metal ions, because final pH of solution (pH = 3) were less than initial pH of solution (pH = 5), therefore ion exchange confirmed to be one of the biosorption mechanisms.

Table 12 Comparison Study on the Uptake of Zn(II) ion by the Normal Condition and Acidified Condition of dry Taro (Biomass)(Batchwise) Based on 50 ppm and Contact Time (Minute) Initial pH = 5, Final pH = 3

Contact Time (min)	Zn(II) concentration (ppm)	
	Normal Condition of drytaro (Biomass)	Acidified Condition of drytaro (Biomass)
15	0.91	98.19
30	0.85	98.31
45	0.81	98.38
60	0.41	99.18
75	0.42	99.16
90	0.42	99.16
105	0.42	99.15

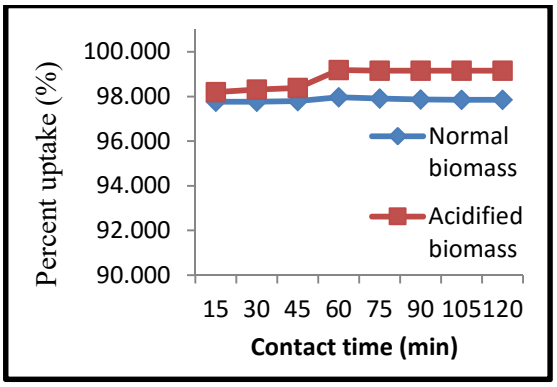

Figure 14 Uptake of metal cation Zn(II) ion by the normal condition and acidified condition of dry taro (Biomass) based on 50 ppm (Batchwise)

Conclusion

The initial amount of Zn(II) ion in plant, water and soil was higher than Pb(II) ion. From the uptake study (Batchwise system) of Pb(II) and Zn(II) ions based on 50, 25 and 10 ppm, both daily and minute by the drytaro (biomass), the uptake capacity of Pb(II) ion was greater than Zn(II) ion. It was observed that with the increases in concentration of heavy metal cations, the percent uptake increases and as the contact time increases, percent uptake increases.The effect of temperature on the uptake of Pb(II) and Zn(II) ions by the drytaro (biomass) was studied at the range between 20ºC and 70ºC based on 50, 25 and 10 ppm. It was found that the percent uptake of Pb(II) ion was higher than Zn(II) ionfor all metal cation concentrations used (50 ppm, 25 ppm and 10 ppm). The maximum uptake of 99.84% for Pb(II) ion and 97.93% for Zn(II) ion at 40ºC based on 50 ppm were observed. There was a decrease in the uptake capacity after 40ºC. The temperature profile indicates that as the

temperature increases the uptake capacity increases to a maximum value and then decreases due to denaturation.

From the comparative study on the uptake of Zn(II) ion by the normal condition and acidified condition of drytaro (biomass) (Batchwise system) based on 50 ppm and contact time (min), the uptake capacity for Zn(II) ion by the acidified condition of the drytaro (biomass) was greater than the normal condition of drytaro (biomass). The maximum percent uptake of Zn(II) ion was 99.18% at 60 min for acidified biomass and 97.95% at 60 min for normal biomass.Based on the results obtained, it can be concluded that the dried biomass of taro has high uptake capacity towards the Pb(II) and Zn(II) metal cations. Hence this property can be effectively utilized for the removal of the heavy metals from the various industrial waste-water since it is of low-cost, save time,abundant and a locally available adsorbent.

Acknowledgements

The authors would like to thank the Myanmar Academy of Arts and Science for accepting this research paper. Profound gratitude is specially expressed to Ministry of Education, Myanmar. We would like to express our sincere thanks to Professor DrTun Cho, Head of Department of Chemistry, Pyay University for providing all the departmental facilities.

References

Grases, F.,Ruiz,J. and Costa-BauZa,A. (1993)."Studies on Lead Oxalate Crystalline Growth".*J. Colloid and Interface Science,*vol155,pp 265-270

Hambali, G.G. (1979)."The Dispersal of Taro by Common Palm Civets".*Proc. Sdt.5th Symp. Inter. Soc. Trop. Root Crops.*Visayas State College of Agriculture (VISCA), Los Banos, Laguna,Philippines:pp 544- 547

Iwuoha, C.I. and Kalu,F.A. (1995). "*Calcium Oxalate and Physicochemical Properties of Cocoyam: Colocasiaesculenta and Xanthosomasagitifocium Tuber Flours as Addected by Processing". Food Chem,*vol54,pp 61-66

Wang,J.K.(1983). *Nutritive Value, Taro; A Review of ColocasiaEsculenta and Its Potentials*.Honolulu: University of Hawaii Press, pp141-144

STUDY ON SOME DERMATOLOGICAL PROPERTIES AND CHEMICAL CONSTITUENTS OF MYANMA NATURAL COSMETIC *Feronia limonia* (L.) SWINGLE (THEE) BARK

Phyu Phyu Zaw[1], Aye Aye Tun[2]

Abstract

This research is concerned with the chemical investigation and some dermatological activity of *Feronia limonia* (L.) Swingle (Thee) bark. *Invivo* antistaphylococcal activities of pet-ether, ethanol and water crude extracts were evaluated by investigating the healing potential on *Staphylococcus aureus* induced excision type cutaneous wounds. All extracts took 6 days to heal wound. No significant difference on wound healing effect between different doses of 2 - 6 mg/day was observed. Control group needed 8 days to heal wound. Skin whitening activity was determined by using a modification of Imokawa Method. In this study, guinea pig was chosen as the experimental animal because its skin histologically and biochemically is similar to the human skin. Pet-ether andethanol extracts, and kojic acid (control) were topically applied on sun rays induced hyperpigmented skin of guinea pigs for three successive weeks. After 3 weeks, pet-ether and ethanol extracts treated portion were found to be whiter than that of untreated hyperpigmented skin. The whitening effect of pet-ether and ethanol extracts were found to be similar, however, lower than that of kojic acid. In chemical investigation, two compounds were isolated from chloroform extract of *Feronia limonia* (Thee) bark. These were: Compound I (Bergapten) (0.0008% yield, mp.188-189ºC) and Compound II (marmesin) (0.0022% yield, mp.160-163ºC).These compounds have been identified by spectroscopic measurement (UV, FTIR,^{1}H NMR and ^{13}C NMR).

Keywords: *Feronia limonia* (L.) Swingle, bergapten, marmesin, skin whitening, antistaphylococcal.

Introduction

Myanmar people frequently use the fragrant liquid powder of the bark of *Feronia limonia* (L.) Swingle (Thee) as a substitute for Tha-nat-khar (a famous natural cosmetic bark). It is recognized to be of great help to bear

1. Dr, Assistant Lecturer, Department of Chemistry, Yangon University of Education
2. Dr, Pro rector, University of Dagon

the heat of sun and thus an ideal cosmetic for those who have to work under direct sunshine. Women who work in paddy fields always wear thick layers of Tha-nat-khar to help themselves tolerate the intense heat of the sun. "Thee" paste also has the same properties as Tha-nat-khar making the skin cool and smooth, having a refreshing and cool fragrance, beautifying the users. It also cures pimples and acne. *Feronia limonia* (L.) Swingle (Figure1) commonly known as Wood apple chosen for present investigation is a tropical fruit plant native to Myanmar, India, Malaysia and Sri Lanka.

Botany of *Feronia limonia* (L.) Swingle

Taxonomical classification

Kingdom	:	Plantae
Division	:	Magnoliophyta
Class	:	Magnoliopsida
Order	:	Sapindales
Family	:	Rutaceae
Genus	:	Limonia

Figure 1: Photograph of *Feronia limonia* (L.) Swingle (Thee) bark in Myanmar.

Material and Methods

Plant Material

Stem bark of *Feronia limonia* (L.) Swingle was collected from Pyay Township, Bago Region. It was cut into small pieces and air-dried at room temperature. Then it was ground into powder and stored in air-tight container to prevent moisture changes and contamination. Authentication of plant was done by the authorized botanist of Department of Botany, Yangon University.

Preparation of Extracts

Four crude extracts of *Feronia limonia* (L.) Swingle bark were prepared by successive extraction of plant material with pet- ether, followed

by chloroform, ethyl acetate finally with ethanol in Soxhlet extractor for 12 h. Water extract was prepared by refluxing the bark with distilled water. These extracts were individually evaporated in rotatory evaporator at 50ºC and subjected to column chromatography and biological activity tests.

Isolation and Purification of Some Chemical Constituents from Chloroform Extract of *Feronia limonia* (L.) SwingleBark

The chloroform extract (5.0 g) was dissolved in minimum volume of pet-ether and thoroughly adsorbed on silica gel (2 g). The adsorbed material after being dried was transferred to a silica gel column. The column was eluted consecutively with pet ether-ethyl acetate solvent system. A quantity of 10 mL was collected for each fraction and checked by TLC using 5% H_2SO_4 solution as spraying reagent. The fractions that showed similar TLC patterns were combined together and concentrated. These fractions were further purified by crystallization and provide the compounds. Fraction F_4 (10 mg) was further chromatographed over a silica gel column (10 g, column 1 cm in diameter) by eluting with danger : acetone (35 : 1) to afford five sub-fractions, F_a to F_e. Fraction F_d was further purified by crystallization with acetone-methanol provided yellow needles (4 mg, 0.0008 % yield; mp.=188-190ºC; R_f=0.56 in benzene: acetone 9:1)which was denoted as compound1. Fraction F_7 provided compound 2 (11 mg; 0.0022% yield; mp (160-163) ºC; R_f = 0.22 in benzene : acetone, 9 : 1) after being crystallized in benzene-acetone.

Screening of *In Vivo* Antistaphylococcal Activity of Different Crude Extracts of *Feronia limonia* (L.) Swingle Bark

PE, EtOH and water extracts of *Feronia limonia* (Thee) bark were used for this activity**.** Twelve rats were randomly divided into four groups; each group contained 3 rats. Surgical wound (2 cm in length and 0.5 cm in depth) were made on dorsal under septic condition. *Staphylococcus aureus* suspension (0.1 ml per wound) was introduced into all rats. Inflammation of infected wounds were observed. Wound inflammation was found to be maximal after 24 h. After 24 h inoculation of *S. aureus*, each extracts (PE, EtOH and H_2O extracts) in three different concentrations (0.2%, 0.4% and 0.6%) were applied topically into inflamed wounds (1 mL/day on a daily basis). For control, 1 mL of ethanol was used.

Evaluation of the Skin Whitening Effect of *Feronia limonia* (L.) Swingle Bark

Skin whitening activity of *Feronia limonia* bark was evaluated via inhibitory effect on sun light-induced hyperpigmentation using guinea pigs (Shigeta *et al.,* 2004).The dorsal skin of the three guinea pigs was washed and about (2 cm x 2 cm) area was cleanly shaved. These guinea pigs were exposed sunlight daily; starting from 11 am to12 am (1h /day) for two consecutive weeks. After two weeks, the hyperpigmentation (tanning) on skin was clearly noticed by naked eye.

Individual guinea pigs (**1**, **2** and **3**) were then treated respectively with PE extract, EtOH extract and kojic acid (control). The hyperpigmented area of each animal was imaginarily divided vertically into two portions (1 cm x 2 cm). The area of left portion on guinea pig **1** was topically applied evenly with the solution of PE extract (0.1mL , i.e., 25 μg extract per cm^2 skin area) and the right portion of it was treated with pet-ether (0.1 mL). Similarly, left portion of guinea pig **2** was treated with EtOH extract (0.1mL , 25 μg/cm^2) and the right side was treated with ethanol (0.1mL). Guinea pig **3** received kojic acid (0.1mL , 10 μg/cm^2) on left portion and ethanol on right portion.

Treatments were continued for three successive weeks one time per day. Finally, the blanching effect of individual samples on hyperpigmented skin was evaluated by viewing with naked eye while comparing with control area.

Results and Discussion

Spectroscopic Identification of Isolated Compounds

Identification of Isolated Compound 1

Study on UV Spectrum

The ultraviolet spectrum of isolated compound 1 in methanol is shown in Figure 2. Isolated compound **1** displayed wavelength of maximum absorption (λ_{max}) at 222, 239, 248, 267 and 310 nm (Table1) characteristic of a coumarin nucleus. A UV maximum near 310 nm suggested a bergaptol or isobergaptol derivatives. The reported λ_{max} for bergapten was 223, 243, 249, 259, 268 and 311 nm (Steck and Bailey, 1969).

Study on FTIR Spectrum

The FTIR spectrum of isolated compound 1 is shown in Figure 3 and the band assignment is reported in Table 2.

FTIR absorption peaks also displayed characteristic of a coumarin nucleus. Peaks in weak intensity at 3110 and 3010 were attributed to the C-H stretching vibration of coumarin. In addition, aliphatic C-H stretching vibration appeared at 2947 cm^{-1}. A strong band at 1720 cm^{-1} that represented C=O stretching vibration revealed the presence of lactone ring in this compound. In addition, C=C stretching vibration appeared at 1604 and 1473 cm^{-1}. The bending vibration of aliphatic C-H groups appeared at 1350 cm^{-1}. Bands at 1141 and 1072 cm^{-1} can be interpreted as C-O stretching vibration. In addition, =C-H out of plane bending vibration of aromatic system was found at 825 cm^{-1}.

Muller *et al.* (2004) reported characteristic absorption peaks of bergapten at $\bar{\nu}$ 3100, 3070, 3050, 1726, 1620, 1602, 1575, 1540 and 885 cm^{-1} and those of xanthotoxin at $\bar{\nu}$ 3110, 3080, 3040, 1705, 1626, 1580, 1540 and 875 cm^{-1}.

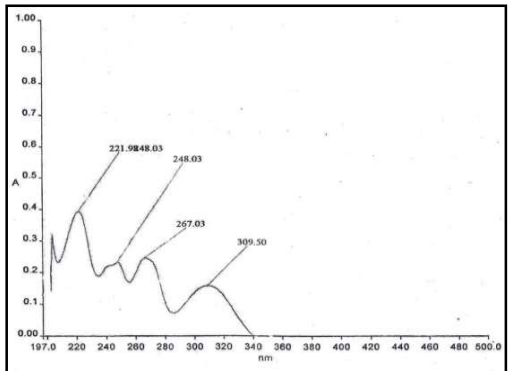

Figure 2: UVspectrum of isolated compound 1 (in MeOH)

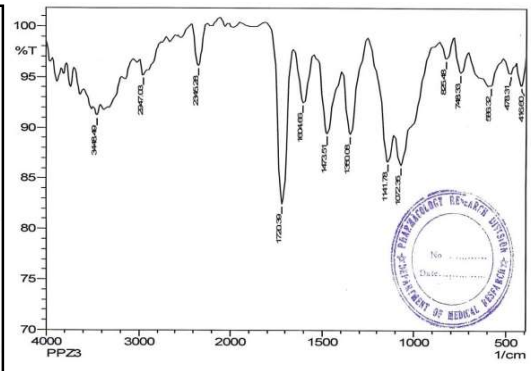

Figure 3: FT IR spectrum of isolated compound 1

Table 1: UV-Vis Spectral Data (λ_{max}) of Isolated Compound 1

Compound	**λ_{max} (nm)** (in MeOH)
Compound	222, 239, 248, 267, 310
Bergapten*	223, 243, 249, 259, 268, 311
Xanthotoxin*	223, 242, 248, 269, 273, 313

* (Muller *et al.*, 2004)

Table 2: FTIR Band Assignment of Isolated Compound 1

Wave number (cm^{-1})	**Band Assignments**
3110, 3010	C-H stretching vibration of coumarin
2947	Aliphatic C-H stretching vibration
1720	C=O stretching vibration of lactone
1604, 1473	C=C stretching vibration
1350	Aliphatic C-H bending vibration
1141, 1072825	C-O stretching vibration
	= CH out of plane bending vibration

Study on ^{1}H NMR Spectrum

The ^{1}H NMR spectrum of isolated compound 1 was measured in $CDCl_3$ and shown in Figure 4 and assignments are presented in Table 3.

The spectrum of compound 1 showed pyrone ring proton signals at δ 8.15 ppm (1H, *d*, *J*=10.0 Hz, H-4) and 6.31 ppm (1H, *d*, *J*=10.0 Hz, H-3), both doublets and coupling with each other with *ortho* coupling constant. H-4 signal at δ > 8.0 indicated substitution occurred at C-5 position. Accordingly, aromatic methoxyl group appeared at δ 4.19 ppm (3H, *s*) would be at C-5. In addition, a benzene ring proton signal at δ 7.26 ppm (1H, *s*, H-8) was observed. The protons on furano ring appeared as two doublets at δ 7.02 ppm (1H, *d*, *J*=2.4 Hz, H-3′) and 7.65 ppm (1H, *d*, *J*=2.4 Hz, H-2′); both protons mutually coupled. Therefore, compound 1 should have the following molecular structure.

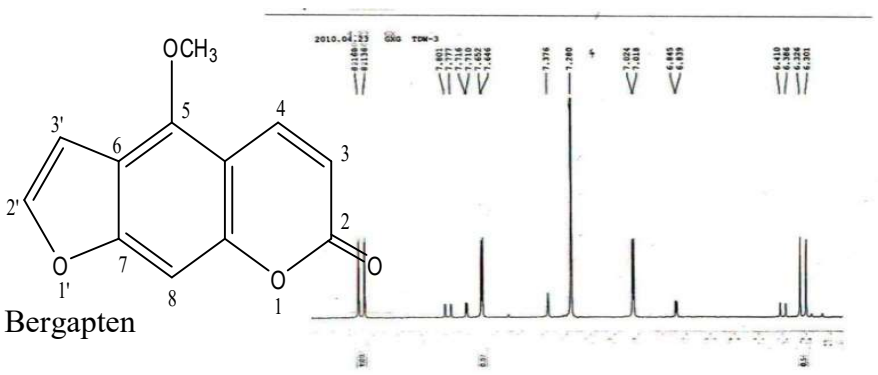

Figure 4: ^{1}H NMR spectrum of isolated compound 1 ($CDCl_3$, 400 MHz)

Table 3: ^{1}H NMR Spectral Data and Peak Assignment of Compound (in $CDCl_3$)

Chemical shift (ppm)	
Observed (Compound 1)	**Literature* (Bergapten)**
8.15 (1H, *d*, *J*=10.0Hz, H-4)	8.16 (*d*, 9.8 Hz)
7.65 (1H, *d*, *J*=2.4Hz, H-2′)	7.60 (*d*, 2.5 Hz)
7.26 (1H, *s*, H-8)	7.16 (*s*)
7.02 (1H, *d*, *J*=2.4Hz, H-3′)	7.01 (*d*, 2.5 Hz)
6.31 (1H, *d*, *J*=10.0Hz, H-3)	6.26 (*d*, 9.8 Hz)
4.19 (3H, *s*, 5-OMe)	4.26 (*s*)

Identification of Isolated Compound 2

Study on UV-Vis spectrum

Figure 5 represents the UV spectrum of compound 2 in methanol. It provided the wavelength of maximum absorption (λ_{max}) at 209, 234, 262, 275, 320 and 360 nm. It could be characterized as a furanocoumarin since absorption at two regions, 290-310 and 240-270 nm appeared (Muller *et al.*, 2004).

Study on FTIR Spectrum

The FTIR spectrum of compound 2 (in KBr) is shown in Figure 6. The band assignments are presented in Table 5. Strong band centered at 3413 cm^{-1} indicated the presence of OH group in this compound. The aromatic C-H stretching vibration was observed at 3100 cm^{-1}. Bands at 2985 and 2880 cm^{-1} were attributed to aliphatic C-H stretching vibrations indicating the presence of methyl groups in this compound. The band at 1680 cm^{-1} was attributed to the C=O stretching vibration of linear furanocoumarin. The bending vibration of aliphatic OH was found at 1407 cm^{-1}. The C-O group was observed as a small band at 1249 cm^{-1}. The out of plane =C-H bending vibration of aromatic system was found at 988 cm^{-1}.

The position of IR bands for marmesin was reported at: 3479 (OH), 2977, 2929, 1703 (α-pyrone ring), 1630, 1572, 1485 (aromatic C=C), 1444, 1404 (CH), 1268, 1132 (C-O), and 819 cm^{-1}.

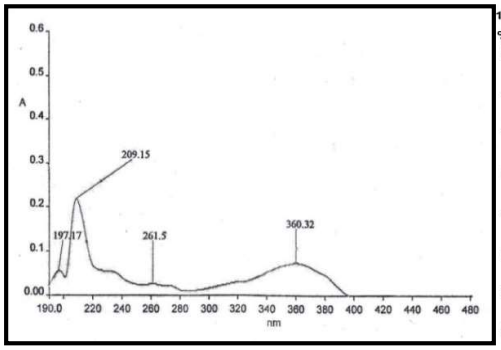

Figure 5: UV spectrum of isolated compound 2

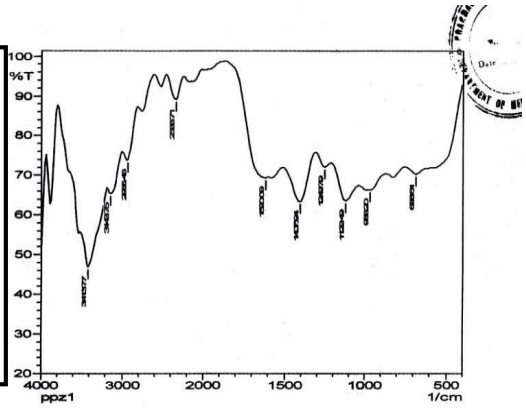

Figure 6: FTIR spectrum of isolated compound 2(inMeOH)

Table 4: UV-Vis Spectral Data (λ_{max}) of Isolated Compound 2

Solvent	Observed λ_{max} (nm)
MeOH	197, 209, 234, 261, 360

Table 5: FT IR Band Assignment of Isolated Compound 2

Wave number (cm^{-1})	**Band Assignments**
3413	O-H stretching vibration
3143	Aromatic C-H stretching vibration
2985, 2880	Aliphatic C-H stretching vibration
1680	C=O stretching vibration
1407	Aliphatic C-H bending vibration
1249, 1122	C-O stretching vibration
988	=CH out of plane bending vibration

Study on ^{1}H NMR Spectrum

The ^{1}H NMR spectrum of isolated compound 2was measured in $CDCl_3$ and shown in Figure7. Band assignment are presented in Table 6. In this spectrum, four aromatic protons were observed. Two doublets appeared at 7.58 (1H, *d*) and 6.19 ppm (1H, *d*), corresponding to H-4 and H-3 protons, were characteristic peaks of α–pyrone ring. Two singlet protons at 7.20 (1H, *s*) and 6.72 ppm (1H, *s*) were assigned to benzene protons that should be situated at *para* position. The former peak corresponded to H-5 and the later peak could be assigned to H-8. Instead, a triplet (1H) and a multiplet (2H) were observed at relatively higher field. Therefore, can be logically thought that furan ring in compound 2 was dihydrogenated. A proton triplet appeared relatively down field at 4.7 ppm was assigned to the proton of C-2′ (i.e. H-2′) that would be adjacent to electronegative oxygen atom. In addition, the splitting pattern revealed H-2′ had two neighbouring protons (two protons on C-3′, i.e. H_2-3′). Accordingly, H_2-3′ protons appeared as multiplet centered at 3.20 ppm (2H). Moreover, no proton should be present at C-4′. Remaining peaks that had not been identified yet were two methyl singlets at 1.21 and 1.38 ppm; and one broad peak at 1.82 ppm. Consequently, these three groups would be at C-4′. Finally compound 2 was assigned as marmesin, linear dihydrofuranocoumarin.

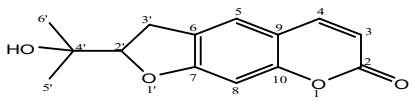

Mermasin(2)

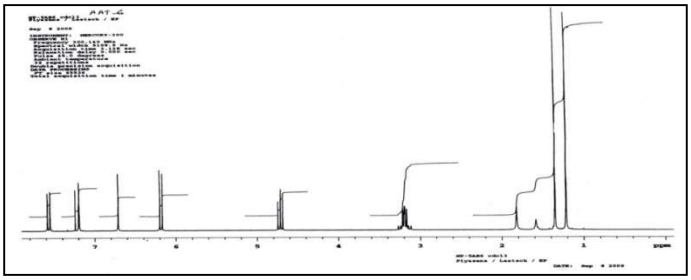

Figure 7: ^{1}H NMR spectrum of isolated compound 2 ($CDCl_3$, 300MHz)

Table 6: ^{1}H NMR Spectral Data and Peak Assignment of Compound (in $CDCl_3$)

Proton No.	Observed data, present work	Marmesin*
H-3	6.19 (1H, *d*)	6.21 (1H, *d*, *J*=9.5 Hz)
H-4	7.58 (1H, *d*)	7.59 (1H, *d*, *J*=9.5 Hz)
H-5	7.20 (1H, *s*)	7.22 (1H, *s*)
H-6	-	-
H-8	6.72 (1H, *s*)	6.74 (1H, *s*)
H-1′	3.20 (2H, *m*)	3.23 (2H, *br d*, *J*= 8.8 Hz)
H-2′	4.72 (1H, *t*)	4.74 (1H, *t*, *J*=8.8 Hz)
H-4′	1.38 (3H, *s*)	1.37 (>Cme_2)
H-5′	1.21 (3H, *s*)	1.23
3′-OH	1.82 (1H, *br*)	1.85 (1H, *br*)

Study on ^{13}C NMR spectrum

The^{13}C NMR spectrum of isolated compound 2 is shown in Figure 8 and peak assignment is reported in Table 7.The ^{13}C NMR spectrum revealed 14 carbon atoms that consistent with the molecular structure explored from ^{1}H NMR spectrum. These carbon peaks were classified as one carbonyl carbon; four quaternary aromatic carbons two of which are oxygenated; one

oxygenated quaternary aliphatic carbon; four aromatic 475 ethane carbons; one oxygenated aliphatic 475 ethane carbon; one methylene carbon; and two methyl carbons.

The down field peak at δ 163.0 ppm was assigned to carbonyl carbon of pyrone ring. Two peaks at 161.9 and 155.5 were corresponded to oxygenated quaternary carbons, C-7 and C-10, respectively. Remaining two aromatic quaternary carbon peaks were observed at 124.9 (C-6) and 112.6 (C-9). In addition, aliphatic quaternary carbon (C-4′) appeared at relatively low field δ 71.6 was due to the presence of –OH group. Four peaks correspond to aromatic CH at 143.5, 123.3, 112.1 and 97.8 ppm were respectively assigned to C-4, C-5, C-9 and C-8. Peak at 91.0 ppm was attributed to C-2′ that attached to electronegative oxygen atom. Peak at 29.5 ppm corresponded to methylene carbon (C-3′). Remaining peaks at 26.1 and 24.3 ppm were assigned to two methyl carbon. The chemical shift of marmesin (Lee *et al.*, 2002) from published data were also presented in Table7. It can be seen from the table that the chemical shift of compound 2 was consistent with that of marmesin {2-(2-hydroxypropan-2-yl)-2H-furo[3,2-g]chromen-7(3H)-one}.

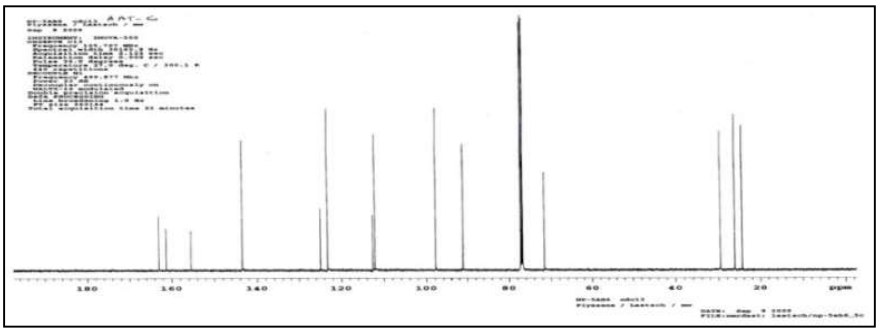

Figure 8: ^{13}CNMR spectrum of isolated compound ($CDCl_3$, 125 MHz)

Table 7: ^{13}C NMR Spectral Data and Peak Assignment of Compound (in $CDCl_3$)

Chemical Shift (δ, ppm)	**Marmesin***
Observed value	**($CDCl_3$, 100 MHz)**
163.0	163.1 (C-2)
161.9	161.0 (C-7)
155.5	155.7 (C-10)
143.5	143.6 (C-4)
124.9	125.0 (C-6)
123.3	123.3 (C-5)
112.6	112.8 (C-9)
112.1	112.3 (C-3)
97.8	97.9 (C-8)
91.0	91.0 (C-2′)
71.6	71.6 (C-4′)
29.5	29.4 (C-3′)
26.1	26.1 (C-6′)
24.3	24.2 (C-5′)

Study on GC-MS spectrum

The GC-MS spectrum of compound 2 is shown in Figure 9. The molecular ion peak was observed at m/z 246 which was consistent with the molecular formula, $C_{14}H_{14}O_4$. The observed m/z values of compound **2** are 246 (M^+), 228, 213, 189, 187, 175, 160, 131, 103, 91, 77, 59 and 43. Reported EI MS data for marmesin m/z (%) 246(M^+,39), 213(20), 188(75), 187(100), 175(15), 160(30), 131(19), 59(66), and 43(7).

On the basis of the spectroscopic data, the isolated compound 2 was identified as marmesin ($C_{14}H_{14}O_4$, molecular mass = 246.26) with the following molecular structure.

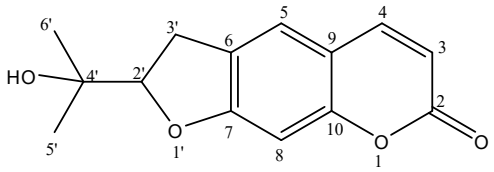

Marmesin (2)

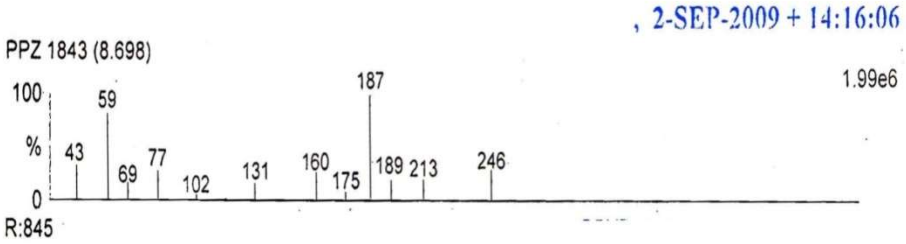

Figure 9: GC-MS spectrum of isolated compound 2

Table 8: Percent Yield and Melting Points of Isolated Compounds from *Feronia limonia* (L.) Swingle Bark

Isolated compounds	% Yield	Appearance	Melting point (°C)
1	0.0008	Yellow needles (Me_2CO-MeOH)	188-190 (sub.)
2	0.0022	White needles (benzene-Me_2CO)	160-163

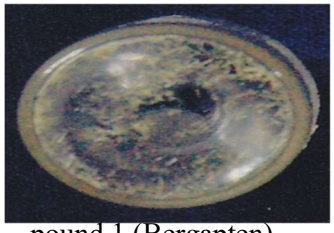

pound 1 (Bergapten)

Compound 2 (Marmesin)

Figure 10: Photographs showing the Crystal form of isolated compounds

Study on *In Vivo* Antistaphylococal Activity of Crude Extracts of *Feronia limonia* (L.) Swingle Bark

In this study, *in vivo* antistaphylococal activities of three different extracts (PE, EtOH and H_2O extracts) of *F. limonia* bark were evaluated by investigating the healing potential on *Staphylococcus aureus* induced excision type cutaneous wounds.

Groups topically treated with any extracts needed 6 days to heal the wound. No significant difference on wound healing effect was observed between different doses of 2-6 mg/wound/day (topical application of 1 mL solution at 0.2-0.6% concentration of sample per day). Control groups (treated with ethanol only) needed 8 days to heal wound. The treated wounds exhibited remarkably dryness of wound margins with tissue regeneration and reduced wound area in comparison to controls.

The wound healing potency of different extracts are presented in Table 9. Figure11 represents the healing potency of *Feronia limonia* bark on staphylococcus induced excision type cutaneous wounds. Since *Feronia limonia* bark possess wound healing activity, it can be used as a traditional wound healer, and as an ingredient in skin cosmetic lotion.

Table 9: *In Vivo* Antistaphylococal Activity (Wound Healing Property on *S. aureus* Induced Excision-Type Cutaneous Wound) of Different Crude Extracts of *Feronia limonia* (L.) Swingle Bark

Concentration (%)	Dose (mg/day)	Time needed to heal wound (day)			
		Gp-1	Gp-2	Gp-3	Gp-4
0.2	2	6	6	6	8
0.4	4	6	6	6	8
0.6	6	6	6	6	8

Gp-1 Topically treated with pet-ether extract of *Feronia limonia* bark

Gp-2 Topically treated with ethanol extract of *Feronia limonia* bark

Gp-3 Topically treated with water extract of *Feronia limonia* bark

Gp-4 Topically treated with ethanol only

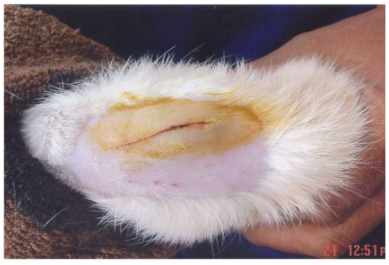

Group 1

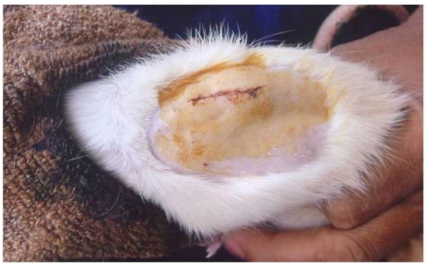

Group 2

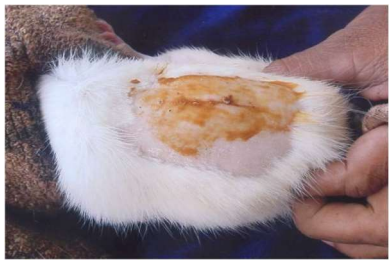

Group 3

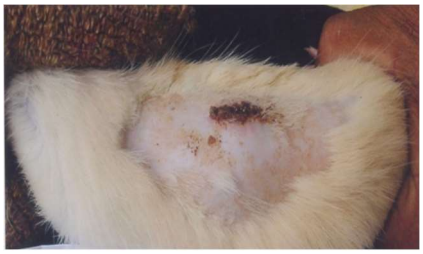

Control

Figure11: *In vivo* antibacterial activity (wound healing property against *S. aureus* induced excision-type cutaneous wounds) of *Feronia limonia* (L.) Swingle bark

Group 1 Healing result after 6 days treatment with pet-ether extract

Group 2 Healing result after 6 days treatment with ethanol extract

Group 3 Healing result after 6 days treatment with water extract

Study on the Skin Whitening Effect of *Feronia limonia* (L.) Swingle Bark

The back of guinea pigs was cleanly shaved and (2 cm x 2 cm) area on shaven skin was exposed to sunlight daily (11-12 AM, 1 h/day) for two consecutive weeks. When the hyperpigmentation on skin was clearly noticed, the area was imaginarily divided into two portions vertically (1 cm x 2 cm). The area of left portion was topically treated with sample solution and the right portion was treated with respective solvent for control purpose. Treatments were continued for three successive weeks one time per day.

Finally, the blanching effect of individual samples on hyperpigmented skin was evaluated by viewing with naked eye while comparing with control area.

Figures 12,13 and 14 represent photographs showing whitening effect of samples (PE and EtOH extracts, and kojic acid) on sun light-induced hyperpigmentation after 21 days of topically application. It can be seen from the figures that the skin of guinea pigs receiving treatment was appeared to be whiter than that receiving treated with respective solvents. The extent of blanching effect of both extracts was seemed to be equal. The whitening level of control kojic acid was seemed to be higher than both extracts.

From this finding, it can be inferred that *F. limonia* bark possessed the ability to blanch hyperpigmentation of the skin and hoped to protect skin from photoaging. The level of UV radiation emitted by the sun is increasing due to the depletion of ozone layer. Skin is more exposed to UV radiation and often suffers from various harmful effects of UV. Melanin production in human skin is an important defense mechanism against UV and a major determinant of skin color. Therefore, this finding was envisaged to be beneficial for exploring plant-based cosmetics.

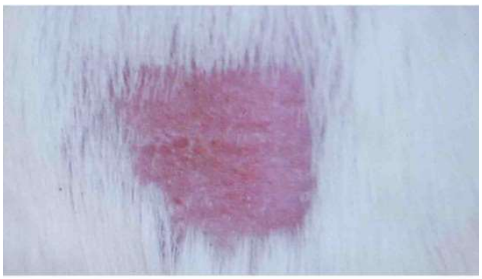

Sun light-induced hyperpigmented skin of guinea pig 1

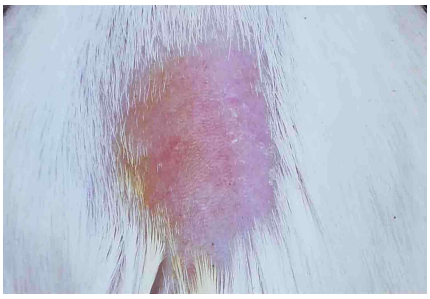

Providing topically treatment on half portion of hyper-pigmented skin

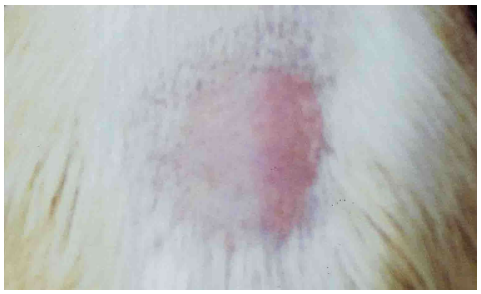

Whitening result after 3 weeks successive treatment

Figure 12 : Whitening effect of pet-ether extract of *Feronia limonia* (L.) Swingle bark on sun light-induced hyperpigmentation

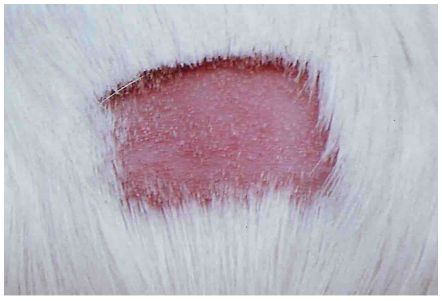

Sun light-induced hyperpigmented skin of guinea pig 2

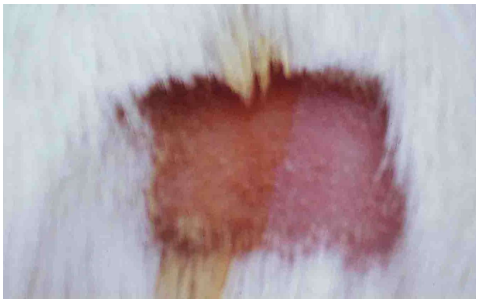

Providing topically treatment on half portion of hyper-pigmented skin

Figure 12 : Whitening effect of pet-ether extract of *Feronia limonia* (L.) Swingle bark on sun light-induced hyperpigmentation

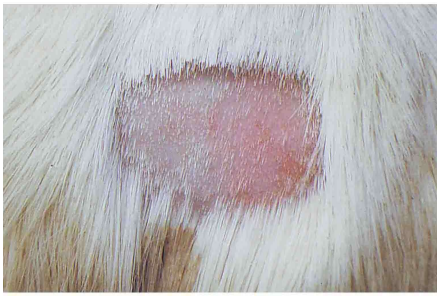

Whitening result after 3 weeks successive treatment

Figure 13: Whitening effect of ethanol extract of *Feronia limonia* (L.) Swingle bark on sun light-induced hyperpigmentation

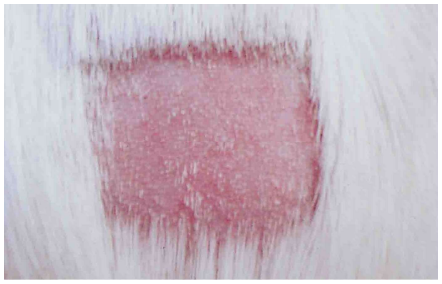

Sun light-induced hyperpigmented skin of guinea pig 3

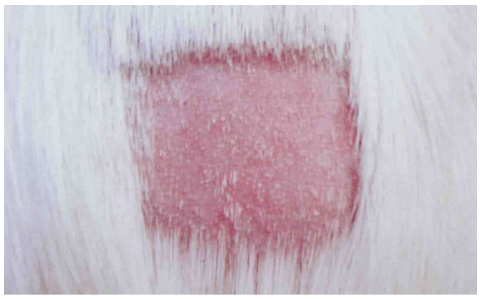

Providing topically treatment on half portion of hyper-pigmented skin

Whitening result after 3 weeks successive treatment

Figure 14: Whitening effect of kojic acid on sun light-induced hyperpigmentation

Conclusion

From the overall assessment concerning with chemical and biological activity investigation on stem bark of *Feromia limonia* (L.) Swingle (Thee in Myanmar), the following inferences may be deduced.

Compound **I** (bergapten) (0.0008% yield, mp 188-189ºC) and Compound **II** (marmesin) (0.0022% yield, mp160-163ºC).*S. aureus* induced excision-type cutaneous wounds when topically treated with PE, H_2O and EtOH extracts needed 6 days to completely cure the wound. No significant difference in wound healing effect between different doses (2-6 mg/day) was observed showing the bark possesses antistaphytococal effect. Control group *needed 8 days to cure wounds.* Skin whitening activity was observed by using sun light induced hyperpigmented guinea pig models. The hyperpigmented skin of guinea pig was topically treated with PE and EtOH extracts, and kojic acid (control) for 3 successive weeks. All extracts provided skin whitening effect but lower than that of kojic acid.

Skin whitening activity is related to inhibition of melanin formulation. Hence topical application of "*Feromia limonia*" bark is envisaged to protect individuals from sun burn, photo-aging and antiwrinkling; and to promote skin whitening by prevention of tanning. In addition, possessing the wound

healing activity of this bark further confirmed the use of this bark as a good candidate for natural cosmeceuticals.

Acknowledgements

The authors would like to thank the Myanmar Academy of Arts and Science for allowing to present this paper and Professor and Head Dr Daw Hla Ngwe, Department of Chemistry, University of Yangon, for her kind encouragement.

References

Lee, S., Kang, S.S. and Shin, K.H. (2002). "Coumarins and a Pyrimidine from *Angelica gigas* Roots". *Nat. Pro. Sci.*, vol. 8(2), pp. 58-61

Muller, M., Byres, M., Jaspars,M., Kumarasamy, Y., Middleton, M., Nahar, L.,Shoeb, M. and Sarker, S.D. (2004). "2D NMR Spectroscopic Analyses of Archangelicin from the Seeds of *Angelica archangelica*". *Acta. Pharm*., vol. 54, pp . 277-285

Steck, W. and Bailey, B.K. (1969). "Characterization of Plant Coumarins by Combined Gas Chromatography, Ultraviolet Absorption Spectroscopy, and Nuclear Magnetic Resonance Analysis". *Canadian J. Chem*, vol. **7**, pp. 3577-3583

Yusutamin, Hideya, .S, Hideya., Atsuko, A., And Naoto, O,(2004). " Skin Whitening Effect of Linoleic Acid is Enhanced by Liposomal Formulations". *Biol. Pharm. Bull*., vol.27(4), pp. 591-594

PREPARATION OF ORGANIC FERTILIZERS USING FOR CROP CULTIVATION

Aung Aung[1], Aye Aye Lwin[2], Thi Thi Aye[3]

Abstract

Organic fertilizers prepared from organic wastes can reduce cost in agricultural sectors and increase soil fertility. This research work concerns with studies for the preparation of organic fertilizers from rice straw, chicken manure and neem leaves, its application for crop cultivation and studies the effect of fertilizer on soil fertility. Rice straw from farmer field, neem leaves from Kun Chan Village in Taungdwingyi Township and chicken manure from Pyay Township were collected. The organic fertilizers were prepared by five different weight ratios (100kg :100kg :100kg), (rice straw, chicken manure, neem leaves) for OF-1(organic fertilizer 1), (200kg : 75kg : 25kg) for OF-2 , (200kg : 25kg : 75kg) for OF-3, (250kg : 30kg : 20kg) for OF-4, and (250kg : 20kg : 30kg) for OF-5. These different fertilizers were prepared by compost heap method. The physicochemical properties and, content of macronutrients and micronutrients were determined by EDXRF, AAS and other modern and conventional methods. It was found that OF-1 contains (2.17%N, 1.523%P_2O_5, 1.663%K_2O), OF-2 (1.70%N, 0.825%P_2O_5, 1.478%K_2O), OF-3 (1.729%N, 0.689%P_2O_5, 1.372%K_2O), OF-4 (1.563%N, 0.913%P_2O_5, 1.346%K_2O), OF-5 (1.241% N, 0.849%P_2O_5, 1.056%K_2O).From EDXRF result, the amount of Ca, K and Si are higher than other elements in five different ratios of organic fertilizers. It was found that, these organic fertilizers contain Ca%, Mg%, Zn%, Cu%, Mn% and Fe% by AAS measurement. According to these results, it was found that OF-1was rich in macronutrients. So OF-1 was chosen to use for crop cultivation and improving the soil fertility. The rice straw based organic fertilizers should be used as effective fertilizer for agricultural section and for reducing the use of chemical fertilizer which can damage the soil fertility.

Keywords: rice straw, chicken manure, neem leaves, organic fertilizers, physicochemical properties, macronutrients, micronutrients

1. 2 PhD, Candidate, Assistant Lecturer, Department of Chemistry, Pyay University
2. Associate professor, Department of Chemistry, Yenangyang Degree College
3. Associate professor, Department of Chemistry, University of Yangon

Introduction

Fertilizer is any organic or inorganic materials of natural or synthetic origin that is added to a soil to supply one or more plants nutrients essential to the growth of plants (Mi Mi Hlaing, 2011). Fertilizer is substance containing some or all of a range of about 20 chemical elements necessary for healthy plant growth, used to compensate for the deficiencies of poor or depleted soil (Auduand Zubairu, 2013).Fertilizers are broadly divided into organic fertilizers (composed of organic matter of plant or animal) or inorganic fertilizers (composed of synthetic chemical and minerals).

Our environment is a houseful of various nutrients which plants require for normal growth and development. Organic wastes or organic fertilizers, many of which are rich in nutrients and organic matter, can be used to replenish soils. Organic fertilizers come from plant and animal sources. These fertilizers have a slower release of nutrients as they need to be decomposed by soil microorganisms. They are easy on plant roots but take longer to become effective. Organic fertilizers are naturally occurring fertilizers(e.g, compost, manure).Organic fertilizers essential for maintaining the soil health (Tha zin Nyo, 2009).Cow dung and chicken manure are excellent source of soil organic matter as well as phorsphorus and potassium. Microorganisms in the soil decompose organic material making its elements available for use by plants(Theingi Shwe, 2007).

Rice is one of the major crops grown throughout the world. Rice straw are an agricultural residue abundantly available in rice producing countries. Rice straw can be converted to fertilizer throughout the process of composting. Components of rice straw are mainly cellulose and hemicellulose encrusted by lignin, in addition to a small amount of protein, which makes it high in C/N ratio. Rice straw compost will be good carrier materials for the inoculants. The biodegradation of such materials to simple sugars provide energy sources for heterotrophic microorganisms such as P- solubilizing and nitrogen fixing bacteria. Rice straw is rich in nitrogen, potassium and silicon (Thida Min, 2005).

Chicken manure provides nitrogen, phosphorus and potassium for plants. Chicken manure is a good source of organic material for composting. Chicken manure is very high in nitrogen and a very desirable fertilizer for

gardens and farms. Chicken manure may be applied to the soil fresh and growth of plants. Chicken manure is an important soil conditioner, and it increases the soil moisture, holding and nutrient holding capacities(Sunarlim, Sahwan and Schuchardt, 1999).

Neem leaves are cheap and useful fertilizer. Neem leaves improve efficiency of fertilizer utilization in crop production by gradual release of nitrogen to crops(Sumaila, 2012).Neem leaves have an adequate quantity of NPK in organic form for plant growth. Neem leaves are 100 % natural fertilizer (Emmanuel, 2013). Rice straw, chicken manure and neem leaves enhance for application to crops and soil as a fertilizing resource, were used as material for biodegradation.

Materials and Methods

Collection of Rice Straw, Chicken Manure, Neem Leaves

The rice strawsample and neem leaves sample were collected from Kun Chan Village in Taungdwingyi Township. The chicken manuresample was collected from Pyay Township.These samples were dried in air, ground and sieved into 80 mesh size and stored in air tight plastic bags.

Preparation of Organic Fertilizers

Five piles were prepared by plastic sheets and the size of each pile was 1.5 m wide, 1.5 m long and 1.5 m high. The prepared organic fertilizers were made by five different ratios. The different types of organic fertilizers(rice straw, chicken manure, neem leaves) wereOF-1 (100kg: 100kg: 100kg), OF-2 (200kg: 75kg: 25kg),OF-3 (200kg: 25kg:75kg), OF-4(250kg: 30kg :20kg), OF-5 (250kg : 20kg : 30kg). Organic fertilizers were prepared by compost heap layer method. Firstly, dry plant materials (strong rice straw) were loosely spread on the bottom of the piles which were used for the foundation layers. The compost heap was made by the three basic layers (first layer, second layer, third layer). First layer was made by rice straw materials. This layer was 25cm thick of the sides. Then, water was sprinkled over this layer. This layer should be moist but not soaked. The second layer was made by neem leaves (green) plant materials. This layer was added on the first layer. The second

layer was 25 cm thick. The third layer was made by chicken manure with 10 cm thick. These three layers were added to the pile in the sequence, first layer, second layer, third layer, until the piles were full of compost making materials. The top of piles were covered with plastic sheets.

After one month, white fungi were appeared on the surface. And then, the piles were turned over. After 3 months, compost making material became black colour and odourless smell. And then, organic fertilizers were obtained.

Study on Physicochemical Properties of Organic Fertilizers

Chemical analyses such as pH, moisture, Organic matter, Total N, P_2O_5, K_2O, Total Ca and Mg, S, Mn, Fe, Zn, Cu and relative composition of elements were carried out on the collected samples and organic fertilizers. The pH was determined by pH meter. Moisture was determined by oven dry method and organic matter was determined by Walkey and Black' titration method. Total N, P_2O_5 and K_2O were determined by Kjeldahl digestion method, visible spectrophotometric method and atomic absorption spectrometric method respectively.Ca, Mg, Mn, Fe, Zn and Cu were also determined by atomic absorption spectrometric method. Total S was determined by turbidity method. Relative composition of elements was determined by energy dispersive –X- ray fluorescence spectrometric method.

Results and Discussion

Total N, P_2O_5 and K_2O Contents of Rice Straw, Neem Leaves and Chicken Manure

Table 1 shows the composition of nitrogen content inrice straw, chicken manure and neem leaves samples. In the present research, totalN of fertilizers contains 0.799%, 0.817% and3.118 %for rice straw, chicken manure and neem leavessamples. As mentioned above,neem leavessample was observed to show higher amounts of nitrogen.

Table 1 shows the composition ofP_2O_5 content inrice straw, chicken manure and neem leaves samples. In this experiment, the amount of P_2O_5in rice straw, chicken manure and neem leavessamples were found to be 0.107%,

2.052% and 0.379%. It can be seen that chicken manure sample was higher in amount of P_2O_5 than rice strawand neem leavessamples. Table 1 shows the composition of K_2O content in three samples. In this work, the amount of potassium in neem leaves sample was higher than rice straw and chicken manuresamples.

Table 1: Total N, P_2O_5 and K_2O Contents of Rice Straw, Chicken Manure and Neem Leaves samples

No.	Sample	Total N (%)	P_2O_5 (%)	K_2O (%)
1	Rice straw	0.799	0.107	0.264
2	Chicken manure	0.817	2.052	0.475
3	Neem leaves	3.118	0.379	1.162

Temperature of Compost During Composting Process

Table 2 shows temperature of prepared compost (OF-1, OF-2 OF-3, OF-4 and OF-5) during composting process. Decomposition of organic wastes produces heat. Compost needs to be kept hot and moist because the plant and animals materials can be broken down quickly and thoroughly. The temperature was measured at (10 am) daily. On one day, the temperature was nearly 32˚C and the temperature gradually increased (~ 50˚C) within at 29 days. And then, the temperature slightly decreased. After 31 days, the temperature gradually increased and reached its optimum (~54˚C) within 55 to 60 days. The temperature gradually dropped to reached26˚C after 84 days. The compost process was finished when the colour of material turned dark. When the temperature reached 26˚C, the dark colour was found. Therefore the compost process was taken between 26˚C to 54 ˚C.

Table 2: Temperature of Compost during Composting Process

Day	Temperature °C					Day	Temperature °C					Day	Temperature °C				
	Of-1	OF-2	OF-3	OF-4	OF-5		Of-1	OF-2	OF-3	OF-4	OF-5		Of-1	OF-2	OF-3	OF-4	OF-5
1	32	32	31	31	32	31	43	42	43	43	42	61	50	51	54	52	52
2	32	33	31	32	32	32	44	42	43	43	42	62	50	51	50	52	50
3	32	33	32	32	33	33	44	44	43	43	42	63	50	51	50	49	50
4	35	33	33	32	33	34	44	44	44	44	43	64	49	48	50	49	47
5	35	35	33	32	34	35	44	44	44	44	43	65	47	48	50	49	47
6	35	35	33	35	35	36	44	44	44	44	43	66	47	44	50	48	47
7	35	36	34	35	36	37	46	45	45	44	43	67	40	44	46	48	47
8	35	36	34	35	36	38	46	45	45	44	43	68	40	42	46	45	43
9	35	36	36	35	36	39	46	45	47	44	45	69	40	42	46	45	43
10	37	37	36	36	36	40	46	45	47	46	45	70	39	40	41	45	43
11	37	37	36	38	36	41	46	46	47	46	45	71	39	40	41	39	41
12	37	37	36	38	37	42	46	46	47	46	45	72	39	40	41	39	41
13	37	37	36	38	37	43	46	47	47	48	45	73	35	34	33	33	36
14	37	37	36	38	38	44	46	47	47	48	46	74	35	34	33	33	36
15	37	38	37	38	39	45	47	47	49	48	46	75	32	34	33	33	32
16	37	38	37	39	39	46	47	47	49	48	47	76	32	34	33	30	32
17	37	38	37	39	39	47	47	47	49	49	47	77	28	27	27	30	29
18	38	38	37	39	39	48	49	48	49	49	49	78	28	27	27	27	27
19	38	38	38	39	39	49	49	48	49	50	49	79	28	27	27	27	27
20	39	38	38	39	39	50	49	49	50	50	49	80	28	27	27	26	27
21	39	38	38	39	39	51	49	50	50	51	49	81	26	27	27	26	26
22	39	38	38	40	39	52	49	50	50	51	50	82	26	26	27	26	26
23	39	38	38	40	41	53	49	50	50	51	50	83	26	26	27	26	26
24	39	39	38	40	41	54	50	50	51	51	50	84	26	26	26	26	26
25	41	39	41	42	41	55	54	53	53	54	54	85	26	26	26	26	26
26	48	40	41	42	41	56	54	53	53	54	54	86	26	26	26	26	26
27	48	49	50	47	47	57	54	54	53	54	54	87	26	26	26	26	26
28	48	49	50	47	47	58	54	54	54	54	52	88	26	26	26	26	26
29	43	40	50	42	47	59	53	54	54	54	52	89	26	26	26	26	26
30	43	42	43	42	41	60	53	51	54	52	52	90	26	26	26	26	26

C/N Ratios of Organic Fertilizers

The C/N ratios in five different ratios of organic fertilizers are shown in Table 3. The C/N ratio of OF-3 was higher than other organic fertilizers. OF-2 and OF-4 were nearly the same amount of C/N ratio. The C/N ratio of (~ 10 to 15) is suitable for crop cultivation and soil fertility.

Table 3: C/N Ratio of Organic Fertilizers

Fertilizers	Organic matter (%)	Organic carbon (%)	Total N(%)	C/N ratio
OF-1	35.629	21.246	2.17	9.523
OF-2	36.766	21.325	1.70	12.543
OF-3	40.09	23.254	1.729	13.448
OF-4	32.859	19.059	1.563	12.19
OF-5	28.19	16.241	1.241	13.175

OF-1= rice straw+chicken manure+ neem leaves (100kg:100kg:100kg)

OF-2= rice straw+ chicken manure+ neem leaves (200kg:75kg:25kg)

OF-3= rice straw+ chicken manure+ neem leaves (200kg:25kg:75kg)

OF-4= rice straw+ chicken manure+ neem leaves (250kg:30kg:20kg)

OF-5= rice straw+ chicken manure+ neem leaves (250kg:20kg:30kg)

pH and Moisture Contents of Organic Fertilizers

Table 4 shows contents of pH and moisture of organic fertilizers. The pH values were slightly acidic as well as alkaline (pH 6.42 to 7.41). The (pH 5.8 to 7.5) are suitable for the plant growth. The moisture contents of OF-5 was higher than other organic fertilizers.

Table 4: pH and Moisture Contents of Organic Fertilizers

Fertilizers	pH	Moisture (%)
OF-1	6.42	6.539
OF-2	6.92	11.573
OF-3	7.41	6.940
OF-4	7.15	8.228
OF-5	7.22	12.648

Relative Abundance of Element in Organic Fertilizers by EDXRF

The presence of silicon, calcium, potassium, iron, sulphur, phosphorous, titanium, manganese, zinc, strontium, copper, chromium, bromine, rubidium, zirconium, vanadium, aluminum and palladium are shown in Figures 1,2,3,4,5 andTable5. Each spectrum indicated that the relevant elements are shift present in organic fertilizers. The amount of silicon, calcium and potassium were higher than other elements in these organic fertilizers.

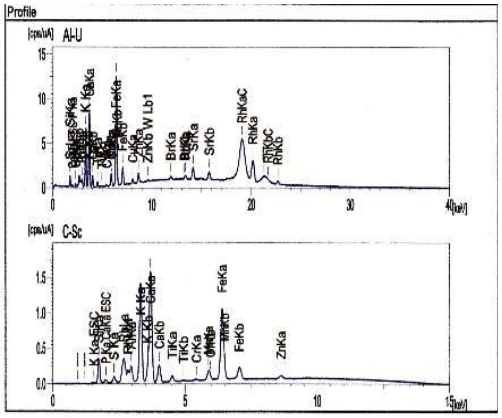

Figure 1: EDXRF Spectrum of OF-1

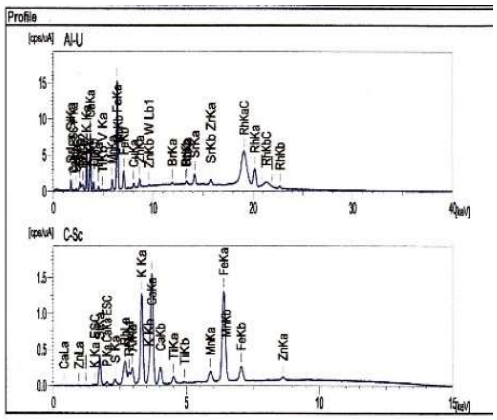

Figure 2: EDXRF Spectrum of OF-2

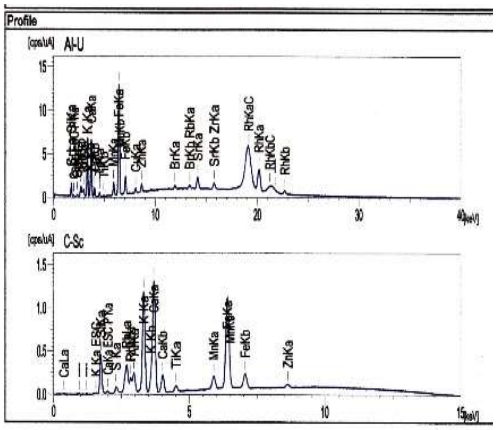

Figure 3: EDXRF Spectrum of OF-3

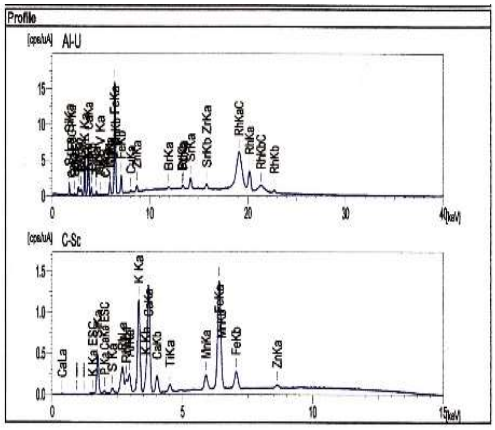

Figure 4: EDXRF Spectrum of OF-4

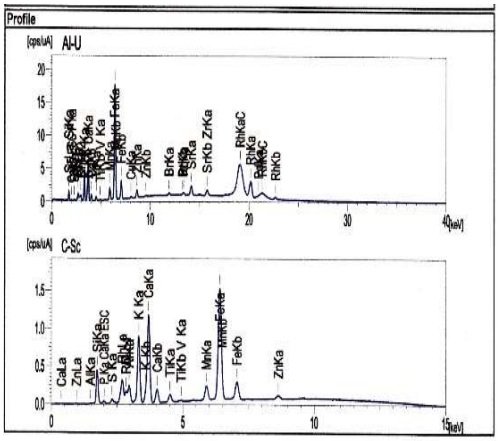

Figure 5: EDXRF Spectrum of OF-5

Table 5: Relative Abundance of Elements in Organic Fertilizers by EDXRF

No.	Elements	OF-1 (%)	OF-2 (%)	OF-3 (%)	OF-4 (%)	OF-5 (%)
1	Si	30.304	36.476	41.408	41.408	44.252
2	Ca	29.117	26.557	23.293	22.665	19.139
3	K	23.994	20.559	20.912	19.688	15.724
4	Fe	7.986	8.785	7.455	8.805	9.394
5	S	2.476	2.072	2.291	1.946	1.803
6	P	2.378	2.056	1.489	1.43	1.729
7	Ti	1.312	1.224	0.965	1.125	1.215
8	Mn	1.145	1.068	1.16	1.253	1.341
9	Zn	0.41	0.379	0.327	0.324	0.376
10	Sr	0.296	0.279	0.257	0.29	0.259
11	Cu	0.203	0.235	0.177	0.093	0.075
12	Cr	0.193	-	-	0.088	-
13	Br	0.096	0.075	0.092	0.083	0.076
14	Rb	0.08	0.08	0.075	0.081	0.066
15	Zr	-	0.104	0.098	0.095	0.121
16	V	-	0.052	-	0.043	0.049
17	Al	-	-	-	-	3.96
18	Pd	-	-	-	-	0.419

Macronutrients and Micronutrients in Prepared Organic Fertilizers

Table6 shows the macronutrients and micronutrients in prepared organic fertilizers. In macronutrients, the total N, P_2O_5, K_2O and S contents of OF-1 were higher than those of other organic fertilizers. The Ca content of OF-3 and Mg content OF-4 were higher than those of other organic fertilizers. In micronutrients, Fe content of OF-1 was higher than those of other organic fertilizers. Mn and Zn contents of OF-5 were higher than those of other organic fertilizers. Cu content of OF-2was higher than those of other organic fertilizers.

Table 6: Macronutrients and Micronutrients in Prepared Organic Fertilizers

Macronutrients	Organic Fertilizers				
	OF-1	OF-2	OF-3	OF-4	OF-5
N(%)	2.170	1.700	1.729	1.563	1.241
P_2O_5(%)	1.523	0.825	0.689	0.913	0.849
K_2O(%)	1.663	1.478	1.372	1.346	1.056
Ca(%)	1.695	2.202	5.100	1.312	3.359
Mg(%)	0.122	0.080	0.038	0.367	0.068
S(%)	0.175	0.162	0.162	0.171	0.166
Micronutrients					
Fe (ppm)	1.203	0.019	0.810	0.562	1.07
Mn(ppm)	0.422	1.102	0.754	0.183	1.201
Zn(ppm)	3.468	3.455	3.752	3.035	5.543
Cu(ppm)	0.280	0.304	0.247	0.138	0.181

Conclusion

In the present work, the selected agricultural wastes (rice straw, chicken manure, neem leaves) were recycled to use as organic fertilizers. During composting process, temperature of prepared organic fertilizers (OF-1,OF-2, OF-3, OF-4, OF-5) ranged from 26°C to 54°C. The moisture content, the pH values, the total organic matter, the total organic carbon and the C/N ratio ranged from6.539 to 12.648, 6.42 to 7.41, 28.19 to40.09, 16.241 to23.254, and 9.523 to 13.448 respectively. According to EDXRF results, the amount of Ca, K and Si are higher than other elements in organic fertilizers. Micronutrients Fe, Mn, Zn and Cu contained in all prepared organic fertilizers. Macronutrients N, P_2O_5, K_2O, Mg and S of OF-1 are higher than OF-2, OF-3, OF-4, OF-5. Primary macronutrients are N, P_2O_5 and K_2O.

Therefore, the prepared organic fertilizers should be used in cultivation of crops and improving the soil fertility.

Acknowledgement

The authors would like to thank the Department of Higher Education (Yangon Office), Ministry of Education, Yangon, Myanmar, for the permission to do this research and Myanmar Academy of Arts and Science for allowing to present this paper. Special thanks are extended to Professor and Head, Dr Tun Cho and Professor Dr Myint Myint Than, Department of Chemistry, Pyay University.

References

Audu, M. and Zubairu, A. (2013).“Analysis of Nutrient Content of Some Organic Materials for Soil Amendment in Sokoto Metroplis”. *Journal of Biology, Agriculture and Health Care,* vol.,4 (18), pp. 8-11

Emmanuel, I.M. (2013).“Comparative Evaluation of Neem Leaf (*Azardirachta Indica* L.), Wood Ash and Modified Neem Leaf Extracts on the Soil Fertility, Growth and Yield of Garden Eggplant(*Solaniummelongena* L.)”. *American Journal of Agricultural Science and Technology*, vol., 1(3), pp .84-92

Mi Mi Hlaing. (2011).*Recycling Wastes into Organic Fertilizers by Vermicomposting using Earthworms*. PhD Dissertation, Chemistry Department, Yangon University

Sumaila, R. (2012).*The Potentiall of Azadirachtaindica Leave Biomass as a Nutrient Source for Maize Cultivation*.M.Sc Thesis, Department of Agroforestry, Kwame Nkrumah University of Science and Technology

Sunarlim, N., Adil, W.H., Sahwan, F.L. and Dan Schuchardt, F. (1999). “The Mineralization of Nitrogen from Two Different Composts in the Soil”.*Indonesian Jou of Crop Science*.Vol.,14(2), pp .34-40

Thazin Nyo. (2009).*Study on Fertilizers prepared from Rice Husk Ash and Tea Residue* .PhD Dissertation, Chemistry Department, University of Yangon

Theingi Shwe. (2007).*Production of Modified Fertilizers from Bat Guano*. PhD Dissertation, Chemistry Department, University of Yangon

Thida Min. (2005). *Quality Assessment of Organic Fertilizers Based on Water Hyacinth and Rice Straw*. PhD Dissertation, Chemistry Department, University of Yangon

EFFECT OF CALCINATION TEMPERATURE ON MORPHOLOGICAL, STRUCTURAL AND THERMAL PROPERTIES OF HYDROXYAPATITE DERIVED FROM GOAT BONE

Lin Lin Naing[1], Ni Ni Sein[2], ThidaWin[3]

Abstract

Hydroxyapatite (HAp) is included in the calcium phosphate compound family having the formula $Ca_{10}(PO_4)_6(OH)_2$.Calcination method was used to extract hydroxyapatite from waste goat bone, a useless resource, after deproteinization. This study focuses the study of HAp derived from waste goat bone subjected to different calcination temperatures (800ºC, 900ºC, 1000ºC and 1100ºC) with regard to their morphological, structural and thermal properties. Calcination treatment has eliminated the collagen and organic compounds from the HAp derived from goat bones. EDXRF spectrum showed the highest amount of calcium and phosphorus in HAp samples at all calcination temperatures. Only a single phase of hydroxyapatite was noted in the XRD pattern at each calcination temperature and the crystal system was indexed as hexagonal. Crystallinity percent increased from 56.77% at 800ºC to 62.73% at 1100ºC. With increase in calcination temperature crystallite size also increased but the increase was not pronounced at higher temperature. The absorption bands of 1548 and 1662 cm^{-1} originated by the collagen disappeared after calcination at 800 ºC. Thermal analysis revealed that the highest weight loss (32.215 %) accompanied by an exothermic peak was observed for uncalcined hydroxyapatitedue to the loss of organic constituents like collagen whereas the weight losses were negligible for the calcined samples.

Keywords: goat bone, hydroxyapatite, calcination method, crystallinity, hexagonal

Introduction

Hydroxyapatite (HAp), a main inorganic crystalline component in bones and teeth, is included in the calcium phosphate compound family having the formula $Ca_{10}(PO_4)_6(OH)_2$. Hydroxyapatite (HAp) crystallizes in a hexagonal system, though with some exceptions in a monoclinic system. The system possesses the hexagonal space group with hexagonal rotational symmetry and a reflection plane and cell

1. Assistant Lecturer , Department of Chemistry, Mandalar Degree College
2. Professor (Retired), Department of Chemistry, University of Yangon
3. Rector, University of Mandalay

parameters of a=b=9.418 Å and c=6.884 Å. HAp structure is formed by a tetrahedral arrangement of phosphate (PO_4^{3-}), which constitute the skeleton of the unit cell. The two oxygens are aligned with the c-axis and the other two are in a horizontal plane (Figure 1).

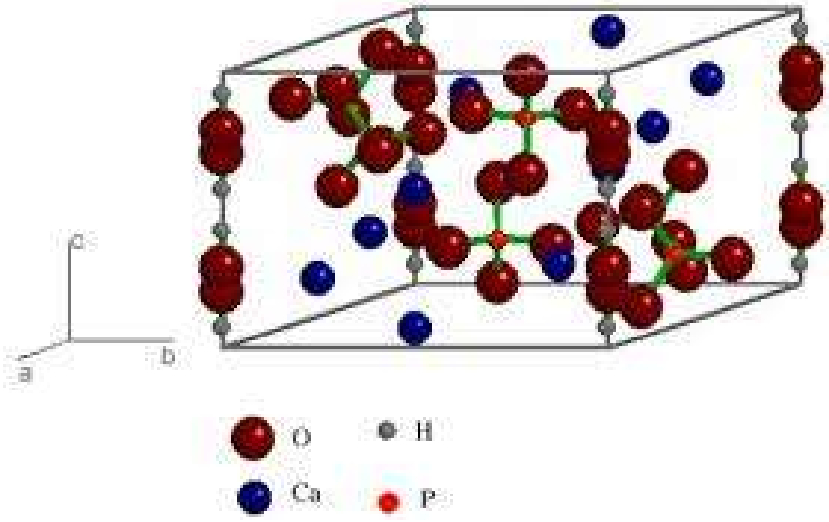

Figure 1: Crystal structure of hydroxyapatite

Hydroxyapatite is one of the most attractive materials for human hard tissue implants because it has close similarities with inorganic mineral component of bone and teeth (Nayak,2010). Naturally occurring HAp is hexagonal in structure with the chemical formula of one unit cell being $Ca_{10}(PO_4)_6(OH)_2$. HAp is also a potential implant material due to its excellent osteoconductive properties. HAp is not only a biocompatible, osteoconductive, non-toxic, non-inflammatory and non-immunogenic agent but also bioactive, *i.e.,* it has got the ability to form a direct chemical bond with living tissues (Fathi *et al*.,2008; Barakat *et al*., 2009).HAp can be derived either from a natural source or by a synthetic method. Both natural and synthetic HAp are widely used as bioceramic in forms of particle, block and coating for the hard tissue repair (Xiaoying *et al*., 2007). HAp having good biocompatibility with human tissues and similarities with the mineral fraction of natural bone is used as a bone graft material in medicine and dentistry. HAp can also be used not only as a bone replacement implants heart valves,

hip extension and other implants in the human body but also as a filler to replace amputated bone or as a coating of metallic prostheses. Besides, HAp are applied for the reconstruction of skull defects, tissue engineering, artificial bone synthesis, biosensor, removal of heavy metals, and as drug carrier (Venkatesan and Kim, 2010).

HAp material manufactured from animal bones can form strong chemical bonds with bone tissues and also it has the advantages of inheriting some properties of the raw materials *viz*. its chemical composition and structure. The composition of HAp from goat bone has similar properties to human bone mineral that it can be used for filling or replacement of bone and teeth. Biowaste such as goat bone is widely available in Myanmar and it can be used as a source of hydroxyapatite. Extraction of hydroxyapatite from goat bone is biologically safe and economic.

The present study is therefore focussed on the preparation of ydroxyapatite from waste goat bone and to study the effect of calcination temperature on its morphological, structural and thermal properties.

Materials and Methods

Sample Collection

The raw goat bone samples were directly collected from a local butcher shop in Mandalay Region.

Sample Preparation

The bones were firstly cleaned with water to remove dirty substances and then cooked in a steel pot on a hotplate for several hours to get rid of any remaining unwanted materials. The dried bones were crushed into small chips and transformed to fine powder (Figure 2).

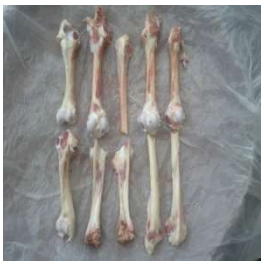

(a) Raw goat bone

(b) Cleaned goat bone

(c) Raw goat bone powder

Figure 2: Preparation of raw goat bone powder

Preliminary Investigation of Raw Goat Bone

Moisture, protein and ash contents were determined by oven drying method, Kjeldahl digestion method and muffle furnace respectively. Phosphorus content was determined with Molybdivanadophosphoric acid method by using UV Vis Spectrophotometer PD-303 UV at Department of Agricultural Research, Ye Zin, Nay Pyi Taw. Calcium content was determined by wet digestion with HNO_3:$HClO_4$ (4:1v/v) followed by measuring with Atomic Absorption Spectrophotometer AA-6200, SHIMADZU at Department of Agricultural Research, Ye Zin, Nay Pyi Taw.

Preparation of Hydroxyapatite from Goat Bone

Hydroxyapatite was prepared according to the procedure of Mondal *et al*.,2012 with some modifications. The collected bones were initially washed with cleaned water to remove dirty substances and then cooked in a steel pot on a hot plate for several hours to get rid of any remaining unwanted materials. The bones were then deproteinized through immersion in 1M hydrochloric acid solution for 24 h at room temperature. Next, the deproteinized goat bones were thoroughly washed several times with distilled water. After that, the bones were immersed in 1M sodium hydroxide solution for 24 h to remove the remaining proteins. Then, the filtered goat bones were thoroughly washed with distilled water again and were dried at 60˚C in hot air oven for several hours. The dried bones were crushed into small chips and transformed to fine powder. Finally, a yellowish white hydroxyapatite powder was obtained. Hydroxyapatite powder was calcined at four different temperatures *viz*., 800ºC, 900ºC, 1000ºC and 1100ºC in a muffle furnace (LEF-103S, DAIHAN LABTECH Group, Korea) for 3 h. The calcined powder samples were cooled and examined the colour. The samples were stored for further studies.

Characterization Techniques

Relative abundances of elements in uncalcined and calcined hydroxyapatite samples derived from goat bone were qualitatively determined by EDXRF analysis using EDX-702 spectrometer (Shimadzu Co. Ltd., Japan) at Universities' Research Center, Yangon. The scanning electron microscope (SEM, JEOL-JSM-5610LV, Japan) was used for the morphological study of uncalcined and calcined hydroxyapatite samples. The phase purity was examined by using Rigaku X-ray diffractometer (Rigaku Co., Japan) with Cu K_α (λ=1.54056 Å) radiation over a range of 2θ angles from 10° to 70°. Various functional groups present in the prepared HA powder as well as the powders calcined at different temperatures were identified by FTIR (Perkin Elmer). Thermal analysis of hydroxyapaptite samples was investigated by TG-DTA employing Thermal Analyzer (DGH-60H), Shimadzu, Japan.

Results and Discussion

Composition of Raw Goat Bone Sample

The experimental results of composition of raw goat bone powder sample are shown in Table 1. The protein and ash contents of the sample were found to be 25.2 % and 2.0 % respectively. The moisture content of the sample was found to be 6.0 %.The calcium and phosphorus contents of the sample was found to be 11.7 % and 11.8 % respectively.

Table 1: Composition of Raw Goat Bone Sample

No	Component	Results (%)
1.	Protein	25.2
2.	Ash	2.0
3.	Moisture	6.0
4.	Calcium	11.7
5.	Phosphorus	11.8

Change of Colour during Calcination

Figure 3 shows the change of colour of hydroxyapaptite samples upon calcination. Before calcination, hydroxyapatite powder was pale yellowish white. After calcination at 800ºC the yellow colour diminished and at temperature 900ºC and above it changed to white colour.

(a)Uncalcined sample (b) 800˚C (c) 900˚C (d) 1000˚C (e) 1100˚C

Figure 3: Colour of hydroxyapatite derived from goat bone (a) uncalcined sample (b) at 800ºC (c) at 900ºC (d) at 1000ºC and (e) at 1100ºC

Relative Abundances of Elements in Hydroxyapatite Samples Derived from Goat Bone

Table 2 shows the relative abundances of elements in uncalcined and calcined hydroxyapatite samples. In all of these samples calcium was found to have the highest percentage followed by phosphorus. Other elements such as iron and strontium were found in all hydroxyapatite samples. Potassium was observed in these calcined samples and zinc and zirconium were found in uncalcined sample and calcined sample at 1000ºC respectively.

Table 2 Relative Abundance of Elements in Hydroxyapatite Samples Derived from Goat Bone at Different Calcination Temperatures

No	Temperature (˚C)	Relative abundance (%)						
		Ca	P	Fe	Sr	K	Zn	Zr
1	Room temperature (uncalcined sample)	77.853	20.332	0.592	1.107	-	0.116	-
2	800	78.813	19.386	0.714	0.426	0.661	-	-
3	900	77.153	21.861	0.560	0.425	-	-	-
4	1000	76.288	21.347	1.248	0.439	0.597	-	0.082
5	1100	76.469	21.638	0.841	0.371	0.682	-	-

Surface Morphology of Uncalcined and Calcined Hydroxyapatite Samples Derived from Goat Bone

The changes of morphology in SEM images of the hydroxyapatite samples derived from goat bone are shown in Figure 4. Densely compacted organic molecules including collagen fibrils along with inorganic mineral structure were observed in uncalcined hydroxyapatite. With increase in calcination temperature the organic polymers were removed and smaller size hydroxyapatite was observed in the SEM image obtained at 800 ºC. Porosity decreased as seen in hydroxyapatite derived from goat bone samples calcined at 800 ºC. At 900 ºC, the particles were found to coalesce and at 1000 ºC necking was observed. As the temperature increased porosity decreased and increased amount of neck formation was observed in the samples calcined at 1100 ºC. The porosity was found to decrease indicating low strength, but as the temperature increased discontinuous cavities were visible due to the formation of neck which increases the strength. This observation was also reported by Pattanayak *et al.,* 2005.

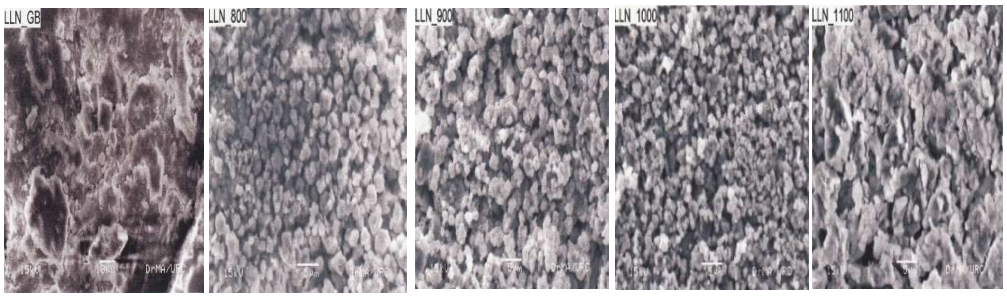

(a) (b) (c) (d) (e)

Figure 4: SEM images of hydroxyapatite samples derived from goat bone (a) uncalcined goat bone and calcined samples at (b) 800ºC (c) 900ºC (d)1000ºC and (e) 1100ºC

X-ray Diffraction Analysis of Hydroxyapaptite Samples Derived from Goat Bone

XRD analysis is a highly trustable technique utilized to investigate the crystalline compounds. Figure 5 shows the XRD spectra of the uncalcined and calcined hydoxyapatite samples derived from goat bone. The XRD spectrum of uncalcined hydroxyapatite sample shows less crystalline peaks and not all the standard hydroxyapatite peaks have been obtained. The intensity of raw goat bone was found to be dispersed by X-ray radiations with a lower intensity and wider peak. This may be due to the presence of extracellular matrix and fibrous collagen. When subjected to calcination at higher temperatures, the broad peak gradually became split into five distinct crystalline peaks, (211), (112), (300), (130) and (222) at 2θ values of 31.805º, 32.234 º,32.936 º, 39.830 º and 46.733 º, respectively, which are similar to the standard HAp (74-0565). Sharp and narrow peaks with high intensity of crystalline patterns were observed. The intensity count of XRD peaks increased due to the detection of more number of diffracted rays developing from the larger number of same group of planes. Therefore, it can be concluded that the calcination treatment has eliminated the collagen and organic compounds from the goat bones and does not affect the molecular skeleton of the hydroxyapatite. The present XRD results suggest that HAp stability has not been affected and no other peaks were observed apart from standard HAp.

Phase purity

Furthermore, X-ray diffraction was employed to evaluate the phase purity and the crystallographic structural properties of the goat bone after calcination at four selected temperatures (800ºC, 900ºC, 1000ºC and 1100ºC). Table 3 shows the phase purity of the hydroxyapatite derived from goat bone at 800ºC, 900ºC, 1000ºC and 1100ºC. It was noted that only single phase of hydroxyapatite with no other phase was found. The well-resolved XRD spectra could be easily indexed on the basis of hexagonal crystal system with equal axial length of 'a' and 'b' and shorter length 'c'.

Crystallinity and crystallite size

Crystallinity percent was calculated by the following equation.

$$\text{Crystallinity \%} = \frac{\text{total crystalline peak area}}{\text{total area of all peaks}} \times 100$$

Crystallinity of the hydroxyapatite derived from goat bone was found to increase with increasing temperature (Table 4). In raw goat bone the crystallinity percent was 26.28 %. The broad peaks in uncalcined hydroxyapatite reflect a poor crystallinity. Increasing the temperature results more intense and sharp peaks corresponding to an increase in the mineral crystallinity. Further increase of the calcinations temperature to 900ºC, 1000ºC and 1100ºC the crystallinity percents were comparable, i.e., about 60%. The increase in crystallinity indicated that organic portions were completely removed from hydroxyapatite.

Crystallite size τ (tau) of the hydroxyapatite powder was evaluated from the peak broadening of XRD patterns based on Scherrer's equation (Landi *et al*., 2000) as follows: $\tau = \frac{0.9\lambda}{\beta \cos\theta}$

in which τ is the crystallite size (nm), λ is the diffraction wavelength (0.154059 nm for Cu K_α radiation) , θ is the diffraction angle (degree) and 'B' is the full width at half maximum (FWHM) for the diffraction peak (radian).

Table 4 shows the changes of crystallite size of hydroxyapatite derived from goat bone before and after calcination. Crystal size increased with increasing temperature and the sizes were not much different at higher calcination temperatures.

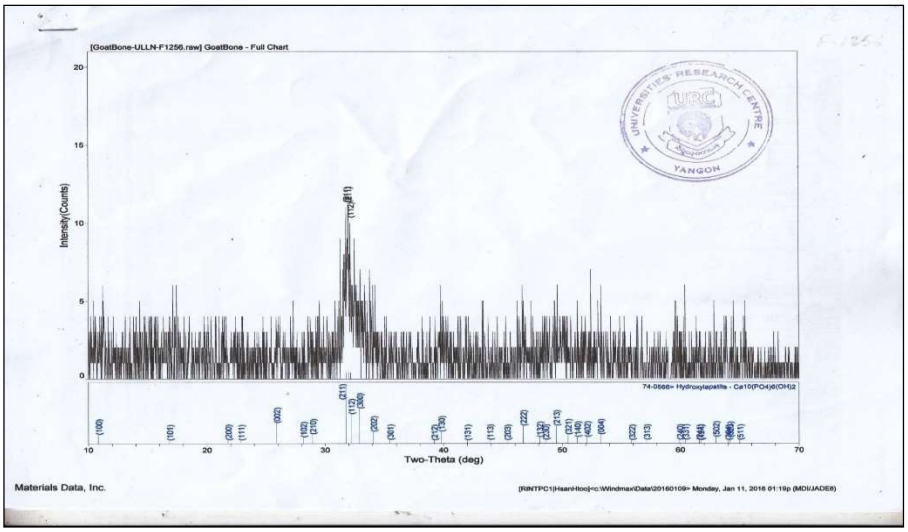

(a)

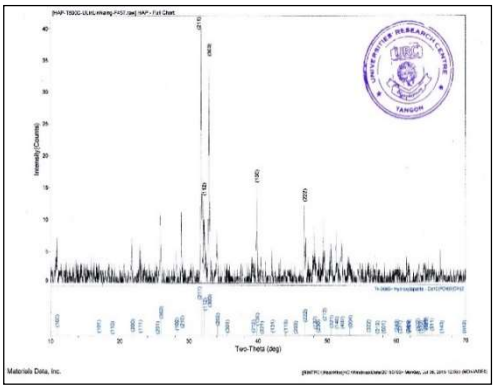

(b)

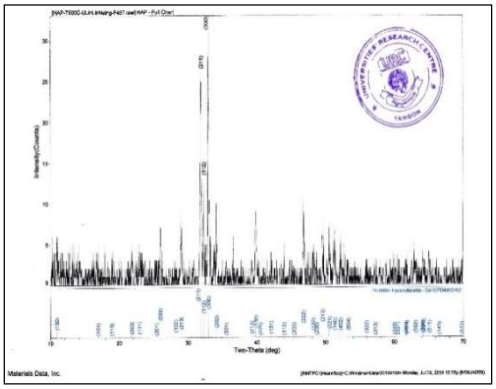

(c)

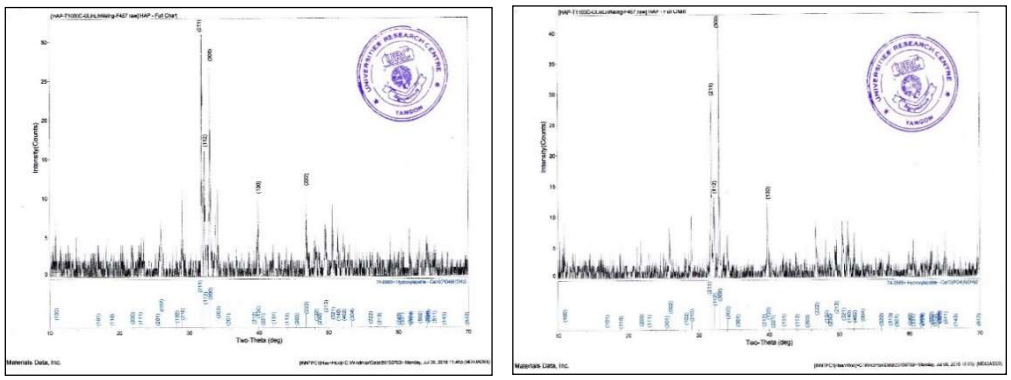

(d) (e)

Figure 5: X-ray diffraction patterns of uncalcined and calcined hydroxyapatite samples derived from goat bone (a) uncalcined sample and samples calcined at (b) 800˚C(c)900˚C(d) 1000˚C (e) 1100˚C

Table 3: Phase Purity and the Crystallographic Structural Properties of Uncalcined and Calcined HAp Samples Derived from Goat Bone

Samples	**Phase**	**Lattice constants (Å)**			**Crystal structure**
		a	**b**	**c**	
UncalcinedHAp	Hydroxyapatite	9.3826	9.3826	6.9600	Hexagonal
HAp at 800^{o}C	Hydroxyapatite	9.4167	9.4167	6.8929	Hexagonal
HAp at 900^{o}C	Hydroxyapatite	9.3893	9.3893	6.8688	Hexagonal
HAp at 1000^{o}C	Hydroxyapatite	9.4062	9.4062	6.8862	Hexagonal
HAp at 1100^{o}C	Hydroxyapatite	9.4168	9.4168	6.8766	Hexagonal

Table 4: Crystallinity Percent and Average Crystallite Size of Uncalcined and Calcined HAp Samples Derived from Goat Bone

No	Temperature (˚C)	Total area of crystalline peaks (nm^2)	Total area of all peaks (nm^2)	Crystallinity (%)	Average crystallite size (nm)
1	Room temperature (Uncalcined sample)	22.6	86.0	26.28	25.45
2	800	43.2	76.1	56.77	74.53
3	900	45.7	77.0	59.35	81.13
4	1000	45.3	75.7	59.84	83.10
5	1100	46.8	74.6	62.73	83.53

FT IR Analysis

The FT IR spectra of the uncalcined and calcined hydroxyapatite samples derived from goat bone are shown in Figures 6, 7,8, 9 and 10. The corresponding spectral data are shown in Table 5. The FT IR spectrum of uncalcined sample shows the characteristic peaks of hydroxyapatite at 563 cm^{-1}, 603 cm^{-1}, 960 cm^{-1} (shoulder) and 1030 cm^{-1}due to phosphate vibrations (Figueiredo *et al*., 2010). The presence of collagen in goat bone was indicated by C=O stretching vibration at 1662 cm^{-1} and N-H in plane bending at 1548 cm^{-1} . The double band at 1415 cm^{-1} and 1454 $cm^{-1}$and also a peak at 871 $cm^{-1}$are attributed to the vibration of carbonate group. Moreover, O-H stretching vibration of hydroxyl group was observed at 3435 cm^{-1}.

After calcination most of the bands due to the phosphate vibrations of hydroxyl apatite have largely increased in intensity. Within 500-700 cm^{-1} region of the spectra of calcined samples, three bands at 632, 601, 570 cm^{-1} were observed whereas in the spectrum of uncalcined sample only two bands were observed. The bands at 630 cm^{-1}appeared with low intensity in the spectra of calcined hydroxyapatite but it is not observed in the uncalcined sample. It is clearly resolved in the spectra of calcined samples. The absorption bands of 1548 and 1662 cm^{-1}due to the presence of collagen disappeared after calcinations at 800 ºC and above. Typical bands of carbonate at 871, 1410 and 1445 cm^{-1} attributed to lattice carbonate vibration

(Landi *et al*., 2003) show small intensity in the spectra of all calcined samples indicating the removal of carbonate.

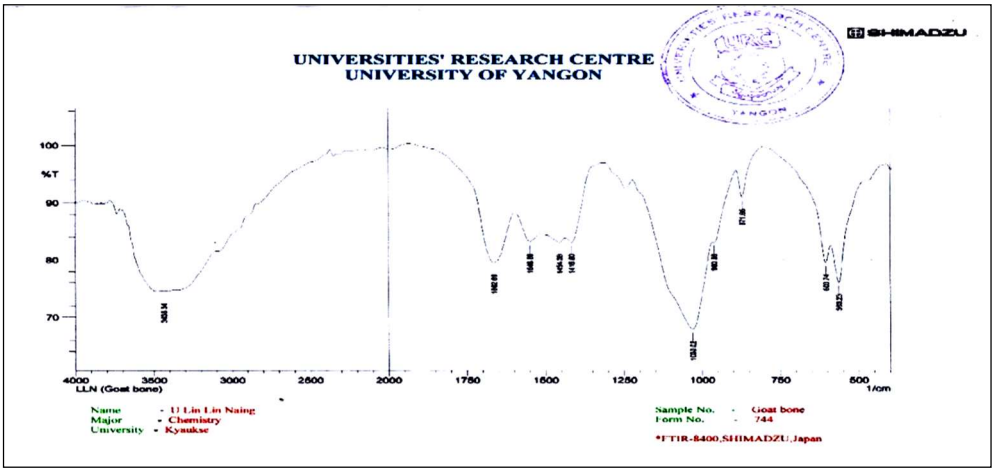

Figure 6: FT IR spectrum of uncalcined HAp sample derived from goat bone

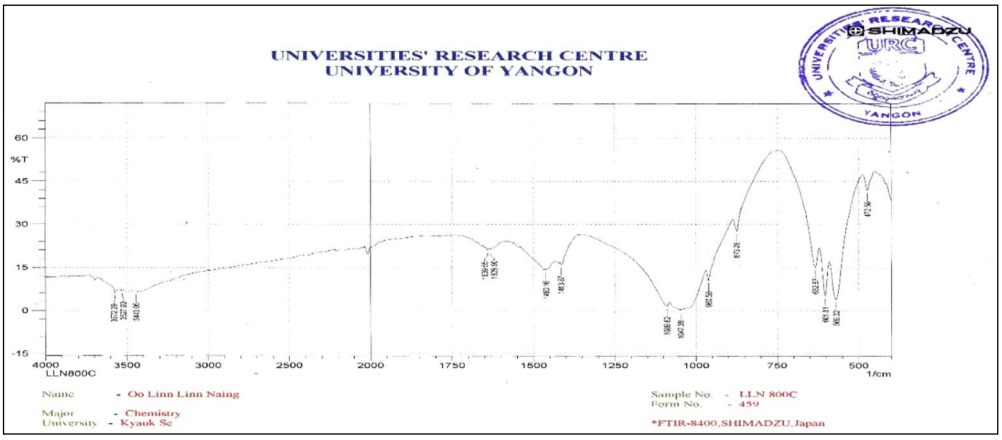

Figure 7: FT IR spectrum of HAp derived from goat bone calcined at 800˚C

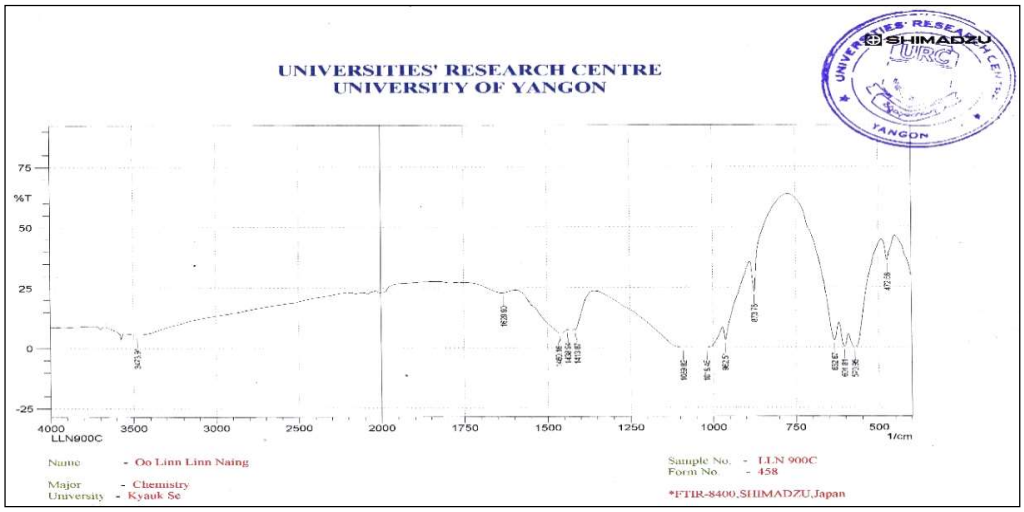

Figure 8: FT IR spectrum of HAp derived from goat bone calcined at 900˚C

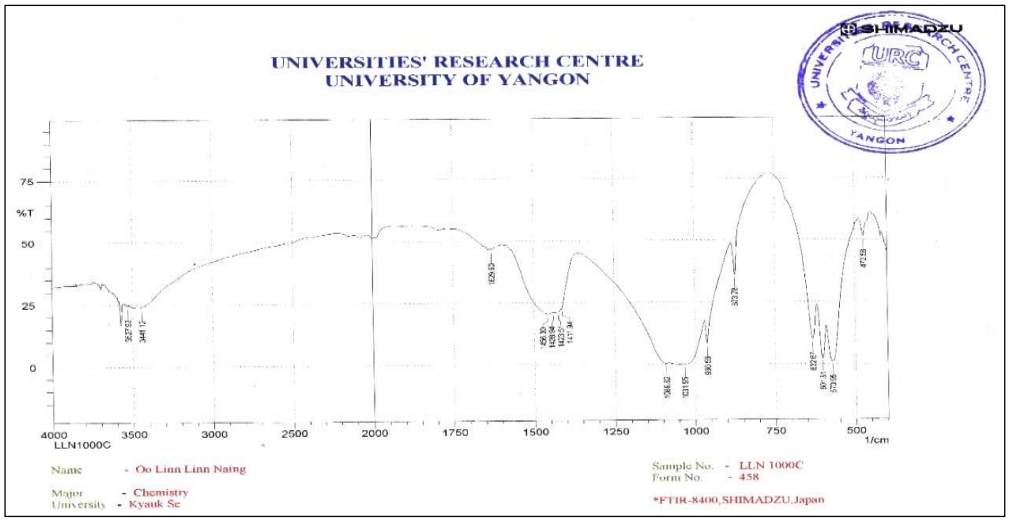

Figure 9: FT IR spectrum of HAp derived from goat bone calcined at 1000˚C

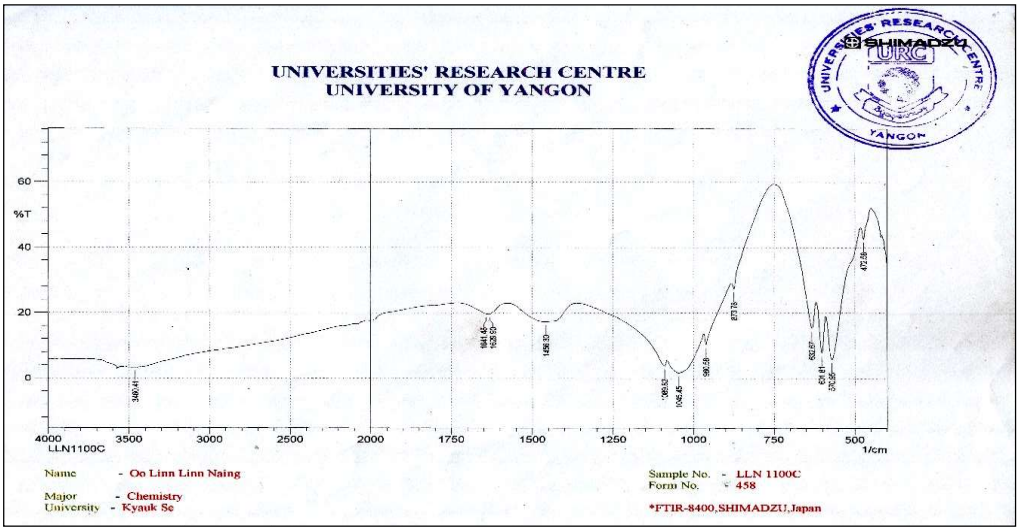

Figure 10: FT IR spectrum of HAp derived from goat bone calcined at 1100˚C

Table 5: FT IR Spectral Data of Uncalcined and Calcined Hydroxyapatite Samples Derived from Goat Bone

No	Wavenumber (cm^{-1})						Remarks
	Uncalcined sample	800˚C	900˚C	1000˚C	1100˚C	Reported values*	
1	3435	-	-	-	-	3100-3500	O-H and N-H stretching
2	-	3443	3473	3441	3460	3100-3500	Stretching vibration of O-H
3	1662	-	-	-	-	1634	Stretching vibration of C=O (Collagen)
4	1548	-	-	-	-	1548	N-H in plane bending (Collagen)
5	1454	1460	1460	1456	1456	1400-1629	Carbonate groups
6	1415	1413	1413	1411	-	1400-1629	Carbonate groups
7	-	1089	1089	1089	1089	900-1200	Stretching P-O
8	1030	1047	1018	1031	1045	900-1200	Stretching P-O
9	960	960	962	960	960	900-1200	Stretching P-O
10	871	873	873	873	873	871	Carbonate group
11	-	632	632	632	632	500-700	Bending P-O
12	603	601	601	601	601	500 - 700	Bending P-O
13	563	569	570	570	570	500-700	Bending P-O

*Figueiredo *et al*., 2010

TG-DTA Analysis

TG-DTA thermogram of hydroxyapatite derived from goat bone is shown in Figure 11(a).

Within the temperature range of 38.96ºC to 90ºC small initial weight loss was observed as 8.045% due to the dehydration of goat bone (surface and bound water). Exothermic peak was observed at 363.72ºC in the temperature range of 90ºC to 445ºC. Appearance of the exothermic peak in DTA curve was due to the combustion of organic component of bone (mainly collagen). So weight loss of 24.324 % was noted in this temperature range. As the

temperature was increased from 445ºC to 601.47ºC unnoticeable weight loss was observed and the TG curve was found to be thermally stable. For calcined hydroxyapatite samples TG-DTA thermograms are depicted in Figures 11 (b,c,d and e).No inflection point was noted in each TG profile of calcined hydroxyapatite sample indicating the stability of the composition of hydroxyapatite. A very small endothermic peak occurred at around 400ºC may be due to the removal of residual organic moieties. The weight losses of the uncalcined and calcined samples subjected to TG analysis are shown in Table 6. The highest weight loss was observed for uncalcined hydroxyapatite (32.215%) due to the loss of organic constituents like collagen. On the other hand, negligible amount was noted for calcined samples. This finding confirmed the decomposition of organic moieties during calcination.

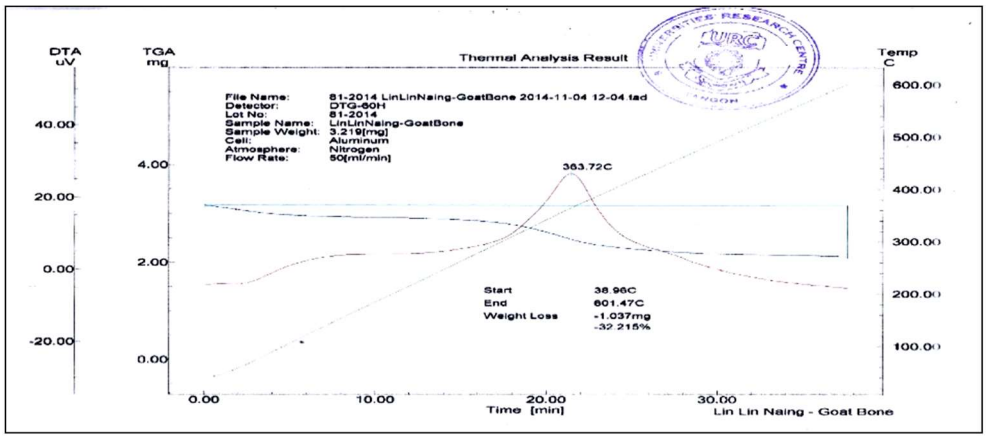

(a)

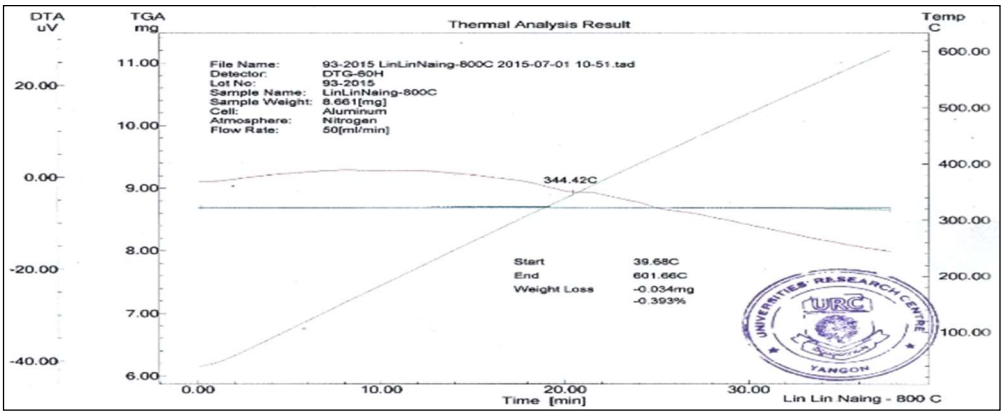

(b)

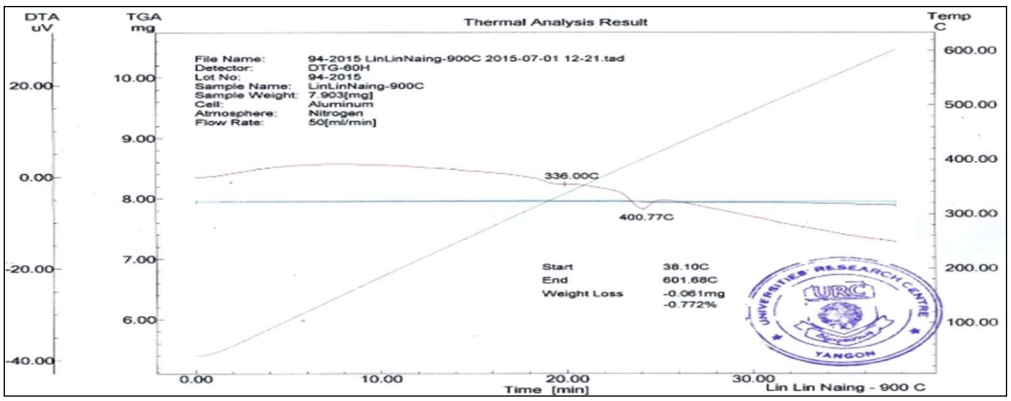

(c)

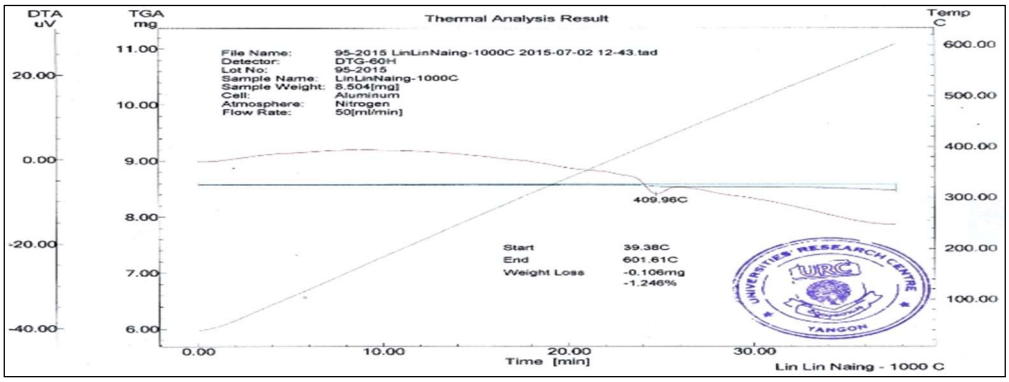

(d)

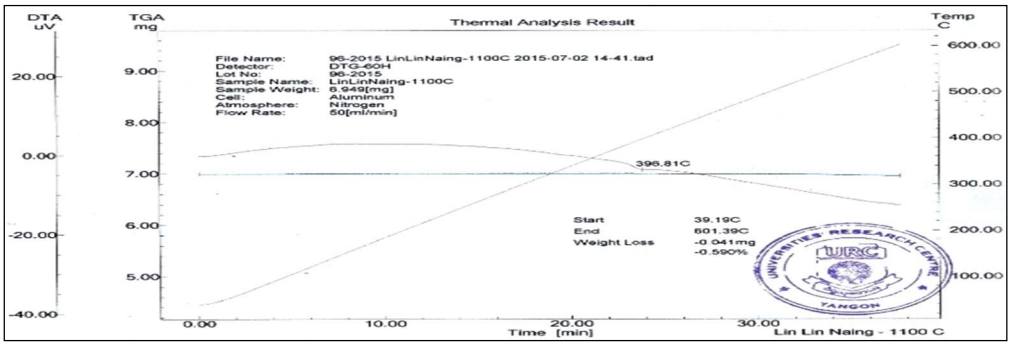

(e)

Figure 11: TG DTA thermograms of uncalcined and calcined hydroxyapatite samples derived from goat bone

Table 6: Weight Loss Percents of Uncalcined and Calcined Hydroxyapatite Samples Derived from Goat Bone after TG-DTA Analysis

No	Samples	Initial weight (g)	Final weight (g)	Weight loss (g)	Weight loss (%)
1	Room temperture	3.219	2.182	1.037	32.215
2	Calcined at 800°C	8.661	8.627	0.034	0.393
3	Calcined at 900°C	7.903	7.842	0.061	0.772
4	Calcined at1000°C	8.504	8.398	0.106	1.246
5	Calcined at 1100°C	6.949	6.908	0.041	0.590

Conclusion

Goat bone hydroxyapatite was prepared from waste goat bone by deproteinization followed by calcination. EDXRF analysis revealed that calcium and phosphorous were present in higher amount both in uncalcined and calcined samples. SEM analysis showed compact and dense structure of both organic and inorganic molecules before calcination of hydroxyapatite 1100 °C densification was observed due to the neck formation between particles.By XRD analysis sharp and narrow peaks with high intensity of crystalline patterns were observed in calcined samples compared to uncalcined sample indicating the elimination of the collagen and organic compounds from the goat bones. Crystallinity percent and crystallite size increased from 800 °C to at 1100 °C but the increases were not much different at high calcination temperatures.The absorption bands due to the presence of collagen (1548 and 1662 cm^{-1}) diminished after calcination. In TG-DTA thermogram of uncalcined sample showed high weight loss of 32.215% which is accompanied by an exothermic peak at 363.72°C. However, samples calcined at 800°C, 900 °C, 1000 °C and 1100 °C showed negligible weight losses indicating the stability of the hydroxyapatite. Among the calcination temperatures of 800 °C, 900 °C, 1000 °C and 1100 °C,morphological, structural and thermal properties were not much different.

This study revealed that calcination is an easy and affordable way to extract hydroxyapatite from waste goat bone resources.

Acknowledgement

The authors would like to thank the Myanmar Academy of Art and Science for allowing to present this paper and Professor and Head Dr Lwin Lwin Myint, Department of Chemistry, Mandalar Degree College for her kind encouragement.

References

Barakat, N.A.M., Khil, M.S., Omaran, A.M.,Sheikh, F.A. and Kim, H.Y.(2009). "Extraction of Pure Natural Hydoxyapatite from the Bovine Bone Biowaste by Three Different Methods". *J. Material Processing Technology,* vol.209(7), pp.3480-3415.

Fathi, M.H., Hanifi, A. and Mortazavi, V. (2008). "Preparation and Bioactivity Evaluation of Bone-like Hydroxyapatite Nanopowder" *J. Material Processing Technology,* vol.202, pp.536-542.

Figueiredo,M., Fernando, A., Martins, G., Freitas, J., Judas, F. and Figueiredo, H. (2010). "Effect of Calcination Temperature on the Composition and Microstructure of Hydroxyapatite Derived from Human and Animal Bones". *Ceramics International*,vol.36, pp. 2383-2393.

Landi, E., Tampieri, A., Celotti, G. and Sprio, S.(2000). "Densification Behaviour and Mechanisms of Synthetic Hydroxyapatites". *J.Eur.Ceram.Soc*., vol.20, pp. 2377-2387.

Landi, E., Tampieri, A.,Celotti, G. and Sprio, S. (2003)." Carbonated Hydroxyapatite as Bone Substitute". *J.Eur.Ceram.Soc*., vol.23, pp. 2931-2937.

Mondal, S., Mondal, B., Dey, A. and Mukhopadhyay, S. S. (2012). "Studies on Processing and Characterization of Hydroxyapatite Biomaterials from Different Bio Wastes". *Journal of Minerals & Materials Characterization & Engineering*, vol.11(1), pp. 55-67.

Nayak, A.K. (2010). "Hydroxyapatite Synthesis Methodologies: An Overview". *International Journal of Chem-Tech Research*, vol.2(2), pp. 903-907.

Pattanayak, D.K., Divya, P., Upadhyay, S., Prasad, R.C., Rao, B.T. and Mohan, T.R. (2005). "Synthesis and Evaluation of Hydroxyapatite Ceramics". *Trends Biomater. Artif. Organs,* vol.18(2),pp. 86-92.

Venkatesan, J. and Kim, S. K. (2010). "Effect of Temperature on Isolation and Characterization of Hydroxyapatite from Tuna (*Thunnus obesus*) Bone". *Materials*, vol.3, pp. 4761- 4772.

Xiaoying, L., Yongbin, F., Dachun, G. and Wei, C. (2007). "Preparation and Characterization of Natural Hydroxyapatite from Animal Hard Tissues". *Key Engineering Materials*, vol.342-343,pp. 213-216.

SORPTION OF ZIRCONIUM AND IRON WITH GRAPHENE OXIDE AND PREPARATION OF GRAPHENE SHELLS FOR ELECTROSORPTION

Naing Min Tun[1], E. G. Rakov[2]

Abstract

The graphene shells were prepared to apply as the electrosorbent for the electrosorption. Firstly, graphene oxide was collected to determine sorption activities of zirconium and iron. The solubility (dispersion in water) of graphene oxide was studied. And then, the interaction of zirconyl chloride solution with the graphene oxide was also determined. Moreover, the sorption of iron with graphene oxide gave the magnetic sorbent. The hollow nanosphere graphene shells with the thickness of 6 – 8 nm were obtained by the methane pyrolysis on spherical SiO_2 particles. The electrosorption of Na^+ ions (NaCl aqueous solution) was carried out on the nanosphere carbon shells electrodes. The electrosorption of Zr ions ($ZrOCl_2$ aqueous solution 1.8 – 5.0 mg/g) on the graphene electrodes was also determined. From the experimental results the maximum sorption capacity was Zr (50.56 mg/g) on graphene electrode.

Keywords: graphene, graphene oxide, electrosorbent, solubility, nanosphere.

Introduction

Graphene and graphene oxide are relatively new carbon materials, in which recent years had attracted much attention of researchers, because of their unusual properties and wide possibilities of practical application in various branch of engineering. Graphite oxide is related to graphene oxide (GO) material, which is often considered an analogue of graphene oxide, and has been obtained for the first time more than 150 years ago (Brodie, 1859; Brodie, 1860), and the first report of it was done twenty years earlier (Schafhaeutl, 1840). The synthesis was based on the oxidation of graphite; oxidation afterwards became the basis of all chemical (covalent) methods of obtaining colloidal dispersions of graphite. The ratio of C:O in the graphite oxide is 1.62 – 2.57 (Buchsteiner *et al*., 2006). For graphene oxide with a few

[1] Dr, Assistant Lecturer, Department of Chemistry, Monywa University
[2] Dr, Professor, Department of Technology of Rare Elements and Nanomaterials, University of Russian Chemical-technology of D.I. Mendeleev

different values: 2 – 4, which correspond to the formula is $C_8O_4H_5$ – $C_8O_2H_3$ (Pei and Cheng, 2011).These materials are closely related to each other but in some properties they are quite different. Graphene is bad wettability on liquid, insoluble in water and organic solvents and is capable of forming very dilute solutions at the expense of the weak interactions with solvents. The study of comparative experimental and molecular dynamics model behavior on changing the pH showed that the GO is protonated at low pH and forms aggregates (Shih *et al*., 2012). Graphene is well electrically conductive and can participate in the electrosorption process (capacitive deionization) – nonchemical form of ion sorption on polarized electrodes in the absence of electrolysis (Hou *et al*., 2006). By reducing and removing of potential, as well as change in sign of the charge and the simultaneous change of the flow direction of fluid, capacitive deionization allows concentrate of salt without cost of reagents (Porada *et al*., 2012). Graphene oxide (GO), in contrast to graphene is capable of forming stable dispersions in water and organic solvents (Nakajima and Matsuo, *1994)*, so far as on the surface contains different functional groups (carboxyl, hydroxyl, phenolic, epoxy, and others) (Lee *et al.,*2010).These groups are easily formed by oxidation of graphene in strongly acidic medium and in aqueous solutions it can participate in the ion exchange process. Since the concentration of ion exchange groups on the surface of the graphene oxide may be very high, on the sorption capacity of graphene oxide is significantly superior to conventional ion exchange resin based on a polymer.

The main aim of this research was to study graphene oxide as an ion-exchange sorbent and graphene as electro-sorbent. In this work several problems were solved:

- Preparation of aqueous dispersions of graphene oxide and study the effect of pH on the solubility of graphene oxide;
- To study the interaction of zirconyl chloride with graphene oxide;
- To synthesise the magnetic sorbents based on graphene oxide and magnetite nanoparticles to facilitate phase separation with ion-exchange sorption;
- To develop the methods for grapheneproducing by pyrolysis of the most accessible of hydrocarbons from methane (town gas) on metal oxides with a large surface area;

- To obtain hollow carbon nanospheres and test created from these electrodes for electrosorption of sodium chloride;
- To study an electrosorption of zirconyl chloride solutions on the graphene electrodes.

Materials and Methods

Materials

Graphene samples were obtained from the plants of Global Co. Ltd. (Davydov *et al*., 2012). Graphene samples have been a specific surface area 1003 m^2/g; 1406 m^2/g 1660 m^2/g and 1906 m^2/g. Additionally, graphene shells were used, which were produced by pyrolysis of CH_4 on SiO_2 at 600˚C for 30 min. Purification of catalyst was performed by hydrofluoric acid (48 wt. %).

Preparation of graphene oxide

Several graphene samples were used for the preparation of graphene oxide. Graphene sample was mixed with a solution of H_2SO_4 and HNO_3 (volume ratio acid 3:1) followed by ultrasonication with the help of dispersant rod for 2 min and then oxidized in a domestic microwave oven (100 – 200 watts) at different times. After cooling, the mixture was centrifuged, the precipitate was diluted with distilled water and again centrifuged 3-4 times until the dispersion was ceased. Thereafter 200 mL of distilled water and 5mL of 38% HCl were added, subjected to ultrasonic treatment and centrifuged. These operations were also repeated several times to obtain colorless overflow. The precipitate was dried at 60˚C.

Ion-exchange sorption method

A weighed amount of the GO is dispersed with a certain volume of water and a solution $Zr(OH)_2Cl_2$, $FeSO_4$, Fe $(NO_3)_3$ and $FeSO_4$ + $FeCl_3$(1:2) was added. After mixing for 1-2 h, the precipitate was filtered on paper and dried at atmosphere. And then it was calcined at 800˚C for 3 h, cooled in the desiccator and weighed the remaining ZrO_2 or Fe_2O_3. The value of pH was measured by pH meter, Martini pH-56.

Carbon coating of metal oxides

Carbon coating of metal oxides was performed by pyrolysis. Pyrolysis was carried out in a tubular quartz reactor using municipal (domestic) gas containing 99% CH_4. Quartz boat with the portion of the precursor SiO_2 particles (250 mg) was added rapidly via the rod in the hot zone heated to a predetermined temperature while feeding it into methane (50–660 mL/min) and maintained within necessary time (20–60 min) and then so-quickly moved into the cold zone. The mass obtained was determined by weighing the sediment product before and after aging for 3 h in air at 750 – 800 ˚C.

Pyrolysis was carried out in a quartz tubular reactor as shown in Figure 1.

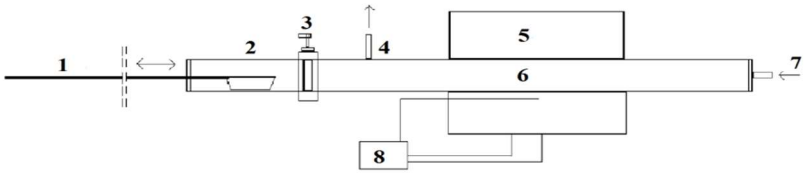

Figure1: Scheme of pyrolytic setting: 1 – boat rod for introducing into the reaction zone; 2 – boat with a substance; 3 – gas seal; 4 – output connection for the reaction gases; 5 – electric furnace; 6 – quartz tube; 7 – inlet for introducing gas; 8 – a device for measuring and regulating the temperature.

Apparatus and equipment

Measurement of specific surface area was carried out by using the apparatus AUTOSORB-1C/MS/TPR (Quantachrom) and SORBI-MS by volume adsorption of N_2.

Electron micrographs (photomicrographs) were obtained by using the scanning microscope (Chem JEOL, JSM-6510LV, Oxford instruments X-Max 20 mm^2,batch switching center, MUCTR) and transparent microscope (FEI Tecnai G^2 30 ST, Institute of Crystallography, Russian Academic Science).

The pH-meter (MARTINI pH-56) was used for measuring pH of sample solution.

The preparation of GO dispersion was carried by using ultrasonic sonicator (dispersant). After centrifugation, the remaining GO particles were dried and weighed. TDS-3 meter was used for the measurement of total dissolved solid(TDS) of solution.

Results and Discussion

Study of the solubility of graphene oxide

Oxidation of graphene was carried out with a mixture of concentrated H_2SO_4 and HNO_3, with a volume ratio is 3:1.

Table 1 shows the GO samples with different solubilities as a function of pH. The solubility of GO samples was found to increase at pH neutral condition.

Table 1: Dependence of Solubility of GO samples on pH.

Sample	pH	Solubility of GO, mg/mL	pH	Solubility of GO, mg/mL
GO -1	2.69	3.27	7.13	10.6
GO -2	2.90	4.06	7.01	11.6
GO -3	2.77	6.10	7.05	14.3
GO -4	3.60	0.30	7.01	1.90
GO -5	2.82	0.57	7.05	2.10
GO -6	2.48	1.70	7.08	6.40
GO -7	3.74	5.40	7.02	7.50
GO -8	2.82	6.82	7.10	14.8
GO -9	3.62	7.30	7.06	7.70

The series of experiment was attained with a more high solubility and were studied the influence of pH value on the solubility. These results are shown in Figure 2.

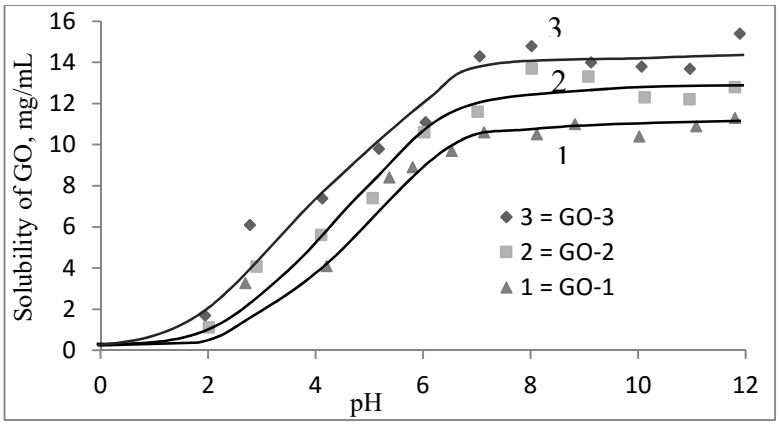

Figure 2: The dependence solubility of three GO samples with different oxidation state on pH value.

The solubility of GO in lower pH value (in strong acid condition) is near to zero. By increasing the pH value from 2–3 to 6–8 which is gradually increased, reached to 11 and even 15 g/L, but after pH value of 8–9 rather fall and then rise.

The most characteristic curves of dependence composition from concentration of zirconyl chloride was obtained with the samples of GO - 4, GO -7, GO -9in Figure 3.

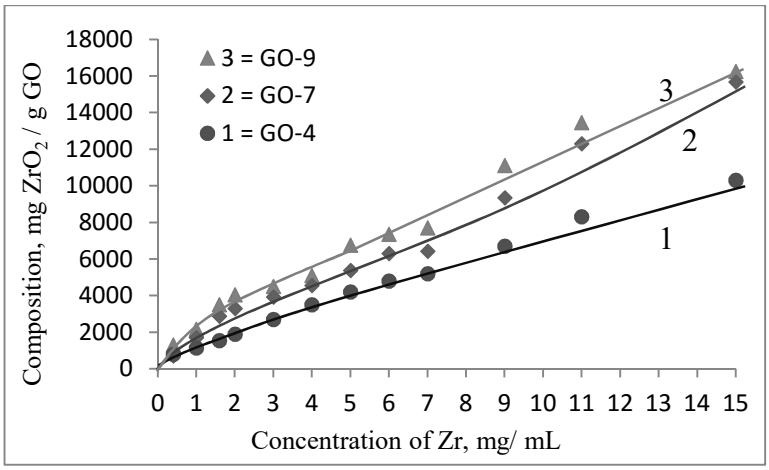

Figure 3: The dependence of composition product, the interaction of GO with the concentration of Zr, at the correlation of mass of GO and volume of Zr solution is 1:10, and the contact time is τ_c = 120 min.

Ion-exchange sorption of Fe^{2+} and Fe^{3+} with graphene oxide

In this research the GO samples with different solubilities in water (concentration in stable colloidal solution) were used. For the determination of metal sorption amount, the dry precipitate was calcined in atmosphere at 750–800˚C for 3 h, and cooled in the desiccator and weighed as an oxide form (Fe_2O_3). The capacity of sorbent in all process conditionally expressed in Fe_2O_3 wt. per 1 g of sorbent.

Figure 4 indicates that as the solid liquid ratio decreases the sorption capacity of GO gradually increases.

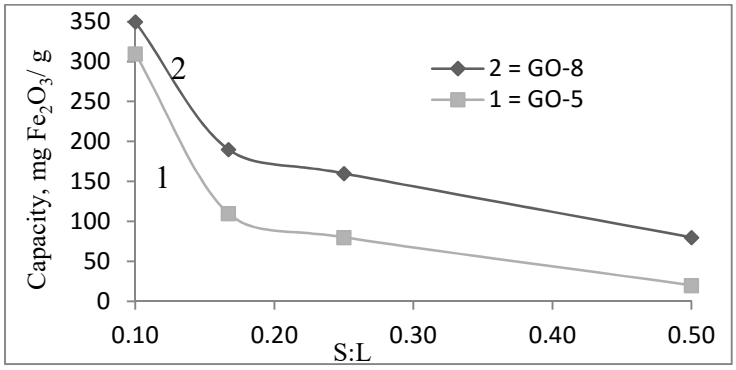

Figure 4: The dependence of capacity of GO-5 (1) and GO-8 (2) on S:L ratio with a concentration of $FeSO_4$ 0.108 g Fe/L, the initial pH value is 4.31 (pH precipitation of solution is 4.36)

The experiments were carried out with the solution of $Fe(NO_3)_3$. Figure 5 shows the equivalence values was settled at 20–30 min and, this means the different sorption capacity of sample GO with a different solubility.

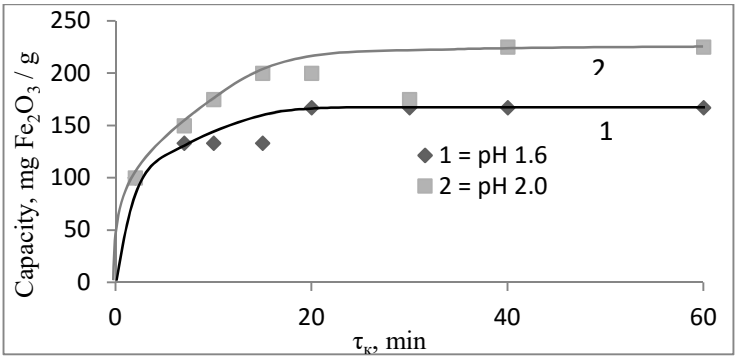

Figure 5: Influence of contact time on the capacity of GO-6 with concentration of $Fe(NO_3)_3$ 0.167 g Fe/L, S:L = 0.58, pH = 1.6 (1) and pH = 2.0 (2).

Preparation of magnetic sorbent from graphene oxide

The mixture solution of $FeCl_3$ (1 g) and $FeSO_4$ (0.5 g) was prepared in 1 L of distilled water, at pH = 3.45 and S:L = 0.1.

The GO dispersion sample was mixed with a given concentration and volume of $FeCl_3$ and $FeSO_4$ (1.5 g/L), after then the contact time was 2 h without any shaking, and obtained then filtered the residue. The obtained residue was dried at 50˚C. Thereafter to get through on 1 h at 350˚C in the flow rate of CH_4 is 588 mL/min.

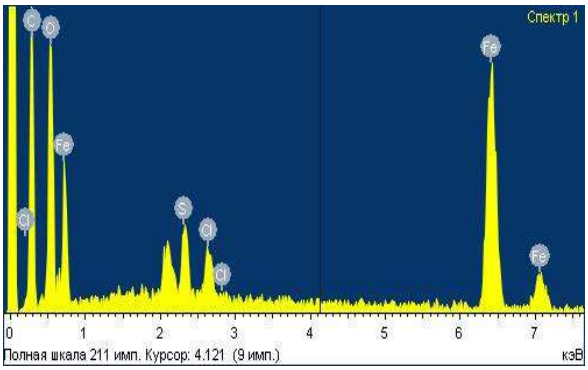

Figure 6: EDX spectrum of magnetic sorbent particles and its composition

The composition of elements in the magnetic sorbent in Table 2 shows the atomic ratio of O:Fe was composed of 1.36 and near to the calculated value for the Fe_3O_4 (1.33). Other impurities of sulfur and chlorine were detected in the precursors.

Table 2: Composition of magnetic sorbent

Element	Mass %	Atom %
C	32.87	57.23
O	17.79	23.25
S	2.42	1.58
Cl	1.73	1.02
Fe	45.18	16.92
Total	**99.99**	**100.00**

Preparation of hollow carbon nanosphere

The SiO_2 initial particles were regular sphere with high scattered diameter as shown in Figure 7.

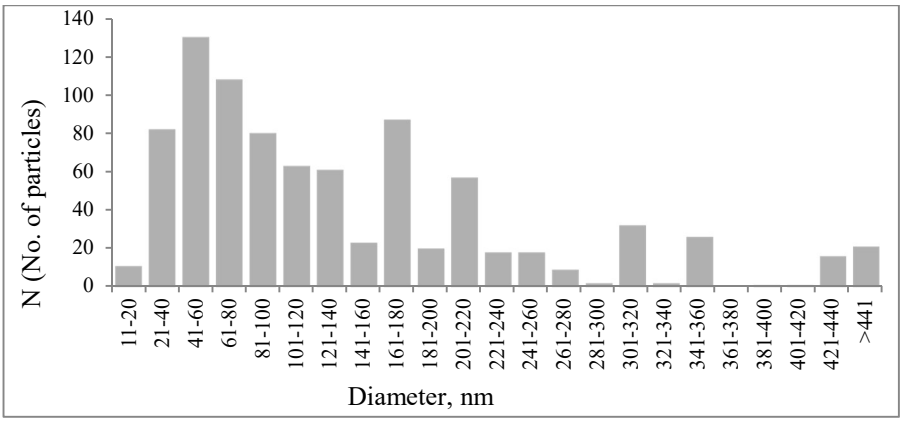

Figure 7: The distribution diameter of spherical SiO_2 particles

The value of N was characterized by the number of particles with defined diameter on photomicrograph.

The CH_4 pyrolysis of SiO_2 was carried out at 500 – 800 °C. The typical dependence of mass increment with time at the two different temperatures is shown in Figure 8 and the influence of gas flow rate is shown in Figure 9.

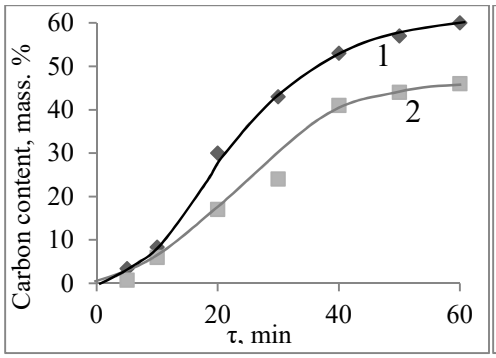

Figure 8: The mass increment on the pyrolysis at temperature 800 °C (1) and 700°C (2)

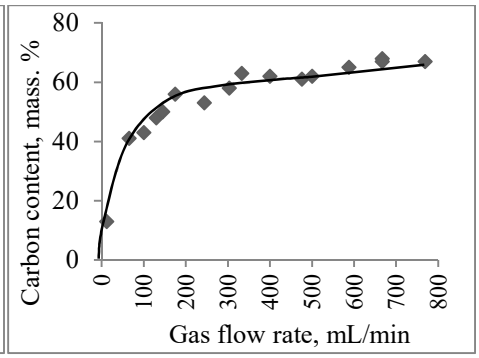

Figure 9: The influence of gas flow rate no mass increment at the pyrolysis temperature of 850 °C for 120 min

The deposition of carbon on SiO_2 becomes steady in the flow rate ranging from 400 to 800 mL/min at pyrolysis temperature 850 ˚C for 60 min. The increment of gas flow rate more than 200–250 mL/min shows the weakly deposit amount of carbon (and, consequently the rate of pyrolysis). The mass increment of maximum amount has reached to 72 mass % at the temperature range of 850 – 900 ˚C. This behavior was attested the catalytic effect of SiO_2 particles, which is weaken the increment of carbon deposit layer thickness on the particles shown in Figure 10.

On the submitted photomicrograph it can be seen in Figure 11 that the spherical form of particles were maintained. This also confirmed the photomicrograph of hollow carbon spheres, obtained by dissolution of SiO_2 in dilute hydrofluoric acid.

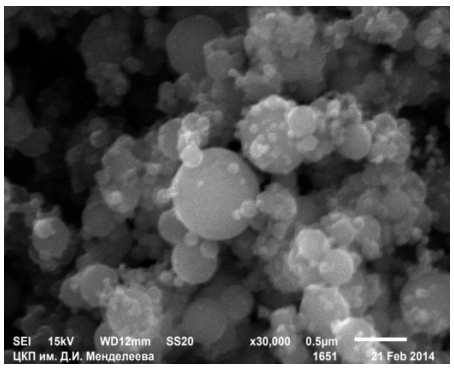

Figure 10: SEM photomicrograph of carbon shells coating on SiO_2 particles

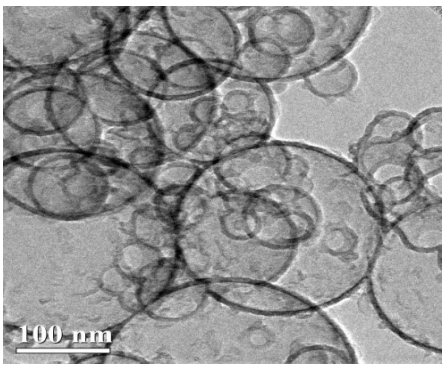

Figure11: TEM photomicrograph of hollow sphere carbon shells

Table 3 shows the calculated values of the carbon shells thickness, obtained by pyrolysis at different temperatures and assumption, that the medium diameter of SiO_2 particles were composed of 60 nm.

Table 3: The Composition of Carbon on SiO_2 Particles at Different Temperatures and Calculated Thickness of Carbon Shells

Temperature, °C	Contact time, min	Carbon content, mass. %	Thickness of shells, (nm) at diameter of SiO_2 particles, (nm)			
			50	60	70	80
550	60	5.0	0.5	0.6	0.7	0.8
600	30*	7.5*	0.6	0.9	1.0	1.2
600	60	10	0.8	1.2	1.4	1.6
650	60	34	3.0	3.6	4.2	4.8
700	60	47	3.5	4.2	4.9	5.6
750	60	65	5.5	6.6	7.7	8.8
800	60	72	5.6	6.7	7.8	8.9

*Gas flow rates 466 mL/min, in other cases 333 mL/min.

The specific surface area (S_{sa}) of carbon nanospheres are 175 m^2/g at 600°C with a specific density of 0.029 g/mLobtained at 850-900°C and with the specific surface area of 12–13 m^2/g (that is near the $S_{sa}$of SiO_2). However, the nanospheres were found to make easier for molecules of solvent permeable.

Study of NaCl electrosorption on carbon nanospheres

For the study of electrosorption one sample was chosen from the obtained carbon microspheres with the specific surface area 175 m^2/g. The total mass of carbon nanospheres in each electrode was composed of280 mg, the intermediate electrical voltage in sorption was 2.0 V, the distance between the two electrodes was 2 cm. For the measurement of concentration of solution were used the analyzer TDS-3 meter (ppm, mg/L). The results of NaCl sorption experiments are shown in Figure 12.

The result were shown for the first time, that the sorption capacity of graphene shells on NaCl sorption proved in this stage that an electro-sorption is likely to take place on another carbon materials. From the results, an electrosorption of the electrode construction occurred relatively slowly, and desorption became faster.

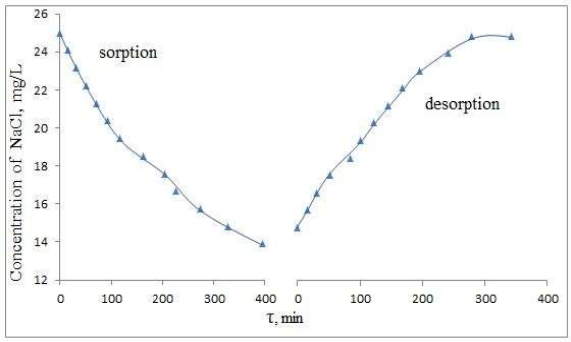

Figure 12: The measurement of NaCl concentration versus time in the aqueous solution at the electrosorption and desorption with mechanical stirring

Study of electrosorption of zirconyl chloride with graphene

For the determination of zirconium content in the solution the gravimetric method, amperometric titration and the pH meter were used.The zirconyl chloride were precipitated with ammonia and dried in vacuum, sintered with the crucible and weighed the remaining oxides.

For carrying on the electrosorption process, the zirconyl chloride solution was preparedwith the concentration in the range of 1.8–5.0 mg Zr/mL. The aliquot was then taken outand were analyzed; its concentration was determined by the gravimetric analysis. Experimental results are shown in Figure 13, the initial voltage 1.47 V, the distance between the two electrodes are 2 cm and the initial concentration of zirconyl chloride 2.0 g/L.

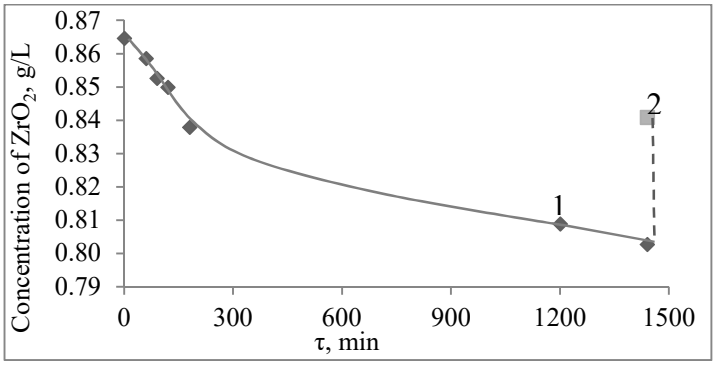

Figure 13: Sorption on one pair of electrode and two parallel connecting batteries, sorption (1) and desorption (2)

The summary of experiment results are shown in table 4.

Table 4: Sorption Capacity of Graphene

Amount of parallel connecting battery on the calculated electrodes	Sorption capacity, mg ZrO_2/ g graphene	Sorption capacity, mg Zr/g graphene
2	47.56	35.20
2	48.86	36.16
3	60.53	44.80
3	68.31	50.56

The most complex and sensitive to the different properties of initial aqueous solution proved an electrosorption process of zirconyl chloride. Therefore the application of graphene have been the definite perspective and for the purification of electrosorption and concentration of technological solution from the different composition.

Conclusion

The study of the solubility (dispersion in water) of GO has shown that it is dependent on the degree of oxidation and gradually rises from nearly pH ~ 1 to pH 8–9the solubility increased 11–15 mg/mL. The interaction of zirconyl chloride solution with the GO at the contact time 120 min were studied; that the product compositions were separated in acidic condition, which depends on the Zr concentration, the solubility of GO, and the ratio of reagents. The highest composition value of ZrO_2 were found to consist of 10 – 16 g/g GO.

When the ion-exchange sorption of Fe^{2+} and Fe^{3+} individually by the GO was investigated, it was found that the sorption capacity of 2.5 g/g was obtained. When the two salts of Fe were used to form Fe_3O_4, using the GO sample, the sorption capacity is found to be 63 mass percent was obtained. At the temperature 500 – 900 ˚C, the pyrolysis of SiO_2 particles in the low density of graphene shells with thickness of 6 – 8 nm was obtained.

The test experiment of Na^+ ions electrosorption was carried out from the aqueous solution of NaCl on the nanosphere carbon shells electrodes, it was shown that the sorption capacity was achieved to 10 – 11 mg/g of C shells. From the aqueous zirconyl chloride solution studied on electrosorption

of Zr ions with the concentration of 1.8–5.0 mg Zr/mL on the graphene electrodes, it showed that the maximum sorption capacity were composed of 50.56 mg Zr/g of C.

Acknowledgements

The authors would like to express their profound gratitude to the Myanmar Academy of Arts and Science for giving permission to submit this paper. I would like to thank Professor and Head, Dr Than Than Win, Chemistry Department, Monywa University for her kind encouragement.

References

Brodie, B.C. (1859). "On the Atomic Weight of Graphite". *Phil. Trans. R. Soc. Lond*.,vol.149, pp. 249–259.

Brodie, B.C. (1860). "Sur le Poids Atomique du Graphite". *Ann. Chim. Phys,* vol.59, pp.466-472

Buchsteiner, A., Lerf, A. and Pieper, J. (2006). "Water Dynamics in Graphite Oxide Investigated with Neutron Scattering". *J. Phys. Chem,* vol.110 (45), pp 22328-22338

Davydov,S.,Yu., Kryukov, A.Yu., Gerya,V.O., Izvol' skii, I.M. and Rakov, E.G. (2012). "Preparation of a Plate Like Carbon Nanomaterial Using MgO as a Template". *Inorg. Mater.* vol..48(3). pp. 244–248.

Hou, C-H., Liang, C., Yiacoumi, S., Dai, S. and Tsouris, C. (2006). "Electrosorption Capacitance of Nanostructured Carbon-based Materials". *J. Colloid Interface Sci,* vol.302(1), pp. 54–61.

Lee, D.W., De Los Santos, V.L., Seo, J.W., Felix, L.L., Bustamante, D.A., Cole, J.M. and Barnes, C.H.W. (2010)."The Structure of Graphite Oxide: Investigation of Its Surface Chemical Groups" . *J. Phys. Chem.* vol.114(17), pp. 5723–5728.

Nakajima, T. and Matsuo, Y. (*1994).*"Formation Process and Structure of *Graphite* Oxide". *Carbon, vol.*32(3), pp. 469–475.

Pei, S. and Cheng, H.M. (2011)."The Reduction of Graphene Oxide". *Carbon,* vol.50 (9).pp. 3210–3228.

Porada S., Bryjak, M., van der Wal, A. and Biesheuvel, P.M. (2012)."Effect of Electrode Thickness Variation on Operation of Capacitive Deionization", *Electrochim. Acta,* vol.75, pp. 148–156.

Schafhaeutl, C. (1840). "On the Combination of Carbon with Silicon and Iron, and Other Metals, Forming the Different Species of Cast Iron, Steel and Malleable Iron". *Phil. Mag,*vol.16(104),pp. 570–590.

Shih, C.J., Lin, S., Sharma, R.,Strano, M.S. and Blankschtein, D. (2012)."Understanding the pH-Dependent Behavior of Graphene Oxide Aqueous Solutions: A Comparative Experimental and Molecular Dynamics Simulation Study". *Langmuir*, vol.28, pp. 235–241.

STRUCTURE ELUCIDATION AND SOME BIOACTIVITIES OF PURE ORGANIC COMPOUND FROM THE STEM BARK OF *DIOSPYROS EHRETIOIDES* WALL.(AUK-CHINSA)

Khaing Khaing Win[1], Htay Htay Shwe[2], Thida Win[3]

Abstract

The stem bark of *Diospyros ehretioides* Wall. (Auk-chinsa) was selected for the phytochemical screening, the determination of the cytoxicity of the crude extract, the isolation of pure organic compound and the identification of the structure of the isolated compound. The cytotoxic activity of the crude extract was determined in HeLa cells by 3-(4,5-dimethylthiazol-2-yl)-2,5-diphenyltetrazolium bromide (MTT) assay and it showed high activity with IC_{50} value of 0.85μg/mL. The pure organic compound (**KKW-1**) was isolated by thin layer and column chromatographic separation techniques. The molecular formula of the isolated compound could be observed according to the HR-MS spectral data. The molecular formula of compound (**KKW-1**) is found as $C_{22}H_{14}O_6$. In addition, the complete structure of naphthoquinone compound (**KKW-1**) was elucidated by applying 1D and 2D NMR spectroscopy.

Keywords: *Diospyros ehretioides,* naphthoquinone, cytotoxic activity, HeLa cells, MTT Assay

Introduction

Herbal medicine is the oldest form of health care known to mankind. Herbs had been used by all cultures throughout history. These historic formulations were created over a period of hundreds of years before the advent of modern medicine.

Most of the people use the traditional indigenous medicinal plants and their usage in therapy play a very important role in Myanmar. A plant can provide thousands of molecules with different biological activities. The persistent use of chemical termiticides is at present of environmental concern

1. Dr.,Assistant Lecturer, Department of Chemistry, Monywa University
2. Dr,Lecturer, Department of Chemistry, University of Mandalay
3. Dr,Rector, University of Mandalay

and has resulted in the need to search for plant-derived compounds as alternatives in termite control (Carter, 1978).

Reports published decades ago had revealed that several wood species possess natural resistance to termite infestation but only a limited number of them had been examined (Sandermann *et al*., 1958).Termite resistant woods are said to contain allelochemicals such as quinones, flavonoids and terpenoids that possess natural repellent and toxic properties (Scheffrahn, 1991).

The family Ebenaceae consists of only three genera, of these, the genus *Diospyros*is by far the largest, with 500 species (Willis, 1966).This genus is widespread in the tropics and the warm temperate regions of the world, of which 24 species are native to India. *Diospyros sylvatica,* also known locally as gatha is a moderate sized tree distributed in the hills of Vizianagram and neighbouring Orissa state (Gamble, 1997).

Chemical examination of Ebenaceae has been generally confined to the genus *Diospyros.* Anumber of *Diospyros* species are used in herbal medicine for the treatment of whooping cough, leprosy, dysentery, menstrual troubles, and abdominal pains and as antibiotics (Watt and Breyer-Brandwijk, 1962). The wood of this genus has considerable economic importance as a source of hard wood timbers and also as edible-fruits (Irvine, 1961).

Chemical studies on a number of species have revealed that the stems and leaves of this genus have been reported to contain triterpenoids (Bhakuni *et al*., 1971), while the roots are well known to contain naphthols and naphthoquinones. The antibacterial, antifungal and termite resistant properties of *Diospyros* have all been attributed to the presence of naphthoquinones (Waterman and Mbi, 1979). In a brief study conducted on the resistance of various timbers of *Diospyros* species, the wood of *D.celebica* was found to be highly resistant to the subterranean termites; *Reticulitermes lucifugus* and *Reticulitermes flavipes* (Sandermann *et. al*., 1957).

The naphthoquinones, 7-methyljuglone and its dimer isodiospyrin isolated from the wood of *D. Virginiana* were reported to possess termiticidal activity against *Reticulitermes flavipes*(Carter *et al*., 1978). Naphthoquinones and naphthalene derivatives have been isolated previously from this genus,

but a survey of the literature revealed that triterpenes namely α– amyrin, lupeol and betulin were the only constituents reported from the bark of this plant.

In this research paper, the pure organic compound (KKW-1) from the stem bark of Auk-chinsa (Figure 1) was isolated by applying column and thin layer chromatographic methods. The molecular formula of the compound (KKW-1) was determined by HR-ESI-MS spectrometry. The complete structure was identified by using modern sophisticated techniques such as ^{1}H NMR, ^{13}C NMR, DQF-COSY, HSQC and HMBC respectively.

Botanical Description

Family name	-	Ebenaceae
Botanical name	-	*Diospyros ehretioides* Wall.
Local name	-	Auk-chinsa
Parts used	-	Stem bark
Medicinal uses	-	anticancer activity, anti HIV activity, antibacterial activity, antimalarial activity, and anti-inflammatory activity

Figure 1: Fruit, leaf and flower of Auk-chinsa

Materials and Methods

General

For column chromatography silica gel 60 (Merck) with a particle size of 63-200 μm was used. Silica gel 60 F_{254} precoated aluminium sheets (0.2 mm; Merck) were used for TLC controls. Melting point was measured by the electric melting point apparatus.

All NMR experiments were recorded on a Bruker Avance 600 (operating at 600.13 MHz for ^{1}H and 150.92 MHz for ^{13}C) at 300 K. The

spectra were recorded in chloroform-d_3 and referenced against residual non deuterated solvent. ESI-MS (LR and HR mode) spectra were measured on a TSQ 7000.

Plant Material

The stem bark of Auk-chinsa was collected from Yezin, Pyinmanar Township, Mandalay Region. The collected sample was washed, dried in air and crushed into small pieces. Then, the dried sample which was stored in a well stoppered bottle was used throughout the experiment.

Extraction and Isolation

The air dried sample of the stem bark of Auk-chinsa (500g) was extracted with pet ether (2000 mL). It was concentrated under reduced pressure. And then it was re-extracted again with ethyl acetate and concentrated by rotatory evaporator. The pet-ether crude extract (1.41 g) and ethyl acetate crude (1.87) g were obtained. The pet-ether portion (1.4g) was fractionated with column chromatography on silica gel as adsorbent and stepwise eluted with n-hexane : EtOAc (4:1) to give pure compound (25.2 mg).

Results and Discussion

Preliminary Phytochemical Test for the Stem Bark of Auk-chinsa

The results of phytochemical tests of crude extract of stem bark of Auk-chinsa are tabulated in Table 1.

Table 1: Phytochemical Constituents of Stem bark of Auk-chinsa

No.	Tests	Reagents	Observation	Results
1.	Alkaloid	1 % HCl, Dragendorff's reagent	Orange ppt	+
2.	Flavonoid	EtOH, Conc. HCl, Mg turnings	Pink color solution	+
3.	Terpenoid	Pet ether, Acetic anhydride, Conc. H_2SO_4	Pink color solution	+
4.	Steroid	$CHCl_3$, Acetic anhydride, Conc. H_2SO_4	Blue color solution	+
5.	Glycoside	H_2O, 10 % Lead acetate	White ppt	+
6.	Reducing Sugar	H_2O, Benedict solution	Brick red ppt	+
7.	Polyphenol	EtOH, 10 % $FeCl_3$, 1 % $K_3Fe(CN)_6$	Greenish blue color solution	+
8.	Saponin	H_2O, shake	Forthing	+
9.	Tannin	H_2O,10 % $FeCl_3$ soluiton, H_2SO_4	Yellowish brown color solution	+

(+) = Presence of constituents (-) = Absence of constituents

According to this Table 1, the stem bark of Auk-chinsa contains many phytochemical constituents.

Antimicrobial Activities of Various Crude Extracts from the Stem Bark of Auk-chinsa

The crude extracts in three solvents (n-hexane, EtOAc, EtOH) were sent to Pharmaceutical Research Department (PRD) for antimicrobial activity measurements by Agar well diffusion method. The resulting data are shown in Table 2.

Table 2: Antimicrobial Activities of Various Crude Extracts from the Stem Bark of Auk-chinsa

Crude Extract	**Diameter of Inhibition Zone (mm)**					
Solvent	I	II	III	IV	V	VI
n- hexane	-	-	-	-	-	-
EtOAc	18 (++)	31 (+++)	25 (+++)	25 (+++)	11 (+)	20 (+++)
EtOH	-	-	11 (+)	-	-	-

Microorganisms

I = *Bacillus subtilis* II = *Staphylococcus aureus*
III= *Pseudomonas aeruginosa* IV = *Bacillus pumilus*
V = *Candida albicans* VI = *Escherichia coli*
Agar well - 10 mm
10 mm~ 14 mm (+); 15 mm ~ 19 mm (++); 20 mm above (+++)

The ethyl acetate extract of stem bark responds high activities on all selected organisms except *Bacillus subtilis* and *Candida albicans*. The n-hexane extract of stem bark has no activity on all organisms. The ethanol extract shows low activity on *Pseudomonas aeruginosa* and no activity on other microorganisms (Figure 2).

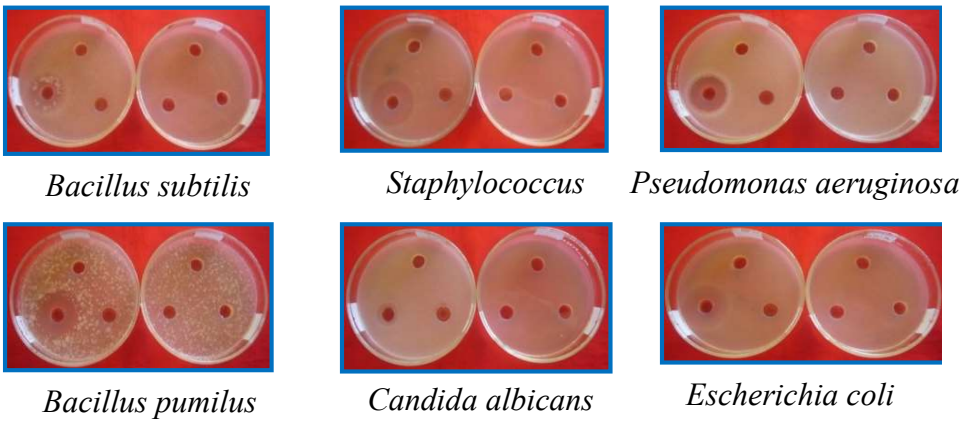

Figure 2: Antimicrobial activities of the crude extracts from the stem bark of Auk-chinsa against six selected microorganisms

Cytotoxic Activity of the Stem Bark of Auk-chinsa

The ethyl acetate crude extract was sent to Pharmaceutical Biology Department, University of Regensburg, Germany for cytotoxicity measurement on HeLa cell by MTT assay. The high IC_{50} value of 0.85 µg/mL shows that this plant has high anticancer activity on HeLa cell (cervical cancer). The resulting data are shown in Figure 3.

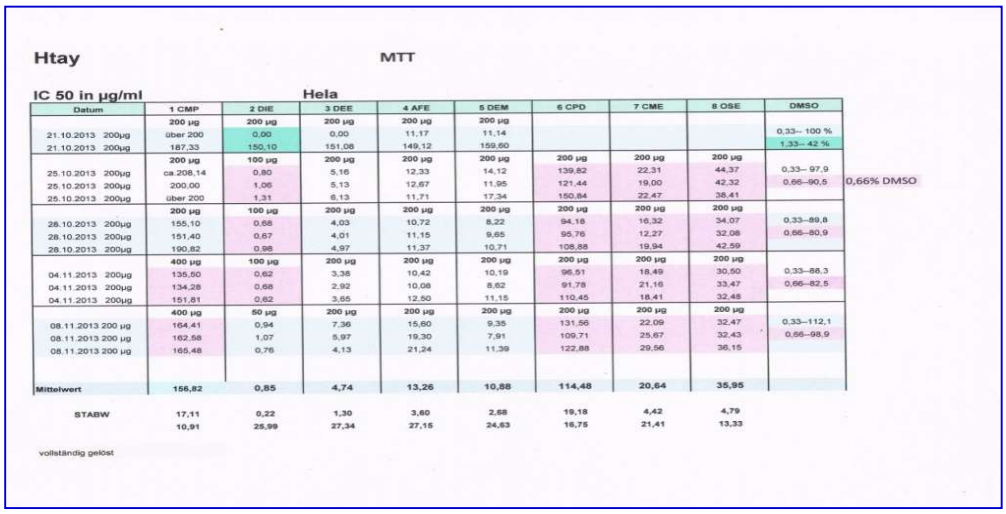

Htay

MTT

IC 50 in µg/ml

Hela

Datum	1 CMP	2 DIE	3 DEE	4 AFE	5 DEM	6 CPD	7 CME	8 OSE	DMSO	
	200 µg	200 µg	200 µg	200 µg	200 µg					
21.10.2013 200µg	über 200	0,00	0,00	11,17	11,14				0,33-- 100 %	
21.10.2013 200µg	187,33	150,10	151,08	149,12	159,60				1,33-- 42 %	
	200 µg	100 µg	200 µg	200 µg	200 µg	200 µg	200 µg	200 µg		
25.10.2013 200µg	ca.208,14	0,80	5,16	12,33	14,12	139,82	22,31	44,37	0,33-- 97,9	
25.10.2013 200µg	200,00	1,06	5,13	12,67	11,95	121,44	19,00	42,32	0,66--90,5	0,66% DMSO
25.10.2013 200µg	über 200	1,31	6,13	11,71	17,34	150,84	22,47	38,41		
	200 µg	100 µg	200 µg	200 µg	200 µg	200 µg	200 µg	200 µg		
28.10.2013 200µg	155,10	0,68	4,03	10,72	8,22	94,18	16,32	34,07	0,33--89,8	
28.10.2013 200µg	151,40	0,67	4,01	11,15	9,65	95,76	12,27	32,08	0,66--80,9	
28.10.2013 200µg	190,82	0,98	4,97	11,37	10,71	108,88	19,94	42,59		
	400 µg	100 µg	200 µg	200 µg	200 µg	200 µg	200 µg	200 µg		
04.11.2013 200µg	136,50	0,62	3,36	10,42	10,19	96,51	18,49	30,50	0,33--88,3	
04.11.2013 200µg	134,28	0,68	2,92	10,08	8,62	91,78	21,16	33,47	0,66--82,5	
04.11.2013 200µg	151,81	0,62	3,65	12,50	11,15	110,45	18,41	32,48		
	400 µg	50 µg	200 µg	200 µg	200 µg	200 µg	200 µg	200 µg		
08.11.2013 200 µg	164,41	0,94	7,36	15,60	9,35	131,56	22,09	32,47	0,33--112,1	
08.11.2013 200 µg	162,58	1,07	5,97	19,30	7,91	109,71	25,67	32,43	0,66--98,9	
08.11.2013 200 µg	165,48	0,76	4,13	21,24	11,39	122,88	29,56	36,15		
Mittelwert	156,82	0,85	4,74	13,26	10,88	114,48	20,64	35,95		
STABW	17,11	0,22	1,30	3,60	2,68	19,18	4,42	4,79		
	10,91	25,99	27,34	27,15	24,63	16,75	21,41	13,33		

vollständig gelöst

Figure 3: Cytotoxic activity result from the stem bark of Auk-chinsa testing with HeLa cells by MTT assay

Structure Elucidation of Isolated Compound

The concentrated pet- ether extract of the stem bark of *Diospyros ehretioides* was separated by column chromatography on silica gel resulted in the isolation of the naphthoquinone compound (KKW-1)with yield % of 1.787% .It was isolated as bright orange amorphous compound with melting point of 296-298°C .The analysis of the ^{1}H- NMR spectral data proton signals at 6.71, 6.72, 6.94, 6.95, 7.3, 7.61ppm revealed that the dimer structure of the aromatic compound(Table 3 and Figure 4). In addition, the four carbonyl carbon signals at 184.43, 184.88, 190.04, 190.31 and other aromatic carbon signals at 113.15, 114.18, 121.34, 125.70, 128.55, 128.75, 130.22, 135.09, 137.65, 138.72, 139.53, 140.11, 145.42, 148.10, 158.55, 161.91 ppm showed the presence of quinone compound (Table 3 and Figure 5). Furthermore , the

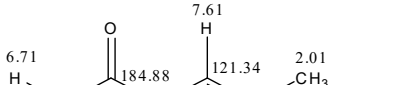

two methyl signals at 2.01, 2.03 and the two phenolic OH protons at 12.1, 12.5ppm described that the two 7- methyl juglone compounds were connected to form dimer type quinone compound. HSQC, HMBC and DQF-COSY experiments were utilized extensively to complete the ^{1}H- and ^{13}C-assignments and the connectivity between the dimer (Figures 6,7 and 8). HR-ESI-MS of the compound displayed a molecular ion $[M + H]^{+}$ at 375.0862 (calculated for $C_{22}H_{15}O_6$, m/z 375.0863) indicating a molecular formula of $C_{22}H_{14}O_6$ (Figure 9). Thus the compound (KKW-1) was determined to be 1',4-dihydroxy-2,3'-dimethyl-1,2'-binaphthyl-5,5',8,8'-tetraone.

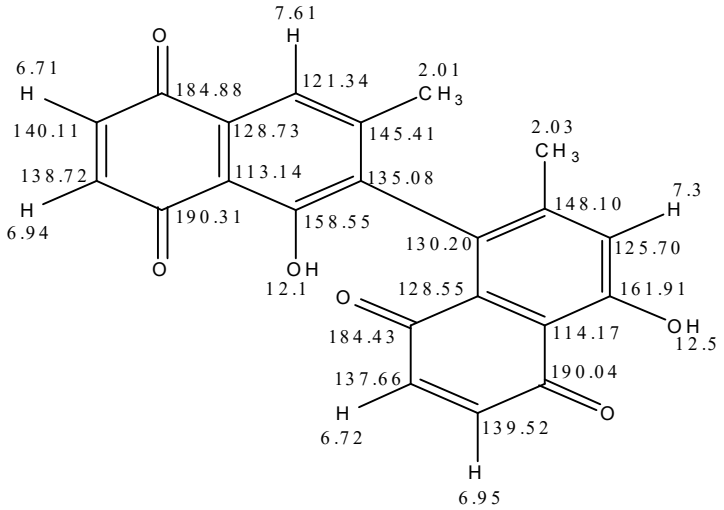

Complete Structure of Compound (KKW-1)

Table 3: NMR data (δ ppm, J in Hz, ^{1}H 600 MHz, ^{13}C 150 MHz 298 K) of the isolated compound (KKW-1)

No. of Proton & Carbon	Chemical shift δ(ppm)	
	H	**C**
C(1)	–	184.88
H–C(2)	6.71 (*d*, *J* = 8.7Hz)	140.11
H–C(3)	6.94 (*d*, *J* = 8.7Hz)	138.72
C(4)	–	190.31
C(5)	–	158.55
C(6)	–	135.08
C (7)	–	145.41
H–C(8)	7.61 (*s*)	121.34
C(9)	–	128.73
C(10)	–	113.14
CH_3(11)	2.01 (3H, *s*)	20.41
C (1')	–	184.43
H–C(2')	6.72 (*d*, *J* = 8.9Hz)	137.66
H–C(3')	6.95 (*d*, *J* = 8.9Hz)	139.52
C(4')	–	190.04
C(5')	–	161.91
C(6')	7.3 (*s*)	125.70
C (7')	–	148.10
H–C(8')	7.61 (*s*)	130.20
C(9')	–	128.55
C(10')	–	114.17
CH_3(11')	2.03 (3H, *s*)	20.60

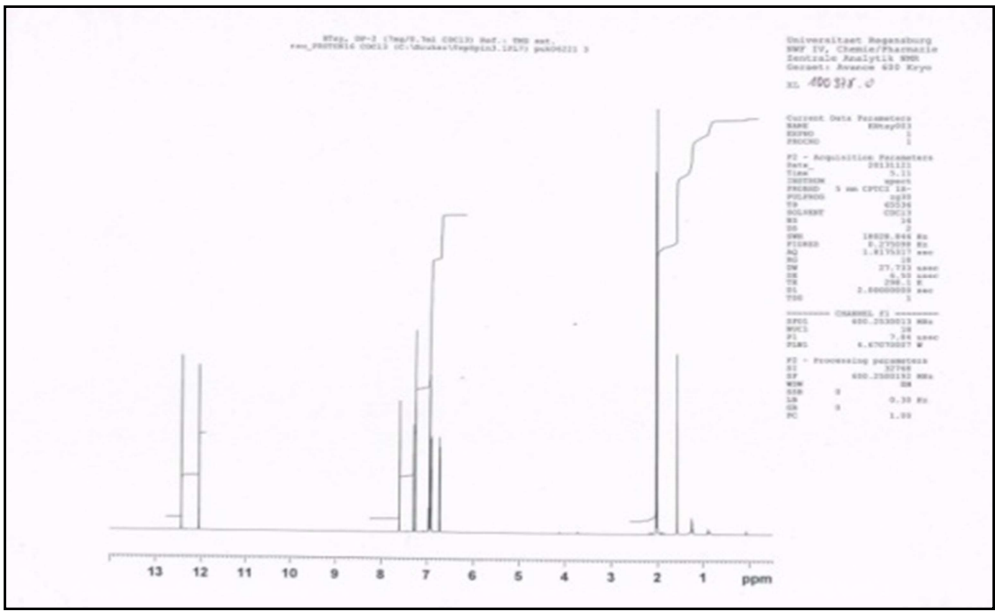

Figure 4: ^{1}HNMR spectrum of isolated compound (KKW-1)

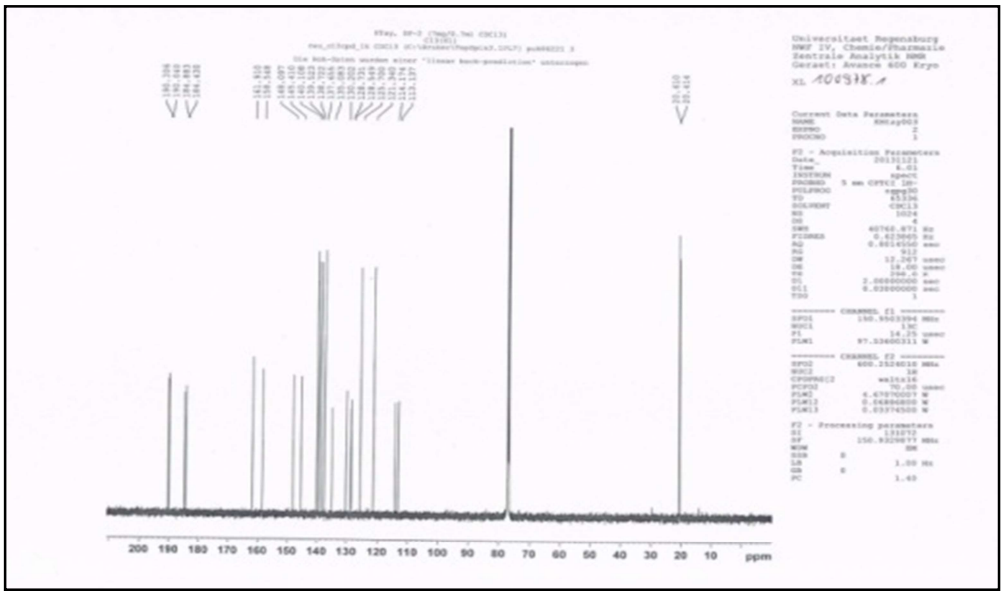

Figure 5: ^{13}CNMR spectrum of isolated compound (KKW-1)

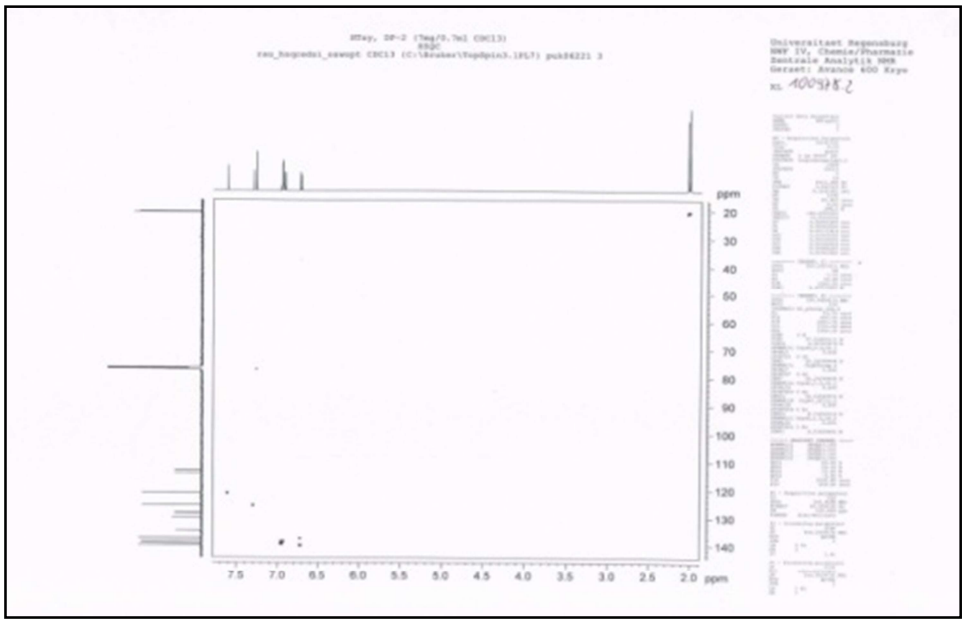

Figure 6: HSQC spectrum of isolated compound (KKW-1)

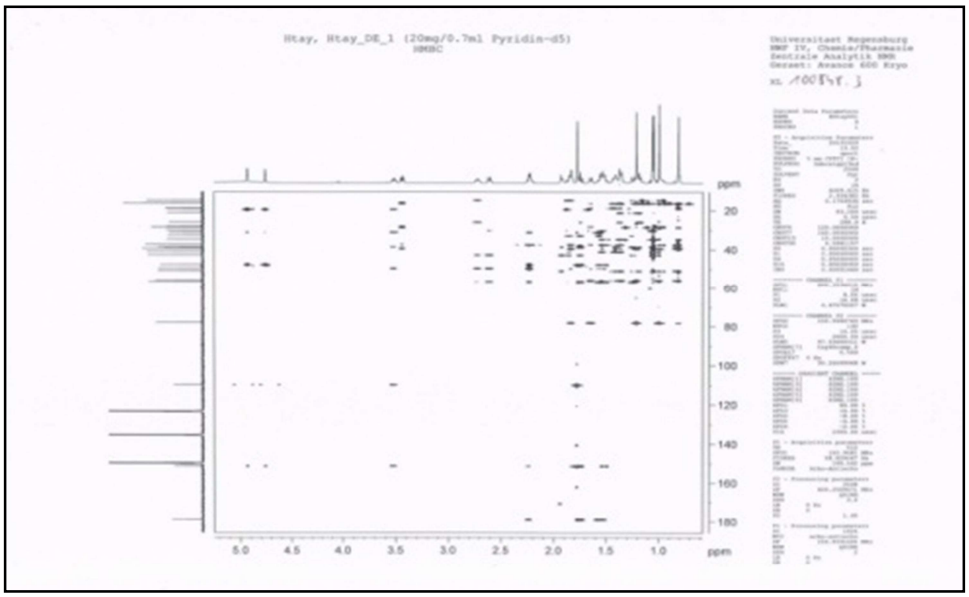

Figure 7: HMBC spectrum of isolated compound (KKW-1)

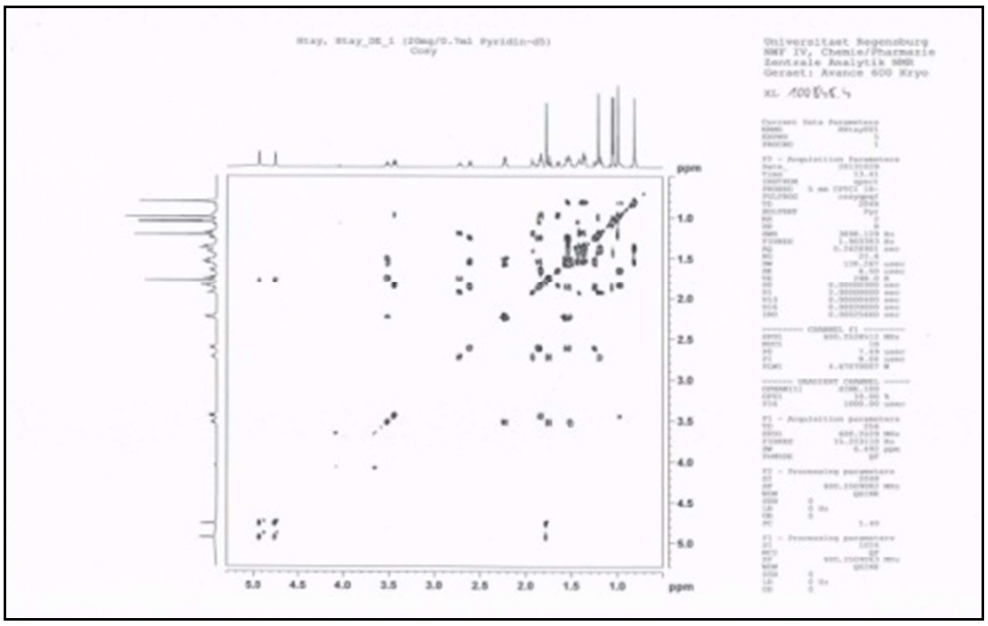

Figure 8: DQF-COSY Spectrum of isolated compound (KKW-1)

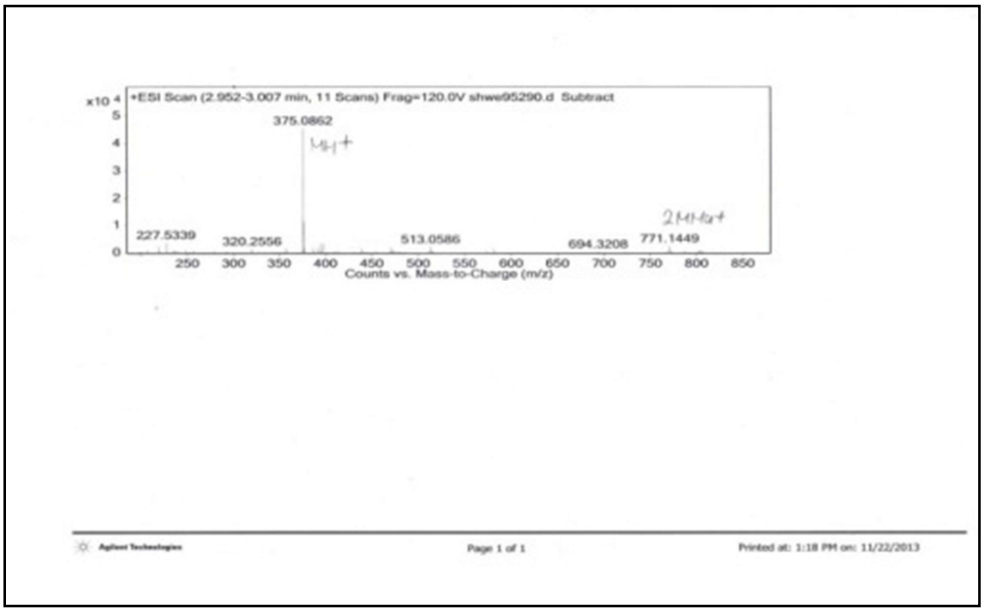

Figure 9: HR-ESI-MS Spectrum of isolated compound (KKW-1)

Conclusion

The stem bark of *Diospyros ehretioides* Wall., (Auk-chinsa) was used to determine the phytochemical constituents, to isolate the pure organic compound and to test the bioactivity and cytotoxicity of the crude extracts. The stem bark of this plant contains alkaloid, flavonoid, terpene, steroid, glycoside, polyphenol, sugar, saponin, and tannin. The high IC_{50} value of 0.85 μg/mL showed that this plant has high anticancer activity on HeLa cell (cervical cancer). The pure organic compound (KKW-1) so was isolated and by thin layer and column chromatographic separation techniques. The melting point of compound (KKW-1) was found to be 296- 298ºC. The yield percent of the isolated pure compound (KKW-1) was 1.787% (25.2 mg) based upon the pet- ether crude extract. The MS of compound (KKW-1) displayed (M^+) at m/z 374 (corresponding to $C_{22}H_{14}O_6$). The ^{1}H-NMR spectrum reflected two methyl groups (δ_H2.01 and 2.03 ppm) corresponding to δ_C 20.41 and 20.60 ppm. The existence of quinone type compound could be confirmed by the ^{13}C- NMR spectral data at four carbonyl carbons at δ_C 184.43, 184.88, 190.04 and 190.31 ppm. The ^{13}C-NMR spectrum reflected the presence of di phenol group at δ_C 158.55 and 161. 91 ppm corresponding phenolic protons at (δ_H12.1 and 12.5 ppm).Thus the compound (KKW-1) was determined to be 1',4-dihydroxy-2,3'-dimethyl-1,2'-binaphthyl-5,5',8,8'-tetraone.

Acknowledgements

We are very thankful to board of editor, of the Myanmar Academy of Arts and Science for allowing the presentation of this research paper. We are indebted to Professor, Dr Than Than Win, Head of Department of Chemistry University of for her permission to do this research.

References

Bhakuni, D. S., Satish, S., Shukla, Y. N. and Tandon, J. S. (1971). ‘‘Chemical Constituents of *Diospyros buxifolia, D. tomentosa, D. ferra, D. lotus, Rhus parviflora, Polygonum recumbens, Balanites aegyptiaca and Pyrus pashia’’. Phytochemistry,* vol.10, pp. 2829-2831

Carter, F. L., Garlo, A. M., Stanely, J. B. (1978).‘‘Termiticidal Components of Wood extracts: 7- methyljuglone from *Diospyros virginiana’’. J. Agric. Food Chem*., vol. 26, pp.869-873

Gamble, J. S. (1997). *Flora of the Presidency of Madras*. Dehradun: Bishen Singh Mahendra Pal Singh Publishers, India, vol.2, pp.772-778

Irvine, F. R. (1961). *Woody Plants of Ghana*. Oxford : Oxford University Press, p. 576

Sandermann, W., Dietrichs, H. H. and Gottwald, H. (1958). “Untersuchungen frühgeschichtlicher Hölzerundderen Bedeutung für den Holzschutz”. *Holz als Roh- und Werkstoff*, vol.16, pp.197-203

Scheffrahn, R. H. (1991). “Allelochemical Resistance of Wood to Termites”. *Sociobiology,* vol.19, pp.257-281

Waterman, P. G. and Mbi, C. N. (1979). “The Sterols and Dimeric Naphthoquinones of the Barks of Three West African *Diospyros species*”. *Planta Med*,vol.37, pp. 241-246

Watt, J. M. and Breyer-Brandwijk, M. G. B. (1962).“Medicinal and Poisonous Plants of Eastern and Southern Africa”. London:2nd Ed., E & S Livingstone, p. 369

Willis, J. C. (rev. H. A. Airy Shaw).(1966). *A Dictionary of Flowering Plants and Ferns*. New York: 7th Ed., Cambridge University Press, p.360